

Topics in Heterocyclic Chemistry 48

Series Editors: Bert Maes · Janine Cossy · Slovenko Polanc

William D. Lubell *Editor*

Peptidomimetics I

 Springer

48

Topics in Heterocyclic Chemistry

Series Editors:

Bert Maes, Antwerp, Belgium
Janine Cossy, Paris, France
Slovenko Polanc, Ljubljana, Slovenia

Editorial Board:

D. Enders, Aachen, Germany
S.V. Ley, Cambridge, UK
G. Mehta, Bangalore, India
R. Noyori, Nagoya, Japan
L.E. Overman, Irvine, CA, USA
A. Padwa, Atlanta, GA, USA

Aims and Scope

The series Topics in Heterocyclic Chemistry presents critical reviews on present and future trends in the research of heterocyclic compounds. Overall the scope is to cover topics dealing with all areas within heterocyclic chemistry, both experimental and theoretical, of interest to the general heterocyclic chemistry community.

The series consists of topic related volumes edited by renowned editors with contributions of experts in the field. All chapters from Topics in Heterocyclic Chemistry are published OnlineFirst with an individual DOI. In references, Topics in Heterocyclic Chemistry is abbreviated as Top Heterocycl Chem and cited as a journal.

More information about this series at <http://www.springer.com/series/7081>

William D. Lubell

Editor

Peptidomimetics I

With contributions by

S. Ballet · F. Cavelier · F. Diness · N.-D. Doan ·
D.P. Fairlie · Y. Garcia-Ramos · A. Geyer · K. Guillemyn ·
E.L. Handy · S. Hanessian · W.D. Lubell · J.Y.W. Mak ·
C. Martin · J. Martinez · M. Meldal · R.W. Newberry ·
R.T. Raines · E. Rémond · S. Schoffelen · B. Schurgers ·
J.K. Sello · D.J. St-Cyr · D. Tourwé · O. Van der Poorten ·
G. Verniest · M.A. Vilchis-Reyes · A. Wuttke · W. Xu



Springer

Editor

William D. Lubell
Département de Chimie
Université de Montréal
Montréal, QC
Canada

ISSN 1861-9282

Topics in Heterocyclic Chemistry

ISBN 978-3-319-49117-2

DOI 10.1007/978-3-319-49119-6

ISSN 1861-9290 (electronic)

ISBN 978-3-319-49119-6 (eBook)

Library of Congress Control Number: 2017942790

© Springer International Publishing AG 2017

This work is subject to copyright. All rights are reserved by the Publisher, whether the whole or part of the material is concerned, specifically the rights of translation, reprinting, reuse of illustrations, recitation, broadcasting, reproduction on microfilms or in any other physical way, and transmission or information storage and retrieval, electronic adaptation, computer software, or by similar or dissimilar methodology now known or hereafter developed.

The use of general descriptive names, registered names, trademarks, service marks, etc. in this publication does not imply, even in the absence of a specific statement, that such names are exempt from the relevant protective laws and regulations and therefore free for general use.

The publisher, the authors and the editors are safe to assume that the advice and information in this book are believed to be true and accurate at the date of publication. Neither the publisher nor the authors or the editors give a warranty, express or implied, with respect to the material contained herein or for any errors or omissions that may have been made. The publisher remains neutral with regard to jurisdictional claims in published maps and institutional affiliations.

Printed on acid-free paper

This Springer imprint is published by Springer Nature

The registered company is Springer International Publishing AG

The registered company address is: Gewerbestrasse 11, 6330 Cham, Switzerland

Preface

Peptide mimicry may be broadly defined as an approach for conceiving molecular structures that can replicate the molecular recognition elements that contribute to the activity of natural peptides [1–3]. The term peptide mimic (peptidomimetic) is used to describe such compounds. Peptidomimetics arise from the combination of chemical synthesis and employment of techniques from various other sciences which are necessary for ascertaining the potential of peptide surrogates. The pursuit of peptidomimetics is propelled by the desire to preserve the remarkable attributes, such as high potency and low toxicity, while simultaneously removing liabilities of the natural parent peptide structures, such as their rapid metabolism, lack of receptor selectivity, and poor bioavailability.

Heterocycles serve fundamental roles in the folding and function of natural peptides. For example, proline drives turn and helical structures by constraining the peptide backbone to a limited set of dihedral angles. Peptide macrocycles adopt commonly well-defined conformations responsible for their activity. The imidazole and indole heterocycle side chains of the amino acids histidine and tryptophan play vital roles for the recognition of various biologically relevant peptides. The various heterocycles used in natural peptides inspire the design of peptidomimetic counterparts.

The application of heterocycle chemistry in peptide mimicry has been paramount to successful designs of peptidomimetics. In addition to adding rigidity to stabilize active conformations and serving as side chain substitutions to improve recognition by targeted receptors, heterocycles have been employed in peptidomimetics to enhance metabolic stability. For example, replacement of amide and disulfide bonds by heterocycles has improved respectively stability against proteolytic cleavage and disulfide bond reduction.

The emphasis of this two-volume set is to illustrate contemporary applications of heterocycles in peptide mimicry. A bias towards the applications of the resulting peptidomimetics in chemical biology and medicinal chemistry is present likely due to the important history of peptides as drugs [4] as well as the boom of investment into peptide-based medicine [5, 6]. Concurrent growth of interest in peptidomimetic science has taken place with the rising employment of peptides in the

pharmaceutical industry, because of two primary goals: to provide probes to gain insight into the biologically active conformation of the native peptide and to furnish prototypes to improve pharmacokinetic properties for drug development. Aspects of heterocycle chemistry in peptide mimicry for other applications such as materials science and catalysis are specifically covered in particular chapters.

Reflecting on advances in peptide mimicry through the employment of heterocycles, different themes emerge from examination of their structural motifs and methods of synthesis. Heterocycles have been typically employed within single amino acid residues and dipeptides, as well as units that nucleate folding to replicate entire secondary structures, such as turns, helices, and sheets [7]. Applications of heterocycles within discrete units that fold into ordered conformations when placed into oligomers, so-called foldamers [8], have been restricted herein to examples that mimic natural peptide geometry, and for more information on alternative non-natural motifs, the interested reader is asked to consult a recent comprehensive review [9]. Similarly, the reader is directed elsewhere for information on heterocyclic frameworks that mimic peptide ligands for diverse receptors, so-called privileged structures [10–14], albeit the potential for diaze- and triazepinones to mimic γ - and β -turn conformations has recently been supported by crystallographic evidence [15, 16 and references therein], and certain heterocycle motifs have served in the *de novo* design of peptide mimics [17, 18]. Methods for making heterocycles and for employing their reactions to prepare constrained peptidomimetics are covered with particular focus on contemporary protocols that exhibit high tolerance for the various functional groups found in natural peptide structures.

The concept of peptide mimicry is broadly applied in this treatise. For example, peptides possessing a single non-natural alteration featuring a heterocycle are included as peptidomimetics in spite of their appearance as selectively modified variants of the natural structure. Similarly, natural products containing non-proteinogenic heterocycles are presented in certain chapters illustrating that nature too makes peptidomimetics. For example, the natural antibiotic penicillin, which inhibits transpeptidase and carboxypeptidase enzymes involved in the construction of the bacterial cell wall material peptidoglycan, functions by mimicking the D-alanine-D-alanine motif of the peptide component [19]. Modified peptide macrocycles are also considered as heterocycles. Finally, some chapters may mention heterocyclic peptidomimetics for which relationships to natural peptide structure and activity have yet to be established. In such cases, the purist is asked to be forgiving of the looseness of the definition and reminded that the goal of the work is to give a contemporary perspective, which aims to inspire future research in a growing field.

Volume I

Peptide backbone geometry is defined by the ϕ , ψ , and ω dihedral angle values of the respective amino acids in the sequence [20]. Local constraints that restrict such dihedral angles about these bonds in a single amino acid or between two amino

acids in a dipeptide can have significant consequences on the global conformation of the entire peptide. For example, a proline residue can favor turn geometry and align the amide bonds of distant amino acid residues in the peptide chain to form ordered hairpin and β -sheet conformations [21]. In longer peptides, such local restrictions combine with hydrophobic effects, van der Waals interactions, and hydrogen bonds to overcome peptide solvation and give rise to relatively stable folded protein three-dimensional structures [22]. Shorter peptides (i.e., <10 residues) may however exist in a dynamic balance of equilibrating conformations. Considering that the entropy penalty for folding into a conformation pre-organized for receptor affinity may be paid by electronic and structural constraints that offset the dynamic equilibrium, heterocycles have been employed strategically to place restrictions on particular dihedral angles with consequences on global geometry.

In Volume I of this treatise, the application of heterocycles that restrain single amino acid and dipeptide conformation are discussed in detail. The importance of the natural amino acid proline has led to various analogs possessing ring substituents to alter ring puckering, as well as to modify the ψ and ω dihedral angles by way of steric and electronic interactions [23–25]. In light of their importance to contemporary research on peptides in chemical biology, medicine, materials science, and catalysis, three chapters of this volume are dedicated to such modified prolines. Illustrating the consequence of a single atom replacement on the global geometry of peptides and entire proteins, Newberry and Raines present the synthesis and conformational analysis of analogs bearing 4-fluoroproline. Substitution of fluorine for hydrogen at the 4-position of proline causes significant inductive effects that influence the ring pucker, as well as the amide bond isomer equilibrium and rate of isomerization of its N-terminal amino acid residue. The consequences of such changes on peptide and protein structures are reviewed in detail with special attention to collagen stabilization. The replacement of the 4-position methylene by a dimethylsilyl group has been explored by Rémond, Martin, Martinez, and Cavalier, who discuss the influence of silaproline on heightening lipophilicity and improving resistance to biodegradation in a variety of peptide targets relevant to medicine and biomaterials science. Finally, the impact of an additional bridging methylene on the conformation of proline is described by Vilchis-Reyes and Hanessian, who detail the challenges in synthesizing such methanoproline and their various applications including serving as a component in the antidiabetic drug Onglyza as well as acting as organocatalysts. Expanding on the theme of proline-like heterocyclic amino acids, the chapter by Handy and Sello presents a review of research on the synthesis and applications of piperazine. This 6-aza-variant of piperazine, a proline homologue, exhibits influence on N-terminal amide geometry and local peptide conformation as a component of many natural products with anti-tumor, anti-HIV, antifungal, and antibacterial activities.

The pyrrolidine and piperidine amino acids, proline and piperolate, feature a bridge between their nitrogen and α -carbon. By moving the bridge from the N- to the C-terminal amino group in a peptide, a lactam ring is created which joins two amino acids ensemble. Such α -amino lactam dipeptide surrogates, so-called

Freidinger-Weber lactams, have been used to explore the conformation of a variety of biologically relevant peptides, since the Merck laboratory employed this heterocycle system to constrain the Gly-Leu fragment of luteinizing hormone-releasing hormone and received an agonist with nearly tenfold greater potency to that of the native hormone for release of luteinizing hormone in a pituitary cell culture system [26]. In two chapters, contemporary advances are featured in the synthesis and application of Freidinger-Weber lactam analogs. Reviewing recent literature on the synthesis of biologically active peptides bearing ring substituted α -amino γ -lactams, St-Cyr, Garcia-Ramos, Doan, and Lubell present recent developments of lactams and their elaboration into aza-variants in *N*-amino-imidazolone and *N*-amino-imidazolidinone dipeptides with particular attention to the influence of a second nitrogen on the conformation of these β -turn mimic analogs. The corresponding seven member α -amino ε -lactams are highlighted by Ballet, Guillemyn, Van der Poorten, Schurgers, Verniest, and Tourwé, who examine various synthetic methods for introducing such azepinone amino acids into medicinally relevant peptides with emphasis on elucidating biologically active conformations.

Azabicyclo[X.Y.0]alkanone amino acids are heterocyclic systems in which the central amide nitrogen of a dipeptide is bridged to the α -carbons of both its N- and C-terminal amino acid residues [27–29] [30 and references therein] [31, 32]. These bicyclic dipeptide mimics combine attributes of proline-like and α -amino lactam structures described above. Since pioneering syntheses of the thia-indolizidinone [31] and thiapyrroloazepinone [32] constrained dipeptides, azabicycloalkanone amino acids have been employed to control peptide folding and to serve as rigid platforms for orienting pharmacophores in peptide science and medicinal chemistry. The development of synthetic methods to access these heterocycles has led to various studies of the influences of their ring sizes, stereochemistry, and ring substituents on peptide conformation. Exploring applications of carbohydrates as building blocks for the effective construction of azabicycloalkanone amino acids possessing polyhydroxylated frameworks, Wuttke and Geyer describe the propensity of such systems to favor turn and loop conformations. The utility of polyhydroxylated bicyclic dipeptides is contrasted with other sugar-amino acid hybrids [33] and highlighted for the ability to stabilize stand-alone peptide hairpins and to mediate protein–protein interactions.

Finally, Volume I concludes with two chapters on five-member heterocycles that have garnered significant use in peptide, protein, and peptidomimetic chemistry. Thiazoles have been employed as amide bond surrogates, pharmacophores, and directing groups in enzyme inhibitors, receptor agonists and antagonists, and mediators of protein–protein interactions. Examining physical properties, such as dipole movement and potential for hydrogen bonding, Mak, Xu, and Fairlie illustrate the utility of thiazoles in peptide mimicry with focus on their importance in natural products and broad applications in drug design in which they serve as the most common 5-membered heterocycle of contemporary pharmaceuticals. Triazoles are emerging rapidly as the most important heterocycle for peptide and protein science in great part because of their effective synthesis by contemporary methods such as copper-catalyzed and strain-promoted azide–alkyne

cycloadditions (CuAAC and SPAAC). Examining the development of triazole chemistry in the context of peptide mimicry, Diness, Schoffelen, and Meldal illustrate how modern synthetic methods have advanced applications of these heterocycles from amide bond isosteres, to disulfide bond mimics, to versatile linchpins for cross-linking various biomolecular entities to peptide structures. Conception of biocompatible approaches for their construction has liberated triazole synthesis from conventional organic methods to empower applications inside live cells to study dynamic biological phenomena.

Volume II

In contrast to Volume I, which focuses predominantly on the local constraints of heterocyclic amino acids, dipeptides, and five-membered ring systems, and their consequences on the global geometry and biological activity of peptides and proteins, Volume II focuses on larger peptide structures. For example, the syntheses of mimics of helices, sheets, and larger folded motifs are discussed in chapters focusing on techniques for their stabilization using multiple heterocycle ring constraints, nucleating units that template hydrogen bonds, as well as cyclic peptides. Methods that assemble multiple rings from iminium ion intermediates are discussed in depth because of their power to add conformational constraint by a single step performed often on the peptide structure late in the synthesis. Peptide macrocycles are discussed within the context of their ability to adopt favored conformations, such as β -sheets. Novel methods for the effective synthesis of macrocycles are reviewed and focus is given to important biologically active macrocycle examples in medicinal chemistry oriented to deliver new antibiotics as well as therapeutics to treat maladies of misfolding, such as Alzheimer's and Parkinson's diseases. Finally, post-translational modification of peptides and proteins by heterocycle structures is discussed with specific focus on the heterocyclic disulfide lipoic acid.

Brief Historical Perspective

The chemistry of peptide mimicry finds origins in pioneering research on heterocycles, amino acids, and peptides. Scholarly appreciation of contemporary research on peptidomimetics in synthetic laboratories around the world at the moment necessitates a knowledge of the relevance of seminal chemistry, much of which was developed over a hundred years ago, to the foundation of modern method discovery. In our age of search engines that tend to juxtapose information without concern for chronological order, the student engaged in the science of peptide mimicry may feel somewhat lost swimming in the sea of knowledge without historical perspective. In this light, the authors of individual chapters

have made important efforts to place research into context by summarizing key discoveries. For the interest of full pedagogic disclosure, some relevant background is now provided with citations to key publications and review articles that may offer a broader stage on which the interested student may build a core of knowledge regarding the origins of heterocycles in peptide mimicry.

The age of the discovery and the characterization of twenty one of the amino acids from proteins started in 1820, when Braconnot isolated glycine from gelatin and continued steadily until the early 1920s when Mueller announced the discovery of methionine from casein [34]. Several milestones in amino acid and peptide science were accomplished during this time period. In particular, one of the first multicomponent reactions was developed by Strecker, who synthesized α -amino nitriles in 1850 [35]. Soon thereafter, Limpricht used this process to synthesize racemic leucine from hydrolysis of the product from valeraldehyde, ammonia, and hydrocyanic acid [34]. Moreover, between 1881 and 1906, Curtius and Fischer employed respectively acid azides and acyl chlorides to make the amide bonds of the first synthetic peptides [36]. During the following hundred years, the science of peptide chemistry was transformed by synthetic methods. Heroic efforts to make important biologically relevant peptides led the way to modern technology for preparing libraries of peptide analogs and effective methods for the assembly of entire proteins from peptides fragments [37]. Key discoveries in the field during this transition included various protecting groups, coupling agents and solid supports [38], pioneering syntheses of oxytocin [39], insulin [40] and HIV protease [41], and revolutionizing technology such as peptide sequencing [42], Merrifield solid-phase synthesis [43], robotic synthesizers [44], and native-chemical ligation [45]. The advent of solid-phase synthesis ushered in the age of peptide analog synthesis, in which residues in the sequence were commonly replaced by other natural and later synthetic amino acids to gain insight into structure-activity relationships [46]. Scanning techniques began to be employed using systematic replacement of each residue of the sequence by a particular amino acid, such as alanine or proline, to gain respectively insight into the importance of side chains and conformation for biological activity [47]. To improve peptide metabolic stability, attention has been turned towards applications of amidation, acylation, *N*-methylation, and cyclization [48], as well as backbone modifications using amide isosteres [49], and replacement of the α -carbons of amino acid residues with nitrogen in so-called azapeptides [50].

In the 1980s, perception in peptide science changed significantly as the application of heterocycle chemistry to control conformation took root. In 1980, Freidinger and Veber demonstrated the power of α -amino lactams for controlling peptide conformation to identify a biologically active conformer and enhance biological activity [26, 51, 52]. Implementation of azabicyclo[X.Y.0]alkanone amino acids to control peptide folding and orient pharmacophores soon followed [27–32]. Industrial interest in harnessing peptides for applications in medicine drove the use of heterocycles to study peptide structures as conformational constraints of the parent sequence [26], in de novo designs of peptidomimetics [53, 54], and in privilege structures that interacted effectively with multiple receptors that bind endogenous peptide ligands [10–14]. Moreover, academic interest gave rise to several designs

of heterocycle templates that nucleated peptide secondary structures [7, 55, 56], such as β -turns [57], β -sheets [58], and α -helices [59]. In addition, the concept of forming side chain to side chain bridges (commonly referred to as “stapled” peptides [47]) was formulated in the 1980s and applied to stabilize α -helical conformations [60]. This decade was particularly rich with innovation for the synthesis of heterocyclic peptidomimetics and paved the way for many creative designs in the decades that followed.

The two treatises that follow provide background on the developments of the field of heterocycles in peptide and protein science since these pioneering discoveries highlight state-of-the-art achievements that define the future to come. In this light, the field of heterocyclic peptidomimetics has grown significantly from its roots in natural product isolation and medicinal chemistry. Analogous to the way methods for peptide synthesis provided impetus for the creation of novel reagents, reactions, and techniques that have advanced the field of organic chemistry in general, modern approaches for assembling heterocycles effectively in the presence of the diverse functional groups common in peptide structures are now influencing the exploration of various domains including chemical biology, materials science, catalysis, and nano-technology.

Montréal, QC, Canada

William D. Lubell

References

1. Marshall GR (1993) A hierarchical approach to peptidomimetic design. *Tetrahedron* 49:3547–3558
2. Hruby VJ, Cai MY, Insel PA (2013) Design of peptide and peptidomimetic ligands with novel pharmacological activity profiles. *Annu Rev Pharmacol Toxicol* 53:557–580
3. Ko E, Liu J, Burgess K (2011) Minimalist and universal peptidomimetics. *Chem Soc Rev* 40:4411–4421
4. Hirschmann R (1991) Medicinal chemistry in the golden-age of biology—lessons from steroid and peptide research. *Angew Chem Int Ed Engl* 30:1278–1301
5. Vlieghe P, Lisowski V, Martinez J, Khrestchatisky M (2010) Synthetic therapeutic peptides: science and market. *Drug Discov Today* 15:40–56
6. Fosgerau K, Hoffmann T (2015) Peptide therapeutics: current status and future directions. *Drug Discov Today* 20:122–128
7. Kemp DS (1990) Peptidomimetics and the template approach to nucleation of beta-sheets and alpha-helices in peptides. *Trends Biotechnol* 8:249–255
8. Gellman SH (1998) Foldamers: a manifesto. *Acc Chem Res* 31:173–180
9. Hill DJ, Mio MJ, Prince RB, Hughes TS, Moore JS (2001) A field guide to foldamers. *Chem Rev* 10:13893–14012
10. Evans BE, Rittle KE, Bock MG, DiPardo RM, Freidinger RM, Whitter WL, Lundell GF, Veber DF, Anderson PS, Chang RSL, Lotti VJ, Cerino DJ, Chen TB, Kling PJ, Kunkel KA, Springer JP, Hirshfield J (1988) Methods for drug discovery: development of potent, selective, orally effective cholecystokinin antagonists. *J Med Chem* 31:2235–2246

- Patchett AA, Nargund RP (2000) Privileged structures — an update. *Annu Rep Med Chem* 35:289–298
- Horton DA, Bourne GT, Smythe ML (2003) The combinatorial synthesis of bicyclic privileged structures or privileged substructures. *Chem Rev* 103:893–930
- Bongarzone S, Bolognesi ML (2011) The concept of privileged structures in rational drug design: focus on acridine and quinoline scaffolds in neurodegenerative and protozoan diseases. *Expert Opin Drug Discovery* 6:251–268
- Welsch ME, Snyder SA, Stockwell BR (2010) Privileged scaffolds for library design and drug discovery. *Curr Opin Chem Biol* 14:347–361
- Dörr AA, Lubell WD (2015) γ -Turn mimicry with benzodiazepinones and pyrrolobenzodiazepinones synthesized from a common amino ketone intermediate. *Org Lett* 17:3592–3595
- Douchez A, Lubell WD (2015) Chemoselective alkylation for diversity-oriented synthesis of 1,3,4-benzotriazepin-2-ones and pyrrolo[1,2][1,3,4]benzotriazepin-6-ones, potential turn surrogates. *Org Lett* 17:6046–6049
- Hirschmann RF, Nicolaou KC, Angeles AR, Chen JS, Smith AB 3rd (2009) The beta-D-glucose scaffold as a beta-turn mimetic. *Acc Chem Res* 42:1511–1520
- Dufour-Gallant J, Chatenet D, Lubell WD (2015) De novo conception of small molecule modulators based on endogenous peptide ligands: pyrrolo-diazepin-2-one γ -turn mimics that differentially modulate urotensin II receptor-mediated vasoconstriction ex vivo. *J Med Chem* 58:4624–4637
- Lee M, Heseck D, Suvorov M, Lee W, Vakulenko S, Mobashery S (2003) A mechanism-based inhibitor targeting the DD-transpeptidase activity of bacterial penicillin-binding proteins. *J Am Chem Soc* 125:16322–16326
- Ramachandran GN, Ramakrishnan C, Sasisekharan V (1963) Stereochemistry of polypeptide chain configurations. *J Mol Biol* 7:95–99
- Lubell WD, Beauregard KS, Polyak F (2012) Peptides and chirality effects on the conformation and the synthesis of medicinally relevant peptides. In: Carreira EM, Yamamoto H (eds) *Comprehensive chirality*, vol 1. Elsevier, Amsterdam, pp 86–104
- Baldwin RL (2007) Energetics of protein folding. *J Mol Biol* 371:283–301
- Duttagupta I, Misra D, Bhunya S, Paul A, Sinha S (2015) Cis–trans conformational analysis of δ -azaproline in peptides. *J Org Chem* 80:10585–10604
- Beausoleil E, Lubell WD (1996) Steric effects on the amide isomer equilibrium of prolyl peptides. Synthesis and conformational analysis of N-acetyl-5-tert-butylproline N'-methylamides. *J Am Chem Soc* 118:12902–12908
- Feytens D, Chaume G, Chassaing G, Lavielle S, Brigaud T, Byun BJ, Kang YK, Miclet E (2012) Local control of the cis–trans isomerization and backbone dihedral angles in peptides using trifluoromethylated pseudoproline. *J Phys Chem B* 116:4069–4079
- Freidinger RM (2003) Design and synthesis of novel bioactive peptides and peptidomimetics. *J Med Chem* 46:5553–5566
- Hanessian S, McNaughton-Smith G, Lombart H-G, Lubell WD (1997) Design and synthesis of conformationally constrained amino acids as versatile scaffolds and peptide mimetics. *Tetrahedron* 53:12789–12854
- Khashper A, Lubell WD (2014) Design, synthesis, conformational analysis and application of indolizidin-2-one dipeptide mimics. *Org Biomol Chem* 12:5052–5070
- Cluzeau J, Lubell WD (2005) Design, synthesis, and application of azabicyclo[X.Y.0]alkanone amino acids as constrained dipeptide surrogates and peptide mimics. *Biopolymers* 80:98–150
- Atmuri NDP, Lubell WD (2015) Insight into transannular cyclization reactions to synthesize azabicyclo[X.Y.Z]alkanone amino acid derivatives from 8-, 9-, and 10-membered macrocyclic dipeptide lactams. *J Org Chem* 80:4904–4918

31. Nagai U, Sato K (1985) Synthesis of a bicyclic dipeptide with the shape of β -turn central part. *Tetrahedron Lett* 26:647–650
32. Wyratt MJ, Tischler MH, Ikeler TJ, Springer JP, Tristram EW, Patchett AA (1983) In peptides, structure and function. In: Hruby VJ, Rich DH (eds) *Proceedings of the 8th American Peptide Symposium*. Pierce Chemical Company, Rockford, p 551
33. Gruner SAW, Locardi E, Lohof E, Kessler H (2002) Carbohydrate-based mimetics in drug design: sugar amino acids and carbohydrate scaffolds. *Chem Rev* 102:491–514
34. Vickery HB, Schmidt CLA (1931) The history of the discovery of the amino acids. *Chem Rev* 9:169–318
35. Wang J, Liu X, Feng X (2011) Asymmetric strecker reactions. *Chem Rev* 111:6947–6983
36. Miranda LP, Alewood PF (2000) Challenges for protein chemical synthesis in the 21st century: bridging genomics and proteomics. *Biopolymers* 55:217–226
37. Kimmerlin T, Seebach D (2005) '100 years of peptide synthesis': ligation methods for peptide and protein synthesis with applications to β -peptide assemblies. *J Peptide Res* 65:229–260
38. Barany G, Kneib-Cordonier N, Mullen DG (1987) Solid-phase peptide synthesis: a silver anniversary report. *Int J Peptide Protein Res* 30:705–739
39. Ottenhausen M, Bodhinayake I, Banu MA, Stieg PE, Schwartz TH (2015) Vincent du Vigneaud: following the sulfur trail to the discovery of the hormones of the posterior pituitary gland at Cornell Medical College. *J Neurosurg* 124:1538–1542
40. Zaykov AN, Mayer JP, Gelfanov VM, DiMarchi RD (2014) Chemical synthesis of insulin analogs through a novel precursor. *ACS Chem Biol* 9:683–691
41. Milton RC, Milton SC, Kent SB (1992) Total chemical synthesis of a D-enzyme: the enantiomers of HIV-1 protease show reciprocal chiral substrate specificity [corrected]. *Science* 256:1445–1448
42. Edman P (1949) A method for the determination of amino acid sequence in peptides. *Arch Biochem* 22:475
43. Merrifield RB (1963) Solid phase peptide synthesis. I. The synthesis of a tetrapeptide. *J Am Chem Soc* 85:2149–2154
44. Mäde V, Els-Heindl S, Beck-Sickinger AG (2014) Automated solid-phase peptide synthesis to obtain therapeutic peptides. *Beilstein J Org Chem* 10:1197–1212
45. Dawson PE, Muir TW, Clark-Lewis I, Kent SB (1994) Synthesis of proteins by native chemical ligation. *Science* 266:776–779
46. Rudinger J (1971) The design of peptide hormone analogs. In: Ariens EJ (ed) *Drug design*, vol II. Academic, New York, p 319
47. Jamieson AG, Sabatino D, Boutard N, Lubell WD (2013) Peptide scanning for studying structure-activity relationships in drug discovery. *Chem Biol Drug Des* 81:148–165
48. Veber DF, Freidinger RM (1985) The design of metabolically-stable peptide analogs. *Trends Neurosci* 8:392–396
49. Spatola AF (1983) Peptide backbone modifications: a structure-activity analysis of peptides containing amide bond surrogates, conformational constraints, and related backbone replacements. In: Weinstein B (ed) *Chemistry and biochemistry of amino acids, peptides, and proteins*, vol VII. Marcel Dekker, New York, pp 267–357
50. Proulx C, Sabatino D, Hopewell R, Spiegel J, García-Ramos Y, Lubell WD (2011) Azapeptides and their therapeutic potential. *Future Med Chem* 3:1139–1164
51. Freidinger RM, Veber DF, Hirschmann R, Paege LM (1980) Lactam restriction of peptide conformation in cyclic hexapeptides which alter rumen fermentation. *Int J Pept Protein Res* 16:464–470

52. Freidinger RM, Veber DF, Perlow DS, Brooks JR, Saperstein R (1980) Bioactive conformation of luteinizing hormone-releasing hormone: evidence from a conformationally constrained analog. *Science* 210:656–658
53. Adang AEP, Hermkens PHH, Linders JTM, Ottenheijm HCJ, van Staveren CJ (1994) Case histories of peptidomimetics: progression from peptides to drugs. *Recl Trav Chim Pays-Bas* 113:63–78
54. Olson GL, Bolin DR, Bonner MP, Bos M, Cook CM, Fry DC, Graves BJ, Hatada M, Hill DE, Kahn M, Madison VS, Rusiecki VK, Sarabu R, Sepinwall J, Vincent GP, Voss ME (1993) Concepts and progression in the development of peptide mimetics. *J Med Chem* 36:3039–3049
55. Hölzemann G (1991) Peptide conformation mimetics (Part 1). *Kontakte (Darmstadt)* 3–12
56. Hölzemann G (1991) Peptide conformation mimetics (Part 2). *Kontakte (Darmstadt)* 56–63
57. Feigel M (1986) 2,8-Dimethyl-4-(carboxymethyl)-6-(aminomethyl)phenoxathiin S-dioxide: an organic substitute for the beta.-turn in peptides? *J Am Chem Soc* 108:181–182
58. Bowen BR, Kemp DS (1988) Synthesis of peptide-functionalized diacylaminoepindolidiones as templates for β -sheet formation. *Tetrahedron Lett* 29:5077–5080
59. Curran TP, Kemp DS (1988) (2S,5S,8S,11S)-1-Acetyl-1,4-diaza-3-keto-5-carboxy-10-thia-tricyclo-[2.8.0^{4,8}]-tridecane, 1. Synthesis of prolyl-proline-derived, peptide-functionalized templates for α -helix formation. *Tetrahedron Lett* 29:4931–4934
60. Felix AM, Heimer EP, Wang CT, Lambros TJ, Fournier A, Mowles TF, Maines S, Campbell RM, Wegrzynski BB, Toome V (1988) Synthesis, biological activity and conformational analysis of cyclic GRF analogs. *Int J Pept Protein Res* 32:441–454

Contents

4-Fluoroprolines: Conformational Analysis and Effects on the Stability and Folding of Peptides and Proteins	1
Robert W. Newberry and Ronald T. Raines	
Silaproline, a Silicon-Containing Proline Surrogate	27
Emmanuelle Rémond, Charlotte Martin, Jean Martinez, and Florine Cavelier	
Proline Methanologues: Design, Synthesis, Structural Properties, and Applications in Medicinal Chemistry	51
Miguel Angel Vilchis-Reyes and Stephen Hanessian	
Structure and Synthesis of Conformationally Constrained Molecules Containing Piperazic Acid	97
Emma L. Handy and Jason K. Sello	
Aminolactam, <i>N</i>-Aminoimidazolone, and <i>N</i>-Aminoimidazolidinone Peptide Mimics	125
Daniel J. St-Cyr, Yésica García-Ramos, Ngoc-Duc Doan, and William D. Lubell	
Azebinone-Constrained Amino Acids in Peptide and Peptidomimetic Design	177
Steven Ballet, Karel Guillemin, Olivier Van der Poorten, Ben Schurgers, Guido Verniest, and Dirk Tourwé	
Polyhydroxylated Cyclic Delta Amino Acids: Synthesis and Conformational Influences on Biopolymers	211
André Wuttke and Armin Geyer	
Thiazoles in Peptides and Peptidomimetics	235
Jeffrey Y.W. Mak, Weijun Xu, and David P. Fairlie	

Advances in Merging Triazoles with Peptides and Proteins	267
Frederik Diness, Sanne Schoffelen, and Morten Meldal	
Index	305

4-Fluoroprolines: Conformational Analysis and Effects on the Stability and Folding of Peptides and Proteins

Robert W. Newberry and Ronald T. Raines

Abstract Proline is unique among proteinogenic amino acids because a pyrrolidine ring links its amino group to its side chain. This heterocycle constrains the conformations of the main chain and thus templates particular secondary structures. Proline residues undergo posttranslational modification at the 4-position to yield 4-hydroxyproline, which is especially prevalent in collagen. Interest in characterizing the effects of this modification led to the use of 4-fluoroprolines to enhance inductive properties relative to the hydroxyl group of 4-hydroxyproline and to eliminate contributions from hydrogen bonding. The strong inductive effect of the fluoro group has three main consequences: enforcing a particular pucker upon the pyrrolidine ring, biasing the conformation of the preceding peptide bond, and accelerating *cis*–*trans* prolyl peptide bond isomerization. These subtle yet reliable modulations make 4-fluoroproline incorporation a complement to traditional genetic approaches for exploring structure–function relationships in peptides and proteins, as well as for endowing peptides and proteins with conformational stability.

Keywords Collagen • Gauche effect • $n \rightarrow \pi^*$ interaction • Pyrrolidine • Stereoelectronic effect

Contents

1	Introduction	2
2	Synthesis	2
3	Conformational Analysis	5
4	Effects on Collagen Stability	10
5	Effects on Peptide Conformation	13

R.W. Newberry and R.T. Raines (✉)
Departments of Chemistry and Biochemistry, University of Wisconsin–Madison, Madison,
WI 53706, USA
e-mail: rtraines@wisc.edu

6	Effects on Protein Folding	15
7	Impact in Medicinal Chemistry	19
8	Outlook	20
	References	21

1 Introduction

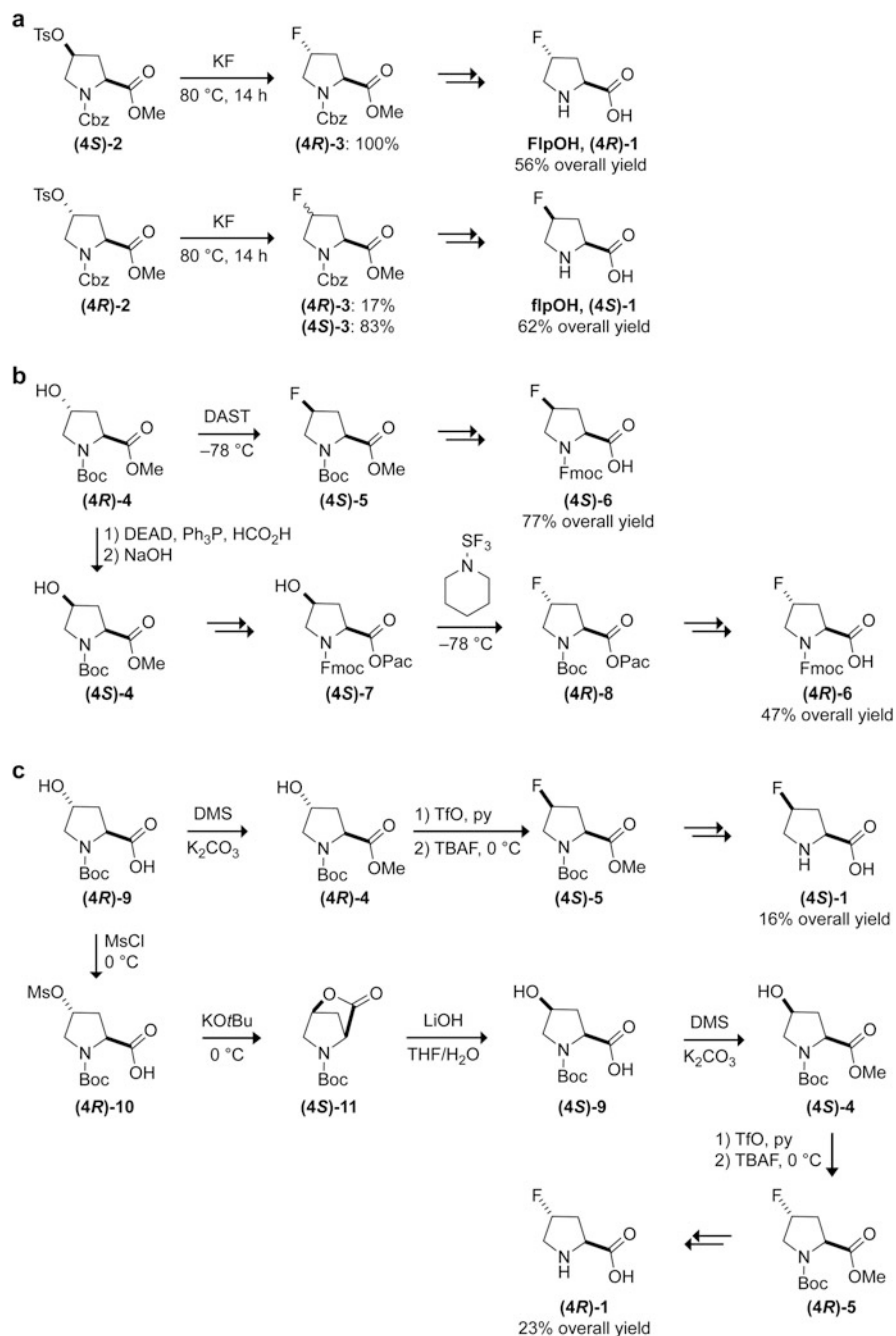
Proline is unique among proteinogenic amino acids because its α -amino group is constrained within a pyrrolidine. This heterocyclic ring restricts the ϕ ($C_{i-1}'-N_i-C_i^\alpha-C_i'$) main-chain dihedral angle, making proline an important determinant of the conformational stability of proteins [1]. Moreover, the pyrrolidine ring promotes population of both the *cis* and *trans* conformation of the preceding peptide bond, thereby enabling structural diversity. The isomerization of this “prolyl amide” bond can limit the folding rate of a protein [2].

Consistent with the conformational restriction imposed by proline relative to other amino acids, proline is prevalent in structural proteins, especially collagen [3]. In 1901, Fischer discovered proline in gelatin hydrolysates [4]. A year later, he discovered therein the product of the earliest known posttranslational modification: 4-hydroxyproline [5]. Within collagen strands, proline residues are oxidized at the 4*R* position by prolyl-4-hydroxylase (P4H [6]), an essential enzyme in animals [7–9]. Attempts to understand this modification led ultimately to the development of a wide variety of proline analogs [10]. Among these, 4-fluoroproline have emerged as powerful tools for studying collagen, as well as for engineering conformationally biased peptides and proteins.

4-Fluoroproline were first employed in 1965 [11], when they were used to investigate the mechanism of collagen hydroxylation and found to be incorporated successfully into collagen proteins [12–15]. Although early studies focused mainly on collagen hydroxylation [11, 16, 17], 4-fluoroproline have now been applied to study a wide variety of systems, some of which have been reviewed previously [18–21]. In this review, the utility of these important heterocycles is presented with a thorough discussion of their synthesis and conformational properties, followed by a detailed examination of their impact on the stability and folding of peptides and proteins. We conclude with an overview of the growing interest of employing 4-fluoroproline for medicinal applications.

2 Synthesis

4-Fluoroproline syntheses have improved significantly since the original report [11]. Nearly all of the syntheses employ displacement of the hydroxyl group of 4-hydroxyproline with a fluoride source. Activation of the hydroxyl group of Cbz-4-hydroxyproline as tosylate **2** before displacement by inorganic fluoride at



Scheme 1 Routes for the chemical synthesis of 4-fluoroprolines. Protecting group manipulations are indicated with *double arrows*. (a) Original synthetic route employing inorganic fluoride [11]. (b) Synthesis of 4-fluoroproline from a single 4-hydroxyproline stereoisomer using sulfur trifluoride reagents [22, 23]. (c) Synthesis of 4-fluoroproline from a single 4-hydroxyproline stereoisomer using organic fluoride [24]

elevated temperatures gave 56–62% yields of (4*S*)- and (4*R*)-*N*-Cbz-4-fluoroprolines **3** to afford, after protecting group removal, (2*S*,4*S*)-fluoroproline (flp, (4*S*)-**1**) from (2*S*,4*R*)-4-hydroxyproline (Hyp) with complete stereochemical inversion, but diastereomeric mixtures of (2*S*,4*R*)-4-fluoroproline (Flp, (4*R*)-**1**) starting from (2*S*,4*S*)-4-hydroxyproline (hyp) (Scheme 1a) [11]. Subsequent reports found difficulty in generalizing this procedure for use of alternative protecting group schemes [22]. Demand existed for syntheses that could provide *both* stereoisomers starting from naturally occurring and relatively less expensive Hyp.

Preliminary work to bypass the alcohol activation step by employing organic fluorinating agents generally resulted in inseparable mixtures of the 4*R* and 4*S* diastereomers [25–28]. Successful syntheses of both 4-fluoroproline diastereomers from a single 4-hydroxyproline diastereomer were first reported in 1998 [22]. Employing diethylaminosulfur trifluoride (DAST) as the fluorine source, both Boc- and Fmoc-flp were prepared in approximately 80% yield from Boc-Hyp-OMe (Scheme 1b). Inversion of the alcohol of (4*R*)-*N*-trityl-4-hydroxyproline methyl ester by a Mitsunobu procedure using benzoic acid as the nucleophile followed by saponification and *N*-protection gave (4*S*)-**5**, which was similarly converted to Fmoc-Flp ((4*R*)-**6**), albeit in <25% yield [22]. Substitution of formic acid for benzoic acid enabled the Mitsunobu reaction in the presence of Boc-amine protection to generate (4*S*)-**4** in 78% yield (Scheme 1b) [23]. Moreover, switching from a methyl to a phenylacetyl (Pac, PhCOCH₂-) ester enabled an orthogonal cleavage with Zn in AcOH in the presence of Boc and Fmoc amine-protecting groups [23]. Fluorination of Pac ester (4*S*)-**7** with morpholiniosulfur trifluoride inverted the alcohol to give 4-fluoroproline (4*R*)-**8** in 79–94% yields. The configuration of Boc-flp was assigned by X-ray diffraction, and chiral HPLC established that the synthesis produced single stereoisomers. Protecting group manipulation then provided Fmoc-fluoroproline starting materials **6** for solid-phase synthesis (Scheme 1b).

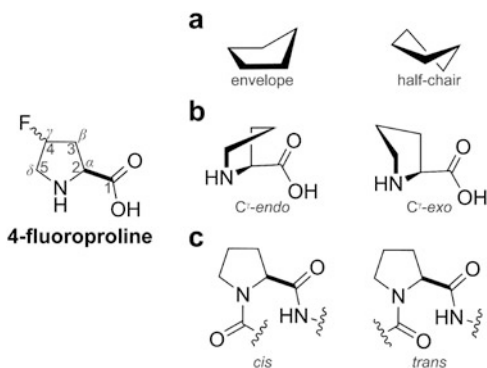
A more scalable and cost-effective synthesis of 4-fluoroproline was later developed, which avoided potentially explosive aminosulfur trifluoride reagents [24]. To generate flp (4*S*)-**1**, Boc-Hyp-OMe (4*R*)-**4** was treated with trifluoromethanesulfonic anhydride to provide a triflate that was treated with tetrabutylammonium fluoride (TBAF). Heating of the resulting protected (4*S*)-**5** with 2*N* HCl at reflux removed the Boc group and methyl ester to provide flp (4*S*)-**1** in 16% overall yield from Hyp (Scheme 1c). Albeit lower-yielding than previous approaches, largely due to inefficiency in the safer fluorination step, this approach was scaled to kilogram quantities. To generate Flp (4*R*)-**1**, rather than employ the Mitsunobu approach, lactone **11** was synthesized by conversion of Boc-Hyp (4*R*)-**9** to methanesulfonate **10** and intramolecular displacement by the carboxylate on treatment with potassium *t*-butoxide. Opening of lactone **11** with lithium hydroxide provided Boc-hyp (4*S*)-**9** in 78% yield from Boc-Hyp (4*R*)-**9**. Conversion of Boc-hyp (4*S*)-**9** to Flp (4*R*)-**1** was performed using a similar protocol by way of triflate to yield (4*S*)-**5**. Alternatively, Hyp was transformed to its 2*R* diastereomer by treatment of with acetic anhydride at 90° C to form an *N*-acetyl lactone which was hydrolyzed in situ with 2*N* HCl at reflux.

The solid-phase synthesis of peptides possessing 4-fluoroproline residues has been achieved by conversion of Hyp residues on resin, a technique called “proline editing” [29, 30]. After coupling Fmoc-Hyp to the peptide chain, the hydroxyl group was protected as trityl ether, and the protected peptide chain was completed by standard Fmoc-based solid-phase peptide synthesis. The trityl group was to be removed selectively using 2% TFA to reveal the free hydroxyl group, which was transformed to its (4*S*)-4-hydroxyproline counterpart by Mitsunobu reaction with 4-nitrobenzoic acid and ester hydrolysis with $K_2CO_3/MeOH$. Transformation of the hydroxyproline containing peptides to their respective 4-fluoroproline peptides was accomplished with inversion of configuration using DAST, prior to resin cleavage and deprotection. Multiple modified proline residues bearing different 4-position substituents in the same peptide may be produced employing alternative and orthogonal protecting group strategies using *tert*-butyldimethylsilyl (TBS) ether and allyloxycarbonyl (Alloc) carbonate groups. In sum, this strategy circumvents the labor required for solution-phase purification of 4-fluoroproline building blocks.

3 Conformational Analysis

Eclipsing interactions deter population of the planar conformer of saturated five-membered rings. Instead, these rings adopt one of two predominant conformations: the envelope conformation, wherein four atoms lie in plane with the fifth distorted away, or the half-chair conformation, wherein two adjacent atoms distort on opposite sides of the plane of the other three (Fig. 1a). Early crystallographic studies [31–33], as well as data from NMR spectroscopy [34], indicated that proline generally adopts the envelope conformation. Although many envelope conformations are possible, crystallographic analysis demonstrates that two predominate: one termed *C^γ-endo*, in which C4 (otherwise, *C^γ*) distorts out of plane to the same side of the ring as the C1 carboxylate, and, another, *C^γ-exo*, in which C4 distorts out of plane to the opposite side of the ring as the C1 carboxylate (Fig. 1b) [35]. These designations are however approximate, and many molecules labeled as “*C^γ-exo*”

Fig. 1 Conformational attributes of proline residues. (a) Conformations of saturated five-membered rings. (b) Pyrrolidine ring puckers. (c) Peptide bond isomers



are better described as C^{β} -*endo*. Moreover, many proline crystal structures display some half-chair character. The C^{γ} -*endo/exo* terminology has become customary and is useful for discussing stereoelectronic effects on proline conformations (*vide infra*), because C^{γ} often experiences the largest change in orientation and because C^{γ} is typically the site of substituent modification.

The energy difference between the *endo* and *exo* puckers is small for proline (~ 0.5 kcal/mol), and the two forms interconvert rapidly at room temperature [36]. Using NMR spectroscopy, an approximately 2:1 *endo/exo* equilibrium population has been determined for Ac-Pro-OMe [36]. Fluorination of C4 serves to bias this equilibrium. Specifically, the C–F bonds in 4-fluoroproline will orient antiperiplanar to adjacent C–H single bonds due to a *gauche* effect. The polarity of the C–F bond makes the substituted carbon electron deficient and therefore a potent electron acceptor. The C–F σ^* orbital is, in particular, highly electrophilic and will accept electron density from antiperiplanar C–H bonding orbitals [37]. The C–F bond in Flp is satisfied by C–H donor orbitals in an orientation that positions the fluoro group toward the opposite side of the ring as the carbonyl carbon, thereby enforcing the C^{γ} -*exo* pucker (Fig. 2a). Conversely, flp exists largely in the C^{γ} -*endo* conformation due to similar hyperconjugation (Fig. 2b). These preferences were first established using $^1\text{H-NMR}$ spectroscopy [38]. The presence of the fluoro substituent disperses the condensed proline proton signals, thereby enabling accurate calculations using the Karplus equation [39]. Refined analysis quantified the preference of flp for the *endo* conformation to be approximately 20:1; analogously, Flp prefers the *exo* conformation at a 6:1 ratio [36].

The reorientation of the pyrrolidine ring between the two puckers influences the structure and stability of proline-containing peptides (*vide infra*). The *exo* pucker reduces the absolute value of the proline ϕ and ψ main-chain torsion angles (Table 1) [37]. Constrained by the pyrrolidine ring, the ϕ dihedral angle varies from approximately -60° in the *exo* pucker to approximately -75° in the *endo* pucker [36]. Although these changes appear modest, they can have a profound effect on the structure and stability of proline-rich peptides (*vide infra*). Two general orientations exist for the ψ ($\text{N}_i\text{-C}_i^\alpha\text{-C}_i'\text{-N}_{i+1}$) main-chain dihedral angle: one near 150° , corresponding to the polyproline type II (PPII) helix, and another near -30° , which is consistent with α -helix geometry. In isolated proline molecules and derivatives, the former ψ value is more common and calculated to be of lower energy [42]. Within the PPII conformer, 4-position fluorination of the pyrrolidine ring has been shown to affect the ψ dihedral angle by as much as 30° , from $\sim 140^\circ$ in the *exo* pucker of Flp to $\sim 170^\circ$ in the *endo* pucker of flp [36].

As a result of the influence of ring pucker on the main-chain dihedral angles, fluorination of C4 can modulate interactions between the N-terminal amide carbonyl and the proline residue carboxamide in peptides. Carbonyl groups of adjacent peptide residues have been shown to engage in so-called $n \rightarrow \pi^*$ interactions [43]. In an $n \rightarrow \pi^*$ interaction, lone-pair (n) electron density delocalizes from the oxygen of one carbonyl group into the π^* antibonding orbital of a proximal carbonyl group (Fig. 2c) [41]. Donation typically occurs from the $i - 1$ residue to the i residue within a polypeptide [44]. Effective orbital mixing requires a distance

Fig. 2 Stereoelectronic effects in 4-fluoroprolines. $\sigma(\text{C-H}) \rightarrow \sigma^*(\text{C-F})$ Gauche interactions stabilizing the (a) C^{γ} -*exo* or (b) C^{γ} -*endo* conformations of Ac-Flp-OMe or Ac-flp-OMe, respectively. (c) The $n \rightarrow \pi^*$ interaction between adjacent carbonyl groups stabilizing the *trans* conformation of the Ac-Flp amide bond in Ac-Flp-OMe

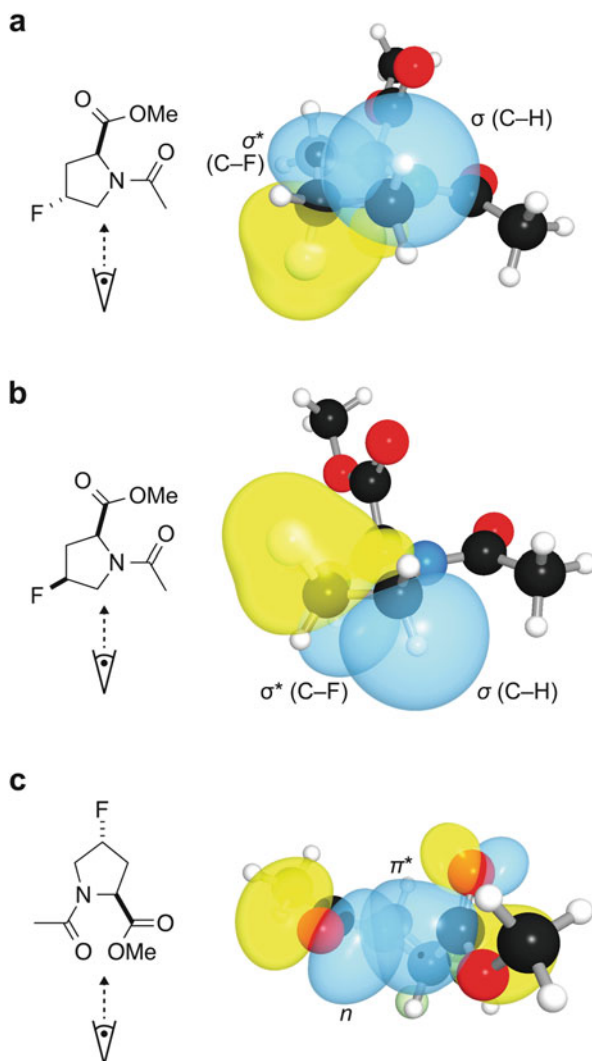


Table 1 Conformational preferences of proline residues

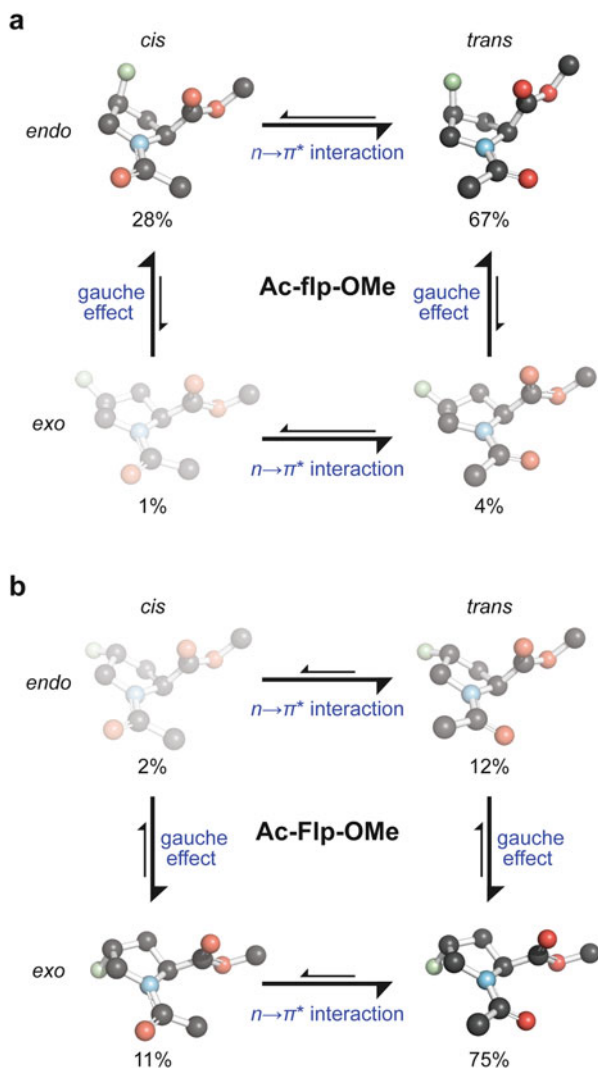
Compound	Ring pucker ^a	ϕ ($^{\circ}$) ^a	ψ ($^{\circ}$) ^a	$K_{trans/cis}$ ^b
Ac-Pro-OMe	<i>endo</i>	-79	177	4.6
Ac-Hyp-OMe	<i>exo</i>	-57	151	6.1
Ac-Flp-OMe	<i>exo</i>	-55	141	6.7
Ac-flp-OMe	<i>endo</i>	-76	172	2.5

^aDetermined with X-ray crystallography [40] or density functional theory calculations (Ac-flp-OMe) [36]

^bMeasured in D_2O at 25 $^{\circ}\text{C}$ with NMR spectroscopy [41]

closer than a van der Waals contact between the donor oxygen and the acceptor carbon along the Bürgi–Dunitz trajectory for nucleophilic addition [45]. The $n \rightarrow \pi^*$ interactions have energies generally greater than 0.27 kcal/mol per interaction [46]. They have been shown to be ubiquitous in proteins [44, 47, 48], particularly about proline residues, in which the pyrrolidine ring pre-organizes the neighboring carbonyl groups to favor the $n \rightarrow \pi^*$ interaction [44]. Fluorination of C4 influences the pyrrolidine ring pucker and the main-chain dihedral angles in ways that have important consequences for the $n \rightarrow \pi^*$ interaction [49] (Fig. 3). Specifically, the distance between the oxygen–carbon donor–acceptor pair of the neighboring carbonyls is generally longer in the *endo* pucker, which leads to a

Fig. 3 (a) Conformational preferences of Ac-flp-OMe. (b) Conformational preferences of Ac-Flp-OMe. Relative populations (%) were measured in dioxane at 25°C with NMR spectroscopy [36]



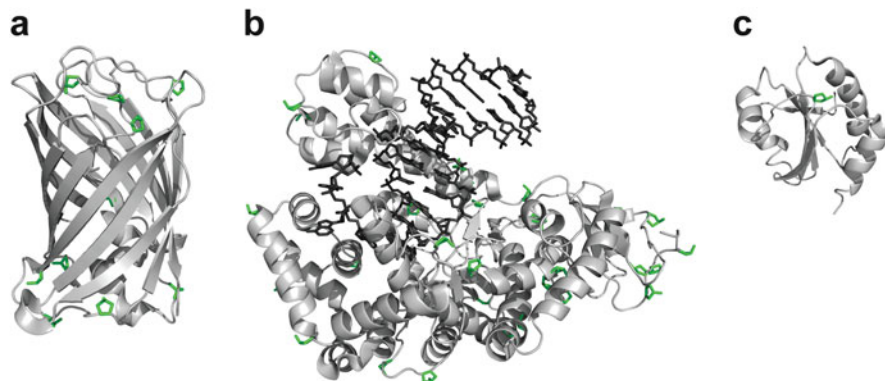


Fig. 4 Three-dimensional structures of representative proteins containing 4-fluoroproline residues (*green sticks*). (a) EGFP containing flp (PDB entry 2q6p) [51]. (b) *Taq* DNA polymerase containing Flp (4dle) [52]. (c) Thioredoxin containing Flp (4hua) [53]

weaker $n \rightarrow \pi^*$ interaction [50]. Conversely, the *exo* pucker is associated with shorter donor–acceptor distances and stronger $n \rightarrow \pi^*$ interactions. In turn, the $n \rightarrow \pi^*$ interaction biases the conformation of the preceding peptide bond. An attractive $n \rightarrow \pi^*$ interaction is only possible in the *trans* conformation of the peptide bond (ω : $C_{i-1}^\alpha-C_{i-1}'-N_i-C_i^\alpha$, Fig. 1c). Accordingly, a higher *trans* peptide bond population correlates with the increased preference for *exo* pucker of the pyrrolidine ring substituted with a 4*R* fluoro group (Table 1, Fig. 4). Notably, the *cis* and *trans* isomers of 4-fluoroprolines have distinct dipole moments, and the *cis*–*trans* ratio of their peptide bonds is sensitive to solvent polarity [54]. In toto, modification of the proline ring with a 4-fluoro substituent has structural consequences on all three backbone dihedral angles in a protein. This principle has been exploited to modulate the conformational stability of peptides and proteins (*vide infra*).

The inductive effect of 4-fluoro substituents has additional consequences on the peptide bond N-terminal to proline residues. Electron withdrawal by the fluoro group reduces the capacity for the proline nitrogen lone pair to contribute double-bond character to the amide N-terminal to proline [40] and thereby diminishes the rotational barrier between the *cis* and *trans* isomers in the peptide [55]. 4-Fluoroprolines have been used to study protein folding kinetics, because isomerization of peptide bonds N-terminal to proline can limit the rate of protein folding [2]. To enhance the influence of a single fluoro substituent, (2*S*)-4,4-difluoroproline (Dfp) has been developed to study protein folding (*vide infra*). Although detailed conformational analysis of Dfp has yet to be performed, its conformational preferences may likely be similar to those of proline.

4 Effects on Collagen Stability

4-Fluoroprolines have been particularly useful in the study of collagen stability [3, 56]. Collagen is the major structural protein in animals, forming a large portion of the dry weight of the skin. Collagen is also prevalent in the extracellular matrix, in which it performs an important structural role. Collagen consists of a distinct triple-helical structure comprised of three polypeptide strands that each have a characteristic Xaa-Yaa-Gly amino acid repeat, in which prolyl residues often occupy the Xaa and Yaa positions. This sequence enables each of the three strands to adopt PPII helices that wrap around one another with an offset of a single amino acid residue [57]. A slice through a collagen triple helix will therefore contain one Xaa, one Yaa, and one Gly residue from different strands. In the PPII secondary structure, the individual peptide chain lacks typically *intra*-strand hydrogen bonding. In a slice of the triple helix, a single interstrand hydrogen bond usually exists between the glycine NH and the carbonyl of the Xaa residue on different peptide chains. The relatively low prevalence of hydrogen bonding raised the question as to the source of the high thermal and mechanical stability of collagen.

One clue as to the source of collagen stability is apparent from its amino acid content. Collagen has a high prevalence of Pro and Hyp residues, which appear at approximately 28% and 38% frequencies in the Xaa and Yaa positions, respectively [58]. The importance of the Hyp hydroxyl group was shown early on by thermal denaturation studies with both synthetic peptides [59] and protocollagen [60], which is the non-hydroxylated precursor to mature collagen. A crystal structure of a collagen-mimetic peptide showed bridging water molecules between the hydroxyl substituent and main-chain carbonyl groups, and these water bridges were proposed to confer stability [61, 62]. The importance of the inductive effect

Table 2 Thermostability of triple-helical CMPs

(Xaa-Yaa-Gly) _n	T _m (°C) ^a	Reference
(Pro-Pro-Gly) ₇	No helix	[63]
(Pro-Hyp-Gly) ₇	36	[41]
(Pro-Flp-Gly) ₇	45	[41]
(Pro-flp-Gly) ₇	No helix	[41]
(flp-Pro-Gly) ₇	33	[64]
(Flp-Pro-Gly) ₇	No helix	[64]
(flp-Flp-Gly) ₇	No helix	[63]
(Pro-Pro-Gly) ₁₀	31–41	[65]
(Pro-Hyp-Gly) ₁₀	61–69	[65]
(Pro-Flp-Gly) ₁₀	91	[65]
(flp-Pro-Gly) ₁₀	58	[66]
(Flp-Pro-Gly) ₁₀	No helix	[66]
(flp-Flp-Gly) ₁₀	30	[67]

^aThe value of T_m refers to the temperature at the midpoint of the thermal transition between the triple-helical and single-stranded states

of the Hyp hydroxyl group was examined by the use of 4-fluoroprolines, which cannot serve as proton donors in hydrogen bonds. In the first synthetic incorporation of 4-fluoroproline into a protein mimetic, the Hyp residues at the Yaa position of a collagen mimetic were replaced with FIp, and circular dichroism (CD) spectroscopy was used to compare the thermostability of the two triple helices (Table 2) [65, 68]. Relative to the Hyp triple helix mimetic, the FIp analog exhibited increased thermostability. Considering that fluoro groups do not form strong hydrogen bonds [69], the data from this comparison refuted the water-bridge proposal. Subsequent molecular dynamics simulations demonstrated the transient nature of bridging water molecules [70]. Moreover, experiments with (2*S*,4*R*)-4-methoxyproline showed that the water bridges actually diminished the stability of the collagen triple helix [71].

Thorough conformational analysis of 4-fluoroproline monomers provided compelling evidence that collagen is stabilized by the stereoelectronic effects of the Hyp residue that are augmented by replacement with the FIp residue [41]. For example, collagen mimetics bearing FIp at the Yaa position exhibited higher thermostability than their Pro counterparts. On the other hand, incorporation of flp at the Yaa position caused a relative decrease in thermostability (Table 2), demonstrating the importance of 4-position stereochemistry. Inspection of available crystal structures indicated a prevalence of *exo* ring puckers in the Yaa position of collagen [61]. The fluoro group in FIp enforces the *exo* ring pucker, which stabilizes collagen by organizing proper dihedral angle orientations. Moreover, FIp favors the prolyl amide *trans* isomer, organizing the proper ω dihedral angle featured in collagen (Table 1) [57]. These effects are evident with even a single Pro \rightarrow FIp substitution within a collagen strand [72]. Increased and decreased stability relative to the parent peptide were respectively observed by CD and NMR spectroscopies upon substitution of Hyp by FIp and flp in a triple-helical model of the $\alpha 1(\text{IV})1263\text{--}1277$ sequence of type IV (basement membrane) collagen, which is known to promote melanoma cell adhesion, spreading, and signaling [73]. Melanoma cell adhesion and spreading on the triple-helical models correlated with stability demonstrating the dramatic influences of fluoro group changes at the Hyp residue [73].

Although FIp-incorporation at the Yaa position increased thermostability in collagen relative to proline in Pro-Yaa-Gly repeats, decreased thermostability was observed with FIp relative to proline in Xaa-Hyp-Gly repeats [64]. Conversely, flp demonstrated respectively stabilizing and destabilizing effects at the Xaa and Yaa positions [66]. Inspection of available crystal structures demonstrated the Xaa residue prefers *endo* ring pucker, which is enforced by flp. The slight preference of Pro for the *endo* pucker is consistent with the stronger effect of FIp at the Yaa position relative to the milder influence of flp at the Xaa position (Table 2).

Although respective incorporation of flp and FIp at Xaa and Yaa residues in the same peptide was predicted to template the appropriate main-chain dihedral angles and confer greater stability than either substitution alone, the resulting collagen triple helix exhibited decreased thermostability relative to the peptide composed of repeats of Pro-Pro-Gly (Table 2) [63, 67]. Molecular modeling revealed a potential interstrand steric clash between the fluoro groups of 4-fluoroproline residues on

adjacent strands that prevented self-association of the peptide. Stable triple helices could be formed by mixing different ratios of (flp-Flp-Gly)₇ and (Pro-Pro-Gly)₇, [63]. The (flp-Flp-Gly)_n sequence binds preferably other collagen strands but not itself. In biological collagen samples, such as in wounds, disrupted helices have provided annealing sites for (flp-Flp-Gly)_n sequences coupled to fluorescent dyes to visualize damaged collagen [74]. Moreover, such annealing strands have been conjugated with moieties, such as growth factors, that modulate the physiology of the surrounding environment to aid in wound healing [75, 76].

Differential scanning calorimetry was employed to provide more insight into the thermodynamics of the influences of fluorination on collagen stability [77]. In comparisons with (Pro-Pro-Gly)₁₀ triple helices, the (Pro-Hyp-Gly)₁₀ and (Pro-Flp-Gly)₁₀ counterparts were shown to retard thermal denaturation by enthalpic and entropic contributions, respectively. Analysis of molecular volumes indicated that the enthalpic contribution to the stability of (Pro-Hyp-Gly)₁₀ was mediated significantly by enhanced water solvation. Water desolvation due to the hydrophobic effect of fluoro substitution may account for the entropic stabilization of (Pro-Flp-Gly)₁₀ because the fluoro group of Flp is a much weaker hydrogen bond acceptor than the hydroxyl group of Hyp [69] and cannot donate a hydrogen bond. This hypothesis was tested in a follow-up study employing Dfp, which retains the hydrophobicity of Flp, but lacks the strong preference for the *exo* ring pucker [56]. Accordingly, if the hydrophobic effect was dominant to triple-helical stability, Dfp and Flp should have similar effects; however, Dfp decreased stability relative to Flp at the Yaa position, arguing against a strong contribution from the hydrophobic effect in driving collagen-mimetic peptide assembly.

Albeit application has been limited to date [78], 4-fluoroprolines have served as NMR probes due to the utility of the ¹⁹F nucleus. For example, the mechanism of strand association and dissociation was studied in a collagen triple helix model possessing a single Flp residue at the central Yaa position using ¹H-¹⁹F and ¹⁹F-¹⁹F exchange experiments to measure populations of native and nonnative structures in solution [79]. As the temperature increased, denaturation of the native collagen strands was observed to give rise to multiple intermediates, contradicting the two-state model often assumed for the denaturation of collagen-mimetic peptides. Isolated monomer strands were found to possess both *cis* and *trans* peptide bonds, but collagen assembly was concluded to take place only from monomers with all-*trans* peptide bonds. Off-pathway intermediates were characterized having misaligned triple helices with more than one residue offset. Misaligned helices required dissociation to all-*trans* monomer strands to convert to the native state.

Besides imparting thermostability and binding specificity to collagen strands, 4-fluoroprolines have also been used to investigate the mechanism by which collagen strands are hydroxylated by proline 4-hydroxylase (P4H). Proline derivatives such as flp, which prefer relatively the *endo* pucker and the *cis* peptide bond conformation, proved better P4H substrates [80]. Enzymatic discrimination during substrate binding and not during turnover was evident from the hydroxylation of peptides bearing flp and the absence of binding to peptide counterparts containing Flp residues. Oxidation of flp to 4-ketoproline (Kep) by P4H was used to develop a

probe of enzymatic activity by measuring fluoride-ion release in a continuous assay [81]. Shedding light on the mechanism of collagen hydroxylation, these studies have provided information for designing inhibitors of P4H to treat fibrotic diseases associated with an overabundance of collagen.

5 Effects on Peptide Conformation

Beyond the triple-helical domain of collagen, the conformations of other peptides, especially polyproline helices, have been explored through incorporation of 4-fluoroprolines. Two major conformations of oligoproline are known: the polyproline type I (PPI) helix, which is marked by *cis* orientation of the peptide bonds, and the aforementioned PPII helix, which features prolyl amide *trans* isomers. The PPII conformation is common in both the folded [82] and unfolded states [83] of proteins and has found utility in molecular rulers [84] and scaffolds [85]. The PPII conformation is favored in relatively polar solvents, such as water. The PPI conformation is formed preferentially in less polar solvents, such as *n*-propanol [86]. The transition between these helices involves isomerization of the peptide bond. Modulating the conformation of the pyrrolidine ring was predicted to have a profound effect on oligoproline structure, because of the connection between pyrrolidine ring pucker and main-chain dihedral angles (vide supra). To evaluate this hypothesis, Pro₁₀, Flp₁₀, and flp₁₀ were synthesized by solid-phase methods and subjected to analysis by CD spectroscopy [87]. In contrast to native Pro₁₀, Flp₁₀ adopted a PPII conformation in both aqueous and organic solutions. Conversely, flp₁₀ exhibited low PPII content in water and a high population of PPI geometry in *n*-propanol. Considering the conformational preferences of the amino acid monomers, the favored *exo* ring pucker of Flp enforced $n \rightarrow \pi^*$ interactions between adjacent carbonyl groups, leading to increased populations of prolyl amide *trans* isomers and PPII helix. Subsequently, (4*R*)- and (4*S*)-fluoroprolines were shown to respectively increase and decrease the transition-state barrier for PPII \rightarrow PPI conversion [88]. This dichotomy was consistent with Flp stabilizing the prolyl amide *trans* isomer. In a follow-up study, the effects of 4-fluoroproline were shown to be more pronounced at the C versus the N terminus of the peptide [89], consistent with polyproline interconversion occurring by a mechanism that initiates at the C terminus [90].

Polyproline helices have attracted interest as motifs, because of their roles in protein–protein interactions [91]. For example, SH3 domains are a ubiquitous peptide module that bind often to proline-rich protein substrates, which adopt PPII conformations [92]. In an effort to design high-affinity ligands to SH3 domains for applications such as cancer chemotherapeutic agents, 4-fluoroprolines were introduced into various proline-rich peptides derived from the hematopoietic progenitor kinase 1 (HPK1) [93]. In affinity assays using the SH3 domain of hematopoietic-lineage cell-specific (HS1) protein, the 4-fluoroproline peptide analogs failed to exhibit enhanced binding, in spite of increasing the population of PPII

conformer, suggesting that ligand recognition involved features beyond secondary structure, albeit the fluoro groups may perturb specific binding interactions.

To study the importance of *exo* ring pucker in the proline–aromatic interaction with Trp64, FIp and fIp were respectively substituted for Pro62 at the N terminus of the C-terminal helix in the subdomain of the villin headpiece (HP36), a small mostly α -helical miniprotein [91]. Although FIp and fIp were respectively expected to enforce and perturb the *exo* ring pucker of Pro62 [92] with consequences of improved and depressed thermostability, thermal unfolding and urea-induced denaturation measurements indicated that the former fluoroproline significantly destabilized HP36 and the latter had little effect on its structure and protein stability, unexpected consequences suggested to be due to steric and hydrophobic effects.

To explore the importance of the *endo* pucker for Pro37 to pack into the hydrophobic core of the Pin1 WW domain, 4-fluoroprolines were incorporated into this small, three-stranded β -sheet protein of about 40 residues [94]. Consistent with the crystal structure of the parent protein [95] and the hypothesis that the native *endo* pucker is preferred for the Pin1 WW domain, FIp decreased thermostability by favoring the *exo* pucker. Although relatively hydrophilic *endo*-favoring prolines, such as hyp and (4*S*)-methoxyproline (mop), destabilized the Pin1 WW domain, fIp increased stability, likely due in part to its hydrophobic nature. Moreover, fIp-incorporation increased the affinity between the protein and its phosphorylated peptide ligand. The advantages of 4-fluoroprolines to perturb selectively pyrrolidine ring conformation were thus highlighted by their capacity to probe peptide structure without complications from hydrogen bonding.

4-Fluoroprolines have been used to study the significance of the *exo* ring pucker of Pro12 in the loop that joins the C-terminal polyproline helix to the N-terminal α -helix in the Trp cage miniprotein [96], a 20-residue peptide that displays tertiary structure and cooperative folding [97], physical characteristics associated with full proteins. Employing proline editing, Trp cage peptides bearing FIp and fIp at position-12 were synthesized and found respectively to increase and decrease thermostability relative to the native proline peptide. The destabilizing effect of fIp was greater than the stabilizing effect of FIp, effects consistent with the *exo* pucker of the native proline, and the sensitivity of small proteins that lack a hydrophobic core.

The critical role of prolyl amide *cis*–*trans* isomerization in the folding of the N-terminal domain of the cysteine-rich terminal region of minicollagen-1 was confirmed by replacement of Pro24 with FIp and fIp, respectively [98]. During the folding of this important structural protein of lower animals, a fully oxidized intermediate accumulates in which the N-terminal domain possesses a prolyl amide *trans* isomer and three disulfide bonds. Conversion to the native folded peptide occurs by slow rate-determining *trans*-to-*cis* isomerization in the absence of enzyme catalysis [99]. Relative to the parent proline peptide, fIp gave efficient folding with formation of the correct isomer and negligible amounts of intermediate, and FIp slowed folding by favoring the *trans* isomer in the folding intermediate. Molecular dynamics simulations and kinetic analyses demonstrated that fIp

decreased the population of the *trans* isomer preventing trapping of nonnative disulfide bonds. Similarly, 4-fluoroprolines were used to investigate stability, and rates of folding and the role of disulfide bond formation in model collagen triple helices [100].

4-Fluoroprolines have been used to modulate the DNA-binding properties of a mimic of the integration host factor (IHF) [101]. Crystal structures of the complex of IHF and a 35-base pair chain of DNA have demonstrated that the so-called α -arm binds the DNA sequence in part by intercalating an *endo*-puckered proline residue between base pairs [102]. In the mimic, a lysine dendrimer was tethered to a cyclopeptide that adopted a β -sheet hairpin conformation, which presented the intercalating proline in homology to the IHF α -arm. Replacement of proline, by flp in the mimic, increased sequence-specific DNA binding.

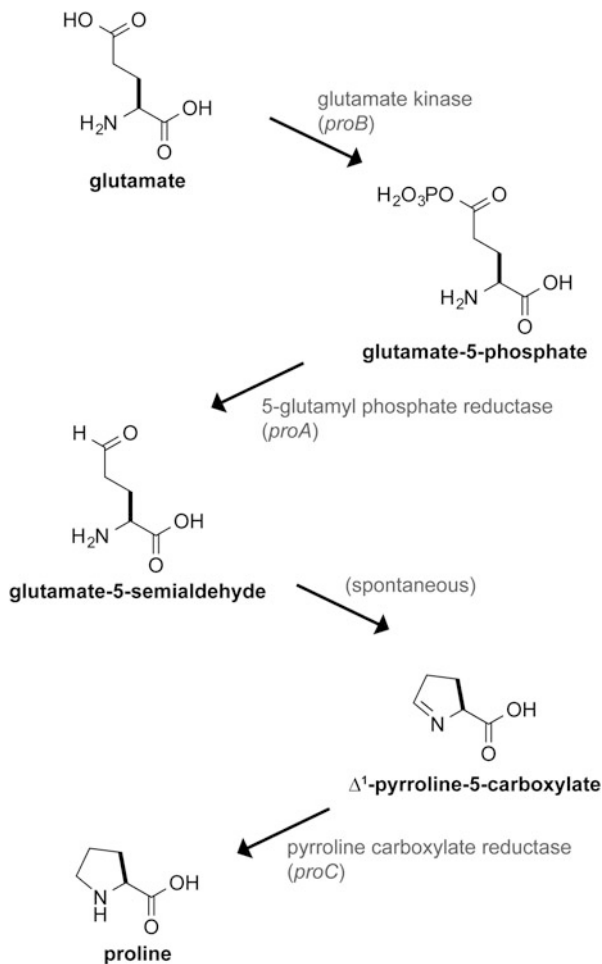
6 Effects on Protein Folding

Broadening the applications of 4-fluoroprolines, methods have been developed to incorporate these heterocyclic amino acids into full-length proteins. For example, selective pressure incorporation (SPI) has resulted in the global substitution of 4-fluoroproline for proline by conditioning bacterial protein synthesis through genetic engineering and the control of environmental factors such as amino acid supply and fermentation parameters [103–108]. Alternatively, the site-specific incorporation of 4-fluoroproline into proteins bearing multiple proline residues has been achieved by the chemical ligation of peptides possessing 4-fluoroproline residues to protein fragments produced by recombinant DNA technology [109].

The first complete replacement of the proline residues in a protein with 4-fluoroprolines was performed on an engineered barstar variant, the cognate inhibitor of a *Bacillus* ribonuclease (barnase) [110]. Wild-type barstar has two prolines, one in each peptide bond conformation. Genetic manipulation yielded a variant containing only the *cis* proline. Efficient recognition of 4-fluoroprolines by the endogenous proline amino-acyl-tRNA synthetase was demonstrated by production of protein with approximately equal efficiency by feeding bacteria proline or either 4-fluoroproline diastereomer. In accordance with their favoring of prolyl *cis* and *trans* isomers, barstar variants containing flp and Flp exhibited respectively higher and lower thermostability than the parent protein. The fluorinated barstar variants were employed to study the mechanism of peptide bond isomerization by peptidyl prolyl *cis*–*trans* isomerases [111].

Bacterial strains with improved efficiency for incorporating 4-fluoroproline have been used to prepare elastin derivatives [112]. In bacterial synthesis of proline from glutamate, the *proA* gene encodes 5-glutamylphosphate reductase to generate glutamate-5-semialdehyde, which spontaneously cyclizes to a Δ^1 -pyrroline intermediate. Proline is produced by reduction of the pyrroline by pyrroline carboxylate reductase, encoded by the *proC* gene (Scheme 2). Knockout of the *proC* gene, followed by supplementation of the growth medium with 4-fluoroproline, resulted

Scheme 2 Route for the biosynthesis of proline from glutamate



in efficient incorporation of 4-fluoroproline throughout the biosynthetic elastin protein, containing eighty proline residues.

Proline residues adopt the central positions of type II β -turns within the [Val-Pro-Gly-Val-Gly] repeats of elastin as the temperature approaches the phase transition of the polypeptide [113]. Elastins substituted uniformly with either Flp or flp were prepared to explore the influence of prolyl residues on the thermodynamics of the phase transition and the physiologically relevant reversible aggregation state of native elastin [114]. Differential scanning calorimetry and CD spectroscopy confirmed that Flp stabilized the structured state and lowered the critical transition temperature, likely by enforcing the *exo* conformation commonly observed in type II β -turns. Conversely, elastins incorporating flp had less stable thermal transitions at a higher temperature, indicating weaker β -turn stability. Analysis of the flp elastin using ^{19}F -NMR spectroscopy detected significant *cis* isomer population at

the valyl-prolyl peptide bond, which may exacerbate the destabilizing effect of this modification.

Ubiquitin has three native proline residues that were replaced with 4-fluoroproline by using the SPI method to study the influence of proline ring pucker on protein folding [115]. Ubiquitylation serves as a key posttranslational modification with a wide variety of cellular effects, notably targeting proteins for proteasomal degradation [116]. The three prolines in native ubiquitin all reside in the *trans-exo* conformation, according to high-resolution crystal structure data [117]. Ubiquitin uniformly incorporating Flp was efficiently expressed from a bacterial auxotroph in high yield; however, attempts failed to incorporate flp, likely due to aggregation or degradation of unfolded protein. Both wild type and Flp-ubiquitin exhibited CD spectra characteristic of native ubiquitin and similar folding pathways involving a single intermediate detected by stopped-flow fluorescence measurements. The barrier between the unfolded state and the intermediate was lower for Flp-ubiquitin, which exhibited slower unfolding from the native state to the intermediate. In thermal and guanidine·HCl-induced denaturation experiments, Flp-ubiquitin exhibited greater stability than the native protein. Furthermore, Flp-ubiquitin served as substrate for ubiquitin-processing enzymes in self-ubiquitylation. In sum, (4*R*)-fluoroproline increased thermostability, accelerated protein folding, and maintained biological function.

Fluoroprolines have also been used to improve the physical properties of antibody fragments for potential uses in therapeutics, diagnostics, and biotechnology [118]. Lack of thermostability relative to their full-length parents has prevented applications of antibody fragments, such as single-chain Fv (scFv) units prepared by linking the variable domains of IgG. Employing the SPI method, anti-c-Met scFv fragments were prepared possessing >90% substitution of 4-fluoroprolines at the five conserved proline positions as determined by mass spectrometric analysis. As observed with ubiquitin, incorporation of Flp and flp resulted respectively in the expression of properly folded soluble and misfolded, insoluble protein. Moreover, Flp-scFv demonstrated higher activity in ELISA assays at elevated temperature compared to the wild-type protein.

Applying this technology to the fluorescent protein EGFP, flp and Flp were fed to a bacterial proline auxotroph to produce respectively soluble, flp-protein, and unfolded Flp-protein that was detectable only in inclusion bodies [51]. Attempts to fold the Flp-protein failed, indicating an irrecoverable effect on the structure, which was unexpected because Flp is known to promote the prolyl amide *trans* isomer found throughout GFP. Characterization of the expressed EGFP containing flp by X-ray diffraction analysis detected no noticeable differences from native protein (Fig. 4a). Moreover, refolding experiments demonstrated that flp-incorporation accelerated the folding of EGFP relative to native protein. The only 4-fluoroproline protein reported to date that folded with flp instead of Flp residues, the flp-EGFP analog may undergo accelerated folding to the wild-type structure, due to the reduced barrier for prolyl amide isomerization of flp relative to Pro [55].

In another fluorescent protein, mRFP1, the opposite trend was observed: flp-incorporation produced only insoluble aggregates, and Flp-incorporation

resulted in a soluble mRFP1, albeit without fluorescence [119]. Molecular modeling demonstrated a steric clash between the chromophore and the fluoro group of Flp63. By genetically mutating Pro63 to alanine before incorporating Flp globally, a fluorescent mRFP1 was obtained which folded faster and exhibited increased thermostability.

Optimized conditions were devised to replace the 32 native proline residues of the 60-kDa KlenTaq DNA polymerase with Flp at 92% efficiency [120]. Attempts to incorporate flp did not result in protein production. The resulting fluorinated enzyme was less thermostable than wild type, but functioned with normal DNA replication kinetics and error rates. A refined preparation of the fluorinated protein with a substitution efficiency of 98% produced crystals of sufficient quality for diffraction to 2.4-Å resolution (Fig. 4b) [52]. The fluoro groups on the exterior of the protein were suggested to improve crystallinity by mediating contacts between individual protein molecules within the lattice. Pucker assignments were possible for 28 out of 32 proline residues in both the Flp and wild-type KlenTaq DNA polymerase crystal structures, which respectively exhibited 89% and 43% *exo* pucker, demonstrating that the strong *gauche* effect in Flp can alter the ring conformation in the context of structural bias from nonlocal interactions. Incorporation of Flp did not alter the two prolyl amide *cis* isomers in KlenTaq DNA polymerase, which adopted *endo* pucker, and accounted for half of the *endo*-puckered residues. Moreover, the electron density for 36% of the prolines in the wild-type polymerase was consistent with a superposition of puckers; only 7% of Flp residues in the fluorinated protein were consistent with multiple puckers in the electron-density map, indicating reduced conformational flexibility of the 4-fluoropyrrolidine ring.

Dissecting the impact of a modification at single residue is challenging using SPI, which inherently results in global substitution. To probe a single-proline position with 4-fluoroproline, a variant of *Escherichia coli* thioredoxin was conceived in which the four *trans* prolines were replaced by alanine, and the single conserved *cis* proline was retained [53]. Both Flp- and flp-proteins were expressed, folded, and shown to be stable in chemical denaturation experiments. Both modifications stabilized the reduced and destabilized the oxidized form of the protein. Both substitutions also improved the cooperativity of folding, which had been compromised by the four proline-to-alanine substitutions. Measures of catalytic activity revealed little effect from fluorination. The lack of significant differences of diastereomeric substitutions was explicable from high-resolution crystal structure analysis of all three single-proline proteins (Fig. 4c). Although Flp and flp favor usually *exo* and *endo* pyrrolidine ring puckers, respectively, both were observed in the *endo* conformation in their respective crystal structures. The Flp residue was predicted to adopt the *endo* pucker to avoid a steric clash between the 4-fluoro substituent and Cys35. The tertiary structure of thioredoxin was suggested to nullify the usual conformational preferences of 4-fluoroproline.

The first total synthesis of a 4-fluoroproline protein was achieved using β 2-microglobulin (β 2m), the causative agent of dialysis-related amyloidosis [121]. In

the native structure of $\beta 2m$, the amide of one of the five proline residues, Pro32, adopts a *cis* isomer [122], which isomerizes to the *trans* conformation in the amyloid, as shown by solid-state NMR spectroscopy [123]. Accordingly, prolyl amide isomerization was predicted to be a key step in the mechanism of amyloid formation. Traditional mutagenic experiments yielded contradictory results: substitution of Pro32 with glycine-induced fibril formation, but substitution with valine or alanine did not [124]. 4-Fluoroprolines (Flp, flp, and Dfp) were employed to subtly and selectively evaluate the role of isomerization in the mechanism of $\beta 2m$ amyloid formation. To incorporate site-specifically the 4-fluoroprolines, $\beta 2m$ variants were produced using native chemical ligation to combine three peptide segments that were generated using solid-phase synthesis. Temporary protection of Cys25 as a thiazolidine allowed for assembly of the full-length protein, which was folded and oxidized into the native structure. Thermal denaturation of the substitution variants demonstrated that *cis*- and *trans*-favoring flp and Flp respectively increased and decreased stability of the folded state relative to wild type. Although Dfp exhibits similar conformational preferences as Pro, the Dfp variant was the least stable of the series. The Dfp variant displayed the least cooperative unfolding, the highest association with a fluorescent probe of unstructured hydrophobic patches on proteins, and the most facile amyloidogenesis. In contrast to wild-type and the monofluoroproline variants, the Dfp variant formed fibrils spontaneously after 2 weeks at neutral pH. Although the relative prolyl *cis* and *trans* isomer populations alone were demonstrated to be insufficient, the rate of amide isomerization appeared key for dictating $\beta 2m$ amyloid formation. Consistent with observations employing a fluorescent probe, rapid *cis*–*trans* isomerization at Pro32 may enhance flexibility of the BC loop to expose hydrophobic regions of the protein and increase the rate of amyloid formation.

7 Impact in Medicinal Chemistry

Fluorination has emerged as a powerful, general strategy for combating the oxidative metabolism of various pharmaceutical candidates [125]. In this light, 4-fluoroprolines are convenient building blocks for introducing fluorine into peptide-based pharmaceuticals [126], such as thrombin inhibitors [127]. Thrombin is an important protease for blood clotting and targeted by inhibitors in therapeutic approaches to treat clotting diseases. Substitution of the central proline residue of a tripeptide inhibitor with flp and Flp gave respectively 200-fold reduced potency and retained potency without oxidative metabolism. In crystal structures of the thrombin·inhibitor complexes, the central proline residue preferred the *exo* ring pucker [128]. These results enabled production of compounds with improved metabolic stability and selectivity toward thrombin over related proteases like trypsin.

4-Fluoroprolines have similarly been employed in the development of peptide inhibitors of Stat3 phosphorylation [129]. Phosphorylation of Stat3 occurs after

cytokines bind to their receptors and results in dimerization and translocation of Stat3 to the nucleus, where it effects changes in gene expression. High activation of Stat3 has been observed in a number of disease states, including cancers, making Stat3 an important pharmaceutical target. Mimics of the SH2 phosphopeptide hold promise as inhibitors of dimerization, because phosphorylation occurs on the SH2 domain of Stat3. Replacement of a key proline residue within a phosphopeptide prodrug with either Flp or Dfp resulted in analogs exhibiting increased potency in cellular assays, in spite of decreased affinity for full-length Stat3 *in vitro*, suggesting that the 4-fluoroproline substitution enhanced potency by retarding deleterious metabolism.

Crystal structures of the complex between neurotensin (NT) and its G protein-coupled receptor (GPCR) NST1 have been used in structure-based drug development programs to yield new analgesics [130]. NT features a key proline residue that binds within a small pocket of NST1 as confirmed by mutagenic studies. To develop selective inhibitors of the related receptor NST2 (which also binds to neurotensin), NT8-13 analogs were produced that contain a variety of proline modifications [131]. A cellular assay was employed to determine the ability of the analogs to inhibit binding of the native ligand and demonstrated a preference of the receptor for *exo*-puckered prolines, including Flp. Further elaboration of the lead peptide with a single peptoid moiety produced a 4-fluoroproline-based ligand with nearly 10^4 -fold selectivity for NST2 over NST1 and provided a probe for ^{19}F MRI imaging.

The effect of a fluoro substituent on ring conformation or peptide bond isomerization is usually the dominant contribution to systems incorporating *N*-acyl-fluoroprolines. Another consequence arises in *N*-alkyl-fluoroproline derivatives. In attempts to develop γ -aminobutyric acid (GABA) reuptake inhibitors related to the *N*-alkyl (*R*)-nipecotic acid drug tiagabine, 4-fluorination of proline and homoproline analogs decreased potency [132], likely due to their decreased amine basicity.

In addition, ^{18}F 4-fluoroproline analogs have begun to be developed as probes for positron emission tomography (PET), due to the relatively short half-life (110 min) of the fluorine isotope, the lack of necessary chelators, and opportunity for incorporation into nascent proteins, such as collagen. In spite of challenges to radio-synthesize, administer, and allow for trafficking and biosynthetic incorporation of the analog, ^{18}F 4-fluoroprolines have been made [133–136], and their pharmacokinetics have been studied [137, 138]. Their future application in imaging of tumors [138–141] or collagen synthesis [142, 143] remains to be advanced.

8 Outlook

Research to date has clearly demonstrated the utility of 4-fluoroprolines for the rational probing of peptide and protein stability, dynamics, and activity. Conformational analysis of 4-fluoroproline monomers has provided predictive insight into

their effects upon incorporation into biopolymers, albeit complications have been observed due to the chemical and structural constraints imposed by these complex molecules. Complementing traditional genetic approaches for exploring protein structure–function relationships, the application of 4-fluoroprolines is expected to continue to find utility for probing key proline residues in a wide variety of proteins due to their subtle yet reliable modulation of polypeptide structure. Incorporation of 4-fluoroprolines has increased conformational stability and accelerated folding of a variety of important proteins. Future application of 4-fluoroprolines is thus well merited to enhance physical, chemical, and biological attributes in the development of chemotherapeutic agents and protein-based technologies.

Acknowledgments This paper is dedicated to the memory of Grant R. Krow (1942–2015), our long-time collaborator on research on 4-fluoroprolines and their analogs. R.W.N. was supported by Biotechnology Training Grant T32 GM008349 (NIH), the Nelson J. Leonard Graduate Fellowship of the ACS Division of Organic Chemistry sponsored by *Organic Syntheses*, and an Eastman Summer Research Award from the Eastman Chemical Company. Work on 4-fluoroprolines in the Raines laboratory was supported by Grant R01 AR044276 (NIH).

References

1. MacArthur MW, Thornton JM (1991) *J Mol Biol* 218:397
2. Brandts JF, Halvorson HR, Brennan M (1975) *Biochemistry* 14:4953
3. Shoulders MD, Raines RT (2009) *Annu Rev Biochem* 78:929
4. Fischer E (1901) *Z Physiol Chem* 33:151
5. Fischer E (1902) *Chem Ber* 35:2660
6. Gorres KL, Raines RT (2010) *Crit Rev Biochem Mol Biol* 45:106
7. Winter AD, Page AP (2000) *Mol Cell Biol* 20:4084
8. Friedman L, Higgin JJ, Moulder G, Barstead R, Raines RT, Kimble J (2000) *Proc Natl Acad Sci U S A* 97:4736
9. Holster T, Pakkanen O, Soininen R, Sormunen R, Nokelainen M, Kivirikko KI, Myllyharju J (2007) *J Biol Chem* 282:2512
10. Mauger AB, Witkop B (1966) *Chem Rev* 66:47
11. Gottlieb AA, Fujita Y, Udenfriend S, Witkop B (1965) *Biochemistry* 4:2507
12. Bakerman S, Martin RL, Burgstahler AW, Hayden JW (1966) *Nature* 212:849
13. Takeuchi T, Prockop DJ (1969) *Biochim Biophys Acta* 175:142
14. Takeuchi T, Rosenbloom J, Prockop DJ (1969) *Biochim Biophys Acta* 175:156
15. Uitto J, Prockop DJ (1974) *Biochim Biophys Acta* 336:234
16. Hutton JJ Jr, Marglin A, Witkop B, Kurtz J, Berger A, Udenfriend S (1968) *Arch Biochem Biophys* 125:779
17. Diegelmann RF, Ondrejickova O, Katz E (1969) *Arch Biochem Biophys* 131:276
18. Yoder NC, Kumar K (2002) *Chem Soc Rev* 31:335
19. Salwiczek M, Nyakatura EK, Gerling UI, Ye S, Koks B (2012) *Chem Soc Rev* 41:2135
20. Merkel L, Budisa N (2012) *Org Biomol Chem* 10:7241
21. Odar C, Winkler M, Wiltshi B (2015) *Biotechnol J* 10:427
22. Demange L, Ménez A, Dugave C (1998) *Tetrahedron Lett* 39:1169
23. Doi M, Nishi Y, Kiritoshi N, Iwata T, Nago M, Nakano H, Uchiyama S, Nakazawa T, Wakamiya T, Kobayashi Y (2002) *Tetrahedron* 58:8453

24. Chorghade MS, Mohapatra DK, Sahoo G, Gurjar MK, Mandlecha MV, Bhoite N, Moghe S, Raines RT (2008) *J Fluor Chem* 129:781
25. Kronenthal DR, Mueller RH, Kuester PL, Kissick TP, Johnson EJ (1990) *Tetrahedron Lett* 31:1241
26. Hudlický M, Merola JS (1990) *Tetrahedron Lett* 31:7403
27. Avent AG, Bowler AN, Doyle PM, Marchand CM, Young DW (1992) *Tetrahedron Lett* 33:1509
28. Hudlický M (1993) *J Fluor Chem* 60:193
29. Thomas KM, Naduthambi D, Tririya G, Zondlo NJ (2005) *Org Lett* 7:2397
30. Pandey AK, Naduthambi D, Thomas KM, Zondlo NJ (2013) *J Am Chem Soc* 135:4333
31. Donohue J, Trueblood KN (1952) *Acta Crystallogr* 5:419
32. Matheison AM, Welsh HK (1952) *Acta Crystallogr* 5:599
33. Mitsui Y, Tsuboi M, Iitaka Y (1969) *Acta Crystallogr* B25:2182
34. Higashijima T, Tasumi M, Miyazawa T (1977) *Biopolymers* 16:1259
35. Allen FH (2002) *Acta Crystallogr* B58:380
36. DeRider ML, Wilkens SJ, Waddell MJ, Bretscher LE, Weinhold F, Raines RT, Markley JL (2002) *J Am Chem Soc* 124:2497
37. Improta R, Benzi C, Barone V (2001) *J Am Chem Soc* 123:12568
38. Grieg JT, McLeod RS (1973) *J Am Chem Soc* 95:5725
39. Karplus M (1959) *J Chem Phys* 30:11
40. Panasik N Jr, Eberhardt ES, Edison AS, Powell DR, Raines RT (1994) *Int J Pept Prot Res* 44:262
41. Bretscher LE, Jenkins CL, Taylor KM, DeRider ML, Raines RT (2001) *J Am Chem Soc* 123:777
42. Jakobsche CE, Choudhary A, Miller SJ, Raines RT (2010) *J Am Chem Soc* 132:6651
43. Hinderaker MP, Raines RT (2003) *Protein Sci* 12:1188
44. Bartlett GJ, Choudhary A, Raines RT, Woolfson DN (2010) *Nat Chem Biol* 6:615
45. Bürgi HD, Dunitz JD, Shefter E (1974) *Acta Crystallogr* B30:1517
46. Newberry RW, VanVeller B, Guzei IA, Raines RT (2013) *J Am Chem Soc* 135:7843
47. Bartlett GJ, Newberry RW, Vanveller B, Raines RT, Woolfson DN (2013) *J Am Chem Soc* 135:18682
48. Newberry RW, Bartlett GJ, Vanveller B, Woolfson DN, Raines RT (2014) *Protein Sci* 23:284
49. Jenkins CL, Lin G, Duo J, Rapolu D, Guzei IA, Raines RT, Krow GR (2004) *J Org Chem* 69:8565
50. Choudhary A, Gandla D, Krow GR, Raines RT (2009) *J Am Chem Soc* 131:7244
51. Steiner T, Hess P, Bae JH, Wiltschi B, Moroder L, Budisa N (2008) *PLoS One* 3:e1680
52. Holzberger B, Obeid S, Welte W, Diederichs K, Marx A (2012) *Chem Sci* 3:2924
53. Rubini M, Schärer MA, Capitani G, Glockshuber R (2013) *ChemBioChem* 14:1053
54. Siebler C, Maryasin B, Kuemin M, Erdmann RS, Rigling C, Grünenfelder C, Ochsenfeld C, Wennemers H (2015) *Chem Sci* 6:6725
55. Eberhardt ES, Panasik N Jr, Raines RT (1996) *J Am Chem Soc* 118:12261
56. Shoulders MD, Kamer KJ, Raines RT (2009) *Bioorg Med Chem Lett* 19:3859
57. Rich A, Crick FHC (1961) *J Mol Biol* 3:483
58. Ramshaw JAM, Shah NK, Brodsky B (1998) *J Struct Biol* 122:86
59. Sakakibara S, Inouye K, Shudo K, Kishida T, Kobayashi Y, Prockop DJ (1973) *Biochim Biophys Acta* 303:198
60. Berg RA, Prockop DJ (1973) *Biochem Biophys Res Commun* 52:115
61. Bella J, Eaton M, Brodsky B, Berman HM (1994) *Science* 266:75
62. Bella J, Brodsky B, Berman HM (1995) *Structure* 3:893
63. Hodges JA, Raines RT (2005) *J Am Chem Soc* 127:15923
64. Hodges JA, Raines RT (2003) *J Am Chem Soc* 125:9262
65. Holmgren SK, Bretscher LE, Taylor KM, Raines RT (1999) *Chem Biol* 6:63

66. Doi M, Nishi Y, Uchiyama S, Nishiuchi Y, Nakazawa T, Ohkubo T, Kobayashi Y (2003) *J Am Chem Soc* 125:9922
67. Doi M, Nishi Y, Uchiyama S, Nishiuchi Y, Nishio H, Nakazawa T, Ohkubo T, Kobayashi Y (2005) *J Pept Sci* 11:609
68. Holmgren SK, Taylor KM, Bretscher LE, Raines RT (1998) *Nature* 392:666
69. Dunitz JD, Taylor R (1997) *Chem Eur J* 3:89
70. Mooney SD, Kollman PA, Klein TE (2002) *Biopolymers* 64:63
71. Kotch FW, Guzei IA, Raines RT (2008) *J Am Chem Soc* 130:2952
72. Persikov AV, Ramshaw JAM, Kirkpatrick A, Brodsky B (2003) *J Am Chem Soc* 125:11500
73. Malkar NB, Lauer-Fields JL, Borgia JA, Fields GB (2002) *Biochemistry* 41:6054
74. Chattopadhyay S, Murphy CJ, McAnulty JF, Raines RT (2012) *Org Biomol Chem* 10:5892
75. Chattopadhyay S, Raines RT (2014) *Biopolymers* 101:821
76. Chattopadhyay S, Guthrie KM, Teixeira L, Murphy CJ, Dubielzig RR, McAnulty JF, Raines RT (2015) *J Tissue Eng Regen Med*. doi:[10.1002/term.1886](https://doi.org/10.1002/term.1886)
77. Nishi Y, Uchiyama S, Doi M, Nishiuchi Y, Nakazawa T, Ohkubo T, Kobayashi Y (2005) *Biochemistry* 44:6034
78. Marsh EN, Suzuki Y (2014) *ACS Chem Biol* 9:1242
79. Kawahara K, Nemoto N, Motooka D, Nishi Y, Doi M, Uchiyama S, Nakazawa T, Nishiuchi Y, Yoshida T, Ohkubo T, Kobayashi Y (2012) *J Phys Chem B* 116:6908
80. Gorres KL, Edupuganti R, Krow GR, Raines RT (2008) *Biochemistry* 47:9447
81. Gorres KL, Raines RT (2009) *Anal Biochem* 386:181
82. Adzhubei AA, Sternberg MJE (1993) *J Mol Biol* 229:472
83. Shi Z, Chen K, Liu Z, Kallenbach NR (2006) *Chem Rev* 106:1877
84. Wilhelm P, Lawandowski B, Trapp N, Wennemers H (2014) *J Am Chem Soc* 136:15829
85. Siebler C, Erdmann RS, Wennemers H (2013) *Chimia* 67:891
86. Kuemin M, Engel J, Wennemers H (2010) *J Pept Sci* 16:596
87. Horng JC, Raines RT (2006) *Protein Sci* 15:74
88. Chiang YC, Lin YJ, Horng JC (2009) *Protein Sci* 18:1967
89. Lin YJ, Horng JC (2014) *Amino Acids* 46:2317
90. Lin L-N, Brandts JF (1980) *Biochemistry* 19:3055
91. Berisio R, Vitagliano L (2012) *Curr Protein Pept Sci* 13:855
92. Feng S, Chen JK, Yu H, Simon JA, Schreiber SL (1994) *Science* 266:1241
93. Ruzza P, Siligardi G, Donella-Deana A, Calderan A, Hussain R, Rubini C, Cesaro L, Osler A, Guiotto A, Pinna LA, Borin G (2006) *J Pept Sci* 12:462
94. Tang HC, Lin YJ, Horng JC (2014) *Proteins* 82:67
95. Wintjens R, Wieruszkeski JM, Drobecq H, Rousselot-Pailley P, Buée L, Lippens G, Landrieu I (2001) *J Biol Chem* 276:25150
96. Naduthambi D, Zondlo NJ (2006) *J Am Chem Soc* 128:12430
97. Neidigh JW, Fesinmeyer RM, Andersen NH (2002) *Nat Struct Biol* 9:425
98. Boulègue C, Milbradt AG, Renner C, Moroder L (2006) *J Mol Biol* 358:846
99. Pokidysheva E, Milbradt AG, Meier S, Renner C, Häussinger D, Bächinger HP, Moroder L, Grzesiek S, Holstein TW, Özbek S, Engel J (2004) *J Biol Chem* 279:30395
100. Barth D, Musiol HJ, Schütt M, Fiori S, Milbradt AG, Renner C, Moroder L (2003) *Chem Biol* 9:3692
101. Scholz S, Liebler EK, Eickmann B, Fritz HJ, Diederichsen U (2012) *Amino Acids* 43:289
102. Rice PA, Yang S-W, Mizuuchi K, Nash HA (1996) *Cell* 87:1295
103. Merkel L, Schauer M, Antranikian G, Budisa N (2010) *ChemBioChem* 11:1505
104. Lepthien S, Merkel L, Budisa N (2010) *Angew Chem Int Ed* 49:5446
105. Hoesl MG, Acevedo-Rocha CG, Nehring S, Royter M, Wolschner C, Wiltschi B, Budisa N, Antranikian G (2011) *ChemCatChem* 3:213
106. Hoesl MG, Budisa N (2011) *ChemBioChem* 12:552
107. Oldach F, Al Toma R, Kuthning A, Caetano T, Mendo S, Budisa N, Sussmuth RD (2012) *Angew Chem Int Ed* 51:415

108. Larregola M, Moore S, Budisa N (2012) *Biochem Biophys Res Commun* 421:646
109. Nilsson BL, Soellner MB, Raines RT (2005) *Annu Rev Biophys Biomol Struct* 34:91
110. Renner C, Alefeldler S, Bae JH, Budisa N, Huber R, Moroder L (2001) *Angew Chem Int Ed* 40:923
111. Golbik R, Yu C, Weyher-Stingl E, Huber R, Moroder L, Budisa N, Schiene-Fischer C (2005) *Biochemistry* 44:16026
112. Kim W, George A, Evans M, Conticello VP (2004) *ChemBioChem* 5:928
113. Debelle L, Tamburro AM (1999) *Int J Biochem Cell Biol* 31:261
114. Kim W, McMillian RA, Snyder JP, Conticello VP (2005) *J Am Chem Soc* 127:18121
115. Crespo MD, Rubini M (2011) *PLoS One* 6:e19425
116. Komander D, Rape M (2012) *Annu Rev Biochem* 81:203
117. Vijay-Kumar S, Bugg CE, Cook WJ (1987) *J Mol Biol* 194:531
118. Edwardraja S, Sriram S, Govindan R, Budisa N, Lee SG (2011) *Mol Biosyst* 7:258
119. Deepankumar K, Nadarajan SP, Ayyadurai N, Yun H (2013) *Biochem Biophys Res Commun* 440:509
120. Holzberger B, Marx A (2010) *J Am Chem Soc* 132:15708
121. Torbeev VY, Hilvert D (2013) *Proc Natl Acad Sci U S A* 110:20051
122. Trinh CH, Smith DP, Kalverda AP, Phillips SE, Radford SE (2002) *Proc Natl Acad Sci U S A* 99:9771
123. Jahn TR, Parker MJ, Homans SW, Radford SE (2006) *Nat Struct Mol Biol* 13:195
124. Eichner T, Radford SE (2011) *FEBS J* 278:3868
125. Park BK, Kitteringham NR, O'Neill PM (2001) *Annu Rev Pharmacol Toxicol* 41:443
126. Tran TT, Patino N, Condom R, Frogier T, Guedj R (1997) *J Fluor Chem* 82:125
127. Staas DD, Savage KL, Sherman VL, Shimp HL, Lyle TA, Tran LO, Wiscount CM, McMasters DR, Sanderson PE, Williams PD, Lucas BJ Jr, Krueger JA, Lewis SD, White RB, Yu S, Wong BK, Kochansky CJ, Anari MR, Yan Y, Vacca JP (2006) *Bioorg Med Chem* 14:6900
128. Tucker TJ, Brady SF, Lumma WC, Lewis SD, Gardell SJ, Naylor-Olsen AM, Yan Y, Sisto JT, Stauffer KJ, Lucas BJ, Lynch JJ, Cook JJ, Stranieri MT, Holahan MA, Lyle EA, Baskin EP, Chen I-W, Dancheck KB, Krueger JA, Cooper CM, Vacca JP (1998) *J Med Chem* 41:3210
129. Mandal PK, Ren Z, Chen X, Kalurachchi K, Liao WS-L, McMurray JS (2013) *Int J Pept Prot Res* 19:3
130. White JF, Noinaj N, Shibata Y, Love J, Kloss B, Xu F, Gvozdenovic-Jeremic J, Shah P, Shiloach J, Tate CG, Grishammer R (2012) *Nature* 490:508
131. Held C, Hübner H, Kling R, Nagel YA, Wennemers H, Gmeiner P (2013) *ChemMedChem* 8:772
132. Zhuang W, Zhao X, Zhao G, Guo L, Lian Y, Zhou J, Fang D (2009) *Bioorg Med Chem* 17:6540
133. van der Ley M (1983) *J Label Compd Radiopharm* 20:453
134. Hamacher K (1999) *J Label Compd Radiopharm* 42:1135
135. Mazza SM (2000) *J Label Compd Radiopharm* 43:1047
136. Azad BB, Ashique R, Labiris NR, Chirakal R (2012) *J Labelled Cpd Radiopharm* 55:23
137. Wester H-J, Herz M, Senekowitsch-Schmidtke R, Schwaiger M, Stöcklin G, Hamacher K (1999) *Nucl Med Biol* 26:259
138. Börner AR, Langen K-J, Herzog H, Hamacher K, Müller-Mattheis V, Schmitz T, Ackermann R, Coenen HH (2001) *Nucl Med Biol* 28:287
139. Langen K-J, Mühlensiepen H, Schmieder S, Hamacher K, Bröer S, Börner AR, Schneeweiss FHA, Coenen HH (2002) *Nucl Med Biol* 29:685
140. Langen K-J, Jarosch M, Hamacher K, Mühlensiepen H, Weber F, Floeth F, Pauleit D, Herzog H, Coenen HH (2004) *Nucl Med Biol* 31:67
141. Langen KJ, Hamacher K, Bauer D, Bröer S, Pauleit D, Herzog H, Floeth F, Zilles K, Coenen HH (2005) *J Cereb Blood Flow Metab* 25:607

142. Zimny M, Klosterhalfen B, Conze J, Hamacher K, Fehler S, Schumpelick V, Coenen HH, Buell U (2002) Nucl Med Commun 23:695
143. Skovgaard D, Kjaer A, Heinemeier KM, Brandt-Larsen M, Madsen J, Kjaer M (2011) PLoS One 6:e16678

Silaproline, a Silicon-Containing Proline Surrogate

Emmanuelle Rémond, Charlotte Martin, Jean Martinez,
and Florine Cavalier

Abstract Silaproline (Sip) is a proline analogue that exhibits similar conformational properties as the natural amino acid in peptides. Moreover, the presence of a dimethylsilyl group confers to silaproline higher lipophilicity as well as improved resistance to biodegradation. The stereoselective synthesis of protected silaproline and two routes to obtain Fmoc-(*L*)Sip-OH on gram scale using chiral HPLC resolution are reported. Silaproline was introduced into the sequences of various natural peptides, and the influence of the silylated proline analogues on bioactivity was studied. In particular, considering the importance of polyproline II helices (PPII) in protein–protein molecular interactions and biology, a series of silaproline oligomers from dimer to pentamer were studied and shown to preferentially populate the polyproline type II secondary structure in both chloroform-*d* and methanol-*d*₄ as shown by circular dichroism (CD), NMR spectroscopy, and molecular modeling.

Keywords Modified bioactive peptides · Peptide structure · Polyproline II helix · Proline surrogate · Silaproline

Contents

1	Introduction	28
2	Synthesis of a Silicon-Containing Proline Surrogate	29
2.1	Racemic Silaproline Synthesis	30
2.2	Diastereoselective Synthesis	33
3	Conformational Studies	33
3.1	Model Peptides	34
3.2	Diketopiperazines	35

3.3 Homopolypeptides	35
4 Silaproline Containing Biologically Active Peptides	41
4.1 Substance P	42
4.2 Octadecaneuropeptide (ODN)	42
4.3 Captopril	43
4.4 Neurotensin	43
4.5 Cell-Penetrating Peptides (CPPs)	45
5 Summary	45
References	46

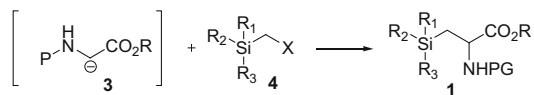
1 Introduction

The need to replace natural amino acids in peptides with non-proteinogenic counterparts, to obtain new pharmacological tools exhibiting better binding to specific receptors and more potent inhibitors of target enzymes, has stimulated a great deal of innovation on synthetic methods. The structural and functional diversity of such modified amino acids is unlimited and useful for the strategic development of new peptide analogues having potentially interesting biological activity.

Non-proteinogenic amino acids derived from natural amino acids and designed and synthesized by chemists are widely used for mimicking interactions of natural peptides [1]. They are important tools for studying the relationships between amino acid structure and peptide conformation [2–4]. Moreover, introduction of non-proteinogenic amino acids into peptides may provide resistance to enzymatic biodegradation [5]. In addition, they may be used either as chiral auxiliaries in asymmetric synthesis [6] or for the preparation of biopolymers [7]. Non-proteinogenic amino acid derivatives of poly- α -amino acids may be used either to prepare fibrous materials and films for studies in the solid state and in solution. For example, analogues of proline have been used in models of polyproline and collagen, which contain a high percentage of proline [8, 9].

The preparation of enantiopure unnatural amino acids remains of great importance in chemistry with wide applications in the life sciences [10–14]. Among the different families of unnatural amino acids (β -amino acids, homo-amino acids, D-amino acids, and *N*-methyl amino acids), we have targeted α -amino acid analogues having a silicon atom serving as an isostere of carbon in order to study biopolymers. Silicon belongs to the crystallogen family and is the most abundant element in the earth's crust after oxygen. In medicinal chemistry, substitution of silicon by carbon within existing drugs is an approach for the synthesis of compounds with original biological properties [15]. In 1979, Tacke and Wannagat reviewed the concept of substituting a carbon atom by silicon [16].

Carbon and silicon share similarities; however, certain differences are notable. For example, although both are tetravalent, silicon is capable of forming penta- and hexa-coordinated complexes possessing stable charges. The size of the two atoms is different: 0.91 and 1.46 Å for the respective atomic radii of carbon and silicon. The lengths of the carbon–carbon and carbon–silicon bonds are, respectively, 1.54 and



Scheme 1 Addition of a glycine anion equivalent to a halomethylsilane

1.87 Å. Silicon is more electropositive (1.8) than carbon (2.5), which induces a difference in bond polarization. Finally, lipophilicity is an important parameter, because silylated compounds are more lipophilic than their carbon analogues, which may facilitate ability to cross cell membranes. Consequently, these differences in size and shape between carbon and silicon influence the pharmacological and pharmacodynamic properties of compounds containing these elements.

Some limitations should be mentioned in incorporating silicon as a carbon isostere. The polarity of the silicon–hydrogen bond leads to an easily cleavable bond in water under non acidic conditions, forming the corresponding silanols. Increased lipophilicity limits water solubility, which is of major importance in medicinal chemistry. In this context, we extended our work to the synthesis and characterization of silaproline polypeptides.

Several publications have described β-silyl α-amino acids with general structures **1** and **2**. The first reported silicon-containing amino acid belongs to this class of compounds, which are accessible using a wide variety of methods and reaction conditions [17, 18].

Moving the silicon atom one more atom further from the carbonyl increased the stability of the C–Si bond [19, 20]. The majority of methods used to synthesize β-silyl amino acids involve alkylation of a glycine anion equivalent **3** with a halomethylsilane **4** (Scheme 1). The resulting β-silyl α-amino acid **1** may undergo cyclization to provide **2** if another halogenated substituent is present on the electrophile.

2 Synthesis of a Silicon-Containing Proline Surrogate

Silaproline (Sip, **2**, R=protecting group or H, Fig. 1) is a proline analogue in which the γ-carbon has been replaced by a dimethylsilyl group. As discussed below, X-ray analysis of model peptides has shown the carbon–silicon bonds in Sip are of about 0.35 Å longer than the carbon–carbon bonds of proline [21]. The C–Si–C angle is significantly small (~93°) relative to that of proline (105°). Furthermore, the presence of the dimethylsilyl group increased lipophilicity, as demonstrated by the octanol–water partition coefficient of Sip that was experimentally determined to be 14 times greater than that of Pro [21].

Increased lipophilicity may facilitate membrane permeability. Reduced sensitivity to enzymatic degradation may also arise from substitution of Sip for Pro in peptides. Moreover, similarities between the two ring systems may result in similar conformational properties for Sip- and Pro-containing peptide analogues.

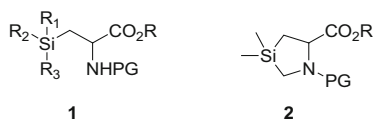
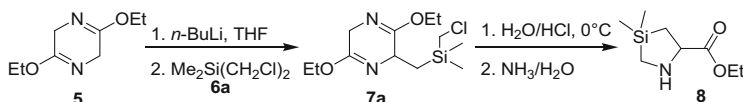


Fig. 1 β -Silyl amino acids



Scheme 2 Synthesis of racemic silaproline starting from 2,5-dihydropyrazine

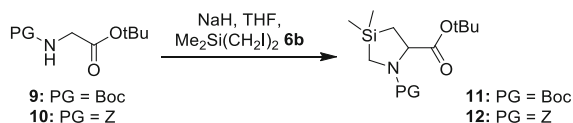
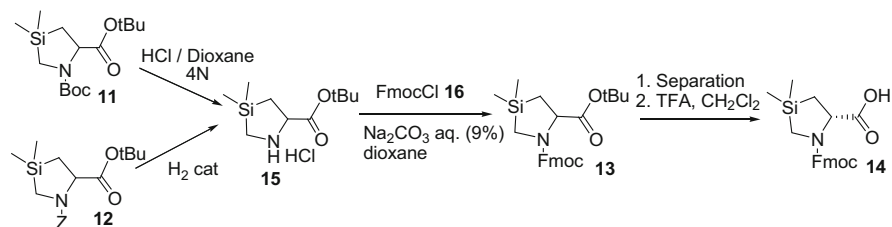
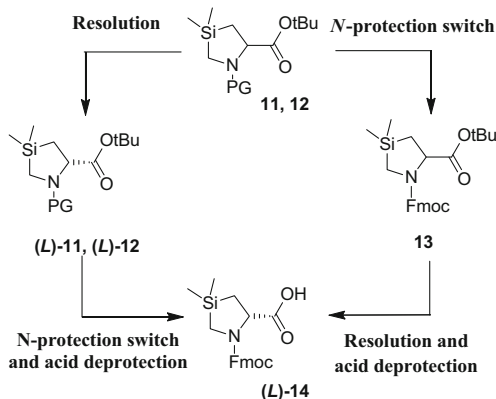
2.1 Racemic Silaproline Synthesis

Protected silaprolines were synthesized in racemic and enantiomerically pure forms by two different research teams in 2000 [22]. In both cases, a glycine equivalent was alkylated initially on carbon followed by nitrogen employing bis-(halomethyl) dimethylsilane. In the racemic case, Tacke and co-workers synthesized silaproline by a route featuring metallation of 2,5-dihydropyrazine **5** with *n*-butyllithium and alkylation with bis-(chloromethyl)dimethylsilane **6a** to afford (pyrazinyl)methylsilane **7a** (Scheme 2) [22]. Treatment with hydrochloric acid opened pyrazine **7a**, which upon washing with ammonia was converted to silaproline ethyl ester (H-(*D,L*)Sip-OEt) **8** in 20% overall yield for the two steps (Scheme 2).

Racemic *N*-(Boc)- and *N*-(Cbz)silaproline *tert*-butyl esters **11** and **12** have been synthesized recently by a strategy featuring alkylation of the corresponding protected glycinates **9** and **10** using bis-(iodomethyl)dimethylsilane **6b** (Scheme 3) [23]. Treatment of glycinates **9** and **10** in anhydrous THF with excess NaH, followed by the silane **6b**, gave, respectively, Boc-(*D,L*)Sip-OtBu (**11**) and Z-(*D,L*)Sip-OtBu (**12**) in 71% and 85% yields after chromatography.

Considering that *N*-(Fmoc)amino acids are commonly used in solid phase peptide synthesis, Fmoc-(*D,L*)Sip-OH (**13**) was prepared by protecting group shuffles from **11** and **12** (Scheme 4) [24], because loss of the base labile Fmoc group rendered alkylation of Fmoc-Gly-OtBu unrealistic. Selective removal of the Boc group from Boc-(*D,L*)Sip-OtBu (**11**) was achieved with anhydrous 4 N HCl in dioxane for 30 min. Alternatively, the Z protecting group was removed from Z-(*D,L*)Sip-OtBu (**12**) by hydrogenolysis. Fmoc-(*D,L*)Sip-OtBu (**13**) was then obtained from H-(*D,L*)Sip-OtBu (**15**) by protection using Fmoc-Cl **16**.

Different strategies were explored for the resolution of the protected racemic silaproline analogues (Fig. 2). For example, racemic Fmoc-(*D,L*)Sip-OtBu **13** was separated into its respective enantiomers by semi-preparative chromatography on a Chiralpak IC column using a mixture of hexane/isopropanol (70/30) as mobile phase. By this method, 200 mg of each enantiomer of **13** was recovered with an ee >99% (Fig. 3). After separation, the *tert*-butyl esters of Fmoc-(*L*)- and (*D*)Sip-

**Scheme 3** Synthesis of racemic silaproline starting from glycine**Scheme 4** Synthesis of Fmoc-(*L*)Sip-OH**Fig. 2** Strategies for the preparation of enantiomerically enriched Fmoc-(*L*)Sip-OH

OtBu [(*L*)- and (*D*)-**13**] were removed quantitatively using TFA in dichloromethane for 30 min.

The second strategy for resolving racemic silaprolines consisted in separation of the enantiomers of Boc-(*D,L*)Sip-OtBu (**11**) and Z-(*D,L*)Sip-OtBu (**12**). Silaprolines **11** and **12** were respectively detected at 220 and 254 nm, as well as with a polarimeter. Employing a Chiralpak IC column and semi-preparative conditions, the enantiomers of **11** and **12** were respectively separated to afford 5 g quantities of each isomer (>99% ee, Fig. 4a,b). Subsequently, Boc-(*L*)Sip-OtBu was converted to Fmoc-(*L*)Sip-OH [(*L*)-**14**] by removal of the acid labile carbamate and ester using 6N HCl followed by introduction of the Fmoc group.

Notably, resolution by chiral HPLC circumvented the need for enantioselective synthesis providing multiple grams of each enantiomer of differently protected silaprolines. The syntheses of racemic Boc- and Z-protected silaprolines were

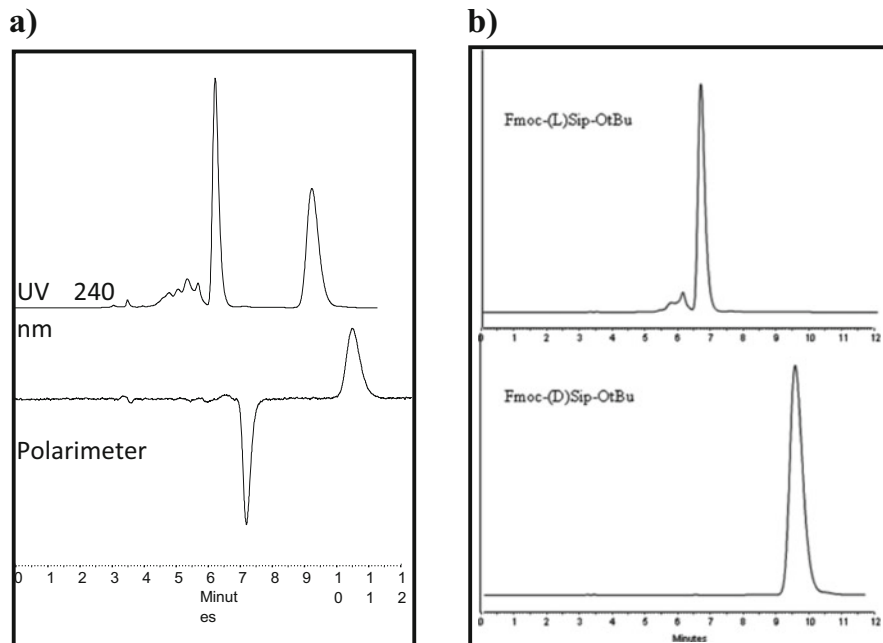


Fig. 3 Separation of the two enantiomers of Fmoc-(*D,L*)Sip-OtBu (**a**) and chromatograms of pure Fmoc-(*L*)Sip-OtBu and Fmoc-(*D*)Sip-OtBu (**b**)

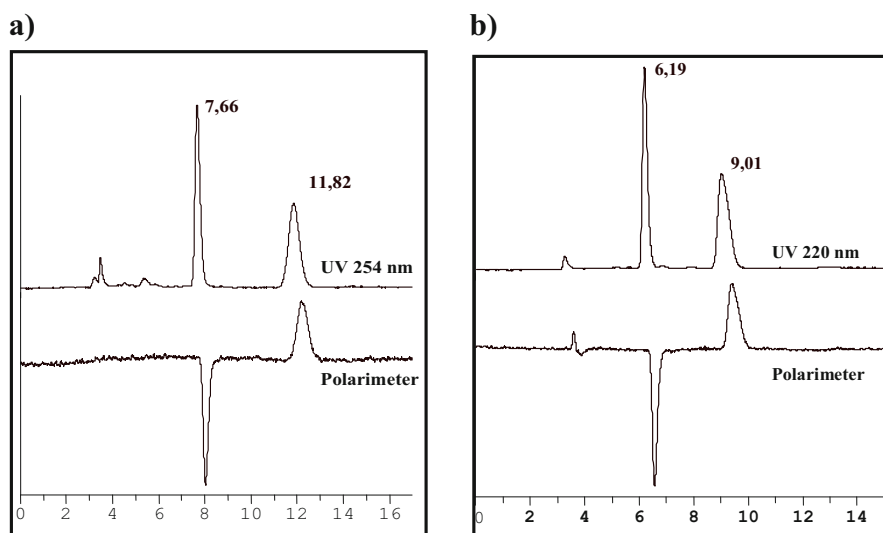


Fig. 4 Separation of enantiomers of Boc-(*D,L*)Sip-OtBu (**a**) and *Z*-(*D,L*)Sip-OtBu (**b**)

straightforward, albeit exchange of protection was necessary for the Fmoc version. The best strategy for obtaining Fmoc-(*L*)Sip-OH [(*L*)-**14**] was to switch the *N*-protection from Boc-(*L*)Sip-OtBu [(*L*)-**11**] after resolution of the corresponding racemic mixture and then regenerate the carboxylic acid function on the enantiomerically pure compound, because separation on the preparative column was only possible with silaproline esters.

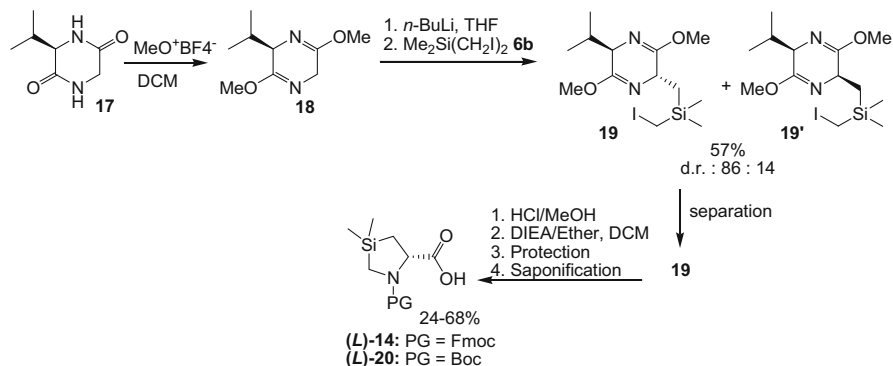
2.2 Diastereoselective Synthesis

Among various methods studied for the asymmetric synthesis of silaproline, the diastereoselective alkylation of the Schöllkopf bis-lactim was the most efficient [25]. The first step consisted in *O*-methylation of the (*D*)Val-Gly diketopiperazine **17** using trimethyloxonium tetrafluoroborate to afford bis-lactim ether **18**, which was deprotonated with *n*-BuLi and alkylated with bis-(iodomethyl)dimethylsilane **6b** to afford piperazine **19** as a 86:14 mixture of separable diastereomers (Scheme 5). After chromatography, each piperazine diastereomer **19** was hydrolyzed using hydrochloric acid, and cyclization with carbon–nitrogen bond formation was achieved by treating the ammonium hydrochloride intermediate with base. After *N*-protection and ester hydrolysis, *N*-(Fmoc)- and (Boc)silaprolines [(*L*)-**14** and (*L*)-**20**] were respectively obtained with 13 and 38% overall yields. Enantiopure silaproline has also been synthesized in 27% overall yield and >99% enantiomeric excess by a similar diastereoselective route from the 3,6-diethoxy-2,5-dihydropyrazine derived from (*D*)Val-Gly diketopiperazine using bis(chloromethyl)dimethylsilane **6a** in the alkylation step [22]. Optimized alkylation conditions of 3,6-dimethoxy-2,5-dihydropyrazine **18** in the presence of bis-(chloromethyl)dimethylsilane have been recently reported in a patent that claims to afford >100 g of enantiopure Boc-(*L*)Sip-OH [(*L*)-**20**] in 60% overall yield (Scheme 5) [26].

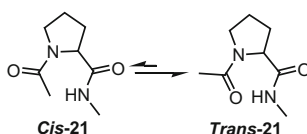
3 Conformational Studies

Proline is the only cyclic essential amino acid. Its pyrrolidine ring restricts local conformational freedom and lowers the molecular flexibility about its side chain and backbone dihedral angles to a fewer number of possible conformers. In addition, in contrast to the amide *N*-terminal to primary amino acids, which exist predominantly as the *trans*-isomer, the tertiary amide *N*-terminal to the pyrrolidine ring of proline, the so-called prolyl amide, may exist in *cis*- and *trans*-isomers separated by a relatively low isomerization barrier (Scheme 6) [27, 28].

Owing to these unique properties, proline plays an important role in biologically active peptides and biological processes, such as protein folding. Therefore, replacement of proline with substituted proline analogues may modify the flexibility of bioactive peptides, providing probes to study the influence of specific conformers on receptor recognition and affinity. Accordingly, numerous surrogates,



Scheme 5 Diastereoselective synthesis of protected silaproline



Scheme 6 *Cis*–*trans*-isomerization of the amide *N*-terminal to proline

mimetics, and analogues of proline have been developed. The first class contains constrained analogues, which are designed with the aim of governing the *cis*–*trans* ratio of peptide bond *N*-terminal to proline. The second class represents unconstrained analogues that conserve the native properties of proline. A typical example of a hindered substituted proline was offered by Lubell, who described δ -*tert*-butylproline for constraining peptide conformation to favor proline-like turns [29, 30]. Pseudoproline residues have also been investigated to control prolyl amide geometry and have proven useful to circumvent solubility problems correlated with hydrophilic side chains during peptide synthesis [31].

The *cis*–*trans*-isomerization of the proline peptide bond has been extensively studied and depends on several factors such as solvent, aromaticity, and the configuration of the residue preceding proline. To modulate the proportion of *cis*- and *trans*-conformers, ring substituents have been used to orientate the amide bond geometry. For example, δ -substituted prolines, such as δ -*tert*-butylproline [29, 30] and δ,δ -dimethylproline [32], have been employed to augment the prolyl amide *cis*-isomer in peptides. Adding to this important field of modified prolines, several studies were reported to compare the structural influence of the replacement of proline by silaproline.

3.1 Model Peptides

To carry out conformational studies, we introduced silaproline in model peptides. We synthesized protected silaproline derivatives (Boc and Piv-Sip-NHiPr),

dipeptides (Boc and Piv-Sip-Ala-NHiPr), and tripeptides containing silaproline, with two sets of epimers [Boc and Piv-(*L* or *D*)Ala-Sip-Ala-NHiPr]. Among the models, Piv-Sip-Ala-NHiPr crystallized and its X-ray structure showed a type II β -turn. This turn conformer is uncommon for homochiral dipeptides and may be stabilized in the crystal by intermolecular interactions between the middle amide groups of two neighboring molecules. Some ring properties due to the silicon atom included long carbon–silicon bonds and a small carbon–silicon–carbon intracyclic angle. The observed $C\beta$ -endo ring puckering consisted of an envelope conformation with four atoms in the same plane and the $C\beta$ atom pointing out of the plane toward the α -carboxamide [33].

Conformational studies were performed on two sets of tripeptides using NMR spectroscopy in solution: Piv-(*L* and *D*)Ala-Pro-Ala-NHiPr and Piv-(*L* and *D*)Ala-Sip-Ala-NHiPr. The percentage of prolyl amide *cis*-isomer was unaffected by the change from proline to silaproline. Amide proton chemical shift differences obtained when switching from DMSO to chloroform and temperature coefficients $\Delta\delta/\Delta T$ in DMSO- d_6 indicated solvent shielded and exposed hydrogens. Notably, both (*L*)Ala-peptides adopted extended conformations. Both (*D*)Ala-peptides adopted folded turn structures, albeit more predominantly for the proline than for the silaproline peptide analogue [21].

3.2 Diketopiperazines

The pyrrolidine ring shape of proline can modulate structural properties, such as the proportion of *cis*- and *trans*-amide isomers, that may play important roles in peptide biological activity. Diketopiperazine models were thus chosen to study the influence of the proline modification on ring shape. In this study, cyclo(Pro-Gly), cyclo(Sip-Gly), and cyclo(Thz-Gly) (Thz=thiazolidine-4-carboxylic acid) were studied by proton NMR spectroscopy (Fig. 5) [34]. We found that relative to proline, which typically exists in a dynamic equilibrium between $C\gamma$ -endo and $C\gamma$ -exo ring puckering, the analogues with γ -position heteroatoms (silicon and sulfur) displayed more rigid five-member rings that slowly interconverted between $C\beta$ -exo and $C\beta$ -endo conformations.

In both linear and cyclic Sip-peptide analogues, both $C\beta$ -exo and $C\beta$ -endo conformations were observed. The $C\delta$ -Si γ -N- $C\alpha$ ring atoms were coplanar. The impact of the methyl groups on silicon does not seem to be important, because the sulfur in (Thz-Gly)DKP had practically the same conformational influence as the dimethylsilyl group in (Sip-Gly)DKP.

3.3 Homopolypeptides

In proline-rich regions, prolyl residues promote formation of extended helical secondary structures, such as type II polyproline (PPII) helices [35, 36]. Involved



Fig. 5 Structure of diketopiperazines

in a wide range of molecular interactions important for biological function, PPII helices have been implicated in signaling, transcription, and immune response. They mediate protein–protein interactions [37] and facilitate cell penetration [38, 39]. These biological properties have stimulated chemists to synthesize PPII mimics for various applications, such as therapeutic agents.

Among proline containing oligomers that fold into conformationally ordered states, oligomers of Ser-Pro dipeptides [40], tricyclic Pro-Pro mimics [41], tri-proline mimics [42], and PTAAAs (proline-templated amino acids) [43–45] all have been used to design PPII helices with modified physical properties such as improved water solubility. A series of silaproline oligomers were synthesized to explore the influences of its alternative ring puckering and hydrophobic nature on PPII conformation.

3.3.1 Polyproline Type II Helix (PPII Helix)

The typical PPII structure is a left-handed helix with all peptide bonds in *trans*-configuration ($\omega = 180^\circ$) and ϕ - and ψ -dihedral angle values of -75° and 145° , respectively. Without intramolecular hydrogen bonds to stabilize the helical structure, backbone solvation has been suggested to be a major determinant of PPII formation [46]. Moreover, the PPII helix has been identified in peptides that do not contain proline residues but adopt similar dihedral angle values [47].

3.3.2 Monodisperse Homopolysilaprolines

Silaproline oligomers were synthesized in solution by a stepwise strategy using *N*-Boc-silaproline as monomer. The dimer was first made in solution by coupling equimolar amounts of *N*-Boc-silaproline with proline benzyl ester hydrochloride in the presence of triethylamine. Chain extension was achieved by selective Boc-deprotection of the dimer and coupling with *N*-Boc-silaproline to afford the trimer. Longer chains were synthesized in a similar fashion (Fig. 6).

Polyproline has been observed to adopt PPII helices in methanol that exhibit far-UV (190–260 nm) CD spectra having two negative maxima at 200 and 232 nm and a positive maximum at 215 nm. Similarly, oligomers **25–28** in methanol exhibited CD curve shapes with negative and positive maxima in the 203–208 nm

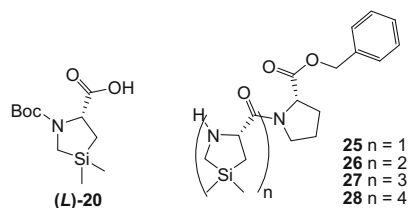


Fig. 6 Silaproline building block and oligomers **25–28**

and 220–230 nm ranges, respectively (Fig. 3a). A subtle change in conformation with increasing chain length was detected by a redshift and increase in per residue molar ellipticity. Pentamer **28** exhibited a PPII-like CD signature with a negative maximum at 207 nm and a positive maximum at 229 nm, which were unaffected by increases in temperature from 20 to 55°C, suggesting a stable silaproline oligomer structure.

Studies of oligomers **25–28** by NMR spectroscopy were performed next in chloroform-*d* and in methanol-*d*₄. A combination of COSY, ROESY, ¹³C-HSQC, and ¹³C-HMBC experiments was used to assign all of the ¹H and ¹³C resonances. Better oligomer solubility and enhanced NMR spectral resolution were observed in methanol-*d*₄, albeit strong NOEs between the ^αCH(*i*) and ^δCH(*i* + 1) protons characteristic of the *trans*-conformation for all oligomers were observed in both solvents. Except in the case of the spectrum of dimer **25**, only the *trans*-conformer was detected in the ¹H NMR spectra of the longer oligomers both in chloroform and methanol. Dimer **25** exhibited *cis*- and *trans*-isomers about the amide bond between silaproline and proline, with ~7% *cis*-isomer detected by ¹H and ²⁹Si NMR in both solvents. Relative to the proline counterpart H-Pro-Pro-OBn, H-Sip-Pro-OBn exhibited more *trans*-isomer in methanol (85% and 93%, respectively). In the spectra of the high molecular weight proline oligomers ($n = 3–5$), the percentage of prolyl amide *trans*-isomer remained relatively constant (90%). As mentioned, no *cis*-isomer was detected in the longer silaproline oligomers starting from the trimer [48].

The NOE data from the NMR studies was used to add restraints in the calculations of the solution structures by a simulated annealing protocol with the AMBER 11 force field. The solution structures of **25**, **26**, **27**, and **28** in methanol were solved using 4, 12, 18, and 24 unambiguously restrained distances, respectively. The 20 lowest-energy NMR structures calculated for each compound demonstrated that the Sip oligomers converged toward PPII structures (Fig. 7). The root mean square deviations (RMSD) on all heavy atoms were 0.03, 0.31, 0.18, and 0.40 Å for **25**, **26**, **27**, and **28**, respectively, when the OBn capping group was omitted. Average values of the backbone dihedral angles for the Sip residue in the polysilaproline helix were $\phi = -74.5 \pm 8.9^\circ$ and $\psi = 143.6 \pm 13^\circ$ after optimization of the NMR structures using the B3LYP/6-31+G(d,p) method. The silaproline PPII helix was left-handed with an axial translation of 3.2 Å composed of three residues per turn, with all peptide bonds in *trans*-configuration ($\omega = 170–175^\circ$).

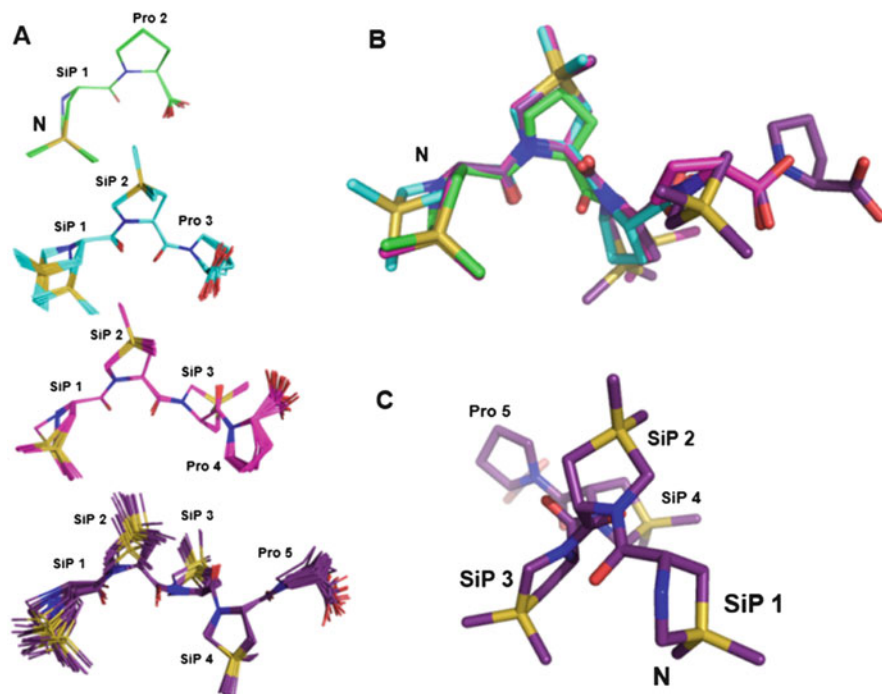


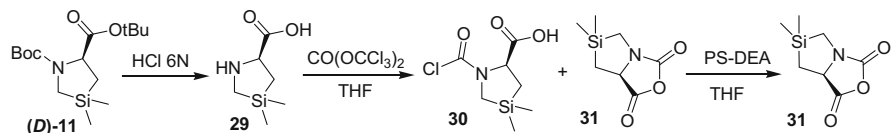
Fig. 7 (a) NMR solution structures of dimer **25** (in *green*), trimer **26** (in *cyan*), tetramer **27** (in *pink*), and pentamer **28** (in *purple*). (b) Overlay of the structures of compounds **25–28** optimized by DFT. (c) Axial view of PII helical structure of the tetramer **4**. Hydrogens and the disordered benzyl group of the *C*-terminal moiety were omitted for clarity

3.3.3 Polydispersed Polysilaproline Oligomers

To synthesize homopolysilaproline having longer chain lengths, the most extensively used method was based on polymerization of silaproline *N*-carboxyanhydride (SiP-NCA).

Synthesis of SiP-NCA

The synthesis of *N*-carboxyanhydrides (NCAs) of common amino acids has been well documented [49]. Reports of NCAs of amino acids with secondary amines are however more rare, in part due to the cyclic structure of such amino acids, which may impose conformational restrictions. For example, unsatisfactory results were obtained in attempt to prepare NCAs from proline by common methods [50], such as treatment with phosgene or a phosgene substitute such as triphosgene (Fuchs–Farthings method) [51]. In the latter case, the *N*-carbamoyl chloride intermediate was relatively stable and required addition of an HCl scavenger, such as silver oxide



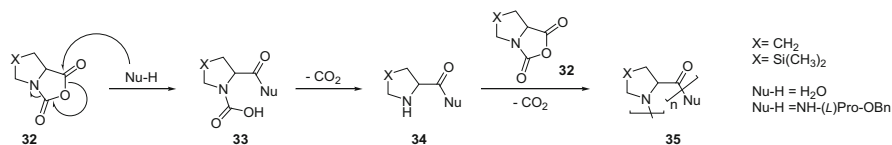
Scheme 7 Synthesis of (*D*)Sip-NCA

or organic bases in order to cyclize. Recently, the synthesis of (*L*)Pro-NCA using triphosgene was achieved effectively with the assistance of *N,N*-diethanolaminomethyl polystyrene (DEAM-PS) to trigger the cyclization without diketopiperazine formation [52]. Removal of the polymer-supported ammonium hydrochloride by filtration facilitated purification of (*L*)Pro-NCA. Inspired by this method, NCAs of (*L*)- and (*D*)-Sip were made using triphosgene and diethylamine polystyrene, respectively. Greater spontaneous cyclization to form NCA was observed for the less constrained five-membered ring of Sip (50%) compared with proline (33%, Scheme 7). Among attempts to optimize cyclization, including variations of stoichiometry, reaction time, and temperature, only the addition of polystyrene-supported diethylaminomethylamine proved effective. With the optimized conditions, (*D*)Sip-NCA **30** was prepared in 72% yield and high purity, such that it could be crystallized and fully characterized [53].

Homopolymerization

Homopolypeptides are commonly obtained by ring opening polymerization (ROP) of NCAs [54]. Several reagents can initiate the polymerization to afford polypeptides with a narrow molecular weight range that is essentially determined by the NCA to initiator ratio. Depending on the relative basicity and nucleophilicity of the initiator, two mechanisms have been described for this reaction: the normal amine mechanism [55] (NAM) and the activated monomer mechanism (AMM) [56]. In the AMM, a significantly basic initiator deprotonates an NCA bearing a proton on nitrogen and the resulting anion may serve as a nucleophile to initiate the ROP. More commonly, the initiator serves as a nucleophile and attacks the C-5 carbonyl of the NCA. Decomposition of the resulting carbamic acid with CO₂ release results in a newly formed amine that propagates polymerization (Scheme 8).

In the particular cases of (*L*)Pro-NCA, and related imino acid NCAs, the AMM cannot occur, because no labile proton is available and the NAM is the only possible mechanism. Initially, precise amounts of water were employed as initiator in THF, at room temperature. Difficulty in verifying the degree of polymerization by NMR spectroscopy of the resulting carboxylic acid [57] and poor polymer purity using water as initiator prompted us to use H-(*L*)Pro-OBn to start the chain reaction, because integration of the benzyl group signal could be employed to check polymer purity and the degree of polymerization. Employing H-(*L*)Pro-OBn to initiate reactions of NCAs derived from (*L*)proline, (*L*)silaproline and



Scheme 8 NAM mechanism for ring opening polymerization of *N*-carboxyanhydrides

(*D*)silaproline gave effectively homopolypeptides with a C-terminal proline benzyl ester.

Conformational Studies

The degree of polymerization of the Pro and Sip homopolymers was measured by ^1H NMR spectroscopy and integration of the aromatic protons of the C-terminal benzyl ester and the C_α protons; the range of the latter, which included two additional protons for the benzyl methylene, was assigned accurately using heteronuclear single quantum coherence spectroscopy (HSQC) experiments. In all cases, this method evaluated consistently the degree of polymerization within the theoretical range determined by the reaction stoichiometry (Table 1).

Both MALDI (matrix assisted laser desorption ionization) and CD (circular dichroism) analyses have been widely used to characterize homopolypeptides. The molecular weight distribution of a homopolymer may be assigned based on the pattern of peaks for the mass of each component in the MALDI analysis. Sample preparation of the matrix influenced however the molecular weight determination of the MALDI-ToF MS experiment, resulting in lower molecular weights than those calculated by NMR spectroscopy. In addition, the abundances were suspected not to reflect the actual distribution, due to limitations of molecular discrimination by MALDI-ToF analysis during ionization.

Polyproline oligomers are known to adopt a type II helical conformation (PPII) in polar solvents such as water, trifluoroethanol, and other fluorinated alcohols. The characteristic PPII circular dichroism signals include a strong negative maximum at 202–206 nm and a weak positive maximum at 225–229 nm [58]. As mentioned earlier, the lipophilic character of homopolysilaproline inhibited solubility in water. We investigated other polar solvents that induced PPII structure to solubilize the polysilaproline oligomers and found the best solvents to be HFIP and TFE; the latter was often used for thermal studies. We recorded circular dichroism spectra of all polymers in TFE at a concentration of 0.1 mg/mL.

The spectrum of polymer P7 showed the typical circular dichroism curve of PPII helix with a strong negative maximum at 207 nm and a weak positive maximum at 228 nm. These results indicated clearly that homopolysilaproline adopted a PPII conformation. Thermal denaturation of the PPII structure was studied next in TFE by heating over the range of 0–70°C in a sealed cell recording CD spectra at 5° intervals (Fig. 8). A slight diminution of the negative maximum at 207 nm was

Table 1 Synthesis of homopolypeptides of different lengths

Polymer	Monomer	Initiator	Monomer/initiator	DPn ^a
P2	(<i>L</i>)Pro-NCA	(<i>L</i>)Pro-OBn	21	24
P4	(<i>D</i>)Sip-NCA	(<i>L</i>)Pro-OBn	5	5
P5	(<i>D</i>)Sip-NCA	(<i>L</i>)Pro-OBn	20	14
P6	(<i>D</i>)Sip-NCA	(<i>L</i>)Pro-OBn	50	44
P7	(<i>L</i>)Sip-NCA	(<i>L</i>)Pro-OBn	10	11

^aDegree of polymerization was determined by NMR integration

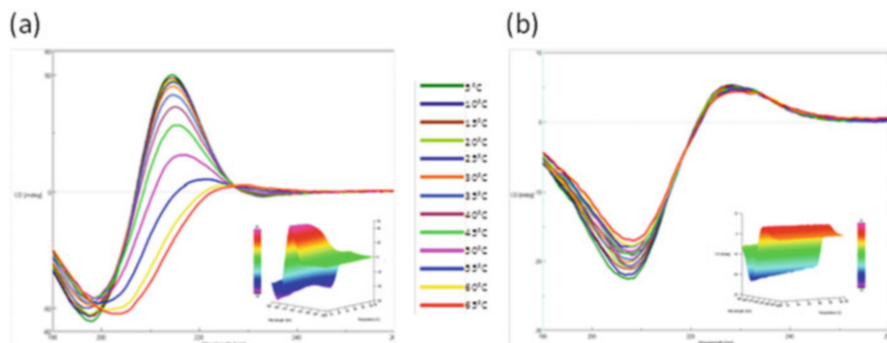


Fig. 8 CD spectra during thermal denaturation experiments of (a) oligoproline **P2** and (b) silaproline oligomers **P7** in TFE

observed, but the positive maximum was unaffected by increasing temperature. In comparison to the polyproline counterpart (Fig. 8a), the PPII helix of polysilaproline was clearly more thermally stable (Fig. 8b).

4 Silaproline Containing Biologically Active Peptides

Innovative building blocks have been used to replace natural amino acids in peptides with non-proteinogenic counterparts to obtain new pharmacological tools, exhibiting better binding to specific receptors and more potent enzyme inhibitors. Constrained amino acid analogues, particularly cyclic amino acid residues such as proline surrogates, have been used to study peptide geometry, because biological activity is often dependent on backbone conformation and side chain orientation [59, 60]. Moreover, unnatural residues may increase the stability and the bioavailability of modified peptides, presumably because they are not well recognized by proteolytic enzymes. In this light, the significance of Sip was studied after insertion into the sequence of several natural biologically active peptides.

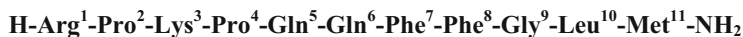


Fig. 9 Substance P (SP) sequence

4.1 Substance P

Substance P (SP) (Fig. 9) is a member of the tachykinin family of natural neuropeptides, which are characterized by a common C-terminal sequence that acts at three different receptor subtypes [61, 62]. Our study focused on SP using assays on the two binding sites associated with its NK-1 receptor, as well as secondary messenger assays on whole cells as previously described [63]. SP and [Pro⁹]SP were taken as reference peptides of the more abundant (NK-1M) binding site, and [pGlu⁶]SP(6–11) and [pGlu⁶, Pro⁹]SP(6–11) were selected as selective peptides of the less abundant (NK-1m) binding site.

Replacing glycine at position 9 by both proline and silaproline led respectively, to SP and C-terminal SP hexapeptide analogues retaining both the whole affinity and activity of the parent peptide. Moreover, in the C-terminal SP hexapeptide, replacement of Gly⁹ with Sip gave a full agonist on the phospholipase C (PLC) pathway that exhibited partial agonist behavior on adenylate cyclase. This latter observation underlines that silaproline is a proline mimetic that may confer a different pharmacological pattern to a biologically active peptide [64].

The stability of the proline- and silaproline-containing SP analogues toward angiotensin-converting enzyme was also examined. After 1 h incubation at 37°C, 80% of SP was degraded; however, [Pro⁹]SP and [Sip⁹]SP remained uncleaved.

4.2 Octadecaneuropeptide (ODN)

The octadecaneuropeptide (ODN; QATVGDVNTDRPGLLDLK), which belongs to the endozepin family, has been previously shown to increase intracellular calcium concentration ([Ca²⁺]_i) in cultured rat astrocytes through activation of a metabotropic receptor positively coupled to PLC [65]. The C-terminal octapeptide, called OP (Fig. 10), is the minimum active ODN sequence, and [(D)Leu⁵]OP possesses weak antagonistic activity [66].

Silaproline analogues of OP, [Sip²]OP and [Sip², (D)Leu⁵]OP, were synthesized by conventional Fmoc solid phase methods and measured for ability to elevate intracellular calcium concentrations. Application of [Sip²]OP (10⁻⁸ M) in the vicinity of an astrocyte provoked a transient and robust increase in [Ca²⁺]_i with an amplitude significantly higher than that induced by ODN at the same dose. A short pulse of [Sip², (D)Leu⁵]OP (10⁻⁸ to 10⁻⁶ M) close to an astrocyte did not affect basal calcium levels, but partially reduced ODN-evoked [Ca²⁺]_i increases with the same efficacy as its non-silylated counterpart, [(D)Leu⁵]OP.

Fig. 10 OP sequence



4.3 Captopril

Angiotensin-I converting enzyme (ACE), a zinc metalloenzyme, plays a fundamental role in blood pressure regulation by converting the inactive decapeptide angiotensin I to the potent vasopressor octapeptide angiotensin II. Captopril [67] is currently used as an oral antihypertensive agent that competitively inhibits ACE [68]. Inhibitory potency is possibly mediated via a hydrophobic interaction with the enzyme. The ring conformation and orientation have been studied by annulation of cyclopropyl and cyclopentyl moieties onto the proline ring [69]. Studying the relevance of the hydrophobic character of the proline moiety, we replaced the proline residue in captopril by the more lipophilic silaproline. Employing the ACE crystal structure [70, 71], a set of silaproline Captopril analogues (Fig. 11) were docked in silico into the Zn catalytic site.

The less hindered analogue of the series (silacaptopril, $R^1=R^2=Me$) was synthesized and tested in vitro for ability to inhibit ACE enzymatic activity. The observed similar inhibition compared to captopril indicated that hydrophobic interactions were either not of significance for interaction with ACE or tempered by steric hindrance, which hampered binding. Docking calculations supported the hypothesis, because silacaptopril exhibited the lowest docking energy in both ACE domains compared to all silylated analogues [72].

4.4 Neurotensin

Neurotensin (NT) (Fig. 12) is a tridecapeptide that is highly expressed in the central nervous system and was first isolated from bovine hypothalamus [73]. Following brain injection along with a cocktail of enzyme inhibitors, NT elicits hypothermic and analgesic responses [74]. The effects of NT have been shown to be differentially mediated by multiple receptors: NTS_{1-3} . For example, NTS_2 has been reported to contribute to the protective effect of NT on pancreatic beta cells [75]. Structure–activity relationship studies have shown the minimal active sequence to be the C-terminal fragment NT(8–13) [76]. Replacement of the arginine residues of NT(8–13) by lysine gave H-Lys-Lys-Pro-Tyr-Ile-Leu-OH (JMV438), which had relatively better affinity and selectivity for NTS_2 (Table 2).

Like many natural peptides, neurotensin has a short half-life in vivo, due to rapid enzymatic degradation. Stability studies in plasma using analysis by electrophoresis have highlighted specific enzymes that cleave specific peptide bonds. To overcome neurotensin instability, several NT analogues have been developed using different approaches including unnatural amino acid incorporations [77–82], peptide bond modifications [83–85], and cyclization [86, 87].

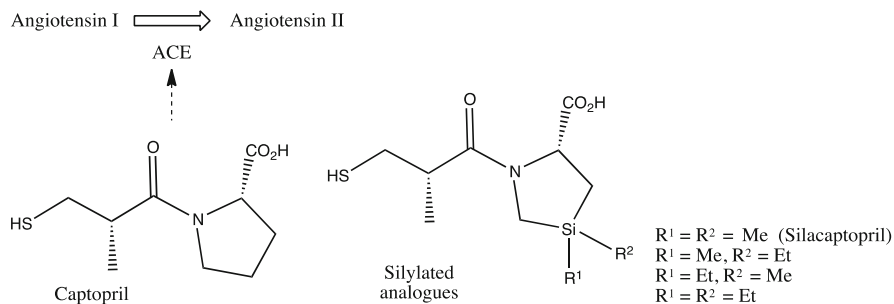


Fig. 11 Role of ACE and structure of captopril

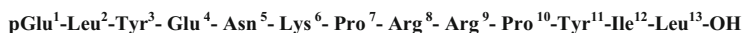


Fig. 12 Neurotensin (NT) sequence

Table 2 Binding of NT and analogues

Agonist	Sequence	NTS1 IC ₅₀ (nM)	NTS2 IC ₅₀ (nM)	Selectivity NTS2
NT	pGlu-Leu-Tyr-Glu-Asn-Lys-Pro-Arg-Arg-Pro-Tyr-Ile-Leu-OH	0.4	4	0.1
NT (8–13)	H-Arg-Arg-Pro-Tyr-Ile-Leu-OH	0.3	2.7	0.11
JMV 438	H-Lys-Lys-Pro-Tyr-Ile-Leu-OH	6.3	2	3.15
JMV 2009	H-Lys-Lys-Sip-Tyr-Ile-Leu-OH	17.5	5	5.83

Few changes are tolerated for Pro¹⁰, which is important for folding into its active peptide conformation, yet is involved in amide bonds that are sensitive to cleavage by endoproteases. Replacement of Pro¹⁰ by hydroxyproline, thioproline, and its 4 and 6 member ring counterparts, azetidine carboxylic acid and pipercolic acid, as well as cyclic aromatic derivatives such as Tic and Aic, all leads to conformational modifications and loss of affinity for the NT receptors. In general, substitutions of Pro¹⁰ are more easily tolerated by amino acids that favor a reverse turn, rather than an extended conformation [88]. For example, information about the bioactive conformation of NT(8–13) has been gained using spiro lactam conformational constraints [89]; however, substituted prolines have been tried without improvement in affinity [90].

The influence of silaproline in position 10 of NT(8–13) was evaluated by insertion into JMV438 to provide H-Lys-Lys-Sip-Tyr-Ile-Leu-OH (JMV2009), which exhibited improved NTS₂ selectivity, albeit with a 2.5-fold drop in affinity (Table 2). The conformations of JMV438 and JMV2009 appeared similar by NMR spectroscopic analysis. Moreover, Sip-containing NT analogue JMV2009

Val-Arg-Lys-Pro-Pro-Sip(Val-Arg-Lys-Pro-Pro-Pro)₂**Fig. 13** Silylated proline-rich peptide designed as CPP

maintained biological activity under conditions in which the natural peptide was rapidly degraded. Central administration of JMV2009 in rats induced dose-dependent antinociceptive responses in a variety of acute, tonic, visceral, and neuropathic pain models [91, 92].

4.5 Cell-Penetrating Peptides (CPPs)

The potential of cell-penetrating peptides (CPPs) to aid therapeutics to cross human membranes has attracted many scientists to the field of drug delivery [93]. Amphipathicity, charged residues, arginine moieties, and hydrophobicity are some of the claimed CPP properties suggested for a successful translocation through cell membranes. Among reported CPPs, proline-rich peptides that form amphipathic polyproline II helices have exhibited promising results as vectors [94, 95]. Replacement of a proline by silaproline on the hydrophobic face of a noncytotoxic CPP was examined to favor the interaction with the amphipathic environment of the cell membrane. Comparative studies using flow cytometry and confocal microscopy techniques showed a 20-fold enhancement in the internalization rate of the peptide Val-Arg-Lys-Pro-Pro-Sip(Val-Arg-Lys-Pro-Pro-Pro)₂ compared to its parent proline peptide [96]. Furthermore, like the parent peptide, the silaproline-containing CPP did not exhibit any cellular toxicity (Fig. 13).

The effect of replacement of Pro by Sip on the secondary structure and aggregation properties of the Pro-rich CPP was further studied by different biophysical techniques. Contact angle measurements, CD spectroscopy, and cellular uptake studies showed a good correlation between amphipathicity and cellular uptake. The CD spectra in water showed the same degree of PPII structure. The transmission electron microscopy (TEM) imaging results indicated the presence of fibrillar superstructures of ~20 nm width and variable length similar to those observed for (Val-Arg-Lys-Pro-Pro-Pro)₃ [97]. The higher hydrophobicity afforded by the Sip derivative resulted in a higher internalization inside HeLa cells due to a retained PPII conformation with increased amphipathic character.

5 Summary

We have described the preparation of enantiomerically pure silaproline (Sip), both by the first diastereoselective synthesis and by large-scale racemic synthesis, followed by resolution using preparative HPLC. Different *N*-protected versions of Sip, useful for the synthesis of oligomers and modified peptides, and the free amino

acid were made by these two methods. Silaproline oligomers were prepared in solution using a stepwise strategy and by polymerization of Sip-NCA. Compared to homopolyproline, homopolysilaproline was found to adopt a more stable PPII structure by CD spectroscopic analysis. Replacement of proline by silaproline in several biologically active peptides led generally to analogues retaining the activity of the parent peptide, as well as greater resistance toward enzymatic degradation. In the case of NT-containing Sip analogues, the *in vivo* biological response was improved, such that they could be used in the absence of a cocktail of enzyme inhibitors. Finally, the higher hydrophobicity afforded by Sip improved internalization of amphipathic proline-rich peptides inside HeLa cells. Considering the power of silaproline to enhance the conformational stability, biological activity, and cell permeability of proline-containing peptides, further use of this silicon-bearing heterocyclic amino acid is merited in applications to make peptide-based probes, receptor ligands, and enzyme inhibitors.

References

1. Gante J (1994) Peptidomimetics—tailored enzyme inhibitors. *Angew Chem Int Ed* 33 (17):1699–1720
2. Dougherty DA (2000) Unnatural amino acids as probes of protein structure and function. *Curr Opin Chem Biol* 4:645–652
3. Horng J-C, Raleigh DP (2003) Φ -Values beyond the ribosomally encoded amino acids: kinetic and thermodynamic consequences of incorporating trifluoromethyl amino acids in a globular protein. *J Am Chem Soc* 125:9286–9287
4. Mendel D, Ellman JA, Chang Z et al (1992) Probing protein stability with unnatural amino acids. *Science* 256:1798–1802
5. Adessi C, Soto C (2002) Converting a peptide into a drug: strategies to improve stability and bioavailability. *Curr Med Chem* 9:963–978
6. Mori A, Abe H, Inoue S (1995) Amino acids, peptides and their derivatives: powerful chiral ligands for metal-catalyzed asymmetric syntheses. *Appl Organomet Chem* 9:189–197
7. Guinn RM, Margot AO, Taylor JR et al (1995) Synthesis and characterization of polyamides containing unnatural amino acids. *Biopolymers* 35(5):503–512
8. Beausoleil E, Lubell WD (2000) An examination of the steric effects of 5-tert-butylproline on the conformation of polyproline and the cooperative nature of type II to type I helical interconversion. *Biopolymers* 53(3):249–256
9. Siebler C, Erdmann RS, Wennemers H (2014) Switchable proline derivatives: tuning the conformational stability of the collagen triple helix by pH changes. *Angew Chem Int Ed* 53 (39):10340–10344
10. Giannis A, Kolter T (1993) Peptidomimetics for receptor ligands—discovery, development, and medical perspectives. *Angew Chem Int Ed* 32(9):1244–1267
11. Ishida H, Inoue Y (1998) Peptides that contain unnatural amino acids: toward artificial proteins. *Rev Heteroat Chem* 19:79–142
12. Najera C (2002) From α -amino acids to peptides: all you need for the journey. *Synlett* 2002:1388–1403
13. Goody RS, Alexandrov K, Engelhard M (2002) Combining chemical and biological techniques to produce modified proteins. *ChemBioChem* 3:399–403
14. Wang L, Schultz PG (2002) Expanding the genetic code. *Chem Commun* 2002:1–11

15. Meanwell NA (2011) Synopsis of some recent tactical application of bioisosteres in drug design. *J Med Chem* 54:2529–2591
16. Tacke R, Wannagat U (1979) Syntheses and properties of bioactive organo-silicon compounds. *Top Curr Chem* 84:1–75
17. Birkofer L, Ritter A (1956) Silicoamino acids and silazanecarboxylic acid esters. *Angew Chem Int Ed* 68:461–462
18. Birkofer L, Ritter A (1958) Silicoamino acid derivatives. *Justus Liebigs Ann Chem* 612:22–33
19. Eaborn C, Feichtmayr F, Horn M et al (1974) The structure and stability of silyl-substituted carbonium ions. *J Organomet Chem* 77(1):39–43
20. Liu G, Sieburth McN S (2005) α -Trialkylsilyl amino acid stability. *Org Lett* 7(4):665–668
21. Cavalier F, Vivet B, Martinez J et al (2002) Influence of silaproline on peptide conformation and bioactivity. *J Am Chem Soc* 124(12):2917–2923
22. Handmann VI, Merget M, Tacke R (2000) Sila-substitution of the α -amino acid proline: synthesis of rac- and (R)-4,4-dimethyl-4-sila-proline ethyl ester. *Z Naturforsch B Chem Sci* 55:133–138
23. Martin C, Vanthuyn N, Miramon H et al (2012) Resolution of protected silaproline for a gram scale preparation. *Amino Acids* 43:649–655
24. Han G, Tamaki M, Hruby V (2001) Fast, efficient and selective deprotection of the tert-butoxycarbonyl (Boc) group using HCl/dioxane (4 M). *J Pept Res* 58(4):338–341
25. Vivet B, Cavalier F, Martinez J (2000) Synthesis of silaproline, a new proline surrogate. *Eur J Org Chem* (5):807–811
26. Dwyer MP, Keertikar KM, Zeng Q, Mazzola RD Jr, Yu W, Tang H, Kim SH, Tong L, Rosenblum SB, Kozlowski JA, Nair AG (2013) WO2013039876
27. MacArthur MW, Thornton JM (1991) Influence of proline residues on protein conformation. *J Mol Biol* 218(2):397–412
28. Wedemeyer WJ, Welker E, Scheraga HA (2002) Proline *cis-trans* isomerization and protein folding. *Biochemistry* 41(50):14637–14644
29. Halab L, Lubell WD (1999) Use of steric interactions to control peptide turn geometry. Synthesis of type VI β -Turn mimics with 5-tert-butylproline. *J Org Chem* 64(9):3312–3321
30. Halab L, Lubell WD (2001) Influence of N-terminal residue stereochemistry on the prolyl amide geometry and the conformation of 5-tert-butylproline type VI β -turn mimics. *J Pept Sci* 7:92–104
31. Keller M, Sager C, Dumy P et al (1998) Enhancing the proline effect: pseudo-prolines for tailoring *cis/trans* isomerization. *J Am Chem Soc* 120(12):2714–2720
32. An SSA, Lester CC, Peng J-L et al (1999) Retention of the *cis* proline conformation in tripeptide fragments of bovine pancreatic ribonuclease a containing a non-natural proline analogue, 5,5-dimethylproline. *J Am Chem Soc* 121(49):11558–11566
33. Vivet B, Cavalier F, Martinez J et al (2000) A silaproline-containing dipeptide. *Acta Crystallogr Sect C Cryst Struct Commun* 56:1452–1454
34. Cavalier F, Marchand D, Mbassi P et al (2006) Conformational studies of proline-, thiaproline- and dimethylsilaproline-containing diketopiperazines. *J Pept Sci* 12(10):621–625
35. Adzhubei AA, Sternberg MJE, Makarov AA (2013) Polyproline-II helix in proteins: structure and function. *J Mol Biol* 425(12):2100–2132
36. Zotti MD, Formaggio F, Crisma M et al (2014) Handedness preference and switching of peptide helices. Part I: helices based on protein amino acids. *J Pept Sci* 20(5):307–322
37. Ball LJ, Kühne R, Schneider-Mergener J et al (2005) Recognition of proline-rich motifs by protein–protein-interaction domains. *Angew Chem Int Ed* 44(19):2852–2869
38. Fillon YA, Anderson JP, Chmielewski J (2005) Cell penetrating agents based on a polyproline helix scaffold. *J Am Chem Soc* 127(33):11798–11803
39. Daniels DS, Schepartz A (2007) Intrinsically cell-permeable miniature proteins based on a minimal cationic PPII motif. *J Am Chem Soc* 129(47):14578–14579
40. Tremmel P, Geyer A (2002) An oligomeric Ser-Pro dipeptide mimetic assuming the polyproline II helix conformation. *J Am Chem Soc* 124(29):8548–8549

41. Zaminer J, Brockmann C, Huy P et al (2010) Addressing protein–protein interactions with small molecules: a Pro-Pro dipeptide mimic with a PPII helix conformation as a module for the synthesis of PRD-binding ligands. *Angew Chem Int Ed* 49(39):7111–7115
42. Raghavan B, Skoblenick KJ, Bhagwanth S et al (2009) Allosteric modulation of the dopamine D2 receptor by Pro-Leu-Gly-NH₂ peptidomimetics constrained in either a polyproline II helix or a type II β -Turn conformation. *J Med Chem* 52(7):2043–2051
43. Zhang R, Brownwell F, Madalengoitia JS (1998) Pseudo-A(1,3) strain as a key conformational control element in the design of poly-L-proline type II peptide mimics. *J Am Chem Soc* 120(16):3894–3902
44. Zhang R, Nickl CK, Mamai A et al (2005) Poly- L-proline type II peptide mimics as probes of the active site occupancy requirements of cGMP-dependent protein kinase. *J Pept Res* 66 (4):151–159
45. Flemer S, Wurthmann A, Mamai A et al (2008) Strategies for the solid-phase diversification of poly-L-proline-type II peptide mimic scaffolds and peptide scaffolds through guanidinylation. *J Org Chem* 73(19):7593–7602
46. Rucker AL, Pager CT, Campbell MN et al (2003) Host-guest scale of left-handed polyproline II helix formation. *Proteins* 53(1):68–75
47. Vila JA, Baldoni HA, Ripoll DR et al (2004) Polyproline II helix conformation in a proline-rich environment: a theoretical study. *Biophys J* 86(2):731–742
48. Zhang R, Madalengoitia JS (1996) Conformational stability of proline oligomers. *Tetrahedron Lett* 37(35):6235–6238
49. Deming TJ (2000) Living polymerization of α -amino acid-N-carboxyanhydrides. *J Polym Sci A Polym Chem* 38(17):3011–3018
50. Leuchs H (1906) Ueber die glycin-carbonsäure. *Chem Ber* 39:857
51. Farthing AC, Reynolds RJW (1950) Anhydro-N-carboxy-DL-phenyl-alanine. *Nature* 165 (4199):647
52. Gulin OP, Rabanal F, Giralt E (2006) Efficient preparation of proline N-carboxyanhydride using polymer-supported bases. *Org Lett* 8(23):5385–5388
53. Martin C, Lebrun A, Martinez J et al (2013) Synthesis of homopolypeptides with PPII structure. *J Polym Sci A Polym Chem* 51(15):3103–3109
54. Hadjichristidis N, Iatrou H, Pitsikalis M et al (2009) Synthesis of well-defined polypeptide-based materials via the ring-opening polymerization of α -amino acid N-carboxyanhydrides. *Chem Rev* 109(11):5528–5578
55. Ling J, Huang Y (2010) Understanding the ring-opening reaction of α -amino acid N-carboxyanhydride in an amine-mediated living polymerization: a DFT Study. *Macromol Chem Phys* 211(15):1708–1711
56. Peggion E, Terbojevich M, Cosani A et al (1966) Mechanism of N-carboxyanhydride (NCA) polymerization in dioxane. Initiation by carbon-14-labeled Amines I. *J Am Chem Soc* 88 (15):3630–3632
57. Kricheldorf HR, Müller D (1983) Secondary structure of peptides: ¹³C NMR cross polarization/ magic angle spinning spectroscopic characterization of solid polypeptides. *Macromolecules* 16:615–623
58. Woody RW (2009) Circular dichroism spectrum of peptides in the poly(Pro)II conformation. *J Am Chem Soc* 131(23):8234–8245
59. Babine RE, Bender SL (1997) Molecular recognition of protein–ligand complexes: applications to drug design. *Chem Rev* 97(5):1359–1472
60. Hruby VJ, Balse PM (2000) Conformational and topographical considerations in designing agonist peptidomimetics from peptide leads. *Curr Med Chem* 7(9):945–970
61. Sagan S, Beaujouan JC, Torrens Y et al (1997) High affinity binding of [³H]propionyl-[Met (O²)¹¹]substance P(7-11), a tritiated septide-like peptide, in Chinese hamster ovary cells expressing human neurokinin-1 receptors and in rat submandibular glands. *Mol Pharmacol* 52(1):120–127

62. Pennefather JN, Lecci A, Cadenas ML et al (2004) Tachykinins and tachykinin receptors: a growing family. *Life Sci* 74(12):1445–1463
63. Sagan S, Karoyan P, Chassaing G et al (1999) Further delineation of the two binding sites (R*(n)) associated with tachykinin neurokinin-1 receptors using [3-Prolinomethionine(11)]SP analogues. *J Biol Chem* 274(34):23770–23776
64. Cavalier F, Marchand D, Martinez J et al (2004) Biological activity of silylated amino acid containing substance P analogues. *J Pept Res* 63(3):290–296
65. de Mateos-Verchere JG, Leprince J, Tonon MC et al (2001) The octadecaneuropeptide [diazepam-binding inhibitor (33-50)] exerts potent anorexigenic effects in rodents. *Eur J Pharmacol* 414(2-3):225–231
66. Leprince J, Gandolfo P, Thoumas JL et al (1998) Structure-activity relationships of a series of analogues of the octadecaneuropeptide ODN on calcium mobilization in rat astrocytes. *J Med Chem* 41(23):4433–4438
67. Ondetti MA, Rubin B, Cushman DW (1977) Design of specific inhibitors of angiotensin-converting enzyme: new class of orally active antihypertensive agents. *Science* 196(4288):441–444
68. Mutahi M, Nittoli T, Guo L et al (2002) Silicon-based metalloprotease inhibitors: synthesis and evaluation of silanol and silanediol peptide analogues as inhibitors of angiotensin-converting enzyme. *J Am Chem Soc* 124(25):7363–7375
69. Hanessian S, Reinhold U, Saulnier M et al (1998) Probing the importance of spacial and conformational domains in captopril analogs for angiotensin converting enzyme activity. *Bioorg Med Chem Lett* 8(16):2123–2128
70. Natesh R, Schwager SL, Evans HR et al (2004) Structural details on the binding of antihypertensive drugs captopril and enalaprilat to human testicular angiotensin I-converting enzyme. *Biochemistry* 43(27):8718–8724
71. Corradi HR, Schwager SL, Nchinda AT et al (2006) Crystal structure of the N domain of human somatic angiotensin I-converting enzyme provides a structural basis for domain-specific inhibitor design. *J Mol Biol* 357(3):964–974
72. Dalkas GA, Marchand D, Galleyrand JC et al (2010) Study of a lipophilic captopril analogue binding to angiotensin I converting enzyme. *J Pept Sci* 16(2):91–97
73. Carraway R, Leeman SE (1973) The isolation of a new hypotensive peptide, neurotensin, from bovine hypothalami. *J Biol Chem* 248(19):6854–6861
74. Doulut S, Dubuc I, Rodriguez M et al (1993) Synthesis and analgesic effects of N-[3-[(hydroxyamino) carbonyl]-1-oxo-2(R)-benzylpropyl]-L-isoleucyl-L-leucine, a new potent inhibitor of multiple neurotensin/neuromedin N degrading enzymes. *J Med Chem* 36(10):1369–1379
75. Béraud-Dufour S, Coppola T, Massa F et al (2009) Neurotensin receptor-2 and -3 are crucial for the anti-apoptotic effect of neurotensin on pancreatic β -TC3 cells. *Int J Biochem Cell Biol* 41(12):2398–2402
76. Kleczkowska P, Lipkowski AW (2013) Neurotensin and neurotensin receptors: characteristic, structure–activity relationship and pain modulation—a review. *Eur J Pharmacol* 716(1–3):54–60
77. Hughes FM Jr, Shaner BE, May LA et al (2010) Identification and functional characterization of a stable, centrally active derivative of the neurotensin (8-13) fragment as a potential first-in-class analgesic. *J Med Chem* 53(12):4623–4632
78. Seebach D, Lukaszuk A, Patora-Komisarska K et al (2011) On the terminal homologation of physiologically active peptides as a means of increasing stability in human serum--neurotensin, opiorphin, B27-KK10 epitope, NPY. *Chem Biodivers* 8(5):711–739
79. Boules M, Liang Y, Briody S et al (2010) NT79: a novel neurotensin analog with selective behavioral effects. *Brain Res* 1308:35–46
80. Pratsch G, Unfried JF, Einsiedel J et al (2011) Radical arylation of tyrosine and its application in the synthesis of a highly selective neurotensin receptor 2 ligand. *Org Biomol Chem* 9(10):3746–3752

81. Einsiedel J, Held C, Hervet M et al (2011) Discovery of highly potent and neurotensin receptor 2 selective neurotensin mimetics. *J Med Chem* 54(8):2915–2923
82. Orwig KS, Lassetter MR, Hadden MK et al (2009) Comparison of N-terminal modifications on neurotensin(8-13) analogues correlates peptide stability but not binding affinity with in vivo efficacy. *J Med Chem* 52(7):1803–1813
83. Dubuc I, Costentin J, Doulut S et al (1992) JMV 449: a pseudopeptide analogue of neurotensin-(8-13) with highly potent and long-lasting hypothermic and analgesic effects in the mouse. *Eur J Pharmacol* 219(2):327–329
84. Doulut S, Rodriguez M, Lugin D et al (1992) Reduced peptide bond pseudopeptide analogues of neurotensin. *Pept Res* 5(1):30–38
85. Couder J, Tourwe D, Van Binst G et al (1993) Synthesis and biological activities of psi (CH₂NH) pseudopeptide analogues of the C-terminal hexapeptide of neurotensin. *Int J Pept Protein Res* 41(2):181–184
86. Sefer AM, He JX, Sawyer TK et al (1995) Design and structure-activity relationships of C-terminal cyclic neurotensin fragment analogues. *J Med Chem* 38(2):249–257
87. Bredeloux P, Cavelier F, Dubuc I et al (2008) Synthesis and biological effects of c(Lys-Lys-Pro-Tyr-Ile-Leu-Lys-Lys-Pro-Tyr-Ile-Leu) (JMV2012), a new analogue of neurotensin that crosses the blood-brain barrier. *J Med Chem* 51(6):1610–1616
88. Heyl DL, Sefer AM, He JX et al (1994) Structure-activity and conformational studies of a series of modified C-terminal hexapeptide neurotensin analogues. *Int J Pept Protein Res* 44(3):233–238
89. Bittermann H, Einsiedel J, Hubner H et al (2004) Evaluation of lactam-bridged neurotensin analogues adjusting psi(Pro10) close to the experimentally derived bioactive conformation of NT(8-13). *J Med Chem* 47(22):5587–5590
90. Held C, Hübner H, Kling R et al (2013) Impact of the proline residue on ligand binding of neurotensin receptor 2 (NTS2)-selective peptide-peptoid hybrids. *ChemMedChem* 8(5):772–778
91. Roussy G, Dansereau MA, Baudisson S et al (2009) Evidence for a role of NTS2 receptors in the modulation of tonic pain sensitivity. *Mol Pain* 5:38
92. Tétreault PB-OÉ, Murza A, Parent A, Bérubé P, René A, Dubuc I, Longpré JM, Beaudet N, Leduc R, Marsault É, Martinez J, Cavelier F, Sarret P (2014) Analgesic potency of a new neurotensin analog in different experimental pain models. Paper presented at the 15th Great lakes GPCR retreat, Bromont, Quebec, Canada, 2–4 October
93. Brooks H, Lebleu B, Vives E (2005) Tat peptide-mediated cellular delivery: back to basics. *Adv Drug Deliv Rev* 57(4):559–577
94. Fernandez-Carneado J, Kogan MJ, Castel S et al (2004) Potential peptide carriers: amphipathic proline-rich peptides derived from the N-terminal domain of gamma-zein. *Angew Chem Int Ed Engl* 43(14):1811–1814
95. Fernandez-Carneado J, Kogan MJ, Pujals S et al (2004) Amphipathic peptides and drug delivery. *Biopolymers* 76(2):196–203
96. Pujals S, Fernández-Carneado J, Kogan MJ et al (2006) Replacement of a proline with silaproline causes a 20-fold increase in the cellular uptake of a Pro-rich peptide. *J Am Chem Soc* 128(26):8479–8483
97. Kogan MJ, Dalcol I, Gorostiza P et al (2002) Supramolecular properties of the proline-rich gamma-Zein N-terminal domain. *Biophys J* 83(2):1194–1204

Proline Methanologues: Design, Synthesis, Structural Properties, and Applications in Medicinal Chemistry

Miguel Angel Vilchis-Reyes and Stephen Hanessian

Abstract In this review, we discuss methanoproline, which are analogues of proline that contain a bridged methylene group at different positions, which we designate herein as *proline methanologues*. Particular emphasis is placed on naturally occurring members, general methods for the stereocontrolled synthesis of different diastereoisomers, functionalized analogues, conformational and stereoelectronic features, as well as their utility as proline congeners in medicinally relevant compounds.

Keywords Conformational analysis • Constrained amino acids • Drug prototypes • Natural products

Contents

1	Introduction	52
2	2,3-Methanoproline	52
	2.1 Synthesis	53
	2.2 Conformational Studies	55
	2.3 2,3-Methanoproline Analogues	56
3	2,4-Methanoproline	57
	3.1 Synthesis	58
	3.2 Conformational Studies	60
	3.3 2,4-Methanoproline Analogues	60
4	3,4-Methanoproline	62
	4.1 Synthesis	63
	4.2 Conformational Studies	67
	4.3 3,4-Methanoproline Analogues	68

5	3,5-Methanoprolines	69
5.1	Synthesis	70
6	4,5-Methanoprolines	73
6.1	Synthesis	74
6.2	Conformational Studies	78
6.3	4,5-Methanoproline Analogues	80
6.4	4,5-Methanoprolines as Metal-Free Organocatalysts	86
7	<i>trans</i> -3,4-Methano-L-azetidine-2-carboxylic acid	88
8	Summary	89
	References	90

1 Introduction

The practice of ring constraint in the field of amino acids and peptides is an important strategy in the design of peptidomimetics and related motifs intended to improve biological activity without compromising the inherent properties of the original substrate [1, 2]. Traditionally ring constraint was intended to simulate the spatial and conformational characteristics of bioactive amino acids and peptides derived from them [3, 4]. In this regard, conformationally constrained mono- and bicyclic amino acids have been incorporated as unnatural counterparts of natural amino acids and peptides [5–7]. Among several advantages of this strategy is the ability to confer favorable pharmacological properties such as better transport and resistance to cleavage by peptidases. The smallest ring motif that can be incorporated in a natural amino acid is the cyclopropane ring [8–12].

In this chapter, we shall focus on methanoprolines as constrained analogues of prolines, which we designate herein as “proline methanologues” focusing on their natural occurrence, synthesis, conformational properties, analogues, and various aspects of their biological activities.

2 2,3-Methanoproline

The discovery that 1-aminocyclopropane-1-carboxylic acid (Acc) was the direct precursor of ethylene, a volatile hormone that regulates many facets of growth and development throughout the life cycle of plants [13], led to the search of naturally occurring amino acids as potential inhibitors of ethylene-forming enzyme (EFE)

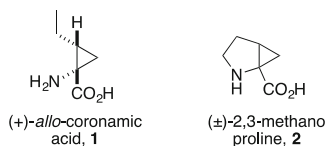
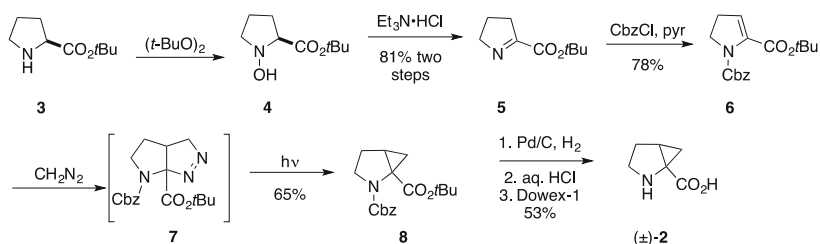


Fig. 1 Structures of naturally occurring and synthetic methano amino acids



Scheme 1 Synthesis of (±) **2** from L-proline *tert*-butyl ester

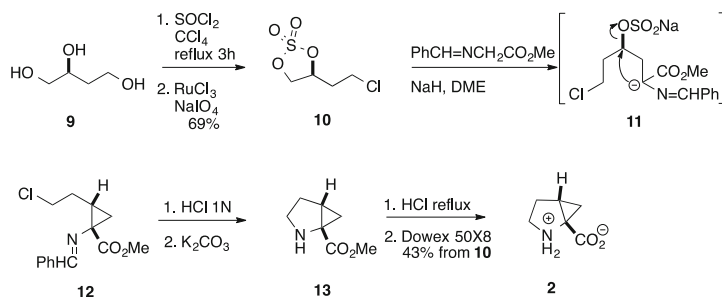
[14–16]. (+)-*Allo*-coronamic acid **1** was found to produce 1-butene at a slower rate compared to the formation of ethylene by Acc (Fig. 1) [17]. Consideration of the functional, stereochemical, and spatial requirements for binding of Acc and its derivatives in the active site of EFE led to the design of 2,3-methanoproline as a potential inhibitor [17]. The active site of the enzyme was reasoned to accommodate this azacyclic constrained analogue of (+)-*allo*-coronamic acid (**1**).

2.1 Synthesis

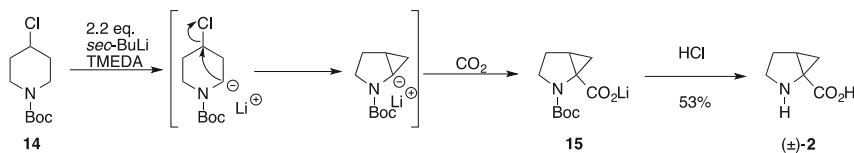
The first synthesis of racemic 2,3-methanoproline **2** was reported by Stammer and coworkers [18], who showed that it was a weak inhibitor of EFE. L-Proline *tert*-butyl ester (**3**) was oxidized to the *N*-hydroxy analogue **4**, which was subjected to elimination. The resulting dehydropyridine *tert*-butyl ester **5** [19] was treated with CbzCl to give 2,3-enamine **6**, which reacted with excess of diazomethane to afford Δ -2 pyrazoline intermediate **7**. Irradiation by means of a 450 W Hanovia medium-pressure Hg lamp afforded protected 2,3-methanoproline **8** which was converted to racemic 2,3-methanoproline **2** as the zwitterion after hydrogenolytic cleavage of the Cbz group, acid cleavage of the *tert*-butyl ester, and ion exchange chromatography on Dowex-1 resin (Scheme 1).

Conversion of **2** to the *N*-acetyl *N'*-methylamide afforded crystalline material suitable for X-ray analysis. The ϕ and ψ angles compared favorable with those of the parent proline amide except for a smaller ψ angle in **2** probably because of the conjugation of the carbonyl group with the cyclopropane ring.

The two crystalline enantiomers of 2,3-methanoproline were prepared by resolution of their *N*-Cbz derivatives using (–)-(*S*)- α -methylbenzylamine [20]. X-ray quality crystals were also obtained from the resolution of the racemic *tert*-butyl ester of 2,3-methanoproline using (+)-tartaric acid.



Scheme 2 Enantioselective synthesis of (–) **2**



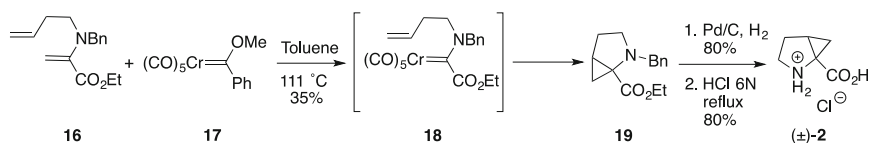
Scheme 3 Racemic synthesis of (±) **2** by ring contraction of a piperidine analogue

The synthesis of (–)-2,3-methano-L-proline was reported by Hercouet and coworkers [21] in 1996, as a sequel to their synthesis of (+)-*allo*-coronamic acid (Scheme 2) [22, 23]. (*S*)-Butanetriol **9** was converted to the 3,4-chlorosulfite ester of 1-chlorobutanetriol and the latter oxidized to the corresponding cyclic sulfate ester **10** according to the Sharpless method [24]. Treatment of **10** with the sodium enolate of *N*-benzylidene methyl glycinate [25] in DME afforded *N*-benzylidene cyclopropane methyl ester **12** in quantitative yield. Remarkably the *cis*-isomer was formed exclusively. Sequential deprotection and intramolecular cyclization afforded 2,3-methano-L-proline methyl ester **13**, which was hydrolyzed to afford (–)-2,3-methano-L-proline (**2**) as the internal salt in 43% overall yield from sulfate **10** without purification of intermediates.

Racemic 2,3-methanoproline was synthesized effectively by a route featuring treatment of *N*-Boc-4-chloropiperidine **14** with 2.2 equiv. of *sec*-BuLi in the presence of TMEDA (*N,N,N',N'*-tetramethylethylenediamine) to cause α -lithiation, intramolecular displacement of the 4-chloro group, and a second α -lithiation [26]. Quenching with carbon dioxide afforded racemic 2,3-methanoproline **2** in 53% yield (Scheme 3).

The original Stammer synthesis of *N*-Cbz-2,3-methanoproline *tert*-butyl ester has been adapted to provide the corresponding benzyl ester, which was prepared for use in β -turn mimetics [27].

Racemic 2,3-methanoproline was targeted in an extension of studies on the synthesis of 1-aminocyclopropane-1-carboxylic acids by reactions of olefins with Fischer dialkylaminocarbene complexes employing an intramolecular variant [28]. Heating a solution containing dehydroamino ester **16** and Fischer carbene **17** in toluene at reflux gave *N*-benzyl-2,3-methanoproline ethyl ester **19** by way of



Scheme 4 Synthesis of (\pm) **2** employing a Fischer carbene complex

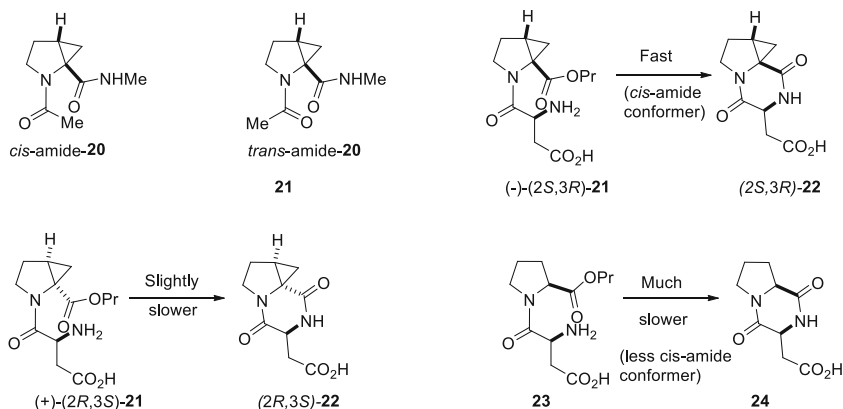
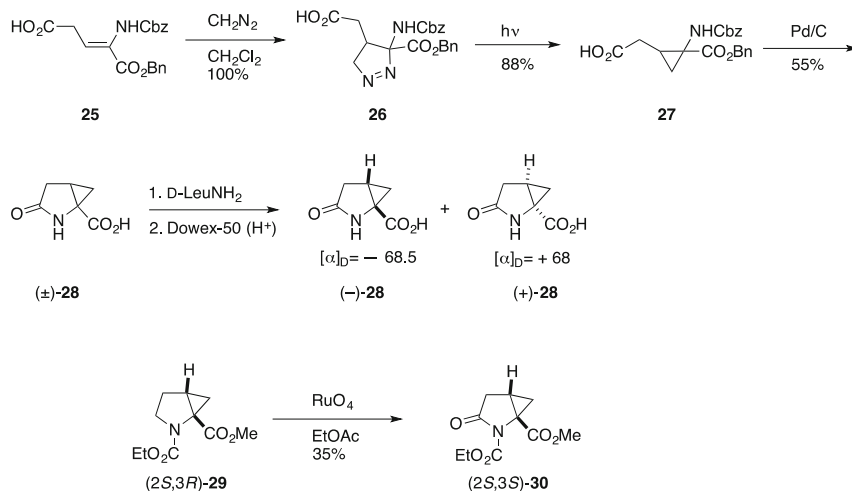


Fig. 2 Diastereomeric 2,3-methano-L-proline analogues and diketopiperazine formation

intermediate **18**. After removal of the protecting groups, racemic 2,3-methanoproline **2** was isolated as the hydrochloride salt (Scheme 4).

2.2 Conformational Studies

N-Acetyl-2,3-methanoproline *N'*-methylamide **20** has been characterized by ^1H -NMR and X-ray crystallography and exhibited in solution slightly higher *N*-terminal amide *cis*-isomer population than its proline counterpart [18]. In the crystalline state, only the *cis*-isomer was observed. Inspired by the highly sweet sugar substitute aspartame (*N*-(*L*- α -aspartyl)-*L*-phenylalanine 1-methyl ester) and a synthetic congener Asp-Acc-OPr (Acc = 1-aminocyclopropane-1-carboxylic acid), the diastereomeric ($-$)-(2*S*,3*R*)- **21** and (+)-(2*R*,3*S*)-**21** *N*-(*L*- α -aspartyl)-*L*-2,3-methanoproline 1-propyl esters were synthesized as constrained analogues. The (2*S*,3*R*)-**21** isomer readily cyclized to the corresponding diketopiperazine (2*S*,3*R*)-**22** at room temperature, while its (2*R*,3*S*)- **21** isomer was slightly slower. Both were readily cyclized at 65°C. *L*-Proline **23** cyclized less readily to **24** than either of the two methano isomers (2*S*,3*R*)-**21** and (2*R*,3*S*)-**21** leading to the conclusion that the latter contained a higher population of the *cis*-amide conformer, which facilitated ring closure (Fig. 2) [20].



Scheme 5 Synthesis of (+) and (-) 2,3-methanopyroglutamic acids

2.3 2,3-Methanoproline Analogues

2,3-Methanopyroglutamic acid has been synthesized and studied in racemic and optically resolved forms [29–31]. Initially, *N*-Cbz-dehydroglutamic acid benzyl ester **25** was converted to the Δ -2-pyrazoline **26**, which on photolysis led to *N*-Cbz-1-amino-2,3-methanopyroglutamate **27** [29]. Catalytic hydrogenation afforded 2,3-methanopyroglutamic acid ((±)-**28**), which was resolved into (+)- and (-)-**28** by the formation of diastereomeric salts, respectively, with D- and L-leucine amide followed by conversion to the free base using Dowex-50 (H^+) (Scheme 5).

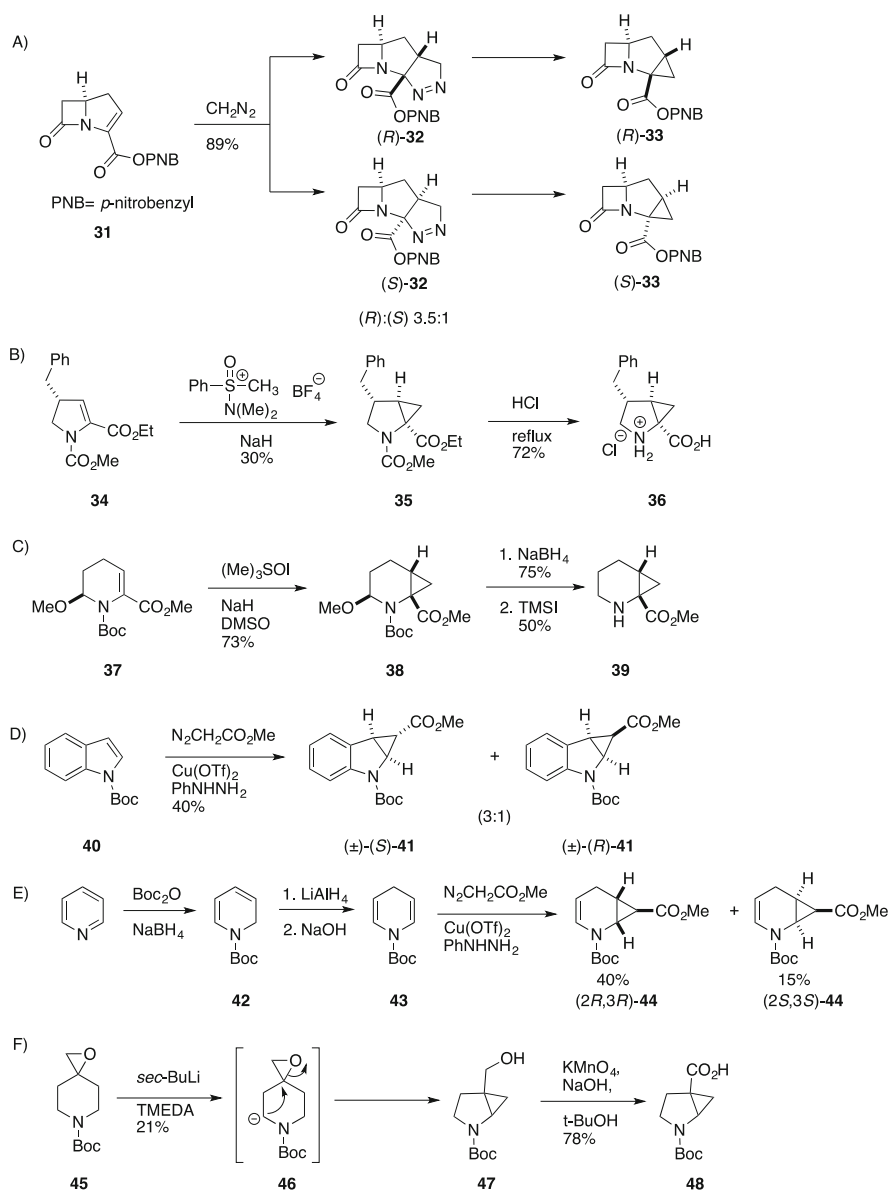
Enantiopure (resolved) (2*S*,3*R*)-*N*-ethoxycarbonyl-methanoproline methyl ester **29** was subjected to oxidation with RuO_4 to give the corresponding (2*S*,3*S*)-*N*-ethoxycarbonyl-2,3-methanopyroglutamic acid methyl ester (2*S*,3*S*)-**30**. The enantiomer (2*R*,3*R*)-**30** was similarly prepared.

Various 2,3-methanoproline and 2,3-methanopipecolic acid analogues have been synthesized (Scheme 6) [32–35]. For example, 1,3-dipolar addition of diazomethane to bicyclic β -lactam intermediate **31** led to a 3.5:1 diastereomeric mixture of Δ -2-pyrazolines **32**, which upon independent thermolysis afforded, respectively, (*S*)- and (*R*)-2,3-methano-7-oxo-1-azabicyclo[3.2.0]heptane carboxylic acids **33** [32].

Michael addition of the sulfoxonium methyl ylide to dehydroproline **34** and solvolysis of the protecting groups with HCl gave 4-benzyl-2,3-methanoproline **36** as the hydrochloride salt [33]. 2,3-Methanopipecolate **39** was prepared by a similar approach [33].

A copper-catalyzed diazoinsertion reaction transformed indole **40** into a 3:1 mixture of racemic diastereomers **41** [34]. Unsaturated 2,3-methanopipecolates **44** were prepared using a similar protocol [34].

Intramolecular epoxide opening of the anion generated from *N*-Boc-piperidine **45** led to *N*-Boc-2,3-methano-3-hydroxymethylpyrrolidine **47**, which was oxidized to the corresponding carboxylic acid **48** [35].



Scheme 6 2,3-Methanoprolines and 2,3-methanopipercolinic acid analogues. See text for details

3 2,4-Methanoproline

In 1980, 2,4-methanoproline (**49**) and 2,4-methano-bridged glutamic acid (1-amino-1,3-dicarboxycyclobutane) (**50**) were isolated and identified as components of seeds isolated from *Ateleia herbert-smithii* Pittier, a legume tree

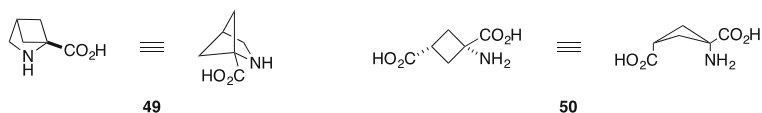
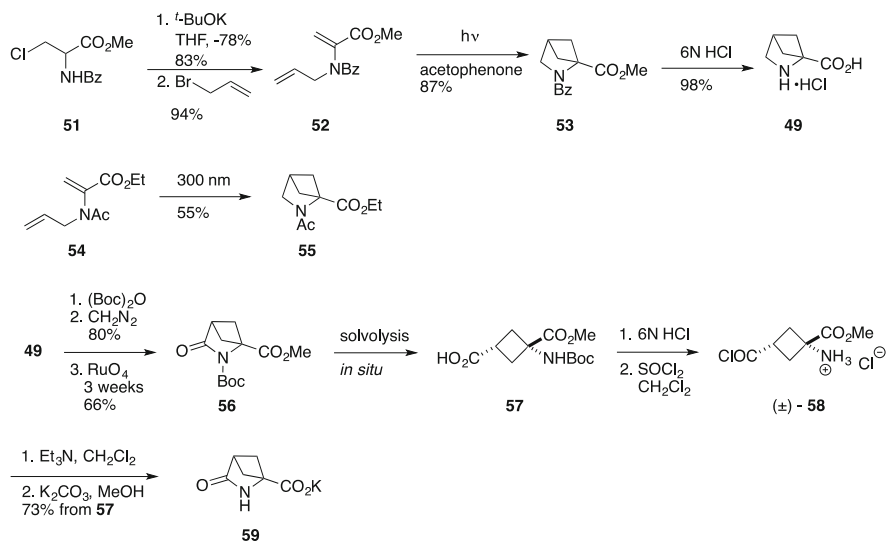


Fig. 3 A naturally occurring 2,4-methanoproline and a 2,4-bridged glutamic acid analogue



Scheme 7 Synthesis of 2,4-methano-L-proline and 2,4-methanopyroglutamate

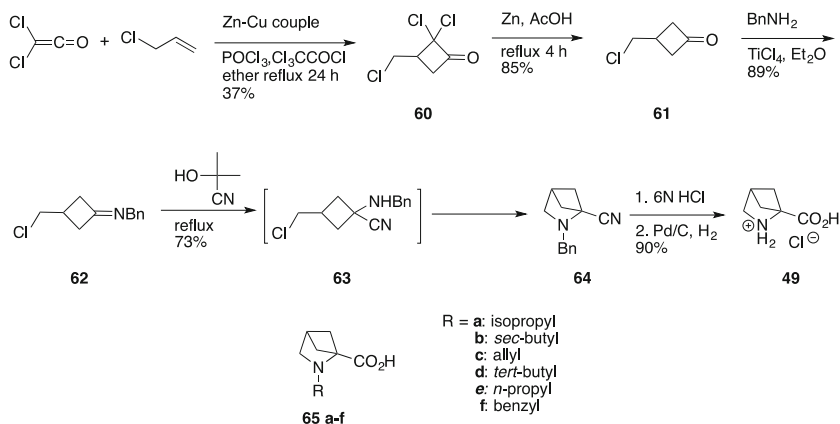
indigenous to Costa Rica [36]. These novel non-proteinogenic amino acids were isolated in minute quantities, and their structures elucidated by X-ray crystallography (Fig. 3). The same two non-proteinogenic amino acids were later isolated from extracts of the legume genus *Bocoa* (Papilionoideae; Swaetzieae) [37]. -2,4-Methanoproline has insect repellent and antifeedant activity against larvae of the cotton leafworm and adults of the cowpea weevil [38].

Replacement of Pro-34 in Ras protein with a 2,4-methano-L-proline, to ensure a locked prolyl amide *trans*-conformation, resulted in a protein with high levels of intrinsic activity and GTPase-activating protein-activated activity in comparison to wild-type Ras [39].

3.1 Synthesis

Formally, approaches to the synthesis of 2,4-methanoproline can consider a core structure having the 2-azabicyclo[2.1.1]hexane system onto which a carboxyl unit is attached at C-1.

2,4-Methanoproline was first synthesized from 2-benzamido-3-chloropropionate (**51**), which was readily obtained from serine (Scheme 7) [40, 41]. Elimination of



Scheme 8 Synthesis of (±) 2,4-methanoproline (**49**) and *N*-alkyl derivatives

chloride using *tert*-BuOK and *N*-allylation provided dehydroalanine **52** in 94% yield. Adopting a photolytic cyclization [42], diene **52** was irradiated with a medium-pressure Hanovia lamp for 12 h in the presence of 0.2% acetophenone in benzene to afford photoadduct **53** in 87% yield.

Treatment of methyl *N*-benzoyl-2,4-methanoprolinate **53** with 6N HCl followed by purification on Amberlite IR-45A gave racemic 2,4-methanoproline (**49**) as the crystalline hydrochloride salt in 68% overall yield from serine. Further optimization of the route from racemic serine gave 2,4-methanoproline in 70% yield over four steps and >20 g scale [43]. In an independent study, ethyl *N*-acetyl-2,4-methanoprolinate **55** was prepared by a similar photochemical [2+3]-cycloaddition (Scheme 7) [44].

Methyl 2,4-methanoglutamate was synthesized as the crystalline hydrochloride salt by conversion of methanoproline **49** to the *N*-Boc methyl ester, followed by oxidation with RuO₄ to afford lactam **56**, which was readily solvolyzed to *N*-Boc-methanoglutamate **57**. Acid hydrolysis gave crystalline methyl 2,4-methanoglutamate hydrochloride. Sequential treatment of **57** with 6N HCl and thionyl chloride followed by lactam formation and ester cleavage led to methanopyroglutamate **59** (Scheme 7) [41].

2,4-Methanoproline and several *N*-alkyl analogues were synthesized starting from a [2+2] cycloaddition between dichloroacetylene and allyl chloride, which gave cyclobutanone **60**, albeit in modest yield [45, 46]. Conversion to 3-(chloromethyl)cyclobutanone **61** followed by treatment with benzylamine led to imine **62**. Acetone cyanohydrin was found to efficiently convert imine **62** to the corresponding α-cyano amine **63** which underwent intramolecular displacement of chloride to give bicyclic **64**. Acid hydrolysis followed by catalytic hydrogenation gave 2,4-methanoproline **49** as the crystalline hydrochloride salt. *N*-Alkyl derivatives **65a–f** were prepared using this method (Scheme 8). Only aminonitrile *cis*-diastereomer **63** can undergo intramolecular cyclization; however, equilibrium is

established using acetone cyanohydrin in refluxing methanol that gives a 3:1 *cis-trans* mixture.

3.2 Conformational Studies

The conformational properties of amides and peptides containing 2,4-methanoproline have been studied by NMR techniques that revealed their predominant prolyl amide *trans*-isomer orientation in aqueous solution [47, 48]. Moreover, *N*-acetyl-2,4-methanoproline *N*-methylamide was observed to adopt the prolyl *trans*-conformer in the solid state by X-ray analysis [48]. Quantum mechanical calculations using the standard CNDO/2 (complete neglect of differential overlap) algorithm were in agreement with these observations [49]. Similarly, a single prolyl amide *trans*-isomer and extended conformation like that of the parent proline analogue was observed for [2,4-methanoproline³]-thyrotropin-releasing hormone (TRH, pGlu-His-Pro) using ¹H- and ¹³C-NMR spectroscopy in polar solvents [50].

3.3 2,4-Methanoproline Analogues

The structural features and conformational properties of 2,4-methanoproline have inspired a number of studies of related analogues with potential biological activities. For example, 4-carboxy-2,4-methanoproline **66** has been used as a constrained congener of glutamic acid to define the structural elements required for inhibitors of sodium-dependent glutamate transporters (Fig. 4a) [51]. Previously, *trans*-L-proline 4-carboxylic acid **67** was found to be a relatively potent competitive inhibitor of sodium-dependent high-affinity excitatory amino acid transporters found in rat brain and hypothesized to mimic a folded conformation of glutamate. Designed to mimic an extended glutamate conformation, 4-carboxy-2,4-methanoproline **66** exhibited inhibitory potency on par with L-glutamate and was translocated at least with L-glutamate supporting the conclusion that **66** embodied the substrate pharmacophore [51].

β -Amino acid homologue **70** of 2,4-methanoproline **49** with a methylene spacer unit at the bridgehead carbon was prepared by S_N2-type displacement of methanesulfonate **68** with cyanide ion and solvolysis of the resulting nitrile **69** [52]. The design and synthesis of molecules such as **71–73** was inspired by the known activity of epibatidine and ABT-594 as nicotinic acetylcholine receptor (nAChR) ligands and the potential of generating more potent analogues; however, their biological evaluation showed no affinity at the $\alpha 4\beta 2$ nor $\alpha 3\beta 4$ nAChR subtypes (Fig. 4b) [53].

Ring-expanded and ring-substituted analogues of 2,4-methanoproline have been synthesized by adopting the method described above from 3-(chloromethyl)

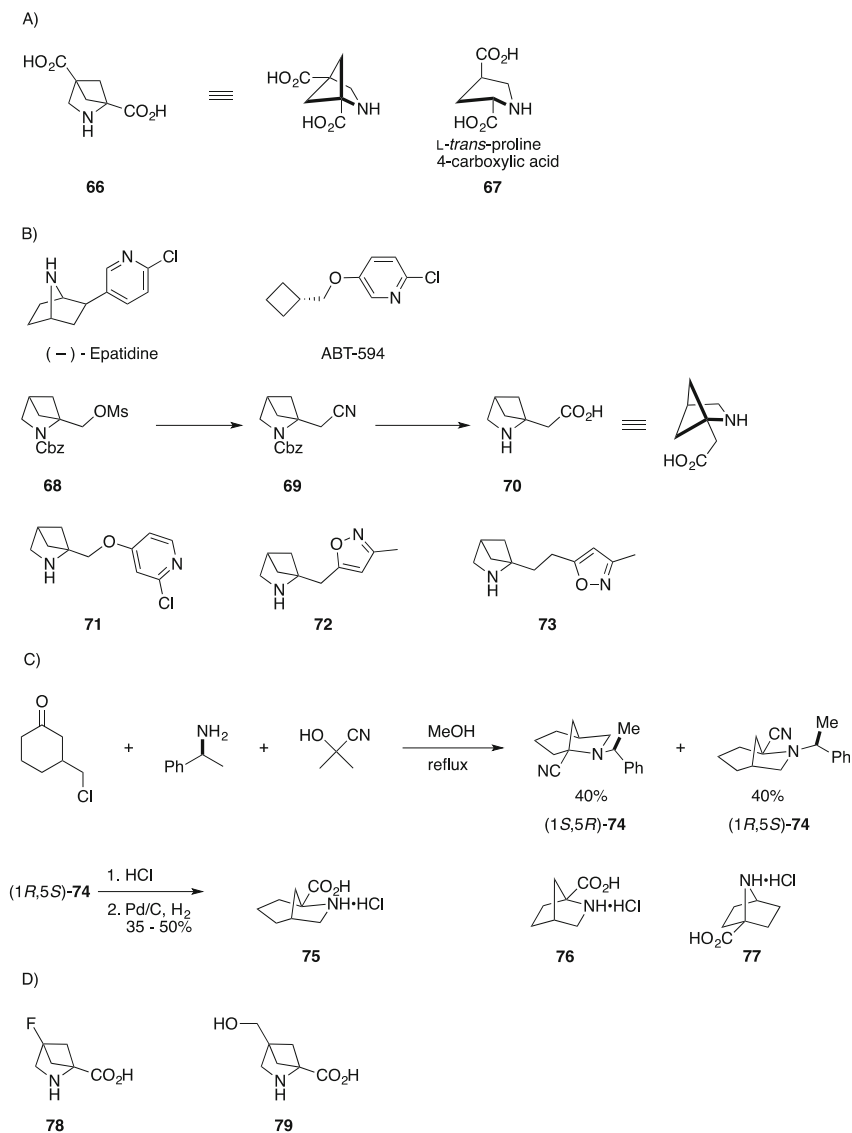


Fig. 4 Selected examples of synthetic 2,4-methanoproline analogues in relation to biologically active compounds

cyclobutanone **61** (Scheme 8) [45, 46] using, respectively, 3-(chloromethyl)cyclopentanone and 3-(chloromethyl)cyclohexanone with (*S*)- α -phenylethylamine and acetone cyanohydrin (Fig. 4c) [54].

Starting with 3-(chloromethyl)cyclohexanone, (*S*)- α -phenylethylamine and acetone cyanohydrin led to a 1:1 mixture of bicyclo[2.3.1]aminonitrile diastereomers (1*S*,5*R*)- and (1*R*,5*S*)-**74** which were separated by column chromatography.

Fig. 5 Naturally occurring *cis*- and synthetic *trans*-3,4-bridged methanoprolines



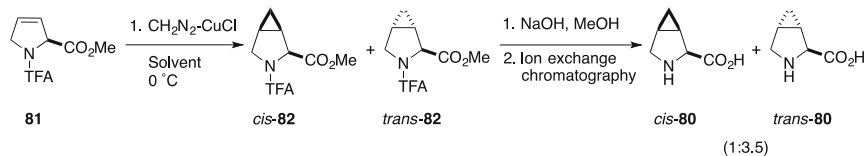
Hydrolysis to the carboxylic acid followed by hydrogenolysis afforded the homologated bicyclic amino acid **75** as the hydrochloride salt. Application of the method to 3-(chloromethyl)cyclopentanone afforded bicyclic compounds **76** and **77**, albeit in modest yields (Fig. 4c). The method could also be adapted to prepare enantiopure 2,4-methano-L-proline [54].

5-Fluoro-2,4-methanoprolinone (**78**, Fig. 4d) was prepared by substituting allyl bromide with 2-fluoroprop-2-enyl methanesulfonate in the [2+2]-photochemical cyclization route described in Scheme 7 [55]. 5-Hydroxymethyl 2,4-methanoprolinone (**79**) was synthesized by a route featuring lactone formation, Curtius rearrangement, and intramolecular alkylation from an oxaspiro[3.3]heptane framework obtained from bis-alkylation of diisopropyl malonate with 3,3-bis(chloromethyl)oxetane [56] (Fig. 4d).

4 3,4-Methanoprolinone

In 1969, *cis*-3,4-methano-L-proline (**80**) was isolated from seeds of *Aesculus parviflora* as a crystalline solid (Fig. 5) [57, 58]. The *cis*-configuration was assigned based on the isolation of *cis*-3-methyl-L-proline as the main product of hydrogenation of *cis*-**80** with Adam's catalyst. *cis*-3,4-Methanoprolinone was also isolated from seeds of *E. foeminea* and *E. foliata* belonging to the *Ephedra* species [59, 60]. (2*S*,3*R*,4*S*)- and (2*S*,3*R*,4*R*)-2-Carboxypropylglycine was also isolated from the abovementioned seeds. Although both *cis*- and *trans*-cyclopropylglycines were isolated, only *cis*-3,4-methano-L-proline was detected in the soluble nitrogen pool of *A. parviflora*. 3,4-Methano-L-prolines have been associated with a number of biological activities such as protection against thermal denaturation of Pro-t-RNA synthetases from *Phaseolus aureus* and *Delonix regia* [61]. Inhibition of proline transport was observed in *E. coli* [62]. Growth of *E. coli* and *S. typhimurium* was inhibited by *cis*- and *trans*-3,4-methano-L-prolines (*cis*- and *trans*-**80**, Fig. 5) with greater efficacy exhibited by the *cis*-isomer, and growth was restored in the presence of L-proline [62]. *cis*-3,4-Methano-L-proline (*cis*-**80**) is a plant male sterlant [63] that exhibits activity independent of 1-aminocyclopropane-1-carboxylic acid (Acc)-induced ethylene biosynthesis which has been associated with male sterility in wheat coleoptile segments [64].

cis-2,4-Methanoprolinone was used in a training set of analogues in a quantitative structure–activity relationship (QSAR) study of the human proton-coupled amino acid transporter 1 (HPAT1) and exhibited a higher K_i value than the reference



Scheme 9 Diazomethane-mediated cyclopropanation of **81**

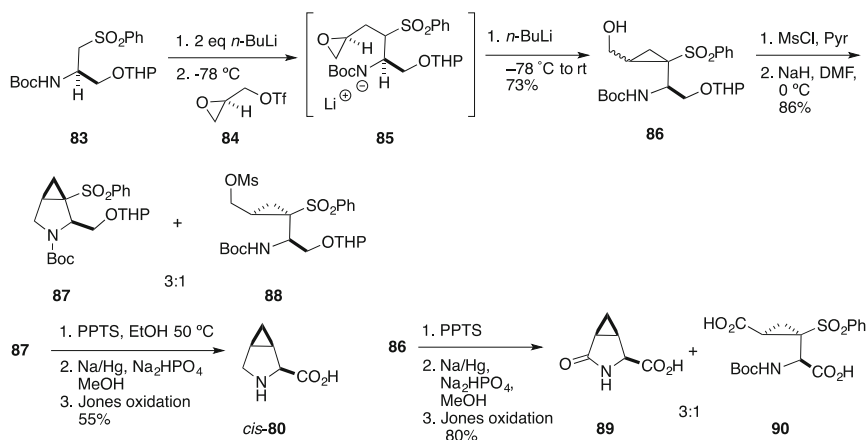
substrate L-proline [65]. As an amide appendage to a pyrrolotriazine, *cis*-3,4-methano-L-prolinol gave moderate pan-Aurora kinase inhibitory activity [66].

4.1 Synthesis

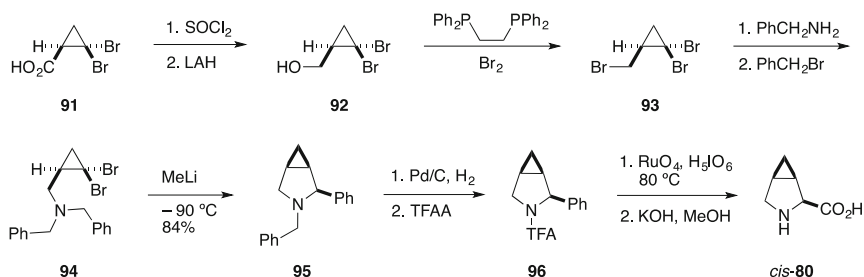
Syntheses and potential biological activities of 3,4-methanoproline and their analogues have been reported in the patent literature (e.g., see [67–71]). The first syntheses of *cis*- and *trans*-3,4-methano-L-proline (*cis*- and *trans*-**80**) were reported by Witkop and coworkers in 1971 [72]. Cyclopropanation of 3,4-dehydro-*N*-trifluoroacetyl-L-proline methyl ester **81** was achieved using the carbene generated from the decomposition of diazomethane in the presence of cuprous chloride to provide a 3.5:1 mixture of *cis*- and *trans*-*N*-trifluoroacetyl-3,4-methano-L-proline (*cis*- and *trans*-**82**) with recovery of unreacted starting material (Scheme 9) [73].

The diastereomers were separated by preparative chromatography and isolated as crystalline solids that were studied by X-ray crystallography, which revealed a boat conformation for the six-membered ring. In the *cis*-diastereomer, the carboxylate group adopted an intermediate position between axial and equatorial orientations. In both cases, the nitrogen atom was situated out of the plane relative to the four carbon atoms of the pyrrolidine ring. The boat conformation of *cis*-3,4-methano-L-proline was determined to be important for inhibition of proline uptake by bacterial proline permease [72].

An enantioselective synthesis of *cis*-3,4-methano-L-proline was achieved via intramolecular displacement of a preformed cyclopropane intermediate [74]. Attack of (*R*)-glycidyl triflate **84** by the lithium anion generated from sulfone **83** led to an intermediate epoxy sulfone **85**, which upon treatment with *n*-BuLi at room temperature afforded the corresponding cyclopropane **86** via a regioselective opening of the epoxide. Mesylation and treatment with NaH led to the 3,4-methanopyrrolidine intermediate **87** which was further elaborated to give *cis*-**80** in 26% overall yield.



Scheme 10 Enantioselective synthesis of *cis*-**80** and the pyroglutamic acid derivative **89**

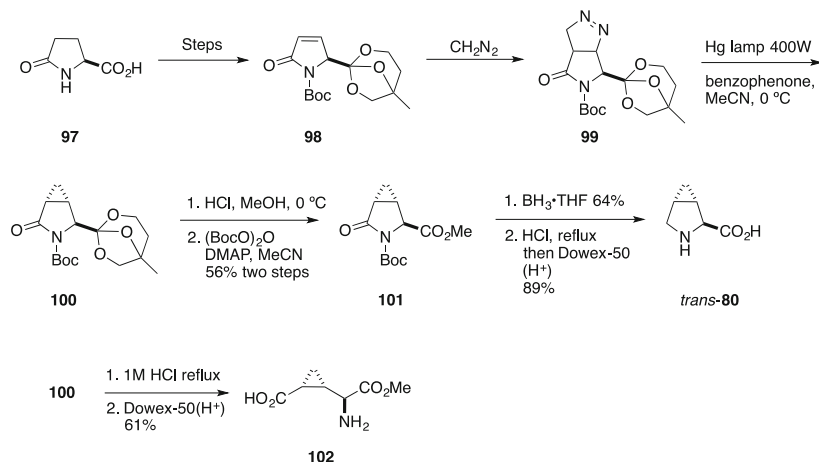


Scheme 11 Enantioselective synthesis of *cis*-**80** from 2,2-dibromocyclopropane carboxylic acid

Applying a similar sequence to cyclopropane **86** gave the corresponding pyroglutamic acid analogue **89** as the major product (Scheme 10).

Effective synthesis of enantiomeric 3,4-methanoglutamic acids has provided tools for studying their activities as NMDA agonist and antagonists [75].

3,4-Methanoproline and its C-4 methyl-substituted analogues were, respectively, prepared from 2,2-dibromocyclopropane carboxylic acid and its 1-methyl analogue, both of which were resolved using dehydroabietylamine [76]. Reduction of acid **91** by way of its acid chloride to alcohol **92** and hydroxyl group activation with the reagent from treating 1,2-bis(diphenylphosphino)ethane with bromine gave tribromide **93** (Scheme 11). Sequential treatment with benzylamine, followed by benzyl bromide, led to tertiary dibenzylamine **94**, which was treated with methyl lithium at $-90\text{ }^\circ\text{C}$. The resulting cyclopropylidene carbenoid intermediate is inserted into the benzylic bond of **94** to give the 2-phenylpyrrolidine **95** as the major product (93% ee). Catalytic hydrogenation removed the *N*-benzyl group, and the secondary amine was *N*-trifluoroacetylated to give *N*-trifluoroacetyl-phenylpyrrolidine **96**, which was oxidized to *cis*-3,4-methano-*L*-proline *cis*-**80** in the presence of catalytic RuO_4 in 40% overall yield. The stereoselectivity of the carbenoid



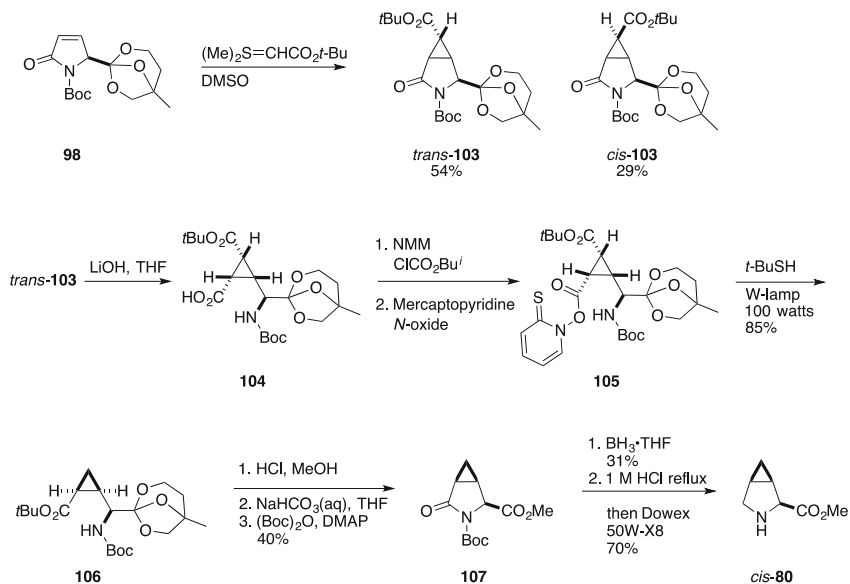
Scheme 12 Diazomethane-mediated cyclopropanation of *N*-Boc-3,4-dehydro-L-pyrroglutamic acid ABO ester **98**

insertion reaction of **94** varied contingent on the choice of amine and C-3 substituents [76].

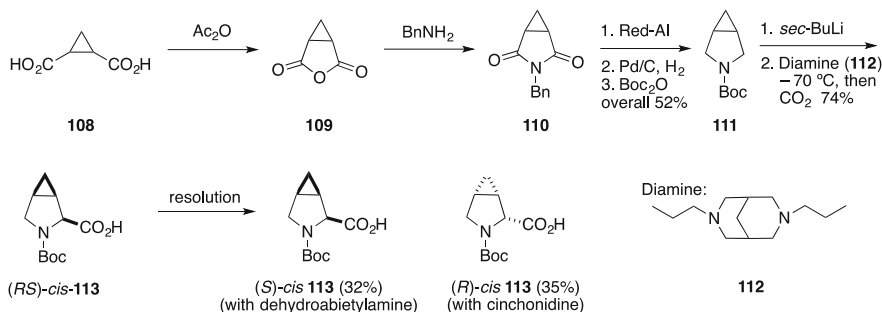
3,4-Methano-L-proline was synthesized from L-pyrroglutamic acid **97**, which was transformed in a few steps into the *N*-Boc-3,4-dehydro-L-pyrroglutamic acid ABO (5-methyl-2,7,8-trioxabicyclo[3.2.1]octyl) ester **98** (Scheme 12) [77]. Treatment of **98** with diazomethane led to Δ^2 -pyrazoline **99**, which upon photolysis afforded the cyclopropane **100**. Cleavage of the ABO ester **100** followed by reduction of the lactam and deprotection gave 3,4-methano-L-proline (*trans*-**80**). Alternatively, acid hydrolysis of **100** followed by purification on a Dowex-50 (H^+) column gave (2*S*,1'*S*,2'*R*)-carboxycyclopropylglycine (L-CCG) **102**.

The common intermediate **98** was used to synthesize different diastereomers of 3,4-methanoglutamic acids, as well as *cis*-3,4-methano-L-proline (Scheme 13). Treatment of lactam **98** with the *S*-ylide derived from *tert*-butylmethylthio acetate led to the *trans*- and *cis*-cyclopropane adducts **103** in 54% and 29% yields, respectively. Ring opening of lactam *trans*-**103** with LiOH and Barton decarboxylation [78, 79] afforded the *cis*-*N*-Boc diester **106** which upon cyclization, lactam reduction, and deprotection afforded *cis*-3,4-methano-L-proline (*cis*-**80**).

All four stereoisomers of *N*-Boc-3,4-methanoproline **113** were prepared by lithiation of azabicyclo[3.2.0]hexane **111**, quenching with CO_2 , and separation of diastereomers by resolution with chiral amines, or by preparative chromatography on a chiral stationary phase [80]. A mixture of *cis*- and *trans*-cyclopropane 1,2-dicarboxylic acid (*cis*- and *trans*-**108**) was converted via the anhydride **109** into *N*-benzyl succinimide **110**, which was reduced to *N*-Boc-3,4-methanopyrrolidine **111** in five steps and 52% overall yield, by following a known procedure



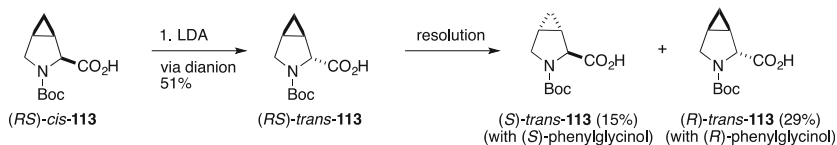
Scheme 13 S-Ylide-mediated cyclopropanation of *N*-Boc-3,4-dehydro-L-pyrroglutamic acid ABO ester **98**



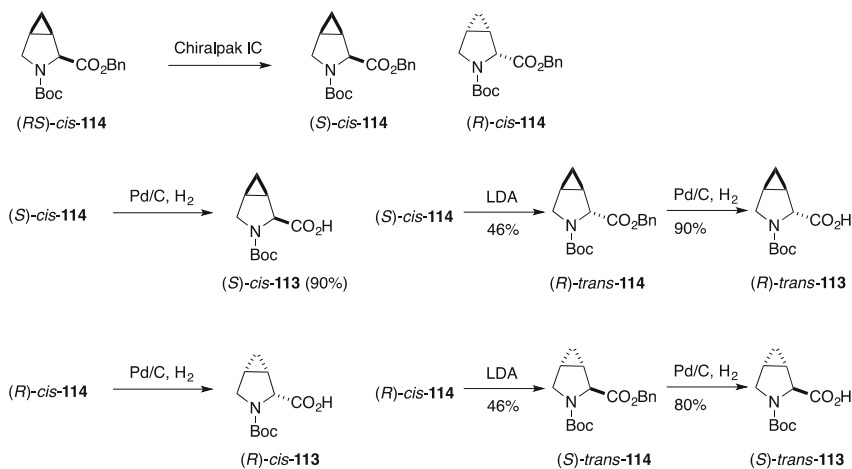
Scheme 14 Synthesis of all four stereoisomers of **113**

(Scheme 14) [81, 82]. Treatment of **111** with *sec*-butyl lithium in the presence of 3,7-dipropyl-3,7-diazabicyclo[3.3.1]nonane (**112**) at -78°C , followed by addition of CO_2 , gave racemic *cis*-3,4-methano-*N*-Boc proline (*RS*-*cis*-**113**) in 74% yield. Other tertiary amines, including sparteine [83] and other chiral bases [84–86], were less stereoselective. Resolution with dehydroabietylamine and cinchonidine gave, respectively, (*S*)- and (*R*)-*cis*-*N*-Boc-3,4-methanoproline **113**, in 32% and 35% yield.

Treatment of racemic *cis*-**113** with LDA led to the corresponding dianion, which upon workup gave racemic *trans*-*N*-Boc-3,4-methanoproline (*RS*)-*trans*-**113**) in



Scheme 15 Conversion of (*S*)- and (*R*)-*cis* **113** via enolate to (*S*)- and (*R*)-*trans* **114**



Scheme 16 Resolution of (*RS*)-*cis*-**114** and epimerization to *trans*-**114** suitable for flow chemistry

51% yield (Scheme 15). Resolution of (*RS*)-*trans*-**113** with (*S*)- and (*R*)-phenylglycinol gave, respectively, (*S*)- and (*R*)-*trans*-*N*-Boc-*L*-3,4-methanoproline [(*S*)- and (*R*)-*trans*-**113**] in 15% and 29% yields.

All four *N*-Boc-3,4-methanoproline diastereomers were isolated by chiral stationary phase column chromatography using conditions previously developed to separate *N*-Boc-proline benzyl esters [80]. Racemic *cis*-*N*-Boc-3,4-methanoproline benzyl ester *cis*-**114** gave the (*S*)- and (*R*)-*cis*-*N*-Boc-3,4-methanoproline enantiomers [(*S*)- and (*R*)-*cis*-**114**] (Scheme 16). Hydrogenation afforded the corresponding *N*-Boc-methanoproline (*S*)- and (*R*)-*cis*-**113**. Epimerization of the respective benzyl ester *cis*-**114** with LDA via the corresponding enolate gave the corresponding *trans*-ester **114**, which were, respectively, hydrogenated to afford (*S*)- and (*R*)-*trans*-**113**. Adapting the method to a flow chemistry reactor with further refinements for large-scale synthesis produced multigram quantities of enantiopure *N*-Boc-3,4-methanoproline diastereomers.

4.2 Conformational Studies

Analysis of the conformation of 3,4-methanoproline by $^1\text{H-NMR}$ spectroscopy in D_2O revealed a strong similarity to *trans*-thujane and bicyclo[3.1.0]hexan-3-ol

[87]. The most favorable conformation was concluded to correspond to a flattened boat form.

4.3 3,4-Methanoproline Analogues

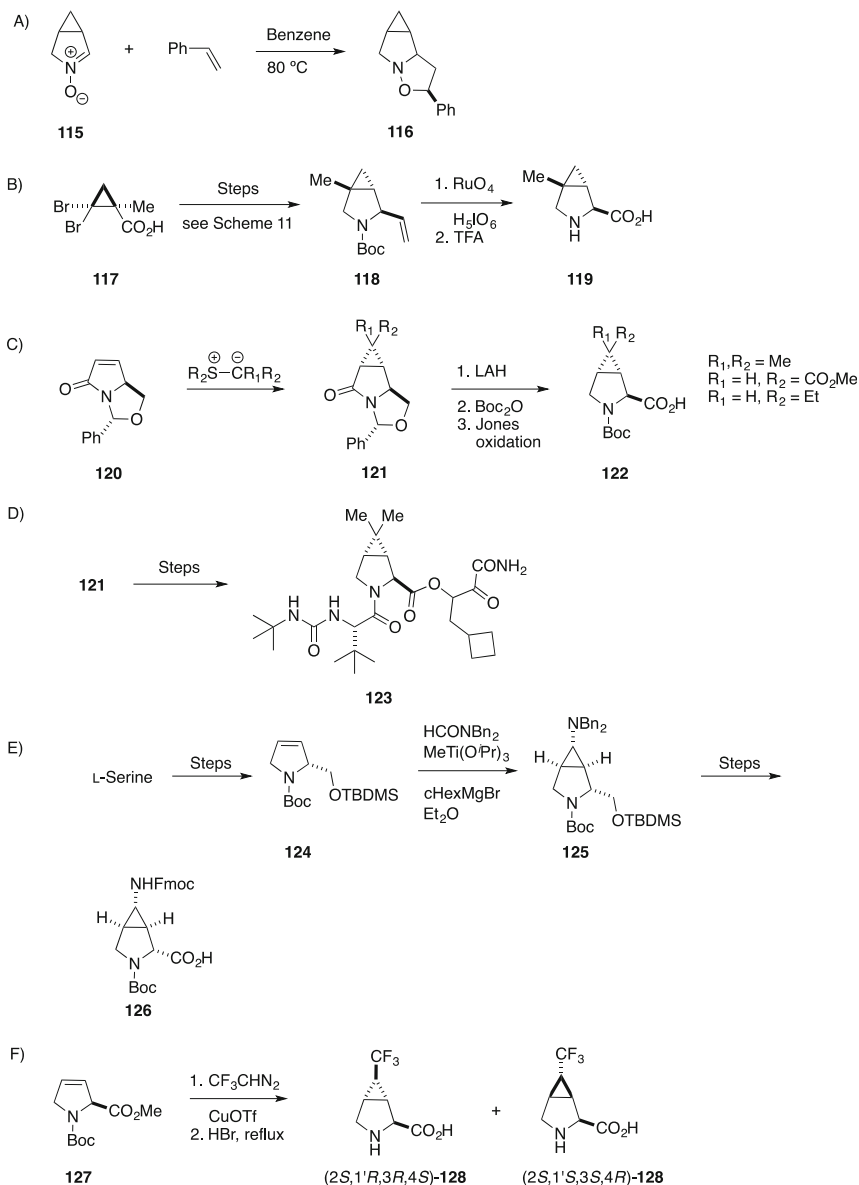
Cycloaddition reactions between azabicyclic nitrone **115** and various olefins have given the corresponding dihydroisoxazoles **116** (Scheme 17a) [81]. 4-Methyl-3,4-methano-L-proline **119** was prepared starting from (*S*)-2,2-dibromo-1-methyl cyclopropane carboxylic acid **117** by a route featuring oxidative cleavage of vinyl *N*-Boc-pyrrolidine **118** (Scheme 17b) [76].

Apically substituted *N*-Boc-3,4-methano-L-prolines have been synthesized starting from L-pyroglutamic acid by routes featuring nucleophilic alkylidene transfer using various *S*-ylides to provide 3,4-methano analogues bearing one and two substituents on the apical carbon of the cyclopropane unit (Scheme 17c) [88]. Cyclopropanations with sulfur ylides on the readily available *N,O*-acetal **120** afforded stereoselectively the corresponding *anti*-adducts **121**, which were converted to *anti*-3,4- *N*-Boc-L-methanoproline analogues **122** that have been studied as constrained *N*-acetyl proline benzyl ester analogues by ¹H-NMR spectroscopy as well as in tripeptides [89]. In CDCl₃ and D₂O, NMR spectroscopic studies of di- and tripeptide models containing proline analogues with the embedded 3-azabicyclo[3.1.0]hexane system found they adopted a flattened boat conformation with backbone and side chain dihedral angles consistent with a poly-L-proline type II conformation: $\phi \sim -70^\circ$, $\psi \sim 131^\circ$, $\chi^1 \sim -57^\circ$, and $\chi^2 \sim -158^\circ$ [90].

gem-Dimethyl-3,4-methano-L-proline was incorporated in peptidomimetics in pursuit of NS3 protease inhibitors [91]. For example, the X-ray structure of methanoproline analogue **123** was solved and illustrated the major interactions between the inhibitor and the enzyme. Moreover, mimic **123** was advanced to phase 1 clinical trials for the treatment of hepatitis C viral disease (Scheme 17d) [91].

3,4-(Aminomethano)-L-proline **126** was synthesized from L-serine by a route featuring diastereoselective titanium-mediated aminocyclopropanation [92, 93] of Δ -3 pyrroline silyl ether **124** (Scheme 17e) [94]. Protecting group shuffling and alcohol oxidation provided *N*^γ-Fmoc-*N*^α-Boc-aminomethanoproline **126**, which was shown to be compatible with solid-phase peptide synthesis.

With the intent to prepare fluorine-labeled prolines for incorporation as NMR probes in proline-rich cell-penetrating peptides, *cis*- and *trans*-3,4-methano-L-prolines **128** were synthesized containing *syn*- and *anti*-trifluoromethyl groups at the apical position of the cyclopropane ring (Scheme 17e) [95]. 3,4-Dehydro-*N*-Boc-L-proline methyl ester **127** was reacted with trifluoromethyl diazomethane in the presence of copper (I) trifluoromethanesulfonate to provide in 15% yield a mixture of *N*-trifluoroethoxycarbonyl trifluoromethyl cyclopropane diastereomers, which were separated by chromatography and deprotected by acid hydrolysis to afford *cis*- and *trans*-methanoprolines **128**.



Scheme 17 Selected examples of 3,4-methano-L-proline analogues

5 3,5-Methanoprolines

As previously discussed, the preferred conformations of proline are important for the functions of proline-containing peptides and proteins [96, 97]. This is particularly relevant in collagen which is the most abundant structural protein found in the extracellular matrix in animals [98]. The repeating collagen-strand sequence consists of three amino acids in which glycine, proline, and 4-hydroxyproline are

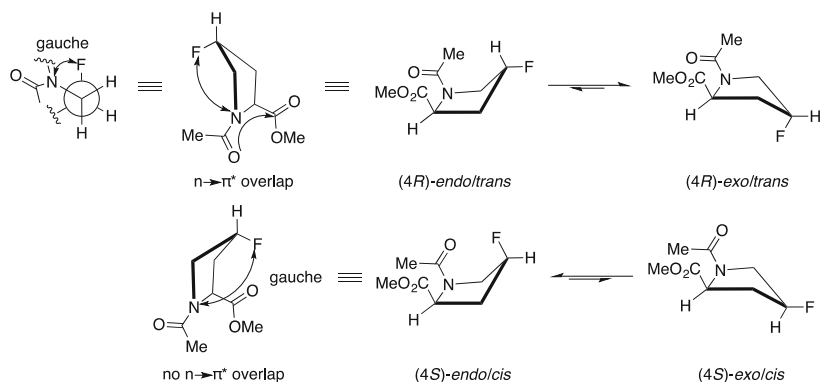


Fig. 6 Conformations of 4-fluoro-*N*-acetyl-*L*-proline methyl ester showing *cis*- and *trans*-amide conformers as well as *endo*- and *exo*-ring puckers

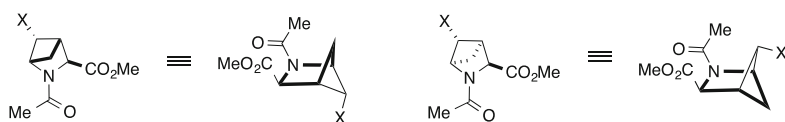


Fig. 7 *N*-Acetyl-3,5-methano-*L*-proline methyl ester (X = H, OH, F) showing *endo*- and *exo*-ring puckers. **Bold lines** indicate a methano bridge between C3 and C5

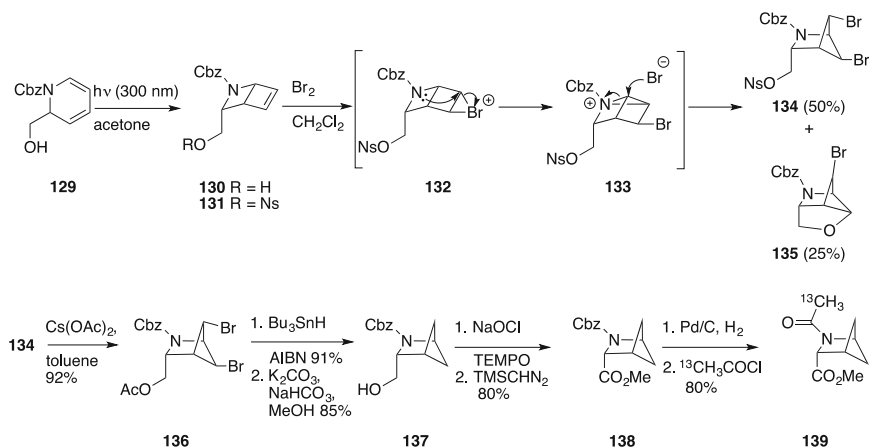
featured. Studies by Raines and coworkers [99–101] and Moroder and coworkers [102] have shown that the nature of the substituent at the 4-position of proline can change its *N*-terminal amide *cis*-/*trans*-conformation ratio. Furthermore, the *endo*- and *exo*-pucker of the pyrrolidine ring are influenced by the 4-position substituent. For example, (4*R*)-fluoro-*N*-acetyl-*L*-proline methyl ester exists predominantly as the 4-*exo trans*-conformer ($K_{T/C} = 6.7$; 86% *exo* conformation), whereas (4*S*)-fluoro-*N*-acetyl-*L*-proline methyl ester has a predominant 4-*endo trans*-conformer ($K_{T/C} = 2.5$; 95% *endo* conformation) (Fig. 6) [103]. These preferences have been in part attributed to the F→N gauche effect [104–106] and $n \rightarrow \pi^*$ overlap between the amide carbonyl as a donor and the ester carbonyl as an acceptor, as shown in the idealized conformation for (4*R*)-fluoro-*N*-acetyl-*L*-proline methyl ester (Fig. 6) [106–108].

Mimics of collagen in which the hydroxyproline residues were replaced with 4-fluoroproline have exhibited extraordinary stability [106–108].

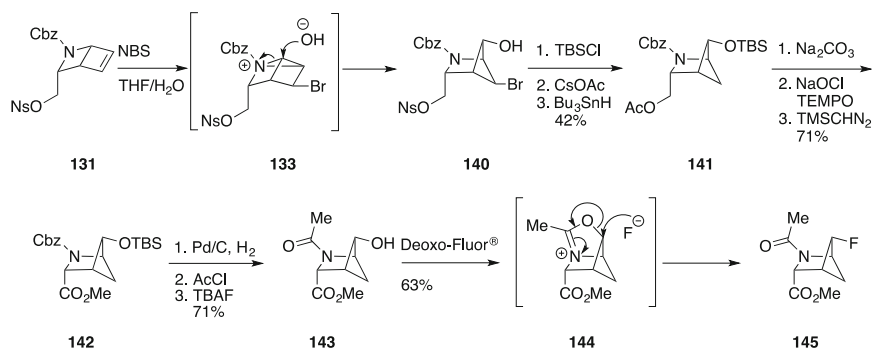
In order to better understand the relationships among ring puckers, inductive and stereoelectronic effects, and peptide backbone conformation, *N*-acetyl-3,5-methanoproline methyl ester and the corresponding 5-hydroxy and 5-fluoro analogues were synthesized and studied by NMR spectroscopy and X-ray crystallography (Fig. 7) [103].

5.1 Synthesis

Racemic *N*-acetyl-4-hydroxy-3,5-methanoproline methyl ester was synthesized by a route featuring the formation of 3-*endo*-hydroxymethyl-2-azabicyclo[2.2.0]hex-



Scheme 18 Synthesis of *N*-¹³C-acetyl-3,5-methanoproline methyl ester (**139**)

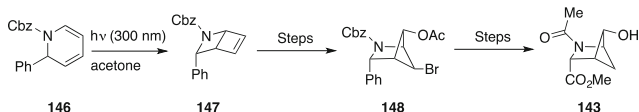


Scheme 19 Synthesis *N*-acetyl-3,5-methanoproline methyl ester analogues **143** and **145** from bicyclic **131**

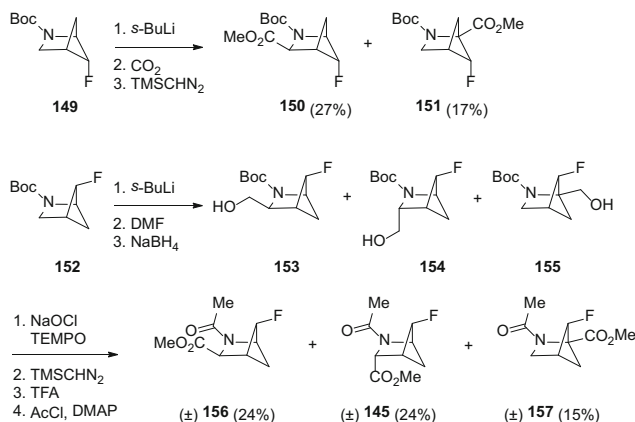
5-ene **130** by UV irradiation of *N*-Cbz-2-hydroxymethyl dihydropyridine (**129**) [103], which was readily available from pyridine (Scheme 18) [109]. Alcohol **130** was protected to give 2-nitrophenylsulfonate (nosylate) ester **131**. Bromination of olefin **131** gave dibromide **134** in 50% yield via intramolecular opening of bromonium ion **132** to form aziridinium ion **133**, which was in turn opened by bromide ion. Dibromide **134** (50%) was accompanied by tricyclic by-product **135** in 25% yield. Displacement of nosylate ester **134** by acetate gave **136**, which was subjected to free-radical debromination and saponification to yield alcohol **137**.

Oxidation to the carboxylic acid, esterification, hydrogenolysis of the Cbz group, and *N*-acetylation gave racemic *N*-acetyl-3,5-methanoproline methyl ester **139**. Use of ¹³C-acetyl chloride in the synthesis provided labeled **139** to facilitate the study of the conformational equilibrium and *cis*-*trans* amide isomerization.

The corresponding racemic *N*-acetyl-4-hydroxy and 4-fluoro-3,5-methanoproline methyl esters were also synthesized from bicyclic **131** as a common precursor (Scheme 19) [103]. Exposure of **131** to NBS in aqueous THF led to



Scheme 20 Synthesis of **143** from bicyclic **147**



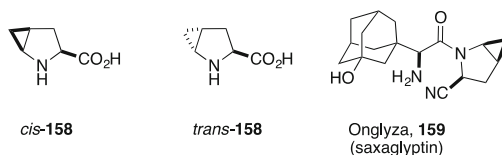
Scheme 21 Synthesis of *N*-(±)-acetyl-4-fluoro-3,5-methanoproline methyl esters (**145**, **156**, **157**)

aziridinium intermediate **133**, which was attacked by water to give the corresponding bromo alcohol **140**. Protection of the hydroxyl group as the TBS ester, displacement of the nosylate with cesium acetate, and free-radical-mediated reductive debromination afforded ester **141**. Cleavage of the ester and oxidation led to acid **142**, which was converted to racemic *N*-acetyl-4-hydroxy-3,5-methanoproline methyl ester **143**. Displacement of the “anti” oriented hydroxyl group with Deoxo-Fluor®, with participation of the *N*-acetyl group via oxazolinium ion intermediate **144**, gave racemic *anti-N*-acetyl-4-fluoro-3,5-methanoproline methyl ester **145**.

Adopting the same methods, but starting with 2-phenyl-1,2-dihydropyridine **146** and irradiation at 300 nm, gave the 2-phenyl-3-*endo*-phenyl-2-azabicyclo[2.2.0]hex-5-ene **147** (Scheme 20). Further steps afforded 2-phenyl-3,5-methanopyrrolidine intermediate **148**, which was converted to hydroxymethanoproline **143** in a relatively shorter synthesis compared to the previous route described above [110].

Expedient routes to stereoisomeric mixtures of racemic *N*-acetyl-4-hydroxy- and 4-fluoro-3,5-methanoproline methyl esters were developed by directed metalation of the racemic fluoro-pyrrolidines **149** and **152** (Scheme 21) [104]. Although inseparable, methyl esters **150** and **151** were obtained from carboxylation of lithiated **149** and quenching of lithiated **152** with DMF, and reduction of the resulting aldehyde with NaBH₄ afforded a mixture of the three separable diastereomers **153**–**155**. Chromatographic separation and further steps led to the corresponding racemic *N*-acetyl-4-fluoro-3,5-methanoproline methyl esters **145**,

Fig. 8 Structures of synthetic *cis*- and *trans*-4,5-methano-L-prolines and the antidiabetic drug Onglyza (saxagliptin)

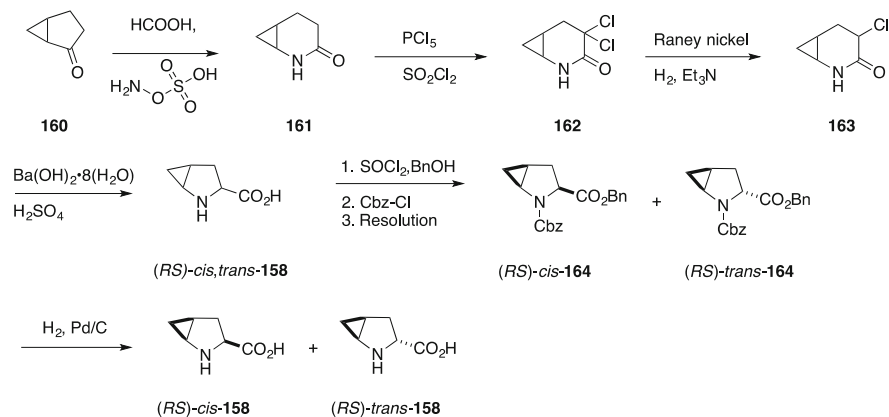


156, and **157**. In this series, the 2-azabicyclo[2.2.1]hexane ring system exemplified the *syn*- (*gauche*) and *anti*-orientations of the fluoro (and hydroxyl) substituents in fixed constrained proline conformations. Minimal $n \rightarrow \pi^*$ orbital interactions involving the amide carbonyl oxygen and the ester carbonyl for the *trans*-amide conformation were observed in NMR spectroscopic studies and calculations of the geometries of the methanoprolines [104], suggesting other forces, such as the nature of the solvent, to be of greater importance in determining their amide *cis*–*trans* isomer equilibrium. The synthesis of methanoproline amides as inhibitors of the complement alternative pathway has been described in a patent [111].

6 4,5-Methanoprolines

As a program directed at the synthesis of constrained analogues of proline [112–119], Hanessian and coworkers reported the first synthesis of enantiopure 4,5-*cis*- and 4,5-*trans*-methano-L-prolines *cis*- and *trans*-**158** [120]. This particular proline congener has since gained considerable relevance, ultimately being incorporated as a *cis*-methano-L-prolylnitrile in the marketed antidiabetic drug Onglyza (saxagliptin) **159** for the treatment of type II diabetes (Fig. 8) [121–123].

The incretins are glucagon-like peptides, such as GLP-1 and glucose-dependent insulinotropic peptide (GIP) [124]. They play a major role in maintaining a balanced glycemic control in the bloodstream. Dipeptidyl peptidase 4 (DPP-4) is a sequence-specific serine protease that is bound to cell surface membranes and expressed in many tissues [125]. Both GLP-1 and GIP are rapidly degraded by DPP-4, which may lead to an imbalance in the management of glucose levels in the bloodstream leading to hyperglycemia [126]. Inhibition of the proteolytic action of DPP-4 has been targeted to increase the levels of incretins leading to insulin secretion in order to improve blood glucose balance. Over the last decade, inhibitors of DPP-4 have emerged as a new class of orally active drugs exemplified by Onglyza (saxagliptin) [123] for the management of type II diabetes [127]. A co-crystal structure of saxagliptin with DPP-4 shows, among other interactions, a covalent imidate adduct formed from the nitrile group of the inhibitor and the alcohol of serine 360 of the catalytic His–Ser–Asp triad [125]. In addition to excellent *in vitro* potency and *in vivo* efficacy, saxagliptin presented good oral activity and extended half-life in pH 7.4 buffer compared to analogues without the methano appendage. This was attributed to a change in conformation, thereby retarding the intramolecular attack of the amino group on the nitrile. Congeners



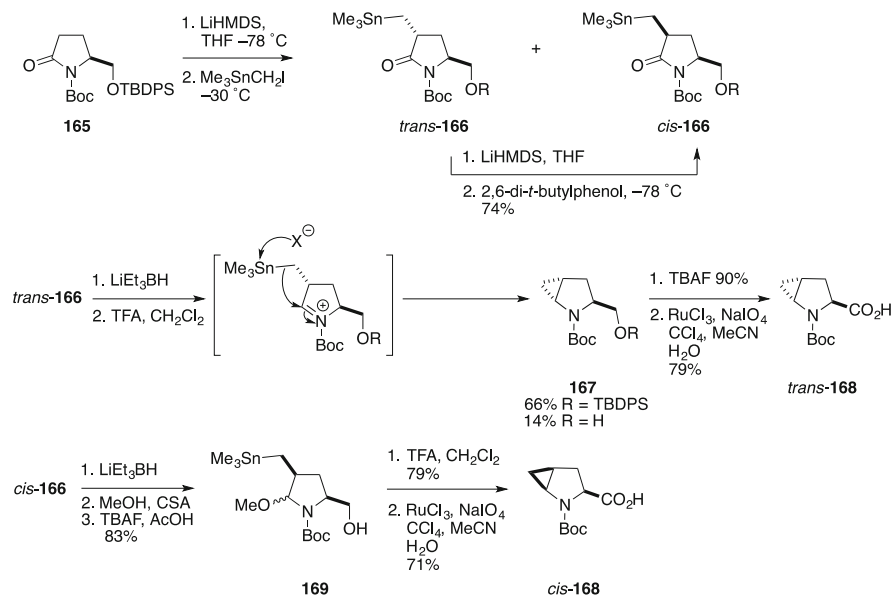
Scheme 22 Synthesis of (±)-*cis*- and *trans*-4,5-methanoproline **158**

that incorporated *trans*-4,5- and *cis*-3,4-pyrrolidine nitriles exhibited shorter half-lives compared to the *cis*-4,5-methano counterpart exemplified by saxagliptin [128]. The deshydroxy variant of saxagliptin was highly active in vitro and in vivo, but suffered from low bioavailability; however, in vivo hydroxylation produced the metabolite (saxagliptin), which became the marketed drug due to its excellent profile.

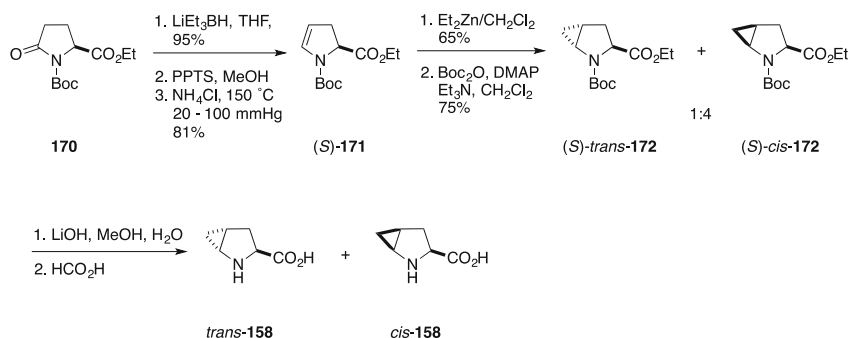
6.1 Synthesis

The synthesis of a mixture of racemic 4,5-methanoproline diastereomers was first disclosed in a patent (Scheme 22) [129, 130].

Stereocontrolled syntheses of *cis*- and *trans*-4,5-methano-*N*-Boc-*L*-proline were reported by Hanessian and coworkers by using a novel intramolecular cyclopropanation reaction (Scheme 23) [120]. Lactam **165** was prepared from commercially available *L*-pyroglutamic acid [131–141]. Conversion of **165** to the corresponding lithium enolate, followed by treatment with trimethylstannyl methyl iodide at low temperature, gave a 3:1 mixture of *trans*- and *cis*-diastereomers **166** in 86% combined yield. Formation of the enolate from *trans*-**166** and quenching with 2,6-di-*t*-butylphenol at -78°C gave the *cis*-**166** in 74% yield. Reduction of lactam *trans*-**166** with lithium triethylborohydride to the corresponding hemiaminal, followed by treatment with TFA in dichloromethane, generated the iminium ion, which was attacked intramolecularly by a synchronously formed “methylene nucleophile” from the trimethylstannyl group (or via the hypervalent trimethylstannyl trifluoroacetate) to give the *trans*-*N*-Boc-4,5-methano-*L*-prolinol **167** in 64% yield, accompanied by 14% of desilylated by-product, which could be reprotected. Silyl ether cleavage and alcohol oxidation gave crystalline *trans*-*N*-Boc-4,5-methano-*L*-proline (*trans*-**168**). In the case of *cis*-**166**, 5-methoxy prolinol



Scheme 23 Intramolecular-mediated cyclopropanation to obtain enantiomerically pure *cis*- and *trans*-4,5-methano-L-prolines **168**

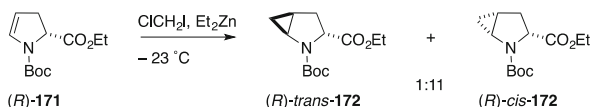


Scheme 24 Simmons-Smith cyclopropanation of **(S)-171**

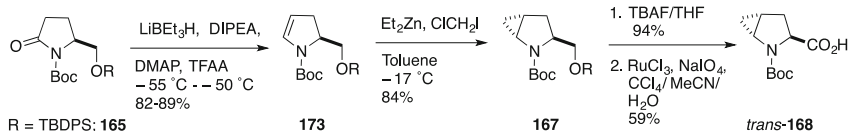
169 was first prepared and subjected to the iminium ion cyclization to afford crystalline *cis*-*N*-Boc-4,5-methano-L-proline (*cis*-**168**). Similar methods proved successful in the synthesis of *cis*- and *trans*-5,6-methano-L-pipecolic acids [120].

A more expedient synthesis of *cis*- and *trans*-4,5-methano-L-prolines was reported by the Hanessian group featuring Simmons–Smith cyclopropanation [142] of enamine **202** (Scheme 24) [143].

Ethyl *N*-Boc-L-pyrroglutamate (**170**) was reduced to the corresponding hemiaminal, transformed to ethyl *N*-Boc-5-methoxy prolinolate, and eliminated with ammonium chloride and heating [144] to give the encarbamate **(S)-171**. Simmons–Smith cyclopropanation of **(S)-171** gave a 1:4 ratio of *trans*- and *cis*-*N*-



Scheme 25 Low temperature Simmons-Smith cyclopropanation of (*R*)-**171**



Scheme 26 Synthesis of *trans*-**168** by steric control-mediated cyclopropanation

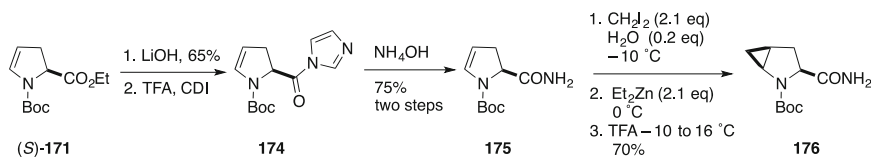
Boc-4,5-methano-L-prolinates (*S*)-*trans*- and (*S*)-*cis*-**172**, which could be efficiently separated by column chromatography. Sequential cleavage of the ester and *N*-Boc groups led, respectively, to *trans*- and *cis*-4,5-methano-L-proline (*trans*- and *cis*-**158**) as crystalline solids. The preponderance of *cis*-diastereomer (*S*)-*cis*-**172** from the cyclopropanation reaction was attributed to coordination of the zinc species by the ester group prior to delivery of the methylene onto the carboxylate face of enecarbamate (*S*)-**171** [145]. Enecarbamate (*S*)-**171** has been prepared more efficiently by reduction of **170** using lithium triethylborohydride at -78°C , acylation with trifluoroacetic anhydride and 2,6-lutidine (or diisopropylethylamine), and elimination on warming to reach room temperature [146].

Ethyl *cis*-*N*-Boc-4,5-methano-L-prolinate ((*S*)-*cis*-**172**) was prepared by diastereoselective cyclopropanation of ethyl *N*-Boc-4,5-dehydro-D-pyrroglutamate ((*R*)-**171**) (Scheme 25) [147] and epimerized to ethyl *trans*-*N*-Boc-4,5-methano-L-prolinate ((*S*)-*trans*-**172**), as previously reported [143].

In the cyclopropanation of ester (*R*)-**171**, chloriodomethane was used instead of diiodomethane [143] at lower temperature (-23°C) with enhanced diastereoselectivity: 11:1 instead of 4:1 *cis*- to *trans*-isomer ratio, respectively. After chromatographic separation, (*R*)-*cis*- and (*R*)-*trans*-**172** were isolated in 84% and 8% yields, respectively. Epimerization of (*R*)-*cis*-**172** using various bases had limited success, because the (*R*)-*cis*-isomer **172** predominated. For example, treatment of (*R*)-*cis*-**172** with *tert*-BuOK in *tert*-BuOH/THF at room temperature led to an equilibrium containing 48% (*R*)-*cis*- and 31% (*S*)-*trans*-**172**, respectively.

Lactam **165** [120] was converted to enecarbamate **173** by dehydration of a hemiacetal trifluoroacetate intermediate and reacted diastereoselectively from the less sterically hindered face in the cyclopropanation to provide *trans*-**167**, which was deprotected and oxidized to *trans*-*N*-Boc-4,5-methano-L-proline (*trans*-**168**) (Scheme 26).

Extensive studies of the Simmons–Smith cyclopropanation reaction were made in an effort to optimize the synthesis of the *cis*-4,5-methano-L-pyrrolidine-2-nitrile



Scheme 27 Synthesis of *cis*-4,5-methano-L-prolylamide

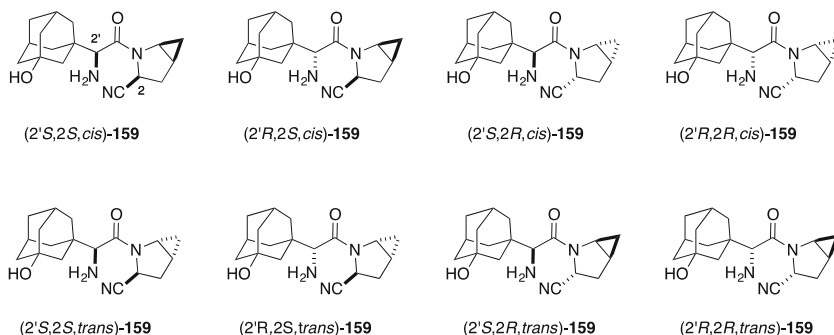
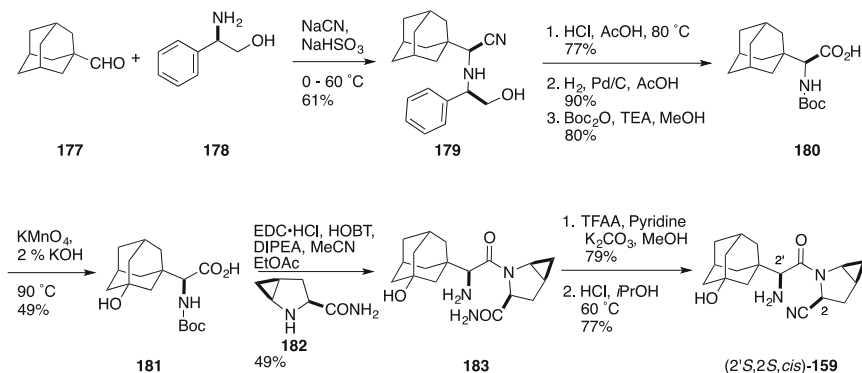


Fig. 9 Structures of all eight stereoisomers of Onglyza (saxagliptin)

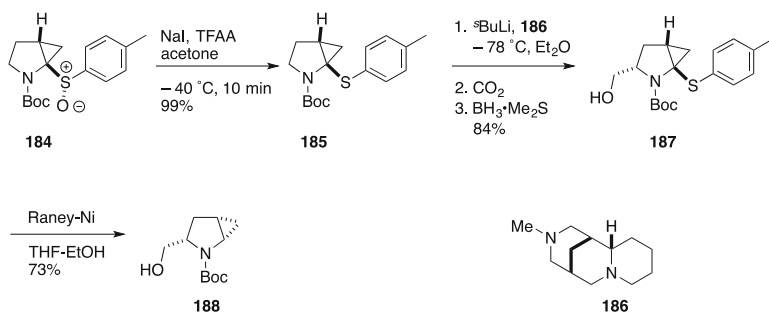
needed for saxagliptin [148]. The strong coordinating power of the carboxamide group was found to favor intramolecular delivery in the cyclopropanation of 4,5-dehydro-*N*-Boc-L-prolylamide (**175**) to provide diastereoselectively *cis*-4,5-methano-L-prolylamide **176** (Scheme 27).

To avoid racemization during the transformation of ethyl ester (*S*)-**171** into amide **175**, a biocatalytic process using a 220 g/L ester feed was developed employing *Candida antarctica* lipase B and ammonium carbamate as ammonia donor, which provided enantiomerically pure (>99.9% ee) amide **175** in 98% yield [149].

All eight stereoisomers of saxagliptin were synthesized and evaluated for inhibitory activity [150] (Fig. 9). The respective couplings of (*R*)- and (*S*)-*N*-Boc-3-hydroxyadamantylglycine (**181**) to *cis*- and *trans*-*N*-Boc-4,5-methanopropyl amides were performed using a patented process [151]. The (*R*)- and (*S*)-adamantylglycine enantiomers **180** were, respectively, prepared by a diastereoselective Strecker reaction sequence employing adamantyl aldehyde (**177**) and (*S*)- and (*R*)-phenylglycinol (**178**) to provide α -aminonitrile **179**, which was hydrolyzed, hydrogenated to remove the auxiliary, and converted to the *N*-Boc derivative **180**



Scheme 28 Synthesis of saxagliptin



Scheme 29 Synthesis of *N*-Boc-*cis*-4,5-methano-L-prolinol (**188**) from sulfoxide **184**

(Scheme 28). Oxidative hydroxylation led to 3-hydroxyadamantyl *N*-Boc-glycine **181**. Amide coupling of (*S*)-**181** with *cis*-4,5-methano-L-prolylamide **182**, dehydration to the nitrile, and deprotection gave saxagliptin (2'*S*,2*S,cis*)-**159**, which exhibited significantly greater potency than the other stereoisomers.

N-Boc-*cis*-4,5-Methano-L-prolinol (**188**) has been synthesized by a route featuring a diastereoselective lithiation of *N*-Boc-2,3-methanopyrrolidine sulfoxide **185** and trapping with carbon dioxide (Scheme 29) [152].

6.2 Conformational Studies

The crystal structure of L-proline shows an *endo*-pucker with a χ angle of 35.5° and a standard deviation from planarity of 0.161 \AA . In contrast, the carbon framework of *cis*-4,5-methano-L-proline (*cis*-**158**) is essentially planar with a root-mean-square

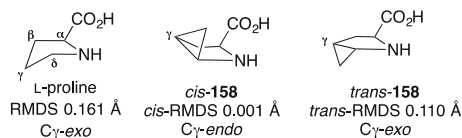


Fig. 10 Ring conformations in L-proline and *cis*- and *trans*-4,5-methano-L-prolines

K_i (nM)	2 ± 0.5	15 ± 1	25 ± 1	29 ± 1	12 ± 1
Stability $t_{1/2}$ (h)	5	4	22	28	2

Fig. 11 In vitro inhibition and solution stability of representative DPP-4 inhibitors

deviation (RMSD) from planarity value of 0.001 Å. The *trans*-isomer (*trans*-**158**) is relatively much less flattened with an RMSD of 0.110 Å (Fig. 10).

The N-C γ (N-C5) bond is equally shorter in the *cis*- and *trans*-4,5-methano-L-proline compared to L-proline which suggests an increased sp^2 character at C-5.

Considering the structures of L-proline and its 4,5-methano congeners, the cyclopropane methylene of the latter may be argued to simulate the C-4 (δ -position) methylene of proline, especially in the flatter pyrrolidine core. The envelope shape of proline may thus be maintained, with consequential changes of ring pucker and bond angles.

In the development of DPP-4 inhibitors, hindered (hydrophobic) alkylamines reduced intramolecular reaction on the nitrile to form cyclic amidine [153]. Cognizant of the observation that the pyrrolidine ring in 4,5-methano-L-proline can be considerably flattened [120], 4,5-methano-L-prolylnitrile amides were examined as DPP-4 inhibitors to improve solution stability [154]. Using a variety of bulky *N*-terminal amino acids, such as isoleucine, valine, *tert*-leucine, and phenylalanine, the corresponding amides were synthesized with selected *cis*- and *trans*-2,3-, 3,4-, and 4,5-methanoprolylnitriles. *cis*-4,5-Methano-L-prolylnitrile amides exhibited increased stability at pH 7.2 and 39.5°C in comparison with the other congeners and with L-prolylnitrile. Although many congeners exhibited nanomolar inhibition of DPP-4 in vitro (Fig. 11), it was decided to develop further saxagliptin as an effective and relatively stable DPP-4 inhibitor [155].

Computational analysis revealed that the ground state conformation of *tert*-leucyl-*cis*-4,5-methano-L-prolylnitrile corresponded to that observed in the single-crystal X-ray structure of its TFA salt [128]. In the prolyl amide *trans*-isomer, the *N*-terminal amino acid residue (*tert*-leucine) ψ -dihedral angle positioned the amine and carbonyl oxygen in a *syn*-coplanar conformation that was also observed in co-crystal studies of DPP-4 inhibitors in complex with the enzyme [156–160]. In another calculated low-energy minima conformation, the prolyl amide *cis*-isomer

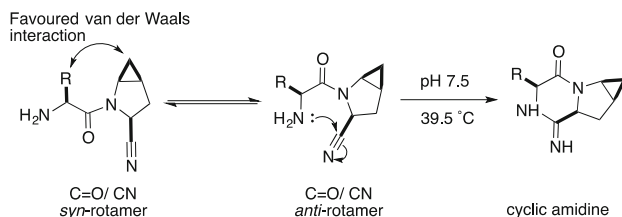


Fig. 12 Prolyl amide *cis*- and *trans*-isomers and cyclic amidine formation

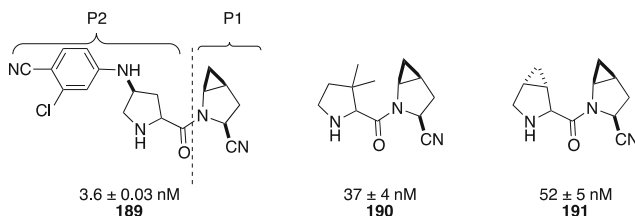


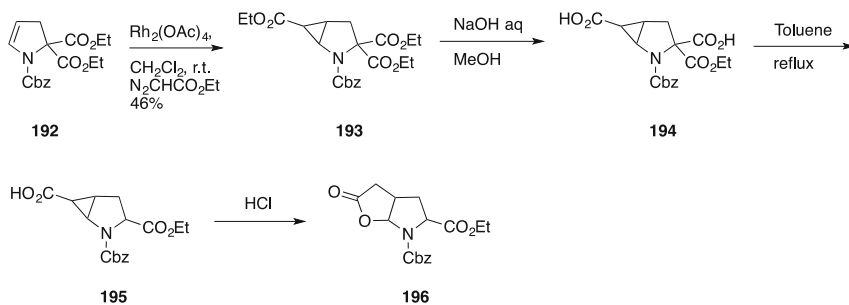
Fig. 13 Examples of L-prolyl-4,5-methano-L-prolylnitriles

oriented the amine and nitrile in close proximity to undergo an intramolecular cyclization, which would result in its conversion to the cyclic amidine and loss of potency (Fig. 12). Further ab initio calculations demonstrated that the energy required to attain the *cis*-conformation could be correlated with the bulk of the side chain of the appended amino acid. In *tert*-leucyl-*cis*-4,5-methano-L-prolylnitrile, the energy barrier to adopt the prolyl amide *cis*-isomer was increased by 0.64 Kcal/mol [128], in part due to a favorable van der Waals interaction between the methano group and the alkyl side chain of the amino acid residue.

Exploring the optimal ring size at the P2-position of inhibitors of DPP-4, a series of *cis*-4,5-methano-L-prolylnitrile amides were prepared and tested [161]. Five-membered rings exemplified by L-prolyl-L-prolylnitrile were well accommodated in the active site leading to promising analogues possessing K_i values ranging from 3.6 to 52 nM (Fig. 13).

6.3 4,5-Methanoproline Analogues

Racemic 4,5-methanoproline analogues have been synthesized by a route involving treatment of diethyl *N*-Cbz-2,3-dihydropyrrole-2,2-dicarboxylate (**192**) [162], with ethyl diazoacetate and catalytic dirhodium (II) tetraacetate to give *N*-Cbz-4,5-methanopyrrolidine **193** [163]. Partial hydrolysis led to the carboxylic acid **194**, which was decarboxylated to furnish racemic *N*-Cbz-4,5-methanoproline ethyl



Scheme 30 Synthesis of **195** and opening of the cyclopropane ring in acidic media to afford lactone **196**

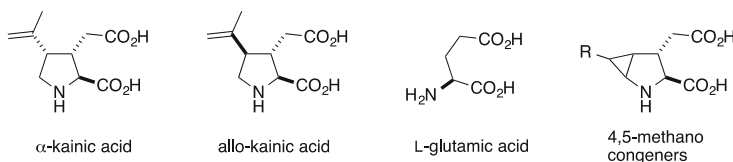
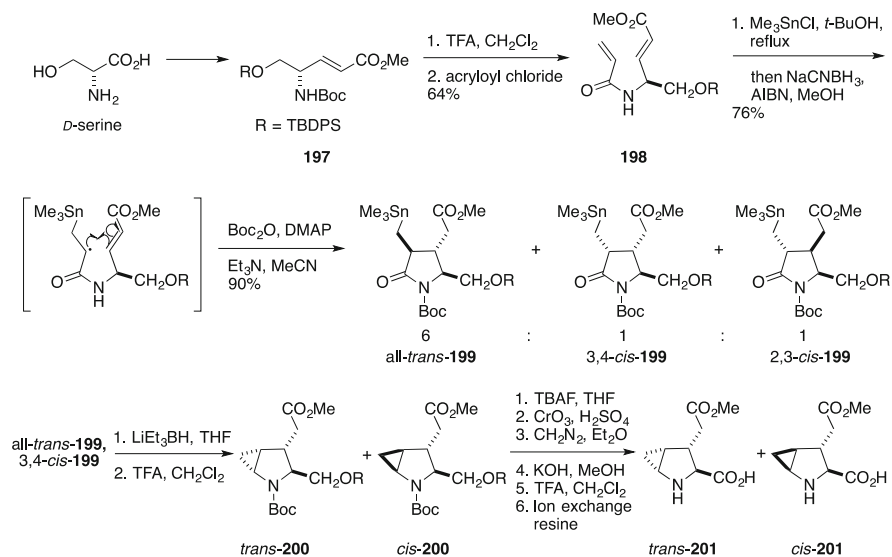


Fig. 14 Naturally occurring kainic acids, glutamate, and a methano congener



Scheme 31 Synthesis of kainic acid 4,5-methanocongeners **201**

ester **195**. However, exposure to aqueous HCl caused ring opening of the cyclopropane to yield bicyclic lactone **196** (Scheme 30).

The excitatory amino acid natural product, kainic acid, acts as a constrained L-glutamic acid analogue on specific subtypes of glutamate receptors (Fig. 14).

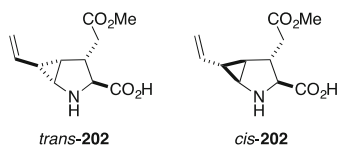


Fig. 15 4,5-Methano kainic acid analogues

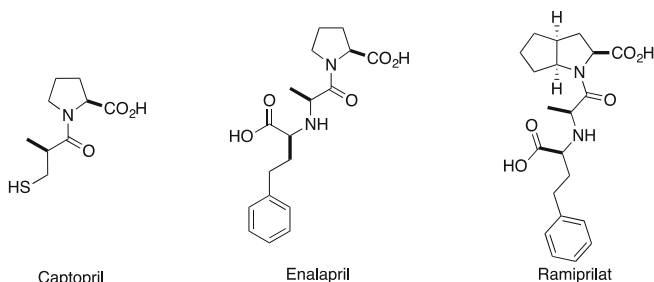


Fig. 16 Examples of marketed ACE inhibitors

Exploring the structural requirements for effective binding to the glutamate receptors, Hanessian and coworkers prepared congeners of α -kainic and *allo*-kainic acids (Scheme 31) [164]. D-Serine was converted in two steps to unsaturated ester **197**, which was acylated to acrylamide **198**. Free-radical carbocyclization followed by conversion to the *N*-Boc derivatives gave mainly (6:1:1) the all-*trans*-stannylmethyl pyrrolidine **199** with the 2,3- and 3,4-*cis*-diastereomers. Sequential treatment of all-*trans*- and 3,4-*cis*-**199** with lithium triethylborohydride, followed by TFA, led respectively to the corresponding 4,5-methanopyrrolidine acetic acid esters (**200**). Liberation and oxidation of the primary alcohol to the carboxylic acid, followed by global deprotection, afforded, respectively, *cis*- and *trans*-4,5-methano-L-proline-3-acetic acid (*cis*- and *trans*-**201**), and the structure and stereochemistry of the former were ascertained by X-ray crystallography.

Employing 2,4-pentadienoic acid in the free-radical cyclization–cyclopropanation reaction sequence furnished substituted vinyl *cis*- and *trans*-4,5-methano-L-prolines *cis*- and *trans*-**202** (Fig. 15).

Neither *cis*- and *trans*-4,5-methano-L-proline-3-acetic acids **201** nor *cis*- and *trans*-**202** exhibited significant binding affinity at the NMDA and AMPA and kainate glutamate receptor subtypes at concentrations as high as 10 μ M.

The discovery of captopril (Fig. 16) as the first marketed inhibitor of angiotensin-converting enzyme (ACE) started an era of antihypertensive drugs inspired by structure-based design [165]. For example, studying the structural requirements of captopril in the enzyme active site, the absolute configuration of the pyrrolidine ring was found to be important for maintaining its ACE-inhibitory activity [166]. With efficient access to *cis*- and *trans*-methano-L-prolines and pipercolates in hand, Hanessian and coworkers launched a program to study constrained captopril analogues [140]. Acylation of the respective amino acids gave, respectively, 4,5-methano-captopril analogues *cis*- and *trans*-**203** and *cis*-

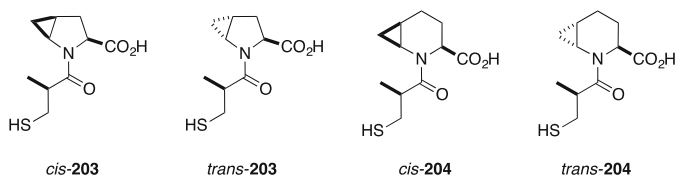
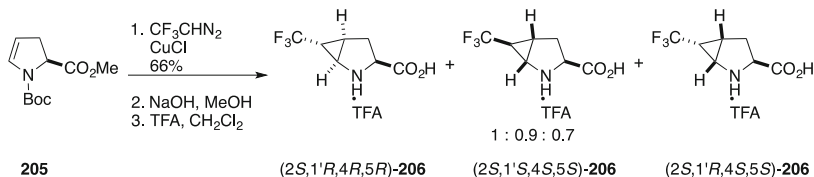


Fig. 17 Examples of 4,5-methano-L-proline and 5,6-methano-L-pipecolic acid analogues of captopril



Scheme 32 Synthesis of trifluoromethyl-substituted 4,5-methanoproline-L-proline (**206**)

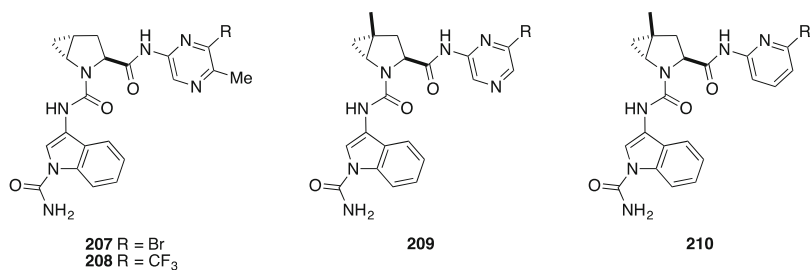


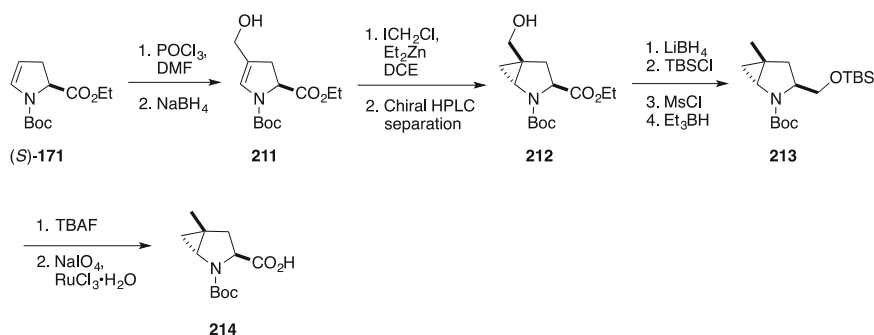
Fig. 18 Examples of inhibitors of the alternative complement pathway containing a 4,5-methano-L-proline unit

and *trans*-**204** (Fig. 17), which exhibited twofold better in vitro inhibitory activity (IC_{50} 5.3–7.6 nM) than captopril (IC_{50} 13.0 nM) [143].

In the co-crystal structure of captopril with ACE [166], space exists to accommodate the cyclopropane ring appended to the pyrrolidine and piperidine portions of **203** and **204**, which may account for the independence of inhibitory activity on the spatial orientation of the fused cyclopropane ring.

Treatment of 4,5-unsaturated *N*-Boc-L-proline methyl ester **205** with excess trifluoromethyl diazomethane in the presence of catalytic CuCl gave a mixture of three diastereomers that were separated by chromatography prior to removal of the ester and carbamate protection to furnish trifluoromethyl-substituted 4,5-methano-L-prolines **206** (Scheme 32) [95].

Incorporation of trifluoromethyl 4,5-methano-L-proline (*2S,1'R,4R,5R*)-**206** in the proline-rich cell-penetrating peptide SAP (VRLPPP)₃ stabilized the polyproline II conformations as observed by concentration- and temperature-dependent circular dichroism (CD) spectroscopy experiments [95].



Scheme 33 Synthesis of 4-methyl-*trans*-4,5-methano-L-proline (**214**)

Inhibitors of the alternative complement pathway including Factor D were prepared containing 4,5-methanoproline amides (Fig. 18) [167]. Vilsmeier formylation of dehydropyrroline (*S*)-**171** followed by reduction gave the allylic alcohol **211**. Simmons–Smith cyclopropanation, followed by purification using chiral HPLC chromatography, led to the *cis*-hydroxymethyl diastereomer **212**. 4-Methyl-*trans*-4,5-methanoproline **214** was prepared by a sequence consisting of ester reduction, selective diol protection, and activation as the *O*-silyl ether methanesulfonylate, reduction, silyl ether cleavage, and oxidation (Scheme 33).

4,5-Methanoproline dipeptide analogues with the general formula **215** (Fig. 19) have been claimed to possess hypotensive effects due to its ability to inhibit angiotensin-converting enzyme (ACE) [129, 130]. 4,5-Methanoproline derivatives, such as **216** and **217** [168–170], and **222** [171, 172], have been claimed to be useful in the treatment of hepatitis C virus (HCV). Similarly, structures **218**, **219** [173], and **220** [174, 175] have been claimed to interfere in the life cycle of HCV, and a series related to **221** have been claimed useful for the treatment of HCV when co-administrated with the undecapeptide cyclosporine A [176].

The 2-(pyrrolidin-2-yl)-1*H*-imidazole core **224** has been obtained by heating *N*-Boc-4,5-methano-L-prolinal **223** in the presence of glyoxal and ammonia in methanol (Scheme 34) [168–171].

Bromination of the imidazole ring of **224** was achieved with NBS, producing a separable mixture of 5-bromo-1*H*-imidazole **225** and 4,5-dibromo-1*H*-imidazole **226**. The 4,5-dibromide **226** was reduced with Na₂S₂O₃ to give **225** [171]. Treatment of **224** with iodine afforded exclusively the 4,5-diiodide, and a similar treatment with Na₂S₂O₃ gave 5-Iodo-1*H*-imidazole [170]. The bromo- and iodoimidazole analogues were subjected to Suzuki–Miyaura cross-coupling reactions to produce the corresponding aryl-imidazole derivatives.

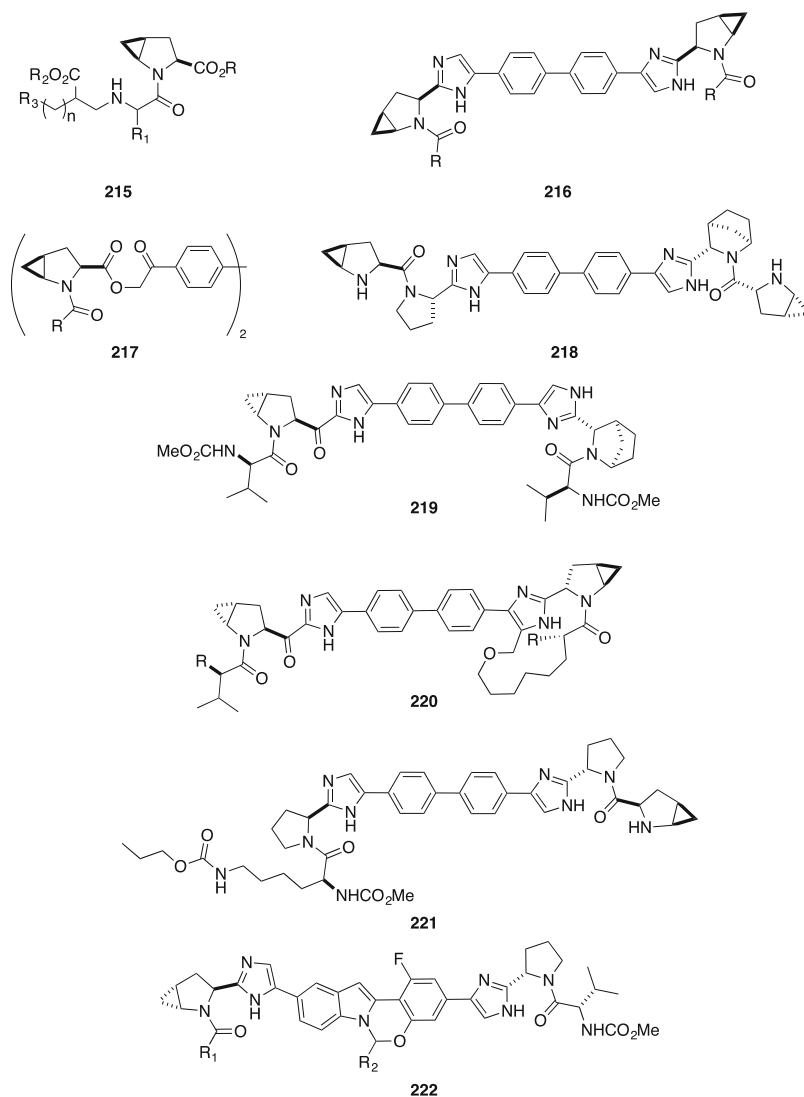
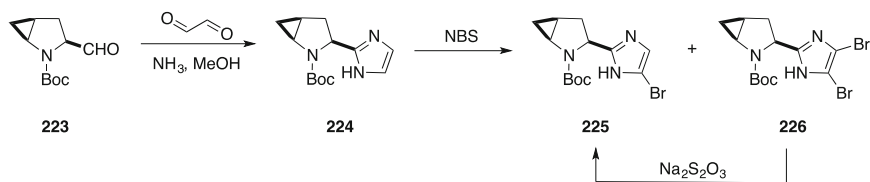


Fig. 19 Examples of bioactive molecules containing 4,5-methano-L-proline units claimed to inhibit angiotensin-converting enzyme



Scheme 34 Synthesis of 5-bromo-1*H*-imidazole derivative **225**

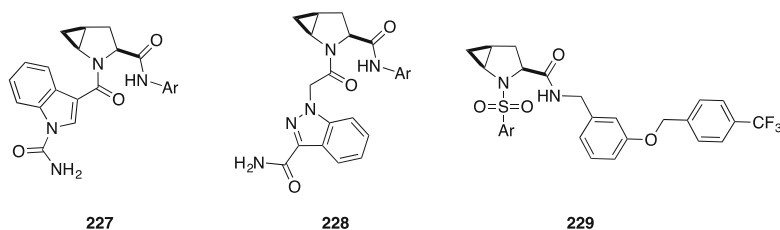
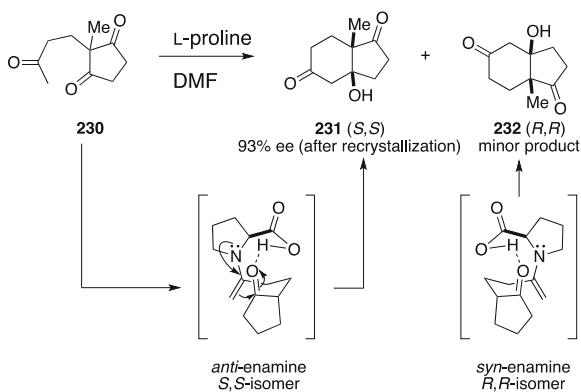


Fig. 20 Examples of indole and indazole bioactive molecules containing a 4,5-methano-L-proline unit claimed for the treatment of age-related macular degeneration

Fig. 21 Enamine catalysis with L-proline

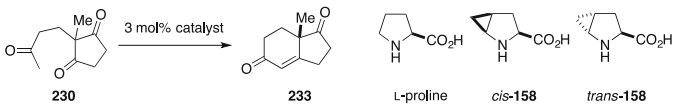


4,5-Methano-L-proline amides containing indole [177] and indazole [178] derivatives, such as **227** and **228** (Fig. 20), have been claimed useful for the treatment of age-related macular degeneration. 4,5-Methano-L-proline amide **229** has been claimed to be an agonist of the transient receptor potential cation channel, member A1 (TRPA1) [179].

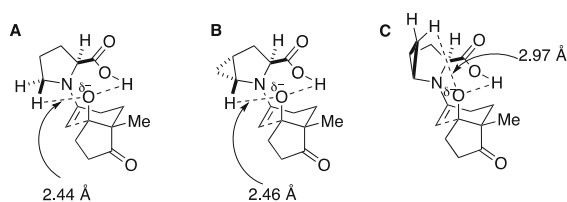
6.4 4,5-Methanoprolines as Metal-Free Organocatalysts

In 1976, scientists at Hoffmann-La Roche [180–182] and Schering A. G. [183, 184] independently reported that L-proline catalyzed the intramolecular aldol reaction of an achiral triketone (**230**) to give a quasi-enantiomerically pure bicyclic product (**231**). The reaction is now known as the Hajos–Parrish–Eder–Sauer–Wiechert reaction (Fig. 21). The mechanism of this transformation has been extensively studied computationally [185, 186] and favors transition-state structures in which the planar enamine is spatially oriented to preferentially attack one of the diastereotopic carbonyl groups.

In collaboration with the Houk laboratory, Hanessian and coworkers [187] reported that *cis*-4,5-methano-L-proline (*cis*-**158**) catalyzed the reaction similar to L-proline, albeit with slower reaction times. In contrast, *trans*-4,5-methano-L-

Table 1 Intramolecular aldol reaction with L-proline and 4,5-methano-L-proline catalysts


Catalyst	Time (h)	Yield (%)	ee (%)
L-proline	48	98	95
<i>cis</i> - 158	140	86 ^a	93
<i>trans</i> - 158	125	67 ^b	83

^a14% Starting material recovered^b28% Starting material recovered**Fig. 22** Transition-state models (**A**, **B** and **C**) in enamine catalysis

proline (*trans*-**158**) gave aldol product **233** in lower yield and enantioselectivity (Table 1).

The lower enantioselectivity with *trans*-4,5-methano-L-proline was attributed to unfavorable energetics related to *anti*- and *syn*-transition structures compared to *cis*-4,5-methano-L-proline and L-proline (Fig. 22) [187, 188].

Electrostatic interactions involving methine hydrogens may contribute to the overall stabilization of the transition states **A** and **B**, although the preference for the planar enamine in the *cis*-4,5-methano-L-proline (as in **C**) may explain the higher enantioselectivity. The energy difference between *syn*- and *anti*-pyramidalized iminium transition structures in the *trans*-isomer was calculated to be smaller ($\Delta H^\ddagger = 1.2$ Kcal) than that of the *cis*-isomer ($\Delta H^\ddagger = 2.2$ Kcal) [187]. The enantioselectivity achieved by the *trans*-isomer may be due in part to an $\text{NCH}^{\delta+} - \text{O}^{\delta-}$ electrostatic interaction stabilizing the *anti*-enamine **B** (compared to **A** and **C**) (Fig. 22).

4,5-Methano-L-prolines were found to catalyze the conjugate addition of 2-nitropropane to cyclohexenone in the presence of 2,5-dimethylpiperazine (Table 2) [188–191]. In this reaction, *trans*-4,5-methano-L-proline was found to be the better catalyst, leading to 99% enantioselectivity. The lower efficiency of the *cis*-isomer was attributed to a steric effect causing a pseudo-axial orientation of the carboxyl group (X-ray) to avoid A^{1,3} strain in the iminium transition structure. The added base has a considerably favorable effect on enantioselectivity compared to L-proline (83% ee) [192, 193]. The corresponding hydroxamic acids **234** and **235**

Table 2 Addition of 2-nitropropane to 2-cyclohexenone in the presence of L-proline and 4,5-methano-L-prolines

Catalyst	ee (%)	Yield (%)
L-proline	89	83
<i>cis</i> - 158	75	52
<i>trans</i> - 158	99	92
 234	75	78
 235	81	65

Scheme 35
Enantioselective Michael addition catalyzed by *trans*-**158**

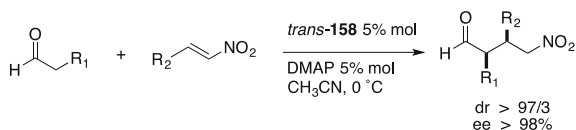
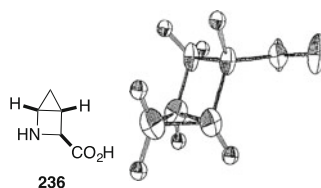


Fig. 23 Structure of SF-1836



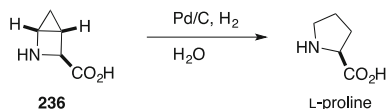
were also effective catalysts, albeit with lower enantioselectivity (Table 2) [190]. (*R*)-3-(2-Nitropropan-2-yl)cyclohexanone was used to synthesize a δ -amino acid that was incorporated in a potent inhibitor of beta-amyloid cleaving enzyme 1 (BACE1) [194, 195].

Michael addition of aldehydes to 2-nitroalkenes have also been reported to be catalyzed by *trans*-4,5-methano-L-proline with high enantioselectivities and generally excellent diastereoselectivity favoring the *syn*-isomer (Scheme 35) [196].

7 *trans*-3,4-Methano-L-azetidino-2-carboxylic acid

An azetidino analogue of 3,4-methano-L-proline was reported as a naturally occurring antibiotic substance (SF-1836), isolated from the culture filtrate of *Streptomyces zaomyceticus* SF-1836 (Fig. 23) [197].

Scheme 36 Hydrogenation of **236** to afford L-proline



The proposed (*S*)-2-azabicyclo[2.1.0]pentane-3-carboxylic acid structure was based on its physicochemical properties and conversion of **236** to L-proline upon catalytic reduction (Scheme 36) [197].

Confirmation of the assigned structure was also secured from an X-ray analysis by direct methods [198]. The third naturally occurring cyclic methano amino acid to be discovered after 2,4-methano-L-proline **49** and *cis*-3,4-methano-L-proline **80**, SF-186 has a highly constrained azabicyclic structure and *trans*-stereochemistry. The biogenesis of SF-186 and its mode of antibacterial action against some *Xanthomonas* species warrant further investigation.

8 Summary

In this review, we have summarized various aspects of the synthesis, structural properties, and applications in medicinal chemistry of methanoprolines, which we have henceforth designated as *proline methanologues*. Racemic 2,4-methanoproline and *cis*-3,4-methano-L-proline have been found in nature and have served as starting points to further explore the chemistry and biology of this class of unusual amino acids. By far the greatest recent interest has been devoted to 4,5-methano-L-proline, with the discovery that they are good surrogates for L-proline itself. In medicinal chemistry, a 4,5-methano-L-proline nitrile amide has been incorporated into a marketed drug for the treatment of type II diabetes. Moreover, a plethora of patents claim 4,5-methano-L-proline analogues for various medicinal applications. In peptide science, substituted methano-L-proline analogues have been shown to stabilize polyproline type II conformations and have been used to probe the stereoelectronic effects of substituted prolines. In addition, 4,5-methano-L-proline analogues have exhibited promising catalytic activities in enantioselective reactions. In light of these interesting properties, proline methanologues merit further study as proline surrogates to advance various fields including natural product synthesis, medicinal chemistry, catalysis, and peptide science.

Acknowledgements We thank CONACyT for a fellowship to Miguel Vilchis and to NSERC for financial support.

References

1. Avan I, Hall CD, Katritzky AR (2014) *Chem Soc Rev* 43:3575
2. Liskamp RMJ, Rijkers DTS, Kruijtzter JAW, Kemmink J (2011) *ChemBioChem* 12:1626
3. Reichelt A, Martin SF (2006) *Acc Chem Res* 39:433
4. Hanessian S, McNaughton-Smith G, Lombart H-G, Lubell WD (1997) *Tetrahedron* 53:12789
5. Trabocchi A, Scarpi D, Guarna A (2008) *Amino Acids* 34:1
6. Hanessian S, Auzzas L (2008) *Acc Chem Res* 41:1241
7. Komarov IV, Grigorenko AO, Turov AV, Khilya VP (2004) *Russ Chem Rev* 73:785
8. Grygorenko OO, Artamonov OS, Komarov IV, Mykhailiuk PK (2011) *Tetrahedron* 67:803
9. Brackmann F, de Meijere A (2007) *Chem Rev* 107:4493
10. Salaün J (2000) Cyclopropane derivatives and their diverse biological activities. In: de Meijere A (ed) *Small ring compounds in organic synthesis VI*, vol 207, *Topics in current chemistry*. Springer, Berlin/Heidelberg, pp 1
11. Milewska MJ (2000) *Pol J Chem* 74:447
12. Stammer CH (1990) *Tetrahedron* 46:2231
13. Adams DO, Yang SF (1979) *Proc Natl Acad Sci U S A* 76:170
14. Pirrung MC (1987) *J Org Chem* 52:4179
15. Wheeler TN, Ray J (1987) *J Org Chem* 52:4875
16. Pirrung MC, McGeehan GM (1986) *J Org Chem* 51:2103
17. Hoffman NE, Yang SF, Ichihara A, Sakamura S (1982) *Plant Physiol* 70:195
18. Switzer FL, Van Halbeek H, Holt EM, Stammer CH, Saltveit ME Jr (1989) *Tetrahedron* 45:6091
19. Häusler J (1981) *Liebigs Ann Chem* 1981:1073
20. Matsui S, Srivastava VP, Holt EM, Taylor EW, Stammer CH (1991) *Int J Pept Protein Res* 37:306
21. Hercouet A, Bessières B, Le Corre M (1996) *Tetrahedron Asymmetry* 7:1267
22. Le Corre M, Hercouet A, Bessieres B (1995) *Tetrahedron Asymmetry* 6:683
23. Hercouet A, Bessières B, Le Corre M (1996) *Tetrahedron Asymmetry* 7:283
24. Gao Y, Sharpless KB (1988) *J Am Chem Soc* 110:7538
25. Stork G, Leong AYW, Touzin AM (1976) *J Org Chem* 41:3491
26. Beak P, Wu S, Yum EK, Jun YM (1994) *J Org Chem* 59:276
27. Kodama H, Yamamoto H, Miyazaki M, Kondo M (1994) Synthesis and beta-turn stabilizing of cyclopropaneprolin analogues. In: Okada K (ed) *Peptide chemistry 1993*, vol 31. Protein Research Foundation, Osaka, pp 61
28. Barluenga J, Aznar F, Gutiérrez I, García-Granda S, Llorca-Baragaño MA (2002) *Org Lett* 4:4273
29. Kodama H, Matsui S, Kondo M, Stammer CH (1992) *Bull Chem Soc Jpn* 65:2668
30. Mapelli C, Elrod LF, Holt EM, Stammer CH (1989) *Tetrahedron* 45:4377
31. Elrod LF, Holt EM, Mapelli C, Stammer CH (1988) *J Chem Soc Chem Commun* 252
32. Bateson JH, Southgate R, Tyler JW, Fell SCM (1986) *J Chem Soc Perkin Trans* 1:973
33. Ezquerro J, Escribano A, Rubio A, Remuiñán MJ, Vaquero JJ (1996) *Tetrahedron Asymmetry* 7:2613
34. Gnad F, Poleschak M, Reiser O (2004) *Tetrahedron Lett* 45:4277
35. Adamovskiy MI, Artamonov OS, Tymtsunik AV, Grygorenko OO (2014) *Tetrahedron Lett* 55:5970
36. Bell EA, Qureshi MY, Pryce RJ, Janzen DH, Lemke P, Clardy J (1980) *J Am Chem Soc* 102:1409
37. Kite GC, Ireland H (2002) *Phytochemistry* 59:163
38. Stevens CV, Smaghe G, Rammeloo T, De Kimpe N (2005) *J Agric Food Chem* 53:1945
39. Chung HH, Benson DR, Cornish VW, Schultz PG (1993) *Proc Natl Acad Sci U S A* 90:10145
40. Hughes P, Martin M, Clardy J (1980) *Tetrahedron Lett* 21:4579
41. Hughes P, Clardy J (1988) *J Org Chem* 53:4793

42. Liu RSH, Hammond GS (1964) *J Am Chem Soc* 86:1892
43. Varnes JG, Scott Lehr G, Moore GL, Hulsizer JM, Albert JS (2010) *Tetrahedron Lett* 51:3756
44. Pirrung MC (1980) *Tetrahedron Lett* 21:4577
45. Rammeloo T, Stevens CV, De Kimpe N (2002) *J Org Chem* 67:6509
46. Rammeloo T, Stevens CV (2002) *Chem Commun* 250
47. Montelione GT, Hughes P, Clardy J, Scheraga HA (1986) *J Am Chem Soc* 108:6765
48. Talluri S, Montelione GT, Van Duyne G, Piela L, Clardy J, Scheraga HA (1987) *J Am Chem Soc* 109:4473
49. Piela L, Nemethy G, Scheraga HA (1987) *J Am Chem Soc* 109:4477
50. Mapelli C, Halbeek HV, Stammer CH (1990) *Biopolymers* 29:407
51. Esslinger SC, Koch HP, Kavanaugh MP, Philips DP, Chamberlin RA, Thompson CM, Bridges RJ (1998) *Bioorg Med Chem Lett* 8:3101
52. Malpass JR, Patel AB, Davies JW, Fulford SY (2003) *J Org Chem* 68:9348
53. Patel AB, Malpass JR (2008) *J Med Chem* 51:7005
54. Grygorenko OO, Artamonov OS, Palamarchuk GV, Zubatyuk RI, Shishkin OV, Komarov IV (2006) *Tetrahedron Asymmetry* 17:252
55. Tkachenko AN, Radchenko DS, Mykhailiuk PK, Grygorenko OO, Komarov IV (2009) *Org Lett* 11:5674
56. Vasiuta RI, Gorichko MV (2014) *Tetrahedron Lett* 55:466
57. Fowden L, Smith A, Millington DS, Sheppard RC (1969) *Phytochemistry* 8:437
58. Fowden L, Lea PJ, Worris RD (1972) *Symp Biol Hung* 13:137
59. Caveney S, Starratt A (1994) *Nature* 372:509
60. Starratt AN, Caveney S (1995) *Phytochemistry* 40:479
61. Norris RD, Fowden L (1972) *Phytochemistry* 11:2921
62. Rowland I, Tristram H (1972) *Chem Biol Interact* 4:377
63. Kerr MW (1984) Rational design of a pollen suppressant for small-grained cereals. In: *British Plant Growth Regulator Group* (ed) *Biochemical aspects of synthetic and naturally occurring plant growth regulators*, vol 11. The Group, Wantage, pp 59
64. Macháčková I, Zmrhal Z (1983) *Biol Plant* 25:394
65. Thondorf I, Voigt V, Schäfer S, Gebauer S, Zebisch K, Laug L, Brandsch M (2011) *Bioorg Med Chem* 19:6409
66. Abraham S, Hadd MJ, Tran L, Vickers T, Sindac J, Milanov ZV, Holladay MW, Bhagwat SS, Hua H, Ford Pulido JM, Cramer MD, Gitnick D, James J, Dao A, Belli B, Armstrong RC, Treiber DK, Liu G (2011) *Bioorg Med Chem Lett* 21:5296
67. Wood DA, Mason RF, Day JA, Searle RJG (1980) *EP* 001 079 9B1
68. Kollmeyer WD (1980) *US* 4 183 857
69. Day JA, Devlin BRJ, Searle RJG (1981) *US* 4 279 821
70. Scholes G, Baardman F (1981) *US* 4 262 124
71. Levy OE, Madison EL, Semple JE, Tamiz AP, Weinhouse MI (2002) *WO* 02/14349
72. Witkop B, Fujimoto Y, Irreverre F, Karle JM, Karle IL (1971) *J Am Chem Soc* 93:3471
73. Fowler FW (1971) *Angew Chem* 83:147
74. Sagnard I, Sasaki NA, Chiaroni A, Riche C, Potier P (1995) *Tetrahedron Lett* 36:3149
75. Pellicciari R, Natalini B, Marinuzzi M, Monahan JB, Snyder JP (1990) *Tetrahedron Lett* 31:139
76. Tverezovsky VV, Baird MS, Bolesov IG (1997) *Tetrahedron* 53:14773
77. Oba M, Nishiyama N, Nishiyama K (2005) *Tetrahedron* 61:8456
78. Barton DHR, Hervé Y, Potier P, Thierry J (1988) *Tetrahedron* 44:5479
79. Barton DHR, Crich D, Motherwell WB (1983) *J Chem Soc Chem Commun* 939
80. Bakonyi B, Furegati M, Kramer C, La Vecchia L, Ossola F (2013) *J Org Chem* 78:9328
81. Tufariello JJ, Milowsky AS, Al-Nuri M, Goldstein S (1987) *Tetrahedron Lett* 28:267
82. Heiser U, Niestroj AJ, Gaertner UT, Demuth HU (2008) *US* 029 3618 A1
83. Kerrick ST, Beak P (1991) *J Am Chem Soc* 113:9708
84. Genet C, McGrath MJ, O'Brien P (2006) *Org Biomol Chem* 4:1376

85. O'Brien P, Wiberg KB, Bailey WF, Hermet J-PR, McGrath MJ (2004) *J Am Chem Soc* 126:15480
86. Gallagher DJ, Wu S, Nikolic NA, Beak P (1995) *J Org Chem* 60:8148
87. Abraham RJ, Gatti G (1970) *Org Magn Reson* 2:173
88. Zhang R, Mamai A, Madalengoitia JS (1998) *J Org Chem* 64:547
89. Zhang R, Madalengoitia JS (1998) *J Org Chem* 64:330
90. Mamai A, Zhang R, Natarajan A, Madalengoitia JS (2001) *J Org Chem* 66:455
91. Venkatraman S, Bogen SL, Arasappan A, Bennett F, Chen K, Jao E, Liu Y-T, Lovey R, Hendrata S, Huang Y, Pan W, Parekh T, Pinto P, Popov V, Pike R, Ruan S, Santhanam B, Vibulbhan B, Wu W, Yang W, Kong J, Liang X, Wong J, Liu R, Butkiewicz N, Chase R, Hart A, Agrawal S, Ingravallo P, Pichardo J, Kong R, Baroudy B, Malcolm B, Guo Z, Prongay A, Madison V, Broske L, Cui X, Cheng K-C, Hsieh Y, Brisson J-M, Prelusky D, Korfmacher W, White R, Bogdanowich-Knipp S, Pavlovsky A, Bradley P, Saksena AK, Ganguly A, Piwinski J, Girijavallabhan V, Njoroge FG (2006) *J Med Chem* 49:6074
92. de Meijere A, Williams CM, Kourdioukov A, Sviridov SV, Chaplinski V, Kordes M, Savchenko AI, Stratmann C, Noltemeyer M (2002) *Chem Eur J* 8:3789
93. de Meijere A, Kozhushkov SI, Savchenko AI (2004) *J Organomet Chem* 689:2033
94. Brackmann F, Colombo N, Cabrele C, de Meijere A (2006) *Eur J Org Chem* 2006:4440
95. Mykhailiuk PK, Afonin S, Palamarchuk GV, Shishkin OV, Ulrich AS, Komarov IV (2008) *Angew Chem Int Ed* 47:5765
96. Reiersen H, Rees AR (2001) *Trends Biochem Sci* 26:679
97. MacArthur MW, Thornton JM (1991) *J Mol Biol* 218:397
98. Nimni ME (ed) (1988) *Collagen*, vol 1–4. CRC, Boca Raton
99. Gorres KL, Edupuganti R, Krow GR, Raines RT (2008) *Biochemistry* 47:9447
100. Eberhardt ES, Panasik N, Raines RT (1996) *J Am Chem Soc* 118:12261
101. Bretscher LE, Jenkins CL, Taylor KM, DeRider ML, Raines RT (2001) *J Am Chem Soc* 123:777
102. Renner C, Alefelder S, Bae JH, Budisa N, Huber R, Moroder L (2001) *Angew Chem Int Ed* 40:923
103. Jenkins CL, Lin G, Duo J, Rapolu D, Guzei IA, Raines RT, Krow GR (2004) *J Org Chem* 69:8565
104. Krow GR, Shoulders MD, Edupuganti R, Gandla D, Yu F, Sonnet PE, Sender M, Choudhary A, DeBrosse C, Ross CW, Carroll P, Raines RT (2012) *J Org Chem* 77:5331
105. O'Hagan D, Bilton C, Howard JAK, Knight L, Tozer DJ (2000) *J Chem Soc Perkin Trans* 2:605
106. Holmgren SK, Taylor KM, Bretscher LE, Raines RT (1998) *Nature* 392:666
107. Holmgren SK, Bretscher LE, Taylor KM, Raines RT (1999) *Chem Biol* 6:63
108. Jenkins CL, Raines RT (2002) *Nat Prod Rep* 19:49
109. Krow GR, Yuan J, Fang Y, Meyer MD, Anderson DJ, Campbell JE, Carroll PJ (2000) *Tetrahedron* 56:9227
110. Krow GR, Lin G, Yu F (2004) *J Org Chem* 70:590
111. Hommel U, Lorthiois ELJ, Maibaum JK, Ostermann N, Randl SA, Vulpetti A (2014) *WO* 2014002057 A1
112. Giannis A, Kolter T (1993) *Angew Chem* 105:1303
113. Giannis A, Kolter T (1993) *Angew Chem Int Ed* 32:1244
114. Gardner B, Nakanishi H, Kahn M (1993) *Tetrahedron* 49:3433
115. Gante J (1994) *Angew Chem* 106:1780
116. Gante J (1994) *Angew Chem Int Ed* 33:1699
117. Adang AEP, Hermkens PHH, Linders JTM, Ottenheijm HCJ, van Staveren CJ (1994) *Recl Trav Chim Pays-Bas* 113:63
118. Curran TP, McEnaney PM (1995) *Tetrahedron Lett* 36:191
119. Müller G, Gurrath M, Kurz M, Kessler H (1993) *Proteins Struct Funct Bioinf* 15:235
120. Hanessian S, Reinhold U, Gentile G (1997) *Angew Chem Int Ed* 36:1881

121. Duez H, Cariou B, Staels B (2012) *Biochem Pharmacol* 83:823
122. Robl JA, Hamann LG (2011) The discovery of the dipeptidyl peptidase-4 (DPP4) inhibitor OnglyzaTM: from concept to market. In: *Accounts in drug discovery: case studies in medicinal chemistry*. The Royal Society of Chemistry, Cambridge, pp 1
123. Augeri DJ, Robl JA, Betebenner DA, Magnin DR, Khanna A, Robertson JG, Wang A, Simpkins LM, Taunk P, Huang Q, Han S-P, Abboa-Offei B, Cap M, Xin L, Tao L, Tozzo E, Welzel GE, Egan DM, Marcinkeviciene J, Chang SY, Biller SA, Kirby MS, Parker RA, Hamann LG (2005) *J Med Chem* 48:5025
124. Baggio LL, Drucker DJ (2007) *Gastroenterology* 132:2131
125. Mentlein R (1999) *Regul Pept* 85:9
126. Nauck M, Stöckmann F, Ebert R, Creutzfeldt W (1986) *Diabetologia* 29:46
127. Neumiller JJ (2015) *Med Clin North Am* 99:107
128. Magnin DR, Robl JA, Sulsky RB, Augeri DJ, Huang Y, Simpkins LM, Taunk PC, Betebenner DA, Robertson JG, Abboa-Offei BE, Wang A, Cap M, Xin L, Tao L, Sitkoff DF, Malley MF, Gougoutas JZ, Khanna A, Huang Q, Han S-P, Parker RA, Hamann LG (2004) *J Med Chem* 47:2587
129. Urbach HD, Henning RD, Becker RD (1985) DE 3324263 A1
130. Urbach H, Henning R, Becker R (1986) US 4 591 598
131. Woo K-C, Jones K (1991) *Tetrahedron Lett* 32:6949
132. Pickering L, Malhi BS, Coe PL, Walker RT (1994) *Nucleosides Nucleotides* 13:1493
133. Shin C, Nakamura Y, Yamada Y, Yonezawa Y, Umemura K, Yoshimura J (1995) *Bull Chem Soc Jpn* 68:3151
134. Arndt H-D, Polborn K, Koert U (1997) *Tetrahedron Lett* 38:3879
135. Rasso G, Carta P, Pinna L, Battistini L, Zanardi F, Acquotti D, Casiraghi G (1999) *Eur J Org Chem* 1395
136. Bunch L, Norrby PO, Frydenvang K, Krogsgaard-Larsen P, Madsen U (2001) *Org Lett* 3:433
137. Arndt H-D, Welz R, Mueller S, Ziemer B, Koert U (2004) *Chem Eur J* 10:3945
138. Shinada T, Hamada M, Kawasaki M, Ohfuné Y (2005) *Heterocycles* 66:511
139. Zanardi F, Sartori A, Curti C, Battistini L, Rasso G, Nicastro G, Casiraghi G (2007) *J Org Chem* 72:1814
140. Zaminer J, Brockmann C, Huy P, Opitz R, Reuter C, Beyermann M, Freund C, Mueller M, Oschkinat H, Schmalz H-G, Kuehne R (2010) *Angew Chem Int Ed* 49:7111
141. Vu H-D, Renault J, Roisnel T, Gouault N, Uriac P (2014) *Eur J Org Chem* 2014:4506
142. Charette AB, Beauchemin A (2004) *Org React* 58:1
143. Hanessian S, Reinhold U, Saulnier M, Claridge S (1998) *Bioorg Med Chem Lett* 8:2123
144. Shono T, Matsumura Y, Tsubata K, Sugihara Y, Yamane S, Kanazawa T, Aoki T (1982) *J Am Chem Soc* 104:6697
145. Charette AB, Marcoux J-F (1995) *Synlett* 1995:1197
146. Yu J, Truc V, Riebel P, Hierl E, Mudryk B (2005) *Tetrahedron Lett* 46:4011
147. Wang G, James CA, Meanwell NA, Hamann LG, Belema M (2013) *Tetrahedron Lett* 54:6722
148. Ramirez A, Truc VC, Lawler M, Ye YK, Wang J, Wang C, Chen S, Laporte T, Liu N, Kolotuchin S, Jones S, Bordawekar S, Tummala S, Waltermire RE, Kronenthal D (2014) *J Org Chem* 79:6233
149. Gill I, Patel R (2006) *Bioorg Med Chem Lett* 16:705
150. Dong J, Gong Y, Liu J, Chen X, Wen X, Sun H (2014) *Bioorg Med Chem* 22:1383
151. Politino M, Cadin MM, Skonezny PM, Chen JG (2006) WO 2005106011
152. Rayner PJ, O'Brien P, Horan RAJ (2013) *J Am Chem Soc* 135:8071
153. Villhauer EB, Brinkman JA, Naderi GB, Burkey BF, Dunning BE, Prasad K, Mangold BL, Russell ME, Hughes TE (2003) *J Med Chem* 46:2774
154. Gwaltney SL, Stafford JA (2005) Inhibitors of dipeptidyl peptidase 4. In: Doherty AM, Bock MG, Desai MC, Overington J, Plattner JJ, Stamford A, Wustrow D (eds) *Annual reports in medicinal chemistry*, vol 40. Academic, San Diego, p 149

155. Traynor K (2009) *Am J Health Syst Pharm* 66:1513
156. Rasmussen HB, Branner S, Wiberg FC, Wagtmann N (2003) *Nat Struct Mol Biol* 10:19
157. Engel M, Hoffmann T, Wagner L, Wermann M, Heiser U, Kiefersauer R, Huber R, Bode W, Demuth H-U, Brandstetter H (2003) *Proc Natl Acad Sci U S A* 100:5063
158. Thoma R, Löffler B, Stihle M, Huber W, Ruf A, Hennig M (2003) *Structure* 11:947
159. Oefner C, D'Arcy A, Mac Sweeney A, Pierau S, Gardiner R, Dale GE (2003) *Acta Crystallogr Sect D* 59:1206
160. Hiramatsu H, Kyono K, Higashiyama Y, Fukushima C, Shima H, Sugiyama S, Inaka K, Yamamoto A, Shimizu R (2003) *Biochem Biophys Res Commun* 302:849
161. Zhao G, Taunk PC, Magnin DR, Simpkins LM, Robl JA, Wang A, Robertson JG, Marcinkeviciene J, Sitkoff DF, Parker RA, Kirby MS, Hamann LG (2005) *Bioorg Med Chem Lett* 15:3992
162. Arenare L, De Caprariis P, Marinozzi M, Natalini B, Pellicciari R (1994) *Tetrahedron Lett* 35:1425
163. Pellicciari R, Arenare L, De Caprariis P, Natalini B, Marinozzi M, Galli A (1995) *J Chem Soc Perkin Trans 1*:1251
164. Hanessian S, Ninkovic S, Reinhold U (1996) *Tetrahedron Lett* 37:8971
165. Smith CG, Vane JR (2003) *FASEB J* 17:788
166. Akif M, Masuyer G, Schwager SLU, Bhuyan BJ, Muges G, Isaac RE, Sturrock ED, Acharya KR (2011) *FEBS J* 278:3644
167. Altmann E, Hommel U, Lorthiois ELJ, Maibaum JK, Ostermann N, Quancard J, Randl SA, Vulpetti A (2014) *WO 2014002054 A1*
168. Bachand C, Belema M, Deon DH, Good AC, Goodrich J, James CA, Lavoie R, Lopez OD, Martel A, Meanwell NA (2009) *US 20090068140 A1*
169. Kim S, Gao Q, Yang F (2010) *US 20100158862*
170. Pack SK, Tymonko S, Patel BP, Natalie JKJ, Belema M (2012) *US 20110269956*
171. Kozlowski JA, Rosenblum SB, Coburn CA, Shankar BB, Anilkumar GN, Chen L, Dwyer MP, Jiang Y, Keertikar KM, Lavey BJ, Selyutin OB, Tong L, Wong M, Yang D-Y, Yu W, Zhou G, Wu H, Hu B, Zhong B, Sun F, Ji T, Shen C, Rizvi R, Zeng Q (2012) *WO 2012041014 A1*
172. Yu W, Tong L, Kozlowski JA, Selyutin O, Chen L, Kim J-H, Sha D, Rizvi R, Shankar B, Hu B, Zhong B, Wai D, Hao J, Wei W, Ji T, Zan S (2014) *WO 2014110705 A1*
173. Or YS, Peng X, Wang C, Ying L, Qiu YL (2011) *WO 2011031904 A1*
174. Qiu YL, Wang C, Cao H, Peng X, Ying L, Gao X, Or YS (2013) *WO 2013052362 A1*
175. Qiu YL, Cao H, Peng X, Chen Z, Or YS (2013) *WO 2013059278 A2*
176. Or YS, Kim IJ, Wang G, Long J (2011) *US 8623814 B2*
177. Altmann E, Hommel U, Lorthiois ELJ, Maibaum JK, Ostermann N, Quancard J, Randl SA, Simic O, Vulpetti A, Rogel O (2012) *WO 2012093101*
178. Altmann E, Hommel U, Lorthiois ELJ, Maibaum JK, Ostermann N, Quancard J, Randl SA, Vulpetti A, Rogel O (2014) *WO 2014002051 A2*
179. Kobayashi K, Suzuki T, Okuzumi T (2014) *WO 2014098098 A1*
180. Hajos ZG, Parrish DR (1976) *US 3975440 A*
181. Hajos ZG, Parrish DR (1971) *DE 2102623 A1*
182. Hajos ZG, Parrish DR (1974) *J Org Chem* 39:1615
183. Eder U, Sauer G, Wiechert R (1971) *DE 2 014 757*
184. Eder U, Sauer G, Wiechert R (1971) *Angew Chem Int Ed* 10:496
185. Cheong PH-Y, Legault CY, Um JM, Çelebi-Ölçüm N, Houk KN (2011) *Chem Rev* 111:5042
186. Armstrong A, Boto RA, Dingwall P, Contreras-Garcia J, Harvey MJ, Mason NJ, Rzepa HS (2014) *Chem Sci* 5:2057
187. Cheong PH-Y, Houk KN, Warriar JS, Hanessian S (2004) *Adv Synth Catal* 346:1111
188. Bahmanyar S, Houk KN (2001) *J Am Chem Soc* 123:11273
189. Hanessian S, Pham V (2000) *Org Lett* 2:2975
190. Hanessian S, Shao Z, Warriar JS (2006) *Org Lett* 8:4787

191. Hanessian S, Govindan S, Warriar JS (2005) *Chirality* 17:540
192. Yamaguchi M, Igarashi Y, Reddy RS, Shiraishi T, Hiramama M (1997) *Tetrahedron* 53:11223
193. Yamaguchi M, Shiraishi T, Igarashi Y, Hiramama M (1994) *Tetrahedron Lett* 35:8233
194. Hanessian S, Shao Z, Betschart C, Rondeau J-M, Neumann U, Tintelnot-Blomley M (2010) *Bioorg Med Chem Lett* 20:1924
195. Hanessian S, Maji DK, Govindan S, Matera R, Tintelnot-Blomley M (2010) *J Org Chem* 75:2861
196. Yu H, Liu M, Han S (2014) *Tetrahedron* 70:8380
197. Shimura M, Iwata M, Omoto S, Sekizawa Y (1979) *Agric Biol Chem* 43:2279
198. Kodama Y, Ito T (1980) *Agric Biol Chem* 44:73

Structure and Synthesis of Conformationally Constrained Molecules Containing Piperazic Acid

Emma L. Handy and Jason K. Sello

Abstract Piperazic acid and its congeners are constituents of many structurally complex natural products. Their conformational rigidity and other advantageous physicochemical properties have motivated the incorporation of these non-proteinogenic amino acids into pharmaceutical agents and drug leads. This review provides an overview of recently published research on piperazic acids, their origins, chemical syntheses, and applications in constrained, biologically active peptides and peptidomimetics.

Keywords Asymmetric α -hydrazination of aldehydes · Aza-Diels–Alder · Peptide mimetics · Piperazic acid · Pyridazine

Contents

1	Introduction	98
2	Biosyntheses of the Piperazic Acids	99
3	Chemical Synthesis of the Piperazic Acids	101
3.1	Aza-Diels–Alder Cycloaddition	101
3.2	Heterocyclization via Tandem Electrophilic Hydrazination/Nucleophilic Displacement	104
3.3	Organocatalytic α -Hydrazination Followed by Heterocyclization	105
3.4	Synthesis of 5-Substituted Piperazic Acids	107
4	Strategies for Syntheses of Peptide Natural Products Containing Piperazic Acid	108
4.1	Acylation of the Reduced Form of Piperazic Acid Followed by Oxidation	108
4.2	Direct Acylation of Piperazic Acid	110
4.3	Acylation of α -Hydrazino Esters Followed by Heterocyclization	112
4.4	Multicomponent Reaction Approach	112
4.5	Synthesis of Peptides with Tandem Piperazic Acids	112

5	Pharmaceutical Agents and Drug Leads Containing Piperazic Acids and Their Syntheses	117
5.1	Cilazapril	118
5.2	Motilin Agonist	119
5.3	Thrombin Inhibitor MOL-376	119
5.4	Pralnacasan	119
5.5	Sangamides	120
5.6	5-Amino-tetrahydropyridazine-3,6-diones	120
6	Conclusion	122
	References	122

1 Introduction

Piperazic acid (Piz) is a non-proteinogenic amino acid characterized by a six-membered ring containing a stable N–N bond. By convention, the α - and β -nitrogen of piperazic acid analogs are referred to as N2 and N1, respectively (Fig. 1). The discovery of piperazic acid was the result of studies of the monamycin peptide natural products, which were isolated from *Streptomyces jamaicensis* in 1959 by Hassall and co-workers [1]. These macrocyclic depsipeptides inhibit the growth of Gram-positive bacteria, including several drug-resistant strains of *Staphylococcus aureus*. Disclosure of the monamycin structures in 1971 [2] marked the first reports of piperazic acid, as well as its 5-hydroxy (γ HOPiz) **3a** and 5-chloro (γ ClPiz) **4a** piperazic acid counterparts (Fig. 1).

Since the discovery of the monamycins, many natural products have been reported that contain piperazic acid and its congeners [3]. These piperazic acid analogs have diverse structures, biological activities, and potential for exploitation in medicine [3]. For example, the luzopeptin cyclic decadepsipeptides have two dehydrohydroxy piperazic acid (HOdhPiz, **3b**) residues and exhibit both antitumor

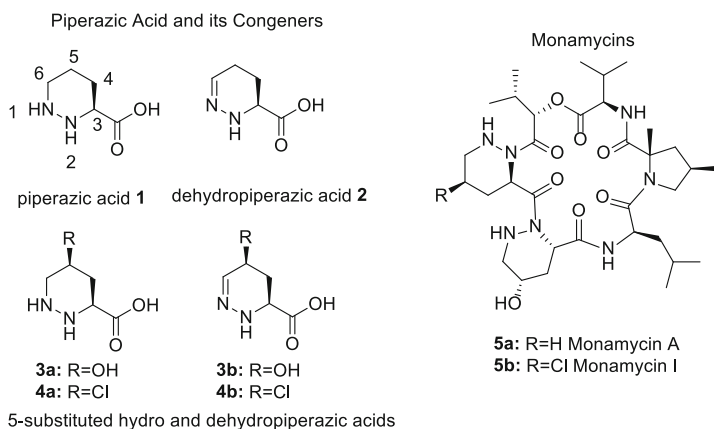


Fig. 1 Structures of piperazic acid, its congeners, and monamycin 5

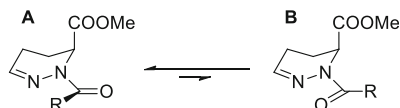


Fig. 2 Piperazine acid conformations

[4] and anti-HIV activity [5]. In contrast, the antrimycins are linear peptide natural products that contain dehydropiperazine acid (dhPiz, **2**) and show antibacterial activity [6].

Piperazine acids may bestow special chemical properties and structural characteristics to peptides, in part because their cyclic structure constrains molecular conformation. Experimental and computational studies indicate that piperazine acid, like proline (Pro) and pipercolic acid (Pip), induces turns in peptides by limiting rotation about the backbone dihedral angles [7]. The dhPiz residue exhibits a greater preference to situate in turn conformations than Pip and Pro (Fig. 2). The *E*-amide isomer *N*-terminal to dhPiz (conformer **A**) is favored over the *Z*-isomer (conformer **B**) in which electrostatic repulsion exists between the carbonyl oxygen and the imino nitrogen [7]. Such properties make dhPiz a promising non-proteinogenic building block for the synthesis of β -turn peptidomimetics.

Their unique structures raise questions about the origins of the piperazine acids and make them challenging targets for chemical synthesis alone and within more complex molecules. In addition to a brief update on biosynthetic studies, an overview of syntheses and applications of the piperazine acids is herein presented with an emphasis on literature published after 2010, because past methods for the synthesis of piperazine acid-containing molecules have been reviewed [3, 8, 9].

2 Biosyntheses of the Piperazine Acids

The mechanism of piperazine acid biosynthesis remains to be completely characterized. Insight into this phenomenon has however emerged from recent studies of the biosynthesis of the kutzneride natural products [10–14]. These actinomycete-derived cyclic depsipeptides have potent antibacterial and antifungal activity. There are nine members of the kutzneride families, each of which contain either a Piz, dhPiz, γ HOPiz, or γ CIPiz residue (Fig. 3) [15].

Biosyntheses of the kutznerides have begun to be elucidated by genetic studies of *Kutzneria* sp. 744. A gene cluster spanning approximately 56 kb has been identified consisting of 29 open reading frames. Seventeen of the gene products have been assigned roles in kutzneride biosynthesis [10]. Within the gene cluster, the *ktzI* gene was shown to encode an enzyme homologous to lysine (Lys) and ornithine (Orn) *N*-hydroxylases, which are responsible for hydroxamic acid formation in siderophore biosynthesis [11]. Considering that no N–O bonds exist in any of the kutznerides, the *ktzI* product was predicted to be involved in the formation of the

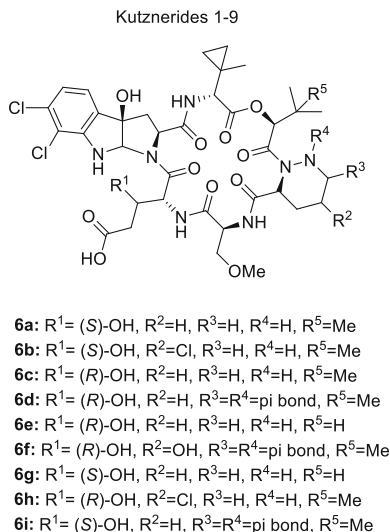
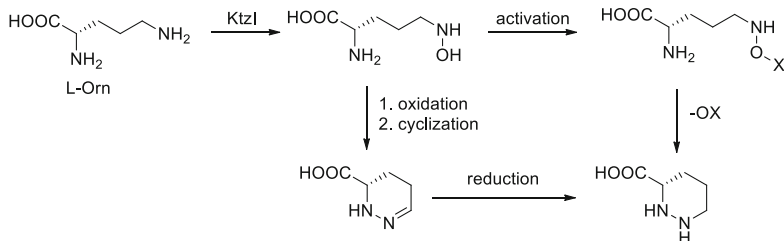


Fig. 3 Structures of the kutzneride natural products



Scheme 1 Possible routes for the biosynthesis of piperazic acid

N–N bond of Piz. Biochemical characterization of purified KtzI confirmed activity as a FAD-dependent *N*-hydroxylase of L-Orn. From stable isotope feeding experiments, ¹³C₅-ornithine and ¹³C₅-*N*-hydroxyornithine were both incorporated into the kutznerides, indicating that KtzI *N*-hydroxylated Orn in an early biosynthetic step to piperazic acid. These results contradicted analogous experiments in which isotopically labeled glutamic acid (Glu) and glutamine (Gln), but not Orn, were incorporated into monamycin and polyoxypeptin [16, 17], suggesting either an alternative pathway for Piz synthesis or that exogenous Orn was not readily taken up by the producing organisms. The steps by which *N*-hydroxyornithine is converted to Piz remain enigmatic because neither spontaneous nor KtzI-mediated cyclization of *N*-hydroxyornithine has been observed [11]. The *N*-hydroxyl group may be activated by phosphorylation or sulfation, or further oxidized to the nitroso counterpart to facilitate cyclization via nucleophilic attack by the α-nitrogen to give respectively Piz or dhPiz (Scheme 1).

Studies of the biosynthetic gene cluster also revealed the origins of the γCIPiz residue in the kutznerides [13]. After determining that none of the three halogenases

(KtzQ, KtzR, KtzD) encoded by the cluster acted on Piz [14], a mononuclear nonheme iron halogenase, named KthP, was found to catalyze regio- and stereo-specific chlorination at C5 of a Piz residue bound via a thioester linkage to the *holo*-thiolation domain, KtzC. The enzyme acted on the fully saturated Piz residue, but not on its activated C4–C5 unsaturated precursor. Although the kutznerides contain (3*S*,5*R*)- γ ClPiz, the product of KthP-catalyzed chlorination was (3*S*,5*S*)- γ ClPiz, suggesting that an epimerization may occur in the biosynthesis of the 5*R*-isomer.

3 Chemical Synthesis of the Piperazic Acids

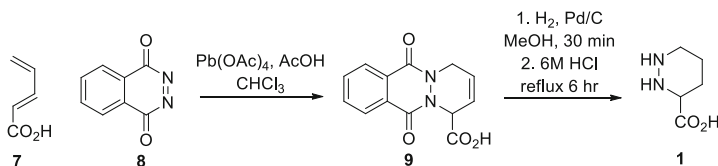
Most syntheses of piperazic acid analogs form the heterocycle via either an aza-Diels–Alder cycloaddition or an intramolecular cyclization of an α -hydrazino carboxylic acid. In the former approach, the challenges have been to control regio- and stereoselectivity. In the latter, formation of the hydrazine precursor with the desired stereochemistry has not been trivial. For both synthetic approaches, the technical challenges have largely been overcome.

3.1 Aza-Diels–Alder Cycloaddition

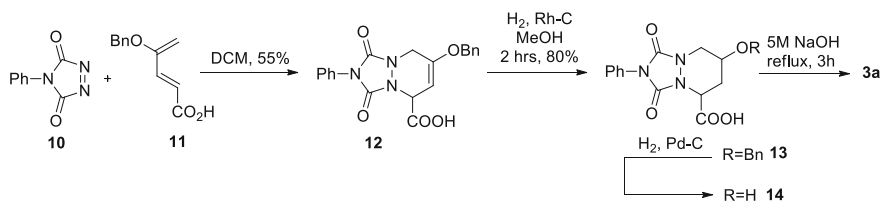
The first reported synthesis of Piz, by Bevan and co-workers in 1971 [18], employed an aza-Diels–Alder cycloaddition of penta-2,4-dienoic acid **7** and phthalohydrazide **8** catalyzed by lead(IV) acetate (Scheme 2). Olefin reduction and acid-catalyzed hydrolysis of the cycloadduct yielded racemic piperazic acid.

Many variations on the aza-Diels–Alder reaction have been reported. For example, the yield was improved when *t*-butyl hypochlorite was used to effect the cycloaddition instead of lead acetate. However, the tendency of the reagent to promote side reactions precluded syntheses of substituted piperazic acids. A cycloaddition in which 4-phenyl-1,2,4-triazoline-3,5-dione **10** was used as the dienophile had a higher yield and could be performed with substituted penta-2,4-dienoic acids (e.g., **11**) to synthesize γ HOPiz (Scheme 3) [19].

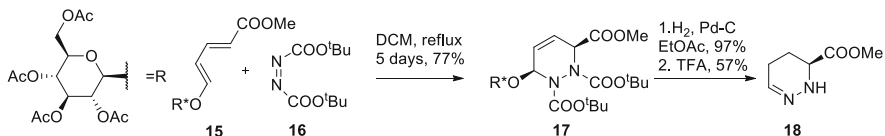
Diastereoselective cycloadditions have been used to produce enantiomerically pure dehydropiperazic acids. For example, the cycloaddition of a diene functionalized with a glucose-derived chiral auxiliary **15** and azodicarboxylate **16**



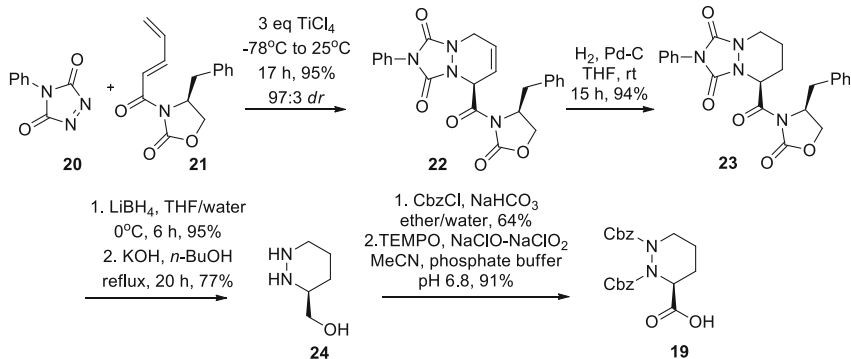
Scheme 2 Aza-Diels–Alder synthesis of racemic D,L-piperazic acid



Scheme 3 Aza-Diels–Alder synthesis of racemic *D,L*-hydroxypiperazic acid



Scheme 4 Diastereoselective synthesis of *dhPiz* via cycloaddition employing a carbohydrate chiral auxiliary

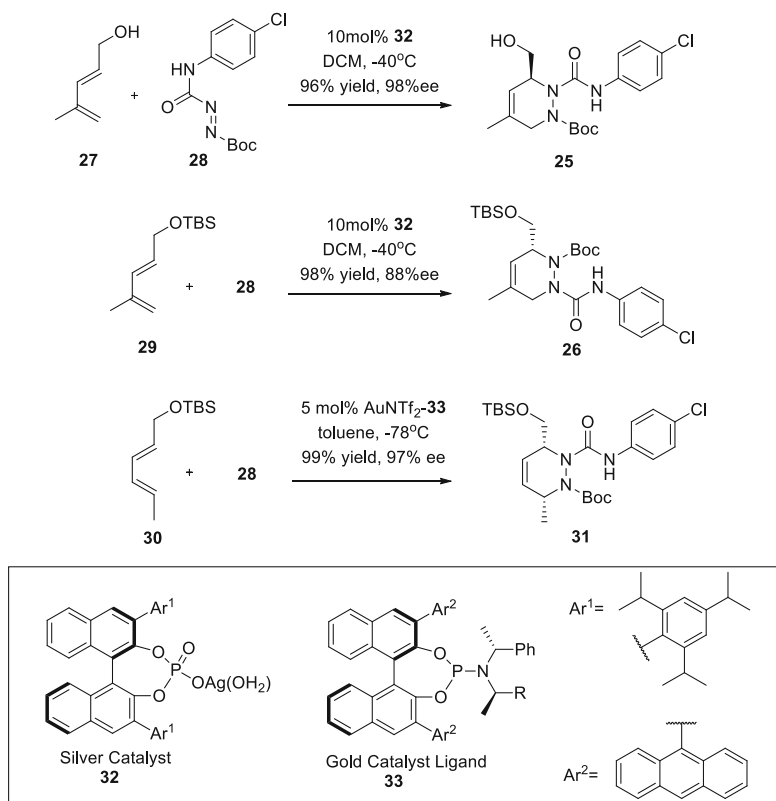


Scheme 5 Diastereoselective Diels–Alder route to *Piz* using oxazolidinone chiral auxiliary

yielded diastereoselectively *dhPiz* **17** (Scheme 4). Subsequent removal of the chiral auxiliary under acidic conditions produced *dhPiz* methyl ester **18** as a single enantiomer [20].

N,N-Di-Cbz-*Piz* **19** was synthesized using a diastereoselective aza-Diels–Alder reaction between 4-phenyltriazoline 3,5-dione **20** and diene **21** possessing a chiral oxazolidinone auxiliary [21, 22] (Scheme 5). Cycloadduct **22** was obtained as a 97:3 mixture of diastereomers in 95% yield. Although the reduction of the double bond was achieved in 94% yield by catalytic hydrogenation, completion of the *Piz* synthesis was circuitous because the conditions for removing the chiral auxiliary necessitated reduction of the carbonyl yielding primary alcohol **24**. The requisite oxidation of the alcohol to the carboxylic acid required protection of the nitrogen atoms with Cbz groups, ultimately yielding protected piperazic acid **19** [22].

Catalytic, enantioselective aza-Diels–Alder reactions have been used to prepare substituted piperazic acid amides [23, 24]. Gold and silver catalysts in complexes with chiral phosphoramidites and phosphates derived from BINOL promoted respectively enantioselective hetero Diels–Alder reactions of diazene dienophiles with various dienes. In the silver phosphate-catalyzed enantioselective hetero Diels–Alder reaction, the presence of a free hydroxy group on the diene could switch the regioselectivity: dienes with free and protected alcohols led respectively to the formation of cycloadducts of types **25** and **26** (Scheme 6). The regioselectivity was explained by formation of a stable complex in which the alcohol of diene **27** was engaged in a hydrogen bond to the oxygen atom of the catalyst's phosphate and coordination to its silver atom. In principle, modification of the resulting alcohol may be used to synthesize various substituted piperazic acid analogs.

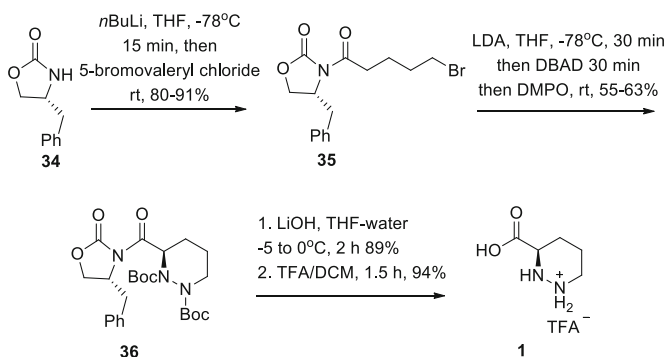


Scheme 6 Enantioselective catalytic hetero Diels–Alder reactions have been catalyzed by silver phosphate and gold phosphoramidite BINOL-derived complexes

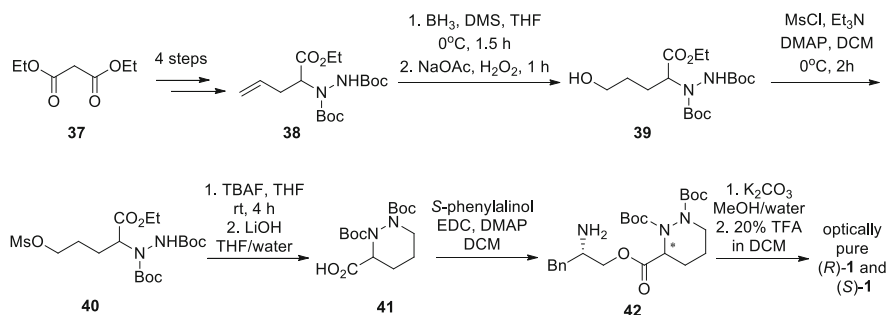
3.2 Heterocyclization via Tandem Electrophilic Hydrazination/Nucleophilic Displacement

Diastereoselective electrophilic hydrazination followed by nucleophilic displacement has provided access to (*R*)-Piz [25]. Acylation of the lithium salt of 4*R*-(benzyl)-2-oxazolidinone **34** with 5-bromovaleryl chloride gave *N*-acyl oxazolidinone **35**, which was treated at -78°C with LDA followed by dibenzylazodicarboxylate (DBAD) and 1,3-dimethyl-3,4,5,6-tetrahydro-2(1*H*)-pyrimidinone (DMPO) to yield protected piperazic amide **36** in 96% diastereoselectivity. The TFA salt of (*R*)-Piz was isolated after saponification of the oxazolidinone auxiliary using LiOH in aqueous THF, followed by removal of the Boc groups using trifluoroacetic acid (Scheme 7). Employing a related γ -benzyloxy analog of oxazolidinone **34**, which was derived from *D*-mannitol, (3*S*,5*S*)- γ HOPiz was prepared by a similar method [26].

Piperazic acid was prepared from a route starting from diethyl malonate (**37**, Scheme 8), which was allylated with allyl bromide and reacted with DBAD to form



Scheme 7 Diastereoselective synthesis of *R*-piperazic acid using an oxazolidinone chiral auxiliary



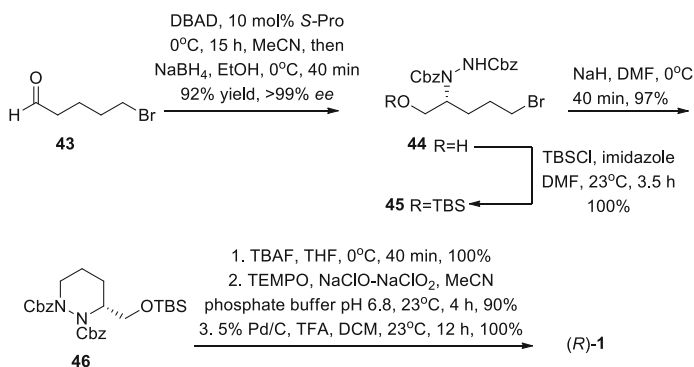
Scheme 8 Synthesis and resolution of Piz from diethyl malonate

the protected hydrazine [27]. Hydroboration and oxidation transformed olefin **38** into alcohol **39** that was subsequently mesylated to effect cyclization. The overall yield of di-Boc-piperazic acid **41** was improved from 16 to 50% by employing dibenzyl and di-*t*-butyl malonate instead of diethyl malonate. Resolution of racemic di-Boc-piperazic acid **41** was achieved by coupling to *S*-phenylalaninol followed by separation of the diastereomeric esters by chromatography. Saponification and removal of the Boc groups provided the TFA salts of (*R*)- and (*S*)-Piz [28].

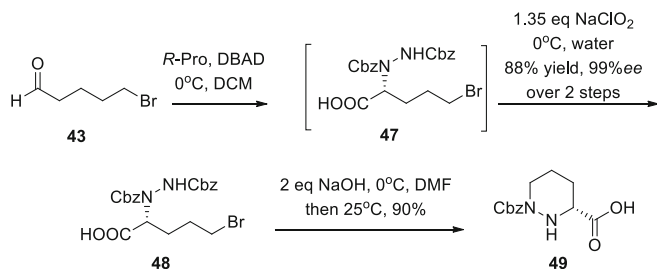
3.3 Organocatalytic α -Hydrazination Followed by Heterocyclization

Routes to *R*- and *S*-piperazic acid that could be scaled up to >50 mmol featured proline-catalyzed asymmetric α -hydrazination of 5-bromopentanal with DBAD (Scheme 9) [29, 30]. Reduction of the aldehyde with NaBH₄ yielded α -hydrazino alcohol **44** in 92% yield with >99% enantioselectivity. Protection of alcohol **44** with TBSCl and sodium hydride-mediated ring closure, silyl ether removal with TBAF, and oxidation of the resulting primary alcohol with TEMPO and NaClO-NaClO₂ yielded (*R*)-di-Cbz-Piz **19**. Employing *R*-Pro in the α -hydrazination step gave similar access to (*S*)-Piz.

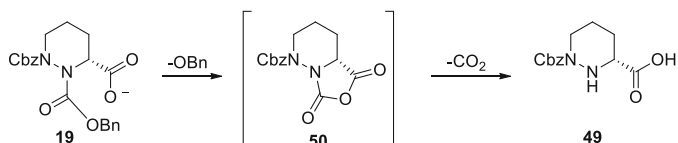
Ma and co-workers reported a scalable modification of this method that could be used to produce the mono-Cbz-protected Piz on a kilogram scale [31]. In this case, pyridazine ring formation and selective deprotection of N2 occur in one pot. After α -hydrazination, aldehyde **47** was oxidized to carboxylic acid **48** using NaClO₂ in 88% yield and >99% *ee* (Scheme 10). Bromo- α -hydrazino acid **48** was treated with hydroxide ion to induce ring closure and removal of the Cbz protection from the 2-position on warming to room temperature before neutralization. At higher temperatures, the α -carboxylate anion reacted with the neighboring N2 carbamate to



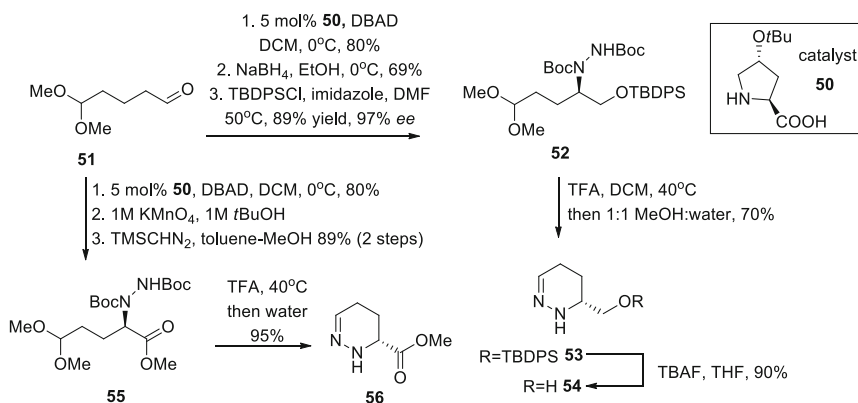
Scheme 9 (*S*)-Proline-catalyzed asymmetric synthesis of *R*-piperazic acid



Scheme 10 Proline-catalyzed asymmetric synthesis of N1-Cbz-Piz acid



Scheme 11 Formation of bicyclic anhydride followed by decarboxylation to yield N1-Cbz-Piz



Scheme 12 *trans*-4-*tert*-Butoxy-L-proline-catalyzed α -hydrazination route to dhPiz methyl ester

yield a bicyclic-ring anhydride. Acid- or base-promoted decarboxylation of the anhydride yielded piperazic acid with the Cbz-protecting group on N1 (Scheme 11).

trans-4-*tert*-Butoxy-L-proline **50** has also been employed as catalyst (5 mol%) in the hydrazination step for the synthesis of dhPiz methyl ester (Scheme 12) [32]. After hydrazination of 5,5-dimethoxy-pentanal **51** with DBAD, the aldehyde was reduced in situ and protected as silyl ether **52**. Acetal and silyl ether cleavage with TFA provided alcohol **54** in 97% *ee* and 69% yield from **52**. Alternatively, the α -hydrazino aldehyde was oxidized with KMnO₄ and esterified to yield α -hydrazino methyl ester **55**. Acetal **55** was treated with TFA to promote

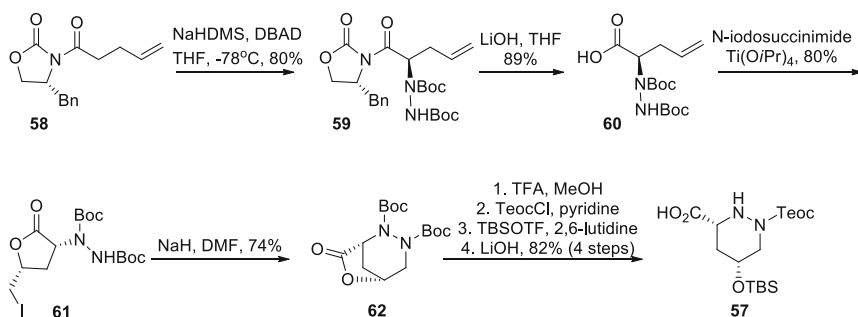
cyclization to dhPiz methyl ester **56**. Piperazic acid derivative **53** was also used as an organocatalyst for hydrazination of **51** in 55% yield and 64% *ee* [32].

3.4 Synthesis of 5-Substituted Piperazic Acids

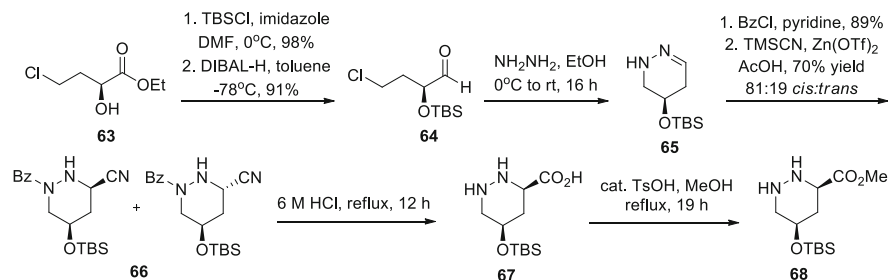
5-Substituted piperazic acids have been synthetic targets due to their presence in natural products. For example, protected γ HOPiz **57** was prepared by a route featuring iodolactonization and iodide displacement, which provided bridgehead bicycle **62** (Scheme 13) [33].

A diastereoselective Strecker reaction on hydrazone **65** provided an 81:19 mixture of *cis/trans* nitriles **66**. Nitrile hydrolysis with aqueous HCl and esterification gave γ HOPiz **68** [34], the synthesis of which was accelerated using microwave irradiation in four key steps (Scheme 14) [35].

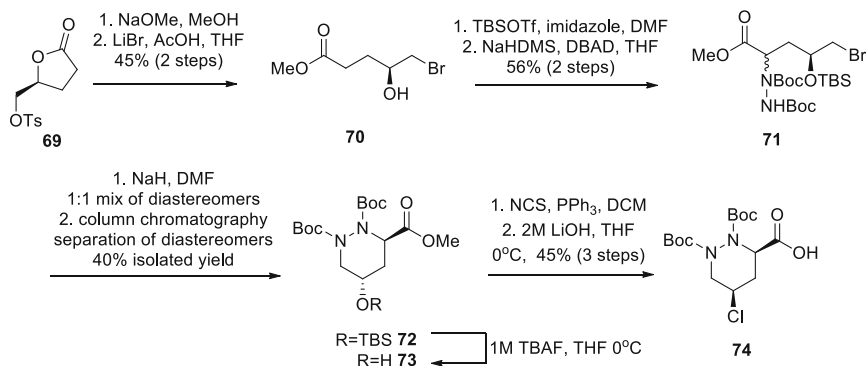
The alcohol of 1,2-di-Boc- γ HOPiz was converted into the corresponding chloride γ CIPiz with inversion of configuration using triphenylphosphine and carbon tetrachloride in acetonitrile [26]. Similarly, after cleavage of silyl ether **72** with TBAF, the alcohol was converted to γ CIPiz **74** using *N*-chlorosuccinimide and triphenylphosphine in dichloromethane (Scheme 15) [36].



Scheme 13 Diastereoselective synthesis of protected γ HOPiz **57**



Scheme 14 Synthesis of protected γ HOPiz **67** by a diastereoselective Strecker reaction



Scheme 15 Diastereoselective syntheses of protected γ HOPiz and γ CIPiz **73** and **74**

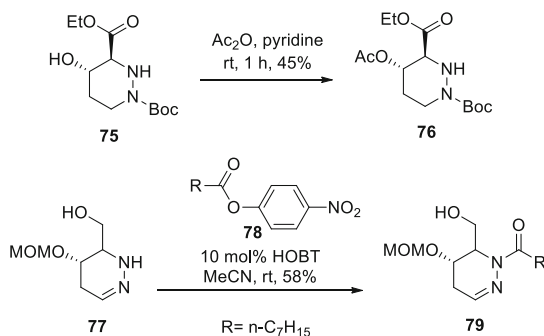
4 Strategies for Syntheses of Peptide Natural Products Containing Piperazic Acid

In most of the known natural products that contain piperazic acid, the N2 position is linked to the peptide backbone. Inconveniently, the N1 position of unprotected Piz is preferentially acylated [8, 37]. Moreover, protection of the N1 nitrogen renders the N2 position difficult to acylate with activated carboxylic acids, such that acyl chlorides are required for acylation [37]. Acylation of dehydro and hydroxy Piz derivatives has also been problematic due to their limited stability under such conditions [39, 40]. By comparison, the reduced hydroxymethyl analog **77** was acylated at the N2 position using 4-nitrophenyl esters and HOBT (Scheme 16) [38]. These observations imply that the problematic acylation of N1 in piperazic acid is likely due to the stereoelectronic effects associated with the neighboring α -carboxylate [38].

Alternative methods have been developed to surmount the poor nucleophilicity of the N2 nitrogen and incorporate piperazic acids into peptides, including acylation of the corresponding hydroxymethyl analogs followed by oxidation, acylation employing reactive acid chlorides, and acylation of α -hydrazino carboxylate derivatives followed by heterocyclization (Fig. 4).

4.1 Acylation of the Reduced Form of Piperazic Acid Followed by Oxidation

Application of the reduced form of N1-protected piperazic acid as a building block in the acylation of N2 followed by oxidation of the primary alcohol to the carboxylic acid, has been used in the total syntheses of the padanamides [41]. These linear



Scheme 16 Attempted and successful acylation at the N2 position of hydroxypiperazic acid **75** and hydroxymethyl counterpart **77**, respectively

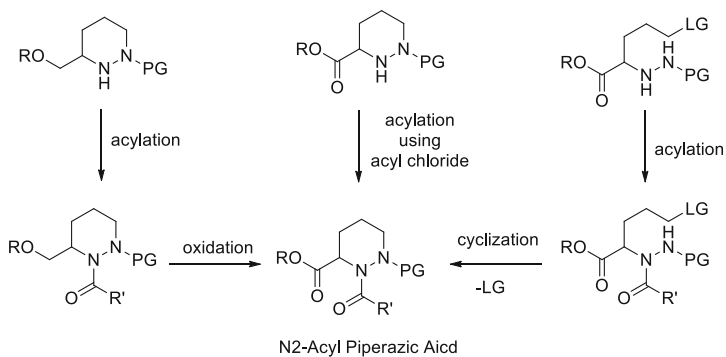


Fig. 4 Common routes to N2-acyl piperazic acid derivatives. *LG* leaving group, *PG* protecting group

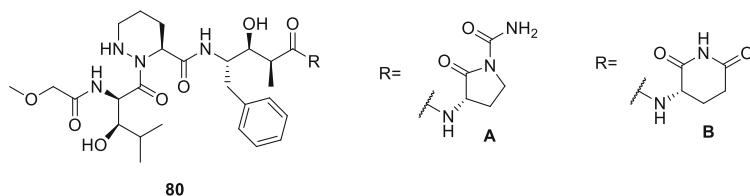
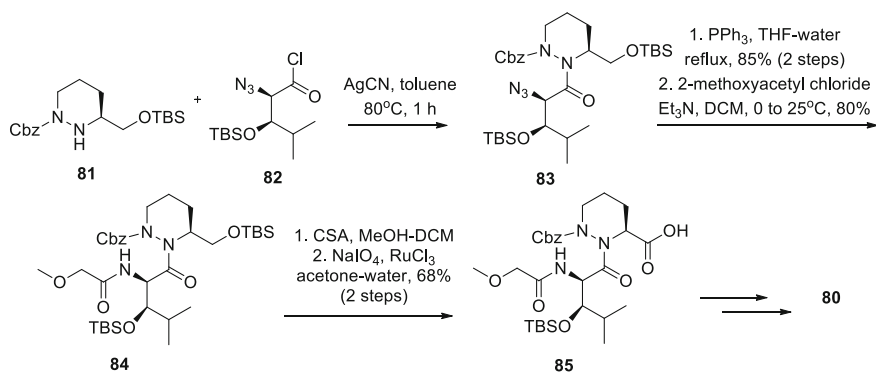


Fig. 5 Structure of padanamides A and B

tetrapeptides (padanamides A and B) were isolated from a *Streptomyces sp* found in marine sediment near Papua New Guinea and differ only in the identity of their C-terminal residue (Fig. 5) [42]. Padanamide B was found to be cytotoxic to Jurkat cells, but its mechanism has yet to be elucidated. Mechanistic studies of padamide A in *Saccharomyces cerevisiae* suggest it inhibits cysteine and methionine biosynthesis in eukaryotes [42].



Scheme 17 Installation of the Piz residue in the padanamides

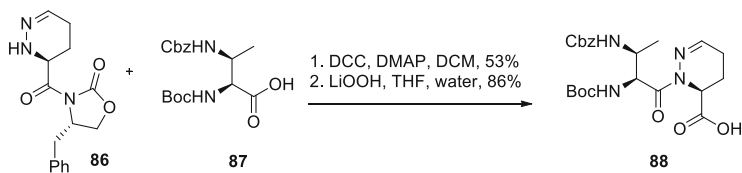
In the total syntheses of the padanamides [41], a TBS-protected form of the reduced piperazic acid was used as a building block to circumvent the reactivity issues of the N2 nitrogen (Scheme 17). After acylation of the N2 position of silyl ether **81** with an acid chloride **82**, the primary alcohol was desilylated and then oxidized to the carboxylic acid **85** with NaIO_4 and catalytic RuCl_3 .

4.2 Direct Acylation of Piperazic Acid

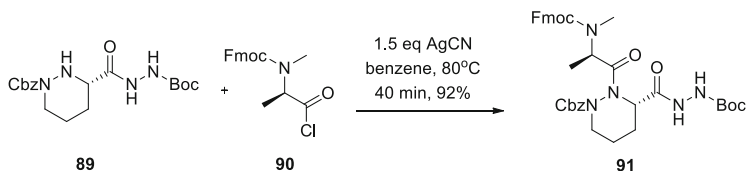
In spite of its poor nucleophilicity, the N2 nitrogen of piperazic acid analogs has been acylated in syntheses of peptide natural products. For example, dhPiz **86** was coupled to amino acid **87** using DCC and DMAP in 53% yield in the total synthesis of antrimyacin (Scheme 18) [43].

Although many standard reagents have failed in the coupling of Piz and dhPiz analogs with N-protected amino acids [8, 37, 39], the reaction of N-protected amino acid chlorides and N1-protected piperazic acid analogs in the presence of silver cyanide has successfully given piperazic acid analogs with acyl groups on the N2 nitrogen [33, 44–46]. For instance, as part of syntheses of azinothricin and kettapeptin [44], Cbz-Piz derivative **89** was coupled to *N*-Fmoc-*N*-methylalanine acid chloride (**90**) with AgCN in a 92% yield (Scheme 19).

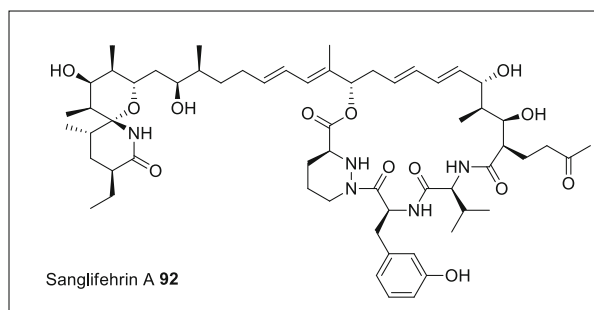
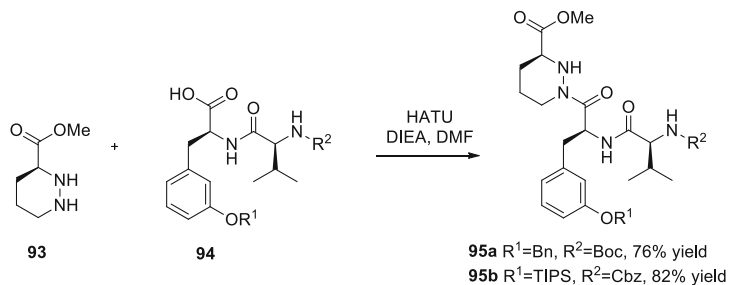
On the other hand, sanglifehrin A (**92**) has a piperazic acid residue that is acylated on the N1 rather than the N2 nitrogen. Identified in a screen for small molecules that bound cyclophilin A, sanglifehrin A is a macrolide that has 20-fold greater affinity for cyclophilin A than the currently marketed immunosuppressive drug cyclosporin A [47, 48]. Total and partial syntheses of sanglifehrin A have taken advantage of the greater reactivity of the N1 over the N2 nitrogen toward acylation, avoiding protection of the latter during coupling reactions with uronium



Scheme 18 DCC-mediated acylation of dhPiz **86** in the total synthesis of antrimycin

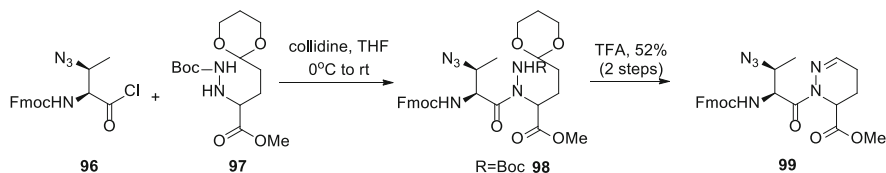


Scheme 19 Silver cyanide-mediated coupling of Cbz-Piz **89** with acyl chloride **90**



Scheme 20 Regioselective N1 acylation of methyl piperazate toward the synthesis of sanglifehrin A

and carbodiimide reagents [49–52]. For example, methyl piperazate (**93**) was respectively coupled to Boc- and Cbz-Phe(*m*-OBn)-Val-OH (**94**) using 1-[bis(dimethylamino)methylene]-1H-1,2,3-triazolo[4,5-b]pyridinium-3-oxide hexafluorophosphate (HATU) in 76% and 82% yields (Scheme 20) [51, 52].



Scheme 21 Formation of dhPiz **99** after acylation of the N2 nitrogen

4.3 Acylation of α -Hydrazino Esters Followed by Heterocyclization

The third strategy that is used commonly for incorporation of piperazic acid into peptide chains for natural product synthesis entails forming the pyridazine ring after acylation of the appropriate nitrogen atom [39, 53–55]. After acylation of the N2 nitrogen of protected hydrazine **96**, dhPiz **99** was synthesized by unmasking acetal **98** using trifluoroacetic acid with concomitant Boc group removal [39] (Scheme 21). Reduction of dhPiz to Piz has been achieved using both NaCNBH_3 in AcOH-MeOH [40] and H_2 and PtO_2 [56].

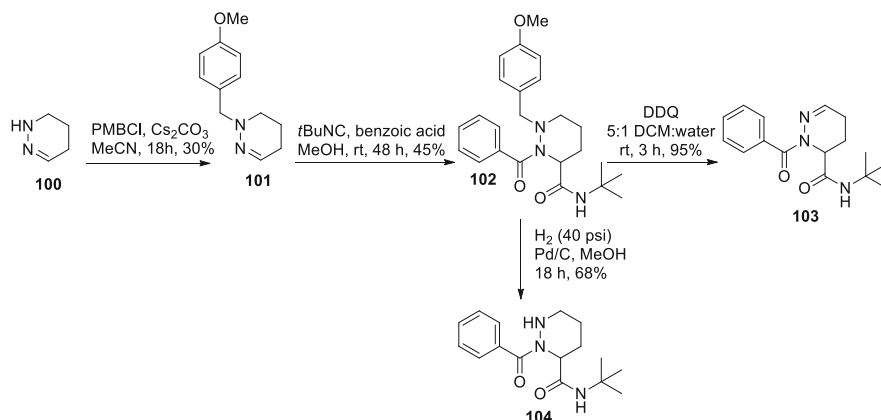
4.4 Multicomponent Reaction Approach

Sello and co-workers have reported an alternative approach for the synthesis of peptides containing piperazic acid, which features a multicomponent reaction that is analogous to the Joullié–Ugi reaction [57]. *N*-*p*-Methoxybenzyl–2,4,5,6-tetrahydropyridazine **101** was condensed with benzoic acid and *tert*-butyl isocyanide to yield *N*-acyl piperazamide **102** (Scheme 22). The *p*-methoxybenzyl N1 substituent was advantageous because it enhanced reactivity of N2 and was removed using both oxidative and reductive conditions to access respectively dhPiz and Piz residues **103** and **104**. The multicomponent strategy has been used to prepare dipeptides and tripeptides containing piperazic acid without stereoselectivity, but the diastereomeric products have been readily separated by chromatography.

4.5 Synthesis of Peptides with Tandem Piperazic Acids

Many natural products contain adjacent Piz residues, and the syntheses of these moieties require special considerations (Fig. 6).

Chloptosin (**107**) was isolated from *Streptomyces* species MK498-98F14 culture broth [58]. Natural product **107** induces apoptotic activity in apoptotic-resistant human pancreatic adenocarcinoma cells, inhibits the growth of Gram-positive



Scheme 22 Multicomponent reaction synthesis of N2-acyl Piz **104** and dhPiz **103**

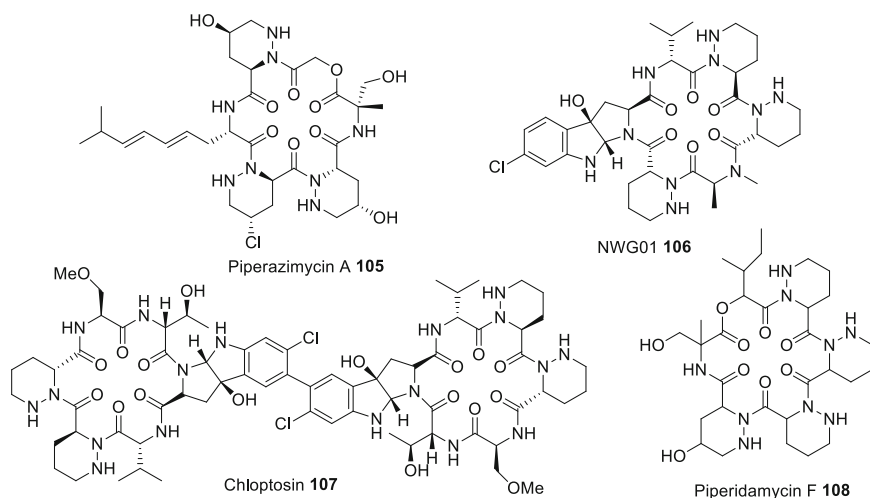
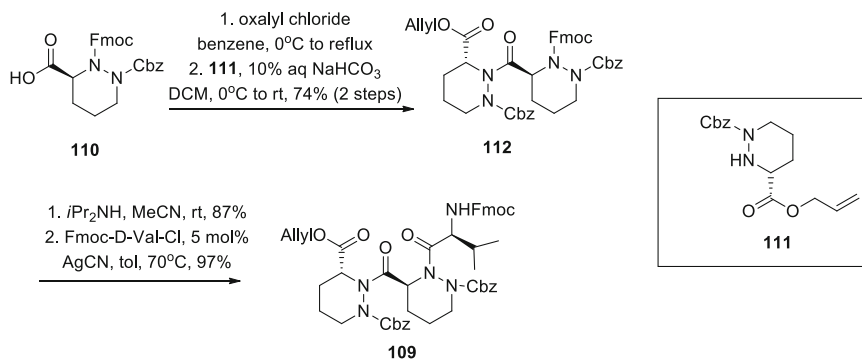


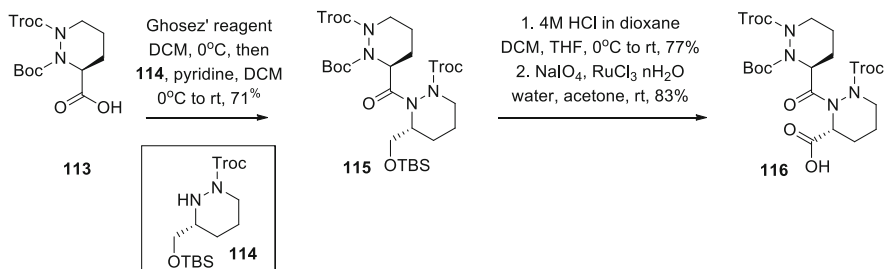
Fig. 6 Representative natural products containing adjacent Piz residues

bacteria, and has a high LD₅₀ value in mice. In one total synthesis of the dimeric cyclic peptide [45], the Piz dipeptide **109** was assembled by the coupling of the acyl chloride derived from Fmoc-Piz(N1-Cbz)-OH (**110**) and H-Piz(N1-Cbz)-*O*-allyl (**111**) in 74% yield [45]. After removal of the Fmoc group from dipeptide **112**, Fmoc-Val-Cl was coupled to the N2 nitrogen in the presence of silver cyanide in 97% yield (Scheme 23).

Alternatively, piperazic acyl chloride derived from Piz **113** was coupled to silyl ether **114** to produce dipeptide **115**, which after liberation and oxidation of the primary alcohol with RuCl₃ and NaIO₄ gave dipeptide acid **116** that was subsequently coupled to allyl *O*-methyl serinate (Scheme 24) [59, 60].



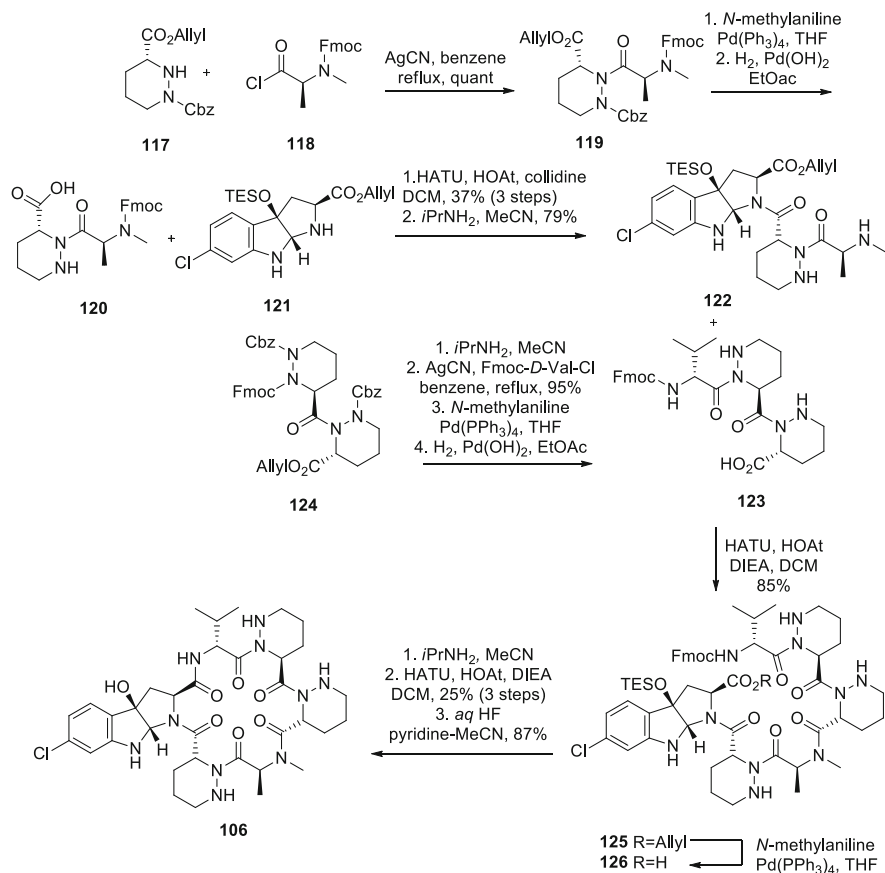
Scheme 23 Synthesis and acylation of piperazic acid dipeptide **109**



Scheme 24 Synthesis of piperazic acid dipeptide, **116**

The cyclic hexadepsipeptide NWG01 contains three Piz residues, two of which are adjacent to each other [61, 62]. Isolated from a broth of *Streptomyces albidoflavus*, NWG01 exhibited potent antibacterial activity against Gram-positive bacteria, including methicillin-resistant *Staphylococcus aureus*. The stereochemistry of the Piz residue adjacent to the pyrroloindoline was originally reported to be *R*, but revised later to be *S* [63]. The revision of stereochemistry was later validated by total syntheses of both epimers [64] in which the diastereoselective hydrazination–cyclization method was used to prepare the Piz residues [25]. Acylation of allyl piperazate **117** with *N*-Fmoc-*N*-methyl-alanine acid chloride and AgCN gave dipeptide **119**, which, after removal of the allyl and Cbz groups, was coupled to pyrroloindoline **121** to afford fragment **122**. Fragment **122** was then coupled to tripeptide **123** [45] using HATU and HOAt in 91% yield [64]. Prior to coupling tripeptide **123**, the Cbz groups were removed because the chlorine atom in the pyrroloindoline moiety did not survive under hydrogenolytic deprotection conditions. The lower nucleophilicity of the N1 nitrogen of tripeptide **123** and aniline of pyrroloindoline **121** was key to the successful acylation of the pyrrolidine moiety (Scheme 25).

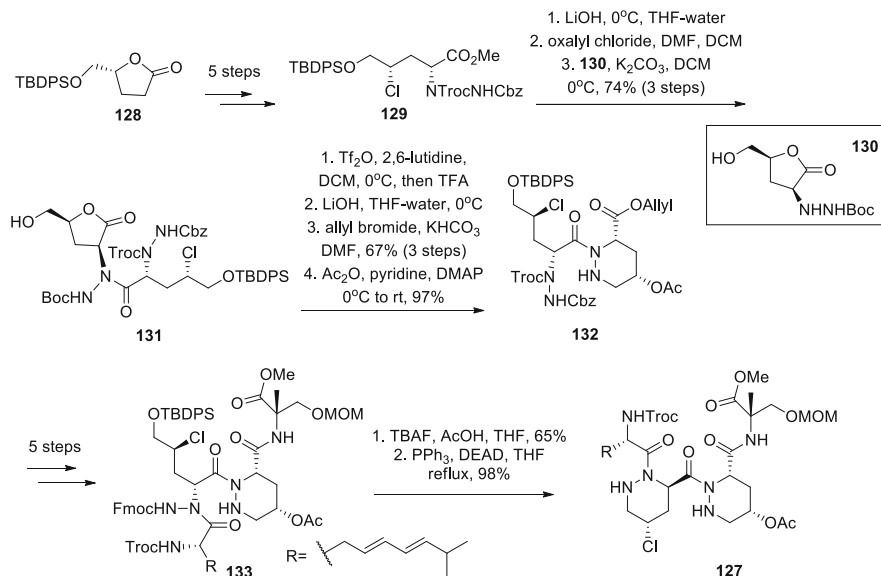
Piperazimycin A (**105**) was isolated from a broth of *Streptomyces* species cultivated from marine sediment near Guam and exhibited in vitro toxicity toward



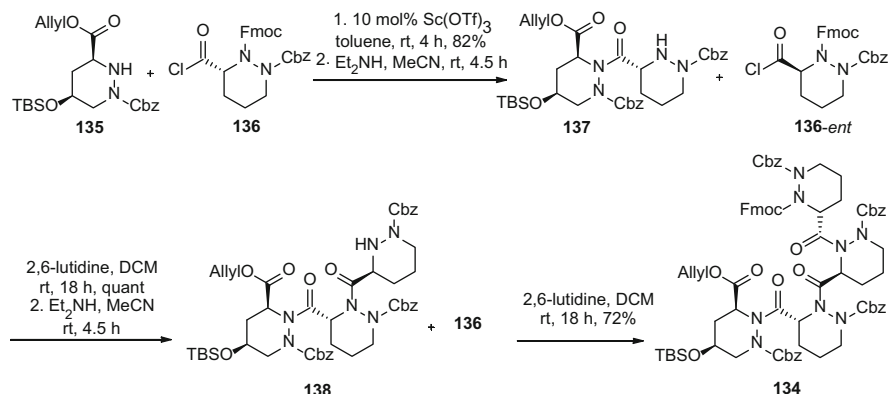
Scheme 25 Total synthesis of NWG01

multiple tumor cell lines [65]. Cyclic hexadepsipeptide **105** contains two γ HOPiz residues, one of which is adjacent to a γ CIPiz residue. The synthesis of the γ CIPiz- γ HOPiz dipeptide proved challenging using common coupling agents [36, 66]. Activation of bis-Boc γ CIPiz as the acid chloride with tetramethylchloroformamidinium hexafluorophosphate (TCFH) and in situ acylation of *N*¹-Teoc-*O*-TBS-Piz methyl ester did provide in 62% yield the corresponding dipeptide, albeit subsequent elaboration was unsuccessful. Instead of coupling to substituted Piz residues, tetrapeptide **127** was prepared by a strategy featuring acylations of hydrazines followed by cyclizations (Scheme 26). In the formation of the second pyridazine by intramolecular *N*-alkylation, initial attempts failed to remove the Fmoc group. However, a route in which deprotection of the alcohol by cleavage of silyl ether **133** with TBAF, followed by cyclization and Fmoc removal under Mitsunobu conditions, provided the desired compound **127** quantitatively [66].

Piperidamycin is an antibacterial cyclohexadepsipeptide natural product that contains four adjacent piperazic acid residues [67]. Although no synthesis of piperidamycin has been reported to date, the tetra-Piz peptide moiety was prepared

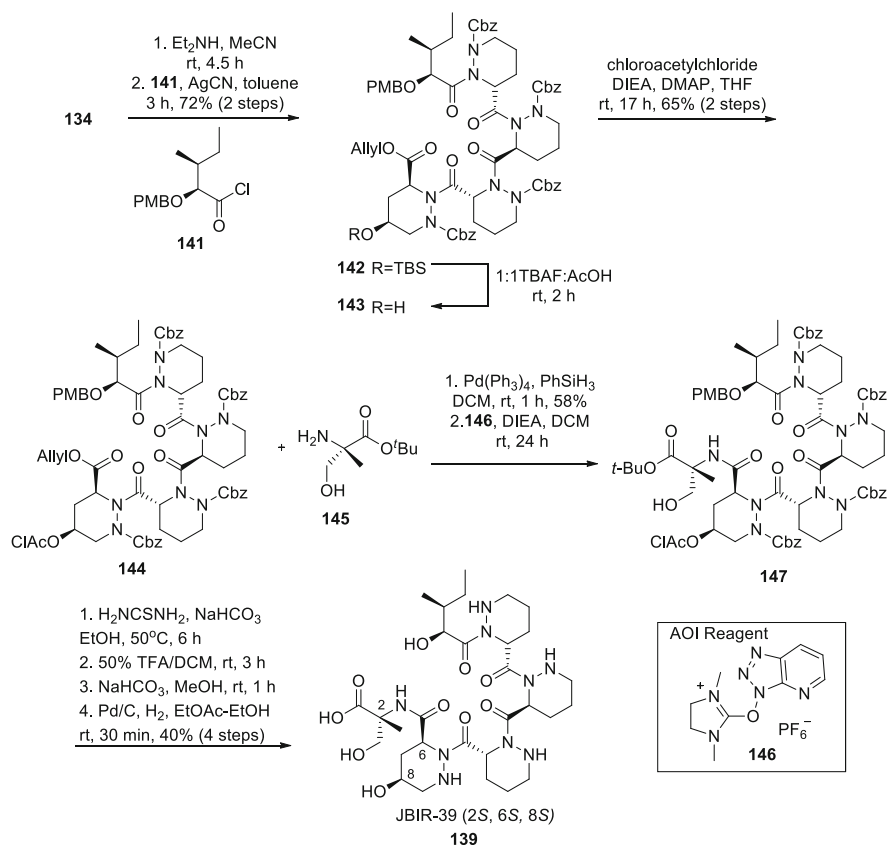


Scheme 26 Synthesis of tetrapeptide **127** in the total synthesis of piperazimycin



Scheme 27 Synthesis of tetra-piperazic acid peptide **134**

as part of the total synthesis of JBIR-39 [68, 69]. Prior to this achievement, there had been no reports of syntheses of tri- nor tetra-Piz peptides. Acid chloride derivatives of Piz were employed in the synthesis; however, low yields and racemization of the α -carbon plagued attempts to couple on the weakly nucleophilic N₂ nitrogen of the γ HOPiz. The application of 10 mol % of Sc(OTf)₃ in the coupling step enabled synthesis of γ HOPiz-Piz dipeptide **137** in 82% yield and with less than 5% epimerization (Scheme 27). Similar conditions proved useful for coupling γ HOPiz to other sterically hindered amino acyl chlorides [69]. Iterative Fmoc deprotections and couplings of N¹-Cbz-N²-Fmoc-piperazic acid chlorides in the absence of the scandium catalyst afforded tetra-Piz peptide **134** in 59% overall yield from **135**.



Scheme 28 Synthesis of JBIR-39

As mentioned, tetrapeptide **134** was used in the total synthesis of JBIR-39 (Scheme 28). To assemble the hexapeptide **139**, pentapeptide **144** was coupled to *R*- α -methylserine *tert*-butyl ester using (7-azabenzotriazol-1-yloxy)tripyrrolidino-phosphonium hexafluorophosphate (AOI reagent, **146**). Prior to coupling, the protection of the γ HOPiz residue hydroxyl group was changed from TBS to chloroacetyl to prevent alcohol predilection and lactonization [69]. The synthesis and comparisons with the spectral data from four diastereomeric hexapeptides led to the unequivocal assignment of the absolute stereochemistry of the natural product [69].

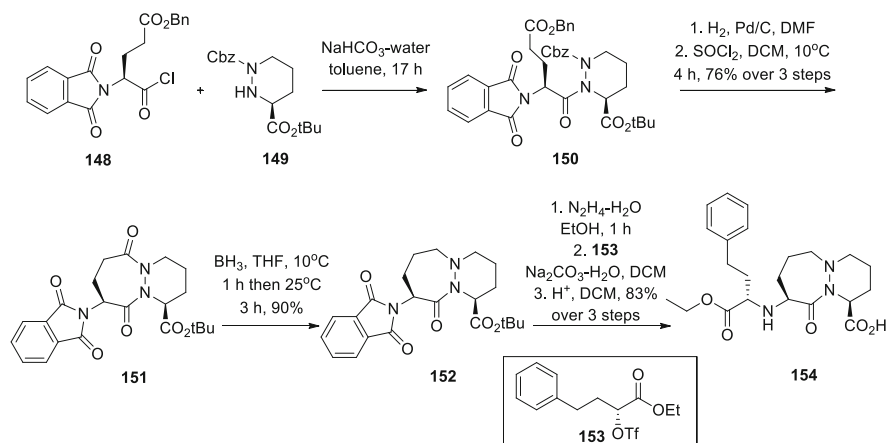
5 Pharmaceutical Agents and Drug Leads Containing Piperazic Acids and Their Syntheses

Piperazic acids have been used as peptide mimetics in several potent pharmaceutical compounds, in part because of their structural rigidity.

5.1 Cilazapril

Cilazapril is marketed for the treatment of hypertension and congestive heart failure. An inhibitor of angiotensin-converting enzyme (ACE) that modulates the renin–angiotensin system, cilazapril contains a bicyclic structure featuring a piperazine acid moiety fused to a seven-membered α -amino lactam. A prodrug that is hydrolyzed to the corresponding dicarboxylate metabolite, cilazapril was designed to achieve three interactions with the active site of ACE: the piperazine acid carboxylate forms a salt bridge with a cationic side chain, the lactam carbonyl accepts a hydrogen bond donor, and the *N*-terminal carboxylate coordinates to the active site Zn ion [70]. In comparisons with other fused ring systems, the 7,6-bicyclic analog exhibited the greatest inhibitor potency and was further developed into cilazapril [71–73].

In the synthesis of cilazapril (**154**), *tert*-butyl *N*¹-Cbz-piperazate was acylated with phthalimide-protected glutamic acid chloride **148** [73]. After hydrogenolytic removal of the benzyl ester, the carboxylate derivative of **150** was converted into the corresponding acid chloride using thionyl chloride to achieve annulation on the N1 nitrogen and form the 7 membered lactam. Selective reduction of the less crowded carbonyl adjacent to the N1 nitrogen was achieved using borane. Phthalimide **151** was deprotected with aqueous hydrazine, and the Zn-binding moiety, ethyl-phenyl butanoate, was introduced by S_N2 displacement of triflate **153** with inversion of configuration (Scheme 29). Bicyclic core structures **151** and **152** were subsequently employed as rigid dipeptide mimetics in the study of the molecular features of ligand binding to major histocompatibility complex class II molecules [74].



Scheme 29 Cilazapril synthesis

5.2 Motilin Agonist

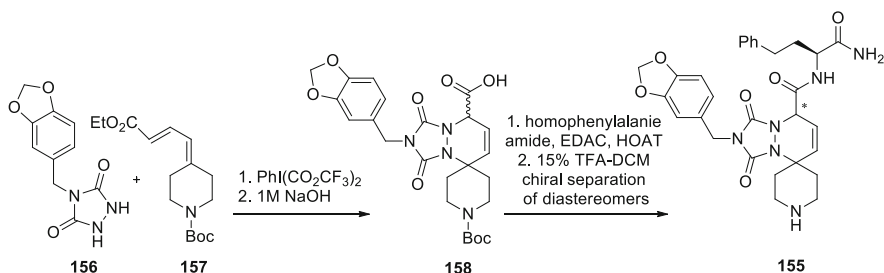
A high-throughput screen of a library of compounds led to the identification of motilin agonist **155** (EC_{50} of 660 nM) containing a piperazic acid bicyclic structure that was synthesized via a [4+2] cycloaddition (Scheme 30) [75].

5.3 Thrombin Inhibitor MOL-376

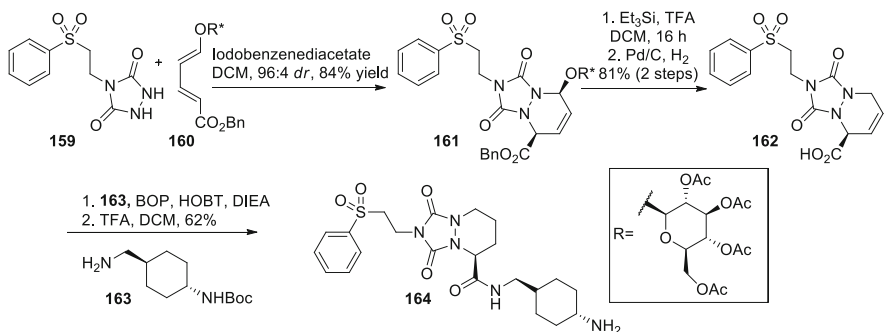
The thrombin inhibitor MOL 376 was developed as a β -strand mimetic. The related potent saturated analog **164** was synthesized by a route employing a glucose-derived chiral auxiliary attached to diene **160** in a diastereoselective aza-Diels-Alder cycloaddition (Scheme 31) [76].

5.4 Pralnacasan

Pralnacasan (**165**, Fig. 7) is an inhibitor of interleukin 1- β converting enzyme that exhibited efficacy in a murine model of osteoarthritis [77–80], but failed in clinical



Scheme 30 Synthesis of motilin agonist containing a bicyclic Piz moiety



Scheme 31 Diastereoselective synthesis of saturated analog **164** of MOL 376

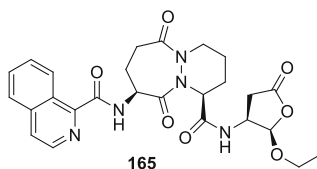


Fig. 7 Pralnacasan

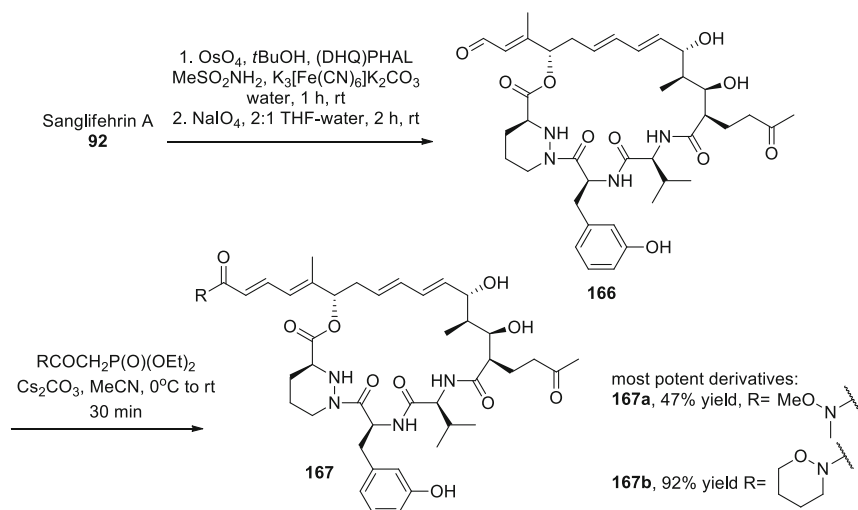
trials as an anti-inflammatory drug candidate [81]. The piperazic acid 7,6-bicyclic peptidomimetic structure of pralnacasan was synthesized by a similar approach as described for cilazapril (Scheme 29). In addition, a MCR route to the piperazic moiety was used to prepare the bicyclic core structure of pralnacasan (Scheme 22) [57].

5.5 Sangamides

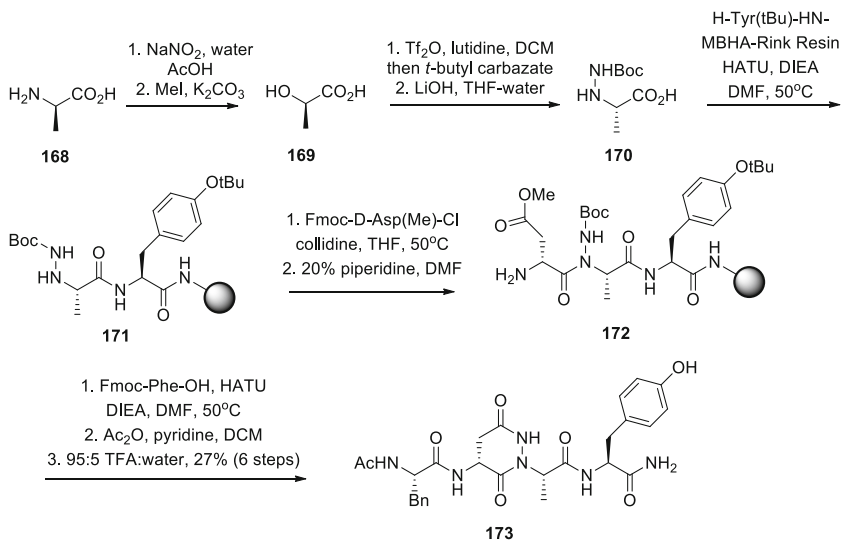
In addition to their immunosuppressive activity, the sanglifehrin natural products were found to have antiviral activity against hepatitis C virus (HCV). The so-called sangamides (**167**) were obtained by cleavage of the aliphatic portion of the natural product from the macrocycle, and retained HCV inhibitory activity, but were no longer immunosuppressive [82]. Truncated analogs **166** were synthesized from natural product **92** by enantioselective dihydroxylation, oxidative cleavage, and Horner–Wadsworth–Emmons coupling to a variety of α -amidophosphonates. Although hydroxamate **167a** was the most potent of the sangamide analogs, tetrahydro-2*H*-1,2-oxazinide **167b** had superior pharmacological properties (Scheme 32).

5.6 5-Amino-tetrahydropyridazine-3,6-diones

5-Amino-tetrahydropyridazine-3,6-diones are close analogs of the piperazic acids also having a N–N bond. They have been explored as structures that could restrict rotation of a peptide backbone, and thus stabilize secondary structures like extended β -strands and β -turns. Recently, Del Valle and co-workers incorporated 5-amino-tetrahydropyridazine-3,6-diones into fifteen different peptides by a solid-phase route (Scheme 33) [83]. In analogy to the piperazic acids, the substrate for the heterocyclization was an acylhydrazine.



Scheme 32 Synthesis of sangamides (**167**) from sanglifehrin A (**92**)



Scheme 33 Solid-phase synthesis of peptide mimetics with tetrahydropyridazidone scaffold using alanine as starting building block

6 Conclusion

Compounds containing piperazic acids include natural products, pharmaceutical agents, and peptidomimetics. Piperazic acid increases conformational rigidity in peptide structures due to a combination of ring constraint and stereoelectronic effects from the hydrazine moiety. The emergence of efficient methods for the synthesis of piperazic acid analogs as well as their insertion into peptides and natural products, bears well for the future application of these heterocyclic amino acids as probes of biological mechanisms of action and as scaffolds for drug discovery.

References

1. Hassall CH, Magnus KE (1959) *Nature* 184:1223
2. Hassall CH, Ogihara Y, Thomas WA (1971) *J Chem Soc* 1971:522
3. Oelke AJ, France DJ, Hofmann T, Wuitschik G, Ley SV (2011) *Nat Prod Rep* 28:1445
4. Rose WC, Schurig JE, Huftalen JB, Bradner WT (1983) *Cancer Res* 43:1504
5. Inouye Y, Take Y, Nakamura S, Nakashima H, Yamamoto N, Kawaguchi H (1987) *J Antibiotics* 50:100
6. Shimada N, Morimoto K, Naganawa H, Takita T, Hamada M, Maeda K, Takeuchi T, Umezawa H (1981) *J Antibiotics* 34:1615
7. Xi N, Alemany LB, Ciufolini MA (1998) *J Am Chem Soc* 120:80
8. Ciufolini MA, Xi N (1998) *Chem Soc Rev* 27:437
9. Kuchenthal CH, Maison W (2010) *Synthesis* 5:719
10. Fujimori DG, Hrvatin S, Neumann CS, Strieker M, Marahiel MA, Wash CT (2007) *Proc Natl Acad Sci U S A* 104:16498
11. Neumann CS, Jiang W, Heemstra JR, Gontang EA, Kolter R, Walsh CT (2012) *ChemBioChem* 13:972
12. Setser JW, Heemstra JR, Walsh CT, Drennan CL (2014) *Biochemistry* 53:6063
13. Jiang W, Heemstra JR, Forseth RR, Neumann CS, Manaviazar S, Schroeder FC, Hale KJ, Walsh CT (2011) *Biochemistry* 50:6063
14. Heemstra JR, Walsh CT (2008) *J Am Chem Soc* 130:14024
15. Pohanka A, Menkis A, Levenfors J, Broberg A (2006) *J Nat Prod* 69:1776
16. Arroyo V, Hall MJ, Hassal CH, Yamasaki K (1976) *J Chem Soc Chem Commun* 1976:845
17. Umezawa K, Ikeda Y, Kawase O, Naganawa H, Kondo S (2001) *J Chem Soc Perkin Trans 1*:1550
18. Bevan K, Davies JS, Hassall CH, Morton RB, Phillips DAS (1971) *J Chem Soc C* 1971:514
19. Davies CR, Davies JS (1976) *J Chem Soc Perkin Trans 1*:2390
20. Aspinall IH, Cowley PM, Mitchell G, Stoodley RJ (1993) *J Chem Soc Chem Commun* 1993:1179
21. Evans DA, Chapman KT, Hung TD, Kawaguchi AT (1987) *Angew Chem Int Ed* 11:1184
22. Makino K, Henmi Y, Terasawa M, Hara O, Hamada Y (2004) *Tetrahedron Lett* 46:555
23. Liu B, Li K-N, Luo S-W, Huang J-Z, Pang H, Gong L-Z (2013) *J Am Chem Soc* 135:3323
24. Liu B, Liu T-Y, Luo S-W, Gong L-Z (2014) *Org Lett* 16:6164
25. Hale KJ, Delisser VM, Manaviazar S (1992) *Tetrahedron Lett* 33:7613
26. Hale KJ, Jogiya N, Manaviazar S (1998) *Tetrahedron Lett* 39:7163
27. Duttgupta I, Goswami K, Sinha S (2012) *Tetrahedron* 68:8347
28. Duttgupta I, Goswami K, Chatla P, Sinha S (2014) *Synth Comm* 44:2510

29. List B (2002) *J Am Chem Soc* 124:5656
30. Henmi Y, Makino K, Yoshitomi Y, Hara O, Hamada Y (2004) *Tetrahedron Asymm* 15:3477
31. Chen Y, Lu Y, Zou Q, Chen H, Ma D (2013) *Org Proc Res Dev* 17:1209
32. Kalch D, Youcef RA, Moreau X, Thomassigny C, Greck C (2010) *Tetrahedron Assymetry* 21:2302
33. Kamenecka TM, Danishevksy SJ (1998) *Angew Chem Int Ed* 37:2995
34. Makino K, Jiang H, Suzuki T, Hamada Y (2006) *Tetrahedron Asymmetry* 17:1644
35. Kennedy JP, Brogan JT, Lindsley CW (2008) *Tetrahedron Lett* 49:4116
36. Kennedy JP, Lindsley CW (2010) *Tetrahedron Lett* 51:2493
37. Hassall CH, Johnson WH, Theobald CJ (1979) *J Chem Soc Perkin Trans* 1:1451
38. Ciufolini MA, Shimizu T, Swaminathan S, Xi N (1997) *Tetrahedron Lett* 28:4947
39. Schmidt U, Riedl B (1992) *J Chem Soc Chem Commun* 1992:1187
40. Ciufolini MA, Xi N (1994) *J Chem Soc Chem Commun* 1994:1867
41. Long B, Tang S, Chen L, Qu S, Chen B, Liu L, Maguire AR, Wang Z, Liu Y, Zhang H, Xu Z, Ye T (2013) *Chem Commun* 49:2977
42. Andrusiak K, Deshpande R, Myers CL, Piotrowski JS, Boone C, Yoshida M, Andersen RJ (2011) *Org Lett* 13:3936
43. Nakamura Y, Ito A, Shin C (1994) *Bull Chem Soc Jpn* 67:2151
44. Hale KJ, Manaviyar S, George JH, Walters MA, Dalby SM (2009) *Org Lett* 11:733
45. Yu SM, Hong WX, Wu Y, Zhong CL, Yao ZJ (2010) *Org Lett* 12:1124
46. Kamenecka TM, Danishevsky SJ (1998) *Angew Chem Int Ed* 37:2997
47. Sanglier JJ, Quesniaux V, Fehr T, Hofmann H, Mahnke M, Memmert K, Schuler W, Zenke G, Gschwind L, Maurer C, Schilling W (1999) *J Antibiot* 52:466
48. Fehr T, Kallen J, Oberer L, Sanglier JJ, Schilling W (1999) *J Antibiot* 52:474
49. Nicolaou KC, Murphy F, Barluenga S, Ohshima T, Wei H, Xu J, Gray DLF, Baudoin O (2000) *J Am Chem Soc* 122:3830
50. Paquette LA, Duan M, Konetski I, Kempmann C (2002) *J Am Chem Soc* 124:4257
51. Radhika L, Chandrasekhar S (2014) *Synth Commun* 44:3602
52. White JD, Suttisintong K (2013) *J Org Chem* 78:2757
53. Boger DL, Ledebauer MW, Kume M, Searcey M, Lin Q (1999) *J Am Chem Soc* 121:11375
54. Boger DL, Ledebauer MW, Kume M (1999) *J Am Chem Soc* 121:1098
55. Boger DL, Ledebauer MW, Kume M, Lin Q (1999) *Angew Chem Int Ed* 38:2424
56. Ciufolini MA, Valognes D, Xi N (2000) *Angew Chem Int Ed* 39:2493
57. Handy EL, Totaro KA, Lin CP, Sello JK (2014) *Org Lett* 16:3488
58. Umezawa K, Ikeda Y, Uchihato Y, Naganawa H, Kondo S (2000) *J Org Chem* 65:459
59. Oelke AJ, Antonietti F, Bertone L, Cranwell PB, France DJ, Goss RJM, Hofmann T, Knauer S, Moss SJ, Skelton PC, Turner RM, Wuitshick G, Ley SV (2011) *Chem Eur J* 17:4183
60. Oelke AJ, France DJ, Hofmann T, Wuitshick G, Ley SV (2010) *Angew Chem Int Ed* 49:6139
61. Guo Z, Shen L, Ji Z, Zhang J, Huang L, Wu W (2009) *J Antibiot* 62:201
62. Guo Z, Ji Z, Zhang J, Deng J, Shen L, Liu W, Wu W (2010) *J Antibiot* 63:231
63. Guo Z, Ji Z, Zhang J, Deng J, Shen L, Liu W, Wu W (2010) *J Antibiot* 63:733
64. Shibahara S, Matsubara T, Takahashi K, Ishihara J, Hatakeyama S (2011) *Org Lett* 13:4700
65. Miller ED, Kauffman CA, Jensen PR, Fenical W (2007) *J Org Chem* 72:323
66. Li W, Gan J, Ma D (2009) *Angew Chem Int Ed* 48:8891
67. Hosaka T, Ohnishi-Kameyama M, Muramatsu H, Murakami I, Tsurumi Y, Kodani S, Yoshida M, Fujie A, Ochi K (2009) *Nat Biotechnol* 27:462
68. Kozono I, Izumikawa M, Motohashi K, Nagai A, Yoshida M, Doi T, Takagi M, Shin-ya K (2011) *J Mar Sci Res Dev* 1:101
69. Yoshida M, Sekioka N, Izumikawa M, Kozono I, Takagi M, Shin-ya K, Doi T (2015) *Chem Eur J* 21:3031
70. Attwood MR (1989) *Br J Clin Pharmacol* 27:133S
71. Hassall CH, Kröhn A, Moody CJ, Thomas WA (1984) *J Chem Soc Perkin Trans* 1:155

72. Attwood MR, Francis RJ, Hassall CH, Kröhn A, Lawton G, Natoff IL, Nixon JS, Redshaw S, Thomas WA (1984) *FEBS Lett* 165:201
73. Attwood MR, Hassall CH, Kröhn A, Lawton G, Redshaw S (1986) *J Chem Soc Perkin Trans 1*:1011
74. Bolin DR, Swain AL, Sarabu R, Berthel SJ, Gillepsie P, Huby NJS, Makofske R, Orzechowski L, Perrotta A, Toth K, Cooper JP, Jiang N, Falcioni F, Campbell R, Cox D, Gaizband D, Belunis CJ, Vidovic D, Ito K, Crowther R, Kammlott U, Zhang X, Palermo R, Weber D, Guenot J, Nagy Z, Olson GL (2000) *J Med Chem* 43:2135
75. Li JJ, Chao H-G, Wang H, Tino JA, Lawrence RM, Ewing WR, Ma Z, Yan M, Slusarchyk D, Seethala R, Sun H, Li D, Burford NT, Stoffel RH, Salyan ME, Li CY, Witkus M, Zhao N, Rich A, Gordon DA (2004) *J Med Chem* 47:1704
76. Matthew J, Farber K, Nakanishi H, Qabar M (2003) *Tetrahedron Lett* 44:583
77. Dolle RE, Prasad CVC, Prouty CP, Salvino JM, Awad MMA, Schmidt SJ, Hoyer D, Ross TM, Graybill TL, Speier GJ, Uhl J, Miller BE, Heaszek CT, Ator MA (1997) *J Med Chem* 40:1941
78. Rudolphi K, Gerwin N, Verzij N, Van der Kraan P, Van den Berg W (2003) *OsteoArthritis Cartilage* 11:738
79. Roubidoux, ALC, Wilson JD, Dieterich P, Storer N, Leonardi S (2004) US Patent 06,703,500
80. Chen MH, Goel OP, Hyun JW, Magano J, Rubin JR (1999) *Bioorg Med Chem Lett* 9:1587
81. MacKenzie SH, Schipper JL, Clark AC (2010) *Curr Opin Drug Discov Devel* 13:568
82. Moss SJ, Bobardt M, Leyssen P, Coates N, Chattergi U, Dejian X, Foster T, Liu J, Nur-e-Alam M, Suthar D, Yongsheng C, Warneck T, Zhang M-Q, Neyts J, Gallay P, Wilkinson B, Gregory MA (2012) *Med Chem Comm* 3:944
83. Kang CW, Ranatunga S, Sarnowski MP, Del Valle JR (2014) *Org Lett* 16:5434

Aminolactam, *N*-Aminoimidazolone, and *N*-Aminoimidazolidinone Peptide Mimics

Daniel J. St-Cyr, Yésica García-Ramos, Ngoc-Duc Doan,
and William D. Lubell

Abstract Among strategies for constraining peptide conformation, the application of 3-amino- γ -lactam (Agl) analogs, the so-called Freidinger-Veber lactams, has played a prominent role in studies of biologically active peptide conformation. Tethering an amino acid side chain to the nitrogen of its neighboring C-terminal residue within a peptide, such lactams constrain backbone ψ - and ω -dihedral angles, as well as side chain χ -torsion angles to induce turn conformation. Reviewing various α -amino lactam analogs as well as their aza-counterparts, the so-called *N*-amino imidazolinone (Nai) and *N*-amino imidazolidinone (Aid) residues, this chapter focuses specifically on the synthesis, conformational analysis, and applications of the 5-membered ring congeners and their variants bearing ring substituents.

D.J. St-Cyr

Département de Chimie, Université de Montréal, C.P. 6128, Succursale Centre-Ville,
Montreal, QC, Canada, H3C 3J7
Institute for Research in Immunology and Cancer, Université de Montréal, Pavillon Marcelle-
Coutu, 2950 chemin de Polytechnique, Montreal, QC, Canada, H3T 1J4

Y. García-Ramos

Département de Chimie, Université de Montréal, C.P. 6128, Succursale Centre-Ville,
Montreal, QC, Canada, H3C 3J7
NuChem Therapeutics Inc., 6100 Royalmount Ave, Montreal, QC, Canada, H4P 2R2

N.-D. Doan

Département de Chimie, Université de Montréal, C.P. 6128, Succursale Centre-Ville,
Montreal, QC, Canada, H3C 3J7
Department of Chemistry, Massachusetts Institute of Technology, 77 Massachusetts Ave,
Cambridge, MA 02139, USA

W.D. Lubell (✉)

Département de Chimie, Université de Montréal, C.P. 6128, Succursale Centre-Ville,
Montreal, QC, Canada, H3C 3J7
e-mail: william.lubell@umontreal.ca

Keywords Amino-imidazolidinone • Amino-imidazolinone • Amino-lactam • Azabicycloalkanone • Azapeptide • Conformation • Dipeptide mimic • Interleukin-1 • Medicinal chemistry • Peptidomimetic

Contents

1	Introduction	126
2	3-Amino- γ -Lactam Peptidomimetic Synthesis, Conformation, and Applications	130
2.1	α -Amino- γ -Lactam Peptides with 5-Position Substituents	132
2.2	α -Amino- γ -Lactam Peptides with 4-Position Substituents	136
2.3	α -Amino- γ -Lactam Peptides with 3-Position Substituents	141
2.4	α -Amino- γ -Lactam Peptides with Multiple Substituents	146
2.5	Conformational Analysis of Substituted α -Amino- γ -Lactam Peptides	150
3	<i>N</i> -Amino-Imidazolin-2-one (Nai) and <i>N</i> -Amino-Imidazolidin-2-one (Aid) Peptidomimetics: Synthesis and Conformational Analysis	154
3.1	Synthesis of Nai Dipeptides with 4-Position Substituents	155
3.2	Synthesis of Nai Dipeptides with 5-Position Substituents	158
3.3	Synthesis of <i>N</i> -Amino-Imidazolidin-2-one (Aid) Peptidomimetics	160
3.4	Conformational Analysis of Nai and Aid Peptides	165
4	Conclusions	168
	References	168

1 Introduction

The science of peptide mimicry employs the power of synthetic chemistry to address questions in various fields, including biology, catalysis, and materials science. Peptidomimetics are valuable tools because they are capable of unlocking the potential inherent in peptide structures for different applications, particularly in medicine, in which they have served to improve potency, selectivity, and pharmacokinetic properties [1–4]. The utility of techniques for peptide mimicry has grown proportionately with the advent of modern design methods for enhancing peptide viability as drugs and chemical probes [5–7]. Modified peptide structures can now be assembled by biological approaches which harness cells to introduce unnatural amino acids by post-translational modifications [8], selective pressure [9], and site-specific incorporation [10–12]. Moreover, combinatorial macrocyclic peptide libraries have been accessed by random nonstandard peptide integrated discovery (RaPID) [13] and split-intein circular ligation of peptides and proteins (SICLOPPS) [14]. The advent of such novel synthetic methodology has revealed a new horizon for exploring peptide mimicry to benefit an expanding array of synergistic opportunities [15].

Templates for peptide mimicry are frequently derived from protein substructures and endogenous peptides [16–19]. For example, the RGD motif recognized by the integrin receptors has provided fertile ground for the development of potent peptidomimetic antagonists [20–22]. Numerous peptides involved in the secretory pathway, such as somatostatin, angiotensin, and substance P, have been leveraged

through peptide mimicry to develop G protein-coupled receptor (GPCR) modulators [23–25]. Moreover, intracellular peptide targets, the functional roles of which may be poised for reassessment [26], offer new vistas for peptidomimetic design.

Interest in peptidomimetics as compelling synthetic targets was galvanized in 1980 by the Merck Sharp and Dohme Research Laboratories team led by Roger Freidinger, Daniel Veber, and Ralph Hirschmann [23, 27, 28]. In particular, investigation of luteinizing hormone-releasing hormone led to the application of an α -amino γ -lactam (a so-called Freidinger-Veber lactam, **1.2**, Fig. 1) to enable constraint about the Gly-Leu residue in mimic **1.1** [27]. The latter exhibited 8.9-fold improved potency in a pituitary cell culture assay, demonstrating by a synthetic analog that the activity of the parent peptide was manifested by a β -turn conformation.

Freidinger-Veber lactams have since inspired the development of diverse analogs (Fig. 2) [24, 34–40], many of which are discussed in other sections of this treatise. For example, 3,4-dihydropyridin-2-ones **1.3** and 5,6-dehydro ϵ -lactam **1.4** were conveniently accessed, respectively, by multicomponent reaction approaches and ring closing metathesis (RCM) [29, 30]. Highly constrained bicyclic and spirocyclic lactam dipeptide mimics in **1.5** and **1.6** have also been deployed to promote β -turn and β -hairpin conformations [31, 32, 41]. In addition, the

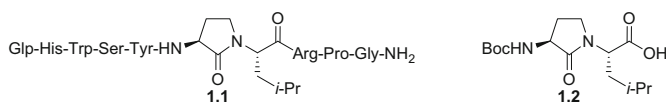


Fig. 1 Peptide mimicry using Freidinger-Veber lactams [27]

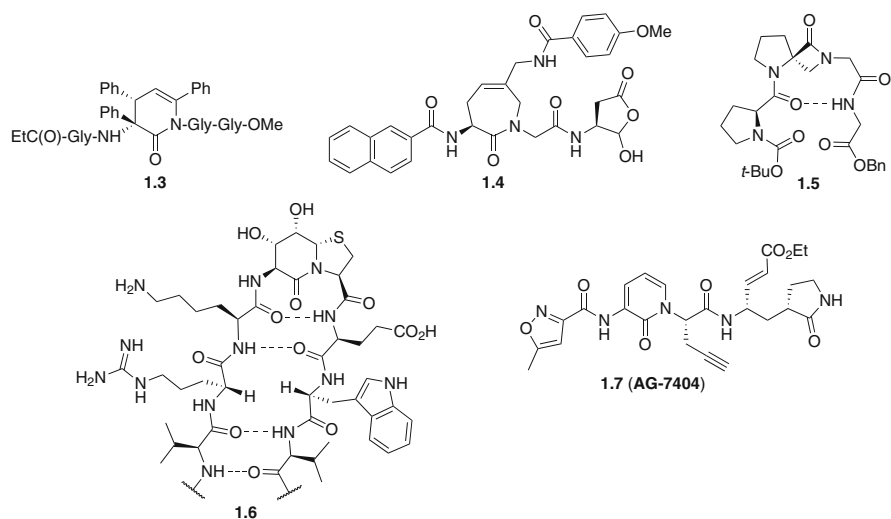


Fig. 2 Structural diversity of 3-amino lactams and related congeners [29–33]

irreversible 3C protease inhibitor 3-amino-2-pyridone **1.7** (AG-7404) was developed as an orally bioavailable analog of AG-7088 (Rupintrivir) by lactam substitution of a flexible ketone motif and subsequently evaluated in clinic for treatment of Rhinovirus infection [33, 42].

Although the original Freidinger-Veber lactams (e.g., **1.1** and **1.2**) featured a simple alkyl chain bridge, substituted lactams have been prepared to offer greater structural and conformational diversity. Various substituted 3-aminolactam scaffolds have been exploited in bioactive molecules from diverse origins. For example, antibiotics such as Loracarbef (**1.8**) were derived from fungal natural products (Fig. 3) [43, 48, 49]. The antihypertensive drug Gemopatrilat (**1.9**) originated from an initial medicinal chemistry strategy involving lactam-constraint [44, 50, 51]. For improved rheumatoid arthritis therapy, tumor necrosis factor- α -converting enzyme (TACE) inhibitor BMS-561392 (**1.10**, a.k.a. DPC-333) was developed, tested in phase II clinical trials, and abandoned due to liver toxicity [45]. During the development of “second mitochondria-derived activator of caspases” (SMAC) mimetics for use as anticancer agents [52], bicyclic ϵ -lactam SM83 (**1.11**) was demonstrated to exhibit synergy with the “TNF-related apoptosis inducing ligand” (TRAIL) protein in an ovarian carcinoma mouse model [46]. Olcegepant is a peptidomimetic agonist of calcitonin gene-related peptide (CGRP) receptor that has shown efficacy in phase II clinical trials [47, 53]. Oral bioavailability was achieved using the caprolactam-based alternative, Telcegepant. To improve the anticipated clinical dose of the latter, augment solubility, and reduce plasma protein binding, imidazole amide isosteres were pursued in conjunction with peripheral modifications to afford the imidazo[1,2-a]azepine derivative, MK-2918 (**1.12**).

Heteroatom substitution in Freidinger-Veber lactams has imparted advantages to enhance synthetic accessibility and conformational constraint (Fig. 4). For example, rhodium-catalyzed anti-Markovnikov hydroformylation of Boc-threoninyl-allylglycine methyl ester led to an adipate-6-semialdehyde intermediate which underwent acid-catalyzed cyclization to afford 5-oxa-1-azabicyclo[4.4.0]decane **1.13** [54]. 6-Oxa-1-azabicyclo[5.3.0]decane **1.14** is a potent “Inhibitor of Apoptosis

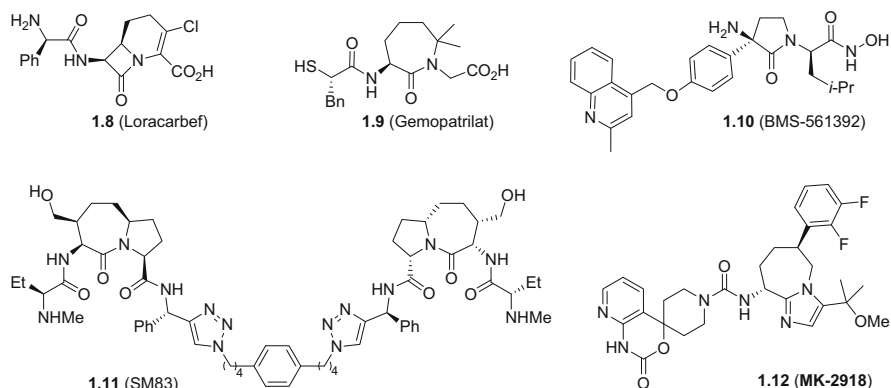


Fig. 3 Bioactive substituted 3-aminolactam peptidomimetics [43–47]

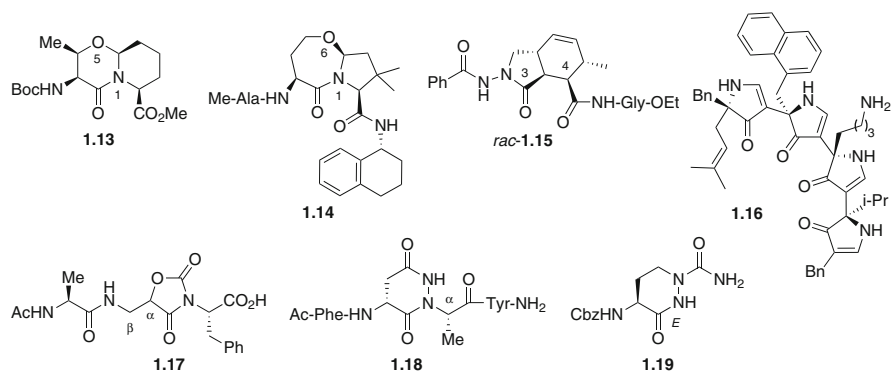


Fig. 4 Oxa- and aza-variants of Freidinger-Veber lactams [54–60]

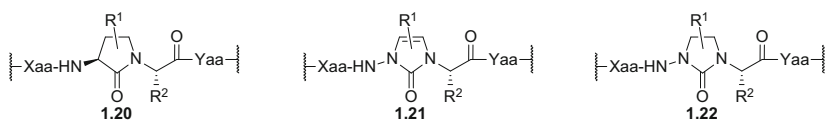


Fig. 5 Compound classes reviewed in this chapter (L-isomers shown)

Protein” (IAP) antagonist which was rapidly accessed using an Ugi reaction of an isocyanotetrahydronaphthalene, Boc-homoserine, ammonia, and a succinaldehyde dimethyl acetal [55].

Bicyclic γ -lactam tetrapeptide mimic **1.15** was synthesized from a *N*-(Boc-amino)-3-oxo-isindole-4-carboxylate intermediate that was obtained by a Diels-Alder cycloaddition involving maleic anhydride and a hexa-2,4-dienylhydrazine [56]. The vinylogous lactam analog, terapyrrolinone **1.16** was designed to mimic the curvature of cyclohexapeptide L-363,301, a potent somatostatin receptor agonist, and synthesized by an iterative method [57].

Solid-supported peptides bearing α -hydroxy- β -amino- and α -hydrazino acid residues respectively underwent regioselective *O,N*- and *N,N'*-acylation using *N,N'*-disuccinimidyl carbonate and D-aspartic acid chloride β -methyl ester as bis-electrophiles to afford oxazolidin-2,4-dione- and tetrahydropyridazine-3,6-dione-constrained mimetics **1.17** and **1.18** [58, 59]. Aza-lactam **1.19** was designed to mimic a dipeptide possessing a *cis* (*E*) amide bond [60].

As illustrated by the many examples above, Freidinger-Veber lactams and their substituted variants represent a vast class of peptidomimetics. This chapter will thus be narrowly focused on the synthesis, conformational analysis, and bioactivity of three classes of Freidinger-Veber lactam analogs: substituted 3-amino- γ -lactams **1.20**, *N*-aminoimidazolinones **1.21** and *N*-aminoimidazolidinones **1.22** (Fig. 5). These three classes of heterocyclic analogs offer different utility for the synthesis of peptidomimetics to explore the orientation of side chain relative to backbone function with stringent precision, as well as to assemble effectively libraries of

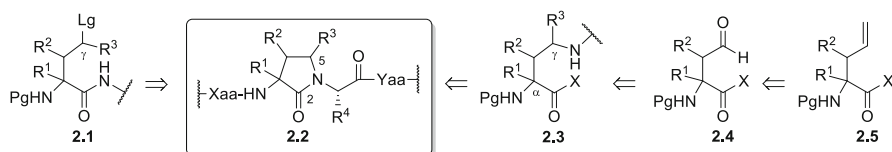
analogues in which conformational constraint is systematically moved along the peptide sequence to identify turn conformations relevant for activity [34].

2 3-Amino- γ -Lactam Peptidomimetic Synthesis, Conformation, and Applications

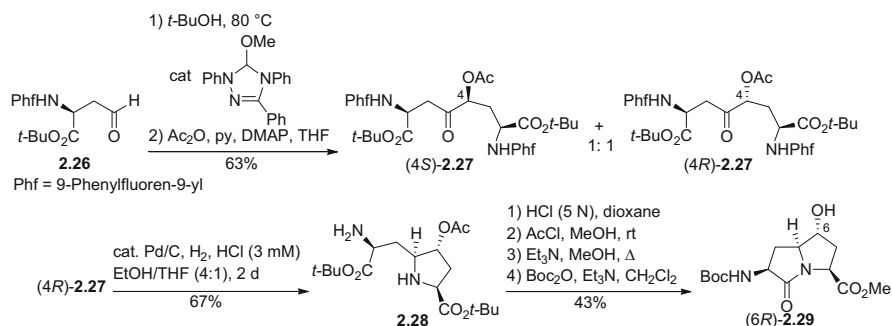
Among methods for synthesizing γ -lactams [61, 62], several have enabled the synthesis of α -amino- γ -lactam (Agl) variants **2.2**, which have proven useful for peptide mimicry (Scheme 1) [24, 34, 36, 37, 40, 63, 64]. For example, the Agl synthesis reported by Freidinger and Veber has been adapted such that the annulation of α -amino amide intermediate **2.1** (Lg = Me₂S⁺) has produced γ -lactams bearing ring substituents (Scheme 12). Although formation of the N-C5 bond by activation of the γ -alcohol **2.1** (Lg = OH) led to *O*-alkylated imidate side product [66, 67], γ -lactam synthesis was achieved from other linear precursors **2.1** bearing alternative electrophiles at the γ -carbon such as aldehydes and ketones (e.g., Scheme 14) [66, 69–78], acetals (Scheme 21) [80], and iodonium ions (Scheme 22). Moreover, ring closure of **2.1** (Lg = H) has been achieved by methods featuring metal-catalyzed C-H bond activation (e.g., Scheme 10).

Substituted γ -lactams are commonly synthesized by reductive amination of aspartate β -semialdehyde **2.4** to generate α,γ -diamino carboxylate **2.3** that undergoes subsequent ring closure by formation of the N-C2 bond. Allylglycine derivatives **2.5** have frequently served as precursors to aldehydes **2.4** in routes that exploit orthogonal alkene oxidation reactions (Schemes 13, 18, and 20) and avoid formation of the γ -lactone side product often encountered using homoserine intermediates [85, 86]. Diastereoselective alkylation has provided access to α,α -disubstituted amino acids **2.5** in enantiopure form (Schemes 12 and 13). Substituted γ -lactam scope has also been expanded by using analogs of amino acid intermediates **2.4**, which harbor various γ -position functional groups such as ketones and ketimines (Scheme 2) [89, 90], Michael acceptors (Scheme 7) [95], and epoxides (Scheme 8) [98].

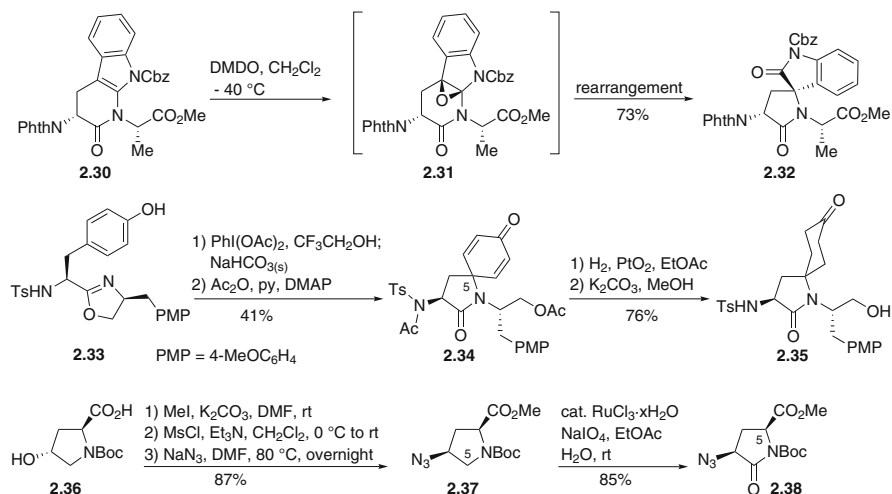
Lactam dipeptide building blocks have often been incorporated into longer peptide sequences (e.g., Schemes 7 and 12). Solid-supported synthesis has been employed to expedite efforts for γ -lactam diversification (e.g., Schemes 8, 19, and 21), including methods which enable the oxidative conversion of alkene **2.5** into aldehyde **2.4** on solid phase [99, 101].



Scheme 1 Common synthetic approaches to substituted α -amino- γ -lactam peptidomimetics

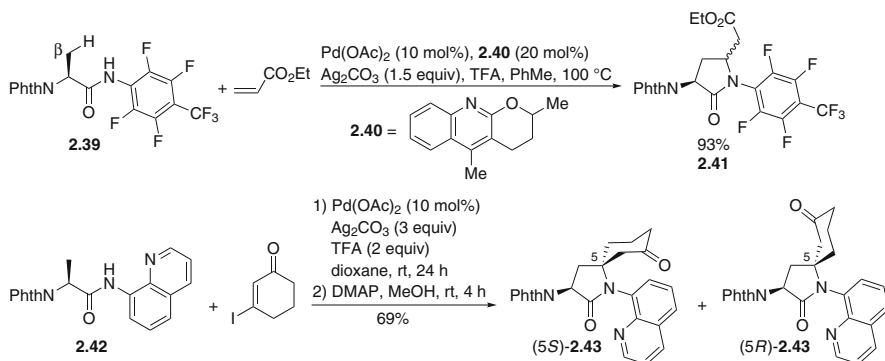


Scheme 2 Synthesis of C5-carbon substituted fused bicyclic 3-amino- γ -lactam [87, 88]



Scheme 3 5-Substituted γ -lactams by routes featuring oxidative ring closure and functionalization [102–104]

Although syntheses of α -amino- γ -lactams involving ring closure by formation of the C3-C4 and C4-C5 bonds, as well as by ring modification have been achieved (e.g., Scheme 3, Fig. 13), such strategies are rarely employed for peptide mimicry. To enable carbon-carbon bond formation during annulation reactions, radical (Scheme 11) [109, 110], bisalkylation (Scheme 15), and metal-catalyzed C-H activation processes all have proven successful (Scheme 4). On the other hand, to generate lactam dipeptides from NH lactam precursors, *N*-alkylation has been achieved, albeit with significant epimerization when chiral secondary electrophiles were used (Scheme 9). In addition, stereogenic quaternary centers at the γ -lactam C3 and C4 positions have been generated by diastereoselective alkylation and amination reactions (Schemes 16 and 17) [91, 118, 119].



Scheme 4 γ -Lactams by metal-catalyzed C-H activation and ring closure [112, 113]

2.1 α -Amino- γ -Lactam Peptides with 5-Position Substituents

In peptide mimicry, 5-substituted γ -lactam motifs have been used abundantly, in part due to their incorporation into fused bicyclic scaffolds (Fig. 6), as elaborated in multiple reviews [36–38, 63, 120, 121]. Several azabicyclo[3.X.0]alkanone amino acid systems bearing 5-substituted γ -lactams have been previously described, including 1-azabicyclo[3.2.0]heptan-2-one (e.g., **2.6**) [36, 121], pyrrolizidin-2-one (e.g., **2.7**, **2.9**, and **2.10**) [37, 38, 63], and indolizidin-9-one (I^9 aa, e.g., **2.8**) amino acids. Scaffolds containing I^9 aa bearing substituents include 2-amino-3-oxohexahydroindolizino[8,7-b]indole-5-carboxylates (IBTM, e.g., **2.11–2.14**) and a series of diastereomeric 4-phenyl indolizidin-9-one amino acids (4-Ph- I^9 aa, e.g., **2.15**) [36, 37, 120].

Related bicyclic systems harboring a second heteroatom linked to C5 of the γ -lactam unit have been made effectively using approaches involving intramolecular trapping of *N*-acyl iminium ion intermediates by the nucleophilic side chains of neighboring residues. For example, adjacent serine and cysteine residues have been employed to respectively afford oxapyrrolizidinone (e.g., **2.16**) and thiapyrrolizidinone (e.g., **2.17** and **2.18**) constrained dipeptides (Fig. 6) [36, 121]. Similar to the more common δ -lactam counterparts [123], thiapyrrolizidinone constraints have been considered as turn mimics and produced by condensation of *L*- or *D*-*N*-Fmoc-aspartate β -semialdehyde (**2.4**, Pg = Fmoc, R^{1-2} = H, X = OH) with cysteinyl-phenylalanyl-leucanyl Wang resin to provide constrained Leu-enkephalin pentapeptide mimics, after separation of the ring fusion diastereomers by HPLC purification [124].

Monocyclic 5-substituted γ -lactams have been investigated for potential as antibiotics (e.g., 5-methyl- γ -lactam **2.19**). In peptide mimicry, 5-substituted γ -lactams have mainly served as synthetic intermediates towards bicyclic targets, such as pyrrolizidinones from 5-iodomethyl γ -lactam **2.20**, and oxapyrrolizidinone 7a-*epi*-**2.16** from 5*R*-methoxy γ -lactam **2.21** [36, 121].

Azabicycloalkanone amino acids bearing 5-substituted γ -lactams have been used to study different peptides, albeit with few active examples. For example,

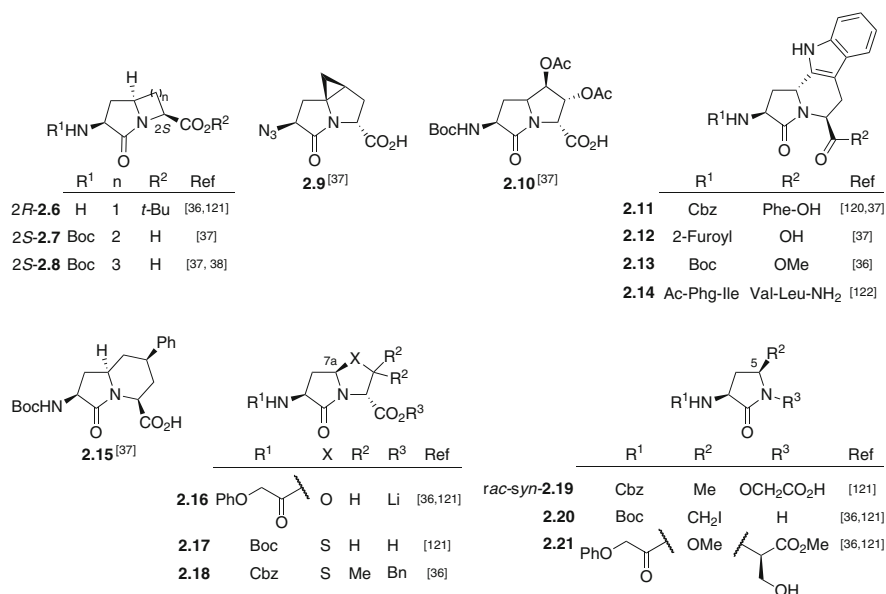


Fig. 6 Representative examples of 5-substituted γ -lactams (cited reviews provide further information) [36–38, 120–122]

substitution of I⁹aa **2S-2.8** for the 6,5-fused δ -lactam counterpart (I²aa) in PDC113.824, a peptidomimetic inhibitor of parturition in mice, led to loss of tocolytic activity [125]. Both I⁹aa **2S-2.8** and 4-phenyl-I⁹aa **2.15** were used to study the conformational requirements for peptide antagonist activity at the Human Calcitonin Gene-Related Peptide 1 Receptor [126]. In addition, IBTM (e.g., **2.14**) was incorporated into a 576-member combinatorial peptide library by using Pictet-Spengler chemistry on solid support [122].

Among syntheses to bicyclic γ -lactams [99, 101, 127, 128], I⁹aa amino acids have been made fused to various aromatic rings. For example, 2-amino-3-oxo-1,2,3,5,6,10b-hexahydropyrrolo[2,1-a]isoquinoline-5-carboxylate **2.22** (AHPIC, Fig. 7) [129] was synthesized by a Pictet-Spengler reaction of aspartate β -semialdehyde **L-2.4** (Pg = Cbz, R¹⁻² = H, X = OMe) and a phenylalaninamide substrate, which on heating forged both the piperidine and γ -lactam rings. Diastereomerically pure products were obtained by chromatographic separation of the resulting mixture of C10b-epimers.

7-Amino-pyrrolo[1,2-a]pyrimidin-6-one-4-carboxylate **2.23** was claimed to be part of a 1,241-member combinatorial library generated on 2-chlorotrityl chloride resin [130]. *N*-Protected amino acids bearing nucleophilic side chains and aspartate β -semialdehyde dimethyl acetal residues were incorporated into peptide sequences, and treated with formic acid to induce cyclization and liberation of the resulting 5,6-fused bicycles from the solid support.

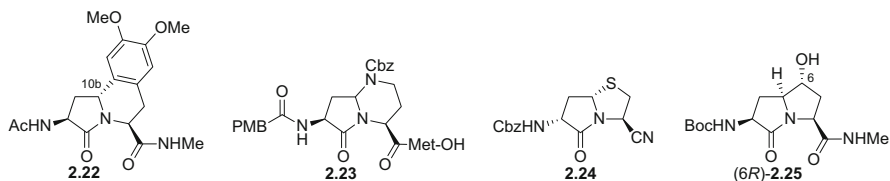


Fig. 7 Fused bicyclic γ -lactam constraints [87, 129–131]

A series of pyrrolizidinone analogs derived from threonine, serine, and cysteine were designed as covalent inhibitors of prolyl oligopeptidase using the docking program FITTED and synthesized in solution. In a HCEC cellular assay, thiaindolizidinone carbonitrile **2.24** gave an IC_{50} of 1.3 μ M [131].

6-Hydroxypyrrolizidinones (6*S*)- and (6*R*)-**2.25** were synthesized and applied in alaninylhydroxyproline dipeptide mimics. X-ray crystallographic analysis of the corresponding methyl ester (5*S*,6*R*)-**2.29** demonstrated backbone dihedral angles which correlated with those of the central ψ^{i+1} and ϕ^{1+2} residues in an ideal type II' β -turn (Scheme 2 and Sect. 2.5) [87]. Using variable temperature NMR spectroscopy in DMSO- d_6 , the *N*-methyl carboxamides **2.25** were shown to exhibit relatively solvent-shielded amide protons indicative of intramolecular hydrogen bonding (see Sect. 2.5). In the synthesis of the hydroxypyrrolizidinone **2.29**, acyloin condensation of aspartate β -semialdehyde **2.26** using *N*-heterocyclic carbene (NHC) catalysis gave a C4-epimeric mixture of 2,7-diamino-5-oxo-4-hydroxysuberates (Scheme 2). *O*-Acetylation and chromatographic separation afforded enantiopure ketones (4*S*)- and (4*R*)-**2.27** [88]. Hydrogenation in the presence of dilute acid caused removal of the amine protection and reductive amination to afford pyrrolidine **2.28** with minimal α - and β -elimination reactions in an optimal 67% yield. Protecting group removal and lactam formation furnished bicycle **2.29** [87].

Spirocyclic 5,5-disubstituted- γ -lactam **2.32** was synthesized on-route to the total synthesis of Chaetominine (Scheme 3). Bicyclic δ -lactam **2.30** was obtained from copper-catalyzed amination of a D-(2-iodotryptophanyl)alanine substrate. Subsequent oxidation of the indole with dimethyldioxirane (DMDO) and rearrangement of epoxide intermediate **2.31** afforded spirocycle **2.32** in 73% yield [102]. 5-Spiro- γ -lactam intermediates have been employed during the syntheses of members of the FR901483 and TAN1251 families of natural products [103, 136–138]. For example, oxazoline **2.33** was prepared by condensation of an amino alcohol and *N*-tosyl L-tyrosine, and subjected to (diacetoxyiodo)benzene oxidation followed by acetylation to afford γ -lactam **2.34** bearing a cyclohexa-2,5-dienone unit at the C5-quarternary center [103, 138]. Platinum-catalyzed hydrogenation and deacetylation gave cyclohexanone derivative **2.35**.

5-Carboxy- γ -lactams are pyroglutamic acid analogs which, in the case of the 4-aminopyroglutamate (Apy), have found application as constrained γ -amino acid residues in longer peptides [139–141]. Among syntheses of γ -lactams bearing carboxylate and hydroxymethyl substituents at the 5-position [142–145], (2*S*,4*R*)-

N-Boc-4-hydroxyproline (**2.36**) has served as chiral educt in an approach to (2*S*,4*S*)-4-azidopyrrolidine-2-carboxylate **2.37** featuring esterification, alcohol methanesulfonation, and nucleophilic displacement with inversion of configuration using sodium azide. Subsequent treatment with catalytic ruthenium(III) chloride in conjunction with sodium periodate as terminal oxidant led to selective C5-oxidation to give γ -lactam-5-carboxylate **2.38** [104].

γ -Lactam **2.41** was synthesized by β -carbon C(sp³)-H activation of alanine amide **2.39** followed by addition to ethyl acrylate using palladium-catalysis in the presence of quinoline ligand **2.40** and oxidant (Scheme 4) [112]. Similarly, by employing palladium(II)acetate as catalyst, *N'*-quinolin-8-yl alanine amide **2.42** reacted with 3-iodocyclohex-2-enone in a tandem cyclization to furnish a cyclohexylalanine derivative in 88% yield. Subsequent lactam formation by Michael addition was achieved using DMAP and DBU for 4 h or 20 min to produce respectively 5.5:1 and 1:2.3 ratios of (5*S*)- and (5*R*)-diastereomers **2.43**, the stereochemistry of which was assigned using crystallography [113]. In related amino acid amide substrates, the 8-amino-5-methoxyquinoline (MQ) alternative to the 8-aminoquinoline (AQ) auxiliary gave lactams which were amenable to *N*-deprotection (see Scheme 10) [81].

Biochemical degradation pathways of peptides and proteins include 5-membered ring condensation reactions of asparagine and aspartate residues to form aspartimide (Asi) intermediates that transform into deaminated, epimeric, and β -linked products [146–148]. Asi-formation has been encountered during peptide elongation with Asp monomers, and mitigated using sterically hindered bases, bulky protecting groups, acid additives, and pseudoproline constraints [149–151]. In a comparison of aspartimide peptidomimetic **2.44** (Fig. 8) and the native octapeptide (IMIKFNRL) as antigens, cytotoxic T lymphocytes (CTL) were raised that displayed minimal cross-reactivity, suggesting a role for Asi-modification in autoimmunity [152]. Moreover, the insulin-potentiating properties of a human growth hormone (hGH) octapeptide were found to correlate with Asi-derivative **2.45**, which was formed during peptide synthesis on Merrifield resin using Boc-Asp (OBn)OH and triethylamine as base [153, 155]. Comparison of Asi-peptide amide **2.46** with its Agl and β -amino- γ -lactam (Bgl) counterparts **2.47** and **2.48** revealed superior stability and biological activity for the Agl derivative [156, 157].

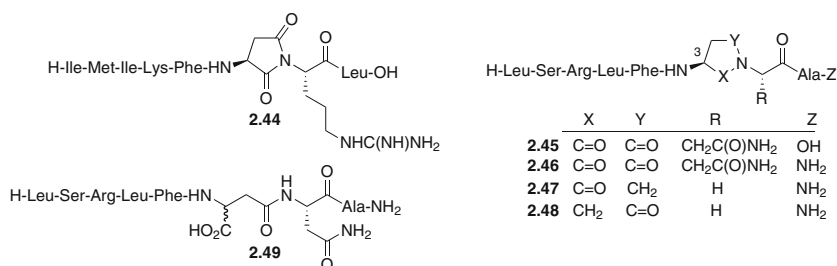


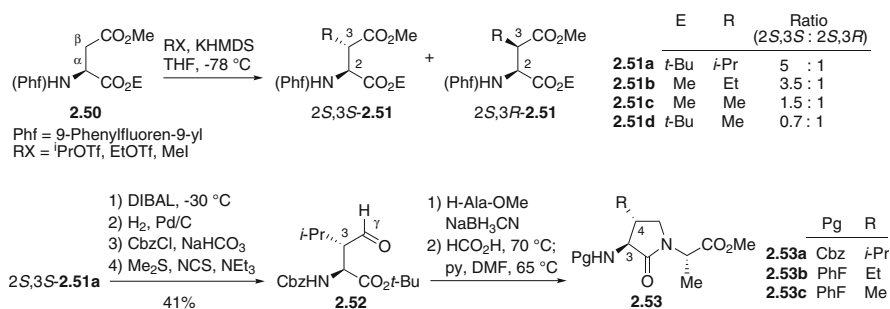
Fig. 8 Peptides bearing succinimide (Asi) bridges and analogs [152–154]

Crystallography, circular dichroism, and NMR spectroscopy, as well as computational analysis, all have suggested that type II and II' β -turn conformations may be stabilized in Asi-bridged peptides, contingent on the C3-configuration [158–161]. The respective presence and absence of secondary structure has been invoked to explain the temperature-dependent variations in the HPLC retention times and peak bandwidths of Asi-peptide **2.46**, which were absent in β -linked aspartate derivative **2.49** [154].

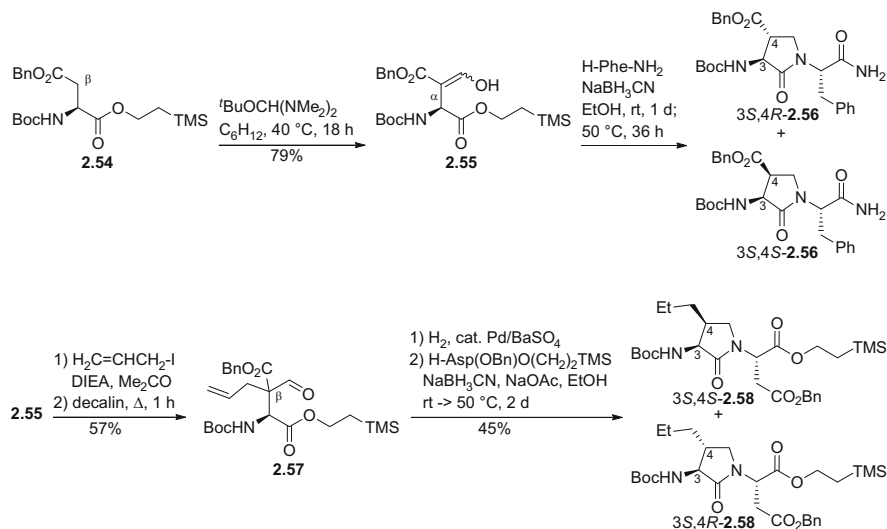
2.2 α -Amino- γ -Lactam Peptides with 4-Position Substituents

Five-membered 3-amino lactams bearing 4-position substituents are a relatively underrepresented class of substituted lactam. Several methods for their synthesis and application have emerged and inspire further exploration of this peptidomimetic category [109].

The synthesis of β -substituted γ -lactams from aspartic acid as chiral precursor has been achieved by judicious application of orthogonal protecting groups. For example, amino acid *N*-protection with the bulky 9-phenylfluoren-9-yl (Phf) group shielded the α -carbon proton [162], such that the β -ester of *N*-Phf-L-aspartate **2.50** (Scheme 5) could be selectively enolized using excess potassium bis(trimethylsilyl) amide and alkylated with isopropyl triflate to afford a 5:1 mixture of C3-diastereomers **2.51a** in 43% yield along with 45% recovered starting material [85]. After chromatography, major *syn*-methyl ester 2*S*,3*S*-**2.51a** was selectively reduced, the nitrogen protecting group was switched to Cbz, and the γ -alcohol was oxidized to the corresponding aldehyde with *N*-chlorosuccinamide and methylsulfide to provide 3*S*-formylleucine **2.52** in 41% yield over four steps. Reductive amination of aldehyde **2.52** with L-alanine methyl ester and lactam formation furnished 4-isopropyl-3-amino- γ -lactam **2.53a** in 32% yield over two steps. 4-Ethyl and 4-methyl-lactam counterparts **2.53b** and **2.53c** were respectively prepared by analogous methods employing ethyl triflate and methyl iodide during



Scheme 5 Synthesis of 4-alkyl-3-amino- γ -lactams from aspartate precursors [85]

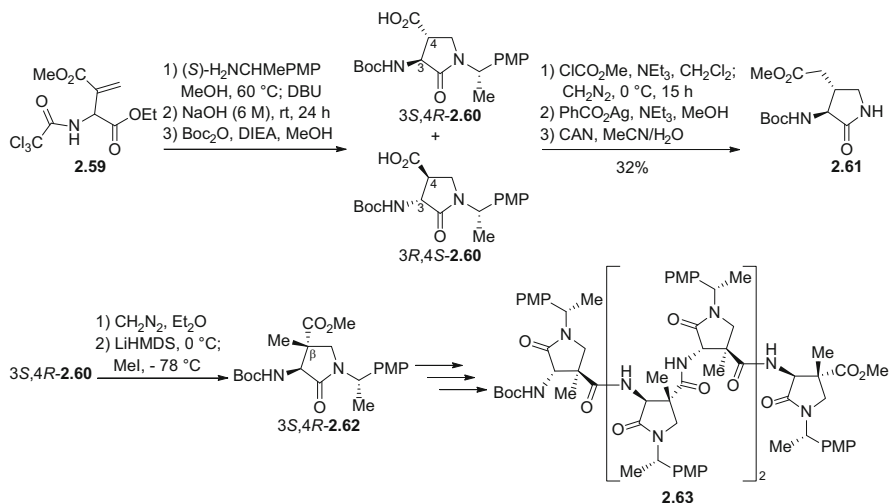


Scheme 6 4-Substituted γ -lactam synthesis by way of aspartate β -formylation [86]

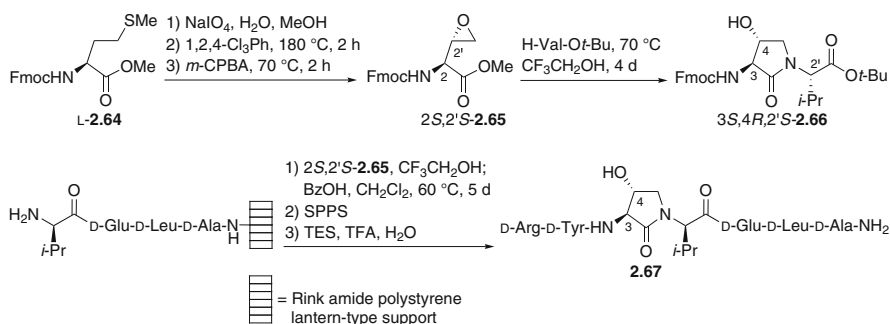
alkylation, albeit with decreased diastereoselectivity in the generation of β -alkyl aspartates **2.51b–d**.

In a related β -functionalization approach (Scheme 6), formylation of aspartate diester **2.54** using *tert*-butoxy-bis(dimethylamino)methane in non-polar medium gave 1,3-dicarbonyl tautomer **2.55** without α -epimerization [86]. Reductive amination with phenylalaninamide, lactam formation on heating, and chromatographic separation gave respectively 3*S*,4*R*- and 3*S*,4*S*- β -benzyloxycarbonyl γ -lactams **2.56** in 41% and 24% yields. During the preparation of the 4-propyl counterpart, allylation of enol **2.55** occurred mostly on oxygen; however, Claisen rearrangement on heating gave β , β -disubstituted aspartate **2.57**. Subsequently, catalytic hydrogenation of olefin **2.57** proceeded with benzyl ester cleavage and decarboxylation to provide a 2-substituted pentanal, which was condensed with β -benzyl α -2-(trimethylsilyl)ethyl aspartate, reduced with sodium cyanoborohydride, and heated to afford a 1:1 mixture of β -propyl γ -lactam diastereomers **2.58**.

Modification of the 4-position carboxylate in γ -lactam **2.60** has provided entry to other 4-substituted derivatives (Scheme 7). For example, constrained glutamic acid amide **2.61** was obtained by Arndt-Eistert homologation of 3*S*,4*R*-**2.60** [92]. A 5-step synthesis was used to prepare a statistical 3*S*,4*R*/3*R*,4*S* mixture of lactams **2.60** in 36% yield in which the diastereomers were separated by chromatography. Electron-rich (*S*)-4-methoxyphenylethylamine was selected as chiral auxiliary for the preparation of **2.60** to enable mild liberation of the lactam nitrogen by cleavage of the chiral auxiliary with ceric ammonium nitrate [93, 163]. The lactam precursor, trichloroacetamide **2.59**, was synthesized in racemic form by an O \rightarrow N rearrangement of a Baylis–Hillman adduct derived from methyl acrylate and ethyl glyoxalate [164].



Scheme 7 Synthesis of 3-amino- γ -lactam 4-carboxylate derivatives [91–94]



Scheme 8 Synthesis of peptides bearing α -amino- β -hydroxy- γ -lactams [96, 97]

γ -Lactam-4-carboxylate **3S,4R-2.60** was esterified, enolized at the β -position, and alkylated with methyl iodide to afford a separable 85:15 mixture of **3S,4R-** and **3S,4S-**diastereomers **2.62** in 75% yield [91]. The configurations of **3S,4R-2.60** and **3S,4R-2.62** were assigned by crystallographic analyses [91, 93]. β -Amino acid oligomer **2.63** was prepared from **3S,4R-2.62** and shown by NMR spectroscopy and molecular modeling to adopt a helical conformation [94, 165].

β -Hydroxy- α -amino- γ -lactam (Hgl) residues were designed to serve as constrained Thr and Ser motifs (e.g., **2.66** and **2.67**, Scheme 8) [96, 166, 167], and shown to induce turn conformation contingent on the C-terminal residue (see Sect. 2.5, Fig. 15) [168]. Employing oxiranylglycine **2.65** as a bis-electrophile in reactions with various α -, β -, and γ -amino esters provided a library of Hgl dipeptides (e.g., **2.66**) in 31–85% yields [96, 97, 166, 168]. Epoxide ring opening by amino esters was favored using 2,2,2-trifluoroethanol as solvent or stoichiometric

amounts of calcium(II) triflate as Lewis acid; lactam formation was achieved on heating and accelerated in the presence of benzoic acid as catalyst [96, 166]. Enantiopure oxiranylglycines **2.65** were prepared respectively from *N*-Fmoc-D- and L-methionine esters **2.64** by a route featuring sulfoxide elimination on heating to provide the corresponding vinylglycinate [169–171], followed by alkene epoxidation. Oxirane formation using *m*-chloroperbenzoic acid yielded a ~5:1 mixture of 2*S*,2'*S*- and 2*S*,2'*R*-diastereomers **2.65**, which was enriched by chromatography.

Allosteric modulation of the interleukin-1 β (IL-1 β) receptor (IL-1R) has been achieved using all D-amino acid heptapeptide rytvela (small letters indicate D-residues) [172–174]. To glean conformation-activity relationships, rytvela analogs were systematically prepared by substitution of each amino acid in the sequence by an α -amino γ -lactam (Agl) residue (Agl positional scanning) [34], and evaluated for potential to antagonize the proliferative effects of IL-1 β on thymocytes [175]. Distinctively reduced activity was found for analogs bearing (*R*)- or (*S*)-Agl at the threonine position, suggesting that turn induction was offset by side chain loss. Application of oxiranylglycine 2*S*,2'*S*-**2.65** in a solid phase approach gave (3*S*,4*R*)-Hgl³ peptidomimetic **2.67** (Scheme 8) [96], which mitigated the loss of activity seen with the Agl³ analogs, and exhibited enhanced inhibitory activity on IL-1 β -induced thymocyte proliferation [97].

Hexahydropyrrolo[3,4-*b*]pyrrol-6(2H)-one substructures **2.68–2.72** (Fig. 9) feature respectively γ -lactams fused to indole and pyrrolidine rings [176–179]. 4-Substituted lactam dipeptide **2.68** was prepared by reductive amination of the condensation product of benzyl 3-formylindole-2-carboxylate and histidine methyl ester, lactam formation, and hydrolysis. Epimerization during the incorporation of acid **2.68** into peptidomimetic **2.69** was avoided by resorting to in situ nitrogen protection using excess Boc anhydride [176]. Angiotensinogen mimic **2.69** inhibited human renal renin with an IC₅₀ of 3.3 nM [180]. After pyrrolidine acylation using a solid-supported mixed anhydride reagent, assignment of the amide isomer and the ring fusion configuration of methoxyphenylacetamides **2.70** was accomplished by 2D NMR spectroscopy [177]. The tachykinin antagonists GR64349 (**2.71**) and GR138676 (**2.72**) employ respectively Agl and pyrrolidine-

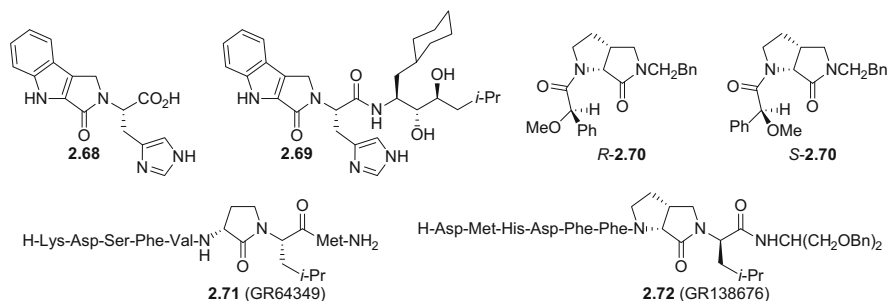
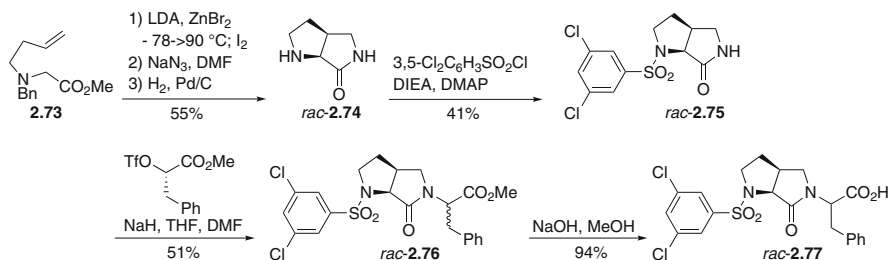
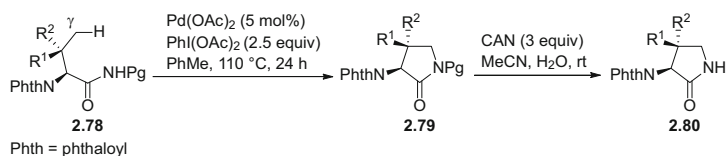


Fig. 9 Diazaoxobicyclo[3.3.0]alkane dipeptide mimics [176–179]



Scheme 9 Synthesis of diazabicyclo[3.3.0]alkanone dipeptide mimic **2.77** [114]



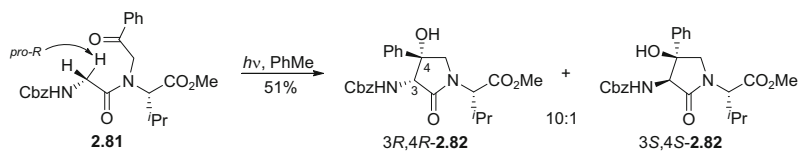
Pg	R ¹	R ²	% yield		
			2.79	2.80	
a	quinolin-8-yl	H	Et	86	-
b	quinolin-8-yl	H	Of-Bu	81	-
c	quinolin-8-yl	Me	Me	94	-
d	5-methoxyquinolin-8-yl	H	Et	87	65
e	5-methoxyquinolin-8-yl	H	Of-Bu	60	71
f	5-methoxyquinolin-8-yl	H	Me	76	62

Scheme 10 γ -Lactam ring closure by C-H activation approaches [81]

fused AgI residues, and were shown to be potent and selective for the neurokinin-2 and -3 receptor subtypes [178, 179]. The pyrrolidine-fused AgI residue possesses rigid ϕ and ψ dihedral angles respectively at $75^\circ \pm 20^\circ$ and $140^\circ \pm 10^\circ$, and was used to restrain the conformation of the glycine residue of the endogenous neurokinin A and B receptor ligands.

Racemic pyrrolopyrrolidinone **2.74** was synthesized from *N*-benzyl *N*-homoallylglycinate **2.73** by a route featuring formation of the zinc enolate, 5-*exo-trig* cyclization and trapping with iodine to provide the 2-iodomethyl proline (Scheme 9) [114, 181]. After displacement of the iodide with sodium azide, hydrogenation removed the benzyl group, reduced the azide to amine, and caused spontaneous lactam formation to give pyrrolidinone **2.74**. Pyrrolidine sulfonylation gave γ -lactam **2.75**, which was alkylated on the pyrrolidinone with triflate that was derived from methyl (L)-3-phenyllactate to give ester **2.76**. Saponification afforded acid **2.77** as a racemate. In the context of ascertaining the active conformation of the potent ($IC_{50} = 1.4$ nM) $\alpha_4\beta_1$ -integrin receptor antagonist 3,5-dichlorophenylsulfonyl-propyl-phenylalanine, a >1,500-fold loss of integrin receptor affinity was observed on examination of 5,5-fused bicycle **2.77** [114].

Intramolecular aliphatic C-H bond activation and cyclization have afforded β -substituted γ -lactams (Scheme 10). 8-Aminoquinolines **2.78a–c** derived from isoleucine, threonine, and *tert*-leucine underwent palladium catalyzed C(sp³)-H bond



Scheme 11 γ -Lactam ring closure by photochemical C-H activation [108]

activation and amidation at the γ -carbon in the presence of stoichiometric amounts of (diacetoxyiodo)benzene as oxidant to afford α -amino- γ -lactams **2.79a–c** [81]. Employment of the 5-methoxy analogs **2.78d–f** enabled oxidative removal of the quinolone using ceric ammonium nitrate to afford the corresponding NH- γ -lactams **2.80d–f**.

A 10:1 diastereomeric mixture of 4-hydroxy-4-phenyl- γ -lactams **2.82** was obtained by photochemical activation of glycinyln-*N*-benzoylmethyl-L-valinate **2.81** by a mechanism involving generation of a singlet diradical, preferred *pro-R*-hydrogen abstraction, and cyclization by radical recombination (Scheme 11) [108]. α,β -Disubstituted γ -lactams were similarly obtained as diastereomeric mixtures using related *N*-benzoylmethyl analogs of Ala-Val and Pro-Ala [182].

2.3 α -Amino- γ -Lactam Peptides with 3-Position Substituents

3-Amino- γ -lactams bearing simple alkyl 3-position substituents and a 1,7-diazaspiro[4.4]nonan-6-one scaffold have been used in medicinal chemistry programs (Fig. 10) [24, 40, 186]. For example, GR 82334 (**2.83**) is a spiro lactam analog that exhibited selective tachykinin NK₁ receptor antagonism [183, 187]. In an *ex vivo* human tonsil tissue proliferation assay, GR 82334 was used to study the role of the “Substance P”-NK₁ pathway in pediatric obstructive sleep apnea [188], highlighting potential for an underexploited non-surgical intervention. In a systematic investigation of the relevance of configuration for the activity of neurotensin peptidomimetics, 2*S*,5′*R*-lactam **2.84** displayed ≥ 100 -fold greater affinity for the neurotensin type 1 (NT1) receptor relative to its diastereomeric spiro lactams and ring opened *N*-(methyl)tyrosine counterparts [184]. The 2*S*,5′*R*-spiro lactam rigidified the proline ψ -dihedral angle to a value of $146 \pm 15^\circ$ favoring an extended β -strand conformation. 3-*sec*-Butyl- γ -lactam **2.85** was designed based on the β -amyloid peptide sequence and exhibited both blood-brain barrier permeability and nanomolar potency against β -secretase 1 (β -site amyloid precursor protein-cleaving enzyme 1, BACE-1); however, lactam **2.85** lacked efficacy in animal models of Alzheimer’s disease [185, 189].

The 3-position substituent has often been incorporated into γ -lactam constraints with stereocontrol by using the “self-reproduction of chirality” alkylation method developed by Seebach [190–193]: e.g., peptidomimetics **2.86–2.88** (Fig. 11). Constraint of the threonine conformation in mimic **2.86** gave ~ 10 -fold reduced affinity for the

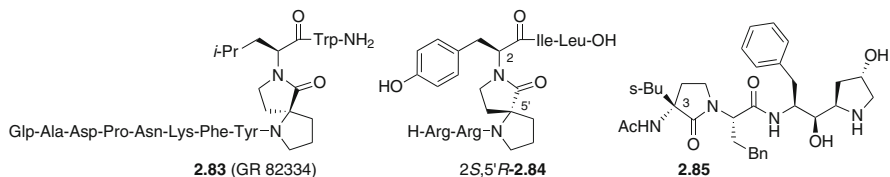


Fig. 10 Bioactive 3-substituted 3-amino- γ -lactams [183–185]

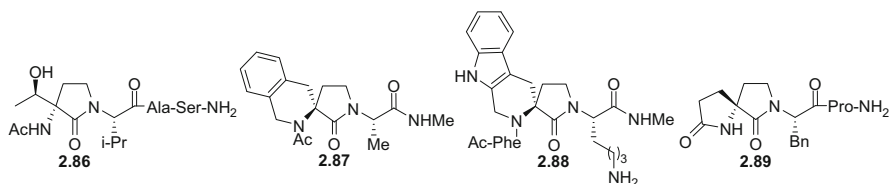
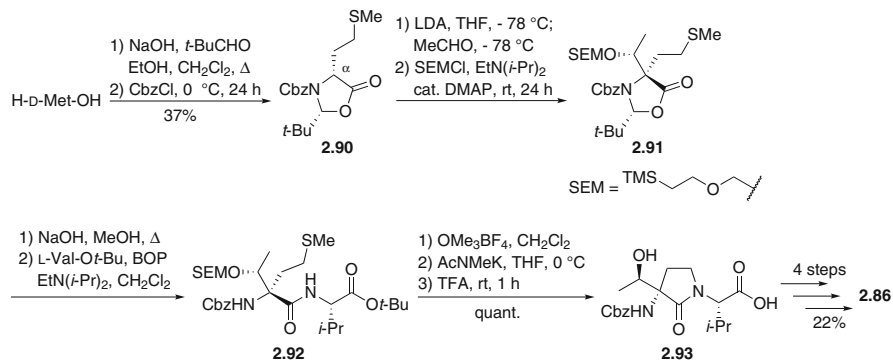


Fig. 11 3-Substituted 3-Amino- γ -Lactams [65, 68, 82, 194]

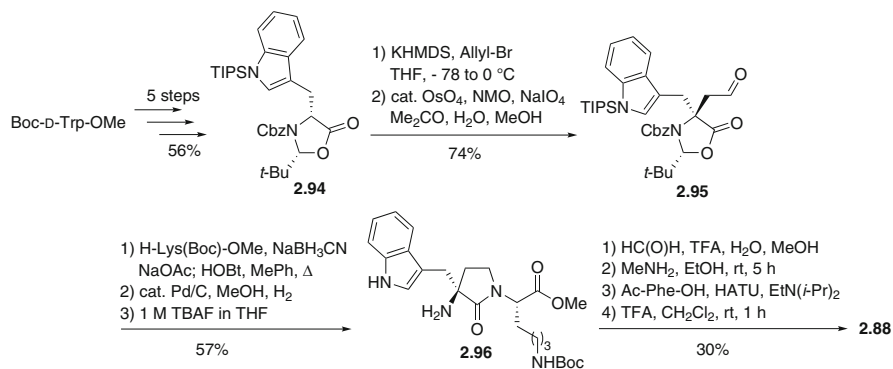
plasminogen activator inhibitor-1 (PAI-1) protein relative to the peptide Ac-TVAS-NH₂ [65]. Constraint of the D-Phe-L-Ala dipeptide in the 2-(2'-oxo-2,4-dihydro-1H-spiro[isquinoline-3,3'-pyrrolidin]-1'-yl)propanoic acid (SIPP) scaffold provided a robust type II' β -turn tetrapeptide mimic **2.87** as demonstrated by IR and NMR spectroscopy, molecular modeling, and crystallography (see Sect. 2.5, Fig. 16) [194]. The Trp residue conformation was constrained in 1,2,3,4-tetrahydro- β -carboline (THBC) analog **2.88**, which lacked affinity for the somatostatin receptor subtypes sst₁-sst₅ [82]. To glean information on the conformation-activity relationships of the thyrotropin-releasing hormone (TRH) tripeptide, lactam analogs of variable size and rigidity were prepared (e.g., **2.89** and **2.100**, Fig. 11 and Scheme 14) [68], but exhibited 3- to 25-fold lower receptor affinity at the TRH receptor-1 relative to the parent analog Glp-Phe-Pro-NH₂.

The synthesis of the lactam in Thr-Val mimic **2.86** was achieved by the Freidinger-Weber method from dipeptide **2.92** (Scheme 12). Aldol adduct **2.91** was prepared by protection of the condensation product of acetaldehyde and the α -anion of D-Met-derived oxazolidinone **2.90**. The Thr configuration resulted from selective *Si*-face addition [65]. Oxazolidinone hydrolysis, peptide coupling, and γ -lactam formation provided dipeptide acid **2.93**, which was incorporated into peptidomimetic **2.86** (Fig. 11).

Diastereoselective alkylation of enolates of oxazolidinones derived from amino acids and pivalaldehyde was employed in the syntheses of 2,6-diazaspiro[4.5]decan-1-ones **2.87** and **2.88** [82, 194]. For example, allylation of D-Trp-derived oxazolidinone **2.94** followed by olefin oxidation gave aspartate β -semialdehyde **2.95**, which underwent reductive amination and lactam formation to give constrained Trp-Lys dipeptide **2.96** (Scheme 13) [82]. Pictet-Spengler reaction of **2.96** and formaldehyde gave subsequently the tetrahydro- β -carboline, which was



Scheme 12 Synthesis of 3-(hydroxyethyl)-3-amino- γ -lactam **2.86** by stereoselective α -alkylation [65]

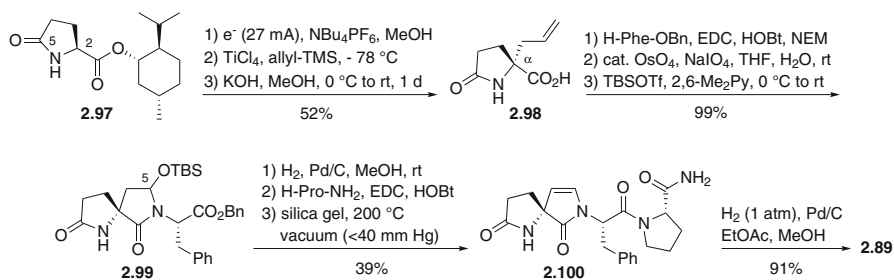


Scheme 13 Synthesis and elaboration of 3-heteroaryl-methyl-3-amino- γ -lactam **2.96** [82]

elaborated at the C- and N-termini and deprotected to afford constrained tripeptide *N*-methylamide **2.88**.

In the synthesis of 1,7-diazaspiro[4.4]nonane-2,6-dione **2.89**, electrochemical oxidation of (+)-menthyl pyroglutamate (**2.97**) gave the 2-methoxy-5-oxopyrrolidine-2-carboxylate, allylation of which led to a 2:1 mixture of α -allyl diastereomers (Scheme 14) [68]. Isolation of the major diastereomer by fractional crystallization and hydrolysis gave 2-allylpyroglutamic acid (**2.98**). Subsequently, peptide coupling, olefin oxidation, and *O*-silylation afforded 5-silyloxylactam **2.99** as a 1:1 mixture of diastereomers. After installation of the C-terminal prolinamide, the silyloxy group was eliminated by adsorption onto silica gel and heating at 200 °C in vacuo to afford unsaturated γ -lactam **2.100**. Hydrogenation gave the tripeptide mimic **2.89**.

3-Substituted γ -lactams have also been synthesized without stereocontrol and resolved [186, 195, 196]. For example, the 4-phenylpropyl moiety of somatostatin mimic **2.101** was synthesized by alkylation of the enolate of ethyl *N*-(acetyl) methioninate with cinnamaldehyde, and the diastereomers were separated after lactam formation on methyl ϵ -Cbz-*L*-lysinate (Fig. 12) [197]. The γ -lactam ring



Scheme 14 Synthesis of a diazaspiro[4.4]nonadione tripeptide **2.89** [68]

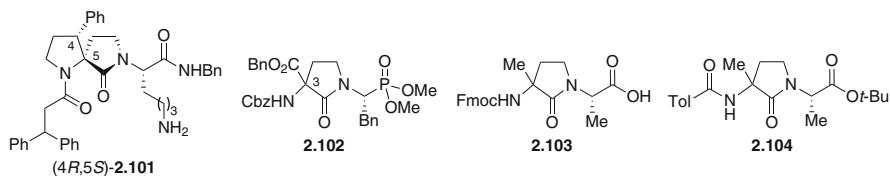


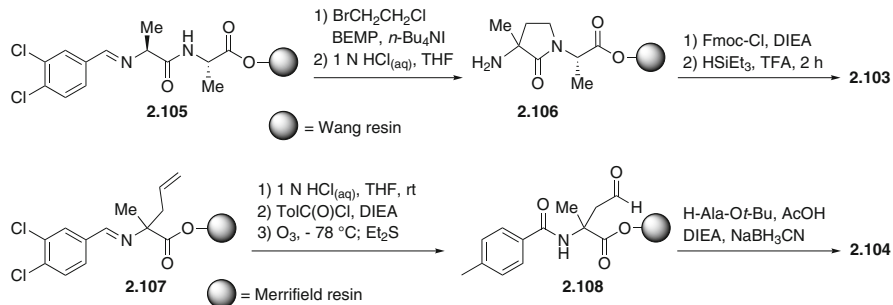
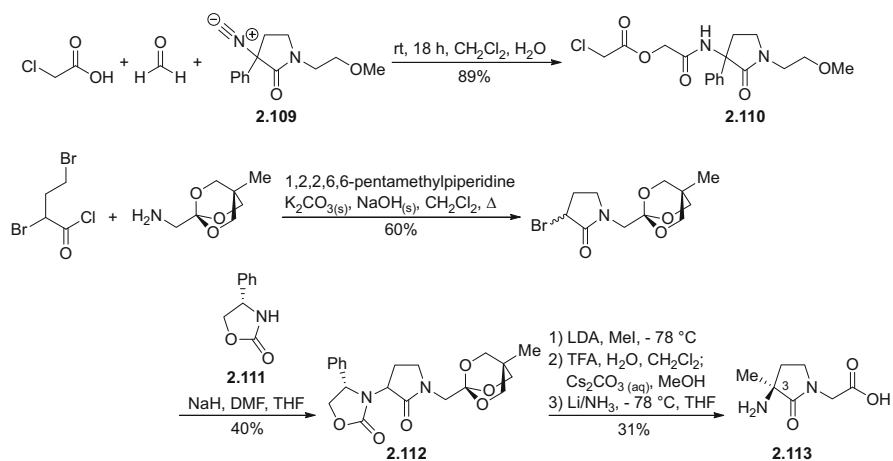
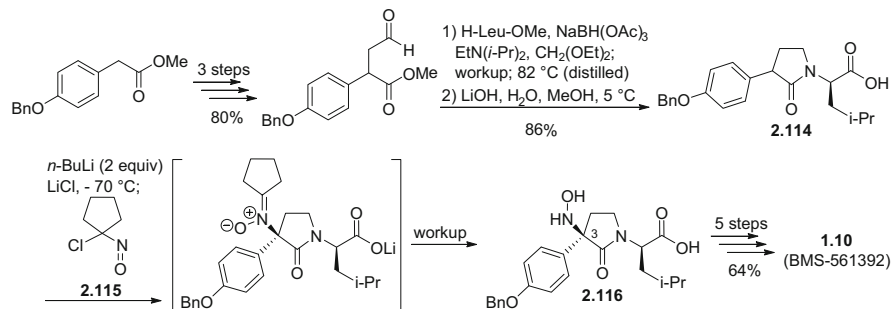
Fig. 12 3-Substituted γ -lactams generated as C3-epimeric mixtures [99, 111, 197, 198]

of α -aminophosphonate **2.102**, a protected precursor of a *N*-methyl-D-aspartic acid receptor antagonist, was forged by *C,N*-bis-alkylation of an amino-malonamide using a 1,2-dihaloethane [198].

γ -Lactam **2.103** was synthesized by a route featuring preparation of 3-amino- γ -lactam **2.106** by alkylation of dichlorobenzylidene dipeptide **2.105** on Wang resin using 1-bromo-2-chloroethane and the phosphazene base BEMP (2-*tert*-butylimino-2-diethylamino-1,3-dimethylperhydro-1,3,2-diazaphosphorine, Scheme 15) [111]. Similar alkylation conditions were used to prepare allylglycinate **2.107** from the benzylidene of alanine bound to Merrified resin [99]. Aspartate β -semialdehyde **2.108** was prepared from allylglycinate **2.107** and used in a route featuring olefin oxidation, reductive amination with alanine *tert*-butyl ester, and resin cleavage with lactam formation to afford γ -lactam diastereomers **2.104** [99].

Ethyl 2-isocyano(phenyl)acetate was alkylated with 1,2-dibromoethane and treated with (2-methoxyethyl)amine to afford 3-isocyanato- γ -lactam **2.109**, which was employed in a Passerini multicomponent reaction with 2-chloroacetic acid and formaldehyde to afford depsipeptide **2.110** (Scheme 16) [115]. (*S*)-(+)-4-Phenyl-2-oxazolidinone **2.111** was employed in a route involving the enolization and diastereoselective C3-alkylation of (3*RS*)-3-amino- γ -lactam **2.112** to afford (3*S*)-3-methyl-3-amino- γ -lactam **2.113** after protecting group manipulation [116].

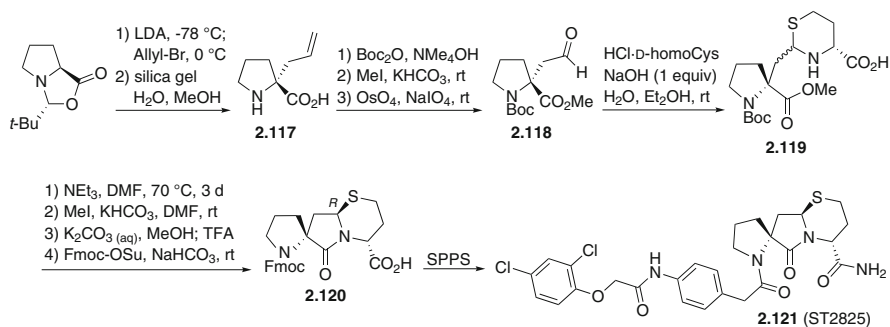
In the synthesis of the “tumor necrosis factor- α converting enzyme” inhibitor BMS-561392 (**1.10**, see Fig. 3 above), amination of the dianion generated from 3-*p*-benzyloxyphenyl- γ -lactam **2.114** using 1-chloro-1-nitrosocyclopentane (**2.115**) in the presence of LiCl provided 3-aryl-3-hydroxylamino- γ -lactam **2.116** in a 92:8 diastereomeric ratio (dr, Scheme 17) [117]. Recrystallization of **2.116** enhanced the dr to >99:1 resulting in 56% overall yield from a 20 kg batch of 3-aryl- γ -lactam **2.114**.

**Scheme 15** Solid-phase syntheses of 3-substituted γ -lactam dipeptides [99, 111]**Scheme 16** 3-Substituted 3-amino- γ -lactam synthesis by multiple component and alkylation routes [115, 116]**Scheme 17** Diastereoselective C3-amination to generate a 3-*p*-benzyloxyphenyl-3-aminolactam intermediate in the synthesis of inhibitor **1.10** [117]

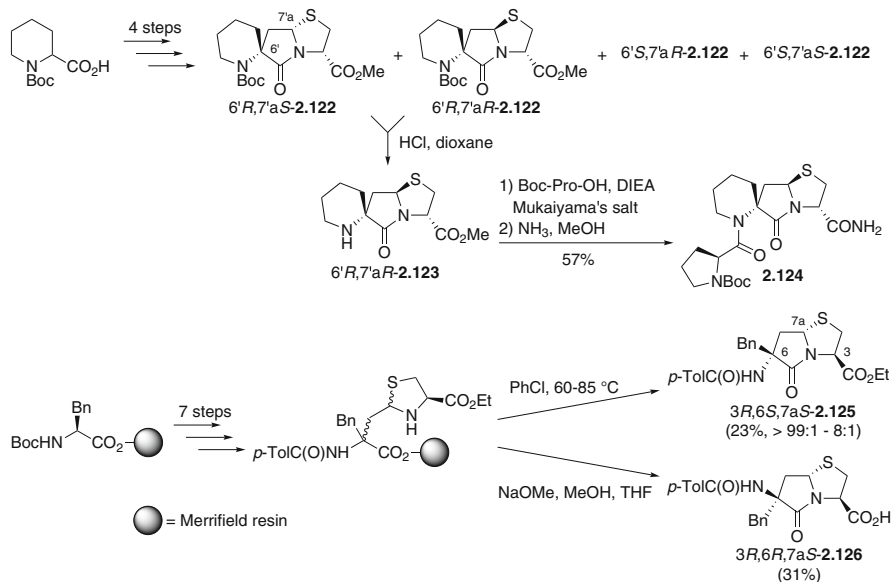
2.4 α -Amino- γ -Lactam Peptides with Multiple Substituents

Demand for constrained scaffolds has driven the pursuit of structures possessing multiple ring systems and substituents. Building on the 3-amino- γ -lactam motif, several of these structures have found use in peptide mimicry. For example, the identification of myeloid differentiation factor 88 (MyD88) inhibitors was enabled by investigation of several β -turn mimics possessing 3-amino- γ -lactam components within multiple ring systems [83]. Signal transduction events triggered by the distinct extracellular ligands of interleukin 1 (IL-1R) and toll-like receptors (TLRs) display a common reliance on MyD88 as adaptor protein. Based on the RDVLPGT sequence of the homo- and hetero-dimerization consensus motifs in MyD88, a peptidomimetic library was generated using solid phase synthesis featuring an Fmoc/*t*-Bu strategy on Rink amide MBHA support. The library was screened for potential to inhibit MyD88 homo-dimerization in a yeast two-hybrid assay and to arrest IL-1 β -induced production of IL-6 in orally dosed mice [83, 199]. Among the active library members, ST2825 (**2.121**) possessed β -turn motif **2.120** (Scheme 18), which was generated from 2-allyl proline **2.117** that was obtained using the “self-reproduction of chirality” method of Seebach [190–192]. Constrained aspartate β -semialdehyde analog **2.118** was prepared from **2.117** by *N*-protection and olefin oxidation. Condensation of **2.118** with D-homoCys provided 1,3-thiazinane **2.119** as a mixture of diastereomers [200]. Only the γ -lactam with the *R*-ring fusion stereochemistry was obtained from heating **2.119** with triethylamine in DMF, such that after protecting group manipulations *N*-Fmoc(amino)-spiro-tricycle acid **2.120** was obtained and deployed in the solid-phase sequence. As a chemical probe in pharmacological studies [201–203], ST2825 has served to decipher the mechanism by which TLR4 mediates vascular remodeling and damage. Exhibiting an influence on NAD(P)H oxidase activity, ST2825 countered angiotensin II-induced oxidative stress in vascular smooth muscle cells [201].

The related 6.5.5-spiro-bicyclic lactams **2.122** and thiazolidine-fused lactams **2.125** have been similarly prepared by sequences involving allylation, olefin



Scheme 18 Synthesis of spirotricycle **2.120** for introduction into ST2825 [83]

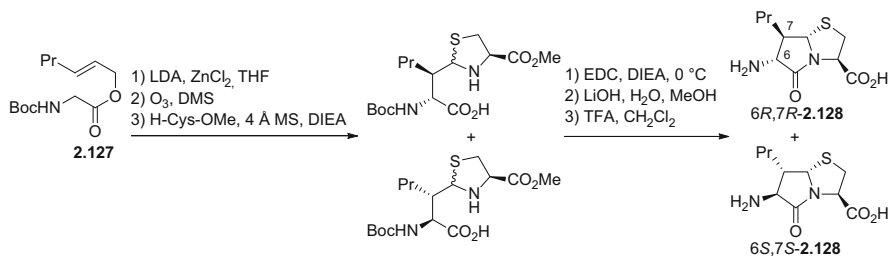


Scheme 19 Diastereoselective approaches to spiro bicyclic γ -lactam dipeptide mimics [99, 100]

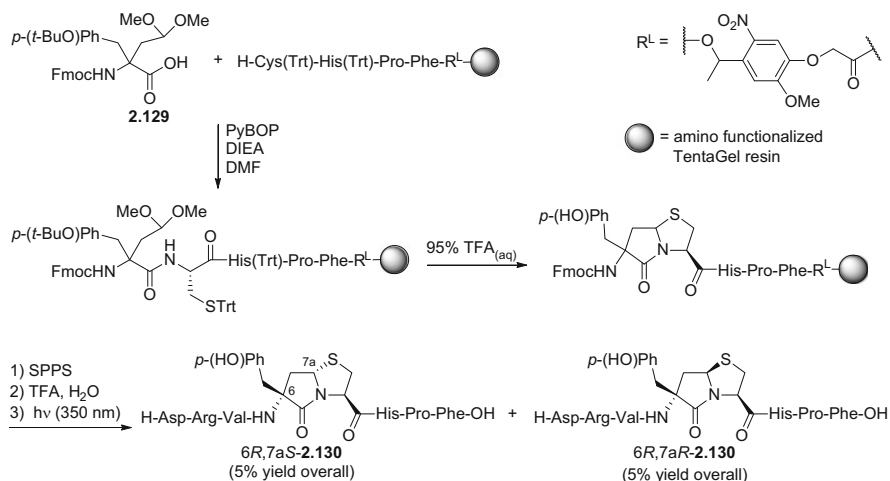
oxidative cleavage, and condensation with cysteine esters under mild conditions (Scheme 19) [99, 100, 204]. Although diastereomers **2.122** could be separated by chromatography, their respective treatment with acid to remove the Boc group caused epimerization of the thiazolidine to afford **6'R,7'aR-2.123**. The quantitative epimerization of the ring fusion stereocenter was consistent with *ab initio* calculations that predicted the isomer obtained to be 3.81 kcal/mol more stable than its epimer. Modification of the C- and N-termini of **2.123** gave peptide mimic **2.124**, which on examination in the solid state and in solution exhibited a β -turn conformation [100].

Stereocontrol of the thiazolidine ring fusion stereochemistry was achieved during lactam formation with resin cleavage by temperature control such that selective resin release at 60–85 °C gave diastereomeric bicycle **3R,6S,7aS-2.125**, the configuration of which was assigned by X-ray crystallography [99]. On the other hand, alkaline methanolysis was claimed to release the C6-epimer as carboxylic acid **3R,6R,7aS-2.126**. In the absence of a quaternary carbon, the C6-position has been epimerized in related thiazabicycloalkane amino acids bearing a tertiary carbon [36].

γ -Lactam diastereomers **2.128** were designed as constrained Nle-Gly dipeptide mimics and prepared by a route featuring Kazmaier-Claisen rearrangement of hex-2-en-1-yl *N*-Boc-glycine (**2.127**), ozonolysis of the resulting alkene to afford an aldehyde, and condensation with cysteine methyl ester (Scheme 20) [84, 205, 206]. Lactam formation, ester hydrolysis, and Boc group removal afforded (6*R*,7*R*)- and (6*S*,7*S*)-thiapyrrolizidinones **2.128** in 50% overall yield as a mixture of separable diastereomers. After conversion to the Fmoc derivatives, bicycles **2.128** were introduced into analogs of the octapeptide SNF 9007 using SPPS. A mimic



Scheme 20 4-Substituted 1-aza-6-thia-bicyclo[3.3.0]octan-2-one-8-carboxylate synthesis [84]



Scheme 21 Bicyclic lactam peptide synthesis by cyclization on solid support [79]

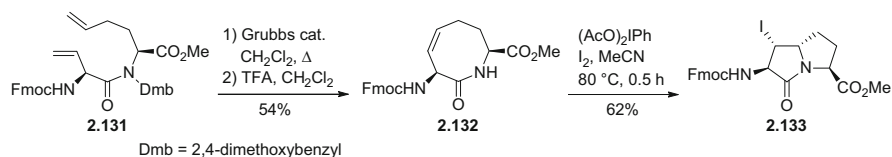
of cholecystokinin, SNF 9007 displayed selectivity for the cholecystokinin-B (CCK-B) receptor and potency against the δ -opioid receptor. Incorporation of (6*R*,7*R*)- and (6*S*,7*S*)-lactams **2.128** into SNF 9007 caused respectively decreased and retained activity against the CCK-B receptor. The synthesis of analogs bearing a phenyl substituent at the 7-position, as well as threonine-derived variants, have been previously reviewed [37].

The construction of azathiabicyclo[3.3.0]alkane constraints within a peptide linked to a TentaGel solid support was enabled by an alternative N-C5 ring closure strategy (Scheme 21) [79]. Targeting angiotensin II analog **2.130**, racemic α -dimethoxyethyl-tyrosine **2.129** was coupled to the N-terminal of cysteine in a peptide sequence attached to a photolabile 4-(1-hydroxyethyl)-2-methoxy-5-nitrophenoxy linker. Exposure to TFA removed the side chain protection to achieve formation of the thiazolidine and lactam rings without premature resin cleavage. Sequence elongation, resin cleavage by UV irradiation, and purification by preparative HPLC afforded peptides (6*R*,7*aR*)- and (6*R*,7*aS*)-**2.130**. Lactams **2.130** displayed extended conformations and maintained low nanomolar affinity for the

angiotensin II receptor without binding to the angiotensin I receptor, indicating the importance of peptide conformation for receptor subtype engagement (see Fig. 17, Sect. 2.5). In addition, angiotensin II analogs harboring related γ -lactam constraints fused to larger 8- and 9-membered rings were prepared from linear precursors which contained His and Tyr residues as spacers between the residues bearing the reactive ω -aldehyde and ω -thiol side chains [207].

Azabicyclo[3.3.0]octanone systems bearing α -amino- γ -lactams have been made by alternative ring closing strategies [67, 208]. In the synthesis of azabicyclo[3.3.0]octan-2-one-8-carboxylate **2.133** (Scheme 22), transannular ring closure of macrocyclic lactam **2.132** set diastereoselectively two chiral centers. Lactam precursor **2.132** was accessed by ring closure metathesis (RCM) of diene **2.131** followed by removal of the 2,4-dimethoxybenzyl group using acid [67]. Although iodamidation failed using iodine alone, addition of (diacetoxyiodo)benzene (DIB) to the reaction mixture converted olefin **2.132** into iodopyrrolizidinone **2.133**. The conformation of the latter was examined using X-ray crystallography (see Sect. 2.5).

Diverse approaches have been developed to access α -amino- γ -lactams fused to aromatic rings (Fig. 13) [209, 210]. Racemic lactams **2.134** and **2.135** were respectively accessed in two- and four-steps from readily available precursors. For lactam **2.134**, a Ugi four-component coupling reaction was employed to assemble ethyl glycinate, acetic acid, 2-iodobenzaldehyde, and methyl isocynoacetate into a linear intermediate which was cyclized by a microwave-assisted intramolecular Buchwald-Hartwig amidation reaction [105]. The synthesis of lactam **2.135** was achieved from isatin by *N*-alkylation, olefination, and aziridination of the unsaturated lactam [106]. Isatin has also provided the framework for construction of lactam **2.136** (Scheme 23) [107, 211]. Addition of allyl Grignard reagent to the imine from condensation of *O*-TBS phenylglycinol and *N*-*p*-methoxybenzylisatin produced diastereoselectively amine **2.137**. Removal of the chiral auxiliary, acetylation, and *N*-allylation afforded diene **2.138**, which upon RCM and olefin hydrogenation gave the spirocycle **2.139**. Conversion to the dipeptide model (*3S*)-**2.136** was accomplished in 15% yield after 11 steps from *N*-*p*-methoxybenzylisatin. Computational analysis



Scheme 22 Synthesis of 1-azabicyclo[3.3.0]alkane dipeptide [67]

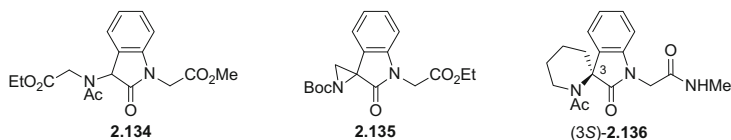
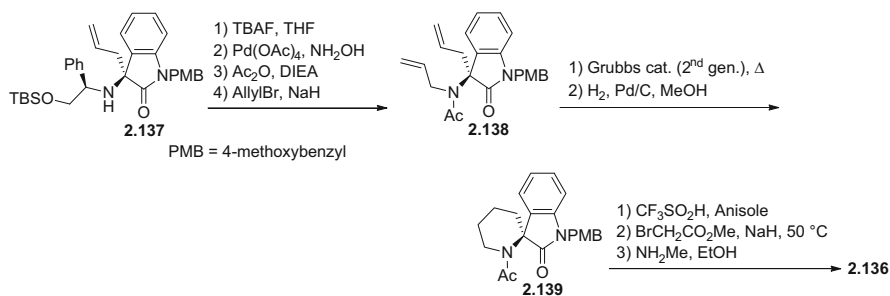
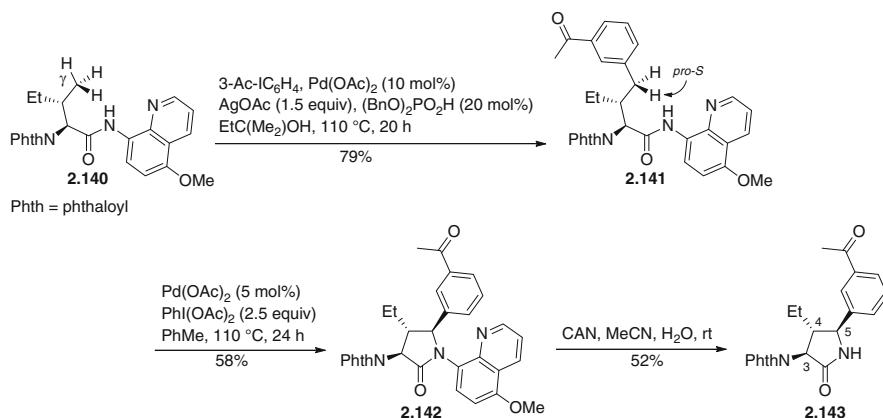


Fig. 13 Representative 4,5-benzene-fused 3-amino- γ -lactams [105–107]



Scheme 23 Synthesis of benzene-fused spirocyclic γ -lactam dipeptide **2.136** [107, 211]



Scheme 24 γ -Lactam synthesis by multiple metal-catalyzed C(sp³)-H activation reactions [81]

and NMR spectroscopy indicated that constrained dipeptide **2.136** adopted a turn conformation (see Sect. 2.5, Fig. 16).

Isoleucinamide **2.140** was converted to 4,5-disubstituted 3-amino- γ -lactam **2.143** by repeated metal-catalyzed functionalization reactions: γ -methyl monoarylation with 3-iodoacetophenone to afford homophenylalaninamide **2.141**, and diastereoselective ring closure through *pro-S* γ -C-H bond activation by palladium to fashion α -amino- γ -lactam **2.142** (Scheme 24) [81]. Oxidative *N*-deprotection with ceric ammonium nitrate gave 3*S*,4*R*,5*S*- γ -lactam **2.143**.

2.5 Conformational Analysis of Substituted α -Amino- γ -Lactam Peptides

Since their conception by Freidinger and Veber, α -amino- γ -lactams have been introduced into peptides to induce turn conformations by constraining rotation specifically about the ψ - and ω -dihedral angles [27]. Peptide turns play vital roles

in molecular recognition events which make them important sources of inspiration in the design of bioactive peptidomimetics [64, 212–216]. In the synthesis of turn mimetics, substituted lactams provide fruitful avenues for the simultaneous control over backbone and side chain topography.

Conformational analysis of α -amino- γ -lactams and their substituted variants has been performed predominantly by using NMR spectroscopy [82, 107, 194], X-ray crystallography [84, 99, 100, 158, 204, 217], computation [68, 92], and combinations thereof [82, 107, 194]. Moreover, circular dichroism (CD) [97, 194, 218, 219] and FT-IR spectroscopy [82, 107, 194] have been used to study the conformation of α -amino- γ -lactams. Although infrequently used to study peptidomimetics, variable temperature HPLC of α -amino- γ -lactam analogs of human growth hormone [6–13] demonstrated that the relative stability of the type II' β -turn structure manifested changes in retention time and bandwidth as a function of temperature (see Fig. 8) [154].

The conformational preference of the parent AgI residue has been reviewed [34, 40, 64]. In brief, contingent on D- or L-stereochemistry of the α -carbon, AgI residues situate typically at the $i + 1$ position of type II and II' β -turns, because the lactam ring constrains the ω -dihedral angle to 180° and the ψ -torsion angle to $125^\circ \pm 10^\circ$ and $-125^\circ \pm 10^\circ$, respectively. Steric interactions between the lactam ring and neighboring residue side chains also restrict backbone geometry to favor turn conformers. For example, X-ray crystallographic studies on a series of analogs of the dopamine D2 receptor allosteric modulator Pro-Leu-Gly-NH₂ in which the central leucine residue was replaced with AgI revealed that bulkier substituents on an N-terminal imidazolidinone and on the C-terminal Gly residue in **2.146** and **2.147** favored turn geometry over the linear conformations observed in **2.144** and **2.145** (Fig. 14) [220–223].

Heterocycle ring substituents may introduce energetic bias to favor specific ring pucker conformers [224, 225]. Although few studies of the conformational preferences of substituted γ -lactam constraints have been reported [168, 194, 204], the influence of hydroxyl substituents on an α -amino- δ -lactam counterpart has been shown to augment the population of particular ring pucker conformers [32]. In particular, thiaindolizidinones with hydroxyl groups on the δ -lactam were shown to have greater conformational rigidity relative to their unsubstituted counterparts [32]. In the case of the X-ray structure of β -hydroxy- α -amino- γ -lactam analog **2.148** (Fig. 15, Scheme 8), the backbone ϕ - and ψ -torsion angles were in agreement with the central residues of a type II β -turn except for the Leu ψ -dihedral angle,

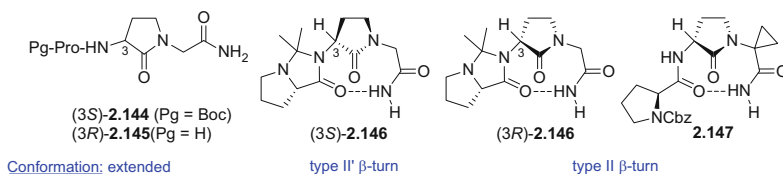


Fig. 14 AgI analogs of Pro-Leu-Gly-NH₂ examined by X-ray crystallography [220–223]

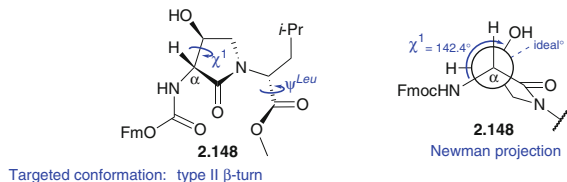


Fig. 15 Influence of β -hydroxy- α -amino- γ -lactam on backbone and side chain geometry [168]

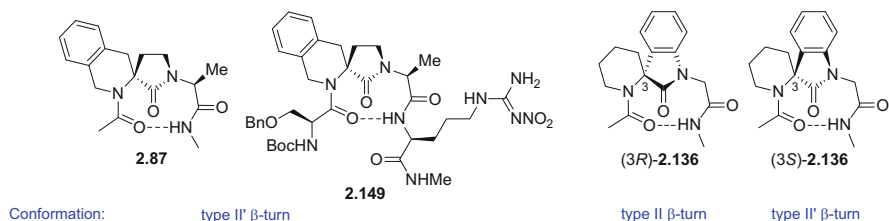
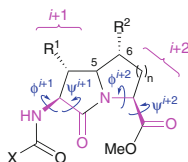


Fig. 16 Spirocycles possessing α -amino- γ -lactams that situate at the $i + 1$ position of β -turns [107, 194]

which was rotated from the ideal conformer likely due to the absence of a C-terminal amide [168]. For the Ser/Thr motif within the β -hydroxy- γ -lactam ring, the χ^1 -dihedral angle value of 142.4° deviated 37.6° from the ideal *trans* conformation (**2.148**, Newman projection) [216].

A spirocycle centered at the α -carbon has provided α -amino- γ -lactams that adopt β -turn conformations as observed by a variety of methods. For example, tetrahydroisoquinoline-based spirocyclic lactam **2.87** was shown to adopt a type II' β -turn conformation by X-ray crystallography, as well as NMR, FT-IR, and CD spectroscopic techniques (Fig. 16) [194]. In the IR spectrum of **2.87** at 2.0 mM in CHCl_3 , an absorption band at $3,352\text{ cm}^{-1}$ was observed indicative of a hydrogen-bonded amide NH stretch. Moreover, in the CD spectrum of spirocycle **2.149** in methanol (0.2 mM), a curve shape for a type II' β -turn was observed featuring two negative minima, one at 203 nm and a second one at 218 nm, and a negative maximum at 209 nm. Similarly, spiro-piperidine-3,3'-oxindole-based peptide isostere (3*R*)-**2.136** was shown by computational analysis to prefer backbone dihedral angles that closely replicated an ideal type II β -turn in which the α -amino- γ -lactam was situated at the $i + 1$ position [107]. In the NMR spectrum of (3*S*)-**2.136** in CDCl_3 at 2.0 mM concentration, titration studies also indicated that the chemical shift of the amide NH remained relatively constant with increasing amounts of DMSO. The presence of a stable intramolecular hydrogen-bonded conformation was supported by a strong nuclear Overhauser effect, which revealed proximity between the acetyl group and the N- CH_2 protons of the piperidine ring.

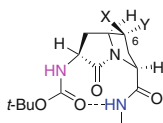
Inside fused pyrrolizidinone and indolizidin-9-one systems **2.150**, **2.29**, and **2.133** (Table 1, see also Schemes 2 and 22), α -amino- γ -lactams have been shown by X-ray crystallography to adopt similar ψ^{i+1} and ϕ^{i+2} dihedral angle values to those of the $i + 1$ and $i + 2$ residues of an ideal type II' β -turn (Table 1). The more

Table 1 Dihedral angle values (in degrees) of fused bicyclic α -amino- γ -lactam ring systems from crystallographic analyses

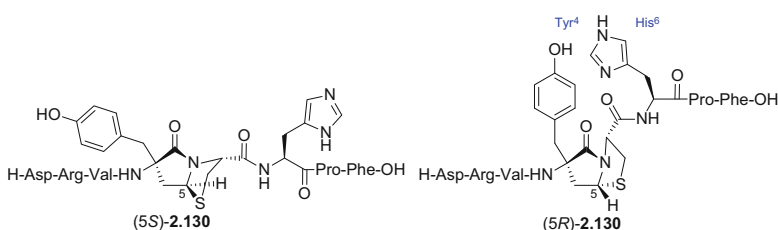
Turn structure	X	R ¹	R ²	<i>n</i>	φ^{i+1}	ψ^{i+1}	φ^{i+2}	ψ^{i+2}	Reference
Ideal inverse γ	–	–	–	–	–	–	–70 to –80°	60–80°	[132–134]
Ideal β -II	–	–	–	–	–60°	120	80°	0°	[135]
Pyrrolizidinone (5 <i>R</i>)- 2.150	Or-Bu	H	H	1	–107°	–149°	–45°	147°	[88]
Hydroxypyrrolizidinone (5 <i>S</i> ,6 <i>R</i>)- 2.29	Or-Bu	H	OH	1	–170°	–141°	–41°	130°	[87]
Iodopyrrolizidinone (5 <i>S</i>)- 2.133-1	OFm	I	H	1	–120°	–141°	–109°	174°	[67]
Iodopyrrolizidinone (5 <i>S</i>)- 2.133-2	OFm	I	H	1	53°	–143°	–109°	170°	[67]
Ideal β -II'	–	–	–	–	60°	–120°	–80°	0°	[135]
Indolizidin-9-one (5 <i>R</i>)- 2.151	Or-Bu	H	H	2	–129°	–141°	–34°	118°	[95]

flexible ϕ^{i+1} and ψ^{i+2} dihedral angle values of these 5,5- and 5,6-fused bicyclic systems varied such that extended as well as turn-like conformers were observed likely because of the presence of a C-terminal ester instead of an amide, as well as crystal packing forces. *N*-Methyl amide derivatives **2.152** and **2.25** were synthesized from pyrrolizidinone **2.150** and (6*R*)- and (6*S*)-hydroxypyrrolizidinones **2.29** (see Fig. 7 and Scheme 2). Examination using variable temperature (VT)-NMR spectroscopy in DMSO-*d*₆ revealed significant differences between the temperature coefficients of the carbamate and amide NH signals (Table 2), suggesting that they exist in two different environments. Although the temperature coefficients of the methyl amide protons were not in the reported range of hydrogen-bonded amides within cyclic peptides and larger proteins [226], they differed significantly from those of the carbamate NH signals indicating their involvement in intramolecular hydrogen bonds.

Thiapyrrolizidinone peptidomimetics **2.130** exhibited selective angiotensin II receptor subtype-2 affinity in the low nanomolar range (Fig. 17, Scheme 21) [79]. Differing respectively at the ring fusion stereochemistry of the 5,5-fused bicycle, both analogs possess the carboxylic acid and amine components on opposite sides of the thiapyrrolizidinone. A combination of computational analysis and NOESY spectroscopy indicated that both isomers adopt extended backbone conformers (i.e., (5*S*)-**2.130** and (5*R*)-**2.130**). In the conformer of the four-fold less

Table 2 Temperature coefficients ($\Delta\delta/\Delta T$ in ppb/T) from VT-NMR studies in DMSO- d_6 of 5,5-fused bicycles

5,5-Fused bicycle	X	Y	BocNH	NHMe	Reference
Pyrrolizidinone 2.152	H	H	-10.2	-5.2	[88]
Hydroxypyrrolizidinone (6R)- 2.25	H	OH	-8.4	-4.3	[87]
Hydroxypyrrolizidinone (6S)- 2.25	OH	H	-11.7	-5.3	[87]

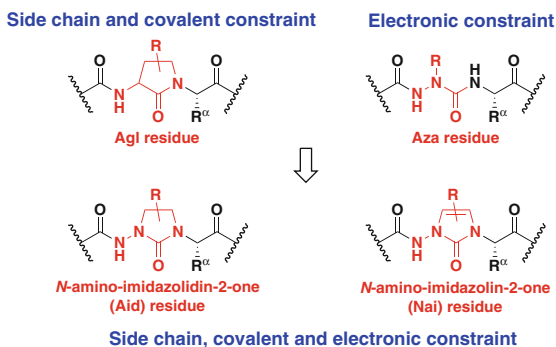
**Fig. 17** Conformers of 5,5-fused thiazabicycloalkane peptidomimetics **2.130** [79]

potent (5R)-isomer, the side chains of the Tyr⁴ and His⁶ residues were observed to have closer proximity.

3 *N*-Amino-Imidazolin-2-one (Nai) and *N*-Amino-Imidazolidin-2-one (Aid) Peptidomimetics: Synthesis and Conformational Analysis

As mentioned above, the Agl residue predisposes the peptide backbone to mimic β -turn secondary structures [175], such as those commonly involved in molecular recognition events of biologically active peptides [212, 213]. Azapeptides, in which the C $_{\alpha}$ H moiety is substituted for a nitrogen atom (Fig. 18), utilize electronic forces to stabilize β -turn conformations [227]. The semicarbazide structure of the azapeptide rigidifies the ψ -dihedral angle, due to the planarity of the urea moiety, and the ϕ -dihedral angle, because of hydrazine nitrogen lone pair-lone pair repulsion [228]. Applications of amino lactam and aza-residues as conformational constraints have provided means for improving receptor affinity by likely diminishing the loss of entropy needed for folding into an active conformer [18, 24, 175, 227, 229].

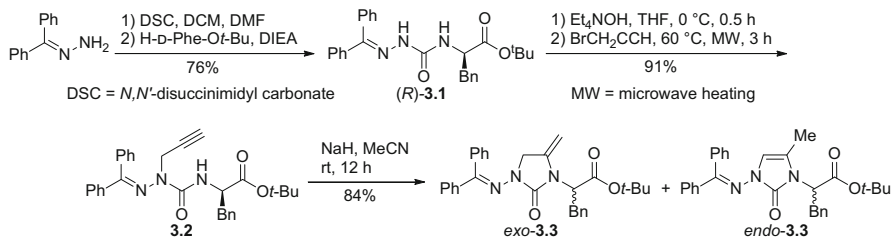
Fig. 18 Design of Nai and Aid peptidomimetics based on Agl and azapeptide counterparts



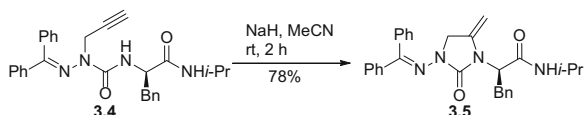
The syntheses of *N*-amino-imidazolin-2-one (Nai) and *N*-amino-imidazolidin-2-one (Aid) peptidomimetics were pursued to blend attributes of Agl and aza-amino acid residues (Fig. 18) [230, 231]. The resulting *N*-amino cyclic ureas enable conformational constraint with potential to facilitate the addition of side chain functional groups onto the heterocycle. By combining the attributes of Agl and Aza residues into a single molecular scaffold, they employ both structural and electronic constraints to restrict rotation about the backbone ϕ -, ψ -, and ω -dihedral angles, consequently favoring β -turn secondary structures [231]. Using X-ray crystallographic and NMR spectroscopic analyses, we have shown that Nai and Aid residues can adopt the central positions of type II' β - and γ -turns [231, 232, 253].

3.1 Synthesis of Nai Dipeptides with 4-Position Substituents

N-Amino-imidazolin-2-one (Nai) residues have been introduced into peptide sequences by an approach featuring 5-*exo-dig* cyclization of an aza-propargylglycine residue using sodium hydride as base [231–233]. Simpler imidazolin-2-ones had previously been prepared from *N*-propargylureas using other bases [232, 234], and transition metal complexes containing respectively palladium [234–236], gold [237] and silver [238]; however, only basic conditions formed successfully 4-substituted Nai analogs. Aza-propargylglycyl dipeptides (e.g., **3.2**, Scheme 25) have been synthesized in solution by alkylation of a semicarbazone protected azaglycine dipeptide with propargyl bromide [231, 232, 240, 241]. The azaglycine dipeptides have been obtained by activation of benzophenone hydrazone with *N,N'*-disuccinimidyl carbonate (DSC) or *p*-nitrophenylchloroformate and coupling to an amino ester or amino amide [239–242]. For example, treatment of benzophenone hydrazone with DSC and reaction with *D*-phenylalanine *tert*-butylester hydrochloride gave aza-dipeptide (*R*)-**3.1** (Scheme 25). Benzhydrylidene aza-glyciny-*D*-phenylalanine *tert*-butyl ester [(*R*)-**3.1**] was alkylated selectively without racemization using tetraethylammonium hydroxide as base and



Scheme 25 Synthesis of imidazolin-2-one by NaH promoted 5-*exo-dig* cyclization of benzhydrylidene aza-propargylglycyl-phenylalanine dipeptide [231, 239]

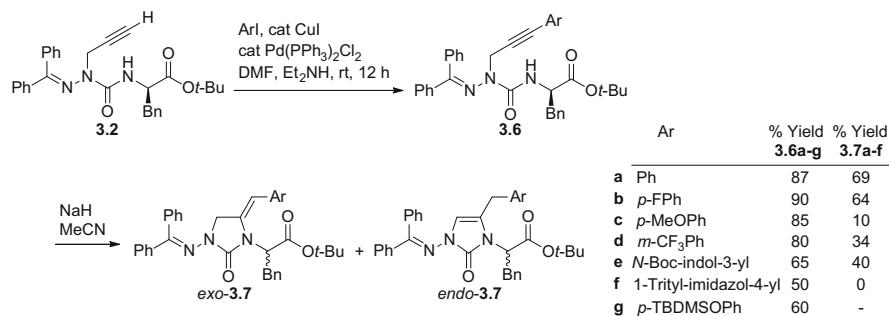


Scheme 26 Cyclization of aza-propargylglycyl dipeptide amide [231]

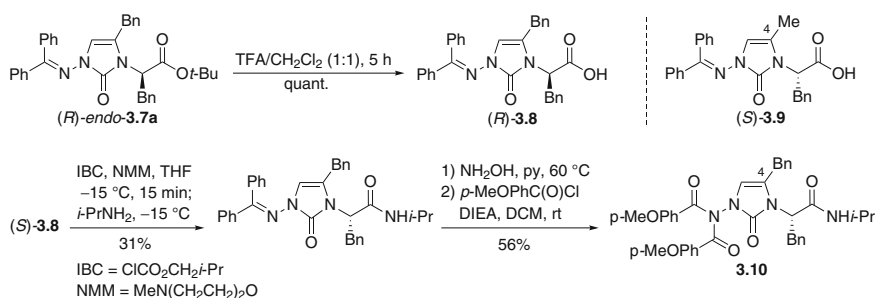
propargyl bromide as electrophile to provide aza-propargylglycyl-D-phenylalanine **3.2** [240, 241].

The 5-*exo-dig* cyclization of aza-propargylglycyl dipeptide **3.2** was successfully achieved using 250 mol% of NaH in acetonitrile. In contrast, attempts to employ gold [(*t*-Bu)₂(*o*-biphenyl)PAuCl] and silver (AgOTf) catalysts failed to effect cyclization [231]. The exocyclic double bond of *exo*-**3.3** was presumed to arise from protonation after cyclization (cyclization may involve an allene intermediate, see: [243, 244]); however, migration occurred spontaneously in solution and was catalyzed by acid, such as silica gel during chromatography, to furnish the thermodynamically more stable endocyclic double bond isomer *endo*-**3.3**. In addition, samples of exocyclic olefin product were observed to convert to the endocyclic isomer on standing as a CDCl₃ solution in a NMR tube. Partial racemization of ester **3.2** occurred under the basic cyclization conditions; the enantiomers of amino-imidazolone *endo*-**3.3** were separated by preparative Supercritical Fluid Chromatography (SFC) on an AD-H column using 15% isopropanol as eluent at 60 g/min and 150 bars [239]. On the other hand, aza-propargylglycyl dipeptide amide **3.4** underwent 5-*exo-dig* cyclization to provide amino-imidazolone **3.5** without racemization and spontaneous double bond migration (Scheme 26).

A set of 4-arylmethyl-1-amino-imidazolin-2-ones was synthesized by introduction of a Sonogashira cross-coupling reaction into the synthetic sequence for arylation of the aza-propargylglycine residue (Scheme 27) [231]. Benzhydrylidene aza-propargylglycyl-phenylalanine dipeptide **3.2** was treated with different aryl iodides, Pd(PPh₃)₂Cl₂, and CuI in 1:1 DMF/Et₂NH to obtain the corresponding aza-arylpropargylglycines **3.6a–g** in 50–90% yields. Notably, *N*-(Boc)-3-iodoindole and *N*-(trityl)-4-iodoimidazole reacted in the Sonogashira cross-coupling to provide the aza-tryptophan and aza-histidine analogs **3.6e** and **3.6f** in 65% and 50% yields, respectively.



Scheme 27 Sonogashira cross-coupling modification of aza-propargylglycyl dipeptides followed by cyclization [231]



Scheme 28 Synthesis of 4-benzyl *N*-amino-imidazolin-2-one peptide **3.10** [231, 232]

Employing the various aza-arylpropargylglycine analogs **3.6** in the *5-exo-dig* cyclization conditions mentioned above gave 4-arylmethyl-1-amino-imidazolin-2-ones **3.7a-f** as mixtures of *endo* and *exocyclic* double bond isomers as observed by NMR spectroscopy (Scheme 27) [231]. For example, aza-phenylpropargylglycine **3.6a** reacted with 250 mol% of NaH in acetonitrile to provide 4-benzyl-1-amino-imidazol-2-one **3.7a** as a mixture of racemic *endo* and *exocyclic* olefin isomers in 69% yield. After purification of 4-benzyl-1-amino-imidazol-2-ones **3.7a** by chromatography, olefin internalization occurred. The enantiomers were later separated using SFC with the conditions described above [239]. 4-Methyl- and 4-benzyl-1-amino-imidazol-2-one *tert*-butyl esters (*S*)-*endo*-**3.3** and (*R*)-*endo*-**3.7a** were converted to their corresponding Nai-dipeptide acids (*S*)-**3.9** and (*R*)-**3.8** using 50% TFA in DCM solution (Scheme 28).

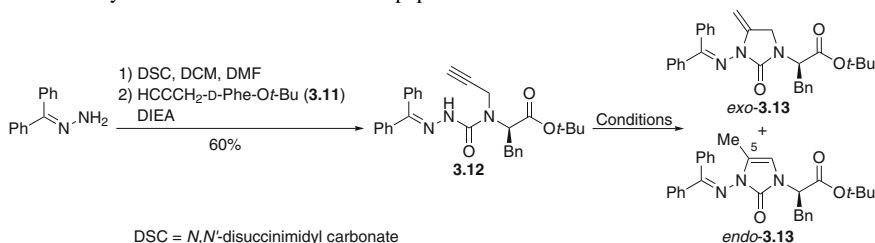
The Nai-dipeptide acids **3.8** and **3.9** have been introduced into peptides [231, 232]. For example, 4-benzyl-Nai dipeptide (*S*)-**3.8** was incorporated into model peptide **3.10** by a route entailing coupling to *iso*-proylamine after activation as a mixed anhydride with *iso*-butyl chloroformate, semicarbazone removal with hydroxylamine hydrochloride in pyridine, and acylation with 4-methoxybenzoyl chloride (Scheme 28) [232]. The conformation of Nai peptide **3.10** was analyzed by X-ray crystallography (see Sect. 3.4, Fig. 21).

3.2 Synthesis of Nai Dipeptides with 5-Position Substituents

5-Substituted Nai analogs have been pursued using 5-*exo-dig* cyclization reactions on aza-glycyl-*N'*-propargylamide derivatives (Y. García-Ramos and W. D. Lubell, unpublished work). For example, 5-methyl-*N*-aminoimidazolin-2-one *endo*-**3.13** was prepared from cyclization of benzhydrylidene aza-glycyl-*N*-propargyl-D-phenylalanine **3.12** (Table 3). The latter was synthesized in 60% yield by acylation of *N*-propargyl-D-phenylalanine *tert*-butyl ester (**3.11**) using the activated carbazate prepared from benzophenone hydrazone and DSC. *N*-Propargyl-D-phenylalanine **3.11** was synthesized in 70% yield with minimal *N,N*-dialkylation side product by alkylation of D-phenylalanine *tert*-butyl ester hydrochloride salt with propargyl bromide in DMF using 2.2 equivalents of lithium hydroxide as base at 0°C [245].

Various conditions gave successfully 5-*exo-dig* cyclization from aza-glycyl-*N*-propargylphenylalanine dipeptide **3.12** to produce the 5-methyl Nai analog *endo*-**3.13** and its exocyclic olefin counterpart *exo*-**3.13**. For example, employing the same basic conditions used in the 5-*exo-dig* cyclizations to make 4-methyl Nai analogs, the NaH treatment gave significant amounts of decomposition and exocyclic olefin *exo*-**3.13** in only 31% (entry 1, Table 3). Transition metal catalyzed conditions gave higher yields of Nai products. Treatment of aza-dipeptide **3.12** in acetonitrile at room temperature with the combination of gold [(*t*-Bu)₂(*o*-biphenyl)PAuCl] and silver (AgOTf) catalysts gave exocyclic olefin *exo*-**3.13** in 94% yield (entry 2). In the absence of the silver catalyst, the gold catalyzed cyclization was

Table 3 Synthesis of 5-substituted Nai dipeptides **3.13**

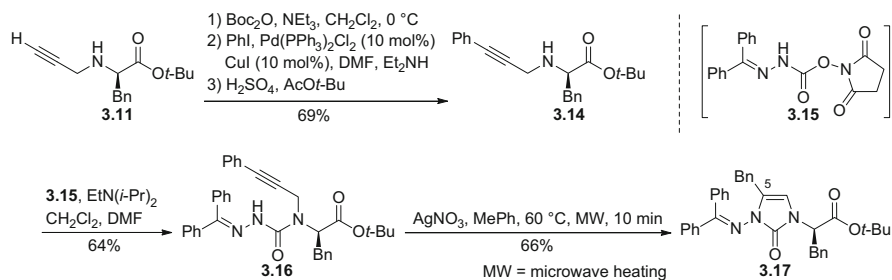


Entry	Conditions	<i>exo</i> - 3.13	<i>endo</i> - 3.13
1	NaH (2 equiv), MeCN, 25°C, 2 h	31%	–
2	[(<i>t</i> -Bu) ₂ (<i>o</i> -biphenyl)P]AuCl (10 mol%), AgOTf (10 mol%), MeCN, 25°C, 12 h	94%	–
3	[(<i>t</i> -Bu) ₂ (<i>o</i> -biphenyl)P]AuCl (10 mol%), MePh, 80°C, 12 h	41%	–
4	AgOTf (10 mol%), MeCN, 80°C, 12 h	65%	–
5	InBr ₃ (10 mol%), MePh, 80°C, 12 h	75%	13%
6	PtCl ₂ (10 mol%), MePh, 80°C, 12 h	30%	25%
7	PdCl ₂ (PPh ₃) ₂ (10 mol%), MePh, 80°C, 12 h	–	59%
8	PdCl ₂ (10 mol%), MePh, 80°C, 12 h	–	68%
9	AgNO ₃ (10 mol%), MePh, 80°C, 12 h	–	87%

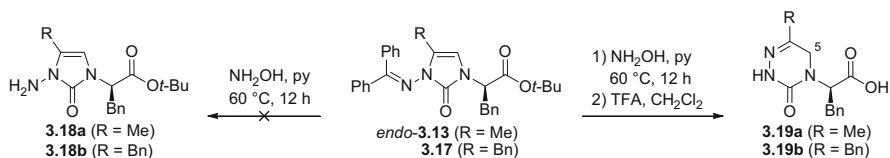
sluggish and required heating to provide exocyclic olefin *exo*-**3.13** in only 41% yield (entry 3) [237]. Silver triflate alone at higher temperature in acetonitrile afforded exocyclic olefin *exo*-**3.13** in 65% yield (entry 4). Indium and platinum catalysts (entries 5 and 6) gave mixtures of *exo* and *endo* olefin isomers, with a preference for the former [246, 247]. On the other hand, palladium catalysis afforded selectively the endocyclic product in 59–68% yields (entries 7 and 8). Silver nitrate in toluene at 80 °C for 12 h proved the best condition for obtaining the endocyclic olefin *endo*-**3.13** in high yield (87%, entry 9). Employing the silver nitrate conditions at lower temperatures or shorter times gave lower yields of *endo*-**3.13** with contamination of the exocyclic olefin *exo*-**3.13**; however, shorter reaction times did give high yields (75–97%) of endocyclic olefin *endo*-**3.13** using silver nitrate and microwave heating at 60 and 80 °C in toluene.

After Boc protection of propargylamine **3.11**, Sonogashira reaction of the resulting *N*-(Boc)-*N*-propargyl-D-phenylalanine *tert*-butyl ester with phenyl iodide gave the *N*-(Boc)-*N*-phenylpropargyl-D-phenylalanine product in 79% yield (Scheme 29) [248]. Selective removal of the Boc group in the presence of *tert*-butyl ester was achieved with sulfuric acid in *tert*-butyl acetate to provide amino ester **3.14** in 93% yield, and in 69% over three steps [249]. Acylation of amine **3.14** with activated carbazate **3.15**, derived from treating benzophenone hydrazone with DSC, gave aza-dipeptide **3.16** in 64% yield. Treatment of aza-glycyl-*N'*-phenylpropargylamide **3.16** with silver nitrate under microwave irradiation provided the endocyclic olefin isomer **3.17** in 66% yield.

Attempts to remove the benzhydrylidene protection from the 5-substituted *N*-imidazolin-2-ones *endo*-**3.13** and **3.17** using hydroxylamine hydrochloride in pyridine failed respectively to provide the desired semicarbazides **3.18a–b** (Scheme 30); instead, 1,2,4-triazin-3(2H)-ones **3.19a–b** were obtained, after ester deprotection, characterized by NMR spectroscopy, and in the case of **3.19a**, crystallized for X-ray analysis (Fig. 19) (Y. García-Ramos and W. D. Lubell, unpublished work). The ¹³C and ¹H NMR spectra of triazinone **3.19a** characterized respectively the ring C5 carbon as a methylene at 58.8 ppm bearing diastereotopic geminal protons appearing as a coupled pair of doublets at 3.85 and 3.72 ppm.



Scheme 29 Synthesis of 5-benzyl-Nai dipeptide **3.17**



Scheme 30 Synthesis of 1,2,4-triazin-3(2H)-ones **3.19a** and **3.19b**

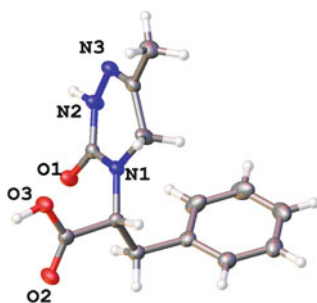
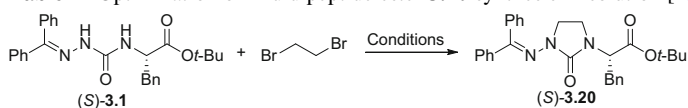


Fig. 19 X-ray structure of 1,2,4-triazin-3(2H)-one **3.19a**

3.3 Synthesis of *N*-Amino-Imidazolidin-2-one (Aid) Peptidomimetics

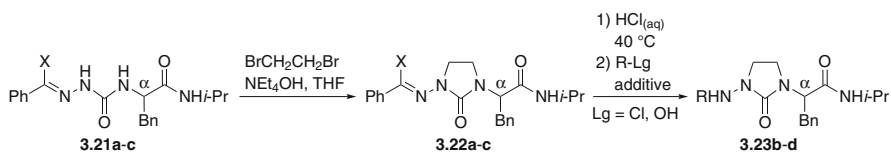
The Aid residue is respectively the saturated and aza-variant of its Nai and Agl counterparts. *N*-Amino-imidazolidin-2-one (Aid) peptidomimetics have been synthesized by a solid-phase method for constructing the cyclic *N*-amino ureas [230]. In contrast to the synthesis of Nai peptidomimetics, which entails 5-*exo-dig* cyclization in solution prior to the application of the resulting Nai dipeptide building blocks [231], solid-phase Aid peptidomimetic synthesis features alkylation of a protected aza-glycinamide residue using 1,2-dibromoethane and base. The synthesis of Aid residues thus offers opportunity for application in combinatorial approaches to study the importance of structural and electronic forces for conformational control, as has been illustrated for related acyclic *N*-alkyl aza-peptide counterparts [250, 251].

In a solution-phase approach to Aid dipeptide esters, attempts to alkylate benzhydrylidene aza-glycyl-phenylalanine *tert*-butyl ester [(*S*)-**3.1**] [240] using 1,2-dibromoethane and tetrabutylammonium hydroxide (TBAH) gave the desired cyclic urea, imidazolidin-2-one (*S*)-**3.20** in 15% yield (Table 4, entry 1) [230]. Switching to tetraethylammonium hydroxide (TEAH) as base improved the yield of **3.20** to 62% (entry 2); however, racemization was detected by examination of the ester product using SFC on a chiral column. Racemization was avoided by decreasing the temperature to 0°C, albeit with lower reaction yield (entry 3).

Table 4 Optimization of Aid dipeptide ester **3.20** synthesis in solution [230]

Entry	Conditions	Yield 3.20 (%)
1	NBu ₄ OH, THF	15
2	NEt ₄ OH, THF	62 ^a
3	NEt ₄ OH, THF, 0°C	21

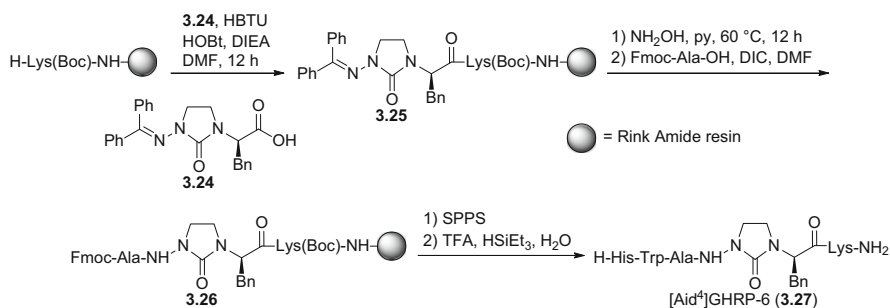
^aPartial α -center epimerization occurred during formation of **3.20**

Table 5 Synthesis of Aid dipeptides **3.22a–c** and incorporation into di- and tripeptide amides **3.23b–d** [230, 252]

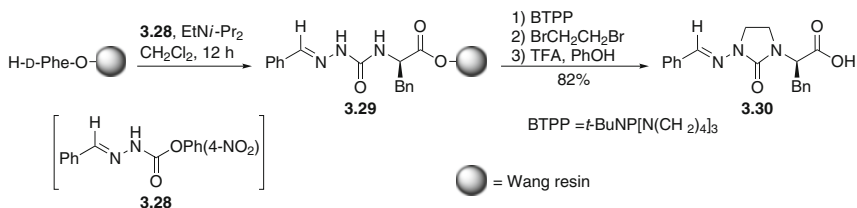
Intermediates 3.22a–c					Products 3.23b–d			
Entry	#	X	α	Yield (%)	#	R-Lg	Additive	Yield (%)
1	a	Ph	<i>R</i>	55	–	–	–	–
2	b	H	<i>R</i>	87	b	<i>p</i> -MeOPhC(O)-Cl	DIEA	89
3	c	H	<i>S</i>	85–87	c	<i>p</i> -BrPhC(O)-Cl	DIEA	74
4	b	H	<i>R</i>	87	d	Fmoc-Ala-OH	DIC	68

In contrast to dipeptide ester **3.1**, alkylation of the isopropyl amide counterpart **3.21a** to afford Aid-dipeptide **3.22a** using the optimal TEAH conditions occurred without racemization and in similar yield (55%, entry 1, Table 5). The yield of Aid-dipeptide **3.22** was enhanced to 87% upon switching the aza-glycine residue protection from benzhydrylidene to benzylidene (entry 2) [230]. The benzylidene group of hydrazone **3.22b** was subsequently removed effectively using 1 N HCl in THF (1:2 v/v) at 40°C to provide the corresponding semicarbazide [253]. The latter was acylated using benzoyl chlorides and DIEA, as well as with the symmetric anhydride prepared from Fmoc-Ala-OH and DIC, to give respectively Aid di- and tri-peptides **3.23b–d** in 68–89% yields overall (Table 5, entries 2–4) [230, 252]. The conformational preferences of Aid peptides **3.23** were probed using X-ray crystallography (see Sect. 3.4, Fig. 22).

Longer Aid peptides have been made using solid-phase chemistry both by employing dipeptide building blocks and by alkylation of aza-glycine residues of peptides linked to the solid support [230]. For example, acid **3.24** was prepared from Aid-dipeptide ester (*R*)-**3.20** using 1:1 TFA/DCM for 2 h, and coupled to Lys (Boc)-Rink amide resin to give support-bound Aid tripeptide **3.25** (Scheme 31). Elongation of the peptide to provide an analog of growth hormone releasing peptide-6 (GHRP-6) was accomplished by chemoselective benzylidene removal,



Scheme 31 Synthesis of [Aid⁴]GHRP-6 (3.27) employing Aid-dipeptide 3.24 [230]

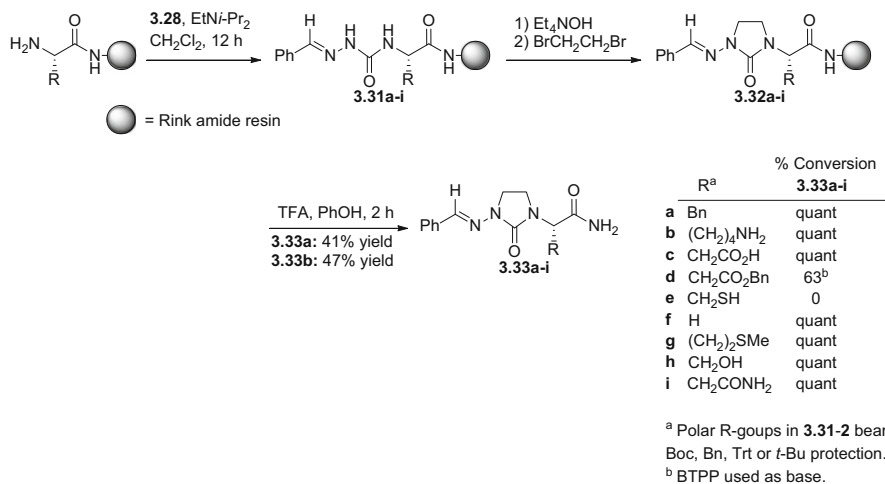
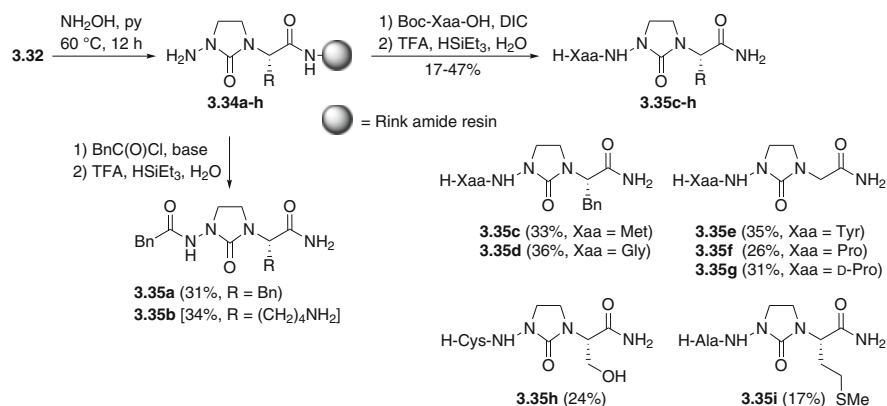


Scheme 32 Solid-phase synthesis of Aid-dipeptide acid 3.30 [230]

employing $\text{NH}_2\text{OH}\cdot\text{HCl}$ in pyridine at 60°C for 12 h [250], followed by acylation with Fmoc-Ala by way of its symmetric anhydride using DIC to give tetrapeptide 3.26. Subsequently, standard solid-phase peptide synthesis (SPPS) protocols were used to complete the Aid peptide [254]. The resin was cleaved with TFA/ H_2O /TES and purification by preparative HPLC to give [Aid⁴]GHRP-6 (3.27) in 13% overall yield [230].

A method for installing Aid residues onto support-bound peptides was developed employing benzylidene aza-glycynyl dipeptides 3.29 and 3.31 possessing a diverse array of C-terminal amino acid residues (Schemes 32 and 33) [230, 250]. To prepare Aid peptide acid 3.30, benzylidene aza-glycynyl-D-phenylalanine 3.29 was synthesized by acylation of D-phenylalaninyl-Wang resin using methyldiene carbazate 3.28, which was generated from benzaldehyde, hydrazine, and *p*-nitrophenylchloroformate (Scheme 32). Alkylation of 3.29 with ethylene dibromide occurred in 82% conversion using the non-nucleophilic base BTTP. Attempts to use TEAH as base were unsuccessful, presumably due to competitive hydrolytic resin cleavage.

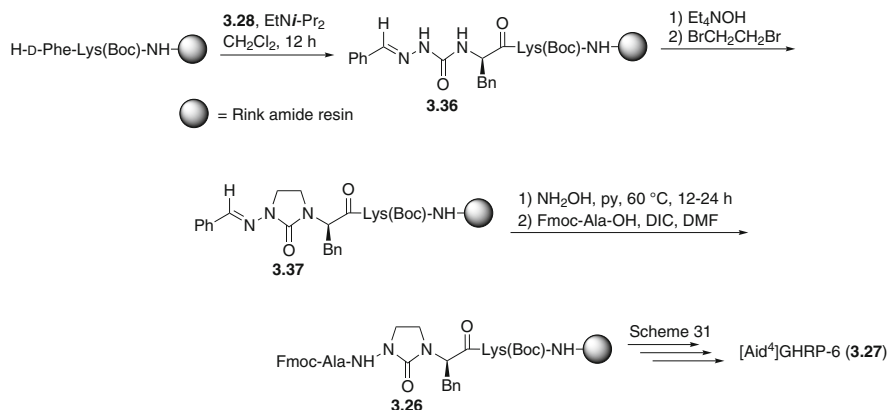
Using Rink amide resin and 3.28, aza-glycynyl dipeptide amides 3.31 were synthesized under similar conditions as described above (Scheme 33) [230]. Alkylation of semicarbazone 3.31 was successfully performed using the ethylene dibromide/TEAH conditions that were optimized in solution. Typically, aza-glycynyl dipeptides 3.31 underwent quantitative bis-alkylation to provide Aid peptides 3.32. After resin cleavage using TFA containing 2% of phenol, benzylidene *N*-amino-imidazolidinones 3.33a and 3.33b were isolated respectively by preparative HPLC in 41% and 47% overall yields. On the other hand, certain amino acids were problematic. For example, the benzyl ester side chain of aspartate

**Scheme 33** Solid-phase synthesis of Aid-dipeptide amides **3.33a-i** [230]**Scheme 34** Solid-phase synthesis of Aid-tripeptides **3.35a-i** [230]

was hydrolyzed during alkylation to afford acid **3.33c**, and multiple attempts failed to synthesize Aid peptide from alkylation of aza-glycine-cysteine(Trt) **3.31e**.

Chemoselective benzylidene removal and liberation of semicarbazide **3.34a-i** was effectively accomplished employing NH₂OH·HCl in pyridine at 60°C for 12 h [250]. Acylation was subsequently performed with phenylacetyl chloride and *N*-protected amino acids activated by way of their symmetric anhydrides [250, 251]. Resin cleavage and side chain deprotection followed by purification by preparative HPLC provided Aid peptides **3.35** in 17–47% overall yields (Scheme 34).

N-Amino-imidazolidin-2-one residues were introduced into the GHRP-6 sequence using the solid-phase alkylation protocol. For example, in the synthesis



Scheme 35 Solid-phase synthesis of [Aid⁴]GHRP-6 peptide by azapeptide alkylation on resin [230]

Table 6 Use of Aid constraints in GHRP-6 peptidomimetics produced using both dipeptide building blocks and solid-phase alkylation of aza-glycine residues [230]

Entry	Peptides	Method ^a	Crude purity (%)	Purity (%)	Isolated yield (%)
1	Aid-D-Trp-Ala-Trp-D-Phe-Lys-NH ₂	A	35	>99	6.8
2	His-Aid-Ala-Trp-D-Phe-Lys-NH ₂	A	51	>99	5.8
3	His-D-Trp-Aid-Trp-D-Phe-Lys-NH ₂	A	51	>99	13.2
4	His-D-Trp-Ala-Aid-D-Phe-Lys-NH ₂ (3.27)	A (B)	44	>99	15.8 (13)
5	His-D-Trp-Ala-Trp-Aid-Lys-NH ₂	A	44	>99	9.7
6	Ala-Aid-D-Phe-Lys-NH ₂	B	72	>99	12.8
7	His-D-Trp-Aid-Trp-D-Phe-NH ₂	B	68	>99	14.0
8	PhAc-Aid-D-Phe-Lys-NH ₂	B	67	>99	11.1

^aScheme 35 procedure for method A, Scheme 31 for method B

of [Aid⁴]GHRP-6 (**3.27**), alkylation of aza-Gly-D-Phe-Lys(Boc)-Rink amide resin **3.36** with 1,2-dibromoethane gave imidazolidin-2-one **3.37** in quantitative conversion (Scheme 35) [230, 250]. Removal of the benzylidene using hydroxylamine hydrochloride in pyridine and acylation with activated *N*-Fmoc-alanine gave semicarbazide resin **3.26**. Subsequent elongation, cleavage, and purification as described above provided [Aid⁴]GHRP-6 (**3.27**) in 44% crude purity and 16% overall yield after HPLC purification (entry 4, Table 6) [230].

Employing the solid-phase alkylation method, four additional [Aid]-GHRP-6 analogs were successfully prepared in 6–13% yields and >99% purity (entries 1–3 and 5, Table 6) [230]. Incomplete alkylation was observed with the longer peptide

sequences and produced side products that complicated HPLC purification of the final Aid-peptides.

3.4 Conformational Analysis of *Nai* and *Aid* Peptides

The influence of *Nai* and *Aid* residues on conformation has been studied on model peptides using ^1H NMR spectroscopy and X-ray crystallography (Figs. 20, 21, and 22, Table 7). For example, model *Nai*-peptides **3.38**, **3.39**, and **3.10** were studied to examine the preferred geometry of the *N*-amino-imidazolin-2-one peptide mimics in solution and the solid state, respectively (Fig. 20, see also Scheme 28). In solution, the 4-methyl *Nai* residue was examined in *N*-(*p*-methoxybenzamido)imidazolin-2-one *iso*-propylamide **3.38** by NMR spectroscopy in CDCl_3 using varying concentrations of DMSO-d_6 (1–100%), which identified respectively solvent shielded and exposed N-H protons for the *iso*-propylamide and *p*-methoxybenzamide hydrogens ($\Delta\delta/\Delta\text{solvent}$ 0.45 and 1.21 ppm) indicative of a turn conformation in which the C-terminal amide is engaged in an intramolecular hydrogen bond [231]. Similar examination of *Aid* peptide **3.23c** (Fig. 20, see also Table 5) identified respectively solvent shielded and exposed hydrogens for the isopropylamide and *p*-bromobenzamide NH signals ($\Delta\delta/\Delta\text{solvent}$: 0.43 and 1.16 ppm). This observation was consistent with a hydrogen-bound *iso*-propylamide proton in a turn conformation.

The solid-state analyses of *Nai* and *Aid* residues in model peptides were consistent with their NMR spectroscopic studies. For example, X-ray analysis of 4-methyl *N*-(benzamido)imidazolin-2-one amide **3.38** identified two different conformers in the crystal lattice: **3.38-1** exhibiting a type II' β -turn possessing a ten-member hydrogen bond, and **3.38-2** adopting an inverse γ -turn encompassing a seven-member hydrogen bond (Fig. 21). In the X-ray structure of the related 4-methyl *N,N*-(bis-*p*-methoxybenzamido)imidazolin-2-one **3.39**, a single

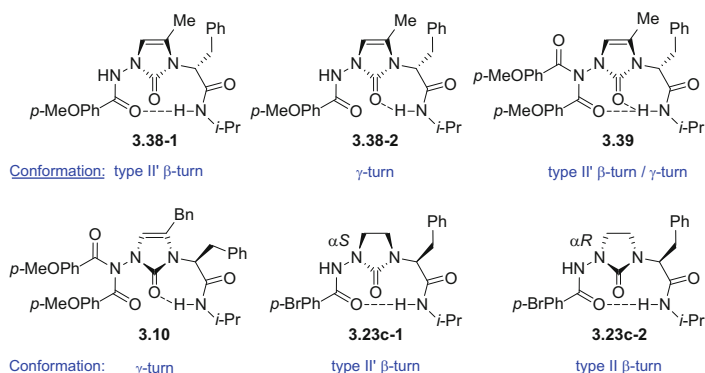


Fig. 20 Turn conformations of *Nai* peptides **3.38**, **3.39**, and **3.10**, and *Aid* peptide **3.23c**

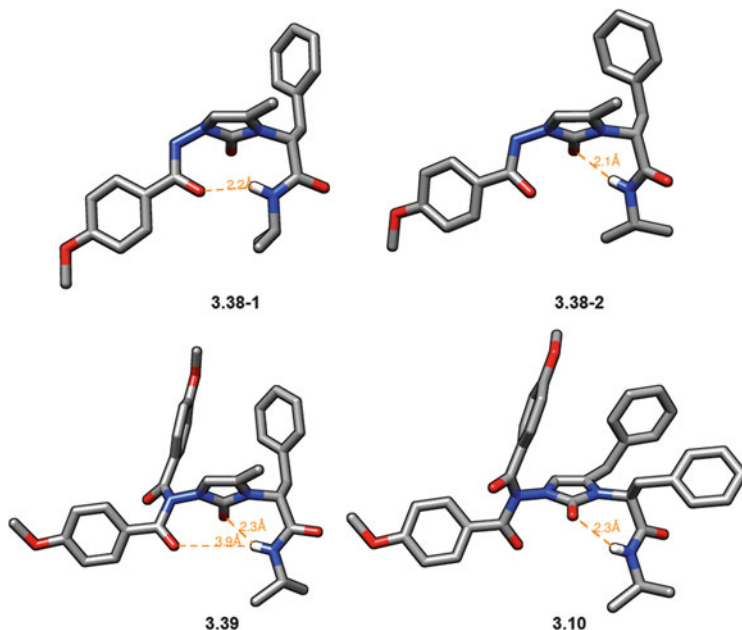


Fig. 21 X-ray structures of 4-benzyl- and 4-methyl Nai peptides **3.38**, **3.39**, and **3.10** [231–232] (For clarity, hydrogen atoms not involved in hydrogen bonding have been omitted)

conformer was observed; however, the ψ^{i+2} dihedral angle value was 31° , midway between the 0° and 60° values of type II' β -turn and inverse γ -turn (Table 7). On the other hand, replacement of the 4-methyl group for a 4-benzyl substituent favored a classic γ -turn geometry as observed in the X-ray structure of 4-benzyl *N,N*-bis-(*p*-methoxybenzamido)imidazolin-2-one **3.10**. The influence of the 4-position substituent was also observed on the χ^1 dihedral angle of the C-terminal phenylalanine side chain, which exhibited respectively *gauche* and *trans* conformers for the 4-methyl and 4-benzyl analogs [216].

X-ray crystallographic analysis of peptide **3.23c** confirmed the preference of the Aid residue to adopt the $i + 1$ position of a β -turn conformation [230–232]. Four different β -turn conformers of **3.23c** were observed in the crystal matrix, all exhibiting intramolecular ten-membered hydrogen bonds between the benzamide carbonyl and *iso*-propylamine NH moieties (residues i and $i + 3$, Fig. 22). Conformer **3.23c-1** exhibited similar dihedral angles to those of an ideal type II' β -turn ($\phi^{i+1} = 60^\circ \pm 6^\circ$, $\psi^{i+1} = -120^\circ \pm 25^\circ$, $\phi^{i+2} = -80^\circ \pm 18^\circ$, $\psi^{i+2} = 0^\circ \pm 9^\circ$); conformer **3.23c-2** had values close to an ideal type II β -turn ($\phi^{i+1} = -60^\circ \pm 6^\circ$, $\psi^{i+1} = 120^\circ \pm 28^\circ$, $\phi^{i+2} = 80^\circ \pm 4^\circ$, $\psi^{i+2} = 0^\circ \pm 23^\circ$, Table 7). The imidazolidinone of the Aid residue was nearly planar; however, *S*- and *R*-configurations were respectively observed for the Aid α -nitrogen in the type II' and II conformers with a slight ~ 0.1 Å distortion from planarity (Fig. 20) [255]. In all

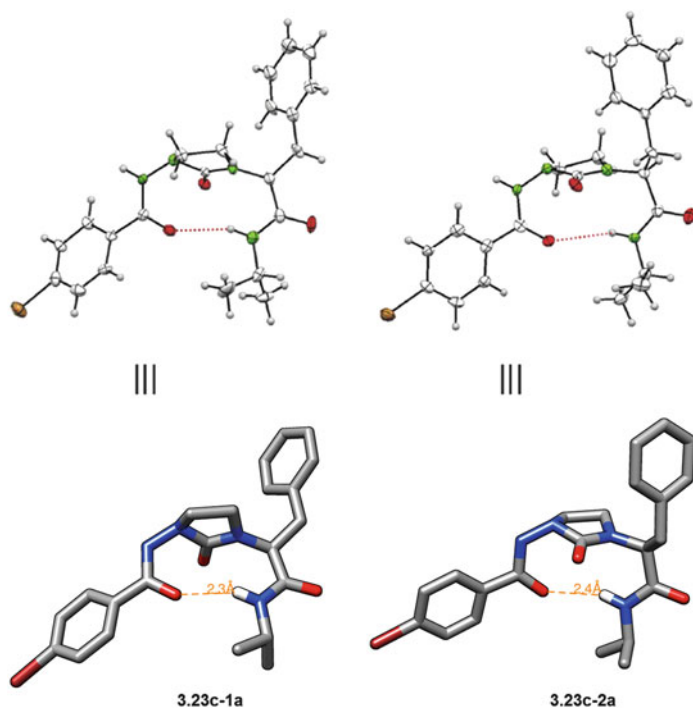
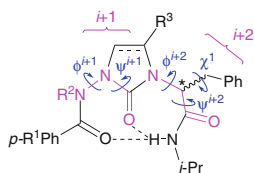


Fig. 22 Select conformers from the crystal structure of Aid peptide mimic **3.23c** [252] (For clarity, hydrogen atoms not involved in hydrogen bonding have been omitted)

Table 7 Dihedral angle values (in degrees) of Nai and Aid peptides from crystallographic analyses



Turn structure	φ^{i+1}	ψ^{i+1}	φ^{i+2}	ψ^{i+2}	Phe χ^1	Reference
Ideal β -II'	60	-120	-80	0	-	[135]
Nai(Me)-D-Phe 3.38-1	59	-153	-69	-5	55	[231]
Nai(Me)-D-Phe 3.38-2	62	-166	-72	66	58	[231]
Ideal inverse γ	-	-	-70 to -80	60-80	-	[132-134]
Nai(Me)-D-Phe 3.39	88	-177	-70	31	68	[232]
Nai(Bn)-L-Phe 3.10	-91	-175	79	-64	-167	[232]
Ideal classic γ	-	-	75	-65	-	[133]
Aid-L-Phe 3.23c-1a	54	-144	-97	19	-58	[253]
Aid-L-Phe 3.23c-1b	56	-149	-98	23	-61	[253]
Ideal β -II	-60	120	80	0	-	[135]
Aid-L-Phe 3.23c-2a	-55	148	79	-9	-60	[252]
Aid-L-Phe 3.23c-2b	-54	147	76	-3	-60	[252]

cases, the Phe side chain χ^1 dihedral angle ($-60^\circ \pm 2^\circ$) was in the *gauche* (–) orientation (Table 7).

Compared to Aid peptide **3.23c**, the Nai ring system (e.g., **3.38**, **3.39** and **3.10**) was flatter due to unsaturation. The absence of ring substituents on the Aid analogs minimized steric interactions enhancing conformational liberty for peptide **3.23c**, which sampled both type II and II' β -turn geometry [232, 250].

4 Conclusions

3-Amino- γ -lactam (Agl) residues combined with their respective substituted and aza-analogs (e.g., Nai and Aid) represent together one of the most employed classes of peptidomimetics for constraining backbone and side chain conformations to study structure-activity relationships. Since the pioneering studies of Freidinger and Veber [27, 28], a diverse array of Agl analogs have exhibited improved properties relative to their parent peptide and small molecule structures. Assembly of substituted Agl analogs has required surmounting various synthetic challenges, such as selective activation of the carbon chain for ring closure, installation of various stereocenters with configurational control, and the preparation of quaternary centers. Innovative methods have been developed to overcome such obstacles to prepare specific 3-amino- γ -lactam targets. Conformational analysis of Agl, Nai, and Aid residues has shown their effective potential to favor turn conformations contingent on their ring structure and electronic constraints, as well as backbone stereochemistry. Applications of cyclic sulfamidates as bis-electrophiles and alkylation of semicarbazones with 1,2-dibromoethane have respectively enabled introduction of Agl and *N*-amino-imidazolidin-2-one (Aid) residues systematically throughout a sequence by solid-phase methods to scan for bioactive turn conformers in peptides [175, 230]. The development of effective synthetic methods for introducing such 3-amino- γ -lactam residues into peptides merits further exploration to help elucidate conformational preferences, structure-activity relationships, and the role of conformers in peptide chemical biology.

References

1. Guarna A, Trabocchi A (2014) Peptidomimetics in organic and medicinal chemistry. Wiley, Weinheim, 308 pp
2. Taylor JW (2002) Biopolymers 66:49
3. Haack M, Beck-Sickinger AG (2007) Multiple peptide synthesis to identify bioactive hormone structures. In: Brase S (ed) Combinatorial chemistry on solid supports, vol 278. Springer, Berlin, p. 243
4. Gante J (1994) Angew Chem Int Ed Engl 33:1699
5. Fosgerau K, Hoffmann T (2015) Drug Discov Today 20:122
6. Giguere S, Laviolette F, Marchand M, Tremblay D, Moineau S, Liang XX, Biron E, Corbeil J (2015) PLoS Comput Biol:11. doi:[10.1371/journal.pcbi.1004074](https://doi.org/10.1371/journal.pcbi.1004074)

7. Vanhee P, van der Sloot AM, Verschueren E, Serrano L, Rousseau F, Schymkowitz J (2011) *Trends Biotechnol* 29:231
8. Armonio PG, Bibb MJ, Bierbaum G, Bowers AA, Bugni TS, Bulaj G, Camarero JA, Campopiano DJ, Challis GL, Clardy J, Cotter PD, Craik DJ, Dawson M, Dittmann E, Donadio S, Dorrestein PC, Entian KD, Fischbach MA, Garavelli JS, Goransson U, Gruber CW, Haft DH, Hemscheidt TK, Hertweck C, Hill C, Horswill AR, Jaspars M, Kelly WL, Klinman JP, Kuipers OP, Link AJ, Liu W, Marahiel MA, Mitchell DA, Moll GN, Moore BS, Muller R, Nair SK, Nes IF, Norris GE, Olivera BM, Onaka H, Patchett ML, Piel J, Reaney MJT, Rebuffat S, Ross RP, Sahl HG, Schmidt EW, Selsted ME, Severinov K, Shen B, Sivonen K, Smith L, Stein T, Sussmuth RD, Tagg JR, Tang GL, Truman AW, Vederas JC, Walsh CT, Walton JD, Wenzel SC, Willey JM, van der Donk WA (2013) *Nat Prod Rep* 30:108
9. Calcott MJ, Ackerley DF (2014) *Biotechnol Lett* 36:2407
10. Passioura T, Katoh T, Goto Y, Suga H (2014) Selection-based discovery of druglike macrocyclic peptides. In: Kornberg RD (ed) *Annual review of biochemistry*, vol 83. Annual Reviews, Palo Alto, p. 727. doi:10.1146/annurev-biochem-060713-035456
11. Lepthien S, Merkel L, Budisa N (2010) *Angew Chem Int Ed* 49:5446
12. Mendel D, Cornish VW, Schultz PG (1995) *Annu Rev Biophys Biomol Struct* 24:435
13. Hayashi Y, Morimoto J, Suga H (2012) *ACS Chem Biol* 7:607
14. Lennard KR, Tavassoli A (2014) *Chem. Eur. J.* 20:10608
15. Grauer A, Konig B (2009) *Eur J Org Chem* 5009. doi:10.1002/ejoc.200900599
16. Hill TA, Shepherd NE, Diness F, Fairlie DP (2014) *Angew Chem Int Ed* 53:13020
17. de Vega MJP, Martin-Martinez M, Gonzalez-Muniz R (2007) *Curr Top Med Chem* 7:33
18. Liskamp RMJ, Rijkers DTS, Kruijtz JAW, Kemmink J (2011) *ChemBioChem* 12:1626
19. Ung P, Winkler DA (2011) *J Med Chem* 54:1111
20. Mas-Moruno C, Rechenmacher F, Kessler H (2010) *Anti Cancer Agents Med Chem* 10:753
21. Danhier F, Le Breton A, Preat V (2012) *Mol Pharm* 9:2961
22. MacDonald M, Aube J (2001) *Curr Org Chem* 5:417
23. Freidinger RM (2003) *J Med Chem* 46:5553
24. Perdih A, Kikelj D (2006) *Curr Med Chem* 13:1525
25. Hoyer D, Bartfai T (2012) *Chem Biodivers* 9:2367
26. Ferro ES, Rioli V, Castro LM, Fricker LD (2014) *EuPA Open Proteom* 3:143
27. Freidinger RM, Veber DF, Perlow DS, Brooks JR, Saperstein R (1980) *Science* 210:656
28. Freidinger RM, Veber DF, Hirschmann R, Paegle LM (1980) *Int J Pept Protein Res* 16:464
29. Scheffelaar R, Nijenhuis RAK, Paravidino M, Lutz M, Spek AL, Ehlers AW, de Kanter FJJ, Groen MB, Orru RVA, Ruijter E (2009) *J Org Chem* 74:660
30. Wang YL, O'Neil SV, Wos JA, Oppong KA, Laufersweiler MC, Soper DL, Ellis CD, Baize MW, Fancher AN, Lu W, Suchanek MK, Wang RL, Schweske WP, Cruze CA, Buchalova M, Belkin M, De B, Demuth TP (2007) *Bioorg Med Chem* 15:1311
31. Macias A, Ramallal AM, Alonso E, del Pozo C, Gonzalez J (2006) *J Org Chem* 71:7721
32. Eckhardt B, Grosse W, Essen LO, Geyer A (2010) *Proc Natl Acad Sci U S A* 107:18336
33. Patick AK, Brothers MA, Maldonado F, Binford S, Maldonado O, Fuhrman S, Petersen A, Smith GJ (2005) *Antimicrob Agents Chemother* 49:2267
34. Jamieson AG, Boutard N, Sabatino D, Lubell WD (2013) *Chem Biol Drug Des* 81:148
35. Khashper A, Lubell WD (2014) *Org Biomol Chem* 12:5052
36. Hanessian S, McNaughton-Smith G, Lombart HG, Lubell WD (1997) *Tetrahedron* 53:12789
37. Cluzeau J, Lubell WD (2005) *Biopolymers* 80:98
38. Halab L, Gosselin F, Lubell WD (2000) *Biopolymers* 55:101
39. Piscopio AD, Robinson JE (2004) *Curr Opin Chem Biol* 8:245
40. Liskamp RMJ (1994) *Recl Trav Chim Pays-Bas* 113:1
41. Nair RV, Baravkar SB, Ingole TS, Sanjayan GJ (2014) *Chem Commun* 50:13874
42. Costenaro L, Kaczmarek Z, Arnan C, Janowski R, Coutard B, Sola M, Gorbalenya AE, Norder H, Canard B, Coll M (2011) *J Virol* 85:10764

43. Brogden RN, McTavish D (1993) *Drugs* 45:716
44. Singh J, Kronenthal DR, Schwinden M, Godfrey JD, Fox R, Vawter EJ, Zhang B, Kissick TP, Patel B, Mneimne O, Humora M, Papaioannou CG, Szymanski W, Wong MKY, Chen CK, Heikes JE, DiMarco JD, Qiu J, Deshpande RP, Gougoutas JZ, Mueller RH (2003) *Org Lett* 5:3155
45. Moss ML, Sklair-Tavron L, Nudelman R (2008) *Nat Clin Pract Rheumatol* 4:300
46. Gatti L, De Cesare M, Ciusani E, Corna E, Arrighetti N, Cominetti D, Belvisi L, Potenza D, Moroni E, Vasile F, Lecis D, Delia D, Castiglioni V, Scanziani E, Seneci P, Zaffaroni N, Perego P (2014) *Mol Pharm* 11:283
47. Paone DV, Nguyen DN, Shaw AW, Burgey CS, Potteiger CM, Deng JZ, Mosser SD, Salvatore CA, Yu S, Roller S, Kane SA, Selnick HG, Vacca JP, Williams TM (2011) *Bioorg Med Chem Lett* 21:2683
48. Frazier JW, Staszak MA, Weigel LO (1992) *Tetrahedron Lett* 33:857
49. Aly AH, Debbab A, Proksch P (2011) *Fungal Divers* 50:3
50. Robl JA, Sun CQ, Stevenson J, Ryono DE, Simpkins LM, Cimarusti MP, Dejneka T, Slusarchyk WA, Chao S, Stratton L, Misra RN, Bednarz MS, Asaad MM, Cheung HS, AbboaOffei BE, Smith PL, Mathers PD, Fox M, Schaeffer TR, Seymour AA, Trippodo NC (1997) *J Med Chem* 40:1570
51. Sagnella GA (2002) *J Renin-Angiotensin-Aldosterone Syst* 3:90
52. Sun HY, Nikolovska-Coleska Z, Yang CY, Qian DG, Lu JF, Qiu S, Bai LC, Peng YF, Cai Q, Wang SM (2008) *Acc Chem Res* 41:1264
53. Bell IM (2014) *J Med Chem* 57:7838
54. Chiou WH, Mizutani N, Ojima I (2007) *J Org Chem* 72:1871
55. Vamos M, Welsh K, Finlay D, Lee PS, Mace PD, Snipas SJ, Gonzalez ML, Ganji SR, Ardecky RJ, Riedl SJ, Salvesen GS, Vuori K, Reed JC, Cosford NDP (2013) *ACS Chem Biol* 8:725
56. Huot M, Moitessier N (2010) *Tetrahedron Lett* 51:2820
57. Smith AB, Charnley AK, Mesaros EF, Kikuchi O, Wang WY, Benowitz A, Chu CL, Feng JJ, Chen KH, Lin A, Cheng FC, Taylor L, Hirschmann R (2005) *Org Lett* 7:399
58. Greco A, Tani S, De Marco R, Gentilucci L (2014) *Chem Eur J* 20:13390
59. Kang CW, Ranatunga S, Sarnowski MP, Del Valle JR (2014) *Org Lett* 16:5434
60. Ottersbach PA, Schmitz J, Schnakenburg G, Gutschow M (2013) *Org Lett* 15:448
61. Martelli G, Orena M, Rinaldi S (2014) *Curr Org Chem* 18:1373
62. Martelli G, Monsignor A, Orena M, Rinaldi S (2014) *Curr Org Chem* 18:1539
63. Belvisi L, Colombo L, Manzoni L, Potenza D, Scolastico C (2004) *Synlett*:1449. doi:[10.1055/s-2004-829540](https://doi.org/10.1055/s-2004-829540)
64. Gillespie P, Cicariello J, Olson GL (1997) *Biopolymers* 43:191
65. Guzzo PR, Trova MP, Inghardt T, Linschoten M (2002) *Tetrahedron Lett* 43:41
66. Gutierrez-Rodriguez M, Garcia-Lopez MT, Herranz R (2004) *Tetrahedron* 60:5177
67. Atmuri NDP, Lubell WD (2015) *J Org Chem* 80:4904
68. Simpson JC, Ho C, Shands EFB, Gershengorn MC, Marshall GR, Moeller KD (2002) *Bioorg Med Chem* 10:291
69. Seufert W, Fleury A, Giese B (2006) *Synlett* 1774. doi:[10.1055/s-2006-944203](https://doi.org/10.1055/s-2006-944203)
70. Pohner C, Ullmann V, Hilpert R, Samain E, Unverzagt C (2014) *Tetrahedron Lett* 55:2197
71. Abell AD, Oldham MD, Taylor JM (1995) *J Chem Soc Perkin Trans* 1:953. doi:[10.1039/p19950000953](https://doi.org/10.1039/p19950000953)
72. Abell AD, Oldham MD, Taylor JM (1995) *J Org Chem* 60:1214
73. Abell AD, Gardiner J (1999) *J Org Chem* 64:9668
74. Shankar R, Scott AI (1994) *Heterocycles* 37:1451
75. Shankar R, Scott AI (1996) *Heterocycles* 42:145
76. Mullersman JE, Bonetti SJ, Preston JF (1991) *Int J Pept Protein Res* 38:409
77. Tian JM, Shen YH, Yang XW, Liang S, Tang J, Shan L, Zhang WD (2009) *Org Lett* 11:1131
78. Harris PWR, Brimble MA, Muir VJ, Lai MYH, Trotter NS, Callis DJ (2005) *Tetrahedron* 61:10018

79. Johannesson P, Erdelyi M, Lindeberg G, Frandberg PA, Nyberg F, Karlen A, Hallberg A (2004) *J Med Chem* 47:6009
80. Hirose T, Sunazuka T, Sugawara A, Noguchi Y, Tanaka T, Iguchi K, Yamamoto T, Gouda H, Shiomi K, Omura S (2009) *J Antibiot* 62:495
81. He G, Zhang SY, Nack WA, Li Q, Chen G (2013) *Angew Chem Int Ed* 52:11124
82. Lesma G, Cecchi R, Cagnotto A, Gobbi M, Meneghetti F, Musolino M, Sacchetti A, Silvani A (2013) *J Org Chem* 78:2600
83. Fanto N, Gallo G, Ciacci A, Semproni M, Vignola D, Quaglia M, Bombardi V, Mastroianni D, Zibella MP, Basile G, Sassano M, Ruggiero V, De Santis R, Carminatit P (2008) *J Med Chem* 51:1189
84. Ndungu JM, Gu XY, Gross DE, Cain JP, Carducci MD, Hruba VJ (2004) *Tetrahedron Lett* 45:4139
85. Wolf JP, Rapoport H (1989) *J Org Chem* 54:3164
86. Garvey DS, May PD, Nadzan AM (1990) *J Org Chem* 55:936
87. Rao M, Pinyol E, Lubell WD (2007) *J Org Chem* 72:736
88. Dietrich E, Lubell WD (2003) *J Org Chem* 68:6988
89. Matsubara R, Nakamura Y, Kobayashi S (2004) *Angew Chem Int Ed* 43:1679
90. Yelin EA, Onoprienko VV (1998) *Bioorg Khim* 24:670
91. Crucianelli E, Galeazzi R, Martelli G, Orena M, Rinaldi S, Sabatino P (2010) *Tetrahedron* 66:400
92. Galeazzi R, Martelli G, Marcucci E, Mobbili G, Natali D, Orena M, Rinaldi S (2007) *Eur J Org Chem* 4402. doi:[10.1002/ejoc.200700300](https://doi.org/10.1002/ejoc.200700300)
93. Galeazzi R, Martelli G, Orena M, Rinaldi S, Sabatino P (2005) *Tetrahedron* 61:5465
94. Galeazzi R, Martelli G, Mazzanti A, Orena M, Rinaldi S (2011) *Chem. Eur. J.* 17:12564
95. Gosselin F, Lubell WD (1998) *J Org Chem* 63:7463
96. St-Cyr DJ, Jamieson AG, Lubell WD (2010) *Org Lett* 12:1652
97. Beauregard K (2012) Université de Montréal, Département de Chimie, Développement de peptidomimétiques antagonistes du récepteur de l'interleukine-1 β , MSc Thesis 17/05/2012: <http://hdl.handle.net/1866/8460>
98. Tashiro T, Fushiya S, Nozoe S (1988) *Chem Pharm Bull* 36:893
99. Scott WL, Martynow JG, Huffman JC, O'Donnell MJ (2007) *J Am Chem Soc* 129:7077
100. Somu RV, Johnson RL (2005) *J Org Chem* 70:5954
101. Nielsen TE, Meldal M (2005) *Org Lett* 7:2695
102. Toumi M, Couty F, Marrot J, Evano G (2008) *Org Lett* 10:5027
103. Ousmer M, Braun NA, Ciufolini MA (2001) *Org Lett* 3:765
104. Craig W, Chen J, Richardson D, Thorpe R, Yuan Y (2015) *Org Lett* 17:4620
105. Bonnaterre F, Bois-Choussy M, Zhu JP (2006) *Org Lett* 8:4351
106. Ammetto I, Gasperi T, Loreto MA, Migliorini A, Palmarelli F, Tardella PA (2009) *Eur J Org Chem* 6189. doi:[10.1002/ejoc.200900891](https://doi.org/10.1002/ejoc.200900891)
107. Lesma G, Landoni N, Sacchetti A, Silvani A (2010) *Tetrahedron* 66:4474
108. Wyss C, Batra R, Lehmann C, Sauer S, Giese B (1996) *Angew Chem Int Ed. Engl.* 35:2529
109. Rancourt J, Gorys V, Jolicoeur E (1998) *Tetrahedron Lett* 39:5339
110. Liu T, Mei TS, Yu JQ (2015) *J Am Chem Soc* 137:5871
111. Scott WL, Alsina J, Kennedy JH, O'Donnell MJ (2004) *Org Lett* 6:1629
112. He J, Li SH, Deng YQ, Fu HY, Laforteza BN, Spangler JE, Homs A, Yu JQ (2014) *Science* 343:1216
113. Wang B, Lu CX, Zhang SY, He G, Nack WA, Chen G (2014) *Org Lett* 16:6260
114. Chang LL, Yang GX, McCauley E, Mumford RA, Schmidt JA, Hagmann WK (2008) *Bioorg Med Chem Lett* 18:1688
115. Sidhoum MA, Dos Santos A, El Kaim L, Legras L (2014) *Eur J Org Chem* 4949. doi:[10.1002/ejoc.201402572](https://doi.org/10.1002/ejoc.201402572)
116. Raghavan B, Johnson RL (2006) *J Org Chem* 71:2151
117. Magnus NA, Campagna S, Confalone PN, Savage S, Meloni DJ, Waltermire RE, Wethman RG, Yates M (2010) *Org Process Res Dev* 14:159

118. Civitavecchia A, Martelli G, Orena M, Rinaldi S (2014) *Amino Acids* 46:1097
119. Amabili P, Amici A, Civitavecchia A, Maggiore B, Orena M, Rinaldi S, Tolomelli A (2016) *Amino Acids* 48:461
120. Garcia-Lopez MT, Gonzalez-Muniz R, Martin-Martinez M, Herranz R (2007) *Curr Top Med Chem* 7:1180
121. Baldwin JE, Lynch GP, Pitlik J (1991) *J Antibiot* 44:1
122. Grimes JH, Angell YM, Kohn WD (2003) *Tetrahedron Lett* 44:3835
123. Nagai U, Sato K, Nakamura R, Kato R (1993) *Tetrahedron* 49:3577
124. Gu XY, Ying JF, Agnes RS, Navratilova E, Davis P, Stahl G, Porreca F, Yamamura HI, Hruby VJ (2004) *Org Lett* 6:3285
125. Bourguet CB, Goupil E, Tassy D, Hou X, Thouin E, Polyak F, Hebert TE, Claing A, Laporte SA, Chemtob S, Lubell WD (2011) *J Med Chem* 54:6085
126. Boeglin D, Hamdan FF, Melendez RE, Cluzeau J, Laperriere A, Heroux M, Bouvier M, Lubell WD (2007) *J Med Chem* 50:1401
127. Allin SM, Towler J, Gaskell SN, Saha B, Martin WP, Page PCB, Edgar M (2010) *Tetrahedron* 66:9538
128. Petersen R, Cohrt AE, Petersen MA, Wu P, Clausen MH, Nielsen TE (2015) *Bioorg Med Chem* 23:2646
129. Landoni N, Lesma G, Sacchetti A, Silvani A (2007) *J Org Chem* 72:9765
130. Kahn M, Eguchi M, Moon SH, Chung JU (2004) β -strand mimetics for use as diagnostic and therapeutic agents, US20040053331A1
131. Lawandi J, Toumieux S, Seyer V, Campbell P, Thielges S, Juillerat-Jeanneret L, Moitessier N (2009) *J Med Chem* 52:6672
132. Madison V, Kopple KD (1980) *J Am Chem Soc* 102:4855
133. Crisma M, De Zotti M, Moretto A, Peggion C, Drouillard B, Wright K, Couty F, Toniolo C, Formaggio F (2015) *New J Chem* 39:3208
134. Toniolo C (1980) *CRC Crit Rev Biochem* 9:1
135. Ball JB, Alewood PF (1990) *J Mol Recognit* 3:55
136. Snider BB, Lin H (1999) *J Am Chem Soc* 121:7778
137. Snider BB, Lin H (2000) *Org Lett* 2:643
138. Ousmer M, Braun NA, Bavoux C, Perrin M, Ciufolini MA (2001) *J Am Chem Soc* 123:7534
139. Sobolewski D, Prah A, Derdowska I, Slaninova J, Kaczmarek K, Zabrocki J, Lammek B (2007) *J Pept Sci* 13:128
140. Kaczmarek K, Williams HJ, Coast GM, Scott AI, Zabrocki J, Nachman RJ (2007) *Biopolymers* 88:1
141. Van CT, Zdobinsky T, Seebohm G, Nennstiel D, Zerbe O, Scherkenbeck J (2014) *Eur J Org Chem* 2714. doi:10.1002/ejoc.201301773
142. Malavasic C, Brulc B, Cebasek P, Dahmann G, Heine N, Bevk D, Grosej U, Meden A, Stanovnik B, Svete J (2007) *J Com Chem* 9:219
143. Bentz EL, Goswami R, Moloney MG, Westawayb SM (2005) *Org Biomol Chem* 3:2872
144. Goswami R, Moloney MG (1999) *Chem Commun* 2333. doi:10.1039/a906297a
145. Javidan A, Schafer K, Pyne SG (1997) *Synlett* 100. doi:10.1055/s-1997-683
146. Geiger T, Clarke S (1987) *J Biol Chem* 262:785
147. Dehart MP, Anderson BD (2007) *J Pharm Sci* 96:2667
148. Brueckner C, Fahr A, Imhof D, Scriba GKE (2012) *J Pharm Sci* 101:4178
149. Subiros-Funosas R, El-Faham A, Albericio F (2011) *Tetrahedron* 67:8595
150. Michels T, Dolling R, Haberkorn U, Mier W (2012) *Org Lett* 14:5218
151. Ullmann V, Radisch M, Boos I, Freund J, Pohner C, Schwarzinger S, Unverzagt C (2012) *Angew Chem Int Ed* 51:11566
152. Chen WS, Ede NJ, Jackson DC, McCluskey J, Purcell AW (1996) *J Immunol* 157:1000
153. Robson VMJ, Rae ID, Ng F (1990) *Biol Chem Hoppe Seyler* 371:423
154. Lee TH, Thompson PE, Milton T, Hearn MTW, Aguilar MI (1997) *J Pept Res* 49:394
155. Thompson PE, Cavallaro V, Hearn MTW (1995) *Lett Pept Sci* 1:263

156. Ede NJ, Rae ID, Hearn MTW (1994) *Int J Pept Protein Res* 44:568
157. Ede NJ, Lim N, Rae ID, Ng FM, Hearn MTW (1991) *Pept Res* 4:171
158. Obrecht D, Bohdal U, Daly J, Lehmann C, Schonholzer P, Muller K (1995) *Tetrahedron* 51:10883
159. Capasso S, Mazzarella L, Sica F, Zagari A, Cascarano G, Giacobozzo C (1992) *Acta Crystallogr Sect B Struct Commun* 48:285
160. Capasso S, Mazzarella L, Zagari A (1995) *Chirality* 7:605
161. Higgins KA, Thompson PE, Hearn MTW (1996) *Int J Pept Protein Res* 48:1
162. Karppanen EJ, Koskinen AMP (2010) *Molecules* 15:6512
163. Galeazzi R, Marcucci E, Martelli G, Natali D, Orena M, Rinaldi S (2008) *Amino Acids* 34:333
164. Galeazzi R, Martelli G, Orena M, Rinaldi S (2004) *Synthesis* 2560. doi:[10.1055/s-2004-831235](https://doi.org/10.1055/s-2004-831235)
165. Menegazzo I, Fries A, Mammi S, Galeazzi R, Martelli G, Orena M, Rinaldi S (2006) *Chem Commun* 4915. doi:[10.1039/b612071g](https://doi.org/10.1039/b612071g)
166. Sicherl F, Cupido T, Albericio F (2010) *Chem Commun* 46:1266
167. Almeida JF, Grande M, Moran JR, Anaya J, Mussons ML, Caballero MC (1993) *Tetrahedron Asymmetry* 4:2483
168. St-Cyr DJ, Maris T, Lubell WD (2010) *Heterocycles* 82:729
169. Afzaliardakani A, Rapoport H (1980) *J Org Chem* 45:4817
170. Organ MG, Xu J, N'Zemba B (2002) *Tetrahedron Lett* 43:8177
171. Lamborelle N, Simon JF, Luxen A, Monbaliu JCM (2015) *Org Biomol Chem* 13:11602
172. Nadeau-Vallee M, Quiniou C, Palacios J, Hou X, Erfani A, Madaan A, Sanchez M, Leimert K, Boudreault A, Duhamel F, Rivera JC, Zhu T, Noueihed B, Robertson SA, Ni X, Olson DM, Lubell W, Girard S, Chemtob S (2015) *J Immunol* 195:3402
173. Rivera JC, Sitaras N, Noueihed B, Hamel D, Madaan A, Zhou T, Honore JC, Quiniou C, Joyal JS, Hardy P, Sennlaub F, Lubell W, Chemtob S (2013) *Arterioscler Thromb Vasc Biol* 33:1881
174. Quiniou C, Sapieha P, Lahaie I, Hou X, Brault S, Beauchamp M, Leduc M, Rihakova L, Joyal JS, Nadeau S, Heveker N, Lubell W, Sennlaub F, Gobeil F, Miller G, Pshezhetsky AV, Chemtob S (2008) *J Immunol* 180:6977
175. Jamieson AG, Boutard N, Beauregard K, Bodas MS, Ong H, Quiniou C, Chemtob S, Lubell WD (2009) *J Am Chem Soc* 131:7917
176. Kempf DJ, Condon SL (1990) *J Org Chem* 55:1390
177. Gao JH, Haas H, Wang KY, Chen ZL, Breitenstein W, Rajan S (2008) *Magn Reson Chem* 46:17
178. Deal MJ, Hagan RM, Ireland SJ, Jordan CC, McElroy AB, Porter B, Ross BC, Stephensmith M, Ward P (1992) *J Med Chem* 35:4195
179. Stables JM, Beresford IJM, Arkinstall S, Ireland SJ, Walsh DM, Seale PW, Ward P, Hagan RM (1994) *Neuropeptides* 27:333
180. Kempf DJ, Rosenberg SH, Plattner JJ, Shan HL, De B (1991) *Heterocyclic renin inhibitors*, US4994477A
181. Karoyan P, Chassaing G (1997) *Tetrahedron Lett* 38:85
182. Sauer S, Schumacher A, Barbosa F, Giese B (1998) *Tetrahedron Lett* 39:3685
183. Ward P, Ewan GB (1990) Preparation of spiro lactam derivatives as intermediates for peptide agonists and antagonists of substance P, EP360390A1
184. Bittermann H, Einsiedel J, Hubner H, Gmeiner P (2004) *J Med Chem* 47:5587
185. Boy KM, Guernon JM, Shi JL, Toyn JH, Meredith JE, Barten DM, Burton CR, Albright CF, Marcinkeviciene J, Good AC, Tebben AJ, Muckelbauer JK, Camac DM, Lentz KA, Bronson JJ, Olson RE, Macor JE, Thompson LA (2011) *Bioorg Med Chem Lett* 21:6916
186. Purandare AV, Wan HH, Laing NM, Benbatoul K, Vaccaro W, Poss MA (2004) *Bioorg Med Chem Lett* 14:4701
187. Otsuka M, Yoshioka K, Yanagisawa M, Suzuki H, Zhao FY, Guo JZ, Hosoki R, Kurihara T (1995) *Can J Physiol Pharmacol* 73:903

188. Gozal D, Kim J, Bhattacharjee R, Goldman JL, Kheirandish-Gozal L (2014) *Chest* 145:1039
189. Thompson LA, Shi JL, Decicco CP, Tebben AJ, Olson RE, Boy KM, Guernon JM, Good AC, Liauw A, Zheng CS, Copeland RA, Combs AP, Trainor GL, Camac DM, Muckelbauer JK, Lentz KA, Grace JE, Burton CR, Toyn JH, Barten DM, Marcinkeviciene J, Meredith JE, Albright CF, Macor JE (2011) *Bioorg Med Chem Lett* 21:6909
190. Seebach D, Boes M, Naef R, Schweizer WB (1983) *J Am Chem Soc* 105:5390
191. Calaza MI, Cativiela C (2008) *Eur J Org Chem* 3427. doi:[10.1002/ejoc.200800225](https://doi.org/10.1002/ejoc.200800225)
192. Bhagwanth S, Mishra RK, Johnson RL, Beilstein J (2013) *Org Chem* 9:204. doi:[10.3762/bjoc.9.24](https://doi.org/10.3762/bjoc.9.24)
193. Hutton CA, Bartlett PA (2007) *J Org Chem* 72:6865
194. Lesma G, Landoni N, Pilati T, Sacchetti A, Silvani A (2009) *J Org Chem* 74:8098
195. Damour D, Herman F, Labaudiniere R, Pantel G, Vuilhorgne M, Mignani S (1999) *Tetrahedron* 55:10135
196. Ward P, Ewan GB, Jordan CC, Ireland SJ, Hagan RM, Brown JR (1990) *J Med Chem* 33:1848
197. Damour D, Barreau M, Blanchard JC, Burgevin MC, Doble A, Pantel G, Labaudiniere R, Mignani S (1998) *Chem Lett* 27:943
198. Takeda H, Takahashi T, Myake M, Shinozaki A, Ishida M (1993) Preparation of (phosphonoalkyl)heterocycle and (phosphonoalkyl)cycloalkanecarboxylic and derivatives, JP05222072A
199. Loiarro M, Capolunghi F, Fanto N, Gallo G, Campo S, Arseni B, Carsetti R, Carminati P, De Santis R, Ruggiero V, Sette C (2007) *J Leukoc Biol* 82:801
200. Khalil EM, Ojala WH, Pradhan A, Nair VD, Gleason WB, Mishra RK, Johnson RL (1999) *J Med Chem* 42:628
201. Hernanz R, Martinez-Revelles S, Palacios R, Martin A, Cachafeiro V, Aguado A, Garcia-Redondo L, Barrus MT, de Batista PR, Briones AM, Salas M, Alonso MJ (2015) *Br J Pharmacol* 172:3159
202. Huang JD, Amaral J, Lee JW, Rodriguez IR (2014) *PLoS One* 9. doi:[10.1371/journal.pone.0100985](https://doi.org/10.1371/journal.pone.0100985)
203. Van Tassell BW, Seropian IM, Toldo S, Salloum FN, Smithson L, Varma A, Hoke NN, Gelwix C, Chau V, Abbate A (2010) *J Cardiovasc Pharmacol* 55:385
204. Khalil EM, Pradhan A, Ojala WH, Gleason WB, Mishra RK, Johnson RL (1999) *J Med Chem* 42:2977
205. Ndungu JM, Cain JP, Davis P, Ma SW, Vanderah TW, Lai J, Porreca F, Hruby VJ (2006) *Tetrahedron Lett* 47:2233
206. Slaninova J, Knapp RJ, Wu JJ, Fang SN, Kramer T, Burks TF, Hruby VJ, Yamamura HI (1991) *Eur J Pharmacol* 200:195
207. Johannesson P, Lindeberg G, Tong WM, Gogoll A, Karlen A, Hallberg A (1999) *J Med Chem* 42:601
208. Berry JM, Doyle PM, Young DW (2005) *Tetrahedron* 61:287
209. Sacchetti A, Silvani A, Gatti FG, Lesma G, Pilati T, Trucchi B (2011) *Org Biomol Chem* 9:5515
210. Soleimani E, Zainali M, Ghasemi N, Notash B (2013) *Tetrahedron* 69:9832
211. Lesma G, Landoni N, Pilati T, Sacchetti A, Silvani A (2009) *J Org Chem* 74:4537
212. Loughlin WA, Tyndall JDA, Glenn MP, Hill TA, Fairlie DP (2010) *Chem Rev* 110:PR32
213. Loughlin WA, Tyndall JDA, Glenn MP, Fairlie DP (2004) *Chem Rev* 104:6085
214. Toniolo C (1990) *Int J Pept Protein Res* 35:287
215. Cowell SM, Lee YS, Cain JP, Hruby VJ (2004) *Curr Med Chem* 11:2785
216. Hruby VJ, Li GG, Haskell-Luevano C, Shenderovich M (1997) *Biopolymers* 43:219
217. Qiu W, Gu XY, Soloshonok VA, Carducci MD, Hruby VJ (2001) *Tetrahedron Lett* 42:145
218. Obrecht D, Altorfer M, Bohdal U, Daly J, Huber W, Labhardt A, Lehmann C, Muller K, Ruffieux R, Schonholzer P, Spiegler C, Zumbunn C (1997) *Biopolymers* 42:575
219. Obrecht D, Abrecht C, Altorfer M, Bohdal U, Grieder A, Kleber M, Pfyffer P, Muller K (1996) *Helv Chim Acta* 79:1315
220. Valle G, Crisma M, Toniolo C, Yu KL, Johnson RL (1989) *J Chem Soc Perkin Trans* 2:83. doi:[10.1039/p29890000083](https://doi.org/10.1039/p29890000083)

221. Valle G, Crisma M, Toniolo C, Yu KL, Johnson RL (1989) *Int J Pept Protein Res* 33:181
222. Baures PW, Ojala WH, Gleason WB, Mishra RK, Johnson RL (1994) *J Med Chem* 37:3677
223. Evans MC, Pradhan A, Venkatraman S, Ojala WH, Gleason WB, Mishra RK, Johnson RL (1999) *J Med Chem* 42:1441
224. Chow WY, Bihan D, Forman CJ, Slatter DA, Reid DG, Wales DJ, Farndale RW, Duer MJ (2015) *Sci Rep* 5:1. doi:[10.1038/srep12556](https://doi.org/10.1038/srep12556)
225. Shoulders MD, Satyshur KA, Forest KT, Raines RT (2010) *Proc Natl Acad Sci U S A* 107:559
226. Kessler H (1982) *Angew Chem Int Ed Engl* 21:512
227. Proulx C, Sabatino D, Hopewell R, Spiegel J, Ramos YG, Lubell WD (2011) *Future Med Chem* 3:1139
228. Lee HJ, Song JW, Choi YS, Park HM, Lee KB (2002) *J Am Chem Soc* 124:11881
229. Boutard N, Turcotte S, Beauregard K, Quiniou C, Chemtob S, Lubell WD (2011) *J Pept Sci* 17:288
230. Doan ND, Hopewell R, Lubell WD (2014) *Org Lett* 16:2232
231. Proulx C, Lubell WD (2012) *Org Lett* 14:4552
232. Proulx C, Lubell WD (2014) *Biopolymers* 102:7
233. Chiu S, Keifer L, Timberlake JW (1979) *J Med Chem* 22:746
234. Lei AW, Lu XY (2000) *Org Lett* 2:2699
235. Fritz JA, Wolfe JP (2008) *Tetrahedron* 64:6838
236. Wolf LB, Tjen K, ten Brink HT, Blaauw RH, Hiemstra H, Schoemaker HE, Rutjes F (2002) *Adv Synth Catal* 344:70
237. Verniest G, Padwa A (2008) *Org Lett* 10:4379
238. Peshkov VA, Pereshivko OP, Sharma S, Meganathan T, Parmar VS, Ermolat'ev DS, Van der Eycken EV (2011) *J Org Chem* 76:5867
239. García-Ramos Y, Proulx C, Camy C, Lubell WD (2012) Synthesis and purification of enantiomerically pure *N*-aminoimidazolin-2-one dipeptide. In: Kokotos G, Constantinou-Kokotou V, Matsoukas J (eds) *Proceedings of the 32nd European peptide symposium*. European Peptide Society, Athens, p. 366
240. Garcia-Ramos Y, Lubell WD (2013) *J Pept Sci* 19:725
241. Garcia-Ramos Y, Proulx C, Lubell WD (2012) *Can J Chem* 90:985
242. Bourguet CB, Proulx C, Klocek S, Sabatino D, Lubell WD (2010) *J Pept Sci* 16:284
243. Menges N, Sari O, Abdullayev Y, Erdem SS, Balci M (2013) *J Org Chem* 78:5184
244. Basceken S, Kaya S, Balci M (2015) *J Org Chem* 80:12552
245. Cho JH, Kim BM (2002) *Tetrahedron Lett* 43:1273
246. Pujanauski BG, Prasad BAB, Sarpong R (2006) *J Am Chem Soc* 128:6786
247. Kwon Y, Cho H, Kim S (2013) *Org Lett* 15:920
248. van Esseveldt BCJ, Vervoort PWH, van Delft FL, Rutjes F (2005) *J Org Chem* 70:1791
249. Lin LS, Lanza T, de Laszlo SE, Truong Q, Kamenecka T, Hagmann WK (2000) *Tetrahedron Lett* 41:7013
250. Sabatino D, Proulx C, Klocek S, Bourguet CB, Boeglin D, Ong H, Lubell WD (2009) *Org Lett* 11:3650
251. Sabatino D, Proulx C, Pohankova P, Ong H, Lubell WD (2011) *J Am Chem Soc* 133:12493
252. Doan ND, Lubell WD (2015) *Biopolymers* 104:629
253. Bourguet CB, Sabatino D, Lubell WD (2008) *Biopolymers* 90:824
254. Lubell WD, Blankenship JW, Fridkin G, Kaul R (2005) *Sci Synth* 21:713. doi:[10.1055/sos-SD-021-00693](https://doi.org/10.1055/sos-SD-021-00693)
255. Bouayad-Gervais SH, Lubell WD (2013) *Molecules* 18:14739

Azepinone-Constrained Amino Acids in Peptide and Peptidomimetic Design

Steven Ballet, Karel Guillemin, Olivier Van der Poorten, Ben Schurgers,
Guido Verniest, and Dirk Tourwé

Abstract Side chain topography of amino acids that are part of a peptide's pharmacophore represents a crucial structural feature in peptidomimetic design. Constraining the side chain dihedral angles (χ angles) may limit the number of low energy conformations and lead to more potent, receptor subtype selective and enzymatically stable peptide ligands. The current chapter describes this strategy for aromatic amino acids such as Phe, Tyr, Trp, and His. The side chains of these residues are incorporated in or mimicked by amino-arylazepinones. A selection of synthetic pathways that were used and developed by our laboratory is described for obtaining conformationally constrained 4-amino-(7-hydroxy)-2-benzazepinones [Aba (or Hba)] and the corresponding amino-indolo- and amino-triazoloazepinones (Aia and Ata, respectively). These azepinone mimics were synthesized from amino acid educts and have been used in various biological applications. Moreover, other heterocyclic amino-azepinones were prepared based on ring-closing metathesis and post-cyclization modifications. Further elaboration of the substitution patterns in these azepinones has rendered them highly versatile building blocks for use in peptidomimetic design. The selected biological applications illustrate their potential for the development of novel peptide-based pharmacological probes and drug candidates.

Keywords 4-Amino-2-arylazepinones · Angiotensin IV · Bradykinin · Conformationally constrained amino acids · Melanocortin · Opioid peptides · Somatostatin

S. Ballet (✉), K. Guillemin, O. Van der Poorten, B. Schurgers, G. Verniest, and D. Tourwé
Research Group of Organic Chemistry, Faculty of Science and Bio-Engineering Sciences,
Vrije Universiteit Brussel (VUB), Pleinlaan 2, 1050 Brussels, Belgium
e-mail: sballet@vub.ac.be; kguillem@vub.ac.be; ovdpoort@vub.ac.be; bschurge@vub.ac.be;
gvernies@vub.ac.be; datourwe@vub.ac.be

Contents

1	Introduction	178
2	Synthesis	180
2.1	4-Amino-1,2,4,5-tetrahydro-2-benzazepin-3-one (Aba) Analogues	180
2.2	4-Amino-1,2,4,5-tetrahydro-2-indoloazepin-3-one (Aia) Analogues	186
2.3	4-Amino-1,2,4,5-tetrahydro-2-triazoloazepin-3-one (Ata) Analogues	188
2.4	Other Heterocycle-Fused Amino-azepinones from Ring-Closing Metathesis	189
3	Conformational Studies	191
4	Biological Applications	192
4.1	Amino-benzazepinones as ACE, Renin, and NEP Inhibitors	192
4.2	Amino-benzazepinones in Opioid Applications	193
4.3	Bifunctional Opioid Agonist – NK1 Antagonist Ligands	197
4.4	Bradykinin (BK)	197
4.5	Somatostatin	198
4.6	Angiotensin IV	200
4.7	α -Melanocyte-Stimulating Hormone (α -MSH)	201
5	Conclusion	203
	References	203

1 Introduction

The biological activity of a peptide is determined not only by its secondary structure, but also by the 3D orientation of key side chain functional groups, which constitute the pharmacophore elements of the peptide ligand. The differences in energy between the low energy staggered conformations of the side chain of an aromatic amino acid and the energy barriers between them are very small such that all three conformational states are usually available. By limiting side chain flexibility, improved selectivity and metabolic stability may be obtained in ways similar to those resulting from main chain cyclized peptides (Fig. 1) [1].

The concept of topographical design in χ -space was introduced to the peptide field in 1988 by Victor Hruby, who used 1,2,3,4-tetrahydroisoquinoline-3-carboxylic acid (Tic) as a side chain-constrained Phe analogue to obtain potent and selective μ -opioid antagonists [2]. Tic was designed to link the backbone α -nitrogen to the aromatic side chain ring by a methylene bridge, thereby restricting the flexibility around the C^α - C^β bond to *gauche*-(-) ($\chi_1 = -60^\circ$) or *gauche*(+) ($\chi_1 = +60^\circ$) conformers and excluding the *trans* ($\chi_1 = 180^\circ$) conformation (Fig. 2). Over the last decades, Tic has been used successfully to obtain potent and selective peptide and peptide mimetic agonists and antagonists [3–6]. Our group has focused on an alternative constraint, which limits the side chain conformations to *gauche*(+) or *trans* conformers. Linkage of the Phe or Tyr aromatic side chain ring by a methylene bridge to the α -nitrogen of the next amino acid at the C-terminal side in the peptide sequence results in the seven-member lactam 4-amino-(7-hydroxy)-1,2,4,5-tetrahydro-2-benzazepin-3-one (Aba, X=H or Hba, X=OH, Fig. 2).

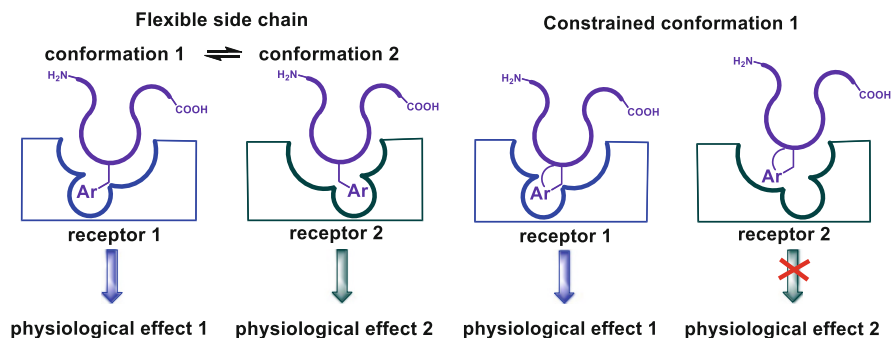


Fig. 1 Side chain flexibility and lack of selectivity (*left*) versus a constrained side chain leading to selectivity (*right*)

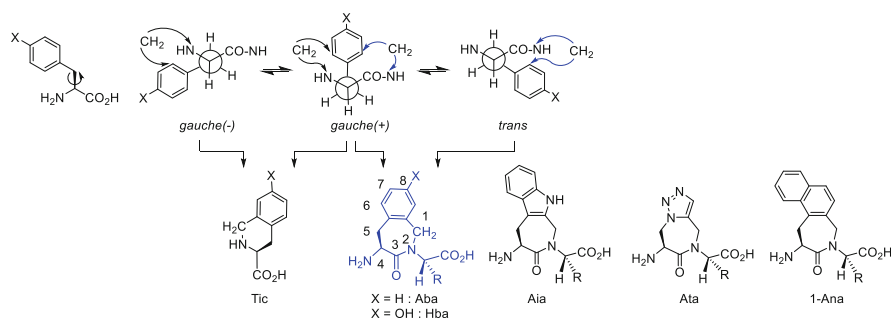


Fig. 2 Low energy conformations around χ_1 of aromatic amino acids and the conformational constrained analogues of Phe (Aba), Tyr (Hba), and their indole (Aia), triazole (Ata), and naphthylalanine (1-Ana) equivalents

Such conformational constraints not only limit the available side chain orientations, but also impose restrictions on main chain dihedral angles. The lactam constraint, including seven-membered ring lactams, has been demonstrated by Roger M. Freidinger and others to induce a turn structure [7, 8].

In this review we describe our efforts to prepare benzazepinone types of constrained analogues of Phe (Aba), Tyr (Hba), Trp (Aia), His (Ata), and Nal (Ana), as well as their use to obtain potent, selective, and blood-brain barrier-penetrating peptides and peptidomimetic analogues and their influence on the overall conformation of the peptide. We report studies dedicated to control the turn-inducing properties of the scaffold by α -methylation and to control the seven-membered ring conformation – and thereby the χ_2 angle – by introducing a 5-position methyl substituent. Finally, a method is reviewed that uses ring-closing metathesis and further modification of chlorinated and methoxycarbonylated alkene precursors to generate new types of heterocycle-fused benzazepinones. The latter extends our efforts to exploit the amino-azepinone heterocycle with various substitution patterns as a privileged scaffold. Indeed, the variety of biological targets

for which high-affinity ligands containing the abovementioned Aba-type scaffolds were obtained, both by other groups and by us, is a clear indication of the privileged scaffold property of the heterocycle.

2 Synthesis

2.1 4-Amino-1,2,4,5-tetrahydro-2-benzazepin-3-one (Aba) Analogues

This section includes the preparation of constrained analogues of Phe (Aba) and Tyr (hydroxy-Aba or Hba).

2.1.1 Retrosynthetic Analysis

The seven-membered azepinone ring of the Aba analogues can be formed either by attack of an aromatic ring onto an *N*-acyliminium ion intermediate (pathway **A**) or by lactam formation (pathway **B**). Iminium ions were formed by treatment of the dipeptide oxazolidinone with Brønsted or Lewis acids or by acylation of an imine. The precursor for lactam formation was obtained by reductive amination of phthaloyl- or oxazolidinone-protected *ortho*-formyl-Phe, which in turn was obtained, respectively, from reduction or oxidation of the corresponding *o*-cyano or *o*-hydroxymethyl counterpart. In a third approach to Aba derivatives, the *ortho*-formyl-Phe was used as substrate in the Ugi-4-component reaction (pathway **C**) (Fig. 3).

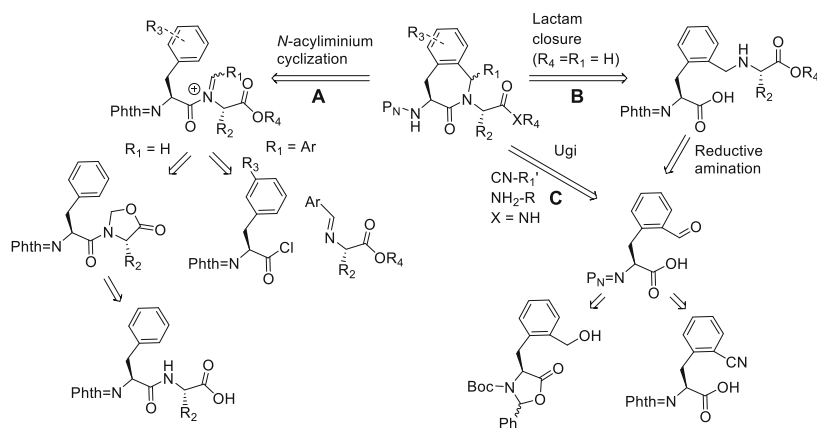


Fig. 3 General retrosynthetic analysis

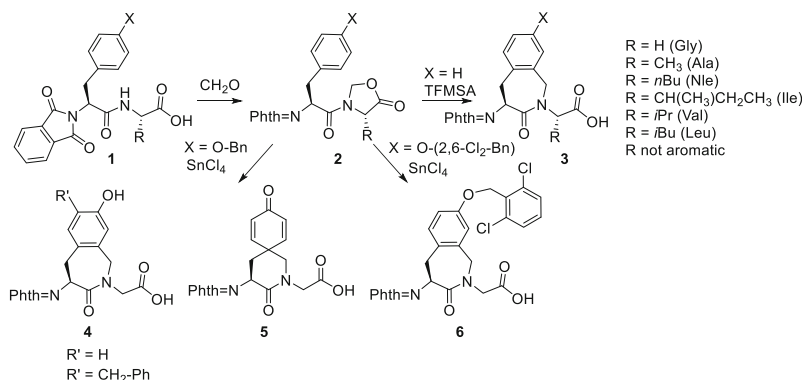


Fig. 4 The oxazolidinone pathway to Aba- and Hba-constrained dipeptides

2.1.2 *N*-Acyliminium Ion Cyclizations: The Oxazolidinone Pathway

To obtain Aba-constrained dipeptides **3** (Fig. 4), the method originally described by Flynn and de Laszlo [9, 10] was applied featuring preparation of oxazolidinone **2** by reacting the phthaloyl-protected dipeptide **1** with formaldehyde. Treatment of oxazolidinone **2** with triflic acid (TFMSA) generated the *N*-acyliminium intermediate which cyclized to the benzazepinone. By carefully controlling the temperature during the workup of the reaction mixture containing TFMSA, the amount of epimerization, which was observed by Flynn and de Laszlo to be as high as 10%, was reduced to less than 2% [4]. We also observed that during the preparation of Phth-Phe-OH using phthalic anhydride in solvent-free conditions, racemization occurred if the temperature of the reaction exceeded 145°C. The preferred method for phthaloyl protection employed methyl ((2-succinimidooxy)carbonyl)benzoate at room temperature [11]. The enantiomeric purity of the phthaloyl-protected amino acids was determined using a chiral HPLC method [12].

Dipeptides **2** possessing sterically hindered C-terminal residues, such as Ile, proved more difficult to cyclize. In such cases, successful cyclization was achieved using microwave heating and Lewis acids such as TiCl_4 and SnCl_4 [13]. The phthaloyl nitrogen protecting group was required to mask the N-terminal amine in a way that was resistant to acidic conditions and prevented addition to the *N*-acyliminium intermediate. The C-terminal residue of **2** should not contain an aromatic side chain (*R*) to avoid competitive reaction on the acyliminium ion to form a six-membered ring (e.g., tetrahydroisoquinoline in the case of Phe).

A variety of Aba-constrained dipeptides were prepared using this pathway: Aba-Gly [4, 9, 10, 13–15], Aba-Ala [13], Aba-Nle [10], Aba-Val [13], Aba-Leu [13], and Aba-Ile [13]. In an attempt to influence the seven-membered ring conformation, the corresponding 5-methyl-substituted Aba isomers were prepared starting from the different β -methyl-Phe stereoisomers [16]. In addition, starting from 1-Nal or 2-Nal, the constrained 4-amino-naphthoazepinones could be

obtained in good yields (Van der Poorten O, Ballet S, Unpublished work; Guillemyn K, Ballet S, Unpublished work).

Our first attempts to prepare the analogously constrained Tyr derivative (Hba) used *O*-benzyl protection of the phenol. This protecting group proved unstable to the TFMSA treatment and was cleaved to generate the starting phenol and benzylated phenol **4** (Fig. 4). Moreover, the unprotected phenol reacted at the *p*-position with the acyliminium ion to give dienone **5** [17]. Successful synthesis of Hba-Gly (**6**) was achieved using the more acid stable 2,6-dichlorobenzyl protection. The best catalyst for this cyclization turned out to be SnCl₄. Remarkably, an *O*-Bn protection was reported later to work smoothly by applying a TFMSA treatment of the oxazolidinone [18]. This *N*-acyliminium ion pathway was not applicable to Phth-Trp-Gly-OH, due to decomposition during formation of the oxazolidinone.

2.1.3 *N*-Acyliminium Ion Cyclizations: *C*-1-Substituted Analogues

1-Methoxycarbonyl-Aba (**10**, R₁ = COOMe, Fig. 5) was prepared by amidoalkylation of Phth-Phe-NH₂ (**7**) with methyl glyoxylate methyl hemiacetal, followed by treatment with TFMSA to induce cyclization [19]. An analogous intramolecular amidoalkylation was described by Rabi-Barakay, using Moc-Phe-NH₂ [20]. For the introduction of other substituents at *C*-1, we used the benzotriazole-mediated aminomethylation method developed by Katritzky [21]. Reacting Phth-Phe-NH₂ (**7**, R=H) and its *m*-methoxy counterpart (**7**, R=MeO) with a range of aromatic aldehydes under these conditions, followed by treatment with AlCl₃ provided in moderate yields 1-aryl-substituted Aba analogues **10** having *cis* relative stereochemistry as confirmed by X-ray crystallography (Fig. 5) [22]. By using *p*-bromobenzaldehyde or *p*-bromo-Phe (**7**, R'=Br), brominated Aba analogues **10** were prepared and further modified using Suzuki, Heck, and Buchwald-Hartwig conditions [23]. Employing this method, the azepinone nitrogen remains unsubstituted. Although *N*-arylation was possible [23], a greater diversity of benzazepinones was obtained by acylation of imines with Phth-Phe-Cl (**11**) (Fig. 6). Employing SbCl₅ as a chloride ion scavenger, *N*-acyliminium ions **13** were generated directly by this method using non-enolizable aldehydes [22]. In contrast to the cyclizations of the benzotriazole adducts, the reactions of acylated imines **13** resulted in *cis* and *trans* isomer mixtures of benzazepinones **14** (both *R*- and *S*-configurations were obtained at the newly formed chiral center).

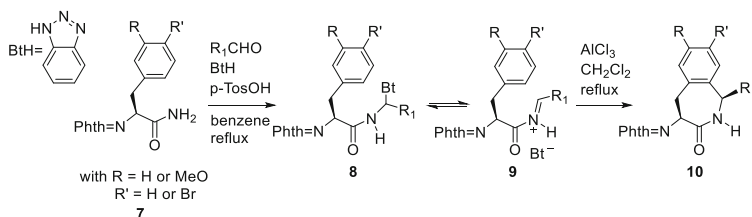


Fig. 5 Benzotriazole adducts for the preparation of 1-substituted Aba structures

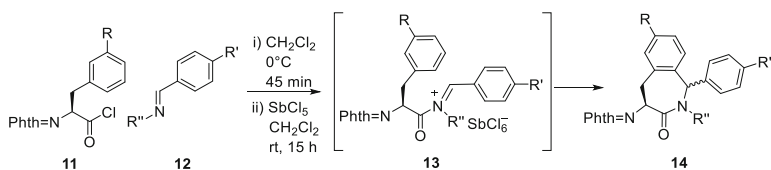


Fig. 6 Formation of 1-aryl-Aba via *N*-acylation of imines

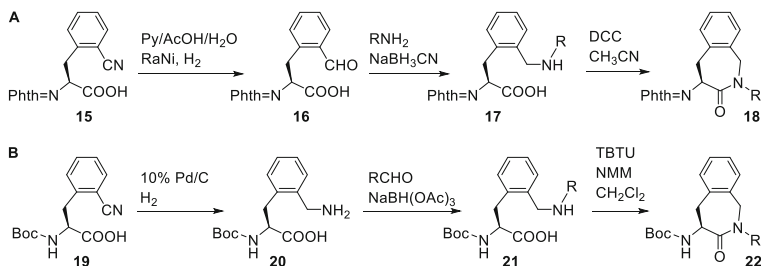


Fig. 7 Intramolecular amide bond formation via *o*-formyl- (A) and *o*-aminomethyl-Phe (B)

2.1.4 Cyclization by Lactam Formation: The *o*-Formyl-Phe Pathway

Formation of oxazolidinone precursors of *N*-acyliminium ions required the presence of an α -amino acid structure. Moreover, acylation of preformed imines suffered from rather modest yields. In certain cases, reductive amination onto phthaloyl-protected *o*-formyl-Phe **16** prior to lactam formation circumvented these limitations. Although *o*-formyl-Phe derivatives had been prepared by ozonolysis of the corresponding *o*-vinyl-Phe [24], we opted to prepare the aldehyde by partial reduction of commercially available *o*-cyano-Phe (Fig. 7) [25]. Phthalimide protection was essential for successful Raney nickel reduction and in situ hydrolysis of the resulting imine to form aldehyde **16**. The corresponding Boc-protected amine was added to the aldehyde to produce the acyliminium ion that underwent subsequent reduction to produce Boc-Tic. Similarly, attempts to prepare the Boc-protected *o*-formyl-Phe by oxidation of the corresponding *o*-hydroxymethyl-Phe **23** resulted in the formation of hemiaminal **24** (Fig. 8). The latter was not observed to be in equilibrium with the ring-opened aldehyde (in contrast to Boc-*o*-formyl-Trp, see Sect. 2.2) and failed to undergo intermolecular reductive amination. In contrast, the reductive method was successfully applied to prepare *N*-Boc-*N*-Me-*o*-formyl-Phe, leading to *N*-Me-Aba analogues (not shown) [25]. Alternatively, hydrogenation of *o*-cyano-Phe **19** over palladium-on-carbon gave *o*-aminomethyl-Phe **20**, which was employed in reductive alkylations with a variety of aldehydes, including α -aminoaldehydes [25]. For the latter method, conditions using solid-supported reagents were developed and used to generate a library of Aba analogues with a variety of substituents on the amine positions [26]. In addition, conditions for performing the reductive

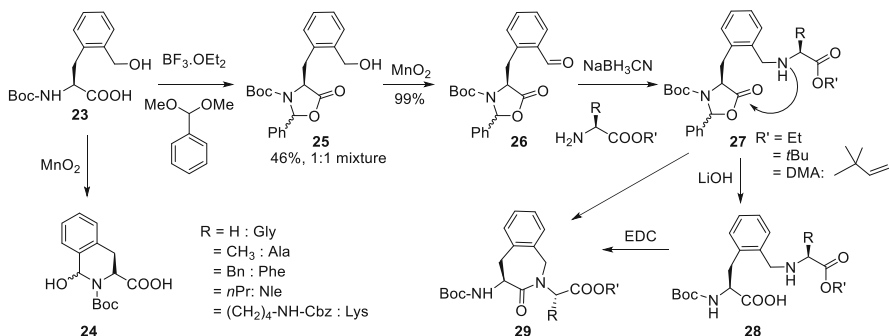


Fig. 8 Aba synthesis via oxidation of oxazolidinone-protected *o*-hydroxymethyl-Phe

amination/cyclization reaction on solid-supported amino acids and peptide fragments were developed and are described in more detail for the Aia analogues below (Fig. 14) [27].

Epimerization was a major concern during the reductive amination/cyclization process. The possibility of epimerization was examined by the synthesis of Phth-(*R,S*)-Aba-Gly-OBn, which after removal of the phthalimide and derivatization with Marfey's reagent, showed two well-resolved peaks by HPLC. In contrast, (*S*)-Aba-Gly-OBn showed only one peak (*ee* > 99%). In addition, in the synthesis of Phth-(*R*)-Aba-(*S*)-Ala-OBn, HPLC analysis showed the presence of only 1.5% of the Phth-(*R*)-Aba-(*R*)-Ala-OBn, which was indicative of a very low degree of racemization at the C_α of Ala [25].

The *o*-formyl-Phe building block was also generated by oxidation of an *o*-hydroxymethyl precursor that was prepared in 90% *ee* using the Oppolzer sultam method [28]. Employing *N*-(Boc)oxazolidinone **25** prevented formation of cyclic hemiaminal during both the oxidation of the benzylic alcohol using MnO_2 and the reductive amination on resulting aldehyde **26** with a variety of amino acid esters. Conversion to lactam **29** entailed saponification of oxazolidinone **27** with LiOH, followed by carboxylic acid activation with EDC or DCC. Bulky esters **27** (e.g., $R' = t\text{-Bu}$) were necessary to avoid competing hydrolysis during oxazolidinone cleavage. Although *t*-butyl protection avoided ester saponification, 1,1-dimethylallyl (DMA) esters were employed, because they were stable under the LiOH conditions and could be later cleaved selectively in the presence of the Boc group [29]. Partial lactam formation was observed during reductive aminations on aldehyde **26** using Lys(Z)-ODMA (15%) and Ala-OEt (45%), and complete conversion was obtained with Gly-OEt to provide Boc-Aba-Gly-OEt in 95% isolated yield.

Efficient syntheses of α -methyl and spirocyclic benzazepinones were developed, because conformational analyses indicated their stronger preference to adopt turn conformations (*vide infra*, Sect. 3) relative to the parent amino-azepinones [30].

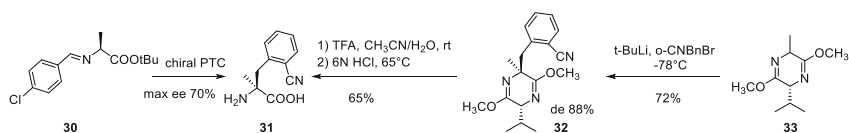


Fig. 9 Synthesis of enantiomerically enriched α -methyl-*o*-cyano-Phe by chiral PTC and by the Schöllkopf method

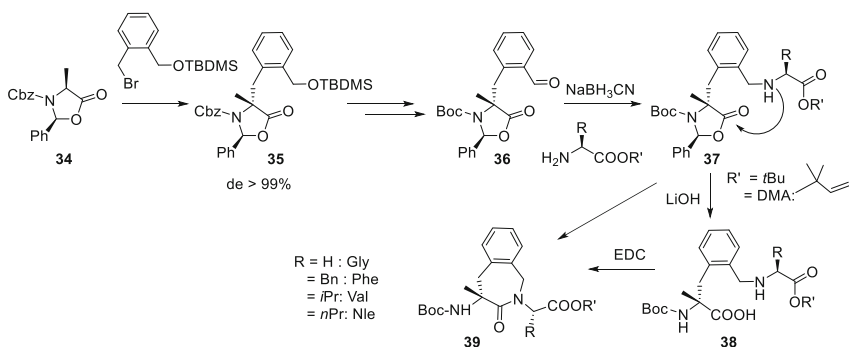


Fig. 10 Efficient synthesis of α -Me-Aba

The synthesis of α -Me-Aba **39** started from the corresponding α -Me-*o*-cyano-Phe (**31**) [30, 31]. Enantiomerically enriched α -Me-*o*-cyano-Phe was synthesized by phase transfer-catalyzed (PTC) alkylation of **30** with *o*-cyanobenzyl bromide using the chiral cinchona-base *O*-(9)-allyl-*N*-2',3',4'-trifluorobenzyl hydrocinchonidinium bromide with CsOH as a base and by employing Schöllkopf's method using bis-lactim ether **33** (Fig. 9) [31]. In contrast, diastereomerically pure **35** (>99% de) was obtained from alkylation of readily available *cis*-(2*S*,4*S*)-2-phenyl-4-methyloxazolidinone **34** and transformed efficiently into α -methyl-Aba analogues using similar methods as those previously described in Fig. 8 (Fig. 10) [32].

Similar to α -methyl-Aba, spirocyclic Aba was found to be an efficient turn inducer that was synthesized by the reductive amination/lactam cyclization approach [33, 34]. α -Alkylation of *N*-Boc- and *N*-Moc-prolines with *o*-cyanobenzyl bromide gave, respectively, (*R,S*)- α -(*o*-cyanobenzyl)-Pro **43** and **40** (Fig. 11). Raney nickel reduction of the Boc-protected analogue of **40** in aqueous pyridinium acetate resulted in a pyrroloisoquinoline carboxylic acid from Boc group cleavage and condensation of the aldehyde intermediate onto the secondary amine. The acid stable Moc group remedied the issues encountered with Boc protection, such that aldehyde **41** reacted with Gly-OBn in the reductive amination-lactam cyclization sequence to provide spirocyclic Aba **42** [34]. Simultaneous removal of the Moc- and benzyl-protecting groups, followed by Boc protection, gave racemic building block **45** suitable for SPPS. Alternatively, spirocyclic Aba **45** was synthesized from Boc- α -(*o*-cyanobenzyl)-Pro **43** by a sequence featuring nitrile reduction to benzyl

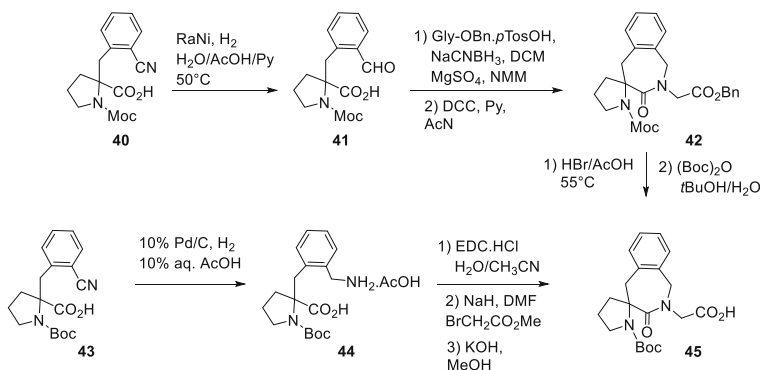


Fig. 11 Synthesis of Boc-spiro-Aba-Gly-OH

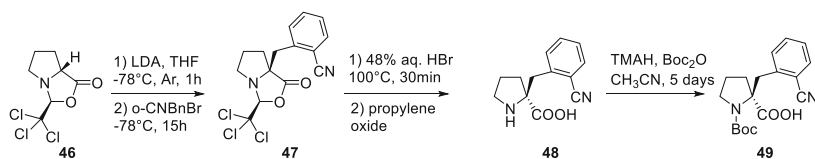


Fig. 12 Enantioselective synthesis of 2-(*o*-cyanobenzyl)pyrrolidine-2-carboxylic acid

amine **44**, lactam formation, and *N*-alkylation with methyl bromoacetate (Fig. 11) [35].

Enantiomerically pure spirocyclic Aba was achieved by a diastereoselective route employing oxazolidinone **46**, which was derived from chloral and *D*-Pro, and alkylated using *o*-cyanobenzyl bromide and LDA (Fig. 12). After hydrolysis of oxazolidinone **47**, the installment of the Boc group onto the secondary amine proved challenging necessitating use of the lipophilic base tetramethylammonium hydroxide (TMAH) and long reaction times to furnish carbamate **49** in 45% yield. Attempts to increase amine nucleophilicity and solubility by silylation using *N*-trimethylsilyl acetamide failed to improve the yield of Boc protection [36]. Transformation of nitrile **49** into enantiomerically pure Boc-spiro-Aba-Gly-OH **45** was performed as described for the racemate.

2.2 4-Amino-1,2,4,5-tetrahydro-2-indoloazepin-3-one (Aia) Analogues

An efficient route was developed for the preparation of 4-amino-3-oxo-3,4,5,10-tetrahydro-1*H*-azepino[3,4-*b*]indol-2-yl acetic acid (Aia), which restricts the side chain of tryptophan to the *gauche*-(+) ($\chi_1 = 60^\circ$) and *trans* ($\chi_1 = 180^\circ$) conformations (Fig. 13) [37].

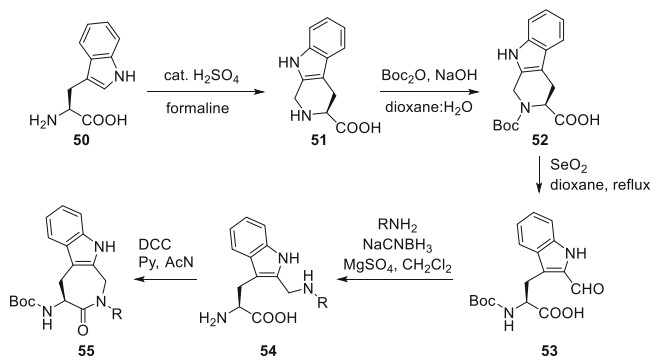


Fig. 13 Synthesis of substituted 4-amino-indoloazepinone (Aia)

An indirect formylation strategy was developed to synthesize 2'-formyl-Trp derivatives **53**, because initially various attempts at formylation of Phth-Trp-OME resulted mostly in formylation of the indole nitrogen [37]. Tetrahydro- β -carboline-3-carboxylic acid **51** (Tcc) was thus prepared by a Pictet-Spengler reaction and was Boc protected. Oxidation of Boc-Tcc (**52**) with SeO_2 gave 2'-formyl-Trp **53** in 76% yield. A series of reductive amination-lactam cyclization sequences were performed to prepare indoloazepinones **55** without purification of the intermediate secondary amines **54** [37]. Although indoloazepinone dipeptidomimetics **55** ($\text{R}=\text{CHR}'\text{CO}_2\text{H}$, Fig. 13) could be effectively introduced into biologically active peptides, increased synthetic efficiency was envisaged by assembly of the Aia motif directly on solid support [38]. This strategy avoided separate solution-phase synthesis of individual Aia-Xxx dipeptide mimetic building blocks. For this purpose, both the reductive amination and the cyclization reactions needed to be adapted to solid phase (Fig. 14). Both Boc- and Fmoc-2'-formyl-Trp derivatives **56** were prepared as described above. In general, the Fmoc strategy provided peptides with variable purity, likely due to the low solubility of the Fmoc-protected aldehyde in dichloromethane. Trimethyl orthoformate (TMOF) was used as a dehydrating agent during the reductive amination. Conversion to the more soluble semicarbazone by applying a semicarbazide facilitated removal of excess aldehyde from the solid support at the end of the reaction [38]. All lactam cyclizations went smoothly with TBTU as coupling reagent. Nevertheless, final peptides with improved purity and better isolated yields were achieved using the Boc strategy. Both strategies allowed effective "Aia-conformational scanning" of Trp-containing peptides [38].

More recently, Boc-2'-formyl-Trp **59** was employed in an Ugi three-component condensation to prepare carboxamide-substituted Aia **60** and derivatives (Fig. 15) [39–41]. This versatile strategy enabled syntheses of azepinone building blocks **60** with three points of diversity. Although substituted Aba building blocks were also prepared using this method (not shown), the Ugi reaction gave lower conversion and reduced stereoselectivity than in the case of the Aia analogues (Jida M, Van der Poorten O, Ballet S, Unpublished work).

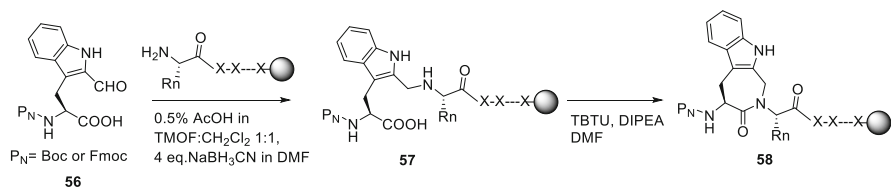


Fig. 14 Solid phase assembly of amino-indoloazepinone (Aia) peptides

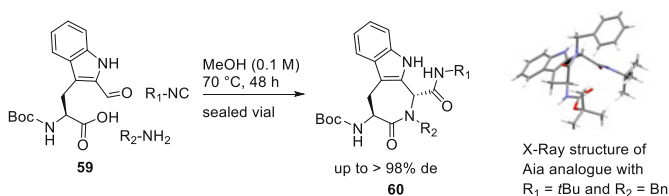


Fig. 15 Three-component Ugi reaction to 1-carbamoyl-4-amino-indoloazepinones **60**

2.3 4-Amino-1,2,4,5-tetrahydro-2-triazoloazepin-3-one (Ata) Analogues

The spectacular emergence of 1,2,3-triazoles in chemical biology and medicinal chemistry [42, 43] motivated the design of our route to assemble amino-triazoloazepinone (Ata) dipeptidomimetics **67** [44]. Even though the hydrogen bonding ability and protonation state of the triazole moiety are quite different from the imidazole in histidine, replacement of the His-Pro dipeptide in angiotensin IV by Ata-Gly gave an equipotent analogue. The Ata heterocycle was therefore validated as a His mimic (vide infra, Sect. 4.6) [44]. Two synthetic routes were investigated to prepare the triazole with 1,5 regiochemistry. The intermolecular route (Route **A** in Fig. 16) employed a ruthenium catalyst to set the desired 1,5-regiochemistry in the Huisgen cycloaddition reaction. Lactam formation with EDC and HOAt provided the dipeptide mimetic **67** with minimal epimerization [45]. Only esters were used in the Ru-catalyzed azide alkyne cycloaddition (AAC) reaction, because of poor compatibility with carboxylic acids. The intramolecular pathway (Route **B** in Fig. 16) was more convergent and provided 1,5-triazoloazepinone without the requisite Ru catalyst. Route **B** was preferred for making Ata-Gly dipeptides **67**; however, yields were reduced, and significant degrees of epimerization (up to 40%) were encountered when making analogues with other C-terminal amino acids. In the latter cases, route **A** was better suited for making Ata-Xaa dipeptides **67**.

Assembly of the Ata motif was also realized using the Ugi four-component reaction (Fig. 17). Conformationally constrained dipeptides have been pursued using Ugi deprotection-cyclization [46, 47] and Ugi activation-cyclization sequences [41]. In our case, after Ugi condensation, the intramolecular thermal Huisgen cycloaddition was used to prepare the triazoloazepinone [48]. This strategy

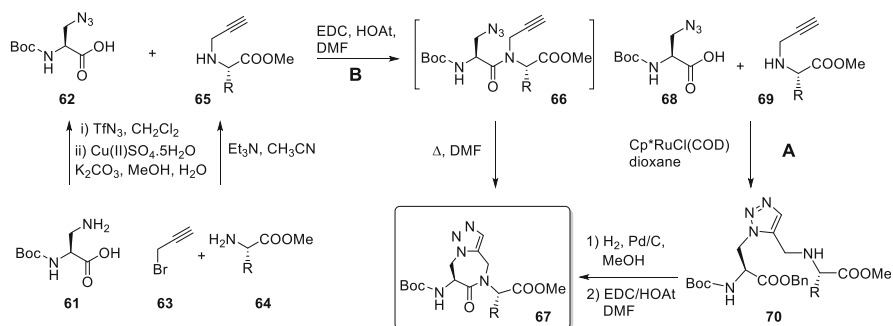


Fig. 16 Synthesis of amino-triazoloazepinones via RuAAC (A) and thermal (B) Huisgen cycloaddition reactions

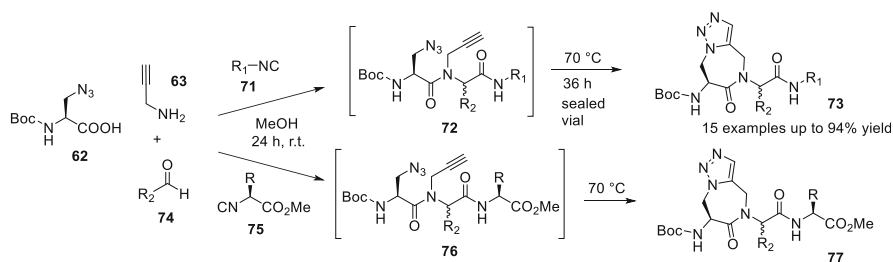


Fig. 17 Constrained di- and tripeptide amino-triazoloazepinones from Ugi-4C reactions

was more convergent, higher yielding, and atom efficient compared to the method depicted in Fig. 16; however, it lacked control over the formation of the new stereocenter from the carbonyl component and gave a mixture of two diastereomers. This one-pot two-step protocol provided Boc-protected tripeptide esters **77** from amino acid-derived isocyanides **75**. After saponification of the ester function of **77**, the tripeptide fragment is compatible in SPPS [48].

2.4 Other Heterocycle-Fused Amino-azepinones from Ring-Closing Metathesis

In addition to benzofused amino-azepinones, 3-amino-1,3,4,7-tetrahydro-2H-azepin-2-ones fused to other heteroaromatic rings may be of interest for peptide mimicry. Aminotetrahydroazepinones **79** and **84** were thus employed as precursors to prepare a series of fused azepinones by modification of their activated double bonds. Starting from racemic allylglycinamides **78** (X=Cl), 6-chloro-3-amino-1,3,4,7-tetrahydro-2H-azepinones **79** were synthesized in good yield by olefin metathesis using either Grubbs II or Umicore M2 catalysts [49]. Unfortunately, olefin metathesis reactions of the corresponding 2-bromoallylated derivatives **78**

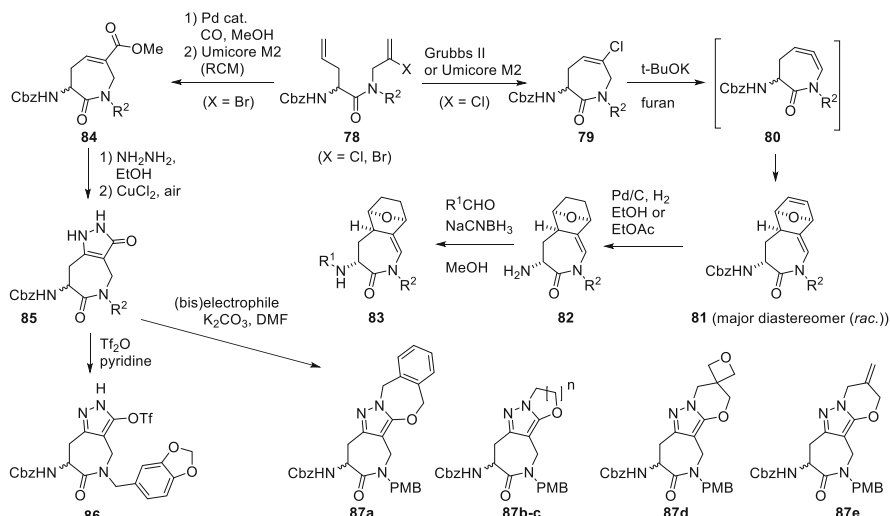


Fig. 18 Ring-closing metathesis routes to heterocycle-fused amino-azepinones

($X = \text{Br}$) did not result in acceptable yields of the corresponding brominated tetrahydroazepinone [50–53]. Bromides **78** ($X = \text{Br}$) were however efficiently methoxycarbonylated using $\text{Pd}(\text{dppf})\text{Cl}_2$ under CO atmosphere in MeOH/THF to afford the corresponding esters **78** ($X = \text{COOMe}$), which underwent ring-closing metathesis to provide azepinones **84** [54].

Treatment of substrates **79** with *t*-BuOK [55–57] in furan resulted in the clean formation of mixtures (2:1 to 96:4) of only two cycloadducts, from which the major isomer was easily separated from the minor regioisomer by column chromatography. The relative stereochemistry of the cycloadducts was confirmed by X-ray analysis and predicted by DFT calculations that indicated the intermediate allenamides **80** reacted diastereoselectively in situ with furan from the face opposite of their 3-aminosubstituents in a regioselective manner to provide the *endo*-enamides **81** (Fig. 18).

Further diversification of cycloadducts **81** was achieved by hydrogenolytic removal of the Cbz group using palladium-on-carbon under H_2 atmosphere and reductive amination reactions with different aldehydes. The enamide functionality remained notably intact after both the hydrogenation and reductive amination protocols. This reaction sequence provides thus an entry to amino oxanorborene azepinone analogues.

On the other hand, α,β -unsaturated esters **84** reacted with hydrazine to furnish with high conversion fused pyrazolidinones, contaminated with minor amounts (<10%) of the corresponding pyrazolones **85**. Therefore, a one-pot protocol toward **85** was developed using an oxidation by air catalyzed by CuCl_2 in DMF [58]. Pyrazolones **85** were however quite insoluble in standard organic solvents, but could be further derivatized into building blocks for peptidomimetic research. For example, reaction of **85** with triflic anhydride provided trifloxy pyrazoles (e.g., **86**), which may be

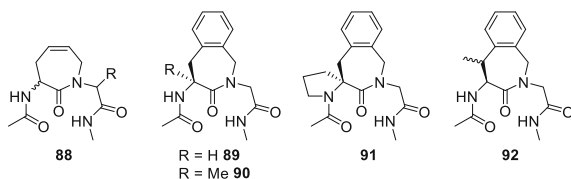
promising building blocks for further Pd-catalyzed cross-coupling reactions. In addition, alkylation of pyrazolones **85** was studied using different electrophiles. The selectivity of *N*- versus *O*-alkylation of pyrazolones was known to be dependent on the substrate, alkylating reagent, and reaction conditions [59–61]. Although methylation reactions did not seem promising, the use of bis-electrophiles gave benzoxazepane-, oxazolidine-, and oxazane-fused heterocycles (e.g., **87a–87c**) via selective *N*-1 and *O*-alkylation without *N*-1,*N*-2 alkylation [62, 63]. The scope was further elaborated by employing dichloroisobutene and 3,3-bis(bromoethyl)oxetane to provide new polyheterocycles (e.g., **87d** and **87e**).

3 Conformational Studies

Since Freidinger demonstrated that a more potent LHRH analogue could be prepared by insertion of a β -turn-inducing five-membered γ -lactam [7], many so-called Freidinger lactams have been prepared and claimed to be β -turn inducers, including six- and seven-member examples [8]. Considering the structural similarity of the described analogues of amino-benzazepinone (Aba) with dehydro-lactam **88** (Fig. 19) [64, 65], we studied the reverse turn-inducing potential of Aba, α -Me-Aba, and *spiro*-Aba scaffolds. For this purpose, they were incorporated into the tetrapeptide models Ac- α -R-Aba-Gly-NHMe (R=H, Me, pyrrolidino) and studied by NMR spectroscopy and molecular modeling [34]. Although no turn formation was indicated for Ac-Aba-Gly-NHMe **89**, the corresponding α -Me and spirocyclic analogues **90** and **91** clearly showed turn structures, as supported by X-ray crystallography [30, 34]. Similarly, in the dermorphin sequence (H-Tyr-D-Ala-Phe-Gly-Tyr-Pro-Ser-NH₂), the application of Aba analogues as Phe³ constraints demonstrated [Aba³]dermorphin to adopt mainly flexible extended conformations, but [(*R*)- α -Me-Aba]dermorphin to prefer a turn conformation [31]. Similar observations were made for a [(*R*)-*spiro*-Aba]endomorphin analogue [33]. These results demonstrated that all lactams may not be considered turn inducers without experimental proof.

Without substituent, the ring conformation of the seven-member Aba lactam was chair-like; that of the α -methyl and *spiro*-substituted Aba analogues were boatlike. Similar to the parent amino-benzazepinone, β -methyl-Aba **92** adopted the chair-like ring conformation [30]. In all cases, the χ_1 dihedral angle corresponded to a *trans* side chain orientation (Fig. 2).

Fig. 19 Lactams as potential turn inducers



4 Biological Applications

This section illustrates the potential of the templates described above for biological applications. In addition to initial efforts on ACE/renin inhibitors and opioid ligands, a wide range of targets have been examined.

4.1 Amino-benzazepinones as ACE, Renin, and NEP Inhibitors

The first reported application of the Aba scaffold consisted of the design of angiotensin-converting enzyme (ACE) inhibitors for the treatment of hypertension [66]. Blockage of the renin-angiotensin-aldosterone system (RAAS) prevents formation of the potent vasoconstrictor angiotensin II. For this reason, the Cbz derivative of the carboxy-terminal tripeptide of the natural ligand angiotensin I, *N*-Cbz-Phe-His-Leu-OH (**93**), was mimicked. Although tripeptide **93** had moderate affinity for ACE (K_i of 10 μ M), diacid **94** inhibited rabbit lung ACE with a K_i of 0.012 nM (Fig. 20). Prodrug **95** proved orally active in rats reducing angiotensin I-induced increase in blood pressure [66]. Relative to these more constrained analogues, Aba **96** was a modest inhibitor ($K_i = 10$ nM) [19].

A second route to control hypertension was realized by inhibition of the aspartyl protease renin [10]. Based on the Merck renin binding site model, conformational restrictions, such as six-membered piperidones and amino-benzazepinones, were introduced into inhibitors. Hydroxyethylene isostere **97** proved to be a potent inhibitor ($IC_{50} = 6.5$ nM) [67]. Replacement of the purported P3 residue of **97** by benzazepinones to decrease the number of rotatable bonds provided analogues **98a–d**, which showed decreased potency. According to molecular modeling studies, the seven-member lactam distorted the preferred extended conformation of the peptide backbone [10].

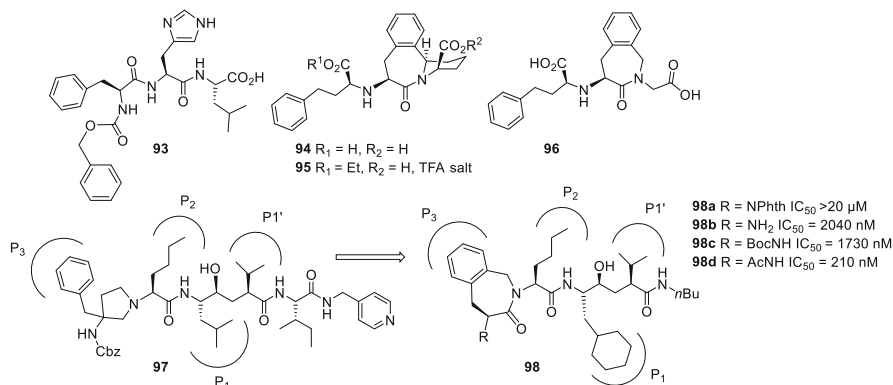


Fig. 20 Angiotensin-converting enzyme and renin inhibitors with their activities

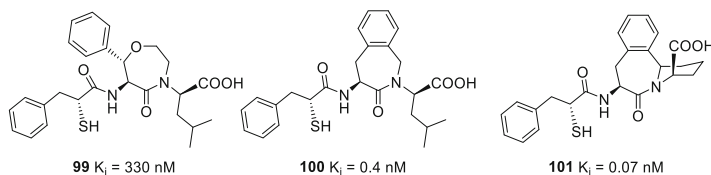


Fig. 21 Neutral endopeptidase inhibitors and their affinities

Similar to ACE blockers, NEP (neutral endopeptidase) inhibitors decrease blood pressure and have been targeted for treatment of hypertension. Commencing with the reported inhibitor oxazepinone **99** (MDL 100,192), which constrained the Phe χ^1 dihedral angle to a *gauche*-(-) conformer, two analogues (**100** and **101**) were prepared using Aba residues to favor the *trans* conformation and exhibited, respectively, 800 and 4,800 times greater potency (Fig. 21) [24].

4.2 Amino-benzazepinones in Opioid Applications

The opioid peptides dermorphin (H-Tyr-D-Ala-Phe-Gly-Tyr-Pro-Ser-NH₂) and deltorphin II (H-Tyr-D-Ala-Phe-Glu-Val-Val-Gly-NH₂) were isolated from the skin of the South American frog *Phyllomedusa sauvagii* [68]. Dermorphin has a high potency and selectivity toward the μ -opioid receptor (MOR), while deltorphin II binds selectively to the δ -subtype receptor (DOR). They have a common N-terminal *message* part and a different C-terminal *address* segment, which is responsible for receptor subtype selection. This receptor selectivity is based on the conformational space available to the peptide [15]. Crucial pharmacophore features involve the relative orientation of the Tyr¹ and Phe³ side chains. To investigate the χ space in dermorphin, Phe³-Gly⁴ was substituted by Aba-Gly [4, 15]. The Phe side chain is constrained to the *trans* conformer in [Aba³] dermorphin, which exhibited increased affinity and activity at the δ -opioid receptor, without significant change of behavior at the μ -opioid receptor.

By truncation of the native dermorphin sequence, the N-terminal tetrapeptide was found to be the minimal requirement for opiate-like activity *in vivo* [69]. The tetrapeptide H-Tyr-D-Ala-Phe-Gly-NH₂ (**102**) has an IC₅₀ value of 36.7 nM at MOR and 1,247 nM at DOR (Table 1) [73]. Introduction of the constrained amino acids into peptide **102** at the 1-position (i.e., Tyr¹ to Hba¹) and 3-position (Phe³ to Aba³) did not dramatically change μ -affinity; however, δ -affinity increased 50- to 100-fold, shifting selectivity to the δ -opioid receptor [14]. All of the analogues showed agonist activity in assays on the guinea pig ileum (GPI, a representative test for MOR agonist activity) and mouse *vas deferens* (MVD, a measure of DOR agonist activity). Among the investigated compounds (Table 1) [14], H-Hba-D-Ala-Aba-Gly-NH₂ **103** was the most potent MOR agonist and selected for *in vivo* analgesia testing (rat tail-flick test). On intrathecal administration, peptide mimetic

Table 1 Affinity and functional activity of selected compounds based on dermorphin

Ligand	MOR affinity K_i (nM)	DOR affinity K_i (nM)	GPI (MOR agonism) IC_{50} (nM)	MVD (DOR agonism) IC_{50} (nM)	EC_{50} [^{35}S] GTP γ S
(102) H-Tyr-D-Ala-Phe-Gly-NH ₂ [73]	36.7 ^a	1,247 ^a	35	263	ND
(103) H-Hba-D-Ala-Aba-Gly-NH ₂ [14]	20.8 ^a	160 ^a	3.64	30.3	ND
(104) H-Tyr-NMe-D-Ala-Phe-NMe-Gly-NH ₂ [70]	28.1 ^a	7.1 ^a	22.0	79.7	ND
(105) H-Dmt-D-Ala-(4S)-Aba-Gly-NH ₂ [30, 71]	0.047 ^b	2.4 ^c	0.0832 ^d	0.17 ^e	ND
(106) H-Dmt-D-Ala-(4R)-Aba-Gly-NH ₂ [16]	0.33 ^b	337 ^c	ND	ND	64.2
(107) H-Dmt-NMe-D-Ala-Aba-Gly-NH ₂ [71]	14.8 ^f	5 ^f	0.00174 ^d	0.016 ^e	ND
(108) H-Dmt-D-Ala-(4S)-Me-Aba-Gly-NH ₂ [16]	4.6 ^b	859 ^c	ND	ND	941
(109) H-Dmt-D-Ala-(4R)-Me-Aba-Gly-NH ₂ [16]	0.3 ^b	63 ^c	ND	ND	288
(110) H-Dmt-D-Ala-(S)- <i>spiro</i> -Aba-Gly-NH ₂ [30]	3.2 ^b	308 ^c	ND	ND	ND
(111) H-Dmt-D-Ala- <i>erythro</i> -(4S,5S)-5-Me-Aba-Gly-NH ₂ [16]	0.025 ^b	1.7 ^c	ND	ND	36
(112) H-Dmt-D-Ala- <i>threo</i> -(4R,5S)-5-Me-Aba-Gly-NH ₂ [16]	0.025 ^b	24 ^c	ND	ND	9.3
(113) H-Dmt-D-Arg-Aba-Lys-NH ₂ [72]	0.61 ^b	38.6 ^g	76	64 (IC_{25})	ND
(114) H-Dmt-D-Arg-Aba-Gly-NH ₂ [72]	0.15 ^b	0.6 ^g	0.32	0.42	ND
(115) H-Dmt-D-Arg-Aba- β -Ala-NH ₂ [27]	1.34 ^b	17 ^g	0.8	0.24	ND

ND not determined

^a IC_{50}

^bDisplacement of [3H]DAMGO

^cDisplacement of [3H][Ile^{5,6}]deltorpin II

^dDisplacement of EC_{50} of agonist properties on forskolin-stimulated cAMP accumulation by MOR

^eDisplacement of EC_{50} of agonist properties on forskolin-stimulated cAMP accumulation by DOR

^fDisplacement of [3H]diprenorphine

^gDisplacement of [3H]DSLET

103 was 40–50 times more potent and possessed a longer duration of action than morphine [14].

Blood-brain barrier (BBB) penetration is notably important for pain relief by activation of the opioid receptors located in the central nervous system [70]. Many opioid peptides are potent analgesics only when applied directly to their site of

action after i.c.v. or i.t. administration. To examine the importance of ring constraints, the antinociceptive effect after intravenous administration of peptide mimetic **103** was compared to that of di-*N*-methyl peptide **104** (H-Tyr-*N*Me-D-Ala-Phe-*N*Me-Gly-NH₂). Both **103** and **104** gave a high antinociceptive effect in the tail-flick test, indicating similar BBB permeation, albeit constrained peptide **103** reached a maximum response after 15 min, twice as fast as flexible **104** [70].

Replacement of Tyr¹ with the unnatural amino acid 2',6'-dimethyltyrosine (Dmt) resulted in compounds with increased potency [3, 74–76]. Therefore, the Hba moiety in tetrapeptide **103** was substituted with Dmt to give H-Dmt-D-Ala-Aba-Gly-NH₂ (**105**), which had subnanomolar affinity for MOR and low nanomolar affinity for DOR [16]. Among variants made starting from di-*N*-methyl dermorphin analogue **104** [14, 71], **107** (H-Dmt-*N*Me-D-Ala-Aba-Gly-NH₂) proved to be one of the most potent, displaying high affinity and extraordinary agonist potency at both the μ - and δ -opioid receptor subtypes [71].

Compared to the parent Aba-Gly peptides, the turn-inducing α -methyl- and spirocyclic Aba-Gly analogues exhibited lower affinity [30, 34]. For example, *spiro*-Aba peptide **110** and α -methyl-Aba peptides **108** and **109** had low nanomolar activity for the μ opioid receptor, but 100-fold reduced δ -affinity, indicating that the turn conformation was less well tolerated by the opioid receptors [30].

All four β -methyl-amino-benzazepinone diastereomers were introduced into the reference sequences **105** and **106** [16] producing ligands with preferred MOR over DOR selectivity. The *erythro*-(4*S*,5*S*)- β -methyl-Aba ligands displayed similarly high μ - and δ -affinity as the parent (*S*)-Aba analogue (**111** vs. **105**). The *threo*-(4*R*,5*S*)- β -methyl-Aba ligand **112** showed the same MOR affinity as **105** in contrast to the observed loss of binding that accompanied a transition from (*S*)- to (*R*)-Aba (**106** vs. **105**) [16, 33, 71]. A similar observation was made for the α -methyl-Aba analogues **108** and **109**, in which the (4*R*)-epimer was more potent than the (4*S*)-counterpart. These results could be explained by molecular docking simulations, which demonstrated that the (4*R*)-Aba isomers could adopt different conformations that were able to bind the opioid receptors [16]. The (*S* and *R*)-Aba-Gly and α -Me-(*S* and *R*)-Aba-Gly dipeptides were also inserted into the full dermorphin sequence providing analogues that retained MOR selectivity [31], albeit lower than the natural ligand. The two analogues incorporating (*S*)-Aba-Gly and (*R*)- α -Me-Aba-Gly were as potent as dermorphin, again illustrating that opposite Aba stereochemistry is preferred in the α -methyl series, compared to that in the α -H series [16, 31]. In NMR spectroscopic studies, [(*S*)-Aba-Gly]dermorphin was shown to be very flexible, and [(*R*)- α -Me-Aba-Gly]dermorphin adopted a well-defined turn conformation [31].

The dermorphin derivative [Dmt¹]-DALDA (Dmt-D-Arg-Phe-Lys-NH₂) developed by Schiller and coworkers [77] has agonist activity, metabolic stability, and high MOR affinity ($K_i^{\mu} = 0.143$ nM, sevenfold higher than morphine) [78]. Based on this peptide, several Aba analogues were synthesized (Table 1) [72]. For example, replacement of Phe³ by Aba in **113** reduced fourfold μ -receptor binding and increased DOR affinity (2,100–38.6 nM). The removal of side chain charge by

substitution of D-Arg² with D-Cit² was tolerated by both receptor types and on replacement of Lys⁴ by Nle⁴, caused a net improvement of μ - and δ -opioid binding. The charged guanidine group was thus not crucial for receptor recognition and activation. Although introduction of an Aba³-Lys⁴ dipeptide was detrimental for MOR and DOR activity, Aba³-Gly⁴ analogue **114** ($K_i^\mu = 0.15$ nM, $K_i^\delta = 0.60$ nM) exhibited notable potency and was later shown to be transported into the brain after intravenous or subcutaneous administration [79]. Peptide **114** exhibited a longer duration of action compared to morphine. Moreover, changing Gly⁴ in **114** to β -alanine⁴ in **115** gave an even more potent peptide in vivo [27].

Endomorphin-2 (H-Tyr-Pro-Phe-Phe-NH₂) is a potent, μ -selective endogenous opioid peptide [80], from which substitution of Pro² by Tic² gave potent TIPP peptides (e.g., **116**, Fig. 22) [6, 81]. In the design of MOR- and DOR-selective peptides, the Tyr-Tic and Dmt-Tic pharmacophores (Dmt = 2',6'-dimethyltyrosine) have been used extensively. For example, the smallest fragment having potent opioid properties is Dmt-Tic-OH [82, 83]. For δ -opioid agonist activity, a third aromatic nucleus was needed at a precise distance from the Dmt-Tic pharmacophore [84]. Albeit Dmt-Aba-OH was reported to be completely inactive [82], the Aba motif **117** (Fig. 22) led to a series of potent analogues with MOR versus DOR selectivity contingent on the $C\alpha_1$ configuration and the (*S*)-stereochemistry at $C\alpha_2$ giving better binding [84]. Replacement of Tic-Gly in δ -selective Dmt-Tic ligands (e.g., H-Dmt-Tic-Gly-NHBn, **119**) for Aba-Gly gave analogues with reversed μ/δ selectivity (e.g., **120**, Fig. 22) [85]. Surprisingly, dimers and trimers of the Aba-pharmacophore proved to be dual and balanced δ/μ antagonists [86]. Replacement of Tic in **119** for L- and D-Aia in **118** gave, respectively, moderate MOR and DOR affinity and a selective μ -agonist with activity comparable to endomorphin-1. In contrast, *N,N*-dimethylation of the Dmt residue in the L-Aia peptide **118** produced potent DOR antagonism [85]. Application of the turn-inducing *spiro*-Aba-Gly motif in the design of endomorphin-2 mimetics gave high MOR selectivity and potency supporting the hypothesis that the parent peptide was recognized by the MOR in a folded conformation [33]. In contrast to endomorphin-2, the spirocyclic derivative was a partial agonist.

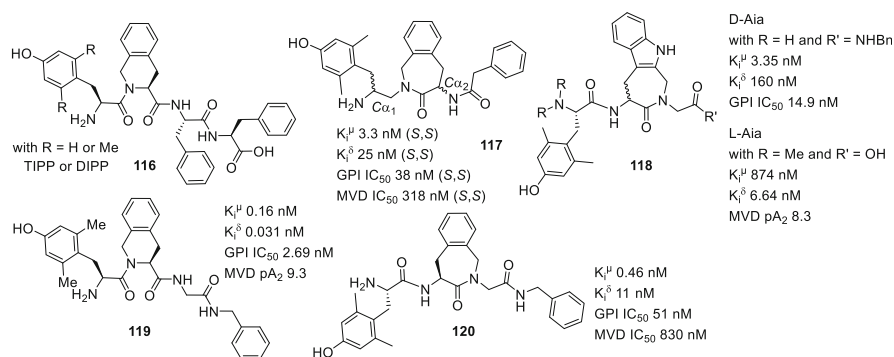


Fig. 22 New motifs mimicking TIPP-like peptides

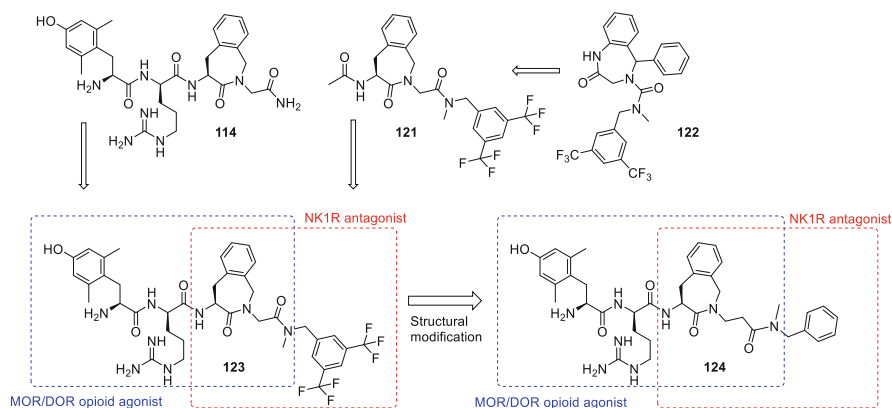


Fig. 23 Peptidomimetic opioid agonist-neurokinin-1 antagonist ligands [27, 79, 101]

4.3 Bifunctional Opioid Agonist – NK1 Antagonist Ligands

One of the major drawbacks of prolonged opioid administration is the development of tolerance. The body finds a way to compensate the opioid activation and increases the release and expression of pronociceptive endogenous ligands and their respective receptors [87, 88]. The development of ligands that target multiple receptors has been considered to counteract these changes [88–90]. This strategy has led to multiple opioid/opioid ligands that combine two opioid pharmacophores [91], as well as opioid/non-opioid hybrids [92]. Earlier reports indicated that an opioid agonist-neurokinin-1 (NK1R) antagonist combination was able to suppress tolerance [93–98]. Linking both pharmacophores into a single chemical entity was used to design a multiple ligand that modulated both targets [90, 99, 100]. Based on reported peptidomimetic NK1R antagonists (e.g., **122**, Fig. 23) [102], various Aba, Aia, Tic, and Tcc mimics were pursued to obtain potent neurokinin antagonism, such as Aba **121**, which exhibited 27 nM NK1R affinity and a pA_2 value of 8.3 [101]. The combination of this neurokinin part with a previously validated opioid sequence **114** (vide supra) led successfully to compact bifunctional opioid-NK1R ligand **123** [101]. This ligand was further modified to identify important structural features in both pharmacophores [27]. In particular, Aba **124** exhibited an improved in vitro opioid profile, but diminished NK1R affinity and antagonism. When tested in acute and neuropathic pain models, both **123** and **124** could induce potent analgesic effects; however, the latter proved more active in the neuropathic pain models and was less toxic at higher doses. Neither **123** nor **124** could abolish tolerance upon chronic administration [27, 79].

4.4 Bradykinin (BK)

Bradykinin (BK, H-Arg-Pro-Pro-Gly-Phe-Ser-Pro-Phe-Arg-OH) is a nonapeptide hormone that is formed by enzymatic cleavage of the plasma precursor kininogen.

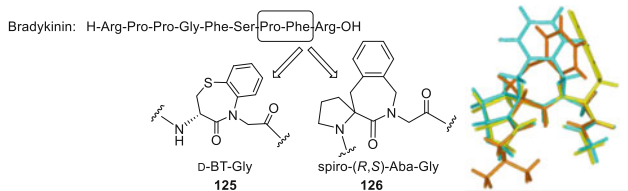


Fig. 24 *Spiro-(R,S)-Aba-Gly* as β -turn-inducing motif in bradykinin and overlap of Pro-Phe (yellow), *D*-BT-Gly (orange), and *spiro-(S)-Aba-Gly* (cyan) [106–109]

Among many biological roles, BK induces inflammation, antinociception, and vascular permeability through the activation of two receptors, B_1 and B_2 [103, 104]. ACE cleaves BK at the Pro⁷-Phe⁸ position. The cardioprotective effects of ACE inhibitors have thus been suggested to be due in part to their ability to prolong BK action [105]. Employment of ACE inhibitory motifs, such as *D*-BT-Gly {(*S*)-[3-amino-4-oxo-2,3-dihydro-5*H*-benzo[*b*][1,4]thiazepin-5-yl] acetic acid} to replace, respectively, the dipeptide residues Pro⁷-Phe⁸ and *D*-Tic⁷-Oic⁸ in BK and in the antagonist HOE 140 (H-*D*-Arg-Arg-Pro-Hyp-Gly-Thi-Ser-*D*-Tic-Oic-Arg-OH), produced potent and selective B_2 receptor ligands which turned out to be agonists [106, 107]. The high affinity of the *D*-BT-containing peptide agonists and demonstration that *D*-BT-Gly adopted a type II' β -turn led to the hypothesis that the latter geometry was important for potency at the B_2 receptor [108]. Structural resemblance (Fig. 24, right) between *D*-BT and *spiro*-Aba-Gly prompted insertion of the spirocyclic scaffold into BK analogue **126**, which in contrast to native BK, HOE 140, and their *D*-BT analogues, exhibited lower B_2 binding [only the (*S*)- and (*R*)-*spiro*-Aba-Gly analogues of HOE 140 produced ligands with K_i values of 3.2 and 25 nM, respectively] [109]. Moreover, switching from Pro-Phe or the *D*-BT moiety to spirocycle **126** gave antagonism. The different orientations (Fig. 24) of the aromatic rings in Phe, *D*-BT, and Aba may thus be important for receptor binding and BK agonist versus antagonist activity [109].

4.5 Somatostatin

Somatostatin (SRIF) is a cyclic 14-amino acid peptide with multiple functions, which are mediated by five subtypes of G protein-coupled receptors: sst₁₋₅. Somatostatin was shown to adopt a β -turn in the region Phe⁷-Trp⁸-Lys⁹-Thr¹⁰. The size of the peptide could be reduced to a cyclic octapeptide in the case of Sandostatin and to cyclic hexapeptides, such as Seglitide (MK678), which all contain a turn-stabilizing and potency-enhancing *D*-Trp⁸ residue [110]. Based on this β -turn pharmacophore model, many peptide mimetics have been prepared, albeit with typically micromolar activities. Potent and subtype selective peptide mimetics have been developed by Merck [111], including the potent and selective sst₂ ligand **L-054,522**, which contains the (2*R*,3*S*)- β -MeTrp residue (Fig. 26) [112]. Noting

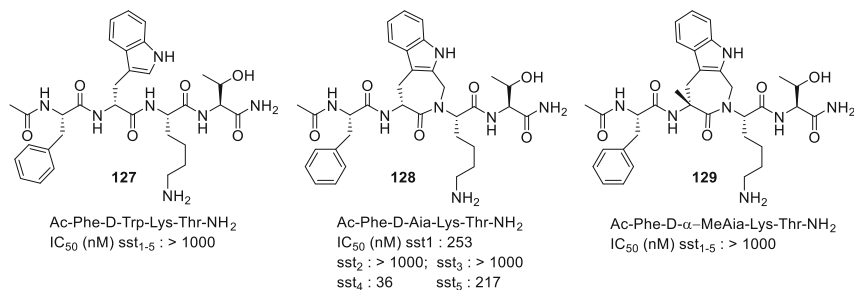


Fig. 25 Somatostatin tetrapeptides and their receptor subtype affinities

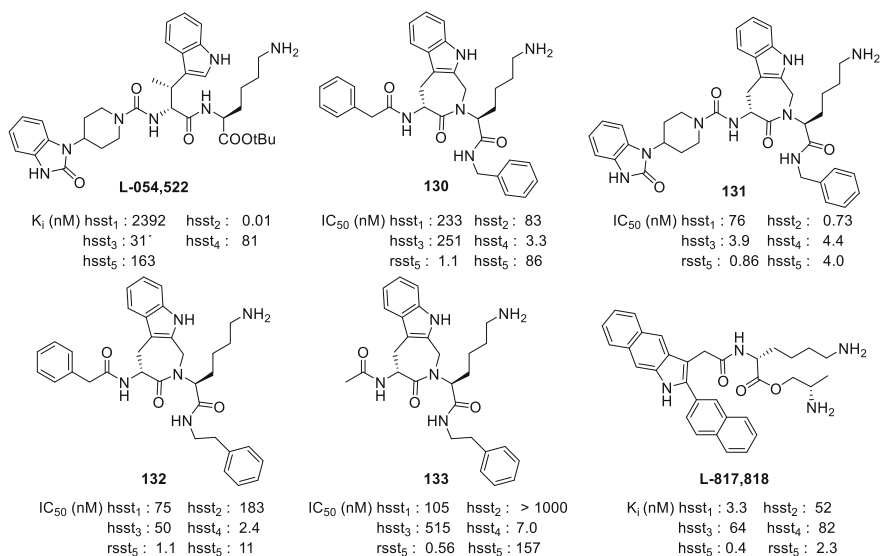


Fig. 26 Somatostatin mimetics and their receptor subtype affinities

that like Aia, (2*R*,3*S*)- β -MeTrp favored a *trans* ($\chi_1 = 180^\circ$) orientation of the D-Trp side chain [113], we replaced D-Trp in tetrapeptide **127** by D-Aia and converted the linear peptide, which did not show any affinity for sst₁₋₅, into ligand **128**, which had low affinity for sst₁ and sst₅ and exhibited a remarkable IC₅₀ of 36 nM for sst₄ (Fig. 25). As mentioned in Sect. 3, the related Aiba model tetrapeptides did not induce β -turn conformations, but their α -methyl analogues adopted turn conformers in solution phase and in the solid state [30, 31, 34]. Racemic α -Me-Aia was thus introduced into tetrapeptides **129**; however, neither epimer exhibited sst receptor affinity (Fig. 25). The α -methyl group may hinder receptor recognition [35].

Based on the results described above, the D-Aia-Lys core was used to prepare other somatostatin mimetics, such as α -*N*-phenylacetyl-D-Aia-Lys-NHBn (**130**, Fig. 26) that had 3.3 nM affinity for sst₄ and 1.1 nM affinity for sst₅ [114]. The subsequent preparation of a focused library using the D-Aia-Lys template with

various *N*- and *C*-substituents gave peptidomimetics with high affinity for different receptor subtypes, including agonist **133** with subnanomolar affinity for *sst*₅ [115]. Initially, *sst*₅ affinity of these mimetics was determined for the rat (*rsst*₅) receptor. Subsequent determination of the affinity for the human *sst*₅ (*hsst*₅) revealed interesting species selectivity. Our analogue **133** was much less potent for the human *sst*₅ in contrast to the Merck *sst*₅-selective **L-817,818** (Reubi JC, Feytens D, Tourwé D, Unpublished work). Hence, the Aia scaffold was used to identify potent-, subtype-, and species-selective peptidomimetics, as well as potent nonselective analogues.

4.6 Angiotensin IV

Angiotensin IV (AngIV, H-Val-Tyr-Ile-His-Pro-Phe-OH) is a metabolite of AngII that improves memory acquisition, inhibits seizures, and has vascular and renal actions. Proposed to interact specifically with the AT₄ receptor, the mechanism of AngIV activity remains unclear; however, AT₄ has also been identified as insulin-regulated aminopeptidase (IRAP). Moreover, AngIV interacts and may be degraded by aminopeptidase-N (AP-N) [116]. Using a β -homo-amino acid scan, we demonstrated that H-(*R*)- β^2 hVal-Tyr-Ile-His-Pro- β^3 hPhe-OH (**134**, AL-11) was a potent and stable AngIV analogue with high selectivity for IRAP versus AP-N and the AT₁ receptor (Fig. 27) [117]. Substitution of His⁴-Pro⁵ by the constrained dipeptides Ata-Gly, Aba-Gly, and Aia-Gly gave equipotent {e.g., [Ata⁴-Gly⁵] AngIV, **135**} [44] and more potent (**136–138**) IRAP ligands [118]. Interestingly, Aba-Gly analogue **136** showed affinity for the AT₁ receptor with a pK_i of 6.85,

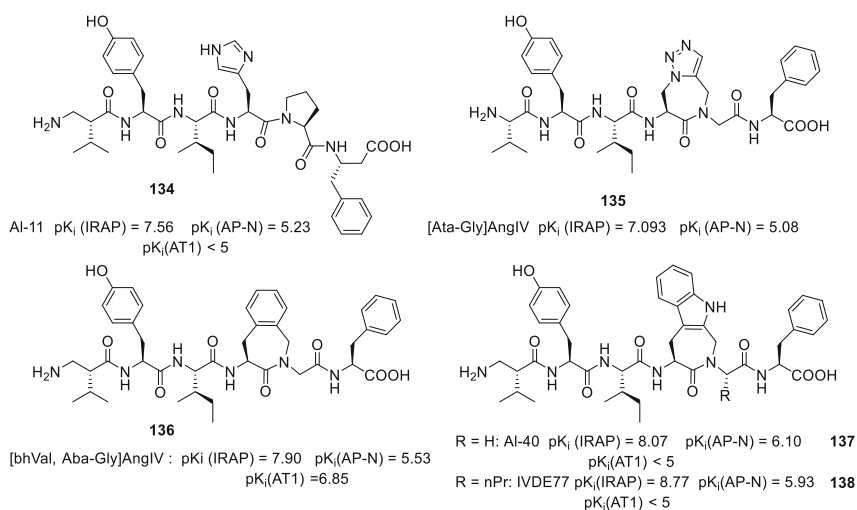


Fig. 27 Angiotensin analogue AL-11 (**134**) and constrained derivatives **135–138**

whereas Aia-Gly analogue **137** did not show any affinity up to a concentration of 10 μM . Therefore, the latter analogue, H-(*R*)- $\beta^2\text{hVal-Tyr-Ile-Aia-Gly-Phe-OH}$ (**137**, AL-40), was found to be the most potent and selective ligand of the series [118]. Substitution of Gly⁵ by Nva⁵ (norvaline) gave **138** (IVDE77), which is the most potent and selective AngIV analogue reported [119]. These results demonstrate the importance of having at hand various azepinone analogues to influence potency and selectivity in bioactive peptides.

4.7 α -Melanocyte-Stimulating Hormone (α -MSH)

The endogenous melanocortin peptides include the α -, β -, and γ -melanocyte-stimulating hormones (MSHs). Derived from posttranslational processing of the pro-opiomelanocortin (POMC) prehormone [120–123], MSHs play roles in a wide range of biological and physiological responses, such as feeding and learning behavior, sexual function, and energy homeostasis. The melanocortin peptides operate through interactions with the G protein-coupled melanocortin receptors (MCRs) in both the peripheral and central nervous system and activate the adenylate cyclase secondary messenger signal transduction cascade [120–123].

The macrocyclic lactam MT-II (Ac-Nle-c[Asp-His-D-Phe-Arg-Trp-Lys]-NH₂) proved to be a nonselective superagonist of human MC1R, MC3R, MC4R, and MC5R [124, 125]. To achieve receptor subtype selectivity, we replaced the His⁶-D-Phe⁷ dipeptide segment in MT-II by Aba-Xxx motifs (**140–142**, Fig. 28) [126]. Molecular modeling indicated backbone overlap of all Aba-containing analogues with the proposed conformation of MT-II [126]. Based on C ^{α} (i)–C ^{α} (i + 3) distances and the lack of proximity between the Asp⁵ carbonyl oxygen and the amide proton of Arg⁸, no β -turn conformation was adopted by these analogues. Gratifyingly, the cyclic lactam analogue **139** with the “Aba⁶-D-Phe⁷” motif proved to be a selective hMC3R antagonist (IC₅₀ of 50 nM at hMC3R). The linear Aba analogue of MT-II (e.g., **139**, Fig. 28) was insufficient at inducing binding up to concentrations of 10 μM , suggesting that MCR ligands with Aba building blocks needed a global conformational constraint [126] (Fig. 29).

Selective linear tetrapeptide MCR ligands with agonist and antagonist activity were identified by the group of Haskell-Luevano by studying various aromatic amino acid surrogates of the D-Phe residue in the sequence Ac-His-D-Phe-Arg-Trp-NH₂ [127, 128]. These observations persuaded us to replace the His residue in the minimal α -MSH pharmacophore – His⁶-Phe⁷-Arg⁸-Trp⁹ – domain by the Aba, Aia, and Ata dipeptidomimetics to evaluate their influence on receptor selectivity and agonist versus antagonist activity [129].

Introduction of the Aia-D-Phe dipeptide mimetic in **143** resulted in weak micromolar antagonist affinity for the hMC1R, allosteric partial agonist activity at hMC3R (EC₅₀ = 52 nM) and hMC4R (EC₅₀ = 0.3 nM), and moderate antagonist activity at the hMC5R. Fluorination of the *para*-position in D-Phe⁷ in **144** led to

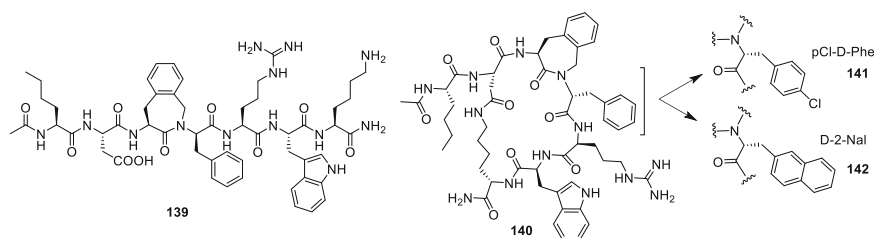


Fig. 28 Linear analogue **139** and cyclic [Aba]MT-II analogues **140–142** [126]

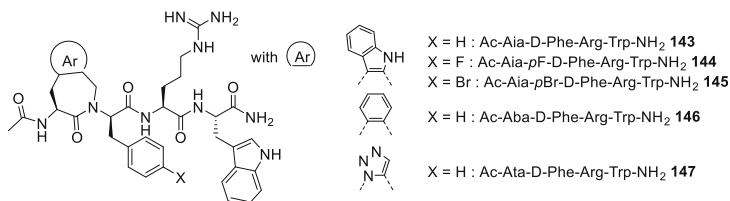


Fig. 29 Constrained melanocortin tetrapeptides **143–147**

enhanced activity, which was most pronounced at *h*MC4R ($IC_{50} = 6.5$ nM; $EC_{50} = 13$ nM, full agonist). In contrast to the *Aia-pF-D-Phe*⁷ tetrapeptide **144**, but similar to **143**, *Aia-pBr-D-Phe*⁷ tetrapeptide **145** gave potent allosteric partial agonist activity at *h*MC4R ($EC_{50} = 0.3$ nM and 80% activity). These affinities reflect the importance of the presence and nature (i.e., van der Waals radius) of the halogen substituent. The *Aba-D-Phe* analogue **146** proved to be a selective antagonist for *h*MC5R ($IC_{50} = 37$ nM), rendering it an ideal template for investigation of *h*MC5R antagonism. Contrary to the *Aia* and *Aba* analogues, the *Ata-D-Phe* analogue **147** showed no specific subtype receptor selectivity. Peptides **144** and **146** were docked into the active state model of *h*MC4R proposed by Mosberg et al. [130]. In comparisons with the earlier proposed binding mode of the His⁶-D-Phe⁷-Arg⁸-Trp⁹ pharmacophore of [Nle⁴,D-Phe⁷]- α -MSH [130], the residues of peptides **144** and **146** interacted less deeply in the binding site. Furthermore, the *pF-D-Phe* residue in peptide **144** was predicted to make contact with more residues of *h*MC4R than *D-Phe* in peptide **146**, which may account for favorable conformational changes to induce agonist activity. Hence, the insertion of constrained aminobenzo- and indoloazepinone-based residues into the core of melanocortin tetrapeptides has resulted in compact and selective human melanocortin receptor ligands with diverse and interesting pharmacological profiles.

5 Conclusion

Versatile synthetic schemes were developed allowing the rapid synthesis of azepinone-constrained analogues of Phe, Tyr, Trp, His, and Nal. These analogues have been demonstrated to give highly potent, selective, and metabolically stable peptides and peptide mimetics. The availability of a diverse set of azepinone-constrained amino acids is important in peptide drug design, because different analogues gave better results contingent on receptor: Aba gave the best results in opioids and NK-1 ligands, and Aia proved to be superior for AngIV and somatostatin ligands. Efforts to obtain diversity in these fused aromatic/heterocyclic systems were validated, because agonist vs. antagonist activity could be modulated by variation of the substitution pattern, stereochemistry, and aromatic residue in the amino-azepinone building blocks (e.g., melanocortin and opioid peptide examples). Finally, amino-azepinones with α -carbon substituents (e.g., α -Me-Aba and *spiro*-Aba analogues) proved to be reverse turn inducers.

References

1. Kessler H (1982) Conformation and biological activity of cyclic peptides. *Angew Chem Int Ed* 21(7):512–523
2. Kazmierski W, Hruby VJ (1988) A new approach to receptor ligand design: synthesis and conformation of a new class of potent and highly selective μ opioid antagonists utilizing tetrahydroisoquinoline carboxylic acid. *Tetrahedron* 44(3):697–710
3. Bryant SD, Jinsmaa Y, Salvadori S et al (2003) Dmt and opioid peptides: a potent alliance. *Biopolymers* 71(2):86–102
4. Tourwe D, Verschueren K, Frycia A et al (1996) Conformational restriction of Tyr and Phe side-chain in opioid peptides: information about preferred and bioactive side-chain topology. *Biopolymers* 38:1–12
5. Wu H, Wacker D, Mileni M et al (2012) Structure of the human kappa-opioid receptor in complex with JD1c. *Nature* 485(7398):327–332
6. Schiller PW, Nguyen TM, Weltrowska G et al (1992) Differential stereochemical requirements of μ vs. δ opioid receptors for ligand binding and signal transduction: development of a class of potent and highly δ -selective peptide antagonists. *Proc Natl Acad Sci* 89(24):11871–11875
7. Freidinger RM, Veber DF, Perlow DS et al (1980) Bioactive conformation of luteinizing hormone-releasing hormone: evidence from a conformationally constrained analog. *Science* 210(4470):656–658
8. Perdih A, Kikelj D (2006) The application of Freidinger lactams and their analogs in the design of conformationally constrained peptidomimetics. *Curr Med Chem* 13(13):1525–1556
9. Flynn GA, Beight DW (1989) Novel antihypertensive agent. European Patent 0249224
10. de Laszlo SE, Bush BL, Doyle JJ et al (1992) Synthesis and use of 3-amino-4-phenyl-2-piperidones and 4-amino-2-benzazepin-3-ones as conformationally restricted phenylalanine isosteres in renin inhibitors. *J Med Chem* 35(5):833–846
11. Casimir JR, Guichard G, Briand J-P (2002) Methyl 2-((succinimidooxy)carbonyl)benzoate (MSB): a new, efficient reagent for N-phthaloylation of amino acid and peptide derivatives. *J Org Chem* 67(11):3764–3768

12. Ilisz I, Ballet S, Van Rompaey K et al (2007) High-performance liquid chromatographic separation of stereoisomers of *N*-phthaloyl-protected amino acids and dipeptidomimetics. *J Sep Sci* 30(12):1881–1887
13. Severino B, Fiorino F, Esposito A et al (2009) Efficient microwave-assisted synthesis of 4-amino-2-benzazepin-3-ones as conformationally restricted dipeptide mimetics. *Tetrahedron* 65(1):206–211
14. Ballet S, Frycia A, Piron J et al (2005) Synthesis and biological evaluation of constrained analogues of the opioid peptide H-Tyr-D-Ala-Phe-Gly-NH₂ using 4-amino-2-benzazepin-3-one scaffold. *J Pept Res* 66:222–230
15. Tourwe D, Verschuere K, Van Binst G et al (1992) Dermorphin sequence with high delta-affinity by fixing the Phe side-chain to trans at alpha-1. *Bioorg Med Chem Lett* 2:1305–1308
16. De Wachter R, de Graaf C, Keresztes A et al (2011) Synthesis, biological evaluation, and automated docking of constrained analogues of the opioid peptide H-Dmt-D-Ala-Phe-Gly-NH₂ using the 4- or 5-methyl substituted 4-amino-1,2,4,5-tetrahydro-2-benzazepin-3-one scaffold. *J Med Chem* 54(19):6538–6547
17. Casimir JR, Tourwé D, Iterbeke K et al (2000) Efficient synthesis of (*S*)-4-phthalimido-1,3,4,5-tetrahydro-8-(2,6-dichlorobenzoyloxy)-3-oxo-2*H*-2-benzazepin-2-acetic acid (Pht-Hba(2,6-Cl₂-Bn)-Gly-OH). *J Org Chem* 65(20):6487–6492
18. Ruzza P, Calderan A, Donella-Deana A et al (2003) Conformational constraints of tyrosine in protein tyrosine kinase substrates: information about preferred bioactive side-chain orientation. *Biopolymers* 71(4):478–488
19. Flynn GA, Burkholder TP, Huber EW et al (1991) An acyliminium ion route to Cis and Trans “Anti” Phe-Gly dipeptide mimetics. *Bioorg Med Chem Lett* 1(6):309–312
20. Rabi-Barakay A, Ben-Ishai D (1994) Intramolecular amidalkylation of aromatics III. Synthesis of conformationally restricted bridged peptide analogues of Phe-Gly. *Tetrahedron* 50(36):10771–10782
21. Katritzky AR, Manju K, Singh SK et al (2005) Benzotriazole mediated amino-, amido-, alkoxy- and alkylthio-alkylation. *Tetrahedron* 61(10):2555–2581
22. Ballet S, Urbanczyk-Lipkowska Z, Tourwé D (2005) Synthesis of substituted 4-amino-2-benzazepin-3-ones via *N*-acyliminium ion cycliations. *Synlett* 18:2791–2795
23. Ballet S, De Wachter R, Maes BUW et al (2007) Derivatization of 1-phenyl substituted 4-amino-2-benzazepin-3-ones: evaluation of Pd-catalyzed coupling reactions. *Tetrahedron* 63(18):3718–3727
24. Warshawsky AM, Flynn GA, Koehl JR et al (1996) The synthesis of aminobenzazepinones as anti-phenylalanine dipeptide mimics and their use in NEP inhibition. *Bioorg Med Chem Lett* 6(8):957–962
25. Van Rompaey K, Van den Eynde I, De Kimpe N et al (2003) A versatile synthesis of 2-substituted 4-amino-1,2,4,5-tetrahydro-2-benzazepine-3-ones. *Tetrahedron* 59(24):4421–4432
26. Van den Eynde I, Van Rompaey K, Lazzaro F et al (2004) Solid-supported solution-phase synthesis of 4-amino-1,2,4,5-tetrahydro-2-benzazepine-3-ones. *J Comb Chem* 6(4):468–473
27. Guillemyn K, Kleczkowska P, Lesniak A et al (2015) Synthesis and biological evaluation of compact, conformationally constrained bifunctional opioid agonist – neurokinin-1 antagonist peptidomimetics. *Eur J Med Chem* 92:64–77
28. Robl JA, Sun CQ (2001) Processes and intermediates for preparing benzo-fused azepinone and piperidinone compounds useful in the inhibition of ACE and NEP. US Patent 6,6235,922
29. Sedighi M, Çalimsiz S, Lipton MA (2006) An improved method for the protection of carboxylic acids as 1,1-dimethylallyl esters. *J Org Chem* 71(25):9517–9518
30. De Wachter R, Brans L, Ballet S et al (2009) Influence of ring substitution on the conformation and β -turn mimicry of 4-amino-1,2,4,5-tetrahydro-2-benzazepin-3-one peptide mimetics. *Tetrahedron* 65(11):2266–2278

31. Vandormael B, De Wachter R, Martins JC et al (2011) Asymmetric synthesis and conformational analysis by NMR spectroscopy and MD of Aba- and alpha-MeAba-containing dermorphin analogues. *ChemMedChem* 6(11):2035–2047
32. Vandormael B (2011) Ph.D. thesis, Vrije Universiteit Brussel, Brussels
33. Tömböly C, Ballet S, Feytens D et al (2008) Endomorphin-2 with a β -turn backbone constraint retains the potent μ -opioid receptor agonist properties. *J Med Chem* 51(1):173–177
34. Van Rompaey K, Ballet S, Tömböly C et al (2006) Synthesis and evaluation of the β -turn properties of 4-amino-1,2,4,5-tetrahydro-2-benzazepin-3-ones and of their spirocyclic derivative. *Eur J Med Chem* 2006(13):2899–2911
35. Feytens D (2009) Ph.D. thesis, Vrije Universiteit Brussel, Brussels
36. Podlech J (2002) In: Goodman M, Felix A, Moroder L, Toniolo C (eds) *Methods of organic chemistry (Houben-Weyl): synthesis of peptides and peptidomimetics*. George Thieme Verlag, Stuttgart/New York, p 141
37. Pulka K, Feytens D, Van den Eynde I et al (2007) Synthesis of 4-amino-3-oxo-tetrahydroazepino[3,4-*b*]indoles: new conformationally constrained Trp analogs. *Tetrahedron* 63(6):1459–1466
38. Feytens D, De Vlaeminck M, Tourwe D (2009) A novel solid phase approach to Aia-containing peptides. *J Pept Sci* 15(1):16–22
39. Jida M, Betti C, Urbanczyk-Lipkowska Z et al (2013) Highly diastereoselective synthesis of 1-carbamoyl-4-aminoindoloazepinone derivatives via the Ugi reaction. *Org Lett* 15(22):5866–5869
40. Domling A (2006) Recent developments in isocyanide based multicomponent reactions in applied chemistry. *Chem Rev* 106(1):17–89
41. Koopmanschap G, Ruijter E, Orru RV (2014) Isocyanide-based multicomponent reactions towards cyclic constrained peptidomimetics. *Beilstein J Org Chem* 10:544–598
42. Angell YL, Burgess K (2007) Peptidomimetics via copper-catalyzed azide-alkyne cycloadditions. *Chem Soc Rev* 36(10):1674–1689
43. Pedersen DS, Abell A (2011) 1,2,3-Triazoles in peptidomimetic chemistry. *Eur J Org Chem* 2011(13):2399–2411
44. Buysse K, Farard J, Nikolaou A et al (2011) Amino triazolo diazepines (Ata) as constrained histidine mimics. *Org Lett* 13(24):6468–6471
45. Han S-Y, Kim Y-A (2004) Recent development of peptide coupling reagents in organic synthesis. *Tetrahedron* 60(11):2447–2467
46. Snieckus V, Singh SP (2014) Synthesis of aminotriazoloazepinone-containing di- and tripeptides. *Synfacts* 10(11):1132–1132
47. Hulme C, Gore V (2003) “Multi-component reactions: emerging chemistry in drug discovery” ‘from xylocain to crixivan’. *Curr Med Chem* 10(1):51–80
48. Barlow TMA, Jida M, Tourwe D et al (2014) Efficient synthesis of conformationally constrained, amino-triazoloazepinone-containing di- and tripeptides via a one-pot Ugi-Huisgen tandem reaction. *Org Biomol Chem* 12(36):6986–6989
49. Schurgers B, Brigou B, Urbanczyk-Lipkowska Z et al (2014) Synthesis of fused 3-aminoazepinones via trapping of a new class of cyclic seven-membered allenamides with furan. *Org Lett* 16(14):3712–3715
50. De Matteis V, van Delft FL, de Gelder R et al (2004) Fluorinated (hetero)cycles via ring-closing metathesis of fluoride- and trifluoromethyl-functionalized olefins. *Tetrahedron Lett* 45(5):959–963
51. Chao W, Weinreb SM (2003) The first examples of ring-closing olefin metathesis of vinyl chlorides. *Org Lett* 5(14):2505–2507
52. Kirkland TA, Grubbs RH (1997) Effects of olefin substitution on the ring-closing metathesis of dienes. *J Org Chem* 62(21):7310–7318
53. Paone DV, Shaw AW, Nguyen DN et al (2007) Potent, orally bioavailable calcitonin gene-related peptide receptor antagonists for the treatment of migraine: discovery of *N*-[(3*R*,6*S*)-6-(2,3-Difluorophenyl)-2-oxo-1-(2,2,2-trifluoroethyl)azepan-3-yl]-4-(2-oxo-2,3-dihydro-1*H*-

- imidazo[4,5-*b*]pyridin- 1-yl)piperidine-1-carboxamide (MK-0974). *J Med Chem* 50(23): 5564–5567
54. Schurgers B, Van Lommen G, Verniest G (2015) Synthesis and selective N, O-functionalization of pyrazolone-fused 3-aminoazepinones. *Eur J Org Chem* 2015(16):3572–3576
 55. Tanaka H, Kameyama Y, Sumida S-I et al (1991) A new short cut route to 3-norcephalosporins. *Synlett* 1991(12):888–890
 56. Farina V, Kant J (1992) A new strategy for the conversion of penams into cephems via allene chemistry. *Tetrahedron Lett* 33(25):3559–3562
 57. Piperno A, Rescifina A, Corsaro A et al (2007) A novel class of modified nucleosides: synthesis of alkylidene isoxazolidinyl nucleosides containing thymine. *Eur J Org Chem* 2007(9):1517–1521
 58. Cheng G, Hu Y (2007) One-pot synthesis of furocoumarins through cascade addition-cyclization-oxidation. *Chem Commun* 31:3285–3287
 59. Zimmermann D, Krogsgaard-Larsen P, Ehrhardt J-D et al (1998) Unambiguous synthesis of 1-methyl-3-hydroxypyrazoles. *Tetrahedron* 54(32):9393–9400
 60. Cottineau B, Toto P, Marot C et al (2002) Synthesis and hypoglycemic evaluation of substituted pyrazole-4-carboxylic acids. *Bioorg Med Chem Lett* 12(16):2105–2108
 61. Holzer W, Kautsch C, Laggner C et al (2004) On the tautomerism of pyrazolones: the geminal 2/*J*[pyrazole C-4, H-3(5)] spin coupling constant as a diagnostic tool. *Tetrahedron* 60(32):6791–6805
 62. Patel MV, Bell R, Majest S et al (2004) Synthesis of 4,5-diaryl-1*H*-pyrazole-3-ol derivatives as potential COX-2 inhibitors. *J Org Chem* 69(21):7058–7065
 63. Zhang Y, Benmohamed R, Huang H et al (2013) Arylazanylpyrazolone derivatives as inhibitors of mutant superoxide dismutase 1 dependent protein aggregation for the treatment of amyotrophic lateral sclerosis. *J Med Chem* 56(6):2665–2675
 64. Piscopio AD, Miller JF, Koch K (1999) Ring closing metathesis in organic synthesis: evolution of a high speed, solid phase method for the preparation of β -turn mimetics. *Tetrahedron* 55(27):8189–8198
 65. Hoffmann T, Waibel R, Gmeiner P (2003) A general approach to dehydro-Freidinger lactams: ex-chiral pool synthesis and spectroscopic evaluation as potential reverse turn inducers. *J Org Chem* 68(1):62–69
 66. Flynn GA, Giroux EL, Dage RC (1987) An acyl-iminium ion cyclization route to a novel conformationally restricted dipeptide mimic: applications to angiotensin-converting enzyme inhibition. *J Am Chem Soc* 109(25):7914–7915
 67. Thaisrivongs S, Pals DT, Harris DW et al (1986) Design and synthesis of a potent and specific renin inhibitor with a prolonged duration of action in vivo. *J Med Chem* 29(10):2088–2093
 68. Montecucchi PC, de Castiglione R, Piani S et al (1981) Amino acid composition and sequence of dermorphin, a novel opiate-like peptide from the skin of *Phyllomedusa sauvagei*. *Int J Pept Protein Res* 17(3):275–283
 69. Melchiorri P, Negri L (1996) The dermorphin peptide family. *Gen Pharmacol* 27:1099–1107
 70. Ballet S, Misicka A, Kosson P et al (2008) Blood-brain barrier penetration by two dermorphin tetrapeptide analogues: role of lipophilicity vs structural flexibility. *J Med Chem* 51(8): 2571–2574
 71. Vandormael B, Fourla D-D, Gramowski-Voß A et al (2011) Superpotent [Dmt¹]Dermorphin tetrapeptides containing the 4-aminotetrahydro-2-benzazepin-3-one scaffold with mixed μ/δ opioid receptor agonistic properties. *J Med Chem* 54(22):7848–7859
 72. Novoa A, Van Dorpe S, Wynendaele E et al (2012) Variation of the net charge, lipophilicity, and side chain flexibility in Dmt¹-DALDA: effect on opioid activity and biodistribution. *J Med Chem* 55(22):9549–9561
 73. Misicka A, Lipkowski AW, Horvath R et al (1992) Topographical requirements for delta opioid ligands: common structural features of dermenkephalin and deltorphin. *Life Sci* 51(13):1025–1032

74. Schiller PW, Fundytus ME, Merovitz L et al (1999) The opioid μ agonist/ δ antagonist DIPP-NH₂[Ψ] produces a potent analgesic effect, no physical dependence, and less tolerance than morphine in rats. *J Med Chem* 42(18):3520–3526
75. Okada Y, Tsuda Y, Fujita Y et al (2003) Unique high-affinity synthetic μ -opioid receptor agonists with central- and systemic-mediated analgesia. *J Med Chem* 46(15):3201–3209
76. Hansen D, Stapelfeld A, Savage M et al (1992) Systemic analgesic activity and delta-opioid selectivity in [2,6-dimethyl-Tyr¹, D-Pen², D-Pen³]enkephalin. *J Med Chem* 35:684–687
77. Schiller P, Nguyen T, Berezowska I et al (2000) Synthesis and in vitro opioid activity profiles of DALDA analogues. *Eur J Med Chem* 35:895–901
78. Szeto HH, Lovelace JL, Fridland G et al (2001) In vivo pharmacokinetics of selective mu-opioid peptide agonists. *J Pharmacol Exp Ther* 298(1):57–61
79. Guillemyn K, Kleczkowska P, Novoa A et al (2012) In vivo antinociception of potent mu opioid agonist tetrapeptide analogues and comparison with a compact opioid agonist - neurokinin 1 receptor antagonist chimera. *Mol Brain* 5(1):4
80. Zadina JE, Hackler L, Ge L-J et al (1997) A potent and selective endogenous agonist for the μ -opiate receptor. *Nature* 386(6624):499–502
81. Wilkes BC, Nguyen TM, Weltrowska G et al (1998) The receptor-bound conformation of H-Tyr-Tic-(Phe-Phe)-OH-related δ -opioid antagonists contains all trans peptide bonds. *J Pept Res* 51(5):386–394
82. Lazarus LH, Bryant SD, Cooper PS et al (1998) Design of δ -opioid peptide antagonists for emerging drug applications. *Drug Discov Today* 3(6):284–294
83. Salvadori S, Attila M, Balboni G et al (1995) Delta opioidmimetic antagonists: prototypes for designing a new generation of ultrasensitive opioid peptides. *Mol Med* 1(6):678–689
84. Van den Eynde I, Laus G, Schiller PW et al (2005) A new structural motif for μ -opioid antagonists. *J Med Chem* 48(10):3644–3648
85. Ballet S, Feytens D, Wachter RD et al (2009) Conformationally constrained opioid ligands: the Dmt-Aba and Dmt-Aia versus Dmt-Tic scaffold. *Bioorg Med Chem Lett* 19(2):433–437
86. Ballet S, Marczak ED, Feytens D et al (2010) Novel multiple opioid ligands based on 4-aminobenzazepinone (Aba), azepinoindole (Aia) and tetrahydroisoquinoline (Tic) scaffolds. *Bioorg Med Chem Lett* 20(5):1610–1613
87. King T, Gardell L, Wang R et al (2005) Role of NK-1 neurotransmission in opioid-induced hyperalgesia. *Pain* 116:276–288
88. Yamamoto T, Nair P, Jacobsen N et al (2010) Biological and conformational evaluation of bifunctional compounds for opioid receptor agonists and neurokinin 1 receptor antagonists possessing two penicillamines. *J Med Chem* 53:5491–5501
89. Morphy R, Rankovic Z (2005) Designed multiple ligands. An emerging drug discovery paradigm. *J Med Chem* 48:6523–6543
90. Morphy R, Rankovic Z (2010) Design of multitarget ligands. In: Lead generation approaches in drug discovery. Wiley, Hoboken, pp 141–164
91. Fujii H (2011) Twin and triplet drugs in opioid research. *Top Curr Chem* 299:239–275
92. Kleczkowska P, Lipkowski AW, Tourwe D et al (2013) Hybrid opioid/non-opioid ligands in pain research. *Curr Pharm Des* 19(42):7435–7450
93. Lipkowski AW (1987) Cooperative reinforcement of opioid pharmacophores. *Pol J Pharmacol Pharm* 39:585–596
94. Lipkowski AW, Carr DB, Misicka A et al (1994) Biological activities of a peptide containing both casomorphin-like and substance P antagonist structural characteristics. In: Brantl V, Teschemacher H (eds) B-casomorphins and related peptides: recent developments. VCH, Weinheim, pp 113–118
95. Bonney IM, Foran SE, Marchand JE et al (2004) Spinal antinociceptive effects of AA501, a novel chimeric peptide with opioid receptor agonist and tachykinin receptor antagonist moieties. *Eur J Pharmacol* 488(1–3):91–99
96. Foran SE, Carr DB, Lipkowski AW et al (2000) A substance P-opioid chimeric peptide as a unique nontolerance-forming analgesic. *Proc Natl Acad Sci* 97(13):7621–7626

97. Yamamoto T, Nair P, Davis P et al (2007) Design, synthesis, and biological evaluation of novel bifunctional C-terminal-modified peptides for δ/μ opioid receptor agonists and neurokinin-1 receptor antagonists. *J Med Chem* 50(12):2779–2786
98. Yamamoto T, Nair P, Vagner J et al (2008) A structure–activity relationship study and combinatorial synthetic approach of C-terminal modified bifunctional peptides that are δ/μ opioid receptor agonists and neurokinin 1 receptor antagonists. *J Med Chem* 51(5):1369–1376
99. Costantino L, Barlocco D (2012) Designed multiple ligands: basic research vs clinical outcomes. *Curr Med Chem* 19(20):3353–3387
100. Gentilucci L (2004) New trends in the development of opioid peptide analogues as advanced remedies for pain relief. *Curr Top Med Chem* 4:19–38
101. Ballet S, Feytens D, Buysse K et al (2011) Design of novel neurokinin 1 receptor antagonists based on conformationally constrained aromatic amino acids and discovery of a potent chimeric opioid agonist-neurokinin 1 receptor antagonist. *J Med Chem* 54:2467–2476
102. Armour DR, Aston NM, Morriss KML et al (1997) 1,4-Benzodiazepin-2-one derived neurokinin-1 receptor antagonists. *Bioorg Med Chem Lett* 7(15):2037–2042
103. Reissmann S, Pineda F, Vietinghoff G et al (2000) Structure activity relationships for bradykinin antagonists on the inhibition of cytokine release and the release of histamine. *Peptides* 21(4):527–533
104. Bock MG, Longmore J (2000) Bradykinin antagonists: new opportunities. *Curr Opin Chem Biol* 4(4):401–406
105. Martorana PA, Kettenbach B, Breipohl G et al (1990) Reduction of infarct size by local angiotensin-converting enzyme inhibition is abolished by a bradykinin antagonist. *Eur J Pharmacol* 182(2):395–396
106. Amblard M, Daffix I, Bedos P et al (1999) Design and synthesis of potent bradykinin agonists containing a benzothiazepine moiety. *J Med Chem* 42(20):4185–4192
107. Amblard M, Daffix I, Bergé G et al (1999) Synthesis and characterization of bradykinin B2 receptor agonists containing constrained dipeptide mimics. *J Med Chem* 42(20):4193–4201
108. Amblard M, Raynal N, Averlant-Petit M-C et al (2005) Structural elucidation of the β -turn inducing (*S*)-[3-amino-4-oxo-2,3-dihydro-5*H*-benzo[*b*][1,4]thiazepin-5-yl] acetic acid (DBT) motif. *Tetrahedron Lett* 46(21):3733–3735
109. Ballet S, De Wachter R, Van Rompaey K et al (2007) Bradykinin analogs containing the 4-amino-2-benzazepin-3-one scaffold at the C-terminus. *J Pept Sci* 13(3):164–170
110. Janecka A, Zubrzycka M, Janecki T (2001) Somatostatin analogs. *J Pept Res* 58(2):91–107
111. Rohrer SP, Birzin ET, Mosley RT et al (1998) Rapid identification of subtype-selective agonists of the somatostatin receptor through combinatorial chemistry. *Science* 282(5389):737–740
112. Yang L, Berk SC, Rohrer SP et al (1998) Synthesis and biological activities of potent peptidomimetics selective for somatostatin receptor subtype 2. *Proc Natl Acad Sci* 95(18):10836–10841
113. Moore SB, Grant M, Rew Y et al (2005) Synthesis and biologic activity of conformationally constrained analogs of L-363,301. *J Pept Res* 66(6):404–422
114. Feytens D, Cescato R, Reubi JC et al (2007) New sst4/5-selective somatostatin peptidomimetics based on a constrained tryptophan scaffold. *J Med Chem* 50(14):3397–3401
115. Feytens D, De Vlaeminck M, Cescato R et al (2009) Highly potent 4-amino-indolo[2,3-*c*]azepin-3-one-containing somatostatin mimetics with a range of sst receptor selectivities. *J Med Chem* 52(1):95–104
116. Chai SY, Fernando R, Peck G et al (2004) The angiotensin IV/AT4 receptor. *Cell Mol Life Sci* 61(21):2728–2737
117. Lukaszuk A, Demaegdt H, Szemenyei E et al (2008) Beta-homo-amino acid scan of angiotensin IV. *J Med Chem* 51(7):2291–2296

118. Lukaszuk A, Demaegd H, Feytens D et al (2009) The replacement of His(4) in angiotensin IV by conformationally constrained residues provides highly potent and selective analogues. *J Med Chem* 52(18):5612–5618
119. Nikolaou A, Van den Eynde I, Tourwe D et al (2013) [³H]IVDE77, a novel radioligand with high affinity and selectivity for the insulin-regulated aminopeptidase. *Eur J Pharmacol* 702(1–3):93–102
120. Hruby VJ, Wilkes BC, Cody WL et al (1984) Melanotropins: structural, conformational and biological considerations in the development of superpotent and superprolonged analogues. *Pept Protein Rev* 3:1–64
121. Cone RD, Lu D, Koppula S et al (1996) The melanocortin receptors: agonists, antagonists, and the hormonal control of pigmentation. *Recent Prog Horm Res* 51:287–317
122. Fan W, Boston BA, Kesterson RA et al (1997) Role of melanocortineric neurons in feeding and the agouti obesity syndrome. *Nature* 385(6612):165–168
123. Huszar D, Lynch CA, Fairchild-Huntress V et al (1997) Targeted disruption of the melanocortin-4 receptor results in obesity in mice. *Cell* 88(1):131–141
124. Al-Obeidi F, Castrucci AM, Hadley ME et al (1989) Potent and prolonged acting cyclic lactam analogues of alpha-melanotropin: design based on molecular dynamics. *J Med Chem* 32(12):2555–2561
125. Al-Obeidi F, Hadley ME, Pettitt BM et al (1989) Design of a new class of superpotent cyclic alpha-melanotropins based on quenched dynamic simulations. *J Am Chem Soc* 111(9):3413–3416
126. Ballet S, Mayorov AV, Cai M et al (2007) Novel selective human melanocortin-3 receptor ligands: use of the 4-amino-1,2,4,5-tetrahydro-2-benzazepin-3-one (Aba) scaffold. *Bioorg Med Chem Lett* 17(9):2492–2498
127. Proneth B, Pogozheva ID, Portillo FP et al (2008) Melanocortin tetrapeptide Ac-His-DPhe-Arg-Trp-NH₂ modified at the para position of the benzyl side chain (DPhe): importance for mouse melanocortin-3 receptor agonist versus antagonist activity. *J Med Chem* 51(18):5585–5593
128. Holder JR, Bauzo RM, Xiang Z et al (2002) Structure–activity relationships of the melanocortin tetrapeptide Ac-His-DPhe-Arg-Trp-NH₂ at the mouse melanocortin receptors: part 2 modifications at the Phe position. *J Med Chem* 45(14):3073–3081
129. Van der Poorten O, Feher K, Buysse K et al (2015) Azepinone-containing tetrapeptide analogues of melanotropin lead to selective hMC4R agonists and hMC5R antagonist (2015) *ACS Med Chem Lett* 6(2):192–197
130. Pogozheva ID, Chai BX, Lomize AL et al (2005) Interactions of human melanocortin 4 receptor with nonpeptide and peptide agonists. *Biochemistry* 44(34):11329–11341

Polyhydroxylated Cyclic Delta Amino Acids: Synthesis and Conformational Influences on Biopolymers

André Wuttke and Armin Geyer

Abstract This review is dedicated to the fitting and functional characterization of polyhydroxylated amino acids into protein environments, noting that systematic compendia of sugar-derived unnatural building blocks can be found in the literature. This review is focused on the local exchange of two sequential amino acids in a peptide or protein for a polyhydroxylated δ -amino acid in various applications ranging from ligand design to the investigation of protein function. Two general strategies are respectively differentiated that delete and retain the peptide backbone. So-called sugar amino acids (SAAs) exchange one peptide bond for a tetrahydropyran or furan ring. Alternatively, polyhydroxylated bicyclic dipeptides encompass an amide bond within their ring system and become integral parts of the peptide backbone (compare SAA and Xaa = Yaa in Fig. 1). In peptides, these polyhydroxylated ring systems may favor turn and loop conformations, modify polarity, and offer handles for ligation methods. The influence of ring substituents on these heterocycles is discussed with respect to their potential to increase the stability of particular conformations with preferred orientations as well as to mediate supramolecular interactions. In addition, examples of the use of polyhydroxylated ring systems to stabilize standalone peptide hairpins and mediate protein–protein interactions will be presented.

Keywords Amino acids · Bicyclic lactams · Peptides · Sugar amino acids

A. Wuttke and A. Geyer (✉)
Fachbereich Chemie, Philipps-Universität Marburg, Hans-Meerwein-Strasse, 35032 Marburg,
Germany
e-mail: geyer@staff.uni-marburg.de

Contents

1	Introduction	212
1.1	Hydroxylated Amino Acids in Nature	213
1.2	Conformational Properties of Hydroxy Amino Acids	215
2	Sugar Amino Acids	215
3	Peptide Constraints Using Lactams, 6,5-Bicyclic Lactams, and Polyhydroxylated Lactams	220
3.1	Lactams and 6,5-Bicyclic Lactams	220
3.2	Polyhydroxylated Lactams	221
4	Synthesis of Polyhydroxylated Bicyclic Lactams	227
4.1	Synthesis of Polyhydroxylated 6,5-Bicyclic Lactam	227
4.2	Synthesis of Polyhydroxylated 7,5-Bicyclic Lactams	228
5	Conclusion	231
	References	231

1 Introduction

Sequence-specific polymers are characterized by an order of building blocks, which matches a characteristic reading frame. The six-atom repeat is a common feature of all three classes of primary biopolymers, the polynucleotides, the proteins, and polysaccharides (e.g., 2,8- α -polysialic acid, Fig. 1). In DNA, the base pair elements for molecular recognition are physically separated from the (deoxy)ribonucleotide

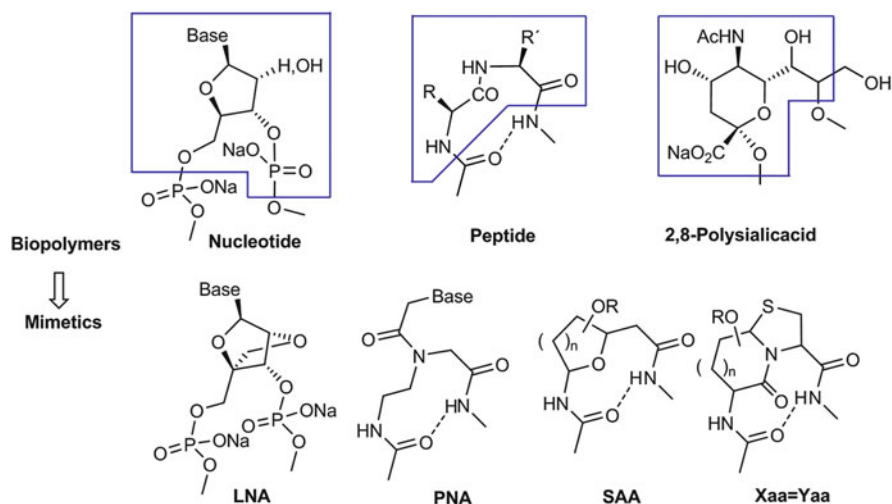


Fig. 1 The six-atom repeats of the three primary biopolymers – DNA, proteins, and carbohydrates – are highlighted by blue boxes. Oligonucleotide and peptide mimetics should preserve the six-atom register. The locked nucleic acid (LNA) is characterized by a bridged furanose ring which restricts the ring pucker to the C3-*endo* conformation. Peptide nucleic acid (PNA) links the nucleobase to an achiral and uncharged oligoamide backbone. Sugar amino acids (SAA) and bicyclic dipeptides (Xaa = Yaa) both may mimic dipeptide repeats and serve as turn mimetics within oligopeptides

backbone. The melting temperature of the double helix reflects directly the pairing affinity, for which a consistent register becomes a constitutional requirement for the development of alternative backbones. Peptide nucleic acid (PNA) has the characteristics of a random-walk chain. Locked nucleic acid (LNA) monomers secure a preferred ring pucker to promote a secondary structure within the homo-oligomer [1, 2]. Albeit the flexible PNA and the oligocyclic restricted LNA are very different oligomers, both conduct base pairing with complementary oligonucleotide chains and preserve a six-atom repeat which may be more important than the backbone composition.

In contrast to oligonucleotide DNA mimics, which adopt primarily helical structures, peptide mimics need to fulfill more complex requirements in part because peptide structures fold into a greater variety of secondary structural elements, e.g., helices, turns, and sheets. Moreover, molecular recognition of peptides involves typically backbone and side chain interactions. The quality of peptide recognition is usually characterized by a greater number of physical parameters than melting temperatures. Instead of two pairs of complementary building blocks for assembling functional DNA oligomers, 20 amino acids are employed in the construction of operative peptides and proteins.

Synthetic monomers have yet to be assembled into folded tertiary structures with the grace exemplified by RNA and proteins, which adopt various types of helices (e.g., polyproline and α -helices), extended structures (e.g., β -sheets), and reverse turns (e.g., β - and γ -turns). Although a set of β -amino acids have been derived from the 20 proteinogenic α -amino acids, their assembly into structures with hypothetical protein-like folds remains a challenge [3]. Inspired by the unique tertiary structures of proteins, discrete molecular chains that fold into ordered states in solution (so-called foldamers) have interfered with molecular recognition processes but, in spite of their structural diversity, have rarely exhibited conformational complexity beyond the helix [4, 5]. Protein folding depends on cooperative organization of linear secondary structures capped by turns and loops. Although it is composed of only four different monomers, RNA is the only known polymer that exhibits structural complexity, which rivals proteins. Every nucleotide in RNA offers a diverse set of possible noncovalent interactions for intermolecular contacts: hydrophobic, π , polar, hydrogen bond, and salt bridges. A handful of different amino acids would be necessary to attain a similar collection of noncovalent interactions. In the search for similarly densely functionalized monomers, carbohydrates represent intriguing building blocks because they possess a functional group on every carbon. Carbohydrate-peptide hybrids offer thus unique promise for designing higher-order structure, because they merge the cyclic polyhydroxylated character of RNA with the backbone rigidity and side chain diversity of peptides.

1.1 Hydroxylated Amino Acids in Nature

In addition to the well-known example of collagen, which becomes a structural protein only after 4-hydroxylation of the second proline of the Pro–Pro–Gly repeat,

numerous other natural peptides are known to possess canonical amino acids that have undergone hydroxylation. For example, α -amino- β -hydroxy acids are frequently observed as the products from posttranslational modifications in antibiotic peptides: β -hydroxytyrosine is found twice in vancomycin [6] and β -hydroxyvaline and β -hydroxyasparagine are found twice in polytheonamide B (Fig. 2) [7]. The presence of a β -position hydroxyl group rigidifies rotation about the side chain χ dihedral angle by introducing a polar group with potential to hydrogen bond. The canonical amino acid, threonine, exhibits restricted rotation about the C_{α} - C_{β} bond and influences the conformational preferences of neighboring residues in a peptide chain.

The thiopeptide antibiotic thiazomycin A is an oligopeptide that has been significantly rigidified by posttranslational modifications (Fig. 3) [8, 9]. In particular, the glutamic acid residue is hydroxylated at the β and γ positions, condensed with its C-terminal cysteine neighbor in a thiazole ring and ligated by way of the

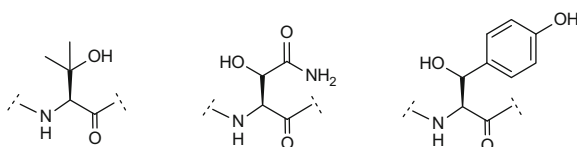


Fig. 2 β -Hydroxyamino acid residues: β -hydroxyvaline (*left*), β -hydroxyasparagine (*middle*), and β -hydroxytyrosine (*right*)

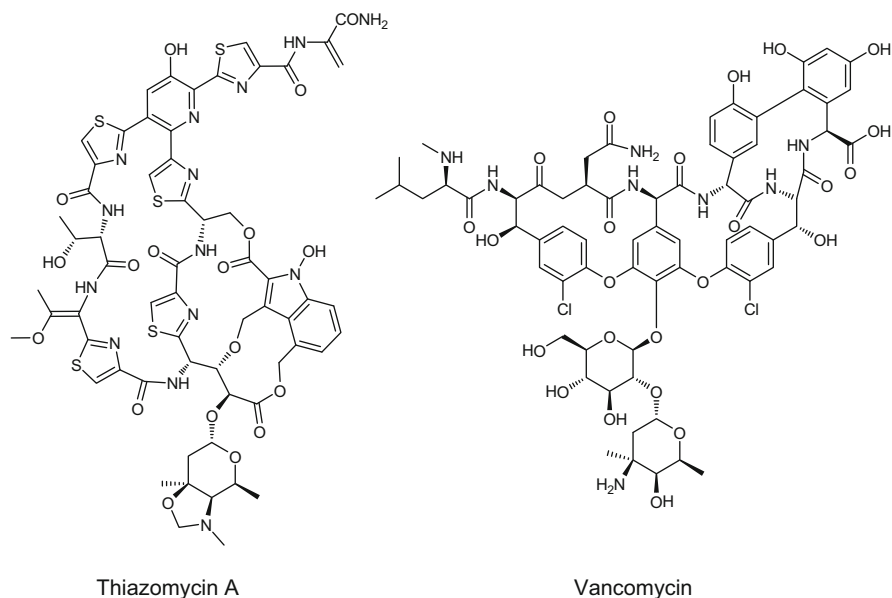


Fig. 3 Vancomycin and thiazomycin A possess hydroxylated amino acid residues obtained from posttranslational modifications

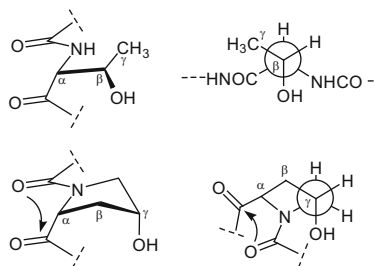


Fig. 4 The *gauche* effect between vicinal electron-withdrawing groups dominate the conformational preferences of the hydroxy amino acids Thr (*above*, in Newman projection) and Hyp (*below*). The polyproline II helical conformation aligns neighboring amide bonds in collagen to favor $n \rightarrow \pi^*$ electronic delocalization

alcohol, amine, and carboxylate functions in ways that provide constraint and glycosylation of the natural product.

The antibiotics vancomycin and thiazomycin A are representative examples of the applications of hydroxylation by nature to control peptide polarity and conformation [10].

1.2 Conformational Properties of Hydroxy Amino Acids

β -Hydroxylation alters the conformational equilibrium about the amino acid side chain. For example, threonine residues adopt the electronically preferred *gauche* arrangement of the α -amino and β -hydroxy groups instead of the antiperiplanar orientation, which may minimize steric interactions, as evidenced by the relatively small $^3J_{\text{H}\alpha\text{-H}\beta}$ coupling constant value (Fig. 4). The so-called *gauche* effect is a vicinal stereoelectronic effect that maximizes the orbital overlap between electronegative substituents and donors in relative antiperiplanar orientations due to σ, σ^* stabilizing interactions [11]. Similarly, the relative *gauche* orientation of the pyrrolidine nitrogen and vicinal δ -hydroxyl substituent orient the ring puckering and backbone of δ -hydroxyproline residues in peptides such as collagen (Fig. 4). The *endo* conformation of the pyrrolidine ring brings two sequential carbonyl groups into a favorable arrangement for $n \rightarrow \pi^*$ electronic delocalization, which contributes to the overall conformational preference of the collagen triple helix [12].

2 Sugar Amino Acids

Sugar-derived δ -amino acid derivatives have been synthesized from tetrahydrofuran and tetrahydropyran monosaccharides and employed as dipeptide isosteres [13, 14]. Initially explored as analogs of polysaccharides [15], the application

of sugar-derived δ -amino acids as dipeptide surrogates in biologically active peptides was first examined by von Roedern and Kessler, who explored glucosyl-uronic acid methylamine (H-Gum-OH) in the synthesis of enkephalin and somatostatin analogs, which proved respectively inactive and 75 times less active than the parent peptides [16]. Subsequently, sugar amino acids (SAAs) having varied ring geometries and substitution patterns were prepared employing the multitude of available monosaccharide precursors [17]. Among these potentially useful carbohydrate building blocks, the scaffolds discussed herein have been studied in peptide environments including linear peptides, cyclopeptides, and homo-oligomers. Examples of SAAs that do not fit the oligopeptide register (Fig. 1) as well as those not investigated in an oligopeptide environment were excluded from this review, because they may alter the peptide reading frame in ways that are not generalizable to other peptide structures.

Azide protection of the amine component of the SAA has often been used for solution-phase peptide synthesis. The azide avoids unwanted lactam formation of activated ω -amino acids similar to the diketopiperazine formation of activated dipeptides. After SAA coupling, the azide may be reduced in situ prior to subsequent peptide synthesis.

Monomers of δ -3,5-*trans*- and *cis*-tetrahydrofuranyl SAAs **1** and **2** have been synthesized in several steps from D-ribose [1, 18]. *O*-Methylation of the alcohols was employed to avoid alcohol acylation and reduce polarity; however, attempts using *O*-*tert*-butyldimethylsilyl and *O*-benzyl ether protection failed to give longer oligomers, likely due to steric hindrance. Homo-oligomers containing an octamer (e.g., **3**) of *trans*-diastereomer **1** and a tetramer (e.g., **4**) of *cis*-diastereomer **2** were obtained by fragment condensations employing dimers activated as pentafluorophenyl esters, followed by hydrogenation of azides to the amines using palladium-black in dioxane (Fig. 5).

Employing Boc protection in a similar approach, *trans*- and *cis*-tetrahydrofuranyl-SAA diastereomers **5** and **6** were coupled to their 4-azido counterparts and the resulting dimers were combined to form tetramers (Fig. 6) [19]. The 4-azido groups were reacted with different alkynes using copper-catalyzed azide-alkyne cycloadditions (Cu-AACs) to afford triazoles bearing different side chain functions (e.g., mannose for oligomers **7** and **8**). The mannose-conjugated glycopeptide mimetics **7** and **8** were recognized by the lectin *Concanavalin A*, albeit

Fig. 5 δ -THF based SAAs **1** and **2** and their corresponding homo-oligomers **3** and **4**

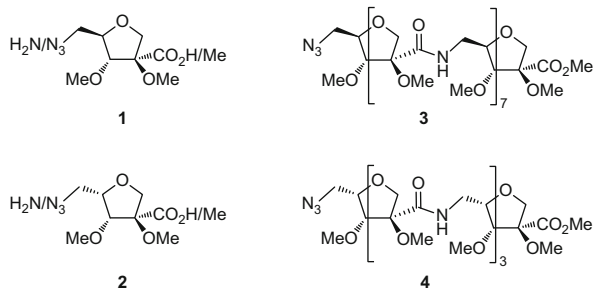
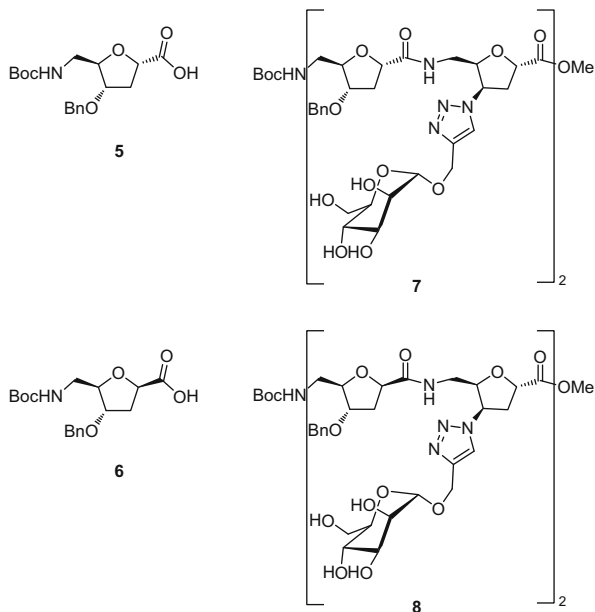


Fig. 6 Boc-protected THF-SAA monomers **5** and **6**, and oligomers **7** and **8**. The backbone was modified via CuAAC chemistry



with less than fourfold lower affinity relative to the natural mannose trimer. In the cases of the *cis*-tertamers bearing azide and mannosyl tetrazole, conformational analysis by NMR spectroscopy indicated nuclear Overhauser effects and solvent exchange indicative respectively of 10- and 16-membered intramolecular hydrogen bonds.

A set of C_2 -symmetric cyclic octapeptide mimics of the type *cyclo*-(SAA-Phe-Leu)₂ on which different cationic amino side chains were examined on the carbohydrate moiety were synthesized from orthogonally protected diamino tetrahydrofuran carboxylates **9** and **10** (with Boc-protected amino groups in side chain R) (Fig. 7) [20]. A detailed NMR analysis of cationic peptides **11–13** and **14–16** was performed in water using ¹H NMR chemical shifts, coupling constants, through-space nuclear Overhauser effects (NOEs), and amide temperature coefficients. The amide protons of the Phe and Saa residues exhibited smaller temperature coefficients than the values for the Leu residues indicative of solvent-shielded and exposed protons. An amphiphilic structure was proposed for macrocycles **11–13** and **14–16** which exhibited antibiotic activities against Gram-positive and Gram-negative bacteria with a greater potency against the former, albeit the more potent analogs exhibited hemolytic activity.

The D-Phe-Pro residue in the antibiotic cyclopeptide gramicidin S [*GS*, *cyclo*-(D-Phe-Pro-Val-Orn-Ile)₂] adopts the central positions of a type II' β -turn conformation and has often been replaced by turn mimetics [21]. Consequently, SAAs have been examined as turn mimics in gramicidin S [1, 22]. Three different ring-sized *O*-benzyl SAAs (**17–19**, Fig. 8) were studied in cyclic decapeptides with the general structure *cyclo*-(SAA-Val-Orn-Leu-D-Phe-Pro-Val-Orn-Leu) [23]. The SAA-GS

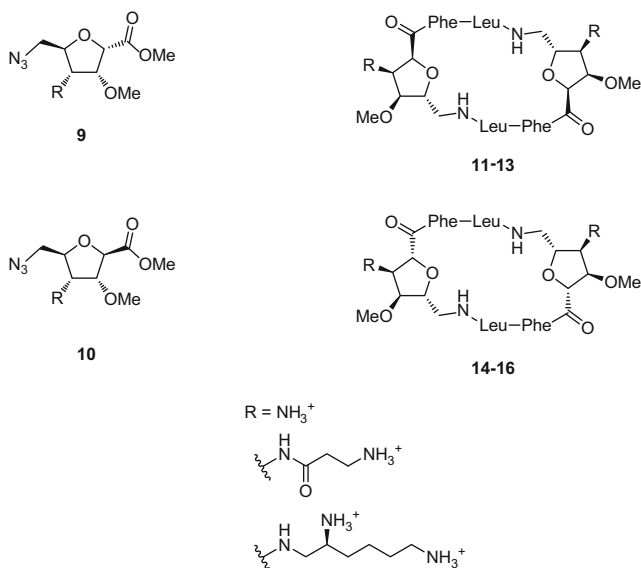


Fig. 7 SAs **9** and **10** were incorporated in cationic antibiotic C₂-symmetric cyclopeptides. The number of positive charges was controlled by different amino substituents (R) of the SAA

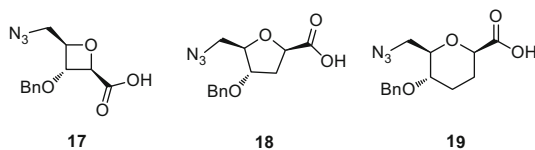


Fig. 8 Oxetane, furanoid, and pyranoid SAAs **17–19** were used as turn mimetics to synthesize gramicidin S analogs

analogues exhibited CD spectra that were influenced more than that of the parent peptide by the change of solvent from water to methanol. The crystal structure of the oxetane GS analog and the solution NMR spectra of all three SAA-GS analogs indicated hydrogen bonding patterns and transfer of magnetization indicative of an antiparallel hairpin shape that resembled the parent amphipathic peptide. Contingent on the bacterial strain, the pyranoid-SAA analog exhibited the same to half the potency of GS with 16-fold less hemolytic activity. The oxetane and furanoid SAA-GS analogs were relatively less active as antibacterial agents [24].

The influence of the polarity of the carbohydrate amino acid on the conformation and activity of gramicidin S analogs was examined by incorporation of dihydroxy, mono-*O*-benzyl, and bis-*O*-benzyl SAAs **20–22** (Fig. 9) into cyclic dodecapeptide ring-extended analogs of gramicidin S with the general structure *cyclo*-(SAA-Leu-Orn-Val-Orn-Leu-D-Phe-Pro-Val-Orn-Leu-D-Orn-Val) [25]. The peptides were assembled by a strategy featuring *N*-Fmoc-amino acids on 2-chlorotrityl chloride (CTC) resin employing *trans*-tetrahydrofuranyl SAAs **20–22**, which were coupled

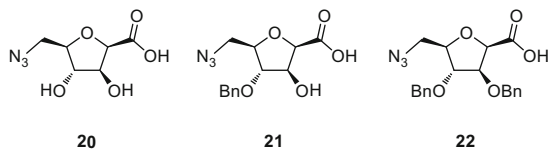


Fig. 9 SAAs **20–22** possessing different numbers of benzyl groups were used as turn mimetics in GS analogs

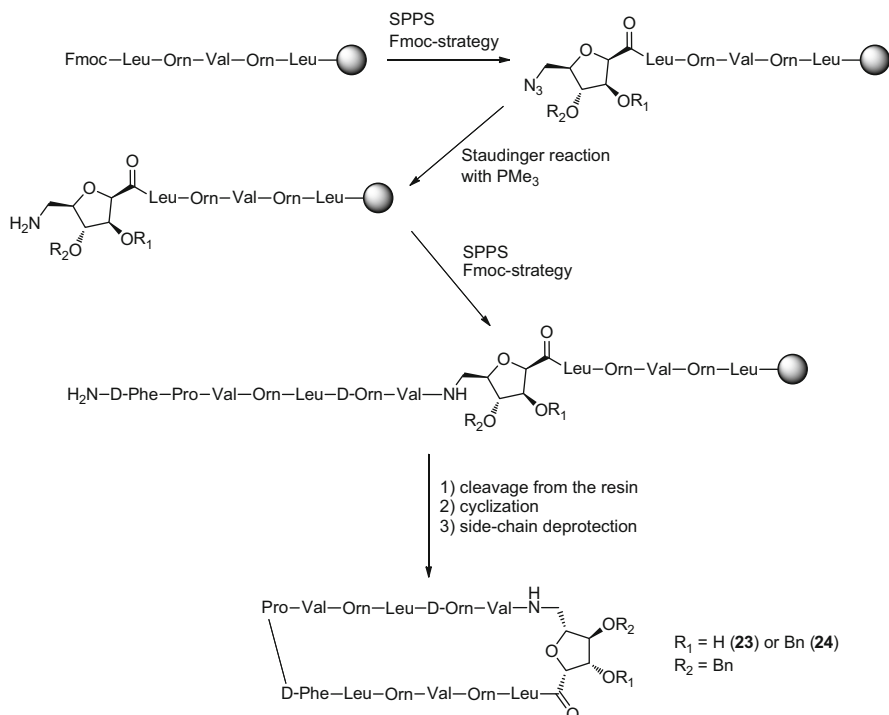


Fig. 10 Synthetic route to gramicidin S analogs **23** and **24** with *O*-benzyl and dibenzyl SAAs on CTC resin

employing standard methods and elongated after reduction of the azide using aqueous trimethylphosphine. The SAA peptides were cleaved without removal of side chain protection under mild acid conditions, and final cyclization was accomplished in solution using benzotriazol-1-yl-oxytripyrrolidinophosphonium hexafluorophosphate (PyBOP, Fig. 10). Although the SAA peptides exhibited coupling constant and chemical shift data similar to the β -sheet/ β -hairpin character of the peptide counterpart, their CD spectra indicated less order. They exhibited promising antibacterial activity and lower hemolytic activity relative to GS. Antibacterial potency declined with the removal of *O*-benzyl groups from the carbohydrate amino acid residue of the cyclic dodecapeptide mimics.

Fig. 11 Fmoc-protected δ -substituted pyranoid SAAs *S*-25 and *R*-25

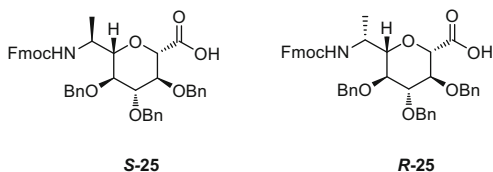
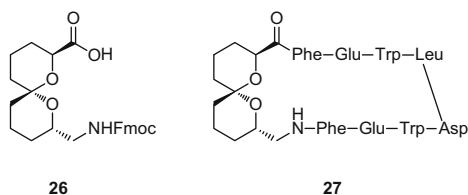


Fig. 12 Fmoc-protected spiroketal SAA **26** and cyclopeptide analog **27**



δ -Substituted pyranoid SAAs *S*-25 and *R*-25 were synthesized by diastereoselective (>10:1) in addition of methyl magnesium bromide to the *tert*-butane-sulfinamide from condensation of a formyl tetra-*O*-benzyl- β -D-*C*-glucopyranoside precursor with *tert*-butanesulfinyl amide, acid-mediated hydrolysis of the chiral auxiliary, and installment of the Fmoc protection (Fig. 11) [26]. The additional δ -substituent may mimic the side chain of Ala and restrict the conformation in a peptide context.

6,6-Spiroketal amino acid **26** was synthesized, introduced into *cyclo*-(SAA-Phe-Glu-Trp-Leu-Asp-Trp-Glu-Phe) **27** by solid-phase peptide synthesis using an Fmoc protection strategy, and found to adopt the *i* and *i* + 1 positions of a β -turn-like structure, instead of the central *i* + 1 and *i* + 2 residues (Fig. 12) [27].

3 Peptide Constraints Using Lactams, 6,5-Bicyclic Lactams, and Polyhydroxylated Lactams

3.1 Lactams and 6,5-Bicyclic Lactams

The concept of employing a lactam to constrain the conformation of a peptide was first applied by Freidinger et al. to study the bioactive conformation of luteinizing hormone-releasing hormone [28]. Side chain to backbone cyclization was subsequently studied using bicyclic dipeptide lactams (e.g., Fig. 13) [21, 22], which were used to constrain peptide conformation in peptides such as gramicidin S, as well as enzyme inhibitors. Subsequently, various bicyclic β -turn mimetics have been synthesized and employed in various applications in medicinal chemistry [29] (and references therein).

The BTD residue has been inserted into larger peptides such as analogs of a zinc finger (25 aa, 2.5 kD) and HIV protease (2×99 aa, 11 kD). In the high-resolution NMR spectroscopic study of the zinc finger analog, the BTD residue adopted the

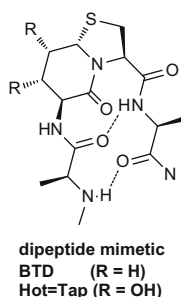


Fig. 13 Schematic representation of bicyclic dipeptides in a peptidic environment. The abbreviation BTD stands for β -turn dipeptide ($R = H$). The Xaa = Yaa six-letter code identifies the six-atom register by combining abbreviations for the two amino acid components, for example, Hot = Tap stands for hydroxythreonine (Hot) fused (=) with thioproline (Tap)

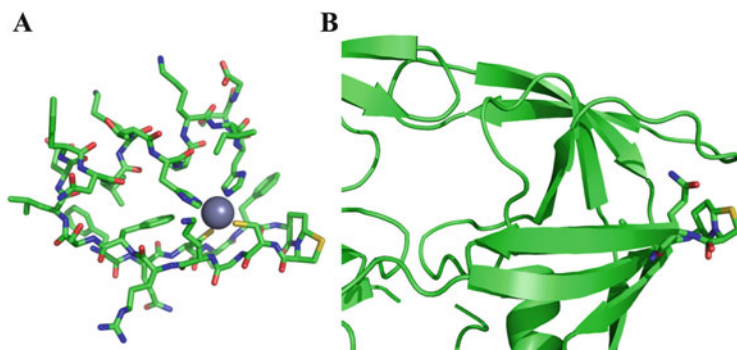


Fig. 14 BTD adopts the central residues of type II' β -turns in (a): zinc finger [30]; (b) HIV protease replacing the Gly¹⁶-Gly¹⁷ residues [31]. BTD is recognizable by the yellow thiazolidine ring at surface-exposed positions

central residues of a type II' β -turn [30]. Similarly, in the HIV-protease analog, BTD replaced effectively Gly¹⁶-Gly¹⁷ at the central position of a type II' β -turn (Fig. 14) [31]. In addition to conserving the structure, both BTD analogs retained function. Although the surface-exposed, flexible Gly-Gly turn in HIV protease and the rigid D-Phe-Pro turn of gramicidin S were both exchanged for BTD without significant modification of function, incorporation at buried positions within the three-dimensional fold of larger proteins may be a greater challenge for such turn mimetics.

3.2 Polyhydroxylated Lactams

The confluence of lactam and SAA moieties through the synthesis of polyhydroxylated bicyclic lactam dipeptides combines backbone constraint with

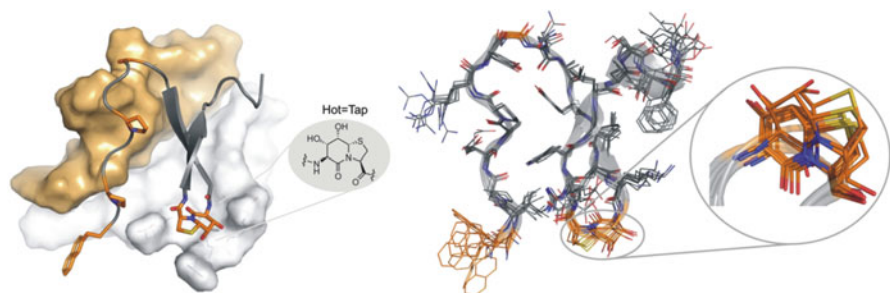


Fig. 15 X-ray structure of the Hot = Tap dipeptide in the miniprotein Foldon. *Left:* Two strands are shown as vdW models (*brown, gray*). The third strand shows the (bi)cyclic amino acids, as well as Nal² and D-Ala. *Right:* Overlay of the six monomers of the two independent Foldons from the asymmetric unit. The expansion shows the Hot = Tap dipeptides

poly-functional side chains. Such a combination offers potential for stabilizing an active conformer and increasing molecular recognition. For example, insertion of the Hot = Tap dipeptide into Foldon (3×27 aa, 10 kD) yielded an analog having one of the two best resolved X-ray structures (PDB Code: [2WW7](#)) among 26 structures deposited for this miniprotein in the pdb databank (Fig. 15) [32]. Foldon comes from the natural trimerization domain of T4 fibrin and has been used as an artificial trimerization domain. In the crystal structure of the miniprotein, Hot = Tap was completely buried and mediated a series of protein-protein contacts. Two independent foldon trimers were identified within the asymmetric unit, which illustrated conformational variability at the N and C termini, but a rigid hydrophobic core for the fibrin–foldon.

In spite of unnatural amino acids, [Δ Gly¹, Nal², Hot¹⁷ = Tap¹⁸]Foldon exhibited a nearly identical conformation to the natural fibrin–foldon fusion protein (PDB Code: [2IBL](#)) [33]. The X-ray structure of [Δ Gly¹, Nal², Hot¹⁷ = Tap¹⁸]Foldon exhibited higher resolution than other natural Foldon protein structures previously deposited in the Brookhaven protein data bank. The twist and hydrogen bonds (I–IV) of the Hot¹⁷ = Tap¹⁸ analog were characteristic of a natural hairpin (Fig. 16), albeit the native and SAA hairpins possessed respectively central Asp–Gly and bicyclic lactam residues in type I' and II' β -turns.

The first high-resolution X-ray analysis of the ring shape of a turn mimetic in a peptide environment, the [Δ Gly¹, Nal², Hot¹⁷ = Tap¹⁸]Foldon structure, provides unique opportunity to study ring torsions of the bicyclic lactam residue (Fig. 17). Similar to other substituted δ -lactones [34], the six-membered ring adopted an envelope (half boat) conformer that placed the C8-hydroxyl group into an axial orientation. In contrast, the five-membered thiazolidine ring exhibited greater conformational flexibility and adopted different puckers for the various structures in the asymmetric unit.

To dissect the influence of the turn mimic from the dynamics of the protein structure, model C₂-symmetric cyclic hexapeptides were synthesized and examined to identify factors affecting their conformational preferences. Such cyclic

Fig. 16 *Left*: [Δ Gly¹, Nal², Hot¹⁷ = Tap¹⁸] Foldon hairpin at 1.05 Å resolution. *Right*: recombinant fibrin–foldon fusion protein hairpin at 1.30 Å resolution [32]

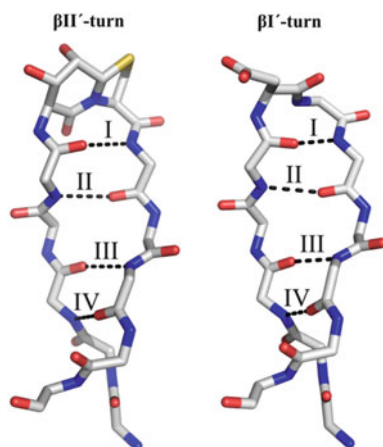


Fig. 17 Average values of ring torsion angles of the six independent Hot = Tap structures in the asymmetric cell of the Foldon structure (PDB Code: 2WW7)

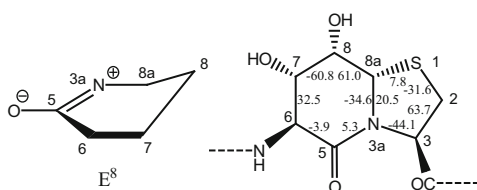
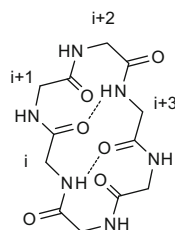


Fig. 18 *cyclo*(Gly)₆



hexapeptides may be considered minimal hairpin and antiparallel β -sheet models, because they adopt typically a minimum energy conformer featuring a rectangular shape with two antiparallel hydrogen bonds (Fig. 18) [35]. Three possible turn positions were accessible in the bicycle, because symmetry rendered the i and $i + 3$ residues equivalent.

Within *cyclo*(Xaa-Yaa-Zaa)₂ cyclohexapeptides, bicyclic dipeptides occupied both the i and $i + 1$ and the $i + 1$ and $i + 2$ positions (Fig. 19). In the latter, the bicycle adopts the central positions of the turn. Bicyclic dipeptides that adopt the i and $i + 1$ positions share conformational preferences with proline, which prefers the $i + 1$ relative to the $i + 2$ position [36]. This shift causes a different orientation of the amide NH protons. Typically, every third NH is involved in an intramolecular hydrogen bond. The other two NH protons are oriented toward solvent. Solvent-exposed amide NH hydrogen exhibit chemical shifts that are influenced more

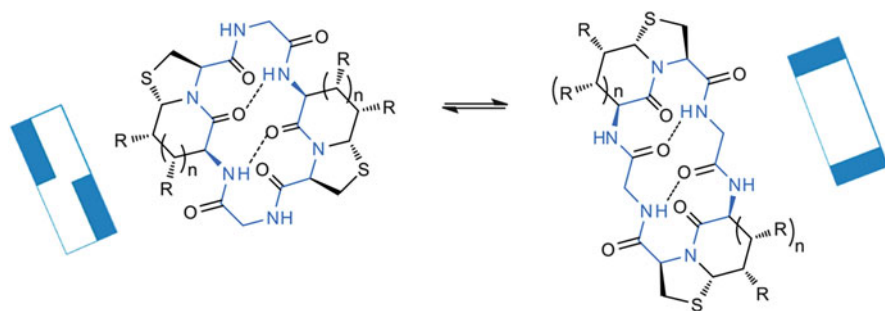


Fig. 19 The two possible orientations of C₂-symmetric cyclic hexapeptides with a bicyclic dipeptide compound. Blue boxes represent simplified illustrations of the bicycle at different positions in the macrocycle

significantly by changes in temperature than solvent-shielded amide NH involved in intramolecular hydrogen bonds. Proton chemical shift dispersion, $^3J_{\text{NH,H}\alpha}$ coupling constants, and through-space transfer of magnetization between neighboring hydrogen were also employed to investigate conformational homogeneity.

Three different C₂-symmetric cyclic hexapeptides were studied: *cyclo*(Gly–BTD)₂, *cyclo*(Gly–Dha = Tap)₂, *cyclo*(Gly–Hot^P = Tap)₂, and *cyclo*(Gly–Hot = Tap)₂ (Fig. 20) [9, 32]. Averaged values were observed for the 3J coupling constants, as well as the amide NH chemical shift and temperature coefficient values for *cyclo*(Gly–BTD)₂ indicative of an equilibrium between similar energy conformers in which the BTD residues occupied the *i* and *i* + 1 or the *i* + 1 and *i* + 2 positions. On the other hand, the NMR data suggested that *cyclo*(Gly–Dha = Tap)₂ adopted a minimum energy conformer in which the Dha = Tap residues resided in the *i* and *i* + 1 positions. Finally, *cyclo*(Gly–Hot = Tap)₂ exhibited NMR spectra demonstrating a single conformer in which the Hot = Tap residues adopted the *i* + 1 and *i* + 2 positions. The coupling constant values of the Hot = Tap residue were indicative of a conformer with dihedral angles well suited for the central position of a type II' β-turn (Table 1).

In the Foldon miniprotein as well as in cyclic hexapeptides, Hot = Tap adopted exclusively the *i* + 1 and *i* + 2 positions of a type II' β-turn. The analytical data obtained from the crystal structure of the protein from water and the NMR data of the model hexapeptides in DMSO draw a complete picture of Hot = Tap in different environments and characterize its reliability as a turn mimetic.

The ring equilibrium of BTD in solution has never been characterized, because there is no diastereotopic assignment possible for the higher-order spin system of the ethylene bridge. It can be assumed that none of the possible valerolactam conformations – boat (B), chair (C), skew (S), half-boat (E), or half-chair (H) – can be excluded or are specially preferred and, therefore, the torque of the neighboring peptide chain dominates the conformation. This adaptive character ranks it among the passive turn mimics which fit the turn, but allow other conformations [38]. Only one conformation is observed in the crystal and in solution for the tricyclic protected Hot^P = Tap, which is characterized by a B_{6,8a} conformation

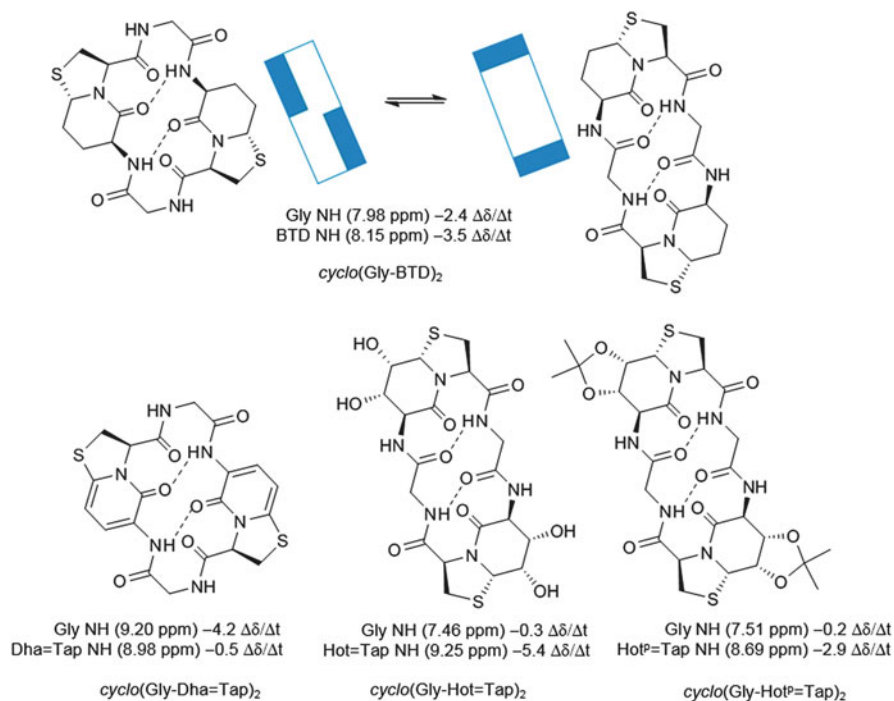
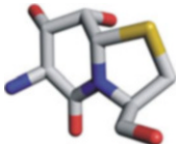


Fig. 20 Structures, chemical shifts, and temperature coefficients in DMSO-*d*₆ for amide NH protons of *cyclo*(Gly-BTD)₂, *cyclo*(Gly-Dha = Tap)₂, and *cyclo*(Gly-Hot = Tap)₂ [9, 32, 37]. The temperature dependency of the amide NH protons identifies the conformation of each cyclic hexapeptide. Hot-NH is characterized by a high chemical shift value around 9 ppm and a strong temperature dependence as expected for a solvent-exposed proton. The Gly-NH in *cyclo*(Gly-HotP = Tap)₂ and in *cyclo*(Gly-Hot = Tap)₂ have values around 7.5 ppm and show a low temperature dependence as expected for a hydrogen-bonded peptide in a cyclic hexapeptide. The opposite is observed for Gly-NH in *cyclo*(Gly-Dha = Tap)₂ where its NH is solvent exposed because Dha = Tap is found in the *i* and *i* + 1 position of the turn. Dha-NH shows a high chemical shift value because of its anilinic character

Table 1 Coupling constant values and calculated structure of *cyclo*(Gly-Hot = Tap)₂

	<i>cyclo</i> (Gly-Hot = Tap) ₂	
	³ J _{6H,7H} (Hz)	8.4
	³ J _{7H,8H} (Hz)	2.3
	³ J _{8H,8aH} (Hz)	1.4
	³ J _{2H,3H} (Hz)	2.2, 6.3

with a flagpole orientation of the amino group [37]. The deprotected Hot = Tap in a peptide environment has already been discussed above in Figs. 15, 16, and 17. β -Branching and several *gauche* effects may account for the turn mimic dominating the shape of its peptide environment (Fig. 21).

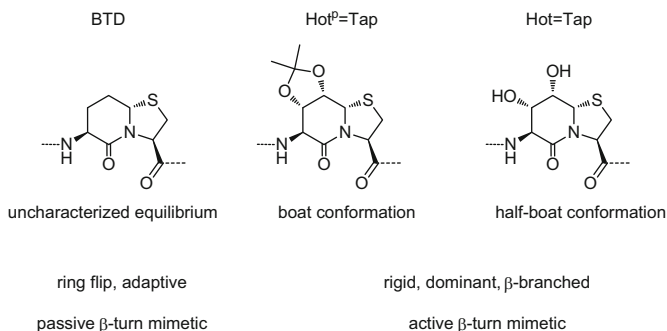


Fig. 21 Comparison of the β -turn mimetics. Hot^P = Tap and Hot = Tap are active mimetics because of their rigid conformation, whereas BTD is more flexible and, therefore, a passive β -turn mimetic [38]

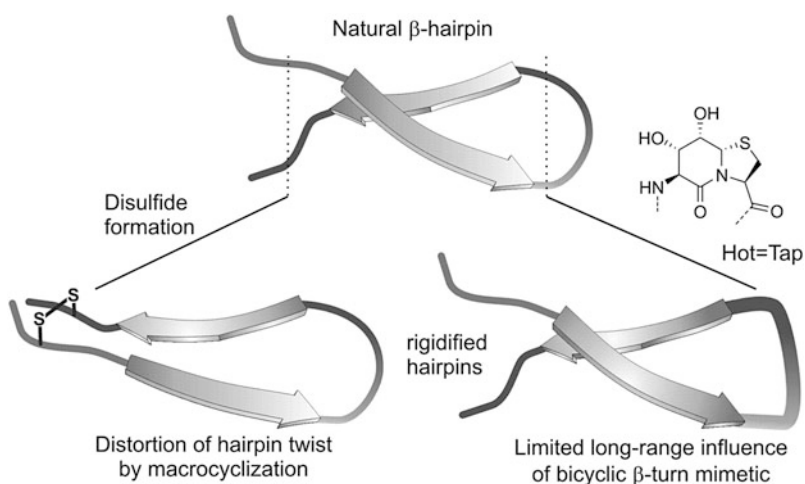


Fig. 22 β -Hairpin-antiparallel β -sheet motifs excised from proteins may be stabilized by end-to-end cyclization using a disulfide bond or employing Hot = Tap

β -Hairpins are usually found as domains in protein structures but have only moderate stability as standalone motifs. For example, a population of approximately 42% hairpin was measured for the isolated Ala-Tyr-Val-Arg-Lys-Asn-Gly-Glu-Trp-Val-Leu-Leu-Ser sequence, which makes up 50% of the structure of the extraordinarily stable miniprotein Foldon [39]. Insertion of Hot = Tap into the sequence augmented the hairpin population to >80% in the peptide Ala-Tyr-Val-Arg-Lys-Hot = Tap-Glu-Trp-Val-Leu-Leu-Ser. In contrast to restriction by macrocyclization by lactam or disulfide formation, which may distort of the hairpin twist, Hot = Tap maintained a more natural conformation (Fig. 22).

4 Synthesis of Polyhydroxylated Bicyclic Lactams

4.1 Synthesis of Polyhydroxylated 6,5-Bicyclic Lactam

In contrast to the synthesis of bicyclic dipeptide analogs such as BTD, which may necessitate amine and carboxylate protection prior to thiazolidine and lactam formation [38], the polyhydroxylated 6,5-bicyclic lactam framework has been assembled directly from uronic acid and cysteine without protection (Fig. 23) [32]. Thiazolidine formation occurred diastereoselectively to provide the (*S*)-ring fusion, likely because the neighboring hydroxyl group guides the addition of the thiol in the attack of the iminium ion intermediate. Conversion of the α -hydroxyl group to the requisite amine may be accomplished with high regioselectivity without protection of the other hydroxyl groups, albeit acetonide protection facilitated purification by column chromatography.

The synthesis of Fmoc-Hot = Tap-OH has been accomplished on multigram scale (Fig. 24) [32]. Ribose was converted to ribonolactone **28**, which was oxidized to the 2,3-isopropylidene-L-riburonolactone with 2-iodoxybenzoic acid (IBX) and treated with cysteine methyl ester hydrochloride to diastereoselectively afford thiaindolizidinone **29**. Acid-induced isomerization to thermodynamically more

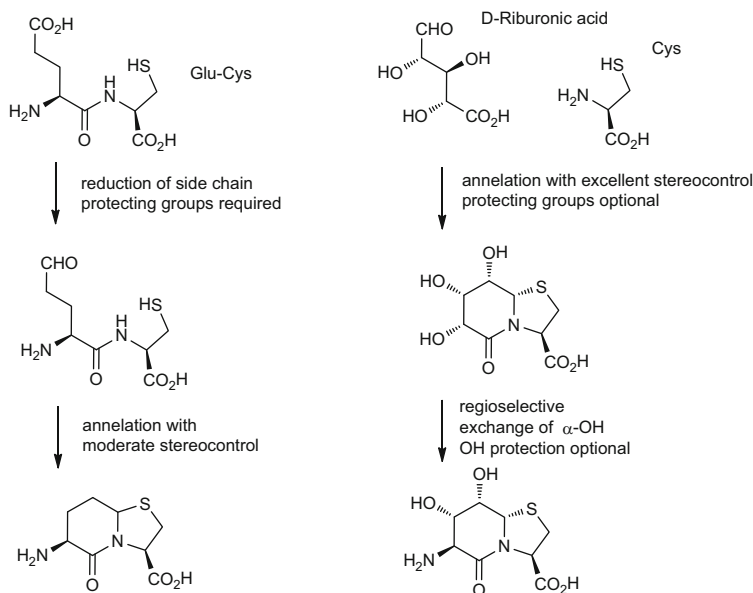


Fig. 23 Two strategies for the synthesis of thiazolidinelactams based on dipeptides. *Left*: The dipeptide strategy that employs a side chain aldehyde necessitates protected intermediates and provides the ring fusion center with moderate diastereoselection [21, 22]. *Right*: The strategy based on uronic acid employs no protecting groups and gives high stereocontrol in the cyclization [32, 40]

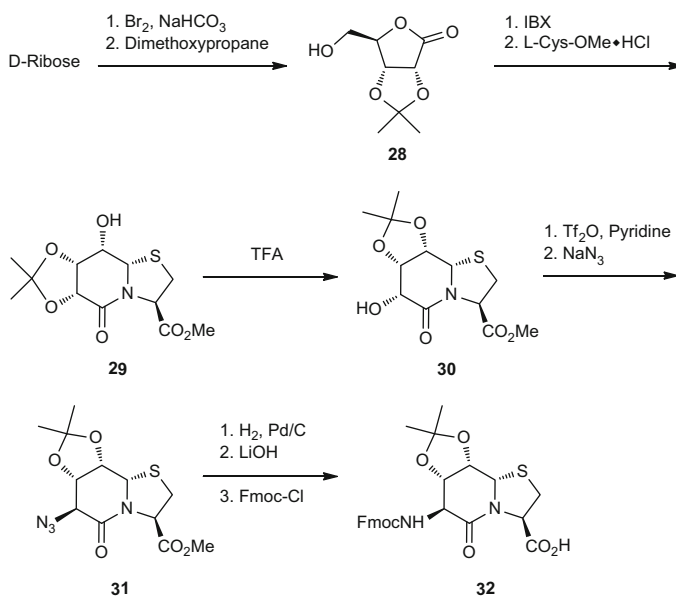


Fig. 24 Multigram scale synthesis of Fmoc-Hot=Tap-OH 32

stable acetonide **30** liberated the α -hydroxyl group, which was activated with trifluoromethanesulfonic anhydride and displaced with inversion of configuration using sodium azide. Although saponification of azido ester **31** may be used to provide a suitable precursor for solid-phase peptide synthesis, to facilitate application of automated synthesizers, the Fmoc counterpart **32** was prepared by azide hydrogenation, ester saponification, and amine acylation with fluorenylmethyl chloroformate.

4.2 Synthesis of Polyhydroxylated 7,5-Bicyclic Lactams

The general strategy for the synthesis of bicyclic lactams from the condensation of a uronic acid and cysteine has also been used to synthesize 7,5-fused ring systems Glc = Tap **33** and Gul = Tap **34** contingent on the starting carbohydrate (Fig. 25) [41–44].

For example, D-glucurono-3,6-lactone (**35**) reacted with L-cysteine methyl ester in a water:pyridine mixture to provide diastereoselectively thiazolidine lactam **36** (Fig. 26) [42]. Regioselective trifluoromethylation of the α -hydroxyl group was achieved without protection of the other secondary alcohols. Displacement of the triflate by sodium azide with retention of configuration, azide reduction with hydrogen sulfide, and Boc protection gave polyhydroxylated dipeptide ester **38** [42].

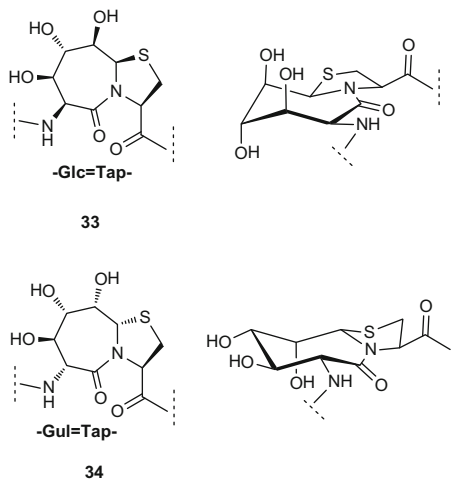


Fig. 25 Glucuronic and mannuronic acids were respectively employed to synthesize 7,5-bicyclic lactams Glc = Tap **33** and Gul = Tap **34**, which possess respectively concave and convex geometry with the amine substituent in an equatorial configuration. Homo-oligomers of Glc = Tap exhibited a polyproline-II-type secondary structure [41]

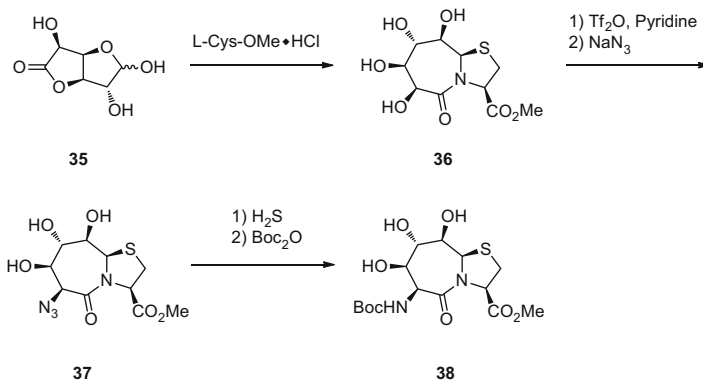


Fig. 26 Synthesis of Boc-protected Glc = Tap methyl ester **38**

Mannurono-3,6-lactone (**39**) was also reacted with L-cysteine methyl ester under similar conditions to give diastereoselectively bicycle **40**, which could be selectively converted to acetonide **41** (Fig. 27) [44]. Methanesulfonylation of the α -hydroxyl group, benzylation of the δ -hydroxyl group, and displacement with sodium azide afforded azido ester **42**, which, after saponification of the ester with lithium hydroxide, was employed to install the Gul = Tap residue into different peptides. In the formation of the thiazolidine ring of both the Glc = Tap and Gul = Tap systems, the δ -hydroxyl group directed the attack of the thiol onto the

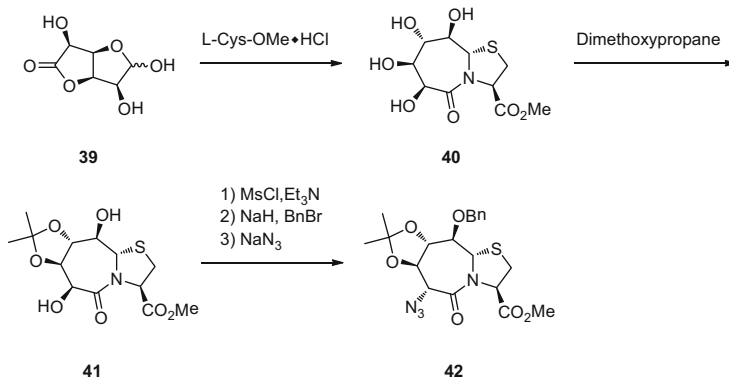


Fig. 27 Synthesis of protected Gul = Tap methyl ester **42**

Table 2 X-ray structure of *cyclo*(Gly–Glc = Tap)₂ (C = green, N = blue, O = red, S = yellow, hydrogens are not shown). Torsion angle values are tabularized along the peptide backbone

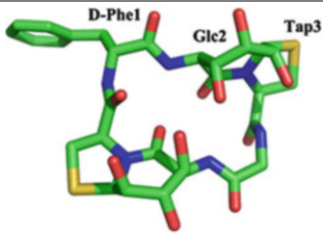
	Amino acid	φ (degree)	ψ (degree)
	Gly1	−113.2	16.4
	Glc2	−157.3	177.4
	Tap3	−57.4	− 16.3
	Gly4	−111.3	9.2
	Glc5	−165.7	−175.6
	Tap5	−57.0	− 33.6

iminium ion intermediate to place both groups on the same face of the lactam ring [42, 44].

The five-membered thiazolidine ring adopted an equatorial orientation in both the Glc = Tap and Gul = Tap residues as observed in the X-ray crystal structure of thiazolidine lactam **33**, in which the carboxylate was observed to assume a pseudo-axial orientation [42]. The seven-membered lactam adopts a chair conformation that places the α -amine substituent in an equatorial orientation (Fig. 25). The conformational preferences of Glc = Tap were examined in the C_2 symmetric cyclopeptide *cyclo*(Gly–Glc = Tap)₂, as well as cyclic hexapeptides in which one of the glycine residues was replaced by L- or D-Phe, respectively (Tables 2 and 3) [43]. In all three cases, Glc = Tap occupied the *i* and *i* + 1 positions of the β -turn, as determined by the characteristic networks of hydrogen bonds identified by NMR spectroscopy.

In the X-ray structure of *cyclo*(Gly–Glc = Tap)₂, the lactam of the Glc = Tap residue aligned nearly perpendicular to the cyclic peptide backbone, bringing hydroxyl groups from opposite sides of the ring into close contact. Two type I β -turns are stabilized by amide NH and ring OH hydrogen bond donors. Nearly ideal C_2 -symmetry was observed by X-ray analysis (Table 2) and maintained in

Table 3 X-ray structure of *cyclo*(D-Phe-Glc = Tap-Gly-Glc = Tap) (C = green, N = blue, O = red, S = yellow, hydrogens are not shown). The table lists the torsion angle values along the peptide backbone. Tap⁶ and D-Phe¹ enclose a β II-turn, while a β I-turn can be seen at the opposite end

	Amino acid	ϕ (degree)	ψ (degree)
	D-Phe1	66.9	16.3
	Glc2	-148.9	179.3
	Tap3	-58.0	-46.9
	Gly4	-100.7	2.8
	Glc5	-158.5	-178.4
	Tap5	-54.2	133.2

solution as observed by NMR spectroscopy. Replacement of glycine by D-Phe provided *cyclo*(D-Phe-Glc = Tap-Gly-Glc = Tap), which was observed by X-ray analysis to possess type II and I β -turns with the D-Phe and Gly residues in the $i + 2$ position (Table 3).

An oligomer of Glc = Tap adopted a polyproline type II helical structure [41]. The Glc = Tap has also been employed as a rigidifying element of non-peptide structures [45].

5 Conclusion

Sugar amino acids and polyhydroxylated bicyclic lactams have proven effective as rigidifying elements to control peptide and protein secondary structures. In particular, the latter have served effectively as β -turn mimics, because of their potential to control both peptide backbone and side chain conformations. Albeit their syntheses may necessitate multiple steps, applications of sugar amino acids to explore the conformations of peptide hormones have provided biologically active analogs. Polyhydroxylated bicyclic lactams have been synthesized with stereocontrol and applied to rigidify conformations of cyclic peptides, small proteins, and polyproline helices. With enhanced methods for their preparation, the applications of sugar amino acids and polyhydroxylated bicyclic lactams are expected to increase in future studies of bioactive peptides and proteins.

References

1. Nielsen PE, Egholm M, Berg RH, Buchardt O (1991) *Science* 254:1497–1500
2. Kaur H, Arora A, Wengel J, Maiti S (2006) *Biochemistry* 45:7347–7355
3. Seebach D, Matthews JL (1997) *Chem Commun* 2015–2022

4. Gellman SH (1998) *Acc Chem Res* 31:173–180
5. Beck-Sickinger AG, Panitz N (2014) *Curr Opin Chem Biol* 22:100–107
6. Nicolaou KC, Mitchell HJ, Jain NF, Winssinger N, Hughes R, Bando T (1999) *Angew Chem Int Ed* 38:240–244
7. Inoue M, Shinohara N, Tanabe S, Takahashi T, Okura K, Itoh H, Mizoguchi Y, Iida M, Lee N, Matsuoka S (2010) *Nat Chem* 2:280–285
8. Zhang C, Zink DL, Ushio M, Burgess B, Onishi R, Masurekar P, Barrett JF, Singh SB (2008) *Bioorg Med Chem* 16:8818–8823
9. Haack M, Enck S, Seger H, Geyer A, Beck-Sickinger AG (2008) *J Am Chem Soc* 130: 8326–8336
10. Just-Baringo X, Albericio F, Álvarez M (2014) *Mar Drugs* 12:317–351
11. Ganguly B, Fuchs B (2000) *J Org Chem* 65:558–561
12. Choudhary A, Gandla D, Krow GR, Raines RT (2009) *J Am Chem Soc* 131:7244–7246
13. Risseuw MD, Overhand M, Fleet GWJ, Simone MI (2013) *Amino Acids* 45:613–689
14. Risseuw MD, Overhand M, Fleet GWJ, Simone MI (2007) *Tetrahedron Asymmetry* 18: 2001–2010
15. Fuchs E-F, Lehmann J (1976) *Carbohydr Res* 49:267–273
16. Graf von Roedern E, Kessler H (1994) *Angew Chem Int Ed Engl* 33:687–689
17. Dondoni A, Marra A (2000) *Chem Rev* 100:4395–4422
18. Simone MI, Edwards AA, Tranter GE, Fleet GWJ (2011) *Amino Acids* 41:643–661
19. Siriwardena A, Pulukuri KK, Kandiyal PS, Roy S, Bande O, Ghosh S, GarciaFernández JM, Martin FA, Ghigo J-M, Beloin C et al (2013) *Angew Chem Int Ed* 52:10221–10226
20. Chakraborty TK, Koley D, Ravi R, Krishnakumari V, Nagaraj R, Chand Kunwar A (2008) *J Org Chem* 73:8731–8744
21. Wyvratt MJ, Tischler MH, Ikeler TJ, Springer JP, Tristram EW, Patchett AA (1983) In: Hruby VJ, Rich DH (eds) *Proceedings of the 8th American peptide symposium*. Pierce Chemical, Rockford, p 551
22. Nagai U, Sato K (1985) *Tetrahedron Lett* 26:647–650
23. Grotenbreg GM, Timmer MSM, Llamas-Saiz AL, Verdoes M, van der Marel GA, van Raaij MJ, Overkleeft HS, Overhand M (2004) *J Am Chem Soc* 126:3444–3446
24. Knijnenburg AD, Tuin AW, Spalburg E, de Neeling AJ, Mars-Groenendijk RH, Noort D, Otero JM, Llamas-Saiz AL, van Raaij MJ, van der Marel GA (2011) *Chem Eur J* 17: 3995–4004
25. Knijnenburg AD, Kapoerchan VV, Grotenbreg GM, Spalburg E, de Neeling AJ, Mars-Groenendijk RH, Noort D, Otero JM, Llamas-Saiz AL, van Raaij MJ (2011) *Bioorg Med Chem* 19:3402–3409
26. Risseuw MDP, Mazurek J, van Langenvelde A, van der Marel GA, Overkleeft HS, Overhand M (2007) *Org Biomol Chem* 5:2311
27. Kueh JTB, Choi KW, Williams GM, Moehle K, Bacsá B, Robinson JA, Brimble MA (2013) *Chem Eur J* 19:3807–3811
28. Freidinger R, Veber D, Perlow D, Brooks JR, Saperstein R (1980) *Science* 210:656–658
29. Khashper A, Lubell WD (2014) *Org Biomol Chem* 12:5052–5070
30. Viles JH, Patel SU, Mitchell JB, Moody CM, Justice DE, Uppenbrink J, Doyle PM, Harris C, Sadler PJ, Thornton JM (1998) *J Mol Biol* 279:973–986
31. Baca M, Kent SBH, Alewood PF (1993) *Protein Sci* 2:1085–1091
32. Eckhardt B, Grosse W, Essen LO, Geyer A (2010) *Proc Natl Acad Sci U S A* 107: 18336–18341
33. Boudko SP, Kuhn RJ, Rossmann MG (2007) *J Mol Biol* 366:1538–1544
34. Brandänge S, Färnäck M, Leijonmarck H, Sundin A (2003) *J Am Chem Soc* 125: 11942–11955
35. Kessler H (1982) *Angew Chem Int Ed Engl* 21:512–523
36. Zimmerman SS, Scheraga HA (1977) *Proc Natl Acad Sci U S A* 74:4126–4129
37. Eckhardt B (2009) *Dissertation, Philipps-Universität Marburg, Marburg*

38. Haubner R, Schmitt W, Hölzemann G, Goodman SL, Jonczyk A, Kessler H (1996) *J Am Chem Soc* 118:7881–7891
39. Körling M, Geyer A (2015) *Eur J Org Chem* 2015:2382–2387
40. Geyer A, Moser F (2000) *Eur J Org Chem* 2000:1113–1120
41. Tremmel P, Geyer A (2002) *J Am Chem Soc* 124:8548–8549
42. Geyer A, Bockelmann D, Weissenbach K, Fischer H (1999) *Tetrahedron Lett* 40:477–478
43. Tremmel P, Geyer A (2004) *Angew Chem Int Ed* 43:5789–5791
44. Hörger R, Geyer A (2006) *Org Biomol Chem* 4:4491
45. Malke M, Barqawi H, Binder WH (2014) *ACS Macro Lett* 3:393–397

Thiazoles in Peptides and Peptidomimetics

Jeffrey Y.W. Mak, Weijun Xu, and David P. Fairlie

Abstract The natural occurrence of the thiazole ring in chemistry and biology has inspired its widespread use in synthetic peptidomimetics as structural templates, biological probes, and pharmaceuticals. Thiazole can be viewed as a dehydrated cyclized derivative of cysteine, incorporated into peptide sequences through chemical synthesis or ribosomal biosynthesis. Thiazoles are planar heterocycles and valuable synthetic templates with a strong hydrogen bond accepting nitrogen, a sulfur atom with extended lone pair electron orbitals, and an aromatic π -cloud. These properties can influence molecular conformation and direct interactions with proteins, leading to development of thiazole-containing peptidomimetics as protein mimicking scaffolds, modulators of cell surface proteins like G protein-coupled receptors (GPCRs), inhibitors of enzymes, and agonists or antagonists of protein–protein interactions. The thiazole ring is the most common five-membered heterocycle present in pharmaceuticals. This perspective article describes important properties of thiazoles in synthetic peptidomimetics and highlights key examples, including some from the last 5 years.

Keywords Amino acid · Conformation · Cyclic peptide · Cysteine · Drug · Heterocycle · Peptidomimetic · Pharmaceutical · Protein structure · Thiazole

Contents

1	From Cysteine to Thiazoles and Peptidomimetics	236
2	Chemistry of Thiazoles	238
	2.1 Syntheses of Thiazoles	238
	2.2 Stereoelectronic Properties of Thiazoles	242
	2.3 Chemical Reactivity of Thiazoles	243

J.Y.W. Mak, W. Xu, and D.P. Fairlie (✉)

Division of Chemistry and Structural Biology, Institute for Molecular Bioscience,
The University of Queensland, Brisbane, QLD 4072, Australia
e-mail: d.fairlie@imb.uq.edu.au

3	Thiazoles as Peptide Surrogates and Synthetic Building Blocks	245
3.1	Thiazoles as Synthetic Building Blocks	245
3.2	Thiazoles as Capping Groups in Peptidomimetics	245
3.3	Thiazole Influences Conformation in Peptidomimetics	246
3.4	Thiazoles as Amide Bond Replacements	249
4	Thiazoles in Peptidomimetics and Cyclic Peptides	250
5	Protein-Binding Thiazoles and Thiazole Drugs	255
5.1	Kinase Inhibition by Dasatinib	256
5.2	p38 α Kinase Inhibitors	258
5.3	Cyclic Dependent Kinase Inhibitor	258
5.4	Thrombin Inhibitor	259
5.5	DNA-Binding Thiazole	259
5.6	Thiazole-Containing Drugs	259
6	Concluding Remarks	262
	References	262

Abbreviations

CCK	Cholecystokinin
CRF	Corticotropin-releasing factor
cSRC	Proto-oncogenic (sarcoma) protein tyrosine-protein kinase
FDA	Food and drug administration (USA)
NSAID	Non-steroidal anti-inflammatory drug
SAR	Structure–activity relationships

1 From Cysteine to Thiazoles and Peptidomimetics

Thiazole (C₃H₃NS) is a five-membered heterocyclic aromatic compound found in many natural products [1–4] including vitamin B1 and has been widely incorporated into synthetic molecules including pharmaceuticals [5], catalysts [6], and dyes [7]. Indeed, thiazole is a more common component of FDA-approved pharmaceuticals than related five-membered heterocycles such as isothiazole, thiophene, furan, isoxazole, and oxazole (Fig. 1). This perspective briefly summarizes thiazole chemistry [8] and focuses on current knowledge of thiazole peptidomimetics and their interactions with proteins.

From a peptidomimetic perspective, thiazole can be viewed as a derivative of cysteine, in much the same way as oxazole can be considered a derivative of serine or threonine (Scheme 1). Within a peptide sequence, a thiazole can be considered to represent a net condensation between the thiolate side chain of cysteine (e.g., in **1**) and the C-terminus of an adjacent amino acid with elimination of water to produce a dipeptide surrogate (Scheme 1). This heterocyclization with dehydration forms a thiazoline (e.g., **3**) that may undergo dehydrogenation to provide the thiazole (e.g., **5**). This set of reactions occurs in both ribosomal and non-ribosomal biosynthesis. The consequences of this condensation include the following: (1) the C-terminal

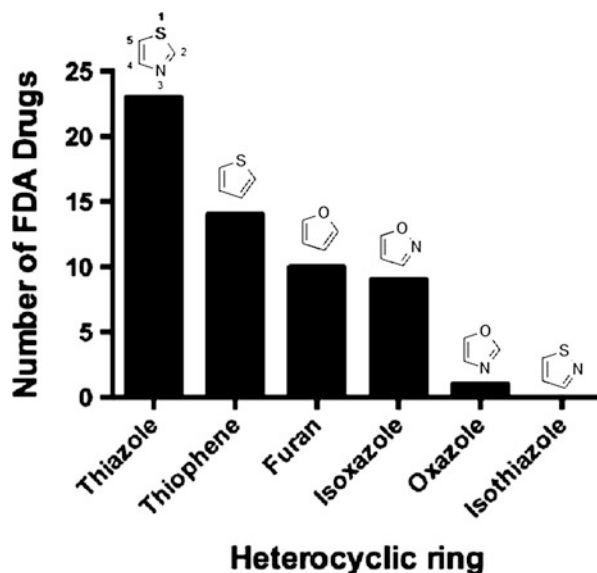
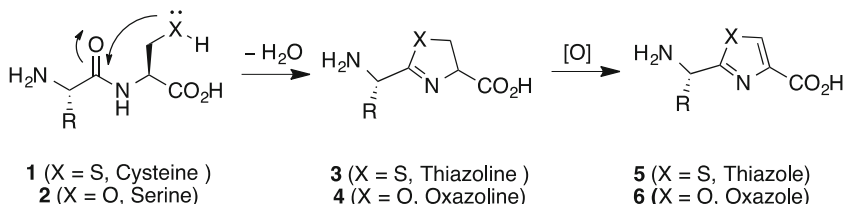


Fig. 1 Number of FDA-approved pharmaceuticals containing a single heterocyclic ring. The FDA1216 database [9] was searched for each heterocyclic ring using the ligand filtering module within Schrödinger software. Numbering convention shown for thiazole



Scheme 1 Condensation of the cysteine (X=S, **1**) and serine (X=O, **2**) side chains to give, respectively, thiazoline **3** and oxazoline **4**, followed by dehydrogenative aromatization to thiazole **5** and oxazole **6** dipeptide surrogates [10]

carboxylate is reoriented due to attachment to the sp^2 carbon of thiazole versus an sp^3 carbon in cysteine; (2) replacement of the N-terminal amide and cysteine thiol by the thiazole reduces polarity and hydrogen bond donors; (3) the cysteine stereochemical center is removed; (4) overall, this cyclization rigidifies the peptide backbone and favors turn conformations that may facilitate peptide cyclization.

The thiazole ring in dipeptide surrogates (e.g., **5**) may be reduced to the thiazoline (one double bond) or thiazolidine (no double bonds) to provide a range of conformational and stereochemical influences on the spatial disposition of the N- and C-terminus of the mimetic, to alter the capacity of the heterocycle to fit into hydrophobic binding sites in proteins, and to modify the hydrogen bonding properties of the heteroatoms. We shall return to peptidomimetics after briefly summarizing the chemistry of the thiazole heterocycle.

2 Chemistry of Thiazoles

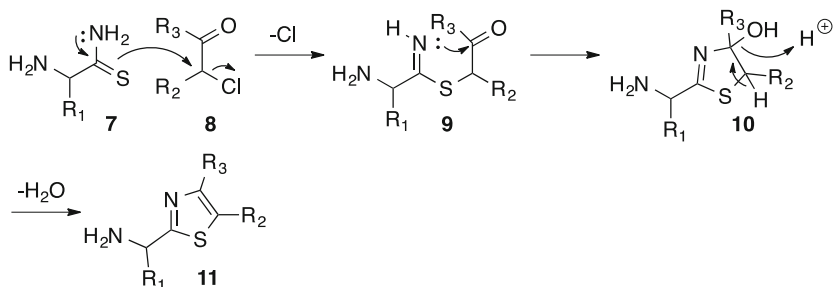
2.1 Syntheses of Thiazoles

The reactivity and synthesis of thiazoles has been previously reviewed [8, 11–16], and only such chemistry relevant to their use as peptidomimetics is presented below. Thiazoles have been traditionally prepared from open-chained components by a number of methods, among which the Hantzsch synthesis is preferred (Scheme 2) [17]. Thioamides (e.g., **7**) and α -halocarbonyls (e.g., **8**) combine to form thiazoles (e.g., **11**) via halide displacement (to give **9**) and subsequent condensation (e.g., **10**) [18]. All three carbons of the components may possess alkyl and aryl substituents, such that various substituted thiazoles may be synthesized [19]. For example, the thioamide component can be replaced by a thiourea to give the corresponding 2-aminothiazole [20].

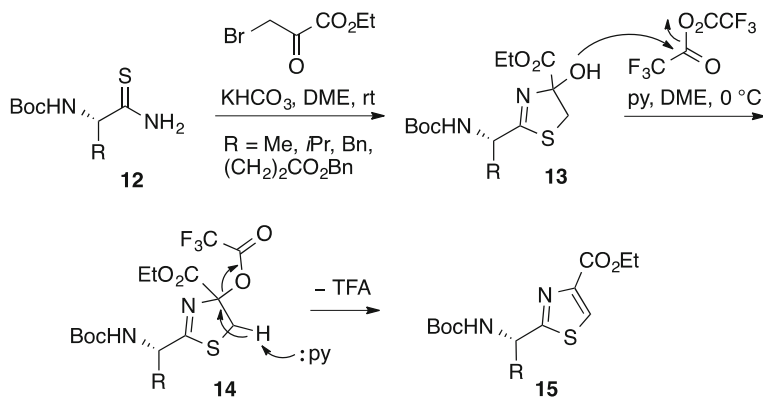
Racemization in the synthesis of thioamides derived from enantiomerically pure α -amino acids has been reported due to base-promoted epimerization [21]. Furthermore, application of α -amino acid-derived thioamides in the Hantzsch synthesis has been suggested to cause racemization from acid-catalyzed imine to enamine equilibrium during cyclization prior to aromatization [22, 23]. A modified Hantzsch synthesis protocol was developed to obtain enantiomerically pure α -amino acid-derived thiazoles (e.g., **15**) [23, 24]. After alkylation of thioamide **12** with ethyl bromopyruvate gave **13**, the hydroxyl group was trifluoroacetylated (to give **14**) and then eliminated in one pot using trifluoroacetic anhydride and pyridine at low temperature (Scheme 3).

The practicality of the Hantzsch synthesis was demonstrated by the preparation of orthogonally protected thiazole diamino acids **21**. β -Alanines **16** were converted to β -keto esters **18** by acylation with Meldrum's acid (**17**) and solvolytic decarboxylation. α -Chlorination of **19** with sulfuryl chloride followed by condensation with thiourea gave 2-aminothiazoles **20**, which were suitably *N*-protected and saponified to give **21** (Scheme 4) [25].

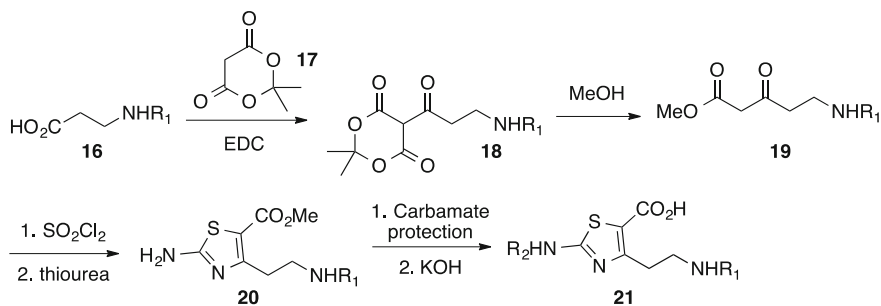
The Hantzsch reaction has also demonstrated utility for peptide macrocyclization (Fig. 2). In the case of macrocycle **22**, the Hantzsch synthesis



Scheme 2 Mechanism of the Hantzsch thiazole synthesis



Scheme 3 Modified Hantzsch thiazole synthesis for production of enantiomerically pure α -amino acid-derived thiazoles



Scheme 4 Synthesis of orthogonally protected thiazole diamino acids **21**

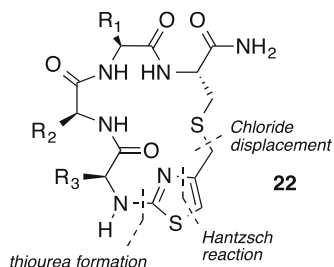
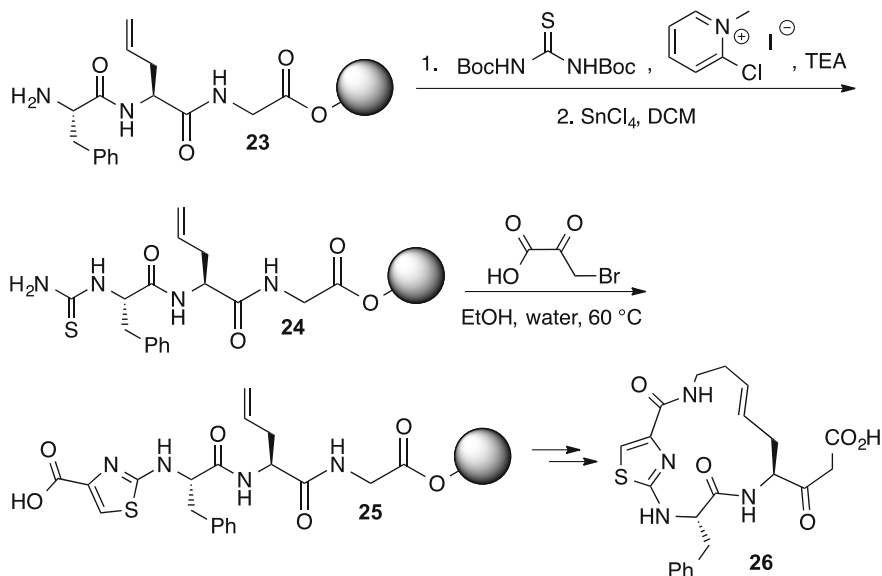


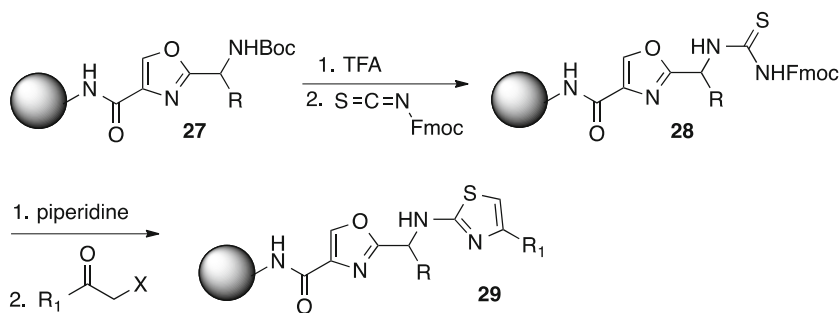
Fig. 2 Hantzsch strategy for the synthesis of peptide macrocycle **22**

installed a cysteine mimetic in the form of a thiazole ring, possessing a 4-position alkyl chloride, which was displaced by the thiol of a cysteine residue in the macrocyclization step [26].

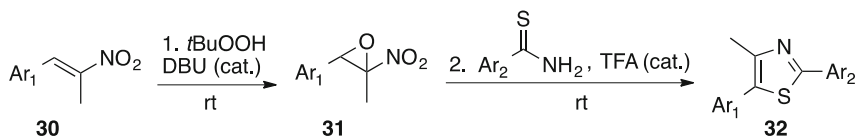
The Hantzsch synthesis has been conducted on solid phase to synthesize thiazole-containing peptide macrocycles [27]. The N-terminus of peptide **23** on solid support was reacted with *N,N'*-di-Boc-thiourea and Mukaiyama's reagent to



Scheme 5 Hantzsch thiazole formation in solid phase macrocycle synthesis



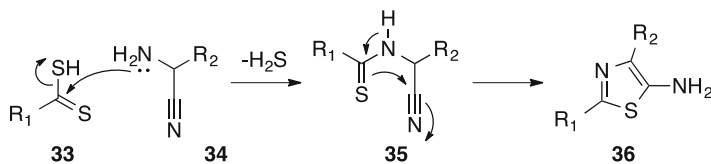
Scheme 6 Solid phase Hantzsch thiazole synthesis with *N*-Fmoc-NCS



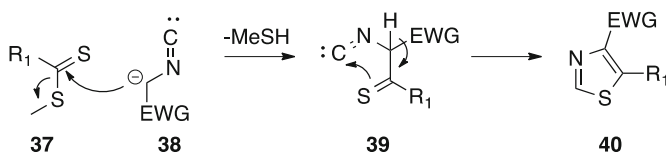
Scheme 7 One-pot synthesis of 2,5-diaryl thiazoles from nitrostyrenes **30**

give thiourea **24**. Subsequent treatment of **24** with α -bromopyruvic acid gave thiazole **25** en route to macrocycle **26** (Scheme 5).

Alternatively, *N*-Fmoc-isothiocyanate has been used to prepare thioureas **28** for solid phase Hantzsch syntheses of thiazoles **29** (Scheme 6) [28].



Scheme 8 Thiazole formation from dithioacid **33** and α -aminonitrile **34** in the Cook–Heilbron synthesis



Scheme 9 Modified Cook–Heilbron synthesis of 4,5-disubstituted thiazoles **40** using activated methylene isocyanides **38**

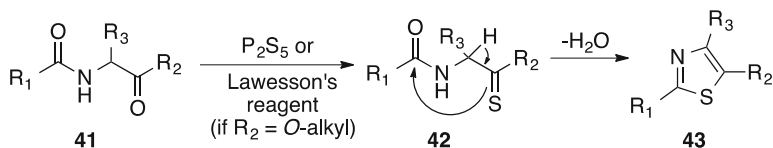
A one-pot formation of 1,3-thiazoles from nitrostyrenes **30** (Scheme 7) was developed based on a Hantzsch strategy [29]. Oxidation of nitrostyrenes **30** gave α -nitro-epoxides **31**, which serves as the α -halocarbonyl equivalent in condensations with thioamides to give the thiazoles **32**, albeit the reaction scope was limited to the formation of 2,5-diaryl thiazoles.

The Cook–Heilbron synthesis gives access to 5-aminothiazoles (e.g., **36**) with 2-position substituents [30–32]. Thioamidation of α -aminonitrile **34** with thiocarbonyl electrophiles, such as carbon disulfide, dithioesters, dithioacids (as exemplified by **33**), and isothiocyanates, provides thioamide intermediate **35**, which cyclizes to 5-aminothiazole **36** (Scheme 8).

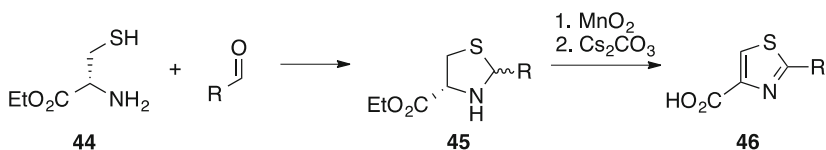
Employment of activated methylene isocyanide **38**, instead of the aminonitrile, in the condensation with dithioester **37** gave access to 4,5-substituted thiazoles **40** by way of thioketone intermediate **39** (Scheme 9) [33].

The Gabriel synthesis features conversion of α -acylamino ketones **41** into the corresponding thioketones **42**, which undergo intramolecular condensation to thiazole **43** [34, 35]. Substitution of Lawesson's reagent in place of phosphorus pentasulfide as thionating agent has expanded the approach to α -amido esters to make 5-alkoxythiazoles (Scheme 10) [36].

2,4-Disubstituted thiazoles **46** have also been synthesized from cysteine. For example, cysteine ethyl ester (**44**) has been condensed with aldehydes to give thiazolidines **45**, which were oxidized with manganese dioxide to give the corresponding substituted thiazoles **46** on multi-gram scale (Scheme 11) [37].



Scheme 10 Simplified mechanism of the Gabriel synthesis of thiazoles



Scheme 11 Synthesis of 2,4-disubstituted thiazoles from cysteine ethyl ester

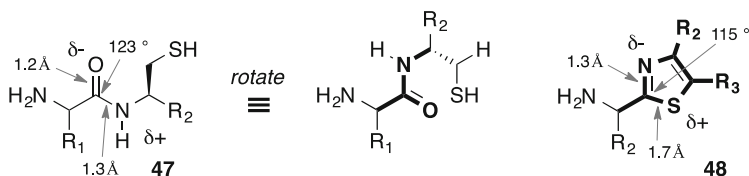


Fig. 3 Selected bond lengths and angles of amide **47** and thiazole **48** with coplanar atoms in *bold*. Bond angles and lengths correspond to unsubstituted thiazole [38]

2.2 Stereoelectronic Properties of Thiazoles

Thiazoles possess a number of stereoelectronic properties that may impact on their peptidomimetic derivatives. Thiazoles are planar aromatic heterocycles in which the relative connectivity of the heteroatoms, the bond lengths, and the bond angles all compare favorably with the planar amide bond in peptides, except that the C–S bond is considerably longer than the carbonyl C=O bond (Fig. 3) [38]. Replacement of a cysteine residue by a thiazole ring forces three additional atoms into the same plane as the amide (Fig. 3, shown in *bold*). Furthermore, a 5-position substituent (R_3) may be introduced, occupying space inaccessible by the cysteine residue.

The thiazole ring structure satisfies Hückel's rule ($n = 1$) courtesy of the delocalization of the lone pair of the sulfur atom. Relative to oxazole, which has little aromatic character, thiazole is considered to be aromatic, due in part to π -electron delocalization of the lone pair on the sulfur atom [39]. Calculations of the electron density distribution in thiazole by many different methods indicate the sulfur and nitrogen atoms have, respectively, net positive and negative charges, and C-2 and C-5 are, respectively, slightly positive, but close to neutral, and slightly negative [40]. The computational results are consistent with experiments indicating nucleophiles attack preferentially at C-2 and electrophiles react with C-5 (Fig. 4).

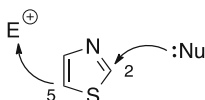


Fig. 4 The 2- and 5-positions of thiazole react preferentially with nucleophiles and electrophiles, respectively

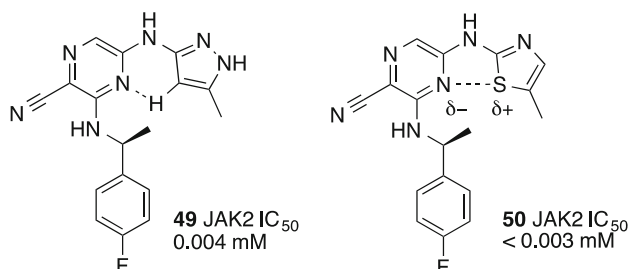


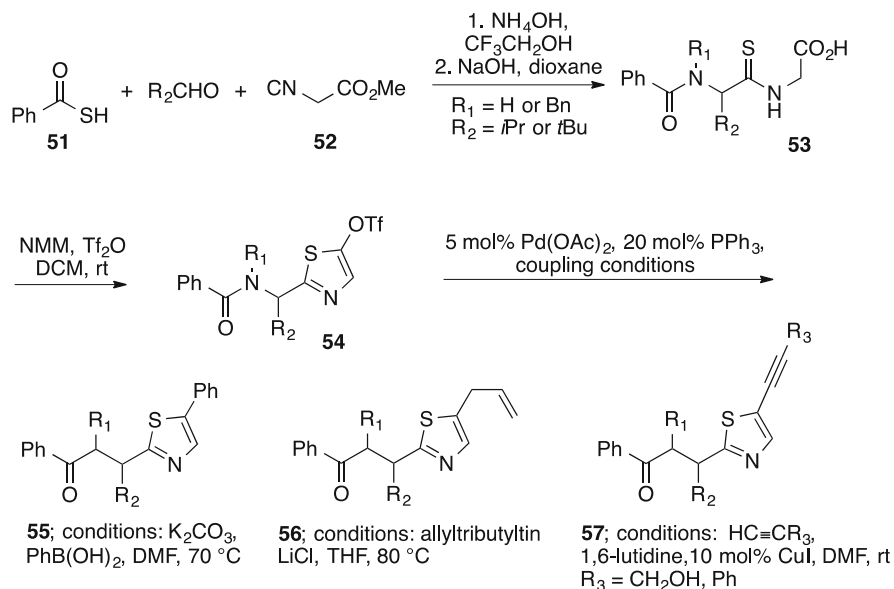
Fig. 5 The predicted N–HC hydrogen bond in pyrazole **49** was successfully replaced by a N–S electrostatic interaction in thiazole **50**

The thiazole sulfur has been suggested to form non-covalent interactions with electron-rich regions of molecules [41]. For example, replacement of a thiazole for the pyrazole ring in Janus kinase 2 inhibitor **49** gave analogue **50**, which exhibited similar potency (Fig. 5). Based on the predicted binding mode, a co-planar electrostatic interaction between the nitrogen (δ^-) of the pyrazine and the sulfur (δ^+) of the thiazole of inhibitor **50** was presumed to replace the hydrogen bond between the pyrazine and 5-position proton of the pyrazole in **49** [41].

The thiazole sp^2 nitrogen is basic. With lone pair electrons sitting outside of the aromatic π -system, the thiazole nitrogen can act as a moderately strong hydrogen bond acceptor, similar to the oxygen of an amide. With a pK_a of 2.5 for the protonated form of unsubstituted thiazole, the nitrogen is typically not protonated under physiological conditions; however, thiazole basicity is affected by ring substitution [42]. Typically, 2-, 4-, and 5-position alkyl groups increase basicity with decreasing potency. For example, the pK_a values of protonated 2-, 4-, and 5-methylthiazoles are 3.4, 3.2, and 3.1, respectively. Protonated 2-aminothiazole has a pK_a of 5.4, due to resonance between the exocyclic amine and the conjugated π system. Protonated benzothiazole and electron-deficient thiazoles, such as nitrothiazole, are relatively more acidic than thiazole.

2.3 Chemical Reactivity of Thiazoles

Unlike their structurally related oxazole counterparts, thiazoles do not usually react in cycloaddition reactions, due to their greater aromaticity [43–45]. Unless activated by electron donating groups (e.g., amino or hydroxyl groups) [46], similar to



Scheme 12 Synthesis of 5-substituted thiazole peptides via the Ugi reaction

π -deficient pyridines, thiazoles typically resist electrophilic attack, due in part to deactivation by the nitrogen [40]. For example, thiazoles are resistant to nitration, sulfonation, and halogenation in strongly acidic media, because nitrogen protonation depletes ring electron density. The C-2 proton possesses greater kinetic and thermodynamic acidity [40], relative to those at C-4 and C-5, and may be deprotonated with alkyl lithium bases [47] and lithium diisopropylamide [48]. Together with thiazole Grignard reagents [47], C-lithiated species have been reacted with various carbon electrophiles. The C-2 position is prone to nucleophilic attack and becomes even more reactive to nucleophiles upon alkylation of the thiazole nitrogen to give the corresponding thiazolium salts [19].

Appropriately functionalized thiazole derivatives have been substrates in palladium-catalyzed reactions, such as Suzuki, Stille, Negishi, Sonogashira, as well as Heck coupling reactions [49, 50], albeit few examples of the latter have been reported [19]. The thiazole tin and zinc reagents serve, respectively, as nucleophilic partners in Stille and Negishi cross-coupling reactions. In Suzuki cross-couplings, however, halothiazoles act typically as the electrophilic component, because of the instability of thiazole boronates, especially those with boron at C-2 [19, 51]. Scalable syntheses of 2-bromothiazole, as well as 2,4- and 2,5-dibromothiazoles from inexpensive commercially available starting materials, have facilitated the use of metallation and palladium-catalyzed reactions [52].

The Ugi reaction has been exploited for the synthesis of thiazole-containing peptides, albeit without stereochemical control [53, 54]. After the Ugi reaction and ester hydrolysis afforded thioamide **53**, treatment with triflic anhydride in CH_2Cl_2 gave thiazole triflate **54**, which was employed in a series of palladium-catalyzed

cross-coupling reactions to prepare thiazoles possessing proton, allyl, acetylenyl and aryl 5-position substituents (e.g., **55**, **56**, and **57**, Scheme 12) [55].

3 Thiazoles as Peptide Surrogates and Synthetic Building Blocks

3.1 Thiazoles as Synthetic Building Blocks

There are many useful thiazole synthetic blocks that are commercially available (e.g., **58–66**, Fig. 6). Thiazoles have found wide application within peptidomimetics, due in part to effective methods for installing substituents at each of the ring carbons [6, 56–58].

3.2 Thiazoles as Capping Groups in Peptidomimetics

Thiazoles have been used to cap the N- and C-termini of peptides and peptidomimetics, such as in the anticancer agent dolastatin-10 (**68**, Fig. 7) [59, 60]. In the PAR2 agonist 2at-LIGRL-NH₂ (**67**, Fig. 7 2at=2-aminothiazol-4-oyl), the aminothiazoyl group was used as a metabolically stable N-terminus cap [61], which may confer additional chemical and biological stability to the peptide [62, 63]. Frequently, the thiazole fits neatly into an indentation in the surface of a protein target, offering interactions with its π cloud or its hydrogen bond accepting nitrogen (see Sect. 5).

2-Aminothiazole was used as a heterocyclic cysteine surrogate in the development of Ras protein C-terminal CAAX tetrapeptide mimetics for the inhibition of

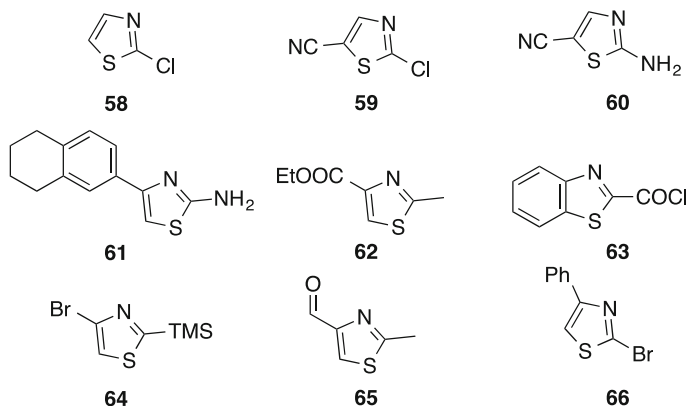


Fig. 6 Useful thiazole-containing synthetic building blocks

Fig. 7 PAR2 agonist 2at-LIGRL-NH₂ (**67**, 2at=2-aminothiazol-4-oyl) and dolastatin-10 (**68**)

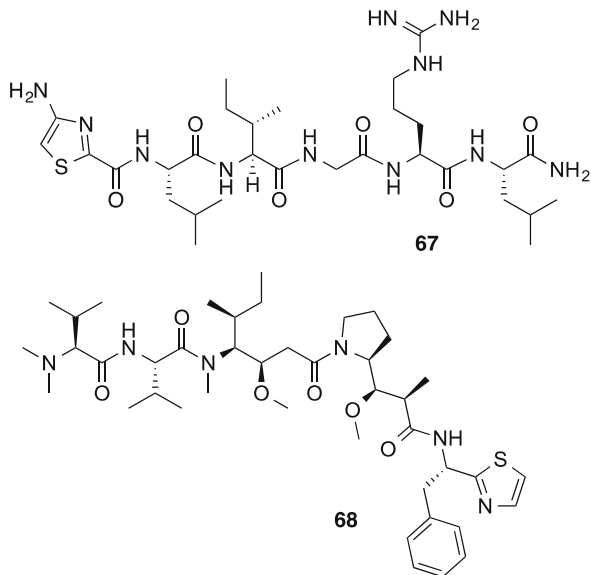
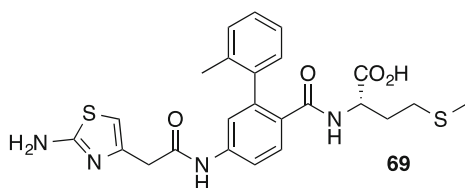


Fig. 8 Based on the C-terminal Ras protein tetrapeptide CAAX sequence, 2-aminothiazole served as a cysteine mimetic in FTase inhibitor **69**



the zinc metalloenzyme farnesyltransferase (FTase, Fig. 8) [64]. In previous studies, a pyridine group had been successfully employed as a metabolically stable cysteine mimetic. The 2-aminothiazole was tested as an alternative, because of its comparable basicity to pyridine, and pronounced properties for forming metal complexes. Thiazole peptidomimetic **69** inhibited FTase activity (IC_{50} 49 nM) and rat smooth muscle cell proliferation (IC_{50} 107 μ M). Described as a potentially promiscuous scaffold [65], 2-aminothiazole is a component of some drugs and has gained significant consideration for employment in drug discovery.

3.3 Thiazole Influences Conformation in Peptidomimetics

Thiazoles exert stereoelectronic effects on adjacent carboxamides that dictate their conformation [66, 67]. The solid-state structures of six thiazole-5-carboxamide analogues have been deposited in the Cambridge crystallographic database. The four thiazole-5-carboxamides **71** possessing a 1,4-relationship between the sulfur and carbonyl oxygen atom exhibited a S–C–O dihedral angle value between

Fig. 9 The dipole moment of the thiazole ring can dictate the conformation of the neighboring amide

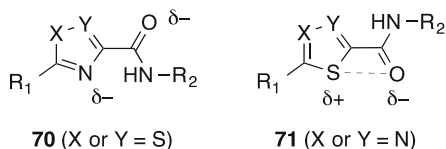
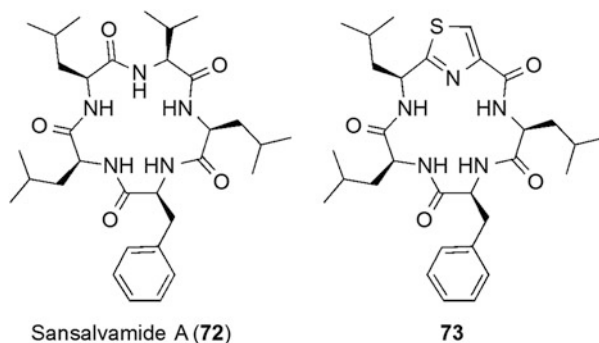


Fig. 10 Sansalvamide A (72) and its thiazole analogue 73



11° and 37° and S–O distances that were less than the sum of the van der Waal radii, suggesting an attractive interaction (Fig. 9). On the other hand, the two thiazole-5-carboxamides **70** with a 1,4-relationship between the thiazole nitrogen and the amide carbonyl oxygen had N–C–C–O torsion angle values of 165° and 173°. On switching locations of the nitrogen and sulfur heteroatoms in thiazole-5-carboxamides **70** and **71** (Fig. 9), the altered dipole and orbital alignments result in opposite amide orientations with different three-dimensional electrostatic surfaces. These differences translated into opposing agonist versus antagonist activity in activating a G protein-coupled receptor (GPCR, i.e., the complement C-3a receptor) on human macrophages [66]. The influence of the heteroatom was confirmed by locking the heterocyclic amide conformation using fused bicyclic rings.

Toward the development of potential anticancer agents, peptidomimetics of the cytotoxic cyclic pentapeptide sansalvamide A (**72**) were prepared employing triazole, oxazole, and thiazole rings as amide bond isosteres (Fig. 10) [68]. Replacement of the Leu-Val residue with thiazole (**73**) gave an analogue with equal cytotoxicity to the parent sansalvamide A (**72**). The relative cytotoxicity of the heterocycle analogues was rationalized on their ability to adopt backbone conformation and side chain presentations similar to the native peptide [68].

4-Amino(methyl)-1,3-thiazole-5-carboxylic acids have served as turn-inducing constraints in peptides such as an analogue of gramicidin S that maintained strong antibacterial activity with reduced hemolytic activity [69]. Oligomers of the 4-amino(methyl)-1,3-thiazole-5-carboxylic acids in γ -peptides adopted a right-handed 9-helix structure [70]. Potent examples of thiazole GPCR ligands include cholecystokinin-1 (CCK1) agonist SR146131 (**74**) and antagonist SR27897 (**75**, IC₅₀ > 0.58 nM CCK; 489 nM CCK2), orally active corticotropin-releasing factor

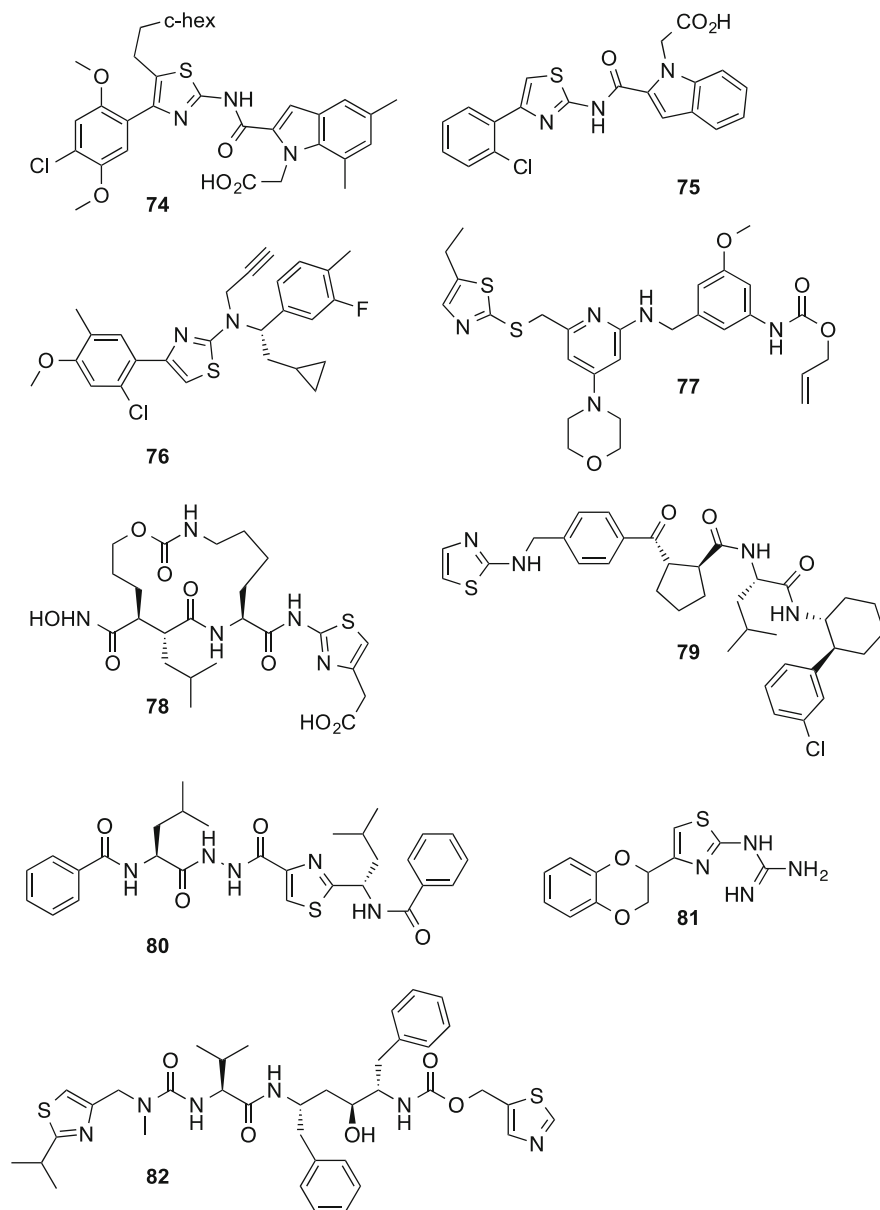


Fig. 11 Thiazole-containing GPCR modulators (74–77) and enzyme inhibitors (78–82)

(CRF) antagonist SSR-125543A (**76**, $K_i = 2$ nM, CRF1), and orally active and brain permeable neuropeptide Y antagonist J-104870 (**77**, $Y_1 < 1$ nM; $Y_2, Y_4 > 10$ μ M; Y_5 6 μ M) (Fig. 11) [71].

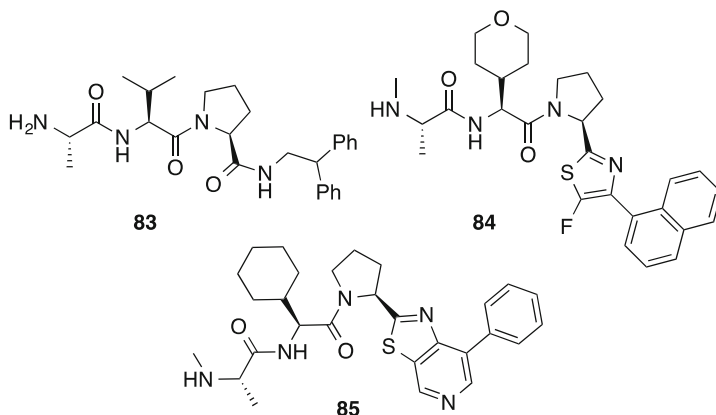


Fig. 12 Thiazoles as amide replacements in IAP antagonists

Thiazoles have served as linkers and capping groups in peptide-mimicking ligands that inhibit enzymes, for example, in tumor necrosis factor- α converting enzyme inhibitor **78** (IC_{50} 0.08 μ M), cyclin-dependent kinase inhibitor **79** (IC_{50} 40 nM, CDK2), cathepsin K inhibitor **79** (K_i 10 nM), ERK inhibitor **81** (K_d 16 μ M, ERK2), and the HIV protease inhibitor ritonavir (**80**, IC_{50} \sim 1 nM, HIV-1 protease) [72].

3.4 Thiazoles as Amide Bond Replacements

Thiazoles have been used as amide bond isosteres. For example, in the development of inhibitors of apoptosis protein (IAP) antagonists, the proline amide bond of lead peptide **83** did not make any specific interactions with the target protein (Fig. 12) [73]. Thus, the amide bond was replaced with thiazole and benzothiazole surrogates to fine-tune the physicochemical properties. The most potent of these thiazole analogues (e.g., **84** and **85**) had K_i values of 20–60 nM against targeted IAPs.

Thiazoles were used as amide bond replacements in the development of peptidomimetic oligomers that modulate the activity of human *p*-glycoprotein [74]. Linear and cyclic trimer oligomers of (*S*)-valine-derived thiazole units **5** ($R = i$ -Pr, Scheme 1) exhibited low micromolar inhibition of human *p*-glycoprotein. Consistent with being effective amide bond replacements, thiazole-based amino acids have also been used to construct peptide secondary structures analogous to those of natural amino acids, such as helical oligomers [70, 75], β -strand mimics [72], and turn mimics [69, 71].

Bi-thiazoles (Fig. 13) may be considered peptide mimics and have served in enzyme inhibitors, protein-binding motifs, and natural products. For example, bi-thiazole-2,2'-diamines (**86** and **87**, Fig. 13) compete against peptide substrates that bind cJun N-terminal kinases (JNKs) [76]. When incorporated into peptide

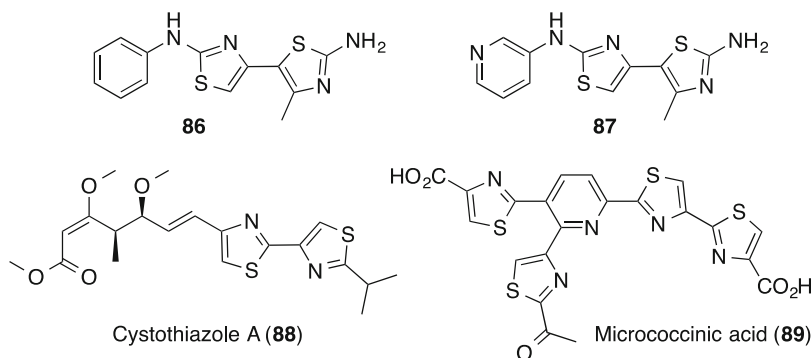


Fig. 13 Bithiazole-2,2'-diamines **86** and **87** and bithiazole natural products cystothiazole A (**88**) and micrococcinic acid (**89**)

sequences, these scaffolds can restrict conformation. The bi-thiazole natural product antibiotic cystothiazole A (**88**) kills human colon cancer and leukemia cells (Fig. 13) [77, 78]. Bi-thiazoles occur in other natural products such as micrococcinic acid (**89**) and macrocyclic peptides (see section below).

4 Thiazoles in Peptidomimetics and Cyclic Peptides

Thiazoles are present in numerous classes of natural products, particularly alkaloids and cyclic peptides [1, 3, 79–81]. Only a few thiazole macrocycles can be accommodated within the size constraints of this article. The first to be considered here is largazole (**90**, Fig. 14), a metabolite from a cyanobacterium that potently inhibits the growth of triple-negative human breast cancer cells ($GI_{50} = 7.7$ nM) [82–86]. Largazole features a macrocycle containing a thiazole fused to a 4-methylthiazoline. An octanoyl moiety is attached to the macrocycle by way of a thioester to the 3-hydroxy-7-mercaptohept-4-enoic acid subunit and serves to produce a prodrug, which on thioester hydrolysis releases the thiolate that potently inhibits histone deacetylase enzymes. The thiazole–thiazoline bicyclic unit serves primarily as a scaffold that orients the other components of the molecule for protein binding.

Bistratamides (e.g., **91–93**, Fig. 15) are a family of thiazole-containing hexapeptide analogues, which were isolated from the aplouso-branch ascidian *Lissoclinum bistratum* [87]. Bistratamides have exhibited antitumour activity against human colon cancer cells [87]. Their cytotoxicity and that of related macrocycles are contingent on the variety of L-amino acid, oxazole, oxazoline, and thiazole components, which leads to different conformational restrictions [88].

Sanguinamides A and B (**94** and **96**, Fig. 16) are thiazole-containing cyclic hepta- and octa-peptide analogues. Sanguinamide A has inspired analogues exhibiting membrane permeation and oral absorption [89–91]. Sanguinamide B

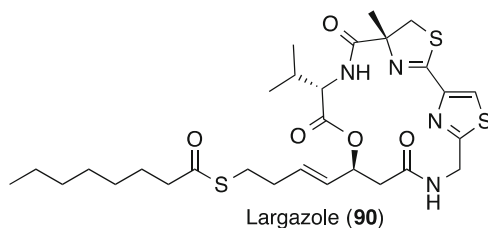


Fig. 14 Largazole (**90**), a thiazole-containing cyclic peptide natural product

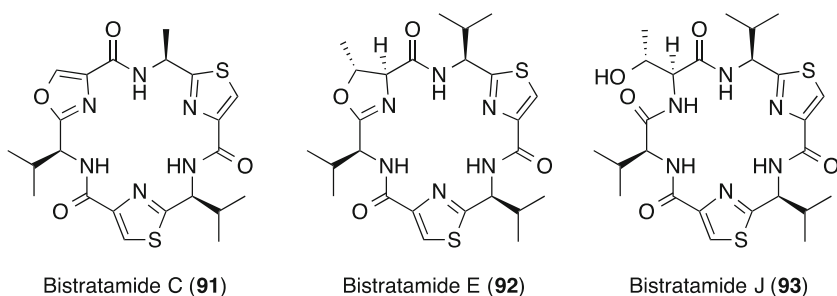


Fig. 15 Bistratamides C (**91**), E (**92**), and J (**93**)

analogues have been the subject of synthetic efforts, due in part to their cytostatic activity [92, 93]. Originally isolated from the sea slug *H. sanguineus* [91], sanguinamide A (**94**) features an isoleucine-thiazole dipeptide surrogate in a 21-member cyclic heptapeptide, *cyclo*-[Ile(Thz)AlaPheProIlePro]. The total synthesis of **94** enabled NMR studies, which revealed two strong intramolecular hydrogen bonds between Ala² and Leu⁵ rigidify the cyclic peptide, which adopts a predominant conformation possessing a prolyl amide *cis*-isomer between Phe³ and Pro⁴ [90]. Replacement of the thiazole constraint by Ala gave a more flexible cyclic peptide with conformers due to *cis*-*trans* isomerization about the Ile⁵-Pro⁶ peptide bond, both retaining the amide *cis*-isomer between Phe³ and Pro⁴ [89]. Guided by amide H-D exchange rates and NMR structures, Ala² was replaced by the bulkier *t*BuGly (i.e., **95**, Fig. 16) to shield solvent-exposed polar atoms, substantially increasing oral bioavailability in rats (7–50%) [89]. Sanguinamide B (**96**, *cyclo*-[Pro-Val-(Ala-Thz)Ile-(ProThzOx)]) was also isolated from *H. sanguineus*. Featuring two prolyl amide *trans*-isomers and an unusual 4,2-oxazole-thiazole unit in a 24-member cyclic octapeptide [92], **96** has exhibited antibacterial (*P. aeruginosa*) and anticancer activity [92–94].

Other thiazole-containing 24-member cyclic octapeptide derivatives include urukthapelstatin A (**97**), patellamide D (**98**), and ascidiacyclamide (**99**) (Fig. 17). Urukthapelstatin A (**97**) was isolated from *Mechercharimyces asporophorigenens* YM11-542 and was characterized by crystallography. The 24-member cycle of **97** contains a sequential oxazole-thiazole moiety that has also been observed in mechercharstatin and telomestatin [95]. Urukthapelstatin A is a potent inhibitor of human cancer cell growth (e.g., IC₅₀ 12 nM, A549 lung fibroblasts).

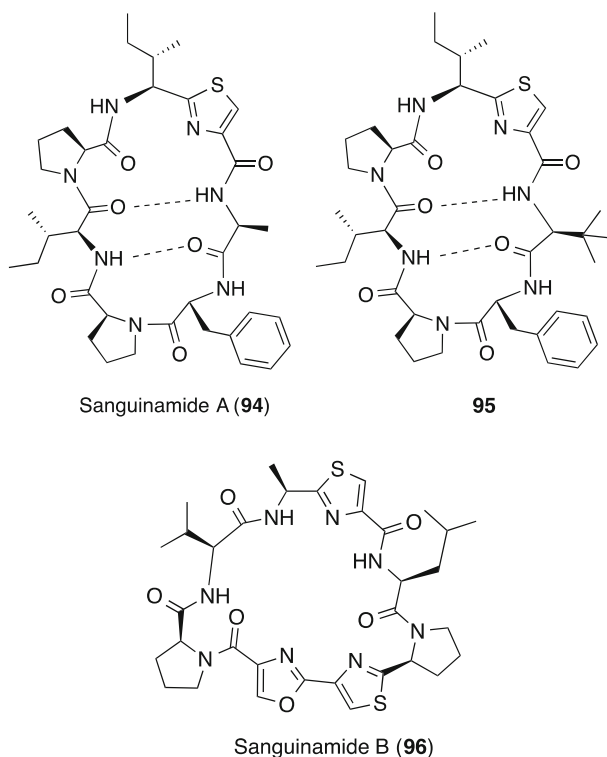


Fig. 16 Sanguinamide A (**94**), *t*BuGly analogue **95**, and sanguinamide B (**96**)

The patellamides are a diverse class of cyclic peptides that exhibit cancer cell cytotoxicity. Biosynthetically produced by enzymes, they possess various oxazoline, oxazole, thiazoline, and thiazole moieties [96–98]. For example, patellamide D (**98**) and ascidiacyclamide (**99**) were isolated from *Lissoclinum patella*, and both have two thiazole and two oxazoline components that create a saddle-shaped conformation that bestows metal binding capability [99]. Each thiazole nitrogen in the cyclic peptide can coordinate to copper, zinc, calcium, and potassium to form one or two metal ion complexes [100]. In complexes with two copper ions, the cyclic peptide can trap carbon dioxide from solution to form a carbonate bridge between the two metal ions [101]. These cleft-forming thiazole peptides can also trap small organic molecules in their cavities [2]. Removal of two of the heterocycles from an ascidiacyclamide analogue completely altered the cleft structure [102] and inspired the use of thiazoles, oxazoles, and their reduced analogues to generate other shapes, including cylindrical and conical structures [103], as well as the preparation of very large macrocycles containing as many as 19 thiazoles and 76 amino acids [104].

There are many larger macrocycles of varying sizes containing thiazoles (Figs. 18 and 19) that are ribosomally derived from complex gene clusters. Most

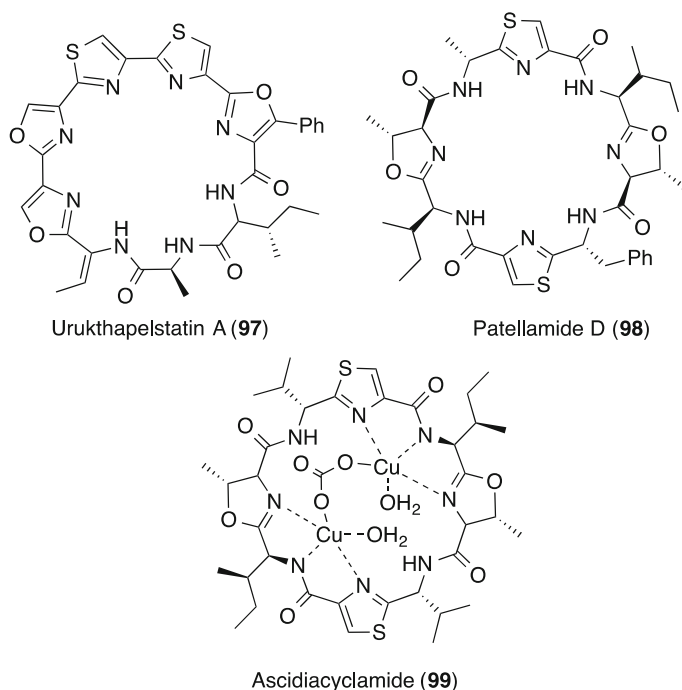


Fig. 17 Thiazole-containing cyclic octapeptide derivatives urukthapelstatin A (**97**), patellamide D (**98**), and ascidiacyclamide (**99**)

notable are the thiopeptide antibiotics, which typically have antibacterial activity against Gram-positive bacteria, and sometimes anticancer, antimalarial, immunosuppressive, and cytotoxic activities at low micromolar concentrations [105]. For example, micrococcin P1 (**100**, Fig. 18) incorporates the four-thiazole unit micrococcinic acid (**89**, Fig. 13), in a 26-member ring that exhibits antimalarial, antiprotozoal, antibacterial, and cytotoxic activities [106]. The natural product GE2270A (**101**) contains five thiazoles and exhibits potent antibacterial activity [107]. The antibiotic GE37468A (**102**) inhibits bacterial protein synthesis. Containing three thiazoles, a thiazoline, an oxazole, and a proline in a 29-member ring, **102** inhibits the growth of a number of bacteria including *Clostridium difficile*. An analogue LFF571 [108] is in clinical trials for treating bacterial infections in the GI tract. Micrococcin P1 (**100**), GE2270A (**101**), and GE37468A (**102**) all have a central pyridine ring. Thiostrepton A (**103**, Fig. 19) is a bis-macrocyclic possessing a dehydropiperidine core linked to one macrocycle comprising of three thiazoles and a thiazoline, a second cycle containing a quinaldic acid macrocycle, and a bis-dehydroalanine tail. Biosynthesis of **103** involves 21 separate genes. Thiostrepton A has also been made by chemical synthesis [109]. Demonstrated to be active against breast cancer cells and Gram-negative bacteria, **103** is an inhibitor of 50S ribosome and 20S proteasome [110], as well as a valuable tool in molecular biology for gene selection in nucleotide metabolism.

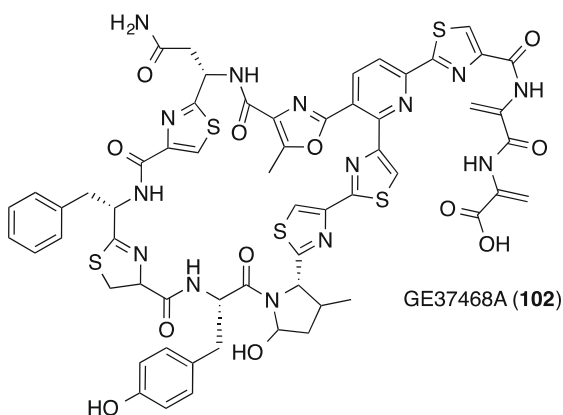
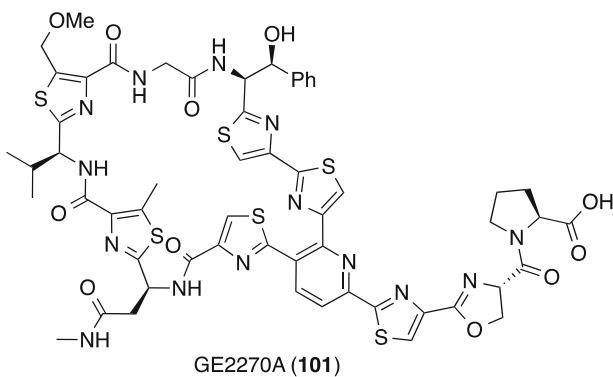
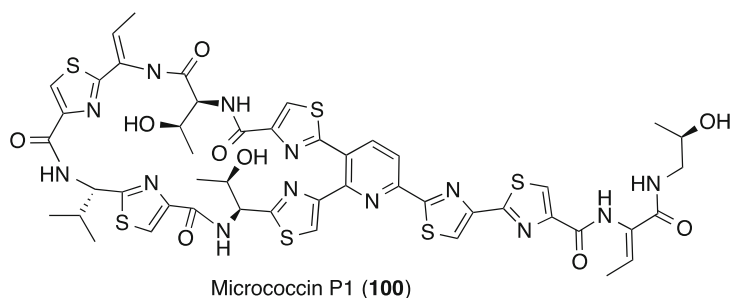


Fig. 18 Micrococcin P1 (thiocillin, **100**), GE2270A (**101**), and GE37468A (**102**)

Although **103** had limited solubility, thiostrepton A is marketed as a drug for treating mastitis and skin infections in domestic animals. The related bis-macrocyclic thiopeptide, nosiheptide (**104**, Fig. 19), is a thiopeptide antibiotic from a marine *actinomycete* strain that has exhibited potency (MIC 0.25 mg/L) against methicillin-resistant *Staphylococcus aureus* (MRSA), drug-resistant clinical isolates, and a virulent strain of *Clostridium difficile*, but was inactive against most

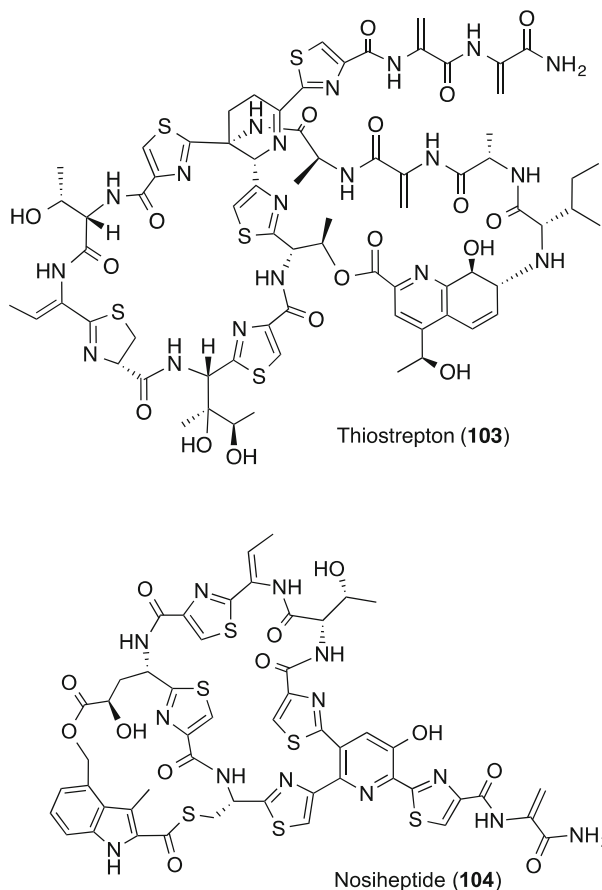


Fig. 19 Thiostrepton (103) and nosiheptide (104)

Gram-negative strains tested [111]. With negligible cytotoxicity against mammalian cells and *in vivo* activity in a murine model of MRSA infection, nosiheptide is marketed for veterinary use as an antibiotic, as well as a food preservative.

5 Protein-Binding Thiazoles and Thiazole Drugs

The thiazole ring is present in biologically active molecules and pharmaceuticals that interact with various proteins [112–114], in part due to the hydrogen bond acceptor ability and aromatic character of the heterocycle. A search of the protein data bank found over 200 crystal structures that feature thiazole–protein interactions exhibiting aromatic π – π , π –cation and π –halogen attractive forces. To exemplify key molecular interactions that underpin biological properties of thiazole

peptidomimetics, eight specific thiazole–protein crystal structures are discussed below including six inhibitors of kinases, a protease inhibitor, and one example of a thiazole bound to DNA: 2GQG [115], 3G5D [116], 2Y6O [117], 3BX5 [118], 3IW8 [119], 3QXP [120], 1A61 [121], and 2R2U [122].

5.1 Kinase Inhibition by Dasatinib

Dasatinib (**105**, Fig. 20a–c) is a kinase inhibitor used to treat chronic myelogenous leukemia (CML) and other cancers. It features a central 2-amido thiazole-5-carboxamide component derived from amino acid **111** (Fig. 21).

Dasatinib (**105**) has been crystallized with several human kinases including BCR-ABL kinase, the human kinase domain of cSrc, erythropoietin-producing hepatocellular EphA4 kinase, Lyn protein kinase [123], and Bruton's tyrosine kinase [124]. A common feature of most dasatinib structures is that the thiazole nitrogen acts as a hydrogen bond acceptor that binds to a protein backbone amide NH, often from a methionine (Fig. 20).

BCR-ABL kinase is activated in chronic myeloid leukemia [115] and inhibited by the drug imatinib (Gleevec); however, kinase mutation leads to resistance. Dasatinib (**105**) is 325-fold more potent than imatinib against wild-type and most mutant forms of BCR-ABL and interacts in the ATP binding site (Fig. 21a, PDB: 2GQG) flanked by the two classical kinase sub-lobes. The 2-amino thiazole component occupies a site normally occupied by the adenine group of ATP. The 2-chloro-6-methyl phenyl moiety binds within a hydrophobic site formed by M290, V299, T315, and K217. The thiazole nitrogen and the proton of its 2-amido nitrogen form respectively hydrogen bonds with the amide and carbonyl oxygen of Met318. A hydrogen bond is also made between the hydroxyl oxygen of Thr315 and the thiazole 5-carboxamide NH of dasatinib. The terminal hydroxyethyl group contacts the backbone carbonyl oxygen of Tyr320 via a hydrogen bond. Comparison of the crystal structures of dasatinib and imatinib bound, respectively, to BCR-ABL led to the suggestion that the higher kinase affinity of the former was due to its ability to recognize multiple states of the enzyme [115].

The kinase cSrc is overexpressed in certain tumors such as glioblastoma, gastrointestinal, and prostate cancers [125–127]. The duration of action of cSrc inhibitors is compromised by the development of drug resistance due to the buildup of substrate pressure on the kinase. Crystallographic analysis of dasatinib (**105**) bound to the human kinase domain of cSrc facilitated development of more effective kinase inhibitors by showing that a T388M mutation, involving a change from a hydrogen bond acceptor side chain to a larger hydrophobic side chain, abolished an important hydrogen bond and caused a steric clash with the known inhibitors (Fig. 21b, PDB: 3G5D) [116].

Erythropoietin-producing hepatocellular kinase EphA4 is associated with axon growth and angiogenesis [128, 129]. Among fourteen known human Eph receptors,

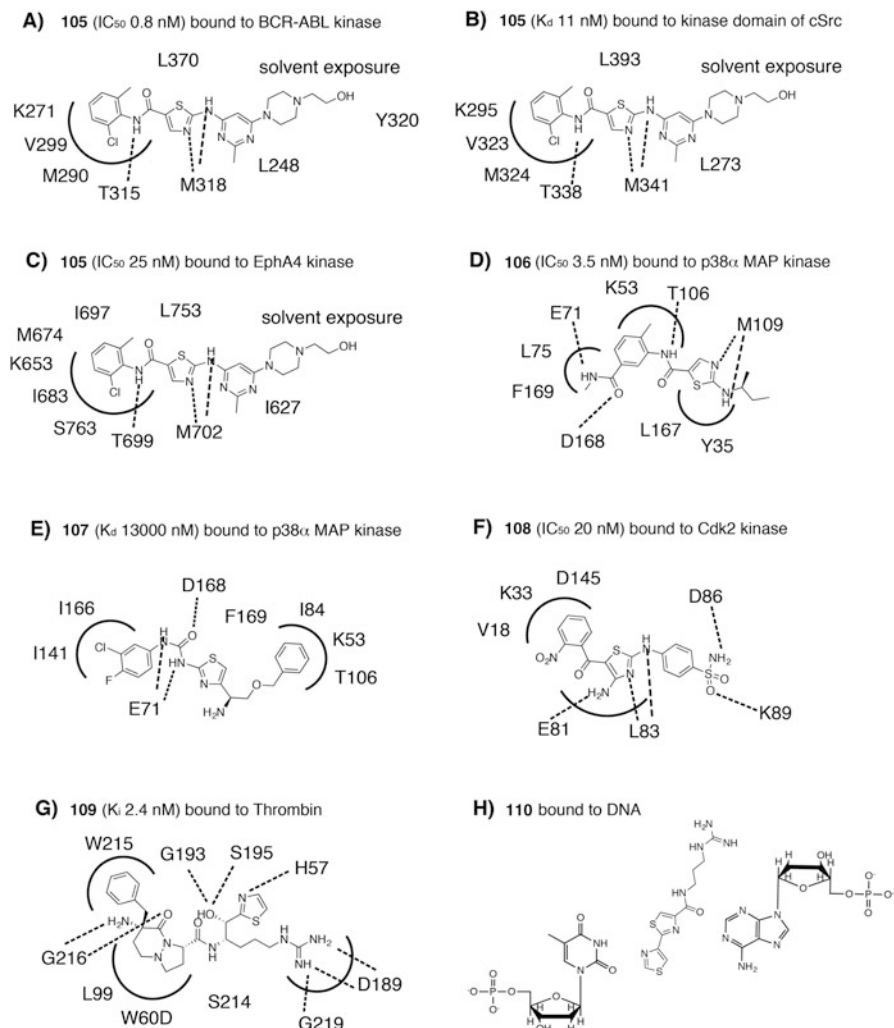


Fig. 20 Interactions between thiazole-containing molecules and their targets in crystal structures: (a–c) dasatinib (**105**) bound to BCR-ABL kinase (PDB: 2GQG), the human kinase domain of cSrc (PDB: 3G5D), and human EphA4 kinase (PDB: 2Y6O); (d) inhibitor **106** bound to p38 α MAP kinase (PDB: 3BX5); (e) inhibitor **107** bound to p38 α MAP kinase (PDB: 3IW8); (f) inhibitor **108** bound to Cdk2 kinase (PDB: 3QXP); (g) inhibitor **109** bound to thrombin (PDB: 1A61); (h) intercalating agent **110** bound to DNA (PDB: 2R2U)

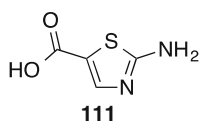


Fig. 21 The central thiazole amino acid of dasatinib

EphA4 is overexpressed in a range of malignant carcinomas, including gastric cancer [130], prostate cancer [131], and cutaneous lymphomas [132]. Crystallographic analysis of the broad-spectrum kinase inhibitor dasatinib (**105**) bound to EphA4 revealed a network of hydrogen bonds between the thiazole ring nitrogen and Met702 amide NH, between the thiazole 2-amido NH with the carbonyl oxygen of Met702, and between the thiazole 5-carboxamide NH and the side chain hydroxyl oxygen of Thr699 (Fig. 21c, PDB: 2Y6O) [117]. Similar to the binding modes of the kinases described above, the 2-chloro-6-methyl phenyl ring is accommodated in a hydrophobic pocket, and the hydroxyethyl piperazine is mainly solvent exposed.

5.2 *p38 α Kinase Inhibitors*

Mitogen-activated protein kinase p38 α (MAPK14) plays an important role in inflammatory stress and conditions such as rheumatoid arthritis, by causing the up-regulation of pro-inflammatory cytokines, such as TNF α and IL-1 β [133]. Iterative structure-activity relationship studies have led to the development of a potent and selective MAPK14 inhibitor BMS-640994 (**106**, IC₅₀ 3.5 nM, [118]) [134]. Crystallographic analysis of the inhibitor-kinase structure has revealed the importance of the amido thiazole carboxamide moiety for the binding of **106** to MAPK14. Stationed in a small hydrophobic pocket lined by Y35 and L167, the thiazole engages in a hydrogen bond with its ring nitrogen to the backbone NH of Met109, and with the amide at its 2-position with the carbonyl of Met109. The linker amide H forms a hydrogen bond with side chain hydroxyl oxygen of T106. In addition, the C-terminal carboxamide of **106** interacts in hydrogen bonds with Glu71 and Asp168 (Fig. 21d, PDB: 3BX5). From such information, orally bioavailable inhibitors were designed exhibiting anti-inflammatory activity in rodent models of inflammatory disease.

Thiazole urea **107** binds an allosteric site of human p38 α MAP kinase in a way that stabilizes an inactive conformation (Fig. 21e, PDB: 3IW8). In the crystal structure, the thiazole ring of **107** does not contribute to hydrogen bonding interactions with p38 α MAP kinase, but forms a π - π contact with F169 [119]. Moreover, the thiazole serves as a pivot that orients the 3-chloro-4-fluoro-phenyl ring toward a hydrophobic pocket, the urea moiety to form two hydrogen bonds with backbone NH of Asp168 and Glu71, and the benzyl ether into a second pocket surrounded by I84, T106 and K53, which are proximal to the gatekeeper residues.

5.3 *Cyclic Dependent Kinase Inhibitor*

Cyclin-dependent kinases (CDK) are a group of Ser/Thr protein kinases that are cell cycle regulators and targets for drug design [135]. Diaminothiazole **108** (IC₅₀

20 nM) proved to be a potent inhibitor of CDK2. In the crystal structure of **108** bound to CDK2, the diamino thiazole is anchored by hydrogen bonds to Glu81 and Leu83; places the *ortho*-nitro phenyl ketone into a hydrophobic pocket consisting of Val18, Ala31, and Lys33; and serves as a hinge-binding scaffold that extends the benzenesulfonamide residue outward to engage in polar interactions in a pocket composed of Gln85, Asp86, and Lys89 (Fig. 21f, PDB: 3QXP).

5.4 Thrombin Inhibitor

Thiazoles have been incorporated into inhibitors of many proteases. For example, thrombin is a serine protease involved in blood coagulation. In the crystal structure of thrombin bound to inhibitor **109**, the thiazole occupies the S1' pocket surrounded by side chains of Cys42, His57, Try60A, Trp60D, and Lys60F (Fig. 21g, PDB: 1A61) [121].

5.5 DNA-Binding Thiazole

A crystal structure for of **110** bound to the 5'-GT containing oligonucleotide d(ATTTAGTAACTAAAT)₂, the bithiazole moiety intercalates between T7 and T9, interfering with stacking of DNA bases, and plays an essential role in DNA cleavage (Fig. 21h, PDB: 2R2U). Thiazoles are often components of DNA-intercalating dyes and other fluorescent dyes, especially when conjugated with aromatic rings that impart useful fluorescence properties [136].

5.6 Thiazole-Containing Drugs

Among FDA-approved drugs that contain thiazole (**105**, **112–133**, Figs. 22 and 23 show twenty-three representative examples), about half are β -lactams that target a penicillin-binding protein, and the remainder target a variety of human and viral enzymes, GPCRs and DNA. Relatively stable from a biological perspective, thiazole drugs have been found to be prone to ring oxidation, as illustrated by the oxidative epoxidation across the C-4–C-5 double bond of **134** (Scheme 13) [137]. Metabolism proceeds by spontaneous rupture of epoxide **135** to form diol **136**, which further ring opens to give dicarbonyl **137** and thioamide **138**, both of which may be further metabolized [138–140].

Ring oxidation was retarded by the addition of substituents at the thiazole C-4 and C-5 positions [141, 142]. For example, the metabolism of the thiazole-containing drug sudoxicam (**139**, Fig. 24) caused oxidative ring opening in vivo

Lactam based Drugs

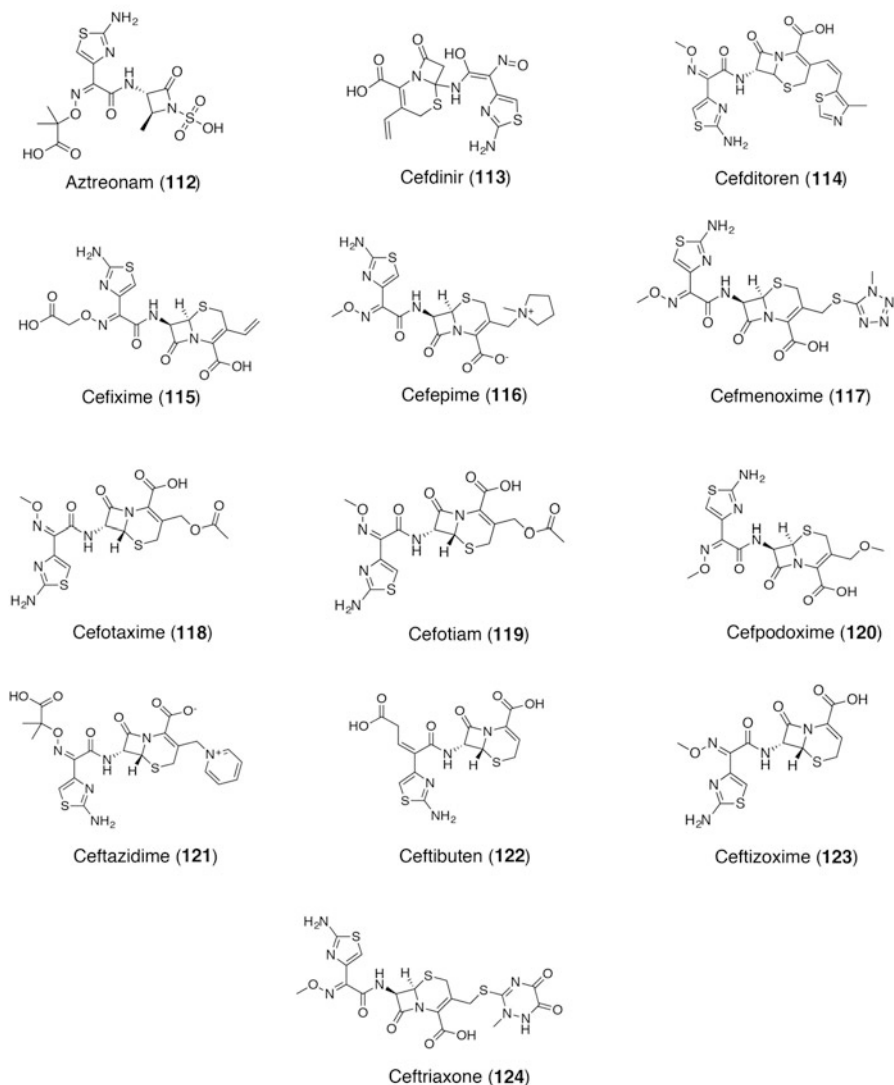
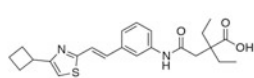


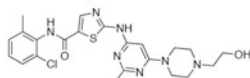
Fig. 22 Lactam-based thiazole-containing antibiotics (**111–124**) that target penicillin-binding protein in bacteria cell walls

in rat, dog, and monkey [143]. The addition of a methyl group to the thiazole 5-position of **139** gave meloxicam (**128**) and switched the oxidative metabolism to the methyl group without epoxidation of the heterocycle leading to little to no ring-opened metabolites [144, 145].

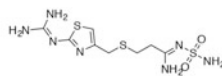
Non-lactam Drugs



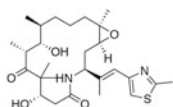
Cinalukast (**125**, anti-arrhythmia)
cysteinyl leukotriene receptor



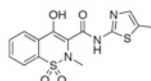
Dasatinib (**105**, anti-cancer)
BCR/ABL and Src family tyrosine kinase



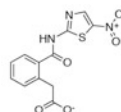
Famotidine (**126**, peptic ulcer)
histamine H2 receptor



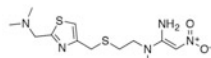
Ixabepilone (**127**, anti-cancer)
tubulin beta-3 chain



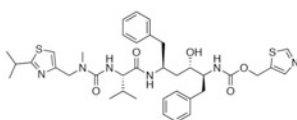
Meloxicam (**128**, NSAID)
Prostaglandin G/H synthase 1 and 2



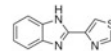
Nitazoxanide (**129**, peptic ulcer)
pyruvate-flavodoxin oxidoreductase (protozoal)



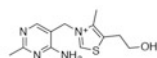
Nizatidine (**130**, peptic ulcer)
histamine H2 receptor



Ritonavir (**131**, anti-viral)
HIV-protease

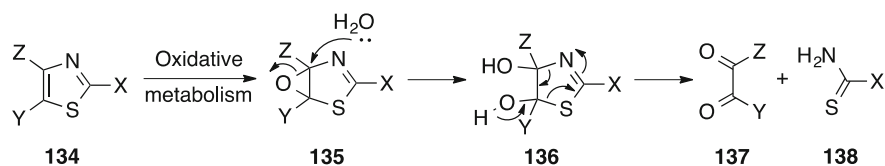


Thiabendazole (**132**, fungicide)
fumarate reductase flavoprotein subunit (E.coli K12)

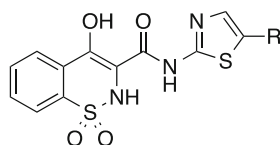


Thiamine (**133**, metabolism)
Thiamin pyrophosphokinase

Fig. 23 Non-lactam thiazole-containing drugs (**105**, **125**–**133**), their uses (in *parentheses*), and protein targets (in *italics*) gathered from <http://www.drugbank.ca/>



Scheme 13 Oxidative metabolism of thiazoles to give dicarbonyl and thioamide metabolites



Sudoxicam (**139**, R = H)
Meloxicam (**128**, R = Me)

Fig. 24 Sudoxicam (**139**) and 5-methyl analogue, meloxicam (**128**)

6 Concluding Remarks

The thiazole ring is present in many peptidic natural products and peptidomimetics. This article has illustrated commonly used approaches to synthesize thiazole derivatives, described their key electronic properties, and highlighted their most important chemical reactivities. A particular focus has been on uses of thiazoles in synthetic peptidomimetics, for example, as a peptide capping group, an amide bond replacement, or a conformational constraint. Importantly, the thiazole ring is the most common five-membered heterocycle present in FDA-approved drugs, strongly supporting future development of additional thiazole-based peptidomimetics. To this end, this perspective assessment of currently known thiazole analogues provides a valuable platform for building new thiazole-based peptidomimetics for the future.

Acknowledgments We acknowledge support from the Australian Research Council (DP130100629, DP150104609, CE140100011) and the National Health and Medical Research Council of Australia (APP1084018). DF is an NHMRC Senior Principal Research Fellow (APP1027369).

References

1. Davyt D, Serra G (2010) *Mar Drugs* 8:2755
2. Donia MS, Schmidt EW (2010) Cyanobactins – ubiquitous cyanobacterial ribosomal peptide metabolites. In: Liu H-W, Mander L (eds) *Comprehensive natural products II*. Elsevier, Oxford, p 539
3. Jin Z (2013) *Nat Prod Rep* 30:869
4. Melby JO, Nard NJ, Mitchell DA (2011) *Curr Opin Chem Biol* 15:369
5. Leoni A, Locatelli A, Morigi R, Rambaldi M (2014) *Expert Opin Ther Pat* 24:201
6. Dondoni A (2010) *Org Biomol Chem* 8:3366
7. Powell RS (1969) In: Kirk-Othmer encyclopedia of chemical technology, 2nd ed, vol 20, p 185
8. Dondoni A, Merino P (1996) Thiazoles. In: Katritzky AR, Rees CW, Scriven EFV (eds) *Comprehensive heterocyclic chemistry II*. Pergamon, Oxford, 373 p
9. Matthews EJ, Kruhlak NL, Benz RD, Contrera JF, Rogers BA, Wolf MA, Richard AM (2008) DSSTox FDA maximum (recommended) daily dose database (FDAMDD): SDF files and documentation, updated version: FDAMDD_v3b_1216_15Feb2008
10. Geyer A, Enck S (2013) Approaches to thiazole dipeptides for the synthesis of thiopeptide antibiotics In: Attanasi OA, Spinelli D (eds) *Targets in heterocyclic systems: chemistry and properties*, vol 16. Royal Society of Chemistry, p 113
11. Wu Y-J, Yang BV (2011) Five-membered ring systems: with N and S (Se) atoms. In: Gordon WG, John AJ (eds) *Progress in heterocyclic chemistry*, vol 23. Elsevier, Oxford, p 267
12. Wu Y-J, Yang BV (2012) Five-membered ring systems: with N and S (Se) atoms. In: Gordon WG, John AJ (eds) *Progress in heterocyclic chemistry*, vol 24. Elsevier, Oxford, p 281
13. Wu Y-J, Yang BV (2013) Five-membered ring systems: with N and S (Se) atoms. In: Gordon WG, John AJ (eds) *Progress in heterocyclic chemistry*, vol 25. Elsevier, Oxford, p 257
14. Wu Y-J, Yang BV (2014) Five-membered ring systems: with N and S (Se) atoms. In: Gordon WG, John AJ (eds) *Progress in heterocyclic chemistry*, vol 26. Elsevier, Amsterdam, p 279

15. Wu YJ, Yang BV (2011) Five-membered ring systems: with N and S (Se) atoms. In: Gordon G, John AJ (eds) *Progress in heterocyclic chemistry*, vol 22. Elsevier, Oxford, p 259
16. Xu Z, Ye T (2011) Thiazoline and thiazole and their derivatives. In: Majumdar KC, Chattopadhyay SK (eds) *Heterocycles in natural product synthesis*. Wiley-VCH, Weinheim, p 459
17. Hantzsch A, Weber JH (1887) *Chem Ber* 20:3118
18. Snyder NL, Boisvert CJ (2011) *Hantzsch synthesis*. Wiley, Hoboken, p 591
19. Ambhaikar NB (2013) Thiazoles and benzothiazoles. In: Li JJ (ed) *Heterocyclic chemistry in drug discovery*. Wiley, Hoboken, p 283
20. Lu J-Y, Riedrich M, Wojtas KP, Arndt H-D (2013) *Synthesis* 45:1300
21. Shalaby MA, Grote CW, Rapoport H (1996) *J Org Chem* 61:9045
22. Holzapfel CW, Pettit GR (1985) *J Org Chem* 50:2323
23. Bredenkamp MW, Holzapfel CW, van Zyl WJ (1990) *Synth Commun* 20:2235
24. Aguilar E, Meyers AI (1994) *Tetrahedron Lett* 35:2473
25. Butler JD, Coffman KC, Ziebart KT, Toney MD, Kurth MJ (2010) *Chem Eur J* 16:9002
26. Nefzi A, Arutyunyan S, Fenwick JE (2010) *J Org Chem* 75:7939
27. Cohrt AE, Nielsen TE (2013) *ACS Comb Sci* 16:71
28. Murru S, Nefzi A (2014) *ACS Comb Sci* 16:39
29. Weiss KM, Wei S, Tsogoeva SB (2011) *Org Biomol Chem* 9:3457
30. Cook AH, Heilbron IM, Levy AL (1947) *J Chem Soc* 1594
31. Cook AH, Heilbron I, Macdonald SF, Mahadevan AP (1949) *J Chem Soc* 1064
32. Ahmad NM (2005) *Cook-Heilbron 5-aminothiazole synthesis*. Wiley, Hoboken, p 275
33. Lingaraju GS, Swaroop TR, Vinayaka AC, Kumar KSS, Sadashiva MP, Rangappa KS (2012) *Synthesis* 44:1373
34. Gabriel S (1910) *Ber Dtsch Chem Ges* 43:134
35. Gabriel S (1910) *Ber Dtsch Chem Ges* 43:1283
36. Kiryanov AA, Sampson P, Seed AJ (2001) *J Org Chem* 66:7925
37. Di Credico B, Reginato G, Gonsalvi L, Peruzzini M, Rossini A (2011) *Tetrahedron* 67:267
38. Nygaard L, Asmussen E, Hoeg JH, Maheshwari RC, Nielsen CH, Petersen IB, Rastrup-Andersen J, Soerensen GO (1971) *J Mol Struct* 8:225
39. Beker W, Szarek P, Komorowski L, Lipiński J (2013) *J Phys Chem A* 117:1596
40. Metzger JV, Vincent EJ (1979) Properties and reactions of thiazoles. In: Metzger JV (ed) *Thiazoles and its derivatives*, vol 1, *The chemistry of heterocyclic compounds*. Wiley, New York
41. Ioannidis S, Lamb ML, Almeida L, Guan H, Peng B, Bebernitz G, Bell K, Alimzhanov M, Zinda M (2010) *Bioorg Med Chem Lett* 20:1669
42. Phan-Tan-Luu R, Surzur JM, Metzger J, Aune JP, Dupuy C (1967) *Bull Soc Chim Fr* 3274
43. Grandberg II, Kost AN (1959) *Zh Obshch Khim* 29:1099
44. Acheson RM, Foxton MW, Miller GR (1965) *J Chem Soc* 3200
45. Reid DH, Skelton FS, Bonthrone W (1964) *Tetrahedron Lett* 1797
46. Zahradnik R, Koutecky J (1961) *Collect Czech Chem Commun* 26:156
47. Metzger J, Koether B (1953) *Bull Soc Chim Fr* 708
48. Florio S, Troisi L, Capriati V (1998) *Tetrahedron Lett* 39:7951
49. Schnürch M, Flasiak R, Khan AF, Spina M, Mihovilovic MD, Stanetty P (2006) *Eur J Org Chem* 2006:3283
50. Schröter S, Stock C, Bach T (2005) *Tetrahedron* 61:2245
51. Schnuerch M, Haemmerle J, Mihovilovic MD, Stanetty P (2010) *Synthesis* 837
52. Grubb AM, Schmidt MJ, Seed AJ, Sampson P (2012) *Synthesis* 44:1026
53. Thompson MJ, Chen B (2009) *J Org Chem* 74:7084
54. Dömling A (2005) *Chem Rev* 106:17
55. Kazmaier U, Persch A (2010) *Org Biomol Chem* 8:5442
56. Just-Baringo X, Albericio F, Alvarez M (2014) *Curr Top Med Chem* 14:1244
57. Nefzi A, Fenwick JE (2011) *Tetrahedron Lett* 52:817

58. Valdomir G, Padrón JI, Padrón JM, Martín VS, Davyt D (2014) *Synthesis* 46:2451
59. Maderna A, Doroski M, Subramanyam C, Porte A, Leverett CA, Vetelino BC, Chen Z, Risley H, Parris K, Pandit J, Varghese AH, Shanker S, Song C, Sukuru SCK, Farley KA, Wagenaar MM, Shapiro MJ, Musto S, Lam M-H, Loganzo F, O'Donnell CJ (2014) *J Med Chem* 57:10527
60. Pettit GR, Hogan F, Toms S (2011) *J Nat Prod* 74:962
61. Boitano S, Flynn AN, Schulz SM, Hoffman J, Price TJ, Vagner J (2011) *J Med Chem* 54:1308
62. Hershko A, Heller H, Eytan E, Kaklij G, Rose IA (1984) *Proc Natl Acad Sci* 81:7021
63. Hollebeke J, Van Damme P, Gevaert K (2012) N-terminal acetylation and other functions of N α -acetyltransferases. *Biol Chem* 393:291
64. Bolchi C, Pallavicini M, Bernini SK, Chiodini G, Corsini A, Ferri N, Fumagalli L, Straniero V, Valoti E (2011) *Bioorg Med Chem Lett* 21:5408
65. Devine SM, Mulcair MD, Debono CO, Leung EWW, Nissink W, Lim SS, Chandrashekar IR, Vazirani M, Mohanty B, Simpson JS, Baell JB, Scammells PJ, Norton RS, Scanlon MJ (2015) *J Med Chem*. doi:10.1021/jm501402x
66. Reid RC, Yau MK, Singh R, Lim JX, Fairlie DP (2014) *J Am Chem Soc* 136:11914
67. Mali SM, Schneider TF, Bandyopadhyay A, Jadhav SV, Werz DB, Gopi HN (2012) *Cryst Growth Des* 12:5643
68. Davis MR, Singh EK, Wahyudi H, Alexander LD, Kunicki JB, Nazarova LA, Fairweather KA, Giltrap AM, Jolliffe KA, McAlpine SR (2012) *Tetrahedron* 68:1029
69. Legrand B, Mathieu L, Lebrun A, Andriamanarivo S, Lisowski V, Masurier N, Zirah S, Kang YK, Martinez J, Maillard LT (2014) *Chem Eur J* 20:6713
70. Mathieu L, Legrand B, Deng C, Vezenkov L, Wenger E, Didierjean C, Amblard M, Averlant-Petit M-C, Masurier N, Lisowski V, Martinez J, Maillard LT (2013) *Angew Chem Int Ed* 52:6006
71. Blakeney JS, Reid RC, Le GT, Fairlie DP (2007) *Chem Rev* 107:2960
72. Loughlin WA, Tyndall JDA, Glenn MP, Hill TA, Fairlie DP (2010) *Chem Rev* 110(6):PR32
73. Cohen F, Koehler MFT, Bergeron P, Elliott LO, Flygare JA, Franklin MC, Gazzard L, Keteltas SF, Lau K, Ly CQ, Tsui V, Fairbrother WJ (2010) *Bioorg Med Chem Lett* 20:2229
74. Singh S, Prasad NR, Kapoor K, Chufan EE, Patel BA, Ambudkar SV, Talele TT (2014) *ChemBioChem* 15:157
75. Dewal MB, Firestine SM (2011) *Curr Med Chem* 18:2420
76. Ngoei KRW, Ng DCH, Gooley PR, Fairlie DP, Stoermer MJ, Bogoyevitch MA (2013) *Biochim Biophys Acta* 1834:1077
77. Ojika M, Suzuki Y, Tsukamoto A, Sakagami Y, Fudou R, Yoshimura T, Yamanaka S (1998) *J Antibiot* 51:275
78. Iwaki Y, Akita H (2007) *Chem Pharm Bull (Tokyo)* 55:1610
79. Bertram A, Pattenden G (2007) *Nat Prod Rep* 24:18
80. Walsh CT, Malcolmson SJ, Young TS (2011) *ACS Chem Biol* 7:429
81. Jin Z (2011) *Nat Prod Rep* 28:1143
82. Bowers A, West N, Taunton J, Schreiber SL, Bradner JE, Williams RM (2008) *J Am Chem Soc* 130:11219
83. Diness F, Nielsen DS, Fairlie DP (2011) *J Org Chem* 76:9845
84. Taori K, Paul VJ, Luesch H (2008) *J Am Chem Soc* 130:1806
85. Taori K, Paul VJ, Luesch H (2008) *J Am Chem Soc* 130:13506
86. Ying Y, Taori K, Kim H, Hong J, Luesch H (2008) *J Am Chem Soc* 130:8455
87. Foster MP, Concepcion GP, Caraan GB, Ireland CM (1992) *J Org Chem* 57:6671
88. Bertram A, Maulucci N, New OM, Mohd Nor SM, Pattenden G (2007) *Org Biomol Chem* 5:1541
89. Nielsen DS, Hoang HN, Lohman R-J, Hill TA, Lucke AJ, Craik DJ, Edmonds DJ, Griffith DA, Rotter CJ, Ruggeri RB, Price DA, Liras S, Fairlie DP (2014) *Angew Chem Int Ed* 53:12059
90. Nielsen DS, Hoang HN, Lohman R-J, Diness F, Fairlie DP (2012) *Org Lett* 14:5720

91. Dalisay DS, Rogers EW, Edison AS, Molinski TF (2009) *J Nat Prod* 72:732
92. Singh EK, Ramsey DM, McAlpine SR (2012) *Org Lett* 14:1198
93. Wahyudi H, Tantisantisom W, McAlpine SR (2014) *Tetrahedron Lett* 55:2389
94. Wahyudi H, Tantisantisom W, Liu X, Ramsey DM, Singh EK, McAlpine SR (2012) *J Org Chem* 77:10596
95. Matsuo Y, Kanoh K, Yamori T, Kasai H, Katsuta A, Adachi K, Shin-Ya K, Shizuri Y (2007) *J Antibiot* 60:251
96. Donia MS, Hathaway BJ, Sudek S, Haygood MG, Rosovitz MJ, Ravel J, Schmidt EW (2006) *Nat Chem Biol* 2:729
97. Koehnke J, Bent A, Houssen WE, Zollman D, Morawitz F, Shirran S, Vendome J, Nneoyiegbe AF, Trembleau L, Botting CH, Smith MC, Jaspars M, Naismith JH (2012) *Nat Struct Mol Biol* 19:767
98. Koehnke J, Bent AF, Houssen WE, Mann G, Jaspars M, Naismith JH (2014) *Curr Opin Struct Biol* 29c:112
99. Comba P, Dovalil N, Gahan LR, Hanson GR, Westphal M (2014) *Dalton Trans* 43:1935
100. van den Brenk AL, Tyndall JDA, Cusack RM, Jones A, Fairlie DP, Gahan LR, Hanson GR (2004) *J Inorg Biochem* 98:1857
101. van den Brenk AL, Byriel KA, Fairlie DP, Gahan LR, Hanson GR, Hawkins CJ, Jones A, Kennard CHL, Moubaraki B, Murray KS (1994) *Inorg Chem* 33:3549
102. Abbenante G, Fairlie DP, Gahan LR, Hanson GR, Pierens GK, van den Brenk AL (1996) *J Am Chem Soc* 118:10384
103. Singh Y, Sokolenko N, Kelso MJ, Gahan LR, Abbenante G, Fairlie DP (2000) *J Am Chem Soc* 123:333
104. Sokolenko N, Abbenante G, Scanlon MJ, Jones A, Gahan LR, Hanson GR, Fairlie DP (1999) *J Am Chem Soc* 121:2603
105. Just-Baringo X, Albericio F, Alvarez M (2014) *Mar Drugs* 12:317
106. Ciufolini MA, Lefranc D (2010) *Nat Prod Rep* 27:330
107. Heckmann G, Bach T (2005) *Angew Chem* 117:1223
108. Trzasko A, Leeds JA, Praestgaard J, Lamarche MJ, McKenney D (2012) *Antimicrob Agents Chemother* 56:4459
109. Nicolaou KC, Zak M, Safina BS, Estrada AA, Lee SH, Nevalainen M (2005) *J Am Chem Soc* 127:11176
110. Zhang F, Kelly WL (2015) *ACS Chem Biol*. doi:[10.1021/cb5007745](https://doi.org/10.1021/cb5007745)
111. Haste NM, Thienphrapa W, Tran DN, Loesgen S, Sun P, Nam SJ, Jensen PR, Fenical W, Sakoulas G, Nizet V, Hensler ME (2012) *J Antibiot* 65:593
112. Huber RG, Margreiter MA, Fuchs JE, von Grafenstein S, Tautermann CS, Liedl KR, Fox T (2014) *J Chem Inf Model* 54:1371
113. Feher M, Schmidt JM (2003) *J Chem Inf Comput Sci* 43:218
114. Li JJ (2013) *Heterocyclic chemistry in drug discovery*. Wiley, Hoboken
115. Tokarski JS, Newitt JA, Chang CY, Cheng JD, Wittekind M, Kiefer SE, Kish K, Lee FY, Borzilleri R, Lombardo LJ, Xie D, Zhang Y, Klei HE (2006) *Cancer Res* 66:5790
116. Getlik M, Grutter C, Simard JR, Kluter S, Rabiller M, Rode HB, Robubi A, Rauh D (2009) *J Med Chem* 52:3915
117. Farenc C, Celie PH, Tensen CP, de Esch IJ, Siegal G (2011) *FEBS Lett* 585:3593
118. Hynes J Jr, Wu H, Pitt S, Shen DR, Zhang R, Schieven GL, Gillooly KM, Shuster DJ, Taylor TL, Yang X, McIntyre KW, McKinnon M, Zhang H, Marathe PH, Doweyko AM, Kish K, Kiefer SE, Sack JS, Newitt JA, Barrish JC, Dodd J, Leftheris K (2008) *Bioorg Med Chem Lett* 18:1762
119. Simard JR, Grutter C, Pawar V, Aust B, Wolf A, Rabiller M, Wulfert S, Robubi A, Kluter S, Ottmann C, Rauh D (2009) *J Am Chem Soc* 131:18478
120. Schonbrunn E, Betzi S, Alam R, Martin MP, Becker A, Han H, Francis R, Chakrasali R, Jakkraj S, Kazi A, Sebti SM, Cubitt CL, Gebhard AW, Hazlehurst LA, Tash JS, Georg GI (2013) *J Med Chem* 56:3768

121. St Charles R, Matthews JH, Zhang E, Tulinsky A (1999) *J Med Chem* 42:1376
122. Goodwin KD, Lewis MA, Long EC, Georgiadis MM (2008) *Proc Natl Acad Sci U S A* 105:5052
123. Williams NK, Lucet IS, Klinken SP, Ingley E, Rossjohn J (2009) *J Biol Chem* 284:284
124. Marcotte DJ, Liu YT, Arduini RM, Hession CA, Miatkowski K, Wildes CP, Cullen PF, Hong V, Hopkins BT, Mertsching E, Jenkins TJ, Romanowski MJ, Baker DP, Silvian LF (2010) *Protein Sci* 19:429
125. Chang YM, Bai L, Liu S, Yang JC, Kung HJ, Evans CP (2008) *Oncogene* 27:6365
126. Du J, Bernasconi P, Clauser KR, Mani DR, Finn SP, Beroukhim R, Burns M, Julian B, Peng XP, Hieronymus H, Maglathlin RL, Lewis TA, Liau LM, Nghiemphu P, Mellinghoff IK, Louis DN, Loda M, Carr SA, Kung AL, Golub TR (2009) *Nat Biotechnol* 27:77
127. Yeatman TJ (2004) *Nat Rev Cancer* 4:470
128. Cheng N, Brantley DM, Chen J (2002) *Cytokine Growth Factor Rev* 13:75
129. Pasquale EB (2008) *Cell* 133:38
130. Gong J, Morishita A, Kurokohchi K, Tani J, Kato K, Miyoshi H, Inoue H, Kobayashi M, Liu S, Murota M, Muramatsu A, Izuishi K, Suzuki Y, Yoshida H, Uchida N, Deguchi K, Iwama H, Ishimaru I, Masaki T (2010) *Int J Oncol* 36:101
131. Ashida S, Nakagawa H, Katagiri T, Furihata M, Iizumi M, Anazawa Y, Tsunoda T, Takata R, Kasahara K, Miki T, Fujioka T, Shuin T, Nakamura Y (2004) *Cancer Res* 64:5963
132. van Doorn R, Dijkman R, Vermeer MH, Out-Luiting JJ, van der Raaij-Helmer EM, Willemze R, Tensen CP (2004) *Cancer Res* 64:5578
133. Kumar S, Boehm J, Lee JC (2003) *Nat Rev Drug Discov* 2:717
134. Choy EH, Panayi GS (2001) *N Engl J Med* 344:907
135. Hall M, Peters G (1996) *Adv Cancer Res* 68:67
136. Sonar MV, Wampole ME, Jin Y-Y, Chen C-P, Thakur ML, Wickstrom E (2014) *Bioconjug Chem* 25:1697
137. Dalvie DK, Kalgutkar AS, Khojasteh-Bakht SC, Obach RS, O'Donnell JP (2002) *Chem Res Toxicol* 15:269
138. Mizutani T, Yoshida K, Kawazoe S (1994) *Drug Metab Dispos* 22:750
139. Mizutani T, Suzuki K (1996) *Toxicol Lett* 85:101
140. Kalgutkar AS, Driscoll J, Zhao SX, Walker GS, Shepard RM, Soglia JR, Atherton J, Yu L, Mutlib AE, Munchhof MJ, Reiter LA, Jones CS, Doty JL, Trevena KA, Shaffer CL, Ripp SL (2007) *Chem Res Toxicol* 20:1954
141. Blagg J (2010) Structural alerts for toxicity. In: Abraham DJ, Protella DP (eds) *Burger's medicinal chemistry, drug discovery and development*, vol 2. Wiley, Hoboken, p 301
142. Barreiro EJ, Kümmerle AE, Fraga CAM (2011) *Chem Rev* 111:5215
143. Hobbs DC, Twomey TM (1977) *Drug Metab Dispos* 5:75
144. Schmid J, Busch U, Trummlitz G, Prox A, Kaschke S, Wachsmuth H (1995) *Xenobiotica* 25:1219
145. Obach RS, Kalgutkar AS, Ryder TF, Walker GS (2008) *Chem Res Toxicol* 21:1890

Advances in Merging Triazoles with Peptides and Proteins

Frederik Diness, Sanne Schoffelen, and Morten Meldal

Abstract Five-membered heterocycles have found extensive use as peptide- and disulfide-bond mimics in peptidomimetics. The application of 1,4- and 1,5-substituted 1,2,3-triazoles has been particularly favored due to their ease of preparation by a variety of “click” methods including the copper(I)-catalyzed azide–alkyne cycloaddition (CuAAC) and the ruthenium-catalyzed azide–alkyne cycloaddition (RuAAC) reactions. These heterocycles are electronically similar to amide bonds and have provided both functional and structural analogues of biologically active peptides. One advantage of triazole ring amide surrogates is their stability toward natural enzyme activity. The quantitative and orthogonal nature of the CuAAC reaction has facilitated its use in peptide macrocyclization reactions. The CuAAC reaction is particularly useful to replace disulfide bonds in order to stabilize bioactive conformations of biologically active peptides. Metal-free cycloadditions promoted by ring strain (SPAAC) have been favored for labeling in living systems in which transition metals are poorly tolerated. A range of in vivo biomolecular “click” reactions have demonstrated the versatility of SPAAC reactions in living cells and even multicellular organisms. Although azides and alkynes can conveniently be introduced in peptides during synthesis, site-specific incorporation of these functional groups into proteins is more challenging. A variety of methods has been developed to make these reactive precursors, including residue-specific replacement and genetic code expansion. Recent developments of new ligands and catalysts for the CuAAC reaction have further contributed to the promising possibilities that triazoles provide for future applications in the peptide and protein field.

Keywords Click reaction • CuAAC • Macrocyclization • Peptide mimetics • Protein labeling • RuAAC • SPAAC • Triazole

F. Diness (✉), S. Schoffelen, and M. Meldal (✉)
Center for Evolutionary Chemical Biology, University of Copenhagen, Universitetsparken 5,
2100 Copenhagen, Denmark
e-mail: fdi@chem.ku.dk; meldal@nano.ku.dk

Contents

1	Introduction	268
2	1,2,4-Triazoles as Peptidomimetics	270
3	Methods for the Synthesis of 1,2,3-Triazole Peptidomimetics	272
3.1	The Huisgen Reaction	273
3.2	Copper(I)-Catalyzed Azide–Alkyne Cycloaddition (CuAAC)	273
3.3	Ruthenium(II)-Catalyzed Azide–Alkyne Cycloaddition (RuAAC)	275
3.4	Strain-Promoted Azide–Alkyne Cycloaddition (SPAAC)	276
3.5	Other Methods	276
3.6	Oligomer Synthesis and Solid-Phase Synthesis	278
4	Structures, Roles, and Applications of Peptide 1,2,3-Triazoles	279
4.1	The 1,2,3-Triazole as Backbone Amide Bond Surrogate	279
4.2	Cyclic Peptides	282
4.3	Side-Chain Mimetics	288
5	Triazoles in Proteins	290
5.1	Strategies for the Introduction of Azides and Alkynes into Proteins	290
5.2	Increasing the Biocompatibility of the Azide–Alkyne Cycloaddition	292
5.3	Triazole-Containing Protein Conjugates Produced In Vitro	294
5.4	Triazole Formation in Cells and Living Organisms	297
6	Conclusion and Perspectives	299
	References	300

1 Introduction

Peptides and proteins, which consist of oligomers of amino acids joined by amide bonds, are among the most abundant classes of biomolecules. In nature, their variety of functions ranges from structural matrices (e.g., collagen and silk) to functional machinery (e.g., receptors and enzymes) [1]. They are also present in a wide variety of toxins, hormones, and other signaling molecules. Their rich properties are tailored by their composition from the 20 canonical amino acids, as well as posttranslational biochemical modifications. The rigid amide bond, the chirality of the amino acids, and the great spectrum of side-chain functionality are here key features that influence the form and function of both peptides and folded proteins alike. The amide bond is well designed to be stable under most physiological conditions, yet easily formed and cleaved by enzymatic reactions to allow for efficient recycling of the amino acid monomers. Altogether, these properties, arising from Nature's powerful evolutionary selection process, explain why peptides and proteins are among the core functional biomolecules in life.

Performing essential roles in all processes of life, peptides and proteins are intriguing and highly relevant subjects of investigation both from a scientific and a pharmaceutical perspective. The inherent conformational flexibility of peptides, as well as their lack of enzymatic stability, has however frequently limited the direct use of peptides and proteins as research tools and pharmaceuticals. A valuable strategy for addressing these problems has been to employ peptidomimetics. Peptidomimetics are defined by general consensus as peptide-

Fig. 1 Five-membered heterocycles as peptide surrogates in peptidomimetics

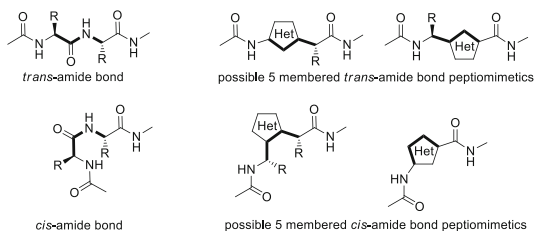
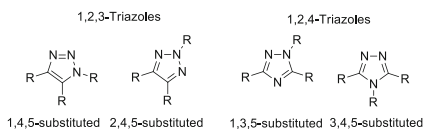


Fig. 2 Substitution patterns for 1,2,3-triazole and 1,2,4-triazole rings



like compounds with regard to structure, function, and chemical/physical properties [2]. Typically, peptidomimetics are generated from the combination of natural and/or artificial amino acids with other organic moieties. In this way, peptide-like compounds are produced, which are able to mimic the binding and activity of peptides *in vitro* and *in vivo*.

A variety of five-membered heterocycles has been employed as peptide surrogates in order to lock the chain into a particular conformation and to enhance resistance toward proteolytic enzyme digestion. As shown in Fig. 1, these five-membered heterocyclic structures can mimic both *trans*- and *cis*-amide conformations.

Triazoles, belonging to the group of five-membered heterocycles, have been found useful for peptide mimicry. The triazole heterocycle can accommodate three substituents in four possible substitution patterns each bearing a group on one of the three nitrogen atoms (Fig. 2). Surveying the scientific literature reveals that both 1,2,3-triazoles and 1,2,4-triazoles have been applied as triazole peptidomimetics. Initially, peptidomimetics based on 1,2,4-triazoles [3, 4] were investigated. However, today the 1,2,3-triazole accounts for almost all of the reported triazole peptidomimetics, and among these the 1,4-disubstituted 1,2,3-triazole has dominated.

Triazoles have entered the peptide field by three distinct waves of innovation. These illustrate the importance of methods to access heterocycles and for facilitating their incorporation into peptidomimetics. The first examples of triazole peptidomimetics became available by using relatively classical condensation chemistry to generate 1,2,4-triazoles from amino acids [3, 4]. In 2001, the discovery of the copper(I)-catalyzed 1,3-dipolar cycloaddition of azides and alkynes (CuAAC reaction) by Tornøe and Meldal revolutionized the synthesis and application of 1,2,3-triazole peptidomimetics [5]. Subsequently, the CuAAC reaction penetrated all fields of organic chemistry and became a mainstay in the peptide field. Interest in the use of the azide–alkyne cycloaddition in protein chemistry and chemical biology initiated the third wave of innovation in the triazole field. Due to toxicity, the application of metal catalysis was initially neither feasible for *in vitro* nor

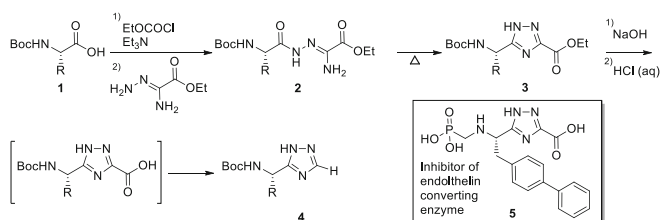
in vivo applications. Hence, the catalyst-free strain-promoted 1,3-dipolar cycloaddition of azides and alkynes (SPAAC) was elaborated, which has advanced the use of triazoles for biological applications [6].

The field of triazole peptidomimetics has been reviewed from different perspectives [7–16], and the chemistry for triazole synthesis has been extensively reviewed [8]. Hence, in this chapter, we present and discuss the generation and application of triazole peptidomimetics as well as the use of triazoles in protein science. Focus is on a selection of significant, state-of-the-art studies, because including all examples would extend beyond the scope of this review. In the sections concerning only 1,2,3-triazoles, the term “triazole” is used in most parts of the chapter to denote a 1,4-disubstituted 1,2,3-triazole, and the term “1,5-disubstituted triazole” is used instead of “1,5-disubstituted 1,2,3-triazole”.

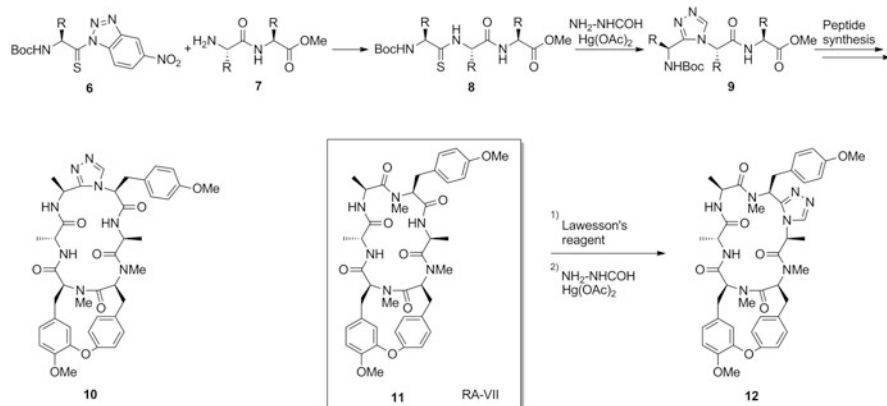
2 1,2,4-Triazoles as Peptidomimetics

The 1,2,4-triazole may be incorporated into the peptide backbone to act as an amide bond surrogate of the *trans*- or *cis*-isomer. Initially, 3,5-disubstituted 1,2,4-triazoles were synthesized from amino acids to serve as dipeptide mimics [4, 17, 18]. The 3,5-disubstituted 1,2,4-triazoles may be considered amide bond isosteres with *trans*-conformation, as confirmed by X-ray crystallography, which revealed the structure of a strand motif in which the 1,2,4-triazole unit made intermolecular hydrogen bonds with neighboring peptides [4]. The 1,2,4-triazole dipeptide mimetics (**3**) were synthesized from *N*-protected amino acids (**1**) without epimerization of the stereochemistry of the α -carbon (Scheme 1) [4]. On saponification of the C-terminal ester **3**, the carboxylic acid was however prone to decarboxylation resulting in low yields and, in some cases, isolation of only the decarboxylated triazole **4** [17, 18]. Despite this challenge, a 1,2,4-triazole dipeptide mimetic was applied in the synthesis of endothelin-converting enzyme inhibitor **5** [17].

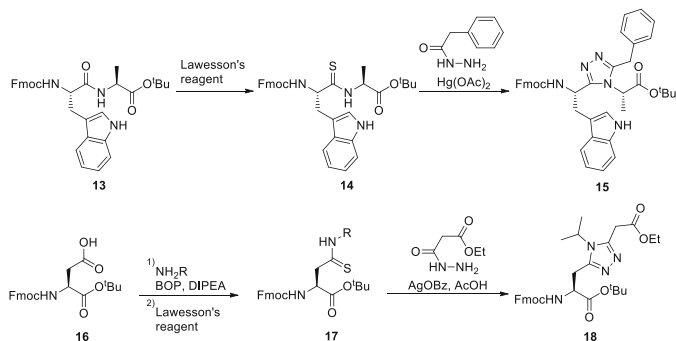
The related 3,4-disubstituted 1,2,4-triazoles have been explored as amide bond *cis*-isomer surrogates [19, 20] and used to determine the overall conformation responsible for the antitumor activity of bicyclic peptide natural products (e.g., **10**, Scheme 2). 3,4-Disubstituted 1,2,4-triazoles have been generated from



Scheme 1 Synthesis and application of 3,5-disubstituted 1,2,4-triazole dipeptide mimetic



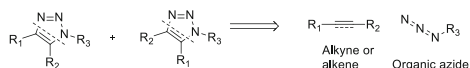
Scheme 2 Synthesis and application of 3,4-d'isubstituted 1,2,4-triazole peptidomimetics



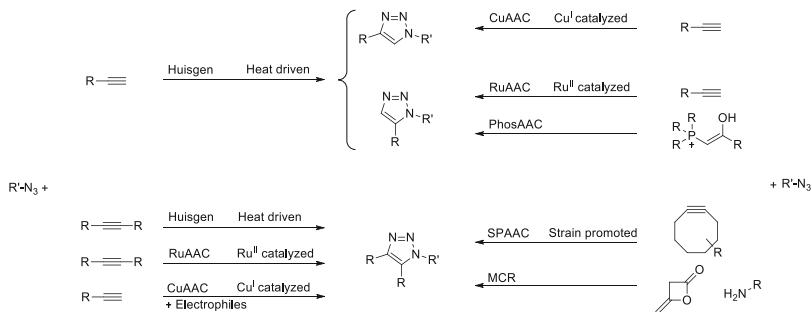
Scheme 3 Synthesis of 3,4,5-trisubstituted 1,2,4-triazole derivatives

thioamides (e.g., **8**) on reaction with formic hydrazide and mercury acetate [19, 20]. The thioamides were synthesized by coupling thiocarbonyl benzotriazole **6** onto the N-terminus of dipeptide **7** or by regioselective thionation of the natural peptide RA-VII (**11**) with Lawesson's reagent.

The reaction of thioamides and hydrazides has also been applied to the synthesis of 3,4,5-trisubstituted 1,2,4-triazole dipeptide derivatives (e.g., **15**, Scheme 3) [3, 21]. Subsequently, the less toxic silver benzoate has been used instead of mercury acetate for the synthesis of aspartate-derived 1,2,4-triazole **18** (Scheme 3) [22, 23].



Scheme 4 Retrosynthesis of 1,2,3-triazoles

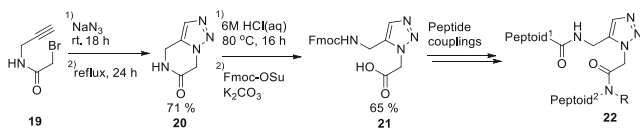


Scheme 5 Overview of 1,3-dipole cycloadditions with azides for the synthesis of disubstituted (*top*) and trisubstituted (*bottom*) triazole peptidomimetics

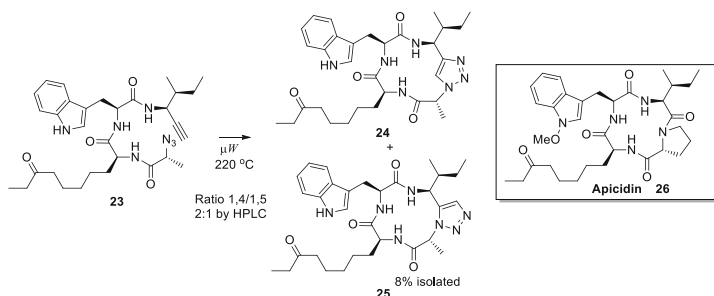
3 Methods for the Synthesis of 1,2,3-Triazole Peptidomimetics

The methods for synthesizing 1,2,3-triazoles as well as the detailed reaction mechanisms of triazole formation have been reviewed elsewhere [8, 24–28]. For peptidomimetic chemistry, few methods of 1,2,3-triazole synthesis have been investigated and only a couple have shown broad utility. Nearly all syntheses of the 1,2,3-triazole heterocyclic core have relied on 1,3-dipolar cycloadditions. The most common synthons used for the generation of 1,2,3-triazoles have been azide and alkyne derivatives. A few recent reports have described the use of alkene instead of alkyne derivatives (see Sect. 3.5). Alternative strategies for 1,2,3-triazole formation have been absent to date, due to the relatively lower efficiency for combining two fragments by ring-closing reactions forming N–N and sp^2 C–C bonds. By comparison, formation of two C–N bonds is more effective for the assembly of 1,2,3-triazoles (Scheme 4).

One advantage of the 1,3-dipolar cycloaddition between organic azides and alkynes is reaction efficiency under both thermal and catalytic conditions (for exceptions see Sect. 3.4) [29]. Moreover, both azide and alkyne may be incorporated into the same molecule prior to intramolecular triazole formation leading to macrocyclization. Another advantage is the relative inertness of organic azides and alkynes toward other reaction conditions, including base- and acid-promoted nucleophilic chemistry [27]. These properties have provided a powerful and versatile research platform for application of 1,2,3-triazoles combined with peptides and proteins. A variety of different methods for triazole formation have been developed to compensate for differences in the reaction environment, the nature of targeted triazole structure, and the function of the triazole. An overview of the different methods is given in Scheme 5.



Scheme 6 Synthesis of dipeptide triazole **21** by Huisgen reaction



Scheme 7 Synthesis of a 1,4- and 1,5-regioisomer mixture of apicidin analogues using thermal conditions for 1,2,3-triazole formation

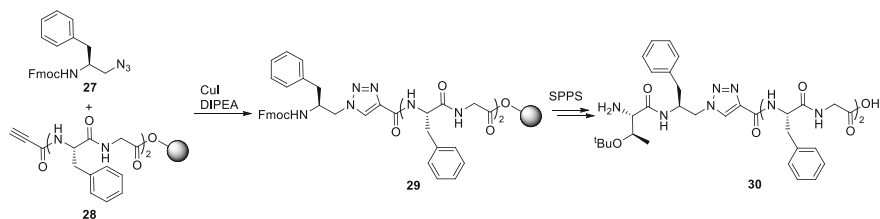
3.1 The Huisgen Reaction

The thermal 1,3-dipolar cycloaddition (Huisgen reaction) of organic azides and alkynes was extensively explored by Rolf Huisgen [30, 31]. The reaction was found to be high yielding but required elevated temperatures and long reaction times [31]. In general, the reaction leads to a mixture of 1,4- and 1,5-regioisomers, which were often difficult to separate. Consequently, the reaction gained marginal interest for the synthesis of peptidomimetics. A few examples of intramolecular ring-closing Huisgen reaction have been reported including the reaction of azide derived from bromide **19** to selectively form 1,5-regioisomer **20**, which was converted to dipeptide mimetic **21** by amide bond hydrolysis (Scheme 6) [32]. Triazole **21** was employed in the synthesis of peptoid **22**, which adopted a hairpin structure.

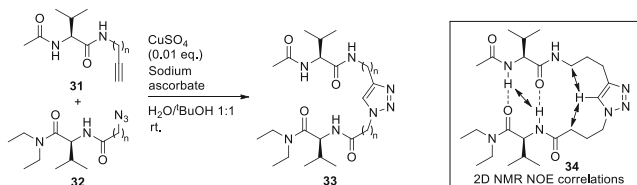
In the synthesis of analogues of the natural product apicidin (**26**), a Huisgen reaction gave the desired macrocycle, albeit as a 2:1 mixture of 1,4- and the 1,5-regioisomers **24** and **25** in low yield (Scheme 7) [33].

3.2 Copper(I)-Catalyzed Azide–Alkyne Cycloaddition (CuAAC)

The copper(I)-catalyzed 1,3-dipolar cycloaddition of organic azides and terminal alkynes (CuAAC reaction) was discovered by the Meldal group during exploration of solid-phase copper(I)-catalyzed couplings of peptide alkynes with azido acid



Scheme 8 First reported formation of a 1,2,3-triazole peptidomimetic



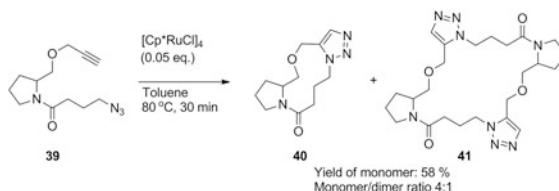
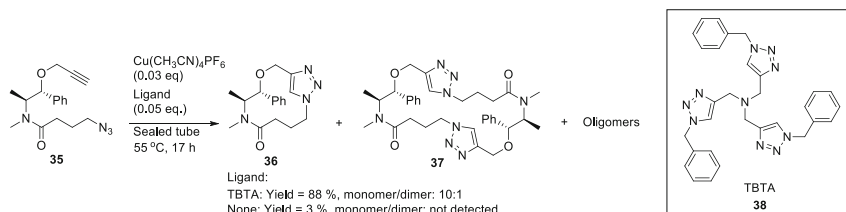
Scheme 9 CuAAC generated 1,2,3-triazoles and their use as turn mimetics in β -hairpin structure

chlorides [5, 34]. The catalytic effect of copper(I) enhanced the reaction rate by a factor of 10^7 compared to the non-catalyzed Huisgen reaction. The copper catalyst empowered 1,3-dipolar cycloaddition at room temperature and reduced reaction time from days to minutes. In addition, the CuAAC reaction was found to be regioselective giving 1,4-disubstituted triazole only (Scheme 8).

Copper iodide was initially applied as the copper(I) source in combination with DIPEA in DMF. However, occasional undesired iodination under these conditions led to examination of copper bromide and other copper(I) salts in later procedures [35]. For example, Cu(I) acetate [36] and dinuclear Cu(I) complexes [37] have been used in efficient CuAAC-catalyst systems.

In 2002, the Sharpless group independently reported the CuAAC reaction. In this case, copper(I) was generated in situ from copper(II) sulfate and ascorbic acid [38]. This aqueous method has also proven to be suitable for the synthesis of triazole peptidomimetics. For example, ligation of azide- and alkyne-functionalized amido amides (e.g., 31 and 32) gave triazoles 33, certain ($n=3$) of which were shown to adopt β -hairpin structure (e.g., 34) by 2D NMR studies (Scheme 9) [39].

In spite of significant progress in mechanistic studies, including finding that more than one copper atom is involved in the reaction transition state, the reaction mechanism for the CuAAC reaction has yet to be fully elucidated [8, 40]. Optimizing the reaction conditions has shown that inert atmosphere or addition of mild reductive agents may be beneficial in order to avoid oxidation of the catalytic copper(I) to inactive copper(II), as well as oxidative side reactions. Copper-coordinating ligands such as tris[(1-benzyl-1*H*-1,2,3-triazol-4-yl)methyl]amine (TBTA) (38, Scheme 10) may also enhance reactivity by preventing copper(I) oxidation and disproportionation and may influence the ratio of intra- versus intermolecular reactions [41–45]. For example, cyclization of azido alkyne 35

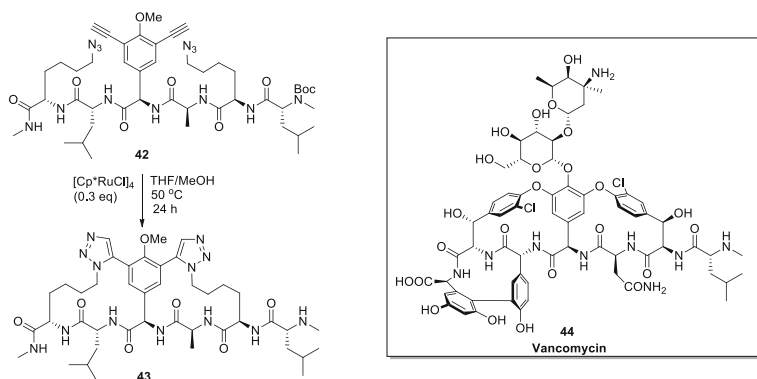


using the CuAAC reaction gave a 10:1 ratio of macrocycle **36** to dimer **37** in 88% yield in the presence of TBTA, but only 3% yield without ligand (Scheme 10) [46].

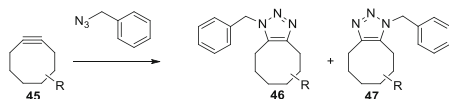
3.3 Ruthenium(II)-Catalyzed Azide–Alkyne Cycloaddition (RuAAC)

The success of the 1,4-regioselective CuAAC reaction stimulated the subsequent development of a 1,5-selective equivalent. The groups of Jia and Fokin mutually solved this challenge by using ruthenium(II) as catalyst to favor 1,5-regioisomer formation in reactions with terminal alkynes [47–49]. The so-called RuAAC reaction is also applicable to disubstituted alkynes at elevated temperatures [50]. The RuAAC reaction has been employed for generation of larger peptidomimetics but most commonly for the synthesis of dipeptide mimics, which were used subsequently as building blocks for incorporation into peptides (see e.g., Scheme 19 in Sect. 3.6). A different example is the synthesis of lactam **40**, which gave 58% yield under optimal conditions, albeit accompanied by substantial amounts of dimer **41** (Scheme 11) [51].

A vancomycin bis-1,5-triazole analogue **43** has also been synthesized in 40% isolated yield by a double RuAAC macrocyclization. The reactions were proven to be completely regioselective, and the product (**43**) was able to bind the D-Ala–D-Ala sequence targeted by vancomycin (**44**), albeit without exhibiting antibacterial activity (Scheme 12) [52].



Scheme 12 RuAAC reactions in the synthesis of a vancomycin analogue **44**



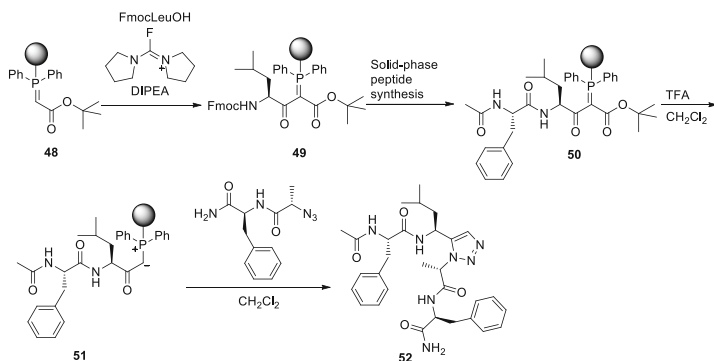
Scheme 13 The catalyst-free SPAAC reaction employed for bioorthogonal conjugation *in vitro* and *in vivo*

3.4 Strain-Promoted Azide–Alkyne Cycloaddition (SPAAC)

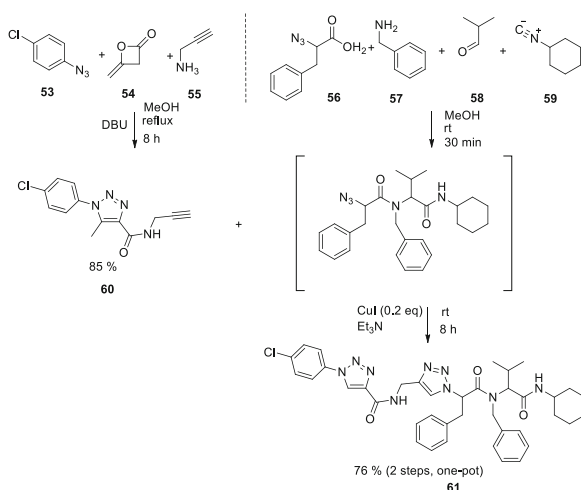
The potential of azide–alkyne cycloaddition reactions for bioorthogonal transformations gained attention due to the stability of azides and alkynes under physiological conditions. The application of metal catalysts was however prohibited by their toxicity and the reduced catalyst stability in oxygen containing biological environments. Bertozzi and coworkers avoided metal catalysis by employing ring strain to distort and polarize the triple bond (e.g., **45**, Scheme 13) [6, 53, 54]. Although the so-called strain-promoted azide–alkyne cycloaddition (SPAAC) has not been employed in peptidomimetic synthesis, this triazole-forming reaction has been used to study the chemical biology of a range of protein substrates [55] (Sect. 5.2).

3.5 Other Methods

Phosphorane-based 1,3-dipolar cycloadditions of the enols of phosphorous ylides (e.g., **51**) and azido dipeptides have been used to make 1,5-disubstituted triazole peptidomimetics by the Rademann group (Scheme 14) [56]. Cyclic peptides were similarly made by employing N-terminal azido peptides bound to phosphorous ylide solid support [57].

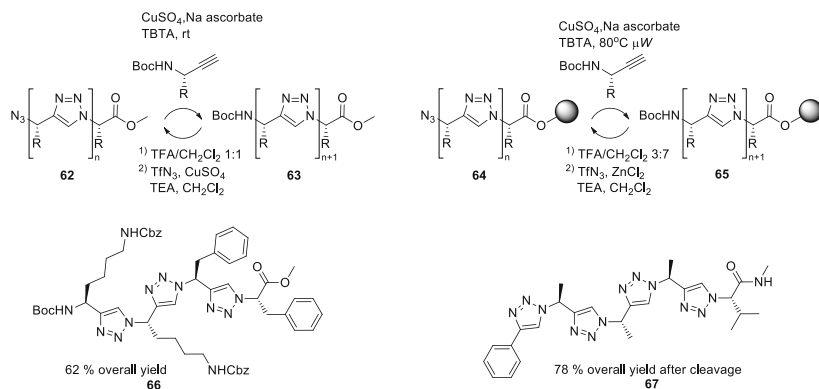


Scheme 14 1,5-Disubstituted triazole peptidomimetic synthesis by phosphorane-based 1,3-dipolar cycloaddition



Scheme 15 Three-step, one-pot assembly of peptidomimetic **61** by combination of multicomponent and CuAAC reactions

Another approach to triazole peptidomimetics employs multicomponent reactions. For example, bis-triazole peptidomimetic **61** has been prepared in 64% yield by a three-step procedure featuring a three-component triazole formation to alkyne **60**, a Ugi four-component reaction to azide **61**, and their combination by a final CuAAC reaction (Scheme 15) [58]. Key to the synthesis of **61** was the three-component triazole formation between azide **53**, diketene **54**, and propargyl amine **56**, because it permitted incorporation of a terminal alkyne into triazole **60** for a subsequent CuAAC reaction to form the second triazole. 1,2,3-Triazoles have also been synthesized from reactions of azides with alkenes, enamines, and enols [25]; however, these approaches have yet to be used for peptidomimetic synthesis.



Scheme 16 Solution-phase and solid-phase synthesis of amino acid-derived triazole oligomers

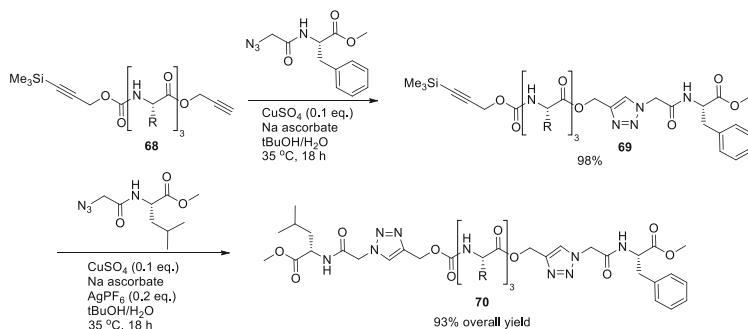
3.6 Oligomer Synthesis and Solid-Phase Synthesis

Inspired by the ability to synthesize larger oligomers using peptide chemistry, several methods have been developed for the synthesis of triazole peptidomimetic oligomers. Oligomers have been synthesized on solid phase and in solution by employing substituted *N*-Boc-propargyl amines derived from amino acids in repetitive CuAAC reaction/Boc removal/diazotransfer sequences (e.g., **66** and **67**, Scheme 16) [59]. By 2D-NMR studies, these compounds were shown to adopt extended structures with the neighboring triazoles pointing in opposite directions [60, 61]. Some compounds were found to be protease inhibitors, albeit with low potency [62].

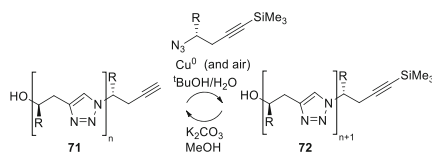
Masking of the terminal alkyne with a trimethylsilyl group has also been applied in methods to generate oligomers. Initially, the strategy was used to mask one alkyne in substrate **68** during CuAAC reaction on another (Scheme 17) [63]. Silyl group removal and sequential coupling of a second azido dipeptide provided selective access to oligomer bis-triazole **70**.

Employing alkyne masking with the trimethylsilyl group to building blocks also containing an azido group enabled synthesis of triazole oligomers (e.g., **71**, $n = 3$) by sequential CuAAC reactions and silyl group removals (Scheme 18) [64].

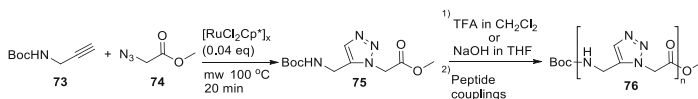
1,5-Disubstituted triazole oligomers have also been generated by peptide couplings of a triazole-containing dipeptide building block (Scheme 19) [65]. Building block **75** was generated by the RuAAC reaction followed by either Boc removal or ester hydrolysis.



Scheme 17 Chemoselective triazole formation using trimethylsilyl alkyne in CuAAC reaction



Scheme 18 Trimethylsilyl masked alkyne-azide building blocks in the synthesis of triazole oligomers



Scheme 19 Synthesis of 1,5-disubstituted triazole dipeptide mimetic and oligomers

4 Structures, Roles, and Applications of Peptide 1,2,3-Triazoles

4.1 The 1,2,3-Triazole as Backbone Amide Bond Surrogate

Triazoles are effective as surrogates for amide bonds, because of their similar size and dipole moment. The 1,4-disubstituted triazole may mimic the *trans*-amide bond and bear either the C- or N-terminal residue at the substituted nitrogen (N-1) giving rise to C–N or N–C orientations, respectively (Fig. 3). Compared to the backbone of a native dipeptide, the chain of the triazole mimic possesses an additional atom [12, 66]. For the C–N type, this results in a 1.2 Å longer distance of about 5 Å between the two α-carbons, such that rotation around the bonds to the triazole 1- and 4-positions may be needed in order to mimic original side-chain interactions for binding to protein targets [67, 68].

The dipole moment of 1,2,3-triazoles is strongly impacted by their substitution pattern [69]. 1,4-Disubstituted triazoles exhibit dipole moments calculated to be around 5 D [66], which is higher than many other azole derivatives [70] and comparable to that of an amide bond (3.7–4.0 D). The direction of the dipole points

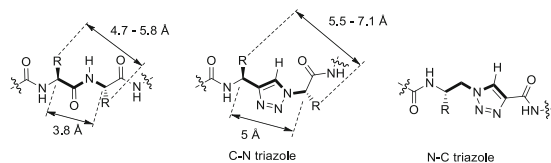


Fig. 3 Conformational mimics of peptide bonds using 1,2,3-triazoles

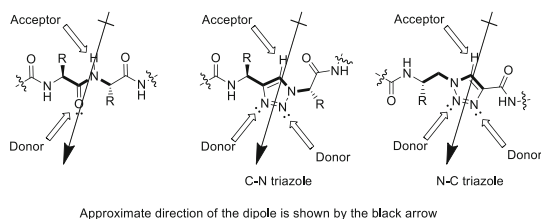


Fig. 4 Dipole and electron donor/acceptor properties of 1,4-disubstituted triazole *trans*-amide bond peptidomimetics

from the 5-position and to a position between N2 and N3 of the triazole ring [71] suggests that the proton in the 5-position may act as an electron acceptor and that both N2 and N3 may act as donors in hydrogen bonds. Electronically, 1,4-disubstituted triazoles constitute ideal mimics of amide bonds in peptides, in part because their dipole moments orient in the same direction (Fig. 4).

In the crystal structure of a 33 amino acid α -helical coiled coil peptide (pLI-GCN4) possessing a C–N triazole dipeptide mimic, the α -helical secondary structure was maintained, and hydrogen bonds were observed from the triazole C5 hydrogen, as well as to the 2- and 3-position nitrogen [72]. Some distortions from the native helical coil were detected in all constructs (Fig. 5a, b), which are likely to account for the lower thermal denaturation values and less-ordered crystal structures. For one of the constructs, a favored extended 1,4-disubstituted triazole backbone caused a frameshift from one helix to the next in the four-helix bundle (Fig. 5b).

With the aim to develop inhibitors toward a recombinant *Leishmania mexicana* cysteine protease, the Meldal group incorporated N–C triazoles into a peptide library from which hits with nanomolar activity were discovered (Fig. 6) [73]. Sequence alignment with the known protease substrate (77) indicated that the triazole (e.g., 79) bound to the S₃–S₂ site instead of the S₁–S₁' binding site [74]. Triazole peptidomimetics may thus bind strongly to protein targets in ways different from the native peptide, due to their extended backbone and mismatch of side-chain orientations.

A 1,4-disubstituted N–C triazole was introduced into a mimic of the antimicrobial BP100, which exhibited increased stability toward proteolytic digestion, albeit activity toward the pathogenic strains was severely reduced compared to native BP100 [75].

As surrogate for backbone amide bonds, 1,5-disubstituted 1,2,3-triazoles position the two α -carbons at a distance of 3.0 Å, which closely resembles the 3.2 Å

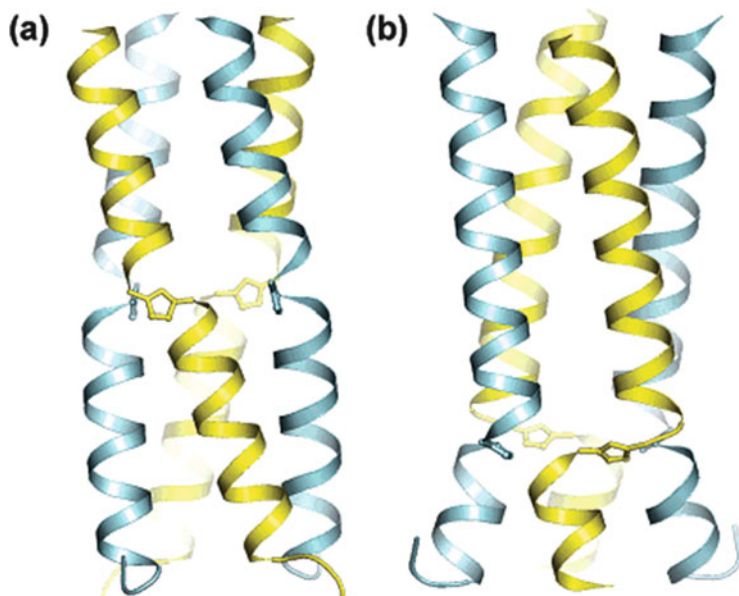


Fig. 5 Crystal structures of two α -helical triazole peptidomimetics

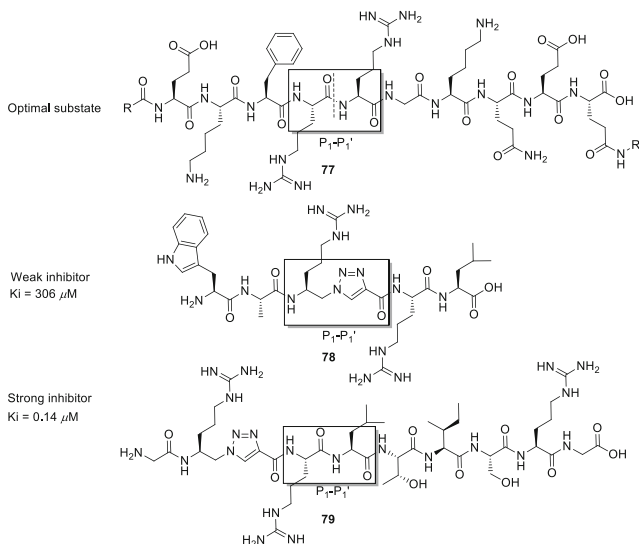


Fig. 6 The P_1 - P_1' binding of substrate and triazole peptidomimetics to *Leishmania mexicana* cysteine protease

distance of a native dipeptide *cis*-amide bond conformation (Fig. 7) [12]. The C-N type of 1,5-disubstituted 1,2,3-triazole separates the N- and the C-terminal residues by four chain atoms equivalent to a native dipeptide unit; however, the dipole

Fig. 7 Dipole and electron donor/acceptor properties of 1,5-disubstituted triazole *cis*-amide bond peptidomimetics

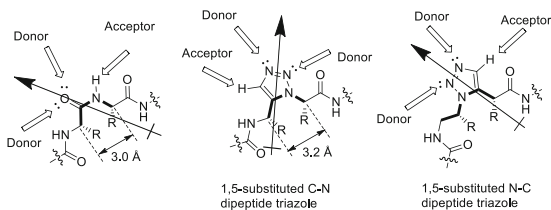
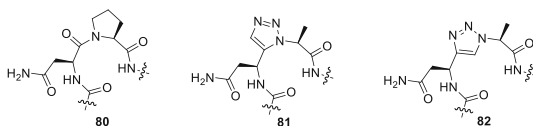


Fig. 8 Stabilization of turn structure by C–N 1,5- and C–N 1,4-disubstituted triazole peptidomimetics



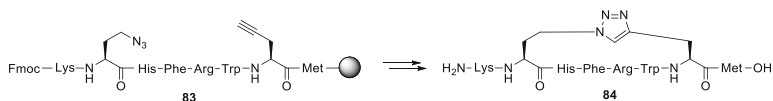
direction is reversed compared to that of the native *cis*-amide bond (Fig. 7). The N–C type of 1,5-disubstituted 1,2,3-triazole has the same dipole direction, but in order to be chemically stable, an additional carbon atom is needed in the dipeptide unit.

The 1,5-disubstituted 1,2,3-triazole has been less explored than its 1,4-disubstituted counterpart as backbone element. In one application, a fully functional RNase A mimic with identical properties to the native enzyme was created by replacement of the native asparagine–proline dipeptide turn sequence (**80**) with Asp-[1,5-triazoly]-Ala motif **81** (Fig. 8) [76]. The 1,5-disubstituted triazole mimetic was initially generated as a dipeptide building block and incorporated into the enzyme by a combination of protein expression, solid-phase synthesis, and native chemical ligation. Similarly, introduction of Asp-[1,4-triazoly]-Ala motif **82** also gave a fully functional enzyme, however, with a reduced thermal stability toward denaturation. Hence, the presented example demonstrated the 1,5-disubstituted C–N-type triazole to be a good structural mimic of the *cis*-prolyl bond. The absence of an electron-accepting proton in the prolyl amide bond may favor mimicry by the 1,5-disubstituted triazole.

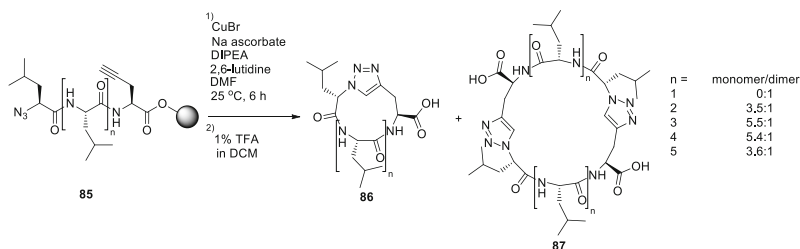
4.2 Cyclic Peptides

Both 1,4- and 1,5-disubstituted 1,2,3-triazoles have been applied in the synthesis of cyclic peptides. The first example was a side-chain to side-chain cyclization of a potential agonist of the G protein-coupled melanocortin-4 receptor (**84**, Scheme 20) [77]. The cyclization was conducted while the peptide was still attached to the solid support, and to illustrate chemical orthogonality with peptide functional groups, the CuAAC reaction was performed successfully with and without protecting groups in 79% and 76% yields, respectively.

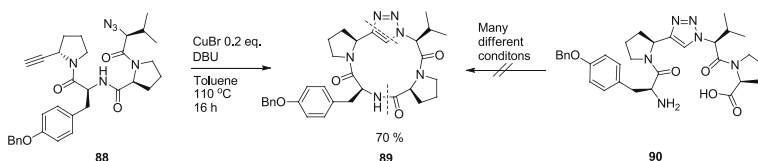
Although orthogonal chemistry empowers linear peptide synthesis followed by selective ring-closing reaction using the CuAAC reaction, the presence of both



Scheme 20 The first reported CuAAC-mediated synthesis of a cyclic peptidomimetic



Scheme 21 Ratio of cyclization to form monomer and dimer depends on peptide length and structure



Scheme 22 Exclusive cyclic monomer formation by ring closure using CuAAC reaction

alkyne and azide on the same linear precursor does not always lead to the desired macrocycle, because triazole formation may occur both intra- and intermolecularly. Cyclodimers have been the major and even exclusive side products from both long and short peptides synthesized on solid phase and in solution. Investigating the effect of peptide length on the preference for formation of cyclic monomer **86** versus cyclic dimer **87** (Scheme 21), short and long peptides, both were found to be more prone to cyclodimerization than peptides of midrange length [78]. Ring strain during cyclization and potential to form intra- and intermolecular backbone hydrogen bonds play important roles in pairing of azide and alkyne components. For example, in longer peptides the formation of antiparallel dimers of β -strands during reaction may account for the high degree of dimer formation [79]. In addition to peptide length and structure, the reaction solvent and resin properties may influence ring closure [80].

The amino acid composition of the linear precursor may also influence the cyclization reaction. For example, tetrapeptide **88** possessing two proline residues yielded macrocycle **89** in 70% yield without dimerization (Scheme 22) [35]. On the other hand, attempts completely failed to form **89** by ring closure using peptide coupling of triazole-containing linear precursor **90**. Cyclization of tetrapeptides by peptide coupling is known to be difficult [81, 82], and as illustrated here, macrocyclization by triazole formation may be a route to solve the problem.

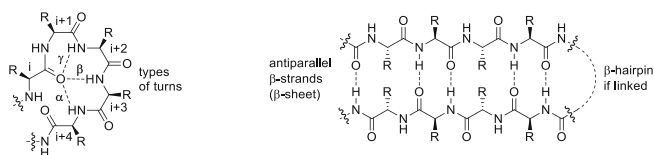


Fig. 9 Schematic overview of peptide turns and antiparallel β -strands

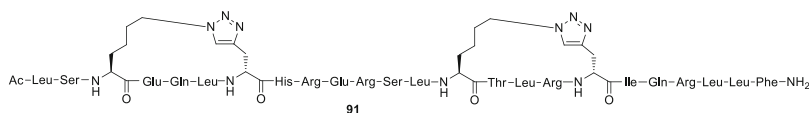


Fig. 10 CuAAC reaction between azide and alkyne side chains provided stable α -helical peptide **91**

4.2.1 Stabilization of Peptide Secondary Structures: Turns, Helices, and Sheets

One of the important functions of peptidomimetics is their ability to stabilize the active structure of natural peptides in a truncated motif. Natural peptides and proteins commonly have secondary structure elements, such as turns, helices, and sheets in their bioactive conformation. Turns are classified by the size of the pseudo-ring constituted by amide hydrogen bonding in the peptide backbone. Among the most common structural elements are the α - and 3_{10} -helices consisting of repeated α - and β -turns, respectively. β -Turns are commonly also found in combination with two β -strand elements, which makes up a β -hairpin motif (Fig. 9).

α -Turns

Triazoles have been applied to stabilize α -turns and α -helices by serving as side-chain to side-chain links in so-called stapled or bridged peptides that are formed by reactions between modified amino acid residues containing azide and alkyne groups [83]. For example, in studies of triazole peptidomimetics of the α -helical binding section of B-cell lymphoma 9 [84], best α -helical structures were obtained by the reaction of L- ϵ -azido-norleucine [Nle(ϵ N3)] and L-propargylglycine residues in the i and $i+4$ position, respectively (Fig. 10). Introducing two such motifs into a 24-residue peptide resulted in mimic **91** exhibiting 99% α -helicity, stronger binding toward the target β -catenin, and enhanced proteolytic stability compared to the native sequence.

In a comparison of a series of different “non-amide bond” linkers, triazole motif **92** proved the best for stabilization of a single α -turn in water, as well as helix conformations in an 18-residue peptide (Fig. 11) [85].

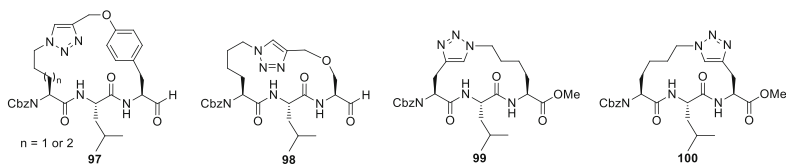


Fig. 13 Stabilized β -strand peptides from triazole formation between the side chains of residues i and $i+2$

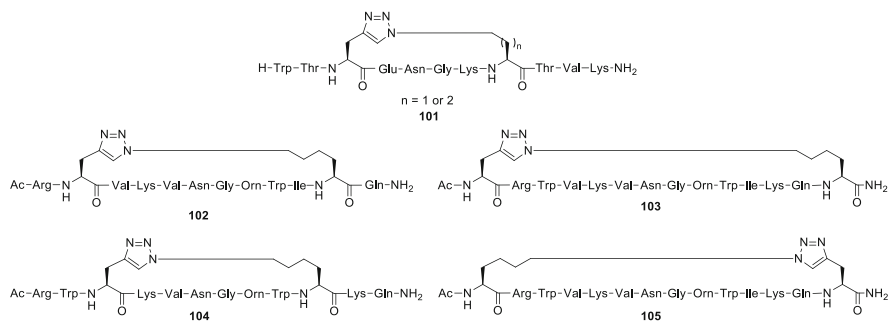


Fig. 14 Peptides with β -hairpin structures induced by triazole side-chain to side-chain cross-links

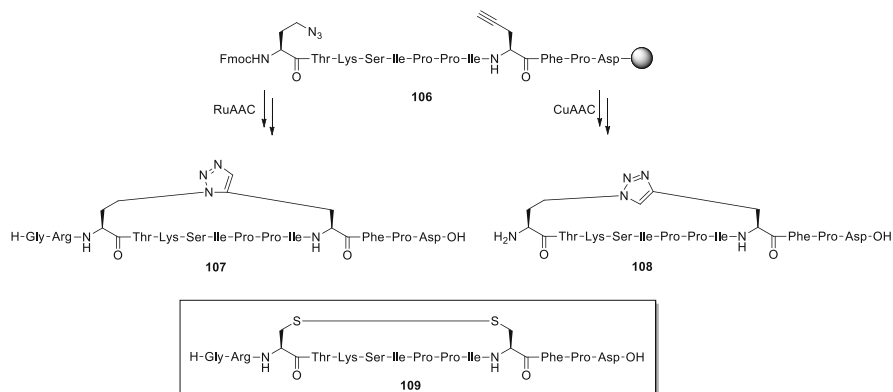
β -Stands and β -Hairpins

Like most other endoproteases, calpain II is known to bind and cleave linear peptides in a β -strand conformation. β -Strand mimics that inhibited calpain II were identified from constrained tripeptides **97–100** featuring triazole links between alkyne and azide side chains of amino acid residues at the i and $i+2$ positions (Fig. 13) [88, 89]. Elaboration on these motifs gave extended β -sheets which self-assembled into nanotubes [89].

Larger macrocyclic triazole peptidomimetics that adopted a β -hairpin consisting of two β -strands were synthesized by linking i and $i+5$ residue side chains in triazole **101** (Fig. 14) [90]. Through studies to determine the optimal side-chain length and triazole placement, the combination of propargylglycine at the i -position and 4-azido-2-amino butyric acid [Dab(N₃)] at the $i+5$ residue was found to best favor β -hairpin structure. Larger macrocyclic triazole peptidomimetics formed by linking propargylglycine and the ω -azide derived from lysine (e.g., **102–105**) also favored β -hairpin structures with up to 14 amino acid residues in the cycle (Fig. 14) [91].

Triazoles as Disulfide-Bond Mimetics

Triazoles have also been used as replacements of natural disulfide bonds. For example, the disulfide in trypsin inhibitor **109** was replaced by triazoles formed



Scheme 24 RuAAC and CuAAC reactions for generation of triazole disulfide-bond mimics

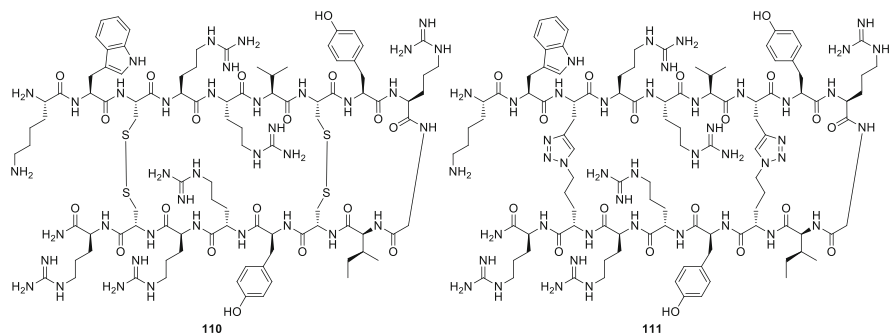
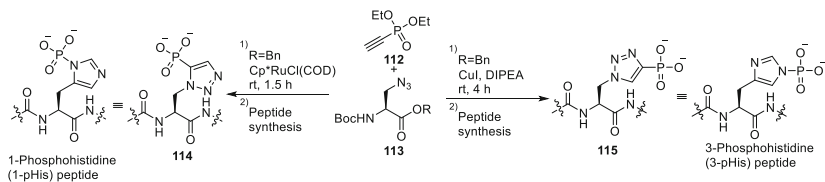


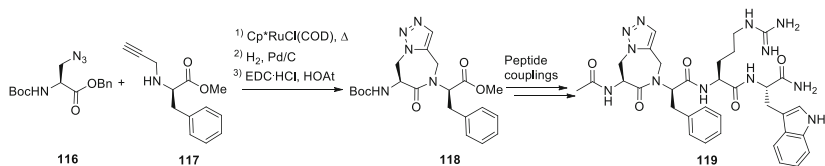
Fig. 15 Tachyplesin 1 from the horseshoe crab (*Tachyplesus tridentatus*) and bis-triazole mimetic **111** in which the disulfide bonds were replaced by 1,2,3-triazoles formed by CuAAC reaction

using CuAAC and RuAAC cyclizations of peptides (Scheme 24) [92]. The RuAAC reaction was performed on protected peptide bound to a solid support and 1,5-disubstituted triazole **107** was isolated in low yield (2%). The CuAAC reaction on the other hand was conducted on the deprotected peptide in solution and provided 1,4-disubstituted triazole **108** in good yield. 1,5-Disubstituted triazole **107** exhibited identical activity as trypsin inhibitor **109** possessing the disulfide bond; however, 1,4-disubstituted triazole **108** was 500 times less potent.

The CuAAC reaction has also been used to replace two disulfide bonds in tachyplesin 1 (**110**), an antibacterial β -hairpin structure from horseshoe crab (*Tachyplesus tridentatus*) (Fig. 15) [93]. Employing a linear peptide with two C-terminal ω -azido amino acid residues and two N-terminal propargylglycines, the CuAAC chemistry gave bis-triazole peptide **111** exhibiting a β -hairpin structure similar to that of the native peptide with comparable if not better activity toward a range of bacterial strains.



Scheme 25 Application of triazoles in phosphohistidine mimics



Scheme 26 Synthesis of a constrained histidine analogue by 1,5-disubstituted triazole formation

4.3 Side-Chain Mimetics

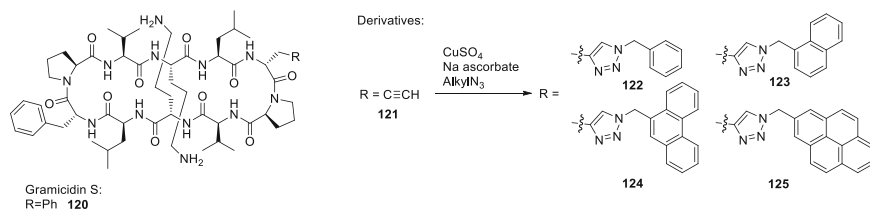
In addition to serving as cross-links, triazoles have mimicked other side-chain functions. For example, phosphohistidine surrogates **114** and **115** were prepared using RuAAC and CuAAC reactions to provide the 1,5- and 1,4-disubstituted triazoles, respectively (Scheme 25) [94]. Similar chemistry was used to prepare the Fmoc-protected phosphohistidine counterparts for solid-phase peptide synthesis [95, 96].

Agonists and antagonists of the melanocortin G protein-coupled receptors (e.g., **119**) have also been synthesized using triazoles in constrained histidine surrogates such as **118** (Scheme 26) [97, 98].

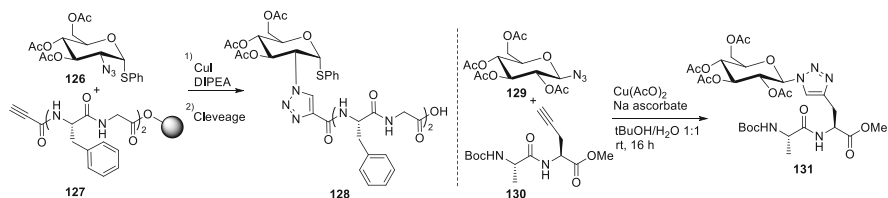
The triazole formation may also serve as a convenient way of testing a range of different side-chain functionalities at a given amino acid position in a larger peptide. Employing propargylglycine in intermolecular CuAAC reactions with common alkyl azides, the structure–activity relationship of the D-phenylalanine residue of the natural antibiotic gramicidin S (**120**, Scheme 27) was studied [99]. The strategy was also applied to a sunflower trypsin inhibitor-1 in order to enhance inhibition of the serine protease matriptase [100].

Many non-ribosomal peptides contain modified side chains that are crucial for bioactivity. CuAAC chemistry has been explored to simplify the synthesis of such analogues. For example, different length triazole tethers were used to attach the polyketide chromophore to the cyclic peptide body of chlorofusin in efforts to enhance the natural tumor-suppressing activity [101].

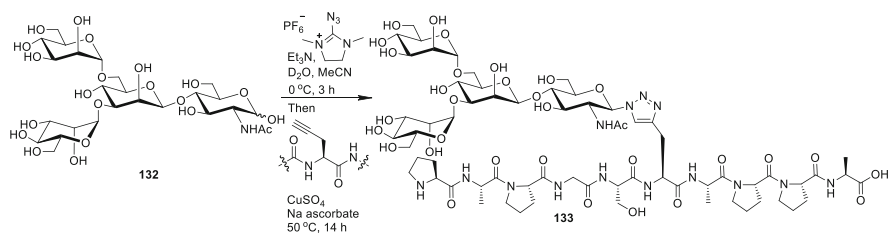
After ribosomal synthesis, the side chains of many peptides and proteins are often enzymatically modified with carbohydrates to produce so-called glycopeptides, which are challenging to synthesize by traditional chemical methods. Alternatively, alkyne-bearing peptides can be readily functionalized by CuAAC reactions with different azidoglycosides (e.g., **128**) on solid phase [34] and in



Scheme 27 Gramicidin S analogues generated by side-chain permutations via triazole formation



Scheme 28 Examples of triazole-linked glycopeptides

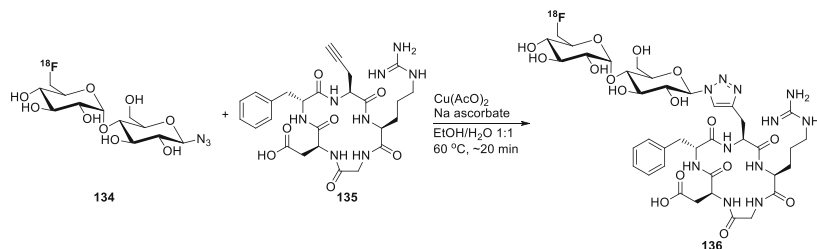


Scheme 29 One-pot synthesis of a glycopeptide from an unprotected reducing oligosaccharide and an alkyne peptide

solution (e.g., **131**) (Scheme 28) [102–104]. Such methods have also been used to synthesize antifreeze glycopeptide analogues [105, 106].

Moreover, complex glycopeptides (e.g., **133**) have been effectively synthesized by employing a one-pot method for converting unprotected reducing sugars (e.g., **132**) into azidoglycosides prior to CuAAC reaction with unprotected peptides bearing alkyne side chains (Scheme 29) [107].

The rapid and quantitative nature of the CuAAC reaction has proven particularly effective for isotopic labeling of peptides. For example, azido-2-fluoro-monosaccharides have been reacted with alkyne side chains to make various triazole-linked amino acids, peptides, and proteins [108], such as ^{18}F -glyco-RGD peptide **136** for in vivo tumor imaging by positron-emission tomography (Scheme 30) [109].



Scheme 30 Synthesis of a radiolabeled construct of fluoroglycosylated RGD peptide by CuAAC reaction

5 Triazoles in Proteins

Proteins possess long polypeptide chains that adopt commonly stable three-dimensional structures. These features distinguish proteins from peptides, which have fewer amino acids and exhibit more dynamic conformational equilibriums. Protein tertiary structure forms the basis for various functions, including catalysis, signal transduction, transport, and structural maintenance.

The combination of 1,2,3-triazoles and proteins has generally not been pursued to alter the molecular properties of the latter but instead to covalently attach another molecule – varying from small fluorophores to large polymers or even other proteins – to the protein of interest. In this section, we discuss examples of triazole-containing protein conjugates that are produced *in vitro*, at the surface and inside living cells. The strategies for site-selective introduction of azide and alkyne functionality into proteins are less straightforward than those used for peptides and are first briefly discussed. Recent advances are summarized for increasing the biocompatibility of the chemistry applied for triazole synthesis noting that among methods discussed in Sect. 3, only CuAAC and SPAAC have been used to modify proteins so far.

5.1 Strategies for the Introduction of Azides and Alkynes into Proteins

The azide–alkyne cycloaddition variants CuAAC and SPAAC have been the two most popular reactions for bioconjugation in protein chemistry and chemical biology. These methods exhibit broad utility, due to the orthogonal reactivity of azides and terminal alkynes, which combine selectively in the presence of proteins under physiological conditions. Moreover, as discussed in Sect. 3, both reactants are stable under most reaction conditions used in peptide synthesis and inert to metabolic processes in cells.

Several techniques are available for introducing azide and alkyne groups into proteins. In the past decades, two distinct methods have been developed for inserting unnatural amino acids bearing azide and alkyne side chains into proteins

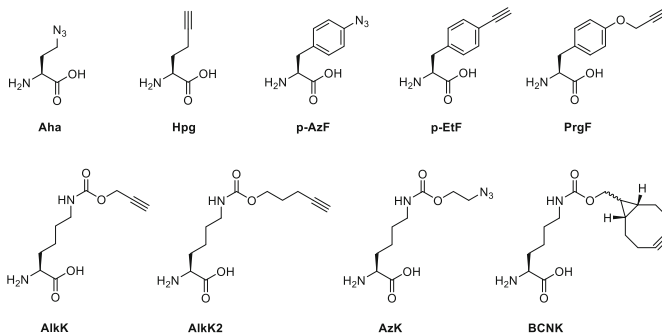


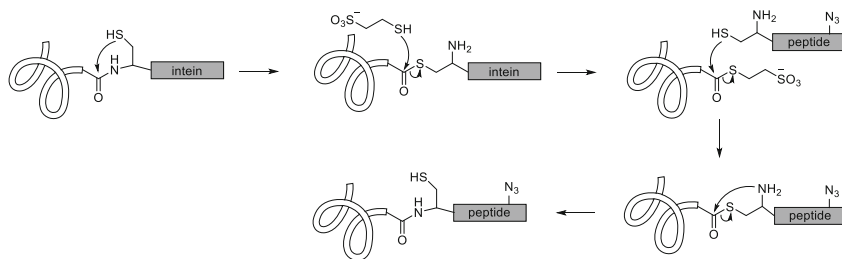
Fig. 16 Representative unnatural amino acids used for functionalization of proteins with azide and alkyne moieties. Aha (azidohomoalanine), Hpg (homopropargyl glycine), p-AzF (*para*-azidophenylalanine), and p-EtF (*para*-ethynylphenylalanine) have been incorporated using the residue-specific replacement method. p-AzF, PrGF (*para*-propargyloxyphenylalanine), and pyrrolysine analogues bearing an aliphatic alkyne (AlkK and AlkK2), aliphatic azide (AzK), and bicyclononyne (BCNK) have been introduced using the site-specific incorporation approach [110]

by manipulation of cellular translational machinery [110]. Residue-specific replacement of a particular natural amino acid with a structurally and electronically similar analogue has been achieved by simply adding the latter to the growth medium of cells that incorporate the unnatural amino acid into all newly synthesized proteins at every position in which the natural residue would normally be incorporated [111, 112]. Genetic code expansion has been used to insert an unnatural amino acid into a defined position in the protein of interest. A so-called blank codon, usually the amber stop codon UAG, is genetically inserted at the desired site of modification in the gene encoding the protein of interest. A tRNA and aminoacyl-tRNA synthetase that recognize the stop codon and the unnatural amino acid, respectively, are co-expressed inside the host cell in order to introduce an extra amino acid in addition to the 20 natural ones, as reviewed in more detail [113, 114]. A broad selection of the unnatural amino acids bearing azide and alkyne side chains have been incorporated using these methods (Fig. 16).

In addition to the incorporation of unnatural amino acids, proteins can be site-specifically labeled using enzymes such as transglutaminase, lipotic acid ligase (Lpl A), and sortase, which have been shown to accept and transfer azide- and alkyne-containing variants of their natural substrates to proteins [115–118].

Intein-mediated protein ligation has been used to combine natural proteins with synthetic peptide sequences [119–122]. The protein is expressed as a fusion to intein, which can undergo cleavage after addition of a thiol reagent, typically 2-mercaptoethanesulfonic acid to provide a protein C-terminal thioester that reacts subsequently with a synthetic peptide containing an N-terminal cysteine (Scheme 31).

Chemical modification of naturally occurring amino acids has also been used to modify proteins with azide and alkyne functionality. For example, lysine residues



Scheme 31 Introduction of a “clickable” azide handle through intein-mediated protein ligation. The reaction starts with an N–S shift followed by thiol-mediated cleavage of the intein, thiol displacement by peptide possessing N-terminal cysteine, and S–N shift

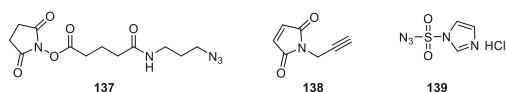


Fig. 17 Reagents used for the chemical modification of naturally occurring amino acid residues in proteins

have been labeled with the *N*-hydroxysuccinimidyl ester of 5-(3-azidopropylamino)-5-oxopentanoic acid (**137**) [41], and cysteine residues have been reacted with *N*-propargyl maleimide (**138**) [123] (Fig. 17). The conversion of amines into azides using imidazole-1-sulfonyl azide hydrochloride (**139**, Fig. 17) offers an efficient and convenient method for the introduction of azides into proteins [124], because under metal-free and pH-controlled conditions, the amine having the lowest pK_a may be selectively modified [125].

5.2 Increasing the Biocompatibility of the Azide–Alkyne Cycloaddition

The greater structural complexity of proteins, compared to peptides, and the concomitant risk of losing protein function necessitate milder conditions for forming the triazole linkage. To avoid the denaturing effect of organic solvents, such as DMF and acetonitrile, triazole-forming reactions are commonly performed in pH-buffered aqueous solution. Moreover, the reaction scale is typically small, because proteins are relatively expensive to produce and used in low amounts. A Cu (II) precursor (e.g., copper sulfate) and excess of reducing agent (e.g., sodium ascorbate) may be employed in CuAAC reactions on proteins, because of difficulties in maintaining an inert atmosphere. Copper can however be detrimental to protein structure, because of its potential to catalyze the generation of reactive oxygen species that oxidize and cleave the polypeptide chain. Moreover, dehydroascorbate and other ascorbate by-products may modify covalently the side chains of lysine and arginine residues and cause protein aggregation [43].

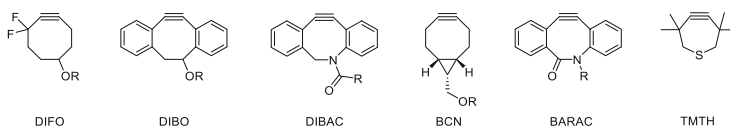


Fig. 18 Examples of cyclooctynes used in the strain-promoted azide–alkyne cycloaddition

Development of the strain-promoted azide–alkyne cycloaddition (SPAAC) has provided a solution to address these issues. The strained cyclooctynes employed in this variant of the azide–alkyne cycloaddition make the addition of a metal catalyst obsolete. Since the first applications of SPAAC reactions to selectively modify biomolecules *in vitro* and on living cells without apparent toxicity by the Bertozzi group in 2004 [6], several cyclooctyne derivatives have been developed: difluorocyclooctyne (DIFO), dibenzocyclooctyne (DIBO), aza-dibenzocyclooctyne (DIBAC), bicyclo[6.1.0]nonyne (BCN), biarylazacyclooctyne (BARAC), and tetramethylthiacycloheptyne (TMTH) (Fig. 18) [126–131].

The high reactivity of strained alkynes has reduced selectivity, and reactions with free sulfhydryl groups can compete with cycloadditions on azides [132, 133]. The necessity for ring strain reduces the structural variety of the triazole product. Moreover, the presence of strained alkynes, such as DIBO, DIBAC, and BARAC, increases lipophilicity and potential for nonspecific interactions with proteins. The commercial availability of cyclooctyne reagents is limited, and their synthesis is relatively challenging. Taking these aspects into account, among the commercially available reagents, BCN has optimal properties, because of its low lipophilicity, high reactivity, and accessible synthesis. Were lipophilicity not a point of concern, the DIBAC-containing probes offer the advantages of higher reactivity compared to BCN and better stability than BARAC and TMTH.

Seeking an alternative solution, copper catalyst formulations have been developed with improved biocompatibility for the CuAAC reaction. Ligand variants have been designed to enhance the water solubility of the Cu(I)-stabilizing TBTA, including the hydroxypropyl derivative THPTA, the 2-ethoxy-2-oxoethyl derivative TEOTA, as well as BTTEs and BTTAAs, both containing two bulky *tert*-butyl groups together with an ethyl hydrogen sulfate or acetic acid group in the third arm, respectively (Fig. 19) [134]. Chelation-assisted CuAAC reactions have been developed that use azide substrates possessing a copper-coordinating moiety [135–137]. By raising the effective copper concentration at the reaction site, such substrates may maintain reaction rates at lower copper concentrations. For example, picolyl azide (**140**, Fig. 19) has been employed to functionalize proteins efficiently at copper concentrations as low as 10–100 μM [135, 136]. After preloading with copper, fluorescently labeled copper-chelating azide **141** (Fig. 19) enabled efficient protein labeling inside living cells at a concentration of 50 μM [137].

Dihydrofolate reductase (DHFR) was used as a model system to test the effect of CuAAC reaction conditions on enzyme activity [138]. Employing genetic code expansion, an amber codon was used to replace a single valine with *p*-ethynylphenylalanine to position an alkyne on the surface of DHFR without perturbing

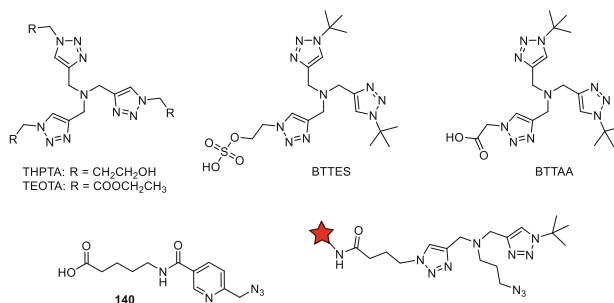


Fig. 19 Water-soluble Cu(I)-chelating ligands and copper-chelating azides improve CuAAC biocompatibility. The star in **141** represents the labeling fluorophore TAMRA

function. The CuAAC reaction was performed with azide-functionalized dye using TBTA and THPTA as Cu(I)-chelating ligands in combination with DTT, TCEP, and ascorbate as reducing agents. By evaluating labeling efficiency and residual enzyme activity as a measure of protein function, optimal CuAAC reaction conditions were established: 1 mM CuSO₄, 1 mM THPTA, and 2 mM ascorbate for 15 min. Optimization of CuAAC chemistry for bioconjugation demonstrated improved efficiency using a fivefold excess relative to copper of THPTA, which acted as a sacrificial reductant that intercepted reactive oxygen species in the coordination sphere of the metal as they were generated [43]. The ligands BTTAA and BTTES showed significantly higher activity compared to THPTA [139]. Moreover, in head-to-head comparisons on purified recombinant glycoprotein and glycoproteins in crude cell lysates, CuAAC-mediated labeling using BTTAA (or BTTES) as ligand proved more efficient than the comparable labeling method using the SPAAC reaction and a BARAC-functionalized probe [139].

5.3 Triazole-Containing Protein Conjugates Produced *In Vitro*

The azide–alkyne cycloaddition reaction has provided controlled and convenient methods for covalent attachment of various molecules to proteins. The resulting triazole protein conjugates have been used to improve function and to add new properties to the protein. Triazole conjugates have also served in the investigation of the structure and function of certain proteins. Moreover, triazole links have been formed between regions of the same protein. To illustrate the wide applicability of the azide–alkyne cycloaddition in the fields of biotechnology, chemical biology, and biomaterials science, this section describes examples of these triazole categories, schematically represented in Fig. 20.

The use of the azide–alkyne cycloaddition reaction for the generation of protein conjugates with improved function is exemplified by the production of site-

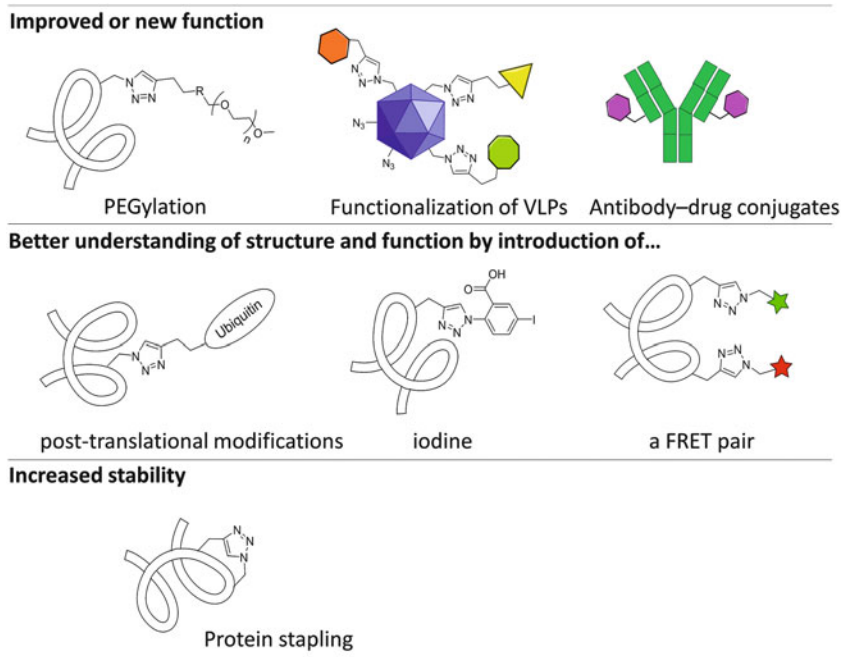


Fig. 20 Selected examples of the application of triazole-containing proteins prepared in vitro

specifically PEGylated interferon β -1b (IFN β) [140]. Poly(ethylene glycol) chains of varying length, all functionalized with an alkyne moiety, were coupled to a mutant of IFN β containing a single azidohomoalanine residue at its N-terminus. The PEGylated IFN β variants displayed increased in vivo efficacy. Among other examples from the area of biopharmaceuticals, antibody–drug conjugates (ADCs) and bio-specific antibodies have been formed with triazole linkages, by exploiting both unnatural amino acid incorporation and enzyme-mediated modification strategies for introduction of the clickable handle, using CuAAC and SPAAC reactions for conjugation [141–143]. Furthermore, oligomers of hemoglobin with a potentially higher resistance to extravasation have been produced through CuAAC-mediated cross-linking [144].

Conjugation of a circular cell-penetrating peptide to green fluorescent protein (GFP) was performed using the CuAAC reaction and resulted in efficient delivery of the protein into live cells [145]. Virus-like nanoparticles (VLPs) have been modified using CuAAC chemistry [146]. The surface-exposed methionines of the self-assembled protein shells of the bacteriophage MS2 and Q β VLPs were replaced, respectively, with azidohomoalanine and homopropargylglycine to provide azide and alkyne side chains [147]. Three different biomolecules (i.e., an iodotypic antibody fragment antigen, a cytokine, and an immunostimulatory oligonucleotide) were coupled in a single step, providing a VLP-based vaccine candidate for treating B-cell lymphoma [147]. Alternatively, the surface of the bacteriophage

Q β VLP has been chemically modified by acylation with the *N*-hydroxysuccinimide ester of 4-pentynoic acid to give alkyne side chains, which were reacted in simultaneous CuAAC-mediated couplings to glycans and porphyrins [148]. The resulting VLPs were designed for targeted photodynamic therapy in which the metalloporphyrins act as photosensitizers, and the glycan binds selectively cells bearing the CD22 receptor [148]. The SPAAC reaction was used to generate protein conjugates with new molecular properties by the synthesis of elastin-like polypeptide–poly(ethylene glycol) (ELP–PEG) conjugates, which self-assembled into micelles at 2.0–3.5 M NaCl encapsulating a fluorescent dye [149].

In higher organisms, protein function is commonly modulated by post-translational modification using glycosyl chains, lipids (e.g., palmitates, myristates, and isoprenoids), and the protein ubiquitin. The CuAAC reaction offers access to protein variants containing such modifications at defined positions for studying their influence on biochemical properties. For example, triazole links have been used to create homogeneously well-defined ubiquitylated proteins [150, 151], ubiquitin dimers (diUbs) [152, 153], and ubiquitin polymers [154]. The diUbs exhibited a native-like binding pattern to a particular Ub-binding domain, validating the triazole as an effective mimic of the natural amide bond between the lysine side chain of one ubiquitin and the carboxylate terminus of another [153]. In addition, CuAAC reactions have been used for site-specific protein glycosylation [155], geranylgeranylation, and palmitoylation [156].

Triazoles have also served as links to attach small-molecule probes to proteins in studies of structure and function. For example, protein iodination was achieved by homopropargylglycine incorporation followed by CuAAC-mediated coupling of 2-azido-5-iodobenzoic acid [157]. A Förster resonance energy transfer (FRET) pair was assembled on the regulatory protein RanBP3 by introduction of alkyne side chains at two distinct positions in the protein and labeling subsequently with two azide-functionalized FRET dyes [158]. Single-molecule fluorescence microscopy provided insight into the disordered confirmation of a specific region of RanBP3, which was not accessible to X-ray crystallography.

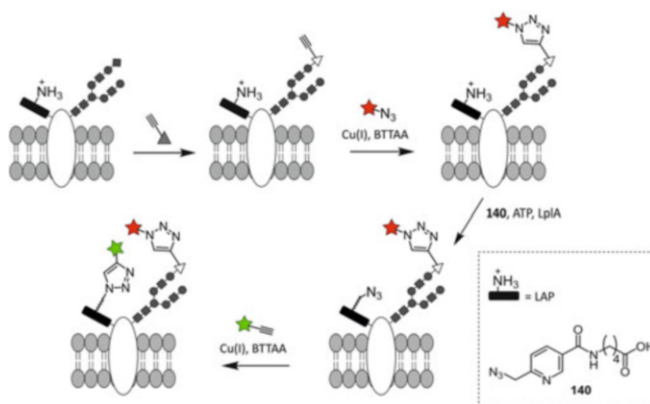
Analogous to side-chain to side-chain ligation of peptides (see Sect. 3), triazoles have been employed to form intramolecular links between azide- and alkyne-bearing amino acids in a recombinant protein [159, 160]. For example, calmodulin was modified with *p*-azido-L-phenylalanine and N⁶-(2-propynyloxy)carbonyl]-L-lysine and expressed in *Escherichia coli* using a combination of quadruplet and amber codons [160]. Triazole formation was achieved using catalytic Cu(I) and bathophenanthroline as ligand and confirmed by gel electrophoresis and MS/MS sequencing, albeit the effect of cyclization on protein structure and stability was not investigated [160].

Azidohomoalanine and *p*-ethynylphenylalanine were introduced into a leucine zipper protein consisting of 68 amino acids. Triazole links were introduced at the center and at the C-terminal regions of the helix, by employing THPTA as a water-soluble, biocompatible ligand, CuSO₄, and ascorbic acid. In both cases, the modified proteins were stabilized by the triazole and retained about 50% helical content at 90°C, a temperature at which the native protein was completely unfolded

[159]. In a second model, the neighboring residues on helix and strand sequences of the core of the globular immunoglobulin G (IgG)-binding domain of protein G (72 amino acids) were linked by a triazole that gave a fourfold enhancement of IgG binding, which was suggested to be due to minimization of the entropic penalty incurred during the binding event [159].

5.4 Triazole Formation in Cells and Living Organisms

As discussed in Sect. 5.2, biocompatible reaction conditions have enabled azide-alkyne cycloadditions on purified proteins, as well as on proteins in cells [134]. - Triazole-mediated labeling in cells has been used to study protein synthesis, localization, trafficking, and dynamics. For example, to study the influence of glycosylation on specific proteins (e.g., integrin $\alpha_x\beta_2$, epidermal growth factor receptor, and transforming growth factor-beta receptor type I) at the surface of living cells, a combination of the global incorporation of an alkyne-functionalized monosaccharide and the site-specific modification of the protein of interest was used to install a FRET acceptor-donor pair (Scheme 32) [161]. The protein of interest was expressed with a 13-amino acid peptide called LAP (lipoic acid ligase acceptor peptide) fused to its extracellular N-terminus. A mutant lipoic acid ligase (LplA) was then used to conjugate a picolyl azide derivative (**140**). The FRET donor (Fluor 488-alkyne) and acceptor (Alexa Fluor 647-azide) were respectively



Scheme 32 Dual-labeling of a membrane protein and its attached glycan for protein-specific imaging of cell surface glycans [161]. First, glycans on various cell surface proteins are labeled by the addition of an alkyne-containing metabolic precursor of sialic acid. Second, the FRET acceptor is attached to the labeled glycans through the BTAA-assisted CuAAC reaction. Third, ATP-dependent ligation by LplA is used to label selectively the N-terminus of the target protein with azide **140**. Finally, the introduced azide is reacted with the FRET donor by another CuAAC reaction

coupled to the azide-modified protein and alkyne-containing glycan by CuAAC reactions using BTTAA as ligand.

For the installation of a FRET donor–acceptor pair into the extracellular domains of epidermal growth factor receptor, three labeling techniques were compared: CuAAC, SPAAC, and inverse-electron demand Diels–Alder (IEDDA) reactions [162]. For this comparative study, pyrrolysine analogues containing a linear alkyne (AlkK2), azide (AzK), or bicyclononyne moiety (BCNK) were incorporated. Dyes functionalized with azide, dibenzocyclooctyne, or tetrazine were used as fluorescent label. Consistent with previous reports [133, 163], labeling using SPAAC resulted in high background fluorescence. Moreover, the efficiency of IEDDA-mediated labeling was lower than the BTTAA-assisted CuAAC reaction.

In addition to cell surface proteins, intracellular proteins have been labeled using triazole formation [163]. In order to selectively detect newly synthesized proteins, fibroblast cells were pulse-labeled with azidohomoalanine. Subsequently, the small, membrane-permeable fluorophore coumarin conjugated to a cyclooctyne was used in SPAAC reactions to visualize this subset of the proteome inside living cells. In a different cell-based approach, the target protein containing the LAP sequence was co-expressed with a mutant of LplA, which was used to attach site-specifically an azide-functionalized substrate. On incubation of the cells with a cyclooctyne-containing fluorophore, the SPAAC reaction was then performed selectively on the azide-bearing proteins [164].

Similar strategies have been employed to label proteins in multicellular organisms [165]. Newly synthesized proteins were tagged in a 7-day-old larval zebrafish by incubation with azidohomoalanine and visualized by CuAAC-mediated conjugation of an alkyne-functionalized dye [166]. Glycans linked to proteins and to lipids inside cells as well as on cell surfaces have been labeled with azides and alkyne moieties using metabolic oligosaccharide engineering [167]. Both SPAAC and biocompatible variants of CuAAC have been employed in these methods, which were initially applied on cultured cells [135, 168], and subsequently proven to be applicable for in vivo imaging of membrane-bound and intracellular glycans in developing organisms. In addition to simple organisms, such as zebrafish [169–171] and *Caenorhabditis elegans* [172], mice have been employed in these applications of triazole formation in living organisms [173]. In the field of nuclear medicine, antibodies are commonly conjugated to radionuclides for imaging and treatment of tumors. In a so-called tumor pre-targeting approach [165], tumor-specific antibodies are modified ex vivo using alkyne or azide moieties and then administered to the body of the living organism, followed by the radionuclide containing the complementary functionality for triazole synthesis. The antibody first locates the tumor and is then reacted with the radionuclide component to image the tumor-bound antibody.

6 Conclusion and Perspectives

Within the last two decades, triazoles have evolved to become one of the most commonly used heterocycles in peptidomimetic and protein chemistry. Although 1,2,4-triazoles were first employed in mimetic synthesis, the field of triazole-based peptide mimicry began to flourish with the discovery of the copper(I)-catalyzed 1,3-dipolar cycloaddition (CuAAC) reaction for making the 1,2,3-counterparts. The CuAAC reaction has become the most frequently employed method for generation of triazole peptidomimetics and has led to a range of related methods relying on the 1,3-dipolar cycloaddition between azides and either alkynes or alkenes. The strain-promoted azide–alkyne cycloaddition (SPAAC) reaction has been valuable for metal-free biocompatible attachment of different molecules to proteins by way of triazole synthesis.

Triazole synthesis is being employed in all fields of peptide and protein chemistry. The size, dipole moment, and electron-donating and electron-accepting properties of the 1,2,3-triazole resemble closely those of the amide bond. 1,2,3-Triazoles have however been used as amide bond surrogates with varying degrees of success due to their less than perfect alignment with the peptide backbone. On the contrary, 1,5-disubstituted C–N-type triazoles have proven effective as structural mimics of the *cis*-prolyl bond. 1,2,3-Triazoles have found greater success as side-chain mimics most importantly as replacement of the disulfide bond in cyclic bioactive peptides. Both CuAAC and RuAAC have found broad application for macrocyclizing of peptides in order to stabilize secondary structures including turns, helices, and strand motifs.

Triazole formation using the CuAAC and SPAAC reactions is bioorthogonal and thus ideal for creation of intra- and intermolecular linkages to cross-link, label, and functionalize peptides and proteins. Such studies have generated triazole analogues with improved function, greater stability, and entirely new properties. Moreover, site-specific labeling has provided triazole probes that have enhanced our understanding of the structure, function, and localization of proteins.

A variety of techniques have enabled introduction of azides and alkynes into proteins. Some of these require genetic engineering in order to introduce, for example, a stop codon for nonnatural amino acid incorporation or a peptide tag that is recognized by ligating enzymes. Other methods are more straightforward involving merely the addition of a nonnatural amino acid analogue to the growth medium of the expression host or a small-molecule reagent for chemical modification. The strategy of choice depends on the desired degree of control over the site of modification and the practical need to genetically engineer the target protein. Biocompatible water-soluble tris(triazolyl)-based ligands and copper-chelating substrates have empowered CuAAC reactions for biological applications. The CuAAC reaction may be an optimal choice, because of its potential for catalyst-controlled triggering of triazole formation using compact terminal alkynes with optimal selectivity, albeit triazole formation without additional reagents may make the catalyst-free SPAAC reaction the preferred method for specific applications.

Considering the variety of available methods and the trajectory of growth of triazole chemistry for peptide mimicry, as well as peptide and protein functionalization, this heterocycle is destined to have lasting impact on these fields and their applications in areas such as chemical biology and medicine. The future wave of peptide-based molecular architectures and proteins with novel functions that may be generated using triazole chemistry both *in vitro* and *in vivo* appears only limited by the imagination of the scientist.

References

1. Yan WY, Zhou JH, Sun MM, Chen JJ, Hu G, Shen BR (2014) *Amino Acids* 46:1419
2. Fletcher MD, Campbell MM (1998) *Chem Rev* 98:763
3. Moulin A, Bibian M, Blayo AL, El Habnoui S, Martinez J, Fehrentz JA (2010) *Chem Rev* 110:1809
4. Borg S, Estenne-Bouhtou G, Luthman K, Csoeregh I, Hesselink W, Hacksell U (1995) *J Org Chem* 60:3112
5. Tornøe CW, Meldal M (2001) Peptidotriazoles: copper(I)-catalyzed 1,3-dipolar cycloadditions on solid-phase. In: Lebl M, Houghten RA (eds) *Peptides 2001, Proc. Am. Pept. Symp.* Kluwer, San Diego, p 263
6. Agard NJ, Prescher JA, Bertozzi CR (2004) *J Am Chem Soc* 126:15046
7. Angell YL, Burgess K (2007) *Chem Soc Rev* 36:1674
8. Meldal M, Tornøe CW (2008) *Chem Rev* 108:2952
9. Tron GC, Pirali T, Billington RA, Canonico PL, Sorba G, Genazzani AA (2008) *Med Res Rev* 28:278
10. Tornøe CW, Meldal M (2009) Dipolar cycloaddition reactions in peptide chemistry. In: Bräse S, Banert K (eds) *Organic azides: syntheses and applications*. Wiley, Chichester, p 285, Chapter 10
11. Holub JM, Kirshenbaum K (2010) *Chem Soc Rev* 39:1325
12. Pedersen DS, Abell A (2011) *Eur J Org Chem* 2011:2399
13. Li X (2011) *Chem Asian J* 6:2606
14. Pasini D (2013) *Molecules* 18:9512
15. Ahmad Fuaad AA, Azmi F, Skwarczynski M, Toth I (2013) *Molecules* 18:13148
16. Valverde IE, Mindt TL (2013) *CHIMIA Int J Chem* 67:262
17. De Lombaert S, Stamford LB, Blanchard L, Tan J, Hoyer D, Diefenbacher CG, Wei D, Wallace EM, Moskal MA, Savage P, Jeng AY (1997) *Bioorg Med Chem Lett* 7:1059
18. Cesar J, Sollner M (2000) *Synth Commun* 30:4147
19. Hitotsuyanagi Y, Motegi S, Fukaya H, Takeya K (2002) *J Org Chem* 67:3266
20. Hitotsuyanagi Y, Motegi S, Hasuda T, Takeya K (2004) *Org Lett* 6:1111
21. Boeglin D, Cantel S, Heitz A, Martinez J, Fehrentz JA (2003) *Org Lett* 5:4465
22. Bibian M, Blayo AL, Moulin A, Martinez J, Fehrentz JA (2010) *Tetrahedron Lett* 51:2660
23. Blayo A-L, Brunel F, Martinez J, Fehrentz J-A (2011) *Eur J Org Chem* 2011:4293
24. Schulze B, Schubert US (2014) *Chem Soc Rev* 43:2522
25. Ramasastry SS (2014) *Angew Chem Int Ed* 53:14310
26. Buckley BR, Heaney H (2012) Mechanistic investigations of copper (I)-catalysed alkyne-azide cycloaddition reactions. In: Košmrlj J (ed) *Click triazoles*. Springer, Berlin, p 1
27. Bock VD, Hiemstra H, Van Maarseveen JH (2006) *Eur J Org Chem* 51
28. Schoffelen S, Meldal M (2014) Alkyne-azide cycloadditions. In: Li CJ, Trost BM (eds) *Modern alkyne chemistry: catalytic and atom-economic transformations*. Wiley, Weinheim
29. Wu P, Fokin VV (2007) *Aldrichchim Acta* 40:7

30. Huisgen R (1963) *Angew Chem Int Ed Engl* 2:565
31. Huisgen R, Szeimies G, Moebius L (1967) *Chem Ber* 100:2494
32. Pokorski JK, Miller Jenkins LM, Feng H, Durell SR, Bai Y, Appella DH (2007) *Org Lett* 9:2381
33. Horne WS, Olsen CA, Beierle JM, Montero A, Ghadiri MR (2009) *Angew Chem Int Ed* 48:4718
34. Tornøe CW, Christensen C, Meldal M (2002) *J Org Chem* 67:3057
35. Bock VD, Perciaccante R, Jansen TP, Hiemstra H, Van Maarseveen JH (2006) *Org Lett* 8:919
36. Shao C, Cheng G, Su D, Xu J, Wang X, Hu Y (2010) *Adv Synth Catal* 352:1587
37. Berg R, Straub J, Schreiner E, Mader S, Rominger F, Straub BF (2012) *Adv Synth Catal* 354:3445
38. Rostovtsev VV, Green LG, Fokin VV, Sharpless KB (2002) *Angew Chem Int Ed* 41:2596
39. Oh K, Guan Z (2006) *Chem Commun* 3069
40. Worrell BT, Malik JA, Fokin VV (2013) *Science* 340:457
41. Wang Q, Chan TR, Hilgraf R, Fokin VV, Sharpless KB, Finn MG (2003) *J Am Chem Soc* 125:3192
42. Chan TR, Hilgraf R, Sharpless KB, Fokin VV (2004) *Org Lett* 6:2853
43. Hong V, Presolski SI, Ma C, Finn MG (2009) *Angew Chem Int Ed* 48:9879
44. Rodionov VO, Presolski SI, Diaz DD, Fokin VV, Finn MG (2007) *J Am Chem Soc* 129:12705
45. Michaels HA, Zhu L (2011) *Chem Asian J* 6:2825
46. Chouhan G, James K (2011) *Org Lett* 13:2754
47. Zhang L, Chen X, Xue P, Sun HHY, Williams ID, Sharpless KB, Fokin VV, Jia G (2005) *J Am Chem Soc* 127:15998
48. Boren BC, Narayan S, Rasmussen LK, Zhang L, Zhao H, Lin Z, Jia G, Fokin VV (2008) *J Am Chem Soc* 130:8923
49. Boz E, Tüzün NS (2013) *J Organomet Chem* 724:167
50. Majireck MM, Weinreb SM (2006) *J Org Chem* 71:8680
51. Kelly AR, Wei J, Kesavan S, Marié JC, Windmon N, Young DW, Marcaurelle LA (2009) *Org Lett* 11:2257
52. Zhang JQ, Kemmink J, Rijkers DTS, Liskamp RMJ (2013) *Chem Commun* 49:4498
53. Blomquist AT, Liu LH (1953) *J Am Chem Soc* 75:2153
54. Wittig G, Krebs A (1961) *Chem Ber* 94:3260
55. Jewett JC, Bertozzi CR (2010) *Chem Soc Rev* 39:1272
56. Ahsanullah, Schmieder P, Kühne R, Rademann J (2009) *Angew Chem Int Ed* 48:5042
57. Ahsanullah, Rademann J (2010) *Angew Chem Int Ed* 49:5378
58. Niu T, Gu L, Wang L, Yi W, Cai C (2012) *Eur J Org Chem* 2012:6767
59. Angelo NG, Arora PS (2005) *J Am Chem Soc* 127:17134
60. Zhang Z, Fan E (2006) *Tetrahedron Lett* 47:665
61. Angelo NG, Arora PS (2007) *J Org Chem* 72:7964
62. Jochim AL, Miller SE, Angelo NG, Arora PS (2009) *Bioorg Med Chem Lett* 19:6023
63. Aucagne V, Leigh DA (2006) *Org Lett* 8:4505
64. Montagnat OD, Lessene G, Hughes AB (2010) *J Org Chem* 75:390
65. Johansson JR, Hermansson E, Nordén B, Kann N, Beke-Somfai T (2014) *Eur J Org Chem* 2014:2703
66. Kolb HC, Sharpless KB (2003) *Drug Discov Today* 8:1128
67. Ko E, Liu J, Perez LM, Lu G, Schaefer A, Burgess K (2011) *J Am Chem Soc* 133:462
68. Ko E, Liu J, Burgess K (2011) *Chem Soc Rev* 40:4411
69. Abboud J-LM, Foces-Foces C, Notario R, Trifonov RE, Volovodenco AP, Ostrovskii VA, Alkorta I, Elguero J (2001) *Eur J Org Chem* 2001:3013
70. Gamovskii AD, Kolodyazhnyi YV, Osipov OA, Minkin VI, Giller SA, Mazheika IB, Grandberg II (1971) *Chem Heterocycl Compd* 7:809

71. Massarotti A, Aprile S, Mercalli V, Del Grosso E, Grosa G, Sorba G, Tron GC (2014) *ChemMedChem* 9:2497
72. Horne WS, Yadav MK, Stout CD, Ghadiri MR (2004) *J Am Chem Soc* 126:15366
73. Tornøe CW, Sanderson SJ, Mottram JC, Coombs GH, Meldal M (2004) *J Comb Chem* 6:312
74. St Hilaire PM, Alves LC, Sanderson SJ, Mottram JC, Juliano MA, Juliano L, Coombs GH, Meldal M (2000) *ChemBioChem* 1:115
75. Güell I, Micaló L, Cano L, Badosa E, Ferre R, Montesinos E, Bardají E, Feliu L, Planas M (2012) *Peptides* 33:9
76. Tam A, Arnold U, Soellner MB, Raines RT (2007) *J Am Chem Soc* 129:12670
77. Roice M, Johannsen I, Meldal M (2004) *QSAR Comb Sci* 23:662
78. Turner RA, Oliver AG, Lokey RS (2007) *Org Lett* 9:5011
79. Jagasia R, Holub JM, Bollinger M, Kirshenbaum K, Finn MG (2009) *J Org Chem* 74:2964
80. Angell Y, Burgess K (2005) *J Org Chem* 70:9595
81. Meutermans WD, Bourne GT, Golding SW, Horton DA, Campitelli MR, Craik D, Scanlon M, Smythe ML (2003) *Org Lett* 5:2711
82. Schmidt U, Langner J (1997) *J Pept Res* 49:67
83. Hill TA, Shepherd NE, Diness F, Fairlie DP (2014) *Angew Chem Int Ed* 53:13020
84. Kawamoto SA, Coleska A, Ran X, Yi H, Yang CY, Wang S (2012) *J Med Chem* 55:1137
85. de Araujo AD, Hoang HN, Kok WM, Diness F, Gupta P, Hill TA, Driver RW, Price DA, Liras S, Fairlie DP (2014) *Angew Chem Int Ed* 53:6965
86. Ingale S, Dawson PE (2011) *Org Lett* 13:2822
87. Jacobsen Ø, Maekawa H, Ge NH, Górbitz CH, Rongved P, Ottersen OP, Amiry-Moghaddam M, Klaveness J (2011) *J Org Chem* 76:1228
88. Pehere AD, Abell AD (2012) *Org Lett* 14:1330
89. Pehere AD, Sumbly CJ, Abell AD (2013) *Org Biomol Chem* 11:425
90. Celentano V, Diana D, De Rosa L, Romanelli A, Fattorusso R, D'Andrea LD (2012) *Chem Commun* 48:762
91. Park JH, Waters ML (2013) *Org Biomol Chem* 11:69
92. Empting M, Avrutina O, Meusinger R, Fabritz S, Reinwarth M, Biesalski M, Voigt S, Buntkowsky G, Kolmar H (2011) *Angew Chem Int Ed* 50:5207
93. Holland-Nell K, Meldal M (2011) *Angew Chem Int Ed* 123:5310
94. Kee JM, Villani B, Carpenter LR, Muir TW (2010) *J Am Chem Soc* 132:14327
95. McAllister TE, Webb ME (2012) *Org Biomol Chem* 10:4043
96. Mukai S, Flematti GR, Byrne LT, Besant PG, Attwood PV, Piggott MJ (2012) *Amino Acids* 43:857
97. Buysse K, Farard J, Nikolaou A, Vanderheyden P, Vauquelin G, Sejer Pedersen D, Tourwé D, Ballet S (2011) *Org Lett* 13:6468
98. Van der Poorten O, Fehér K, Buysse K, Feytens D, Zoi I, Schwartz SD, Martins JC, Tourwé D, Cai M, Hruba VJ, Ballet S (2014) *ACS Med Chem Lett* 6:192
99. van der Knaap M, Lageveen LT, Busscher HJ, Mars-Groenendijk R, Noort D, Otero JM, Llamas-Saiz AL, van Raaij MJ, van der Marel GA, Overkleeft HS, Overhand M (2011) *ChemMedChem* 6:840
100. Fittler H, Avrutina O, Glotzbach B, Empting M, Kolmar H (2013) *Org Biomol Chem* 11:1848
101. Qiu HB, Chen XY, Li Q, Qian WJ, Yu SM, Tang GL, Yao ZJ (2014) *Tetrahedron Lett* 55:6055
102. Kuijpers BHM, Groothuys S, Keereweer AR, Quaedflieg PJLM, Blaauw RH, Van Delft FL, Rutjes FPJT (2004) *Org Lett* 6:3123
103. Kuijpers BH, Groothuys S, Hawner C, Dam J, Quaedflieg PJ, Schoemaker HE, Delft FL, Rutjes FP (2008) *Org Process Res Dev* 12:503
104. Huang W, Groothuys S, Heredia A, Kuijpers BH, Rutjes FP, van Delft FL, Wang L-X (2009) *ChemBioChem* 10:1234
105. Miller N, Williams GM, Brimble MA (2009) *Org Lett* 11:2409
106. Capicciotti CJ, Trant JF, Leclere M, Ben RN (2011) *Bioconjug Chem* 22:605

107. Kowalczyk R, Brimble MA, Tomabechi Y, Fairbanks AJ, Fletcher M, Hay DL (2014) *Org Biomol Chem* 12:8142
108. Boutoureira O, D'Hooge F, Fernández-González M, Bernardes GJ, Sánchez-Navarro M, Koeppe JR, Davis BG (2010) *Chem Commun* 46:8142
109. Maschauer S, Haubner R, Kuwert T, Prante O (2013) *Mol Pharm* 11:505
110. Lang K, Chin JW (2014) *Chem Rev* 114:4764
111. Ngo JT, Tirrell DA (2011) *Acc Chem Res* 44:677
112. Johnson JA, Lu YY, Van Deventer JA, Tirrell DA (2010) *Curr Opin Chem Biol* 14:774
113. Davis L, Chin JW (2012) *Nat Rev Mol Cell Biol* 13:168
114. Liu CC, Schultz PG (2010) *Ann Rev Biochem* 79:413
115. Matsumoto T, Tanaka T, Kondo A (2012) *Biotechnol J* 7:1137
116. van Geel R, Debets MF, Lowik DWPM, Pruijn GJM, Boelens WC (2012) *Amino Acids* 43:1251
117. Fernandez-Suarez M, Baruah H, Martinez-Hernandez L, Xie KT, Baskin JM, Bertozzi CR, Ting AY (2007) *Nat Biotechnol* 25:1483
118. Witte MD, Cragnolini JJ, Dougan SK, Yoder NC, Popp MW, Ploegh HL (2012) *Proc Natl Acad Sci U S A* 109:11993
119. Lin PC, Ueng SH, Tseng MC, Ko JL, Huang KT, Yu SC, Adak AK, Chen YJ, Lin CC (2006) *Angew Chem Int Ed* 45:4286
120. Kalia J, Raines RT (2006) *ChemBioChem* 7:1375
121. Govindaraju T, Jonkheijm P, Gogolin L, Schroeder H, Becker CFW, Niemeyer CM, Waldmann H (2008) *Chem Commun* 3723
122. Steinhagen M, Holland-Nell K, Meldal M, Beck-Sickinger AG (2011) *ChemBioChem* 12:2426
123. Dirks AJ, Van Berkel SS, Hatzakis NS, Opsteen JA, Van Delft FL, Cornelissen JJLM, Rowan AE, Van Hest JCM, Rutjes FPJT, Nolte RJM (2005) *Chem Commun* 4172
124. van Dongen SFM, Teeuwen RLM, Nallani M, Van Berkel SS, Cornelissen JJLM, Nolte RJM, Van Hest JCM (2009) *Bioconjug Chem* 20:20
125. Schoffelen S, van Eldijk MB, Rooijackers B, Raijmakers R, Heck AJR, Van Hest JCM (2011) *Chem Sci* 2:701
126. Debets MF, Van Berkel SS, Schoffelen S, Rutjes FPJT, Van Hest JCM, Van Delft FL (2010) *Chem Commun* 46:97
127. Dommerholt J, Schmidt S, Temming R, Hendriks LJA, Rutjes FPJT, Van Hest JCM, Lefeber DJ, Friedl P, Van Delft FL (2010) *Angew Chem Int Ed* 49:9422
128. Ning XH, Guo J, Wolfert MA, Boons GJ (2008) *Angew Chem Int Ed* 47:2253
129. Jewett JC, Sletten EM, Bertozzi CR (2010) *J Am Chem Soc* 132:3688
130. de Almeida G, Sletten EM, Nakamura H, Palaniappan KK, Bertozzi CR (2012) *Angew Chem Int Ed* 51:2443
131. Baskin JM, Prescher JA, Laughlin ST, Agard NJ, Chang PV, Miller IA, Lo A, Codelli JA, Bertozzi CR (2007) *Proc Natl Acad Sci U S A* 104:16793
132. Kim EJ, Kang DW, Leucke HF, Bond MR, Ghosh S, Love DC, Ahn JS, Kang DO, Hanover JA (2013) *Carbohydr Res* 377:18
133. van Geel R, Pruijn GJM, Van Delft FL, Boelens WC (2012) *Bioconjug Chem* 23:392
134. Yang MY, Li J, Chen PR (2014) *Chem Soc Rev* 43:6511
135. Uttamapinant C, Tangpeerachaikul A, Grecian S, Clarke S, Singh U, Slade P, Gee KR, Ting AY (2012) *Angew Chem Int Ed* 51:5852
136. Uttamapinant C, Sanchez MI, Liu DS, Yao JZ, Ting AY (2013) *Nat Protoc* 8:1620
137. Bevilacqua V, King M, Chaumontet M, Nothisen M, Gabillet S, Buisson D, Puente C, Wagner A, Taran F (2014) *Angew Chem Int Ed* 53:5872
138. Lim SI, Mizuta Y, Takasu A, Kim YH, Kwon I (2014) *PLoS One* 9:e98403
139. Besanceney-Webler C, Jiang H, Zheng TQ, Feng L, del Amo DS, Wang W, Klivansky LM, Marlow FL, Liu Y, Wu P (2011) *Angew Chem Int Ed* 50:8051

140. Nairn NW, Shanebeck KD, Wang AJ, Graddis TJ, VanBrunt MP, Thornton KC, Grabstein K (2012) *Bioconjug Chem* 23:2087
141. Dennler P, Chiotellis A, Fischer E, Bregeon D, Belmont C, Gauthier L, Lhospipe F, Romagne F, Schibli R (2014) *Bioconjug Chem* 25:569
142. Kim CH, Axup JY, Dubrovskaya A, Kazane SA, Hutchins BA, Wold ED, Smider VV, Schultz PG (2012) *J Am Chem Soc* 134:9918
143. Wagner K, Kwakkenbos MJ, Claassen YB, Maijoor K, Bohne M, van der Sluijs KF, Witte MD, van Zoelen DJ, Cornelissen LA, Beaumont T, Bakker AQ, Ploegh HL, Spits H (2014) *Proc Natl Acad Sci U S A* 111:16820
144. Wang AZ, Kluger R (2014) *Biochemistry* 53:6793
145. Nischan N, Herce HD, Natalia F, Bohlke N, Budisa N, Cardoso MC, Hackenberger CP (2015) *Angew Chem Int Ed* 54:1950
146. Smith MT, Hawes AK, Bundy BC (2013) *Curr Opin Biotechnol* 24:620
147. Patel KG, Swartz JR (2011) *Bioconjug Chem* 22:376
148. Rhee JK, Baksh M, Nycholat C, Paulson JC, Kitagishi H, Finn MG (2012) *Biomacromolecules* 13:2333
149. van Eldijk MB, Smits FCM, Vermue N, Debets MF, Schoffelen S, Van Hest JCM (2014) *Biomacromolecules* 15:2751
150. Schneider D, Schneider T, Rosner D, Scheffner M, Marx A (2013) *Bioorg Med Chem* 21:3430
151. van Treel ND, Mootz HD (2014) *J Pept Sci* 20:121
152. Eger S, Scheffner M, Marx A, Rubini M (2010) *J Am Chem Soc* 132:16337
153. Weikart ND, Sommer S, Mootz HD (2012) *Chem Commun* 48:296
154. Schneider T, Schneider D, Rosner D, Malhotra S, Mortensen F, Mayer TU, Scheffner M, Marx A (2014) *Angew Chem Int Ed* 53:12925
155. van Kasteren SI, Kramer HB, Jensen HH, Campbell SJ, Kirkpatrick J, Oldham NJ, Anthony DC, Davis BG (2007) *Nature* 446:1105
156. Yi L, Abootorabi M, Wu YW (2011) *ChemBioChem* 12:2413
157. Dong SL, Moroder L, Budisa N (2009) *ChemBioChem* 10:1149
158. Milles S, Tyagi S, Banterle N, Koehler C, VanDelinder V, Plass T, Neal AP, Lemke EA (2012) *J Am Chem Soc* 134:5187
159. Abdeljabbar DM, Piscotta FJ, Zhang SY, Link AJ (2014) *Chem Commun* 50:14900
160. Neumann H, Wang KH, Davis L, Garcia-Alai M, Chin JW (2010) *Nature* 464:441
161. Lin W, Du YF, Zhu YT, Chen X (2014) *J Am Chem Soc* 136:679
162. Yang Y, Lin SX, Lin W, Chen PR (2014) *ChemBioChem* 15:1738
163. Beatty KE, Fisk JD, Smart BP, Lu YY, Szychowski J, Hangauer MJ, Baskin JM, Bertozzi CR, Tirrell DA (2010) *ChemBioChem* 11:2092
164. Yao JZ, Uttamapinant C, Poloukhine A, Baskin JM, Codelli JA, Sletten EM, Bertozzi CR, Popik VV, Ting AY (2012) *J Am Chem Soc* 134:3720
165. Borrmann A, Van Hest JCM (2014) *Chem Sci* 5:2123
166. Hinz FI, Dieterich DC, Tirrell DA, Schuman EM (2012) *ACS Chem Neurosci* 3:40
167. Rouhanifard SH, Nordstrom LU, Zheng TQ, Wu P (2013) *Chem Soc Rev* 42:4284
168. Hong V, Steinmetz NF, Manchester M, Finn MG (2010) *Bioconjug Chem* 21:1912
169. del Amo DS, Wang W, Jiang H, Besanceney C, Yan AC, Levy M, Liu Y, Marlow FL, Wu P (2010) *J Am Chem Soc* 132:16893
170. Laughlin ST, Baskin JM, Amacher SL, Bertozzi CR (2008) *Science* 320:664
171. Jiang H, Zheng TQ, Lopez-Aguilar A, Feng L, Kopp F, Marlow FL, Wu P (2014) *Bioconjug Chem* 25:698
172. Laughlin ST, Bertozzi CR (2009) *ACS Chem Biol* 4:1068
173. Chang PV, Prescher JA, Sletten EM, Baskin JM, Miller IA, Agard NJ, Lo A, Bertozzi CR (2010) *Proc Natl Acad Sci U S A* 107:1821

Index

A

- ABT-594, 60
Acetyl-4-fluoro-3,5-methanoproline methyl esters, 72
N-Acetyl-2,4-methanoproline *N*-methylamide, 60
Aesculus parviflora, 62
AG-7088, 127
Aid peptides, 161, 165
Aldehydes, 72, 88, 105, 106, 129–136, 147, 149, 182–190, 241
 α -hydrazination, asymmetric, 97
Alkaloids, 250
4-Alkyl-3-amino- γ -lactams, 136
Amide bond isosteres, thiazoles, 249
8-Amidoquinolines, 140
Amino acids, azepinone-constrained, 177
 constrained, 51, 177
 cyclic delta, polyhydroxylated, 211
 non-proteinogenic, 97
Amino-arylazepinones, 177
Amino-benzazepinones (Aba), 177, 180, 193
1-Aminocyclopropane-1-carboxylic acid (Acc), 52
1-Amino-1,3-dicarboxycyclobutane, 57
4-Amino-(7-hydroxy)-tetrahydro-2-benzazepin-3-one, 178
Aminoimidazolidinones, 125, 160
Aminoimidazolinones, 125
Amino-indoloazepinones, 177
3-Amino- γ -lactam 4-carboxylates, 138
3-Amino- γ -lactams (Agl), 142
 analogs, 125
8-Amino-5-methoxyquinoline (MQ), 135
4-Amino(methyl)-1,3-thiazole-5-carboxylic acids, 247
Amino-3-oxo-hexahydropyrrolo[2,1-*a*]isoquinoline-5-carboxylate, 133
4-Amino-3-oxo-tetrahydro-1*H*-azepino[3,4-*b*]indol-2-yl acetic acid, 186
Aminopeptidase-N (AP-N), 200
3-Amino-2-pyridone, 127
4-Aminopyroglutamate (Apy), 134
7-Amino-pyrrolo[1,2-*a*]pyrimidin-6-one-4-carboxylate, 133
4-Amino-tetrahydro-2-benzazepin-3-one (Aba), 180
4-Amino-tetrahydro-2-indoloazepin-3-one (Aia), 186
4-Amino-tetrahydro-2-triazoloazepin-3-one (Ata), 188
5-Amino-tetrahydropyridazine-3,6-diones, 120
Aminothiazoles, 238, 241, 245
Amino-triazoloazepinones, 177
Amphipathicity, 45
Amyloidosis, 18
Analgesics, 20, 43, 194, 197
Angiotensin-converting enzyme (ACE), 42, 43, 82, 84, 118, 192
Angiotensinogen, 139
Angiotensins, 126, 177, 188, 192, 200
Apicidin, 273
3-Aryl-3-hydroxylamino- γ -lactam, 144
Ascidia cyclamide, 251–253
Ateleia herbert-smithii, 57
Aza-Diels–Alder cycloaddition, 97, 101
7-(Azabenzotriazol-1-yloxy)tripyrrolidinophosphonium hexafluorophosphate (AOI), 117

Azabicycloalkane, 125
 amino acids, 132
 Azabicyclo[3.2.0]hexane, 65
 Azabicyclo[2.1.0]pentane-3-carboxylic acid, 89
 Azapeptides, 125, 154, 164
 Azepinones, 177
 Azide-alkyne cycloadditions, 216, 267–299
 biocompatibility, 292
 Azidohomoalanine, 296
 2-Azido-5-iodobenzoic acid, 296
 Azinotricin, 110
 Azodicarboxylate, 101

B

Bacillus ribonuclease (barnase), 15
 BCR-ABL kinase, 256
 2-Benzamido-3-chloropropionate, 58
 Benzotriazoles, 182, 271
 Benzotriazol-1-yl-
 oxytripyrrolidinophosphonium
 hexafluorophosphate (PyBOP), 219
 4-Benzyl *N*-amino-imidazolin-2-one, 157
 4-Benzyl *N,N*-bis-(*p*-methoxybenzamido)
 imidazolin-2-one, 166
 Bicyclic lactams, 211
 Biodegradation, 27
 Bis(chloromethyl)dimethylsilane, 30, 33
 Bis(dimethylamino)methylene]-1*H*-1,2,3-
 triazolo[4,5-*b*]pyridinium-3-oxide
 hexafluorophosphate (HATU), 111
 Bistratamides, 250, 251
 Bi-thiazoles, 249
 Blood clotting, 19
 BMS-561392, 127
 BMS-640994, 258
N-Boc-3,4-dehydro-L-pyroglytamic acid ABO
 (5-methyl-2,7,8-trioxabicyclo[3.2.1]
 octyl) ester, 65
N-Boc-*cis*-4,5-methano-L-prolinol, 78
Bocoa, 58
 BP100, 280
 Bradykinin, 177, 197
 Butoxyproline, 106
 Butylproline, 34

C

Calcitonin gene-related peptide (CGRP)
 receptor, 127, 128, 133
 Calpain II, 286
 Captopril, 43, 83

1-Carbamoyl-4-amino-indoloazepinones, 188
 Carbohydrate-peptide hybrids, 213
 4-Carboxy-2,4-methanoproline, 60
 5-Carboxy- γ -lactams, 134
N-Carboxyanhydrides (NCAs), 38
 Catenin, 284
N-Cbz-2-hydroxymethyl dihydropyridine, 71
 Cell membrane, 45
 Cell-penetrating peptides (CPPs), 45
 Chloptosin, 112
 Cilazapril, 118
 Cinchonidine, 66
 Click reaction, 267
 Clotting diseases, 19
 Collagen, 2, 10–20, 28, 69, 213
 4-fluoroprolines, 1, 10
 mimics, 70
 synthesis, 20
 Concanavalin A, 216
 Conformational analysis, 51
 Cook-Heilbron synthesis, 241
 Copper(I)-catalyzed azide-alkyne
 cycloaddition (CuAAC), 216, 267, 273,
 282, 287
 Coronamic acid, 53
 Cyclin-dependent kinases (CDK), 258
 Cyclophilin A, 110
 Cyclosporin A, 110
 Cysteine, 14, 109, 148, 214, 227, 235–246, 292
 protease, 280
 Cystothiazole A, 250

D

Dasatinib, 256
 Dehydroabietylamine, 66
 5,6-Dehydro ϵ -lactam, 126
 Dehydropiperazic acids, 99, 101
 Dehydro-*N*-trifluoroacetyl-L-proline methyl
 ester, 63
Delonix regia, 62
 Deltorphan II, 193
 Dermorphin, 193
 Diabetes, 73
 2,5-Diaryl thiazoles, 240
 Diazabicyclo[3.3.0]alkane dipeptide mimic,
 140
 Diazaspiro[4.4]nonadione tripeptide, 144
 1,7-Diazaspiro[4.4]nonane-2,6-dione, 143
 Diethyl *N*-Cbz-2,3-dihydropyrrole-2,2-
 dicarboxylate, 80
 Diethylaminosulfur trifluoride (DAST), 4
 Difluoroproline, 9

Dihydropyrazine, 30
Dihydropyridinones, 126
Diisopropyl malonate, 62
Diketopiperazines, 35
Dimethyldioxirane (DMDO), 134
Dimethyl-3,4-methano-L-proline, 68
Dimethylpiperazine, 87
Dimethylproline, 34
Dimethylsilane, 30
Dimethyltyrosine, 195
Dimethoxy-pentanal, 106
Dipeptide mimics, 125
Dipeptidyl peptidase 4 (DPP-4), 73
Disulfide-bond mimetics, 286
DNA, mimics, 213
Drug prototypes, 51

E
EGFP, 17
Elastin-like polypeptide-poly(ethylene glycol) (ELP-PEG), 296
Elastins, 16
Endomorphin-2, 196
Endozepins, 42
Encarbamate, 77
Ephedra, 62
Epibatidine, 60
Erythropoietin-producing hepatocellular kinase EphA4, 256
Ethyl 2-isocyano(phenyl)acetate, 144
Ethyl *cis*-*N*-Boc-4,5-methano-L-prolinate, 77
Ethyl *N*-Boc-L-pyroglytamate, 75
Ethylene-forming enzyme (EFE), 52

F
Factor D, 84
Farnesyltransferase (FTase), 246
5-Fluoro-2,4-methanoproline, 62
4-Fluoro-3,5-methanoproline methyl esters, 71
4-Fluoroprolines, 1
2-Fluoroprop-2-enyl methanesulfonate, 62
Foldamers, 213
FR901483, 134
Freidinger-Weber lactams, 125, 127
Fuchs-Farthings method, 38

G
G protein-coupled melanocortin-4 receptor, 282
G protein-coupled receptors (GPCRs), 20, 235, 247, 259
Gabriel synthesis, 242

Gamma-aminobutyric acid (GABA), 20
Gauche effect, 1
GE2270A, 253
GE37468A, 253
Gemopatrilat, 127
Glucose-dependent insulinotropic peptide (GIP), 73
Glucosyluronic acid methylamine (H-Gum-OH), 216
Glutamate-5-semialdehyde, 15
5-Glutamylphosphate reductase, 15
GR138676, 139
GR64349, 139
Gramicidin S, 217–221, 247, 288

H

Hairpins, 15, 127, 211, 222, 226, 273
Hajos-Parrish-Eder-Sauer-Wiechert reaction, 86
Halomethylsilane, 29
Hantzsch synthesis, 238–241
HCV inhibitory activity, 120
Hematopoietic-lineage cell-specific (HS1) protein, 13
Hematopoietic progenitor kinase 1 (HPK1), 13
Hepatitis C virus (HCV), 120
3-Heteroarylmethyl-3-amino- γ -lactam, 143
Heterocycles, 235
HIV, 99
 protease, 220, 221, 249
Homopolypeptides, 35, 39
Huisgen reaction (thermal 1,3-dipolar cycloaddition), 273
Human calcitonin gene-related peptide 1 receptor, 133
Human growth hormone (hGH), 135
Human proton-coupled amino acid transporter 1 (HPAT1), 62
Hydrazination, 104, 107, 114
 β -Hydroxy- α -amino- γ -lactam (Hgl), 138
Hydroxylation, 2, 12, 78, 213
4-Hydroxy-4-phenyl- γ -lactams, 141
4-Hydroxyproline, 1, 2, 5, 44, 69, 70, 135, 215
Hydroxypyrrolizidinones, 134
 β -Hydroxytyrosine, 214
Hyperglycemia, 73

I

Imatinib, 256
Imidazo[1,2-*a*]azepine, 127
Incretins, 73
Inhibitors of apoptosis protein (IAP) antagonists, 249

- Insulin-regulated aminopeptidase (IRAP), 200
- Integration host factor (IHF), 15
- Interleukin-1, 119, 125
IL-1 β receptor (IL-1R), 139, 146
- 3-Isocyanato- γ -lactam, 144
- Isopropylidene-L-riburonolactone, 227
- J**
- J-104870, 248
- Janus kinase 2 inhibitor, 243
- JBIR-39, 116
- Jun N-terminal kinases (JNKs), 249
- K**
- Kainic acids, 81
- Kettapeptin, 110
- Kinases, 249, 256, 258
inhibition, 256
- KlenTaq DNA, 18
- Kutznerides, 99
- L**
- Lactams, 220
bicyclic, 227
polyhydroxylated, 221
- Largazole, 251
- Leishmania mexicana* cysteine protease, 280
- Leucyl-4,5-methano-L-prolylnitrile, 79
- Lipoic acid ligase (LplA), 297
- Lissoclinum bistratum*, 250
- Lissoclinum patella*, 252
- Loracarbef, 127
- Luteinizing hormone-releasing hormone, 220
- Luzopeptin, 98
- M**
- Macrocyclization, 226, 267, 275, 283
- Mannurono-3,6-lactone, 229
- MAPK14, 258
- Mechercharimyces asporophorigenens*, 251
- Melanocortin, 177, 202
- Melanocyte-stimulating hormone (MSH), 201
- Meloxicam, 260
- Menthyl pyroglutamate, 143
- Methano-L-azetidine-2-carboxylic acid, 88
- Methano kainic acid analogues, 82
- Methanologues, proline, 51
- Methano-7-oxo-1-azabicyclo[3.2.0]heptane
carboxylic acids 56
- Methanopipelic acid, 56
- Methanoprolines, 52, 57, 62, 69, 73
- Methano-L-prolylamide, 77
- Methano-L-prolylnitrile amides, 79, 80
- Methanopyroglutamic acid, 56
- Methano-L-pyrrolidine-2-nitrile, 77
- Methionine, 109, 139, 256, 295
- N-p*-Methoxybenzyl-tetrahydropyridazine, 112
- 4-Methyl *N*-(benzamido)imidazolin-2-one
amide, 165
- Methyl *N*-benzoyl-2,4-methanopropionate, 59
- Methyl 2,4-methanoglutamate, 59
- Micrococcin P1 (thiocillin), 253, 254
- Micrococcinic acid, 250, 253
- Microglobulin, 18
- MK-2918, 127
- MOL-376, 119
- Monamycin, 98
- Motilin, agonist, 119
- MT-II, 201
- N**
- Nai dipeptide, 158, 165
- Natural products, 51
- Neurokinin-1 antagonist, 197
- Neuropeptide Y antagonist, 248
- Neurotensin (NT), 20, 43
- Neutral endopeptidase (NEP), inhibitors, 193
- Nicotinic acetylcholine receptor (nAChR), 60
- Nipecotinic acid, 20
- Nosiheptide, 254, 255
- Nucleic acids, 212, 213
locked (LNA), 212, 213
- NWG01, 114
- O**
- Octadecanoneuropeptide (ODN), 42
- Opioid agonist-neurokinin-1 (NK1R)
antagonist, 197
- Opioid peptides, 177, 193
receptor, 148
- Osteoarthritis, 119
- 5-Oxa-1-azabicyclo[4.4.0]decane, 127
- 6-Oxa-1-azabicyclo[5.3.0]decane, 127
- Oxapyrrolidinone, 132
- Oxaspiro[3.3]heptane, 62
- Oxazolidinone, 102
- Oxiranylglycines, 138

P

- p38 α kinase inhibitors, 258
- Padanamides, 108
- Pan-Aurora kinase inhibition, 63
- Patellamide D, 251–253
- Penta-2,4-dienoic acid, 101
- Peptide nucleic acid (PNA), 212, 213
- Peptides, cyclic, 235, 250, 282
 - mimetics, 97, 267
 - modified bioactive, 27
 - stapled/bridged, 284
 - structure, 27
- Phaseolus aureus*, 62
- 2-Phenyl-3-endo-phenyl-2-azabicyclo[2.2.0]hex-5-ene, 72
- 4-Phenyl-1,2,4-triazoline-3,5-dione, 101
- Phospholipase C (PLC), 42
- Phthalohydrazide, 101
- Piperazic acid, 97–122
 - acylation, 110
- Piperazic amide, 104
- Piperazimycin A, 114
- Polyproline helices, 13
 - type I (PPI), 13
 - type II (PPII), 6, 27, 35, 36, 45, 89, 215, 229, 231
- Polysilaproline, 38
- Polytheonamide B, 214
- Pralnacasan, 119
- Pro-opiomelanocortin (POMC) prehormone, 201
- Proline, 1, 52, 99, 105
 - methanologues, 51
 - surrogate, 27
- Proline *tert*-butyl ester, 53
- Proline 4-carboxylic acid, 60
- Prolyl-4-hydroxylase (P4H), 2
- Proteins, iodination, 296
 - labeling, 267
- Pyridazine, 97, 112, 115
- Pyrrolidine, 1, 33, 63, 134, 140, 215
- Pyroline carboxylate reductase, 15

R

- RA-VII, 271
- Random nonstandard peptide integrated discovery (RaPID), 126
- Renin, 192
- Renin-angiotensin-aldosterone system (RAAS), 192
- RNase A mimic, 282

- Ruthenium-catalyzed azide–alkyne cycloaddition (RuAAC), 267, 275
- Rytvela, 139

S

- Sangamides, 120
 - Sanglifehrin, 110, 121
 - Sanguinamides, 250
 - Sansalvamide A, 247
 - Saxagliptin, 73, 77
 - Seglitide (MK678), 198
 - Semialdehydes, 15, 128–134, 142, 144, 146
 - Semicarbazide, 163
 - Silacaptopril, 43
 - Silanols, 29
 - Silaproline, 27
 - Silicon-containing proline surrogate, 29
 - Silyl amino acids, 29
 - SM83, 128
 - Somatostatin, 126, 129, 142, 177, 198–200, 216
 - Sparteine, 66
 - Split-intein circular ligation of peptides and proteins (SICLOPPS), 126
 - SR146131, 247
 - SR27897, 247
 - SSR-125543A, 248
 - Stat3, 19
 - Stereoelectronic effect, 1
 - Strain-promoted azide–alkyne cycloaddition (SPAAC), 267, 276
 - Streptomyces jamaicensis*, 98
 - Streptomyces zaomyceticus* SF-1836, 88
 - Substance P (SP), 42, 126, 141
 - Sudoxicam, 259
 - Sugar amino acids (SAAs), 211, 215
-
- T**
 - Tachykinin, 139
 - Tachyplesin 1, 287
 - TAN1251, 134
 - Tartaric acid, 53
 - Telcagepant, 127
 - Tetrahydro- β -carboline (THBC), analog, 142
 - Tetrahydro- β -carboline-3-carboxylic acid (Tcc), 187
 - Tetrahydroisoquinoline-3-carboxylic acid (Tic), 178
 - Tetrahydro-2*H*-1,2-oxazinide, 120
 - Thiaindolizidinone, 227

- Thiazole-5-carboxamides, 246
 - Thiazoles, 235, 238
 - DNA-binding, 259
 - Thiazolidines, 227
 - lactams, 228
 - Thiazomycin A, 214
 - Thioamides, 238, 271
 - Thiopropine, 44
 - Thiostrepton A, 253–255
 - Thrombin, 19, 257
 - inhibitors, 19, 119, 259
 - Tiagabine, 20
 - Transient receptor potential cation channel,
 - member A1 (TRPA1), 86
 - Triazoles, 267, 270
 - Triazoloazepinone, 188
 - Triphosgene, 38
 - Tris[(1-benzyl-1*H*-1,2,3-triazol-4-yl)methyl]
 - amine (TBTA), 274
 - Trypsin, 19
 - inhibitor, 286–288
 - Tumor necrosis factor- α converting enzyme
 - inhibitor, 249
- U**
- Ubiquitin, 17, 296
 - Ubiquitylation, 17
 - Urukthapelstatin A, 251–253
- V**
- Vaccines, 295
 - Vancomycin, 214, 275
 - Virus-like nanoparticles (VLPs), 295
- Z**
- Zinc, 76, 244, 252
 - Zinc enolate, 140
 - Zinc finger, 220
 - Zinc metalloenzyme, 43, 246